Geologic and geochemical attributes of the Beaver River Diabase and Greenstone Flow: Testing a possible intrusive-volcanic correlation in the 1.1 Ga Midcontinent Rift

A THESIS SUBMITTED TO THE FACULTY OF THE GRADUATE SCHOOL OF THE UNIVERSITY OF MINNESOTA BY

Michael Sean Doyle

IN PARTIAL FULFILMENT OF THE REQUIREMENTS FOR THE DEGREE OF MASTER OF SCIENCE

Advisor: Dr. James Miller

February 2016

ACKNOWLEDGEMENTS

This work would not be completed – nor would the idea driving this research be conceived of, for that matter – without the extensive knowledge and expert guidance of my advisor, Dr. James Miller. His experience in the field and ability to see the bigger picture led to this undertaking and I am grateful for all his guidance and suggestions that helped to shape and refine this document. Thank you as well to my committee members, Drs. John Goodge and Paul Siders, whose input was both invaluable and appreciated. My sincerest thanks to Drs. George Hudak and Dean Peterson who helped teach me how to operate as a geologist in the field and to Dr. Bryan Bandli who provided me with expert training and guidance on the SEM. Financial support for this project was provided through research grants by the Institute on Lake Superior Geology, the Society of Economic Geologists, the Geological Society of America, the Precambrian Research Center at UMD, the Mesabi Range Geological Society, and the Department of Earth and Environmental Sciences at UMD. Thank you all for your generous support.

I would also like to thank my family and friends for all of thier support during this process. Thanks especially to my mother, Ellen Shown, who travelled to UMD for my defense and experienced a true Duluth winter. Thank you as well to Cortney Alexander, Paul Fix, Aubrey Lee, Matt Grotte, and Bo Betzler who listened intently and with the utmost “interest” as I expounded on the intricate details of spider diagrams, the mysteries of Adobe Illustrator, and all things basalt. Lastly, my sincerest apologies to my poor guitar who suffered the indignity of disuse these past three years - to you I say: the work is done, let’s jam.

ABSTRACT

Over the last century, numerous geological studies have reasonably resolved the overall tectonomagmatic evolution of the 1.1 Ga Midcontinent Rift (MCR). The structural complexity, duration of magmatic activity, and relative scarcity of continuous exposure, however, have thus far hindered efforts to correlate the numerous MCR flood basalts with their intrusive feeder systems. Providing such correlations is essential to furthering our understanding of the magmatic processes that operated during rifting. This study provides field, petrographic, and geochemical evidence of one such intrusive-volcanic correlation between the Beaver River diabase (BRD) and Greenstone Flow (GSF) – two of the largest igneous systems associated with the MCR.

The BRD is an extensive, multiply-intrusive, composite dike and sill network and the most extensive intrusive phase of the Beaver Bay Complex (BBC) in northeastern Minnesota. The GSF is an enormous (> 2,000 km^3), similarly composite flood basalt exposed on Isle Royale and the Keweenaw Peninsula in northern Michigan. The notion that these two systems might be related was first suggested by Miller and Chandler (1997) based on the recognition that very large (≤ 400m) inclusions of anorthosite, interpreted to be xenoliths derived from the lower crust, occur in BRD dikes and sills at hypabyssal depths. Because vertical conduits wide enough to accommodate such large xenoliths traversed the crust to shallow depths, these intrusions likely reached the Earth's surface to erupt extraordinarily large lava flows. Likewise, the GSF may possibly be the product of this venting, as supported by several lines of circumstantial evidence: 1) overlapping U-Pb ages - 1094.0 ± 1.5 Ma for the GSF (Davis and Paces, 1990) and

1095.8 ± 1.2 Ma for the BRD (Paces and Miller, 1993); 2) similar ranges in lithologies – ophitic olivine diabase/basalt to ferromonzodiorite; and 3) similar enormous sizes. This study seeks to more rigorously evaluate a possible comagmatic link between these two systems by carefully comparing their field, petrographic, and geochemical attributes.

The BRD is composed of a network of ophitic olivine diabase dikes and sills that intrude the medial section of the North Shore Volcanic Group and host numerous, smaller composite intrusions of variably fractionated lithologies. In the southern BBC near Silver Bay, MN, these composite intrusions occur as a series of singularly emplaced, concentrically-zoned bodies of vari-textured ferromonzodiorite cored by foliated ferrogabbro/diorite, which are collectively termed the Silver Bay Intrusions (SBI). In the northern BBC, composite intrusions in the BRD range from intergranular gabbro to ferrodiorite and have been interpreted by Miller and Chandler (1997) to have been emplaced in at least two intrusive pulses into BRD diabase dikes.

The GSF is composed predominantly of ophitic to subophitic, olivine tholeiitic basalt which can be divided into upper and lower zones. The core of the GSF, here termed the Heterolithic Zone, separates the ophitic zones and contains a heterogeneous suite of evolved rocks ranging from intergranular gabbro to prismatic ferromonzodiorite. Field observations and petrographic data suggest that the core of the initial tholeiitic basalt flow was intruded, inflated, and partially displaced by one or possibly two intrusive pulses of evolved magma. Previous workers (e.g. Cornwall, 1951) have suggested that the occurrence of evolved lithologies in the core of the GSF resulted from *in situ* differentiation. However, evidence for composite emplacement of evolved magmas

within the GSF, presented here, is given by: 1) abrupt changes in mineralogy, texture, mineral chemistry, and lithogeochemistry over centimeter to meter scale; 2) inclusion relationships between evolved and ophitic GSF lithologies; and 3) the occurrence of remnant blocks of initially crystallized GSF ophitic basalt interlayered with evolved lithologies within the Heterolithic Zone.

Petrographic observations show that the comparable rock types in the BRD and GSF are nearly indistinguishable in terms of modal mineralogy and texture. Most notably are the similar occurrences of distinctive clustering of plagioclase, and the occurrence of coarse-grained plagioclase megacrysts in both the BRD ophitic diabase and GSF ophitic basalt. The presence of plagioclase megacrysts in the GSF ophitic basalt with similar anorthite contents (up to 81 mol%) as reported for the anorthosite inclusions in the BRD (An_{54-80}; Morrison et al., 1983) strongly supports the interpretation that these crystals are xenoliths derived from a similar source as those in the BRD ophitic diabase.

Geochemical data are also consistent with the interpretation that the various rock types in the BRD and GSF crystallized from chemically similar parental magmas. SEM-EDS analyses of mafic mineral compositions show considerable overlap in the mean and range of En' contents in augite and Fo contents in olivine between comparable rock types in the BRD and GSF systems. Compositional overlap is also observed in whole rock analyses of trace element abundances and ratios between comparable rock types in each system.

Concluding from the field, petrographic, and geochemical data that the BRD dike and sill network acted as the intrusive feeder system for the GSF lava flow implies that

previous estimates of the volume of the GSF (White, 1960; Long, 1984) are grossly underestimated. Projecting the GSF westward under Lake Superior from exposures on Isle Royale and the Keweenaw Peninsula to the proposed feeder system on the Minnesota shore implies that the GSF has an areal extent of roughly 20,000 km^2 and a total volume of at least 2,000 km^3. These estimates indicate that the GSF is possibly the largest single lava flow on Earth.

Table of Contents

List of Tables

List of Figures

1.0 INTRODUCTION

The 1.1 Ga Midcontinent Rift (MCR) is a failed attempt at continental rifting characterized by extensive flood basalt volcanism and the emplacement of comagmatic intrusions in what is now the Lake Superior region of North America (Fig. 1). Over the last century, numerous geological, geochemical, geochronological, and geophysical studies have been conducted in the MCR (see Miller and Nicholson (2013) for a recent compilation). In particular, high-resolution aeromagnetic, gravity, and deep-crustal seismic data, as well as geochemical, isotope, and high-precision U-Pb age data, collected in the last quarter-century, has greatly improved our overall understanding of the three-dimensional structure and tectonomagmatic evolution of the rift (Fig. 2).

By virtue of the MCR's failure to evolve to a full continental separation, and because of subsequent structural inversion by later compression (Fig. 2), a nearly complete vertical section of the rift is exposed in the Lake Superior region (Fig. 1). This provides a unique opportunity to study the 4-dimensional tectonomagmatic evolution of an intracontinental rift, including the relationship between subvolcanic intrusions and the volcanic units fed by those intrusions. Although comagmatic links between flood basalts and their intrusive feeder vents have been documented in other large igneous provinces (e.g. Martin, 1989; Wright et al., 1989), such correlations are difficult to make in the MCR because of the considerable duration of magmatic activity, structural complexity, and scarcity of continuous exposure as compared to other flood basalt provinces.

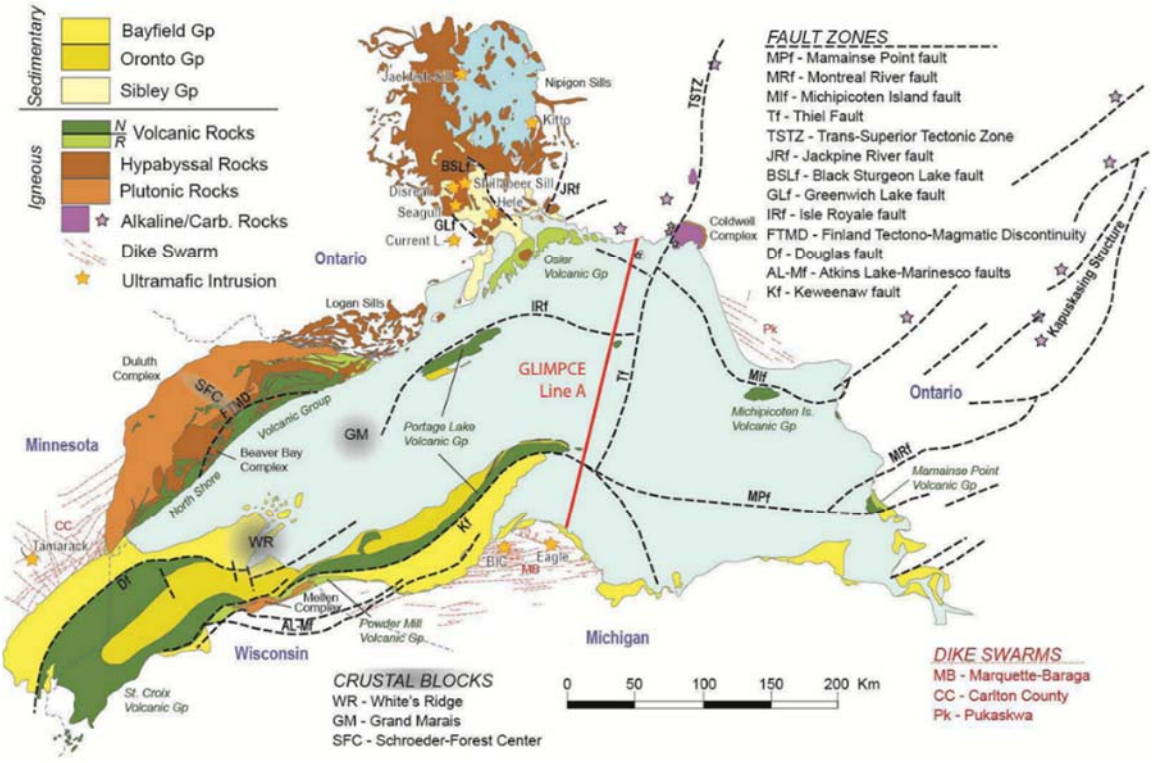

Figure 1. Geology of the Midcontinent Rift in the Lake Superior region. Major volcanic and intrusive units, faults, dike swarms, and pre-MCR crustal blocks are labeled (from Miller and Nicholson, 2013).

One such intrusive-volcanic link in the MCR, may be between the Beaver River diabase (BRD) and the Greenstone Flow (GSF). The BRD is an extensive, composite dike and sill complex in northeastern Minnesota that is part of the Beaver Bay Complex. The GSF is an enormous (at least 1,650 km^3) flood basalt exposed on Isle Royale and the Keweenaw Peninsula in northern Michigan that is part of the Portage Lake Volcanic Group (Fig. 1). This correlation is suggested by not only the extensive volume and areal extent of each, but also by an overlap in U-Pb zircon ages reported for the BRD (1095.8 ± 1.2 Ma; Paces and Miller, 1993) and the GSF (1094.0 ± 1.5 Ma; Davis and Paces, 1990) and by their similar range of lithologies (ophitic olivine diabase/basalt to prismatic ferromonzonite) (Longo, 1984; Miller and Chandler, 1997). More circumstantial, but

compelling evidence for this link comes from the existence of numerous, large (up to 400 m in diameter), lower-crustal anorthosite xenoliths hosted by the BRD dikes and sills (Morrison et al. 1983; Miller and Chandler, 1997). The presence of these large xenoliths implies that at one time, at least some of the BRD dikes reached nearly a half a kilometer in width within just a few kilometers of the Earth's surface. The possibility that these large hypabyssal dikes and sills might have breached the surface to vent enormous outpourings of lava, such as would have created the GSF, is intriguing.

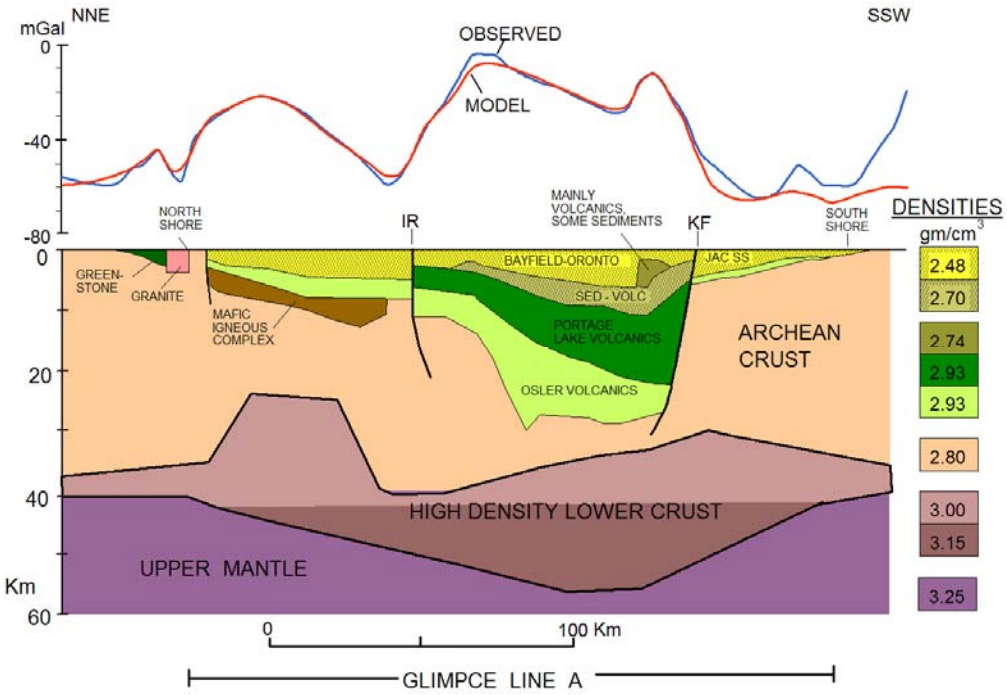

Figure 2. Geologic crustal model across the central part of Lake Superior based on seismic reflection data along GLIMPCE Line A (shown in Fig. 1) and Bouguer gravity data (after Trehu et al., 1991 and Thomas and Teskey, 1994). IR and KF denote the Isle Royale and Keweenawan faults, respectively. High density crust is interpreted to be underplated mafic material (from Miller and Nicholson, 2013).

1.1 Geologic Setting

1.1.1 Midcontinent Rift

The BRD and GSF are two of the most extensive igneous bodies associated with the Mesoproterozoic Midcontinent Rift. As mentioned above, the MCR represents the initiation and subsequent failure to open of an incipient ocean basin in what is now the Lake Superior region of North America (Fig. 1). This structurally intact continental rift records up to 30 million years of extension, subsidence, and volcanism (Heaman et al., 2007) during which time the Earth's crust was nearly totally separated (Cannon, 1992). During rifting, up to 25 kilometers of subaerial volcanic and 8 kilometers of fluvial and lacustrine rocks were deposited into a deep central graben (Cannon, 1992). These stratified MCR volcanic and sedimentary rocks, exposed only in the Lake Superior region, are collectively termed the Keweenawan Supergroup (Morey and Green, 1982). High-precision U-Pb zircon ages (Davis and Sutcliffe, 1985; Davis and Paces, 1990; Heaman and Machado, 1992; Paces and Miller, 1993; Davis and Green, 1997; Zartman et al., 1997; Hoaglund, 2010) indicate that the bulk of MCR magmatic activity occurred between 1109 Ma and 1086 Ma, although rift-related activity can reasonably be extended to at least 1115 Ma (Heaman et al., 2007).

Cannon (1992) gave a conservative estimate of 2 million km^3 for the original volume of erupted material during the MCR, a volume that is comparable with other continental flood basalt provinces. For example, it is estimated that 1-3 million km^3 of volcanic rocks were erupted during Deccan volcanism (Sen, 2001), although Deccan volcanism occurred during a considerably shorter time period (~1-3 m.y.; Courtillot, 1988) than in the MCR. It is now generally accepted that the initiation of rifting was caused by the interaction of

an upwelling mantle plume with the base of the lower crust (Hutchinson et al., 1990; Nicholson and Shirey, 1990; Cannon and Hinze, 1992; Shirey et al., 1994; Miller and Nicholson, 2013) although that interpretation has recently been challenged (Hollings et al., 2012; Hollings and Heggie, 2014). What is clear is that early extension during rifting was followed by compressional stresses during the waning stages of MCR development, possibly due to the far-field effects of the Grenville orogeny (Cannon, 1994).

Though mostly obscured by Paleozoic sedimentary rocks, the full 2,000 kilometer geophysical signature of the MCR is traceable from southeastern Michigan, through the Lake Superior region, and then southward into central Kansas (King and Zeitz, 1971; Hinze et al., 1992). Deep seismic reflection, refraction, and gravity profiles across Lake Superior show that a complex system of deep, asymmetrical grabens and sag basins were formed during extension (Cannon et al., 1989; Chandler et al., 1989; Mariano and Hinze, 1994A and B; Allen et al., 1997). Seismic profiles across Lake Superior (e.g., GLIMPCE Line A, Fig. 1) and Bouguer gravity data indicate that the deepest portion of the rift occurs in the western Lake Superior region where subsidence and infill reached depths of up to 36 kilometers with volcanic rocks comprising the bulk of the accumulated material (Figure 2; Trehu et al., 1991; Thomas and Teskey, 1994; Allen et al., 1997).

The development of the MCR is commonly subdivided into several stages distinguished by variations in the frequency and rates of eruption, as well as the chemical compositions of the magmatic products (Miller and Vervoort, 1996; Nicholson et al., 1997; Vervoort et al., 2007; Heaman et al., 2007). Correlating the lithostratigraphy, chemostratigraphy, and chronostratigraphy of the intrusive and volcanic suites throughout

the rift, Miller and Nicholson (2013) proposed an updated tectonomagmatic model which subdivides MCR activity into six stages spanning 75 million years (Figure 3).

Stage I (1115-1110 Ma) – *Initiation Stage* – Previous models of rift development (e.g. Cannon, 1992; Miller and Vervoort, 1996; Nicholson et al., 1997; Vervoort et al., 2007) reasoned that the mantle plume thought to be responsible for rifting contacted the base of the lithosphere around 1110-1109 Ma, the earliest age of most reversed-polarity MCR volcanic and intrusive rocks. However, the recent discovery of a mix of mafic to ultramafic intrusions in the Nipigon Embayment (Fig. 1) with ages between 1115-1110 Ma (Heaman et al., 2007) and undepleted-mantle chemical signatures (Hollings et al., 2007a and 2007b) suggest that plume interaction may have occurred as early as 1115 Ma. The arrival of the plume head likely caused significant doming of the crust (Campbell and Griffiths, 1990; Campbell, 2001) prior to the onset of volcanism. Fracturing of the crustal dome would have allowed for the rapid rise of deep-mantle magmas and the eruption of primitive (picritic) lavas. Although picrites are found at the bases of many flows throughout the rift (Nicholson et al., 1997) their ages are unknown and they represent only a minor percentage of the total volume of MCR volcanic rocks. Miller and Nicholson (2013) suggested that the relative scarcity of volcanic rocks older than ~1109 Ma may indicate a period of rapid erosion from the uplifting crustal dome.

Stage II (1110-1105 Ma) – *Early Magmatic Stage* – Magmatic activity during this stage is characterized by the rapid eruption of reversely-polarized plateau style flood basalts over a broad area throughout the Lake Superior region (Cannon, 1992) and

the emplacement of ultramafic to felsic igneous intrusions. All of the lava sequences erupted during this period show similar chemostratigraphic sequences where early primitive basalts (mg# >50) give way to more diverse compositions displaying evidence of crustal contamination (e.g. negative ε_{Nd} values, Th:Yb > 1). The progressive evolution and increasing contamination of the volcanic rocks during this period is interpreted to be the result of the progressive embedding of the plume head into the base of the subcontinental lithospheric mantle. Primitive mantle melts encountering the density transition of the mantle-crust interface would have caused the onset of magma underplating of the crust, which is evident in geophysical models (Fig. 2). Ponding of mantle melts in the lower crust would have resulted in contamination of these mafic magmas and in intense heating and anatectic generation of felsic melts.

Stage III (1105-1101 Ma) – *Hiatus Stage* – During this stage, broad-scale magmatic activity had largely ceased with the exception of intermittent rhyolitic eruptions. Several authors (Miller and Vervoort, 1996; Vervoort et al., 2007; Miller and Nicholson, 2013) attributed this volcanic quiescence to a period of continued mantle plume melting and storage of those melts in the lower crust by crustal underplating. Felsic melts, generated by the anatexis of the crust, would have formed a rheological and density barrier preventing the ponded mafic magmas from rising through the crust. At lower crustal pressures (~8-10 kb), plagioclase would be buoyant relative to basaltic liquids (Kushiro, 1980) and would have resulted in the flotation of plagioclase to create pure anorthosites and settling out of mafic phases to create

peridotites. Once this underplating had begun, the subcrustal mafic magma chambers would continue to expand by a feedback mechanism of felsic melts trapping additional plume-generated melts, causing more widespread heating and melting of the lower crust, causing more trapping. The expansion of the lower crustal underplate during this stage and the lack of magmatic heating of the upper crust likely resulted in decoupling of the upper and lower crust with all extension taken up by the lower crust.

Stage IV (1101-1094 Ma) – *Main Magmatic Stage* – This stage is thought to represent the onset of separation of the upper crust, and the subsequent emptying of the subcrustal magma chambers formed during the volcanic hiatus. After most felsic melt barriers had been removed, mafic magmas were able to rise through the upper crust, generating enormous amounts of flood basalts, which were erupted into rapidly subsiding, asymmetrical grabens flanking the main rift axis (Cannon et al., 1989; Cannon, 1992; Dickas and Mudrey, 1997; Miller and Nicholson, 2013). These flood basalts are best represented by the nearly 10 km thick sequence of normally polarized lavas of the North Shore Volcanic Group (NSVG) in Minnesota (Green, 1972; Davis and Green, 1997; Green, 2002) and the 5 km thick Portage Lake Volcanics (PLV) in northern Michigan (discussed below) (Huber, 1973; Paces, 1988; Davis and Paces, 1990; Nicholson and Shirey, 1990). The compositions of the initial basalts were variably evolved from primitive melts and commonly plagioclase-phyric, however compositions became progressively less evolved as volcanism continued. This change in composition is interpreted to be the result of the

progressive maturation of the MCR plumbing system, which allowed for shorter residence times for mantle-derived magmas.

This stage also saw the emplacement of numerous mafic to ultramafic intrusions including the bulk of the Duluth and Beaver Bay Complexes in Minnesota (discussed below) (Paces and Miller, 1993; Miller and Ripley, 1996; Miller and Chandler, 1997; Miller and Green, 2002; Miller and Severson, 2002; Hoaglund, 2010). Many of the earliest magmas generated during the main stage were plagioclase-phyric that created the anorthositic series of the Duluth Complex. Miller and Weiblen (1990) interpreted these early plagioclase crystal mushes as being derived from lower crustal magma chambers where plagioclase is buoyant. They further speculated that the anorthosite xenoliths found in the BRD were derived from the roof zones of these deep-seated chambers and either floated or were carried to their present positions within the BRD dikes.

Stage V (1094-1080 Ma) – *Late Magmatic Stage*– Waning magmatism signaled the thermal decline of the mantle plume during this stage, possibly as the result of the decoupling of the plume head due to plate motion (possibly shortly after it embedded in the lithosphere during Stage II). The central rift graben continued to subside and was filled with a thick accumulation of alluvial fan, fluvial, and lacustrine sediments to form the Oronto Group (Figs. 1 and 2). Magmatic activity, characterized during this stage as localized, intermittent, intermediate to felsic volcanism, is thought to have ceased by 1086 Ma although subsidence and sedimentation continued until around 1080 Ma.

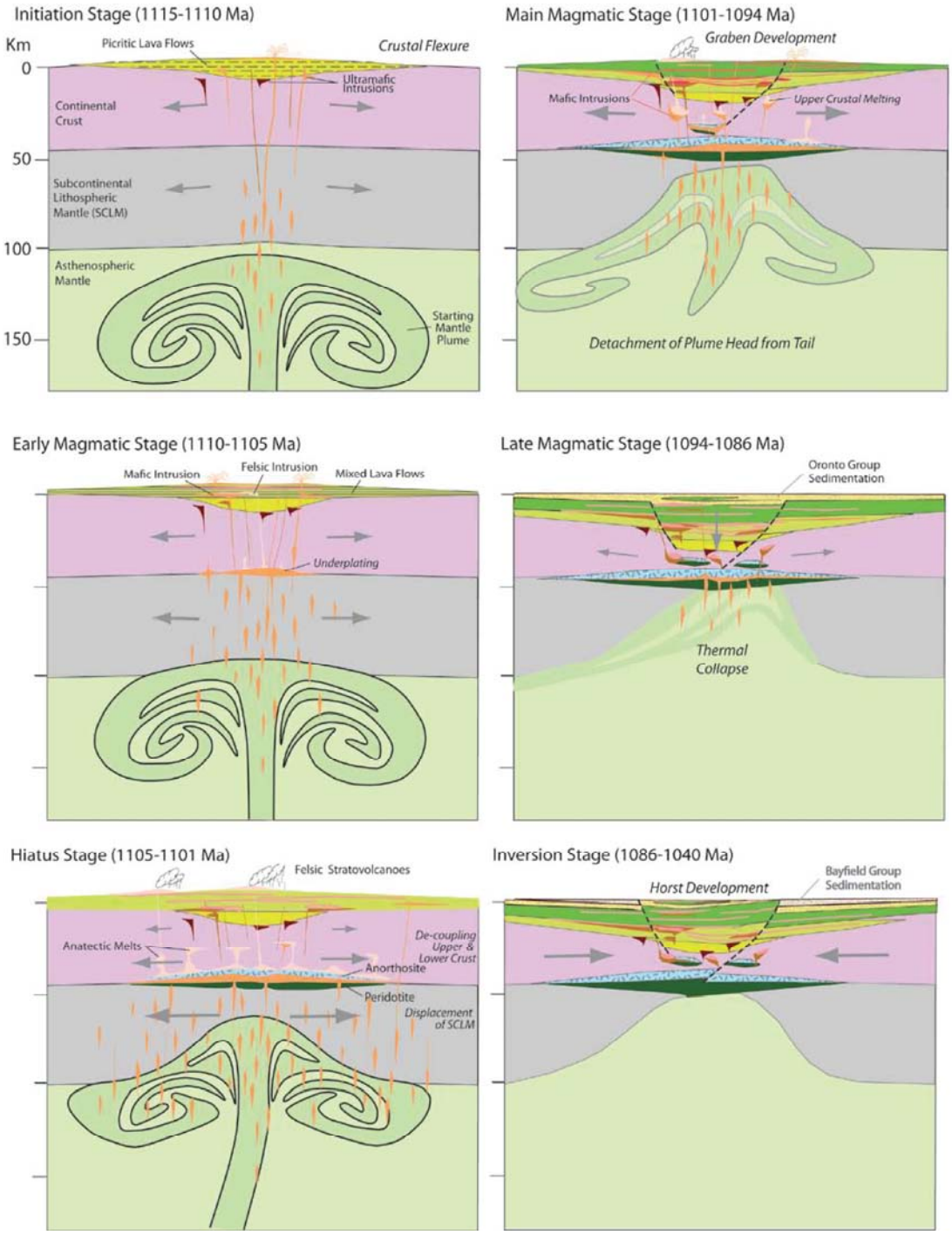

Figure 3. Six-stage model for the tectonomagmatic evolution of the Midcontinent Rift (from Miller and Nicholson, 2013).

Stage VI (1080-1040 Ma) –*Inversion Stage* – Reverse faulting along originally normal graben-bounding faults is thought to have begun around 1080 Ma which coincides with the onset of the compressive effects of the Grenville orogeny (Cannon, 1994). Reverse faulting culminated at around 1060 Ma, but may have persisted until around 1040 Ma (Cannon, 1994). Compressive stresses caused approximately 30 km of crustal shortening and a central horst along the southwest arm of the rift (Figs. 1 and 2) (Cannon, 1994). Sediments derived from this central horst accumulated into flanking basins to form the Bayfield Group (Fig. 1).

1.1.2 North Shore Volcanic Group

The rift-filling volcanic and sedimentary rocks exposed along a roughly 150-kilometer-long section of the north shore of Lake Superior in northeastern Minnesota (Fig. 4) are collectively called the North Shore Volcanic Group (NSVG) (Green, 1972, 2002). The NSVG form an arcuate stack of plateau lavas that are slightly tilted toward the rift axis and grossly define a gently-dipping (10-20°), bowl-shaped structure. Flows in the northeast portion are tilted gently to the south while those in the southwest dip to the east and the central Schroeder-Lutsen sequence tilts southeast (Fig. 4). Locally, this gentle tilt is disrupted by intrusions of the Duluth Complex into the base of the volcanic pile and Beaver Bay Complex emplaced into the medial section of the edifice.

The NSVG are broadly subdivided into two stratigraphic sections, a southwest limb and northeast limb (Figs. 4 and 5). A paleomagnetic reversal (R-N) has long been recognized in both limbs and has been used to further subdivide them into a reversely-polarized lower sequence and a normally-polarized upper sequence. A capping sequence

of normally-polarized basalts, the Schroder-Lutsen sequence, unconformably straddles the hinge dividing the upper southwest and northeast limbs. High-precision U-Pb zircon ages from NSVG basalts and rhyolites, reported by Davis and Green (1997) and presented in Figure 5, demonstrate that the majority of reversed-polarity volcanism occurred during the early magmatic stage of the MCR, while the majority of normal-polarized lavas were erupted during the main magmatic stage (Figs. 3 and 5). Green (2002) noted that in both the southwest and northeast limbs, there exists a significant time gap, which corresponds to the hiatus stage (Fig. 3) of the MCR. This time gap is evident in the U-Pb zircon ages from volcanics straddling the upper (N-polarized) and lower (R-polarized) sequences in the northeast limb. The two flows dated are separated by less than 500 meters within a 6,500 kilometer stratigraphic section, yet are separated in time by roughly 7 million years (1107.6 ± 2.5 to 1100.5 ± 1.9 Ma; Davis and Green, 1997; Figure 5). Another significant unconformity occurs near the top of the NSVG where the Schroder-Lutsen basalts, with a polymict conglomerate at their base, rest in angular unconformably atop upper units of the SW (Figs. 4 and 5). Moreover, the Schroeder-Lutsen basalts are not intruded by the Beaver Bay Complex (discussed below), which pervasively cuts the SW NSVG sequence and was emplaced as late as 1095.8 ± 1.2 Ma (Paces and Miller, 1993). Unfortunately, attempts to date the Schroder-Lutsen basalts have been unsuccessful.

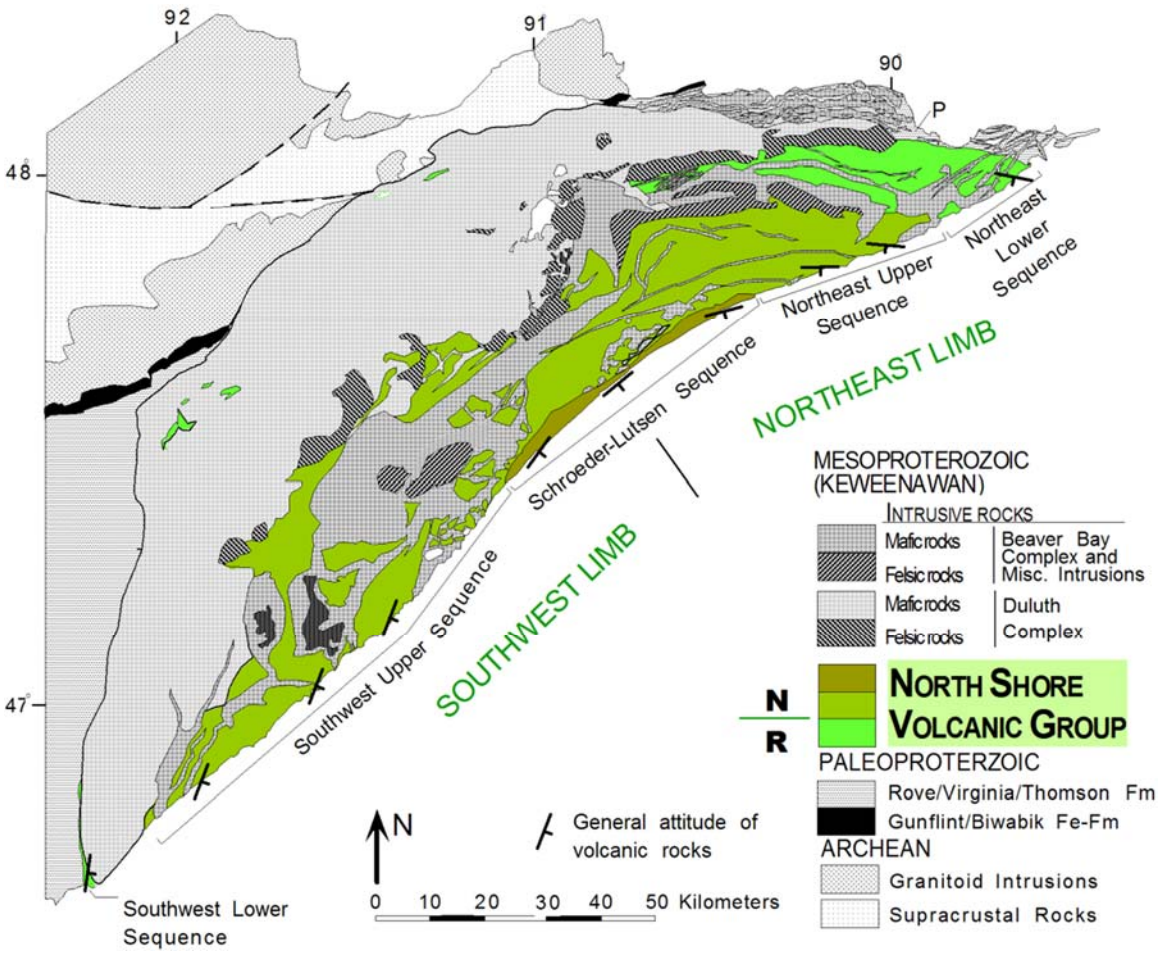

Figure 4. Exposure area of the North Shore Volcanic Group in northeastern Minnesota showing the lithostratigraphic subdivision into limbs and sequences based on magnetic polarity (N- normal, R-reversed; after Green, 2002).

Looking at the detailed stratigraphy of the SW and NE limbs, however, reveals that the lithostratigraphy and chemostratigraphy of lavas comprising each limb is distinct (Fig. 5). Perhaps the most obvious difference is in the inconsistent abundances of felsic lava compositions. Along the northeast limb, rhyolite composes up to 25% of the volcanic sequence, but makes up only 10% of the southwest limb (Green, 1972). With the exception of the monotonously primitive basalts of the Schroeder-Lutsen sequence, no individual lava flow or lava package can be correlated from the SW to the NE limb,

giving each a unique lithostratigraphic column (Fig. 5). The cumulative stratigraphic thickness is also variable, measuring 9.7 kilometers along the southwest limb and 7.2 kilometers along the northeast limb (Green, 2002). The lack of correlation and the variability in the compositions and attitudes of the flows led Green (1972, 2002) to conclude that the rocks in the two limbs accumulated independently into separate basins during rifting. This interpretation is consistent with the interpretation of a large crustal ridge of Archean basement, the Schroeder-Forest Center ridge (SFC; Figure 1), which corresponds to a pronounced saddle in the Bouguer gravity over northeast Minnesota and roughly underlies the divide between the NSVG limbs. Several workers (Boerboom, 1994; Miller and Chandler, 1997; Peterson and Severson, 2002) have speculated that this ridge is the buried eastward projection of the Late Archean rocks of the Giant's Range batholith and exerted significant structural control over the focus of both the volcanic and intrusive activity during rifting.

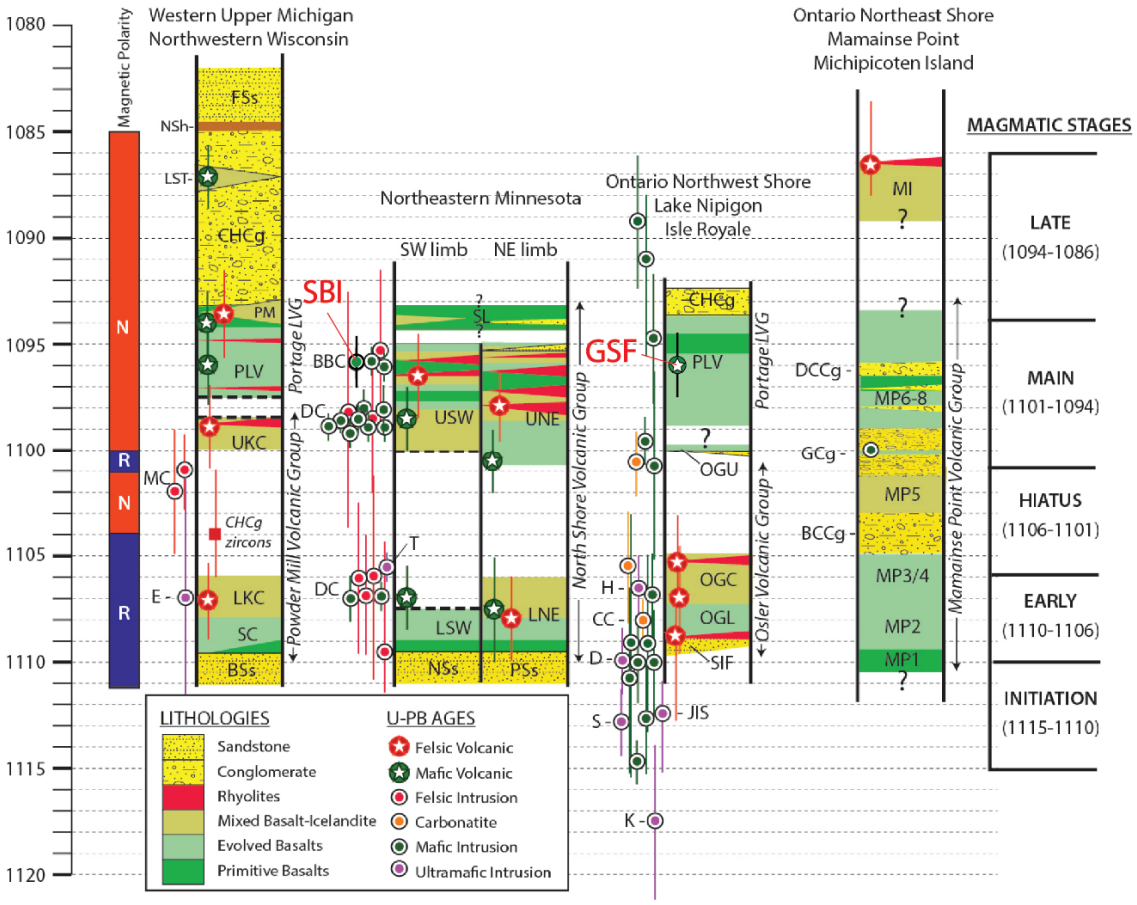

Figure 5. Chronostratigraphic correlation of the main volcanic sequences and bounding sedimentary units of the MCR in the Lake Superior basin from Miller and Nicholson (2013). Also shown are main polarity intervals and U-Pb ages for volcanic and intrusive rocks (ages from Davis and Sutcliffe, 1985; Palmer and Davis, 1987; Davis and Paces, 1990; Heaman and Machado, 1992; Paces and Miller, 1993; Davis and Green, 1997; Zartman et al., 1997; Smyk et al., 2006; Vervoort et al., 2007; Heaman et al., 2007; Hoaglund, 2010; Ding et al., 2010; Goldner, 2011; Hollings et al., 2010; and Swanson-Hysell et al., 2011). Ages of intrusion are plotted to the left of volcanic sequence or pre-rift terranes into which they are intruded. Labels for Greenstone Flow (GSF) and Silver Bay Intrusions (SBI) are highlighted in red. U-Pb ages for GSF (1094.0±1.5 Ma) are reported by Davis and Paces, 1990. U-Pb zircon age of SBI intrusions in BRD (1095.8±1.2 Ma) reported by Paces and Miller, 1993. Labels for other intrusion ages are: MC-Mellen Complex, E-Eagle, BBC-Beaver Bay Complex, DC-Duluth Complex, T-Tamarack, H-Hele, CC-Coldwell Complex, D-Disreali, JIS-Jackfish Lake Sill, S-Seagull, K-Kitto. Simplified lithostratigraphies of the four main volcanic-sedimentary packages are schematically portrayed. The bold dashed lines indicate where the sequence is truncated by intrusions or major faults. Question marks indicate that the upper or lower age limit of the unit is unknown.

Unit abbreviations for the Upper Michigan/NW Wisconsin package are: BSs-Bessemer Quartzite, SC-Siemens Creek Volcanics, LKC-Lower Kallander Creek Volcanics, UKC- Upper Kallander Creek Volcanics, PLV-Portage Lake Volcanics, SCV-St. Croix Volcanic Group, PM- Porcupine Volcanics, CHCg-Copper Harbor Conglomerate, LST-Lake Shore traps, NSh-Nonesuch Shale, and FSs-Freda Sandstone. For the North Shore Volcanic Group (NSVG) in northeastern Minnesota, which Green (2002) subdivides into two lithologically distinct, structural limbs, the unit abbreviations are: NSs-Nopeming Sandstone, PSs-Puckwunge Sandstone, LSW-Lower southwest sequence, LNE-Lower northeast sequence, USW-Upper southwest sequence, and UNE-Upper northeast sequence. The UNE and USW sequences are unconformably capped by the Schroeder-Lutsen sequence (SL). For the northwestern shore of Ontario (Black Bay Peninsula), the unit abbreviations are: SIF-Simpson Island formation, OVL-Osler Volcanic Group-lower suite, OLC-Osler Volcanic Group-central suite, and OLU-Osler Volcanic Group-upper suite. Upsection of the Osler Volcanics, southeast-dipping basalt flows on Isle Royale can be lithologically (and seismically) correlated with the northwest-dipping Portage Lake Volcanics (PLV) and overlying Copper Harbor Conglomerate (CHCg) exposed on the Keweenaw Peninsula (Fig. 1) and thus are given the same unit names (Huber, 1973). For volcanics of the Mamainse Point Volcanic Group exposed along the northeast Ontario shoreline, Klewin and Berg (1990) subdivide the sequence into 8 numbered intervals based on their lithologic and geochemical attributes. Several thick interflow volcaniclastic conglomerate units within the Mamainse Point section include: BCCg-basalt clast conglomerate, GCg-great conglomerate, and DCCg-Deadman's Cove conglomerate. The Michipicoten Island Formation described by Annels (1974) is identified as MI.

1.1.3 Duluth Complex

The Duluth Complex (Fig. 6) is the largest intrusive phase of the MCR and consists of a nearly 5,000 km^2, semi-continuous mass of multiply-intruded tholeiitic mafic to felsic intrusions that were emplaced into the lower portions of the NSVG (Weiblen and Morey, 1980; Miller and Severson, 2002). Gravity data suggest that the Duluth Complex extends to depths of up to 13 kilometers (Allen et al., 1997) implying a total volume of between 35,000 km^3 and 40,000 km^3 (Miller and Nicholson, 2013). The footwall of the Duluth Complex is composed of the Neoarchean granitoid and supracrustal rocks of the Wawa Granite-Greenstone Belt and the Paleoproterozoic sedimentary rocks of the

Animikie Group (Peterson and Severson, 2002). Geochronological evidence indicates that the separate intrusions of the complex were emplaced during two major magmatic episodes at ~1108 Ma and ~1099 Ma, corresponding to the early and main magmatic stages of the MCR, respectively (Paces and Miller, 1993; Hoaglund, 2010).

The Duluth Complex is routinely divided into four series – felsic, early gabbroic, anorthositic, and layered – distinguished by bulk composition, age, and internal structure (Weiblen and Morey, 1980; Miller and Severson, 2002). The earliest intrusive phases comprise the felsic series and early gabbroic series. They are reversely-polarized and have U-Pb zircon ages between 1109-1106 Ma (Paces and Miller, 1993; Vervoort et al., 2007) which corresponds to the early magmatic stage of the MCR (Fig. 3). The felsic series consists of a semi-continuous mass of granophyric granite and smaller amounts of intermediate rocks emplaced along the eastern and central roof zones of the complex (Fig. 6). The early gabbroic series is a sequence of evolved gabbroic mafic layered intrusions that occur along the northeastern contact of the complex (Fig. 6). Although similar in age to the felsic series (~1109 Ma; Paces and Miller, 1993; Vervoort et al., 2007), field relationships consistently imply that the emplacement of the felsic series rocks preceded the mafic intrusions of the early gabbroic series (Miller and Nicholson, 2013).

The bulk of the exposed Duluth Complex (>75%) is made up of the rocks of the anorthositic series and layered series (Fig. 6; Miller and Severson, 2002). The rocks in both series are normally-polarized and were emplaced during the main magmatic stage of the MCR (~1099 Ma, Fig. 3). The anorthositic series consists of a structurally complex

suite of foliated, plagioclase-rich gabbroic intrusions which were emplaced throughout the entirety of the Duluth Complex (Fig. 6; Miller and Severson, 2002).

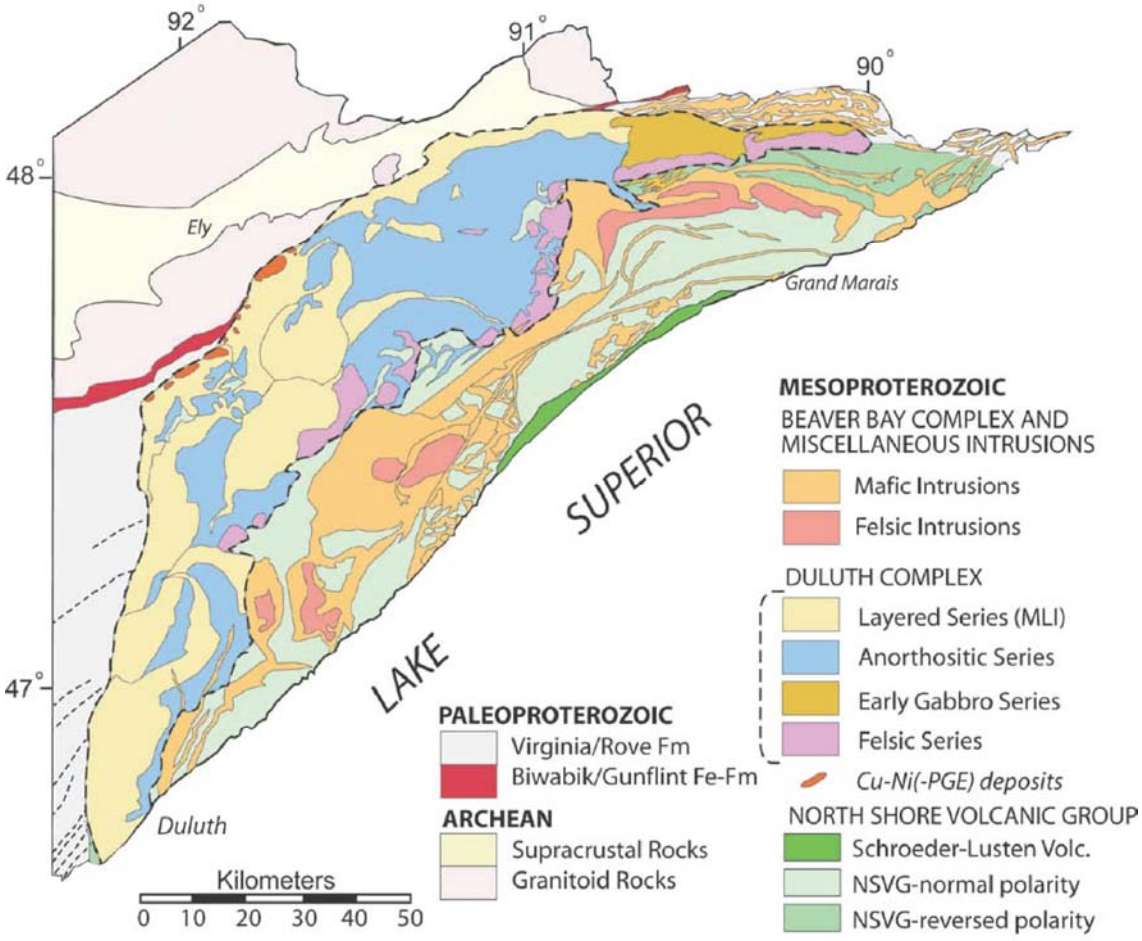

Figure 6. Geology of northeast Minnesota showing the exposure areas of the Duluth Complex and other Midcontinent Rift-related rocks and older terranes (from Miller and Nicholson, 2013).

Citing field, petrographic, and mineral chemical evidence, Miller and Weiblen (1990) proposed that the rocks of the anorthositic series were formed from multiple intrusions of plagioclase crystal mushes (basaltic magmas physically enriched in intratelluric plagioclase) which were sourced from lower crustal magma chambers where plagioclase would be buoyant (Kushiro, 1980). The layered series consists of a suite of at

least 11 variably differentiated mafic intrusions that occur mostly along the base of the Duluth Complex (Miller and Ripley, 1996). Although U-Pb zircon ages from the layered intrusions are irresolvable from those of the anorthositic series (Paces and Miller, 1993; Hoaglund, 2010), field relationships indicate that the rocks of the anorthositic series were emplaced prior to those of the layered series (Miller and Nicholson, 2013).

1.1.4 Beaver Bay Complex

The Beaver Bay Complex (BBC; Fig. 7) is a hypabyssal, multiply-intrusive igneous complex that was emplaced into the medial and upper portions of the NSVG edifice (USW and UNE sequences in Fig. 5) during the main magmatic stage of MCR activity (1101-1094 Ma, Fig. 3) (Miller and Chandler, 1997; Miller and Green, 2002). As defined by Miller and Chandler (1997), the BBC comprises all of the intrusive rocks that occur throughout a roughly 600 km^2 area extending between Split Rock Point and Grand Marais and as much as 30 kilometers inland from Lake Superior (Fig. 7). Thirteen separate intrusive units have been identified within the BBC, representing at least six major magmatic episodes (Fig. 7; Miller and Chandler, 1997). With the exception of the Finland granophyre, BBC intrusions are generally gabbroic to dioritic in composition, becoming progressively less evolved in successively younger intrusions (Miller and Chandler, 1997). This increasingly primitive trend is also evident in lithostratigraphic sequences in the NSVG (Green, 1983) and interpreted as a reflecting a maturation of the magma conduit system of the MCR (Green, 2002).

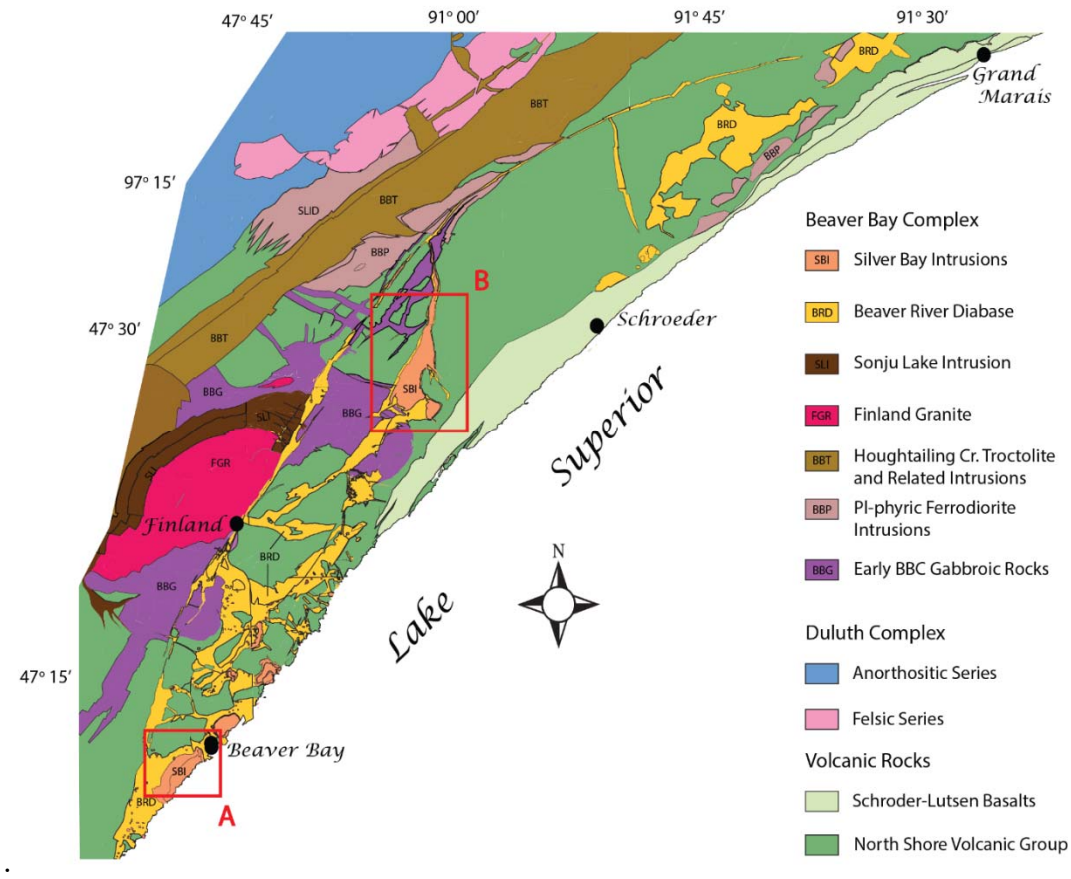

Figure 7. Geology of northeast Minnesota showing the exposure area of the Beaver Bay Complex and other Midcontinent Rift-related rocks (modified from Miller, 1989). Bedrock mapping and sampling locations are denoted by red boxes. A- southern BBC near Beaver Bay, MN and B- northern BBC near Cramer, MN.

U-Pb zircon ages of several intrusions in the BBC, including the Finland granophyre. (1097.8 ± 4.4 Ma; Vervoort and Wirth, 2004), the Sonju Lake intrusion (1096.1 ± 0.8 Ma; Paces and Miller, 1993) and Silver Bay intrusions (1095.8 ± 1.2 Ma; Paces and Miller, 1993), indicate that the BBC intrusions are generally younger than the ~1099 Ma intrusions of the Duluth Complex. Hoaglund (2010), however, recently reported a high-precision U-Pb zircon ages of 1098.62 ± 0.5 Ma for the Houghtaling Creek troctolite (Fig. 7), a northeast-trending macrodike which defines the exposed northwest boundary

of the BBC. This age is within analytical error of the 1099.0 ± 0.5 Ma age reported by Paces and Miller (1993) for the anorthositic and layered series of the Duluth Complex and may indicate an overlap in timing between BBC and Duluth Complex magmatism.

With the exception of the Houghtaling Creek troctolite and Sonju Lake intrusions (Fig. 7), the hypabyssal BBC intrusions are distinct from the deeper-seated Duluth Complex intrusions in that they tend to occur as narrow (< 1 km wide/thick) dikes, sills, or sheet-like bodies and are intrusive into volcanic rocks rather than other intrusions (Miller and Chandler, 1997). Although locally layered, most BBC intrusions generally do not display igneous foliation, cumulate textures, or cryptic layering indicative of magmatic differentiation (Miller and Green, 2002). Those that do display evidence of differentiation are either especially thick (e.g. the Houghtaling Creek troctolite); situated under an insulating cap of granophyre (e.g. the Sonju Lake intrusion); and/or late composite phases (e.g. the Silver Bay intrusions) (Miller and Green, 2002).

Because of uncertainties in correlating individual intrusive units over its extensive exposure area, the BBC is usually described in terms of three broad areas – southern, northern, and eastern (Fig. 7; Miller and Chandler, 1997). The shapes of the intrusions differ markedly throughout the BBC. In the northern BBC, the intrusions are generally focused into northeast-trending linear dikes while those in the southern and eastern areas occur as a mixture of dikes, sills, and sheet-like bodies, the latter of which are especially common among the younger intrusions. Miller and Chandler (1997) proposed that this change in geometry between the southern and northern BBC is due to the focusing of repeated magma injections into a narrow conduit cutting the Schroeder-Forest Center

ridge (Fig. 1). This conduit may have formed along the southwest margin of the ridge or along an earlier-formed fault through the structure. Miller and Green (2002) further suggested that the ridge may have acted as a barrier to rift-parallel migration of magma in the upper crust resulting in the ponding of BBC magma into sheet-like intrusions southwest and northeast of the structure

1.1.5 Beaver River Diabase

The Beaver River diabase (BRD) is the most extensive intrusive phase of the BBC (Fig. 7). It forms an interconnected network of composite dikes, sills, and sheet-like intrusions which are found in contact with every other intrusive phase of the BBC with the exception of the Houghtaling Creek troctolite (Miller and Chandler, 1997). The western and northern extent of the BRD is marked by a continuous dike (or dike set) which is traceable in outcrop along a roughly 110-kilometer-long arcuate path. This bounding dike, termed the Finland Tectonomagmatic Discontinuity (FTMD) (Figs. 1 and 7), is interpreted to have been emplaced along a normal growth fault during the main magmatic stage of the MCR (Miller et al., 1995). Based on the offset of the early gabbroic rocks of the BBC (BBG unit in Fig. 7), Miller et al. (1995) estimated up to 5 kilometers of downward displacement of the riftward blocks. Inboard of the FTMD, the BRD forms a series of bifurcating dikes and sheets which dip gently to the southeast. In the vicinity of the town of Beaver Bay at the southern extent of the BBC (Fig. 7), steeply-dipping BRD dikes up to 110 meters-thick feed nearly horizontal sheets which form prominent table-top highlands along the Lake Superior shore (Miller, 1988; Miller et al., 1989; Miller and Chandler, 1997). Progressing into the northern BBC (Fig. 7), the BRD

intrusions become focused into a series of linear composite dikes that merge into a single, generally northerly-trending dike (Boerboom and Miller, 1994; Miller and Chandler, 1997).

Over its large extent, the main lithologic phase of the BRD is remarkably homogeneous. Typically, it is a medium-grained ophitic olivine diabase that grades into coarser grained and more subophitic to locally intergranular oxide gabbros in the medial portions of thicker dikes and sills (Shank, 1989; Miller and Chandler, 1997). Oikocrysts of clinopyroxene range from less than a centimeter across near the chilled margins to as much as 10 centimeters in diameter in the thicker dikes and sills. The diabase is strongly chilled against the volcanic footwall rocks although it retains its ophitic texture (Shank, 1989). In the Beaver Bay area (Fig. 7), Shank (1989) reported distinct textural variations between poikilitic and more common granular olivine within sills. He also noted the local occurrence of very coarse-grained gabbroic segregations at the transition between these two varieties. Miller and Chandler (1997) noted the occurrence of a less common phase of the BRD containing quartz and feldspar megacrysts and abundant, large inclusions of anorthosite, granite, felsite, and basalt in a dense, aphanitic groundmass which occurs at the margins of some thicker dikes and sills. Mapped as an inclusion-rich diabase (*brid* unit of Miller, 1988), Miller and Chandler (1997) interpreted this phase to represent the brecciation and partial assimilation of the country rocks during the initial emplacement of the diabase.

Perhaps the most intriguing feature of the BRD is the occurrence of numerous xenoliths of nearly pure anorthosite ranging in size from polycrystalline aggregates of

less than a centimeter in length to enormous blocks over 400 meters in diameter (Fig. 8). The inclusions are particularly common in the upper and lower portions of the larger diabase sheets in the southern BBC but are relatively scarce in the in the more linear BRD dikes in the northern part of the complex (Miller and Chandler, 1997). The anorthosites are typically massive, coarse-grained, and consist of tabular, calcic plagioclase (An_{54-80}) and locally display brecciation and recrystallization textures (Morrison et al., 1983).

Figure 8. Anorthosite xenoliths in the Beaver River diabase. A.) Large angular xenolith in Highway 61 roadcut exposure. B.) Google Earth image of Carlton Peak, near Tofte, MN which is composed of two large (up to 400 meters in diameter) and two smaller anorthosite xenoliths.

With the exception of Lawson (1893), who thought that the anorthosites were the exposed tops of deeply-rooted Archean mountains around which Keweenawan lavas had flowed, most early workers recognized the xenolithic nature of the anorthosite. Grout and Schwartz (1939) suggested that the inclusions had been derived from the anorthositic gabbros of the Duluth Complex though they noted several inconsistencies with this interpretation including their coarser texture and lighter color. Morrison et al. (1983) analyzed the petrographic and geochemical compositions of the inclusions and, based on

ambiguous isotopic signatures, suggested that the inclusions were derived from older (~1.9 Ga) anorthosites which had been contaminated by interaction with Keweenawan magmas.

X-ray diffraction studies by Miller (1980; unpublished data) indicated that the plagioclase in the inclusions had a higher state of structural disorder compared to the anorthositic Duluth Complex rocks, indicating a deep crustal source (Miller and Chandler, 1997). Miller and Chandler (1997) suggested that a lack of chilled margins indicated that the xenoliths were emplaced within the BRD diabase at deeper levels in the crust before the inclusions had fully cooled. Several studies by Miller and others (Miller and Weiblen, 1990; Miller and Vervoort, 1996; Miller and Chandler, 1997) suggested that the anorthosite inclusions are Keweenawan in age and are related to the flotation and accumulation of plagioclase in the roof zones of lower crustal magma chambers during the hiatus stage of the MCR (1105-1101 Ma, Fig. 3). Under the high pressures of the lower crust, plagioclase should be buoyant in basaltic magmas (Kushiro, 1980), allowing for the emplacement of the anorthosite xenocrysts and xenoliths into their present position within the diabase by flotation and/or intratelluric transport after the onset of main stage magmatism.

The youngest group of intrusions in the BBC, recognized by field mapping (Boerboom and Miller, 1994; Miller, 1988; Miller et al., 1989, 1993, 1994, 2006) and confirmed by U-Pb zircon ages of 1095.8 ± 1.2 Ma (Paces and Miller, 1993), are a series of small, moderately to highly differentiated intrusions that occur within or directly adjacent to the BRD dikes and sills. In the southern BBC, these intrusions typically occur

as concentrically zoned, lensoidal bodies and are collective termed the Silver Bay Intrusions (SBI, Fig. 7; Miller, 1988; Miller et al., 1989). Lithologies within the SBI bodies range from ophitic olivine gabbro to ferrogranite (Shank, 1989), but are, on average, intermediate in composition (Miller and Chandler, 1997). Well-zoned intrusions typically grade from an outer marginal zone of coarse-grained, vari-textured, granophyric olivine ferromonzodiorite to a core of medium-grained, foliated and locally layered olivine ferrodiorite (Shank, 1989; Miller and Chandler, 1997). Similar intrusions occur within BRD dikes in the northern and eastern BBC although the range in these intrusions (ophitic olivine gabbro to ferrodiorite) is not as wide as in the SBI (Miller and Chandler, 1997).

Petrological modelling by Shank (1989) demonstrated that the compositional variation observed in the rocks of the SBI and the intrusions in the northern and eastern BRD dikes could have been generated by the progressive fractionation of BRD parental magma. Although this differentiation could have occurred in situ, detailed field mapping (Miller, 1988; Miller et al., 1989, 1993, 1994, 2006; Boerboom and Miller, 1994) led Miller and coworkers to conclude that they were formed by the composite emplacement of progressively fractionated magma. Miller and Chandler (1997) cite several lines of evidence to support the composite nature of these intrusions. The SBI and other small intrusions in the southern BBC typically occur within or directly adjacent to the BRD dikes and sills suggesting that they were emplaced along the same conduits as the surrounding diabase. Similarly, the intrusions in the northern and eastern BBC are usually confined within the axial traces of the BRD dikes. The sharp, unchilled contacts between

the various intrusive lithologies offer perhaps the most compelling evidence of composite emplacement. Contacts between the various lithologies are typically very abrupt on a centimeter to meter scale. Moreover, they are marked by abrupt changes in texture and mineralogy, and a distinct compositional hiatus as opposed to the smooth gradational contacts that would be expected had the evolved lithologies formed through *in situ* differentiation of the diabase. Large, angular inclusions of ophitic olivine diabase are also common in the marginal zones of the SBI, suggesting brecciation and engulfment of the host diabase during the emplacement of the SBI magmas. Furthermore, the lack of discernable chilled margins with and the occurrence of abundant inclusions of the host diabase indicate that the intermediate magmas which formed the SBI and northern composite intrusions were emplaced into the BRD after it had crystallized but before it had fully cooled.

1.1.6 Portage Lake Volcanic Group

On the southern shore of Lake Superior, the Portage Lake Volcanic Group (PLV) occurs as a 3- to 5-kilometer-thick sequence of normally polarized (Green, 1982), dominantly basaltic volcanic flows and terrigenous clastic rocks that comprise the upper portions of the Keweenawan Supergroup on the Keweenaw Peninsula and Isle Royale of Upper Michigan (Fig. 1). Being host to economic native copper deposits that were mined from 1842 to 1972, the volcanic stratigraphy of the PLV sequence is very well documented by geologic mapping and drill core logging (Paces, 1988). The PLV succession contains several hundred alkaline to subalkaline tholeiitic basalt flows and smaller amounts of interflow sedimentary rocks (Lane, 1893, 1911; Huber, 1973; Paces,

1988). Davis and Paces (1990) reported U-Pb zircon ages of 1096.2 ± 1.8 Ma and 1094.0 ± 1.5 Ma for the Copper City flow near the base of the exposed sequence and the Greenstone flow near the top, respectively (Fig. 9). This implies that the bulk of the PLV flows were emplaced over a roughly 5-million-year period during the main magmatic stage of the MCR.

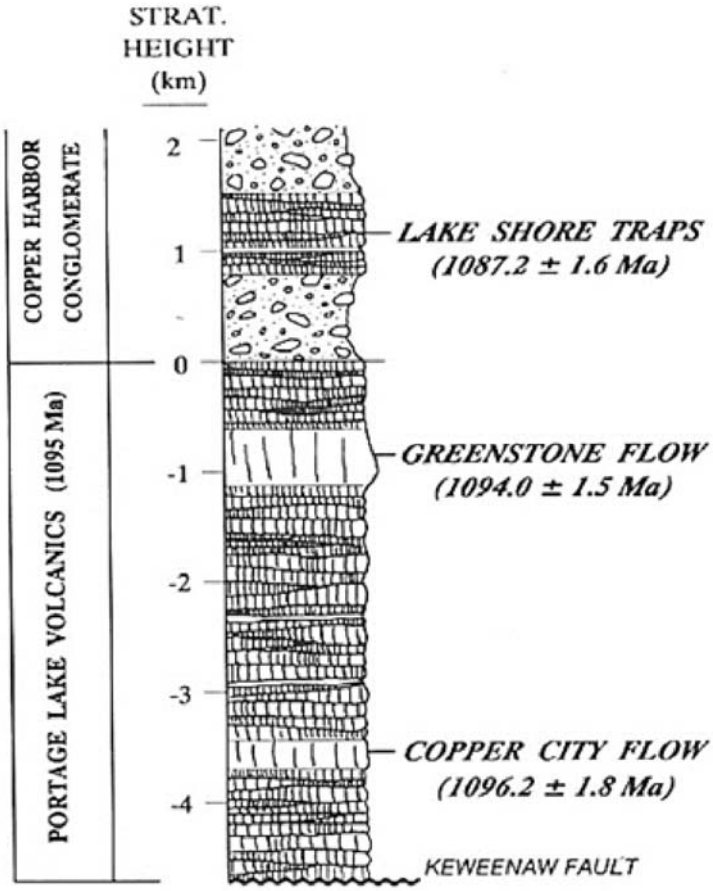

Figure 9. Stratigraphic column for the Portage Lake Volcanics and a portion of the overlying Copper Harbor Conglomerate exposed on the Keweenaw Peninsula. U-Pb zircon ages of select basaltic lava flows are labeled. From Davis and Paces (1990).

The PLV are best exposed on Michigan's Upper Peninsula where they extend for over 200 kilometers from the Michigan-Wisconsin border to the tip of the Keweenaw Peninsula (Figure 1; White, 1960). Where exposed, they form a 3-5-kilometer-thick

sequence although the lower part of the section is truncated by the high-angle reverse Keweenaw fault (Figs. 1 and 9) obscuring the true thickness of the PLV sequence. Seismic reflection profiles suggest that the PLV underlie much of Lake Superior where they may attain a thickness of 6-7 km near the axis of the Lake Superior syncline (Fig. 2).

Similarities in the stratigraphic sequences of the PLV on the Keweenaw Peninsula and Isle Royale (Fig. 1), recognized by workers as early as 1851, led Lane (1893, 1911) to conduct the first thorough study of the rocks in each location. Lane's research led to the correlation of several specific rock units between the two locations. Aeromagnetic studies and field mapping conducted by Books (1968, 1972) and Huber (1973), respectively, and, more recently, geochemical analyses conducted by Longo (1984) support Lane's correlations of PLV units across Lake Superior.

Structurally, the PLV occupies an asymmetrical graben, the Portage Lake Volcanic basin, which is bounded by high-angle reverse faults; the Keweenaw fault to the southeast and the Isle Royale fault to the northwest (Fig. 1; Halls and West, 1971). Although originally thought to be entirely contained between these faults, integrated modelling of gravity, magnetic, and seismic data in western Lake Superior (Allen et al., 1994) identified two areas to the north and south of the axis of the Lake Superior syncline where the volcanic sequence pinches out. These areas, termed White's Ridge and the Grand Marais block (Fig. 1), are presumed to be large blocks or ridges of granitic crust that may have become isolated during crustal separation and may have acted as structural highs which exerted control over the shape of the grabens into which MCR lavas accumulated (Allen et al., 1994; Sexton and Henson, 1994; Miller and Chandler, 1997).

Allen et al. (1994) demonstrated that the synformal axis of the Portage Lake basin, which has historically been termed the Lake Superior syncline (Irving, 1883) is deflected around the Grand Marais block, curving from a southwest trend between Isle Royale and the Keweenaw Peninsula to a west-northwest trend between the two crustal blocks (Fig. 1). Miller and others (Miller et al., 1995; Miller and Chandler, 1997) have suggested that the axial trace of the northwestern segment of the Portage Lake basin may project onto the Minnesota shore, terminating in the cusp of the FTMD described above as a normal growth fault intruded by the BRD dike complex (Figs. 1 and 7). They further speculated that the Schroeder-Lutsen basalts (Figs. 4 and 5), which occupy the upper part of the North Shore Volcanics and lie unconformably on older NSVG lavas that have been intruded and structurally deformed by the Beaver Bay Complex, may be correlative with the lower portion of the Portage Lake Volcanic sequence.

1.1.7 Greenstone Flow

The Greenstone Flow (GSF) is the largest lava flow in the PLV. It has an exposure area of over 5,000 km^2 (White, 1960) and an estimated volume of at least 1,650 km^3 (Longo, 1984). This estimate may be conservative, however, due to the uncertainty of the western extent of the flow. The GSF forms the precipitous ridge which runs roughly 90 kilometers along the length of the Keweenaw Peninsula (Fig. 1) and achieves a maximum thickness of 450 meters (White, 1960). The GSF has been correlated across Lake Superior to Isle Royale (Lane, 1893, 1911; Huber, 1973; Longo, 1984) where it also forms a prominent ridge and reaches a thickness of roughly 250 meters (Huber, 1973).

Throughout most of the Keweenaw Peninsula, the GSF is underlain by a moderately-coarse, cupriferous, felsitic conglomerate – the Allouez Conglomerate – which is typical of the conglomeratic rocks of the Michigan copper district. Beneath the conglomerate is a series of lava flows which display ophitic to plagioclase-porphyritic texture. Similar stratigraphic units are found underlying the GSF on Isle Royale. On the southwest end of the island, Lane (1893) and Huber (1973) describe a sedimentary conglomerate, termed the Allouez Conglomerate Correlative, which is in turn underlain by a series of ophitic to plagioclase-porphyritic lava flows. These two units are important stratigraphic markers that were used by Lane (1893, 1911) to correlate the GSF between the Keweenaw Peninsula and Isle Royale. The presence of the Allouez Conglomerate Correlative unit is obscured by glacial debris over the remaining part of Isle Royale but Longo (1984) reported the occurrence of a series of thin, highly-oxidized ophitic to plagioclase-porphyritic lava flows underlying the GSF near the Palisades (Fig. 14) at the northeastern end of the island. These rocks are thought to be correlative with the underlying flows on the southwestern part of the island. Directly above the GSF on Isle Royale is a pyroclastic breccia unit which contains subrounded lithic clasts that range in size from 1-10 cm and have been interpreted to be fragments of the GSF flow top (Huber, 1973). Similarly, on the Keweenaw Peninsula, the GSF is directly overlain by a pyroclastic-breccia unit, termed the Mesnard Epidote by Lane (1911). This unit has been interpreted by Lane (1911) and Huber (1973) to be correlative with the pyroclastic breccia overlying the GSF on Isle Royale.

The immense thickness and lithological variation within the GSF led many earlier workers to regard it as an intrusive sill (e.g. Van Hise and Leith, 1911). However, convincing observations from field exposures and drill core provide convincing evidence of its volcanic nature. These observations include: 1) the presence of a hackly and locally scoriaceous flow top (Huber, 1973; Longo, 1984); 2) the presence of pyroclastic breccia units directly overlying the GSF on both Isle Royale and the Keweenaw Peninsula (Lane, 1893, 1911; Huber, 1973); and 3) the consistently concordant stratigraphic position of the GFS which is never observed to cross-cut the underlying conglomerates or overlying pyroclastic units (Lane, 1893, 1911; Broderick 1935, 1946; Huber, 1973).

Recognizing the lithological variation inherent in the thicker portions of the flow, many authors have subdivided the GSF into separate lithostratigraphic zones based on mineralogical and textural attributes of the dominant rock types. Cornwall (1951) offered the first rigorous examination of the lithological variation and divided the GSF into four separate zones (Fig. 10) – lower ophitic, pegmatoid, upper ophitic, and amygdaloidal – which has been adopted by subsequent authors.

The upper and lower ophitic zones are essentially identical in terms of mineralogy and texture; each being composed of ophitic olivine basalt. The basalts of the lower ophitic zone tend to be slightly coarser than in the upper ophitic zone, but grain sizes in both coarsen away from the flow margins with augite oikocryst ranging in diameter from less than a millimeter to over two centimeters (Huber, 1973; Longo, 1984). Cornwall (1951) reported localized layering near the base of the lower ophitic zone as being

defined by variations in the size and concentration of augite oikocrysts and foliation of the groundmass plagioclase crystals with sharp contacts separating successive layers.

The pegmatoid zone is a lithologically heterogeneous interval composed of medium- to coarse-grained, subophitic to subprismatic granular gabbros which host numerous en echelon lenses or layers of coarse-grained to very coarse-grained, granophyric gabbro or "pegmatoids". This term is equivalent to the term "dolerite" used by Lane (1893, 1911) to describe these and similar rocks in other flows of the PLV. Although no modal rock type classification has been applied to these rocks, they are typically described as being well-laminated and composed of an interlocking mat of albite-oligoclase (An_{5-15}) with smaller amounts of interstitial augite, ilmenite, magnetite, chlorite, and apatite (Lane, 1893, 1911; Cornwall, 1951, Huber, 1973; Longo, 1984). These lenses, or layers, are typically aligned parallel to the base of the flow and range in thickness from a few centimeters to several tens of meters in thickness (Lane, 1893, 1911; Cornwall, 1951, Huber, 1973; Longo, 1984). Huber (1973) reported that the contacts between the various rocks in the GSF are typically very sharp but are locally gradational with intermingling of the separate rock types occurring over intervals of a few meters or less. On Isle Royale, the pegmatoid zone is considered to be a continuous stratiform feature (Huber, 1973) although it tends to pinch out in the thinner portions of the GSF on the Keweenaw Peninsula (Lane, 1893, 1911; Cornwall, 1951). The amygdaloidal zone is composed of fine-grained, massive to amygdaloidal basalt and represents the exposed flow top of the GSF (Cornwall, 1951).

Since Lane's (1893) work it has been interpreted that the lithological variation within GSF, as well as in other flows of the PLV, is the result of the *in situ* differentiation of the

GSF flow sheet. Lane (1893, 1911) suggested that the pegmatitic rocks were formed by the accumulation of water or some other "mineralizer" in certain layers that facilitated the crystallization of plagioclase. Broderick (1935) and Cornwall (1951), citing observational and wet chemical analyses, supported Lane's interpretation that the pegmatitic rocks are the likely result of the late stage accumulation of volatile-rich fluids, likely derived from the GSF basalts. Cornwall (1951) offered several hypothetical models to describe the mechanism of formation of the pegmatoid rocks and argued that the whole-rock geochemistry of all of rock types in the PLV could be generated by differentiation of the marginal GSF composition, thus concluding that all PLV lithologies could have been generated from a single parental magma. Cornwall (1951) also posited that the obvious differentiation of GSF may have been formed from magmas that evolved in separate staging chambers at different levels in the crust and were then successively erupted.

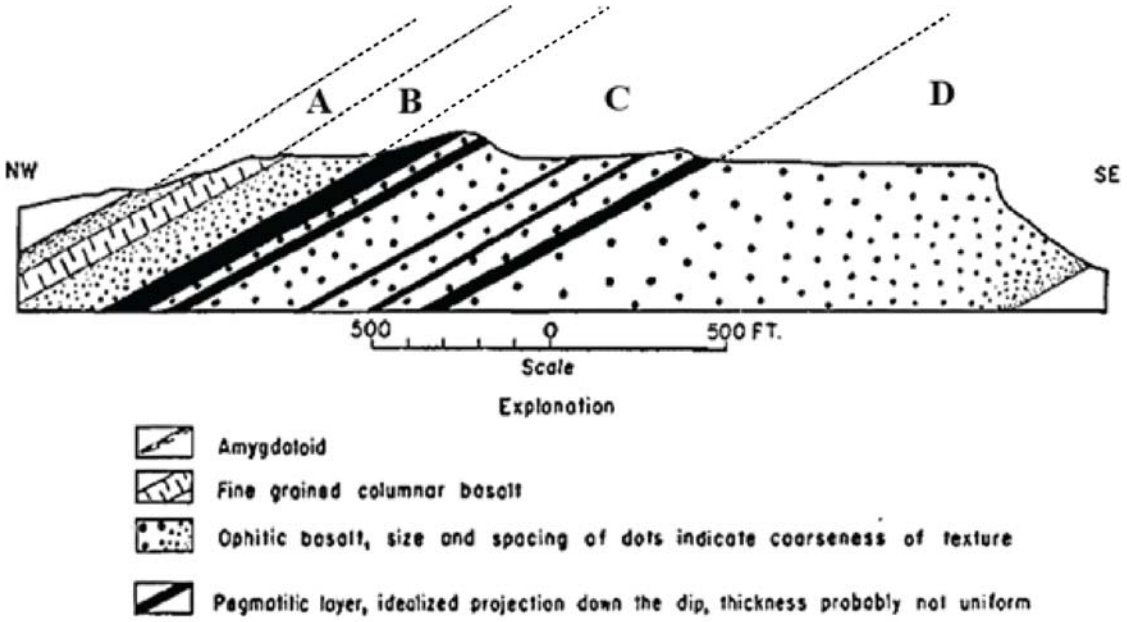

Figure 10. Idealized cross section of the Greenstone Flow near Phoenix, MI on the Keweenaw Peninsula (from Cornwall, 1951). Principal rock units distinguished are:

A) *amygdaloidal zone;* B) *upper ophitic zone*; C) *pegmatoidal zone*; and D) *lower ophitic zone*.

1.2 Objectives of Study

The main goal of this research is to evaluate the plausibility that the Beaver River diabase dike and sill network acted as the magmatic feeder system to the Greenstone Flow lava sheet. Correlating these two extensive igneous bodies will provide substantial insight into the relationships between the intrusive and volcanic systems during main stage MCR activity and will help to develop a more robust interpretation of the overall tectonomagmatic evolution of the rift.

This study seeks to document the petrographic, mineral chemical, and lithogeochemical attributes of samples collected along several profiles of each unit in order to compare them for a comagmatic relationship. The specific objectives of this study are as follows:

1) Conduct field mapping and sampling of the BRD-SBI intrusions and GSF lava sheet. This mapping will focus especially on the contact relationships between the various lithologies in the GSF to determine whether they likely formed *in situ*, as interpreted by others (e.g. Lane, 1893, 1911; Cornwall, 1951), or by composite emplacement as has been interpreted for the BRD-SBI intrusions (Shank, 1989; Miller and Chandler, 1997).
2) Conduct detailed petrographic and mineral chemical analyses of BRD-SBI and GSF samples to compare and contrast the mineralogical and textural attributes of comparable lithologies in each.

3) Conduct whole-rock lithogeochemical analyses to determine whether the chemical compositions of the various lithologies in the BRD-SBI and GSF support a comagmatic link.

2.0 METHODS OF INVESTIGATION

2.1 Terminology and Nomenclature

The terminology and nomenclature used to describe the lithological, textural, and mineralogical attributes of rocks in this study follows the definitions set out in the American Geological Institute's *Glossary of Geology* (Nuendorf, 2005). Rock types are classified based on the criteria recommended by Miller et al. (2002) for the field and petrographic identification of rocks in the BBC.

Although the plagioclase-olivine-pyroxene scheme of Streckeisen (1974) (Fig. 11A) and the quartz-alkali feldspar-plagioclase feldspar-feldspathoid classification scheme of Streckeisen et al. (1976) (Fig. 11B) are the standard methods for the classification of igneous rocks, there are several practical problems that arise when applying them in a field based or petrographic study. The first involves distinguishing between intermediate (diorite) and mafic (gabbro) lithologies. The generally accepted criteria for this determination is a change in the anorthite content in plagioclase from less than 50% (diorite) to greater than 50% (gabbro). This determination is often problematic during petrographic analysis and is impossible during field-based studies because it usually requires a chemical analysis. A second problem arises when trying to determine the relative modal abundances of rocks containing micrographic quartz and alkali feldspar, which are common throughout the BBC and in the pegmatoid unit of the GSF. The terms *granophyre* or *granophyric*, which are traditionally used to describe these rocks are problematic in that they are commonly used both as compositional and textural modifiers. Because of this, Miller et al. (2002) suggests the use of the term *felsic mesostasis* to describe what is defined by Miller et al., (1993, 1994) as the fine-grained, typically pink

matrix composed of micrographically intergrown quartz and K-feldspar with minor Fe-silicates, Fe-Ti oxides and hydroxides, and accessory minerals such as apatite, epidote, zircon, calcite, and titanite. The term *granophyric*, however, will still be used informally to describe rocks containing this material. For the reasons stated above, mafic and intermediate lithologies in this study are classified based on the criteria recommended by Miller et al. (2002) and presented in Tables 1 and 2.

Table 1. Criteria for distinguishing mafic and intermediate lithologies in the BBC. From Miller et al., (2002).

	Mafic Mineral Habit	Felsic Mesostasis
Intermediate	Prismatic, subprismatic	> 5%
Mafic	Granular to poikilitic	< 5%

Table 2. Criteria for classifying intermediate and felsic lithologies in the BBC. From Miller et al., (2002).

Criteria	Diorite-quartz diorite	Monzodiorite- quartz monzodiorite	Quartz monzonite (granodiorite?)	Granite
Percent felsic mesostasis	5-15	15-35	>35	>50
percent mafic mineral phases	>25	>15	35-10	<20
visible quartz	No-diorite Yes-quartz diorite	No-monzodiorite Yes-quartz monzodiorite	Yes	Yes

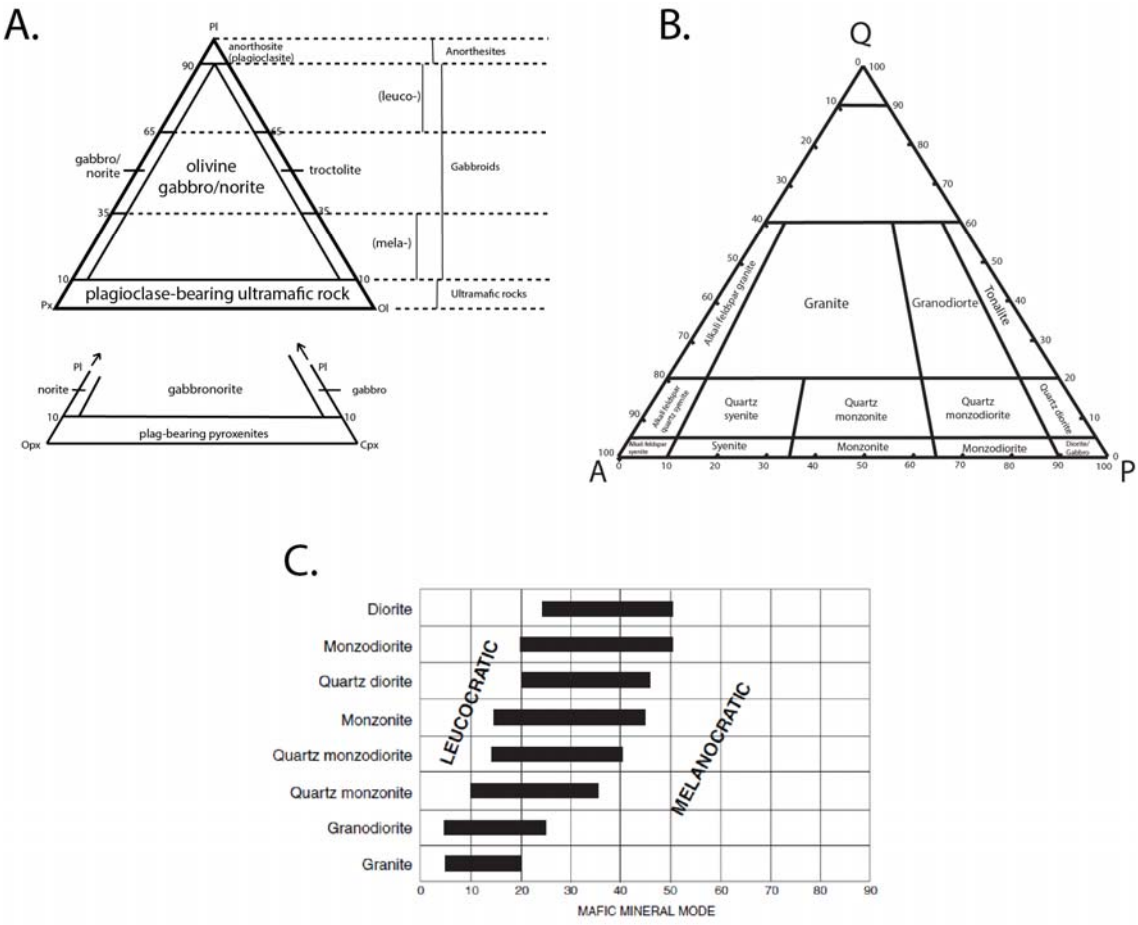

Figure 11. A). Olivine-plagioclase feldspar-pyroxene classification scheme for gabbroic rocks (after Streckeisen, 1974); B). Quartz-alkali feldspar-plagioclase feldspar (QAP) classification scheme for phaneritic igneous rocks (after Streckeisen, 1976); C). Expected range of mafic mineral abundances in intermediate and felsic rocks (modified Streckeisen, 1976).

The absolute grain-sizes of rocks in this study are determined based on the average length of plagioclase laths. Plagioclase was chosen because the relative size of pyroxene oikocrysts in ophitic rocks can often be a misleading indicator of grain size as these rocks are often composed of fine-grained primocryst minerals enclosed by much coarser-grained pyroxene oikocrysts. Grain-size classifications are based on Winter (2014) and are as follows:

aphanitic: crystals are too small to distinguish with the naked eye;

fine-grained: < 1 mm in diameter or length;

medium-grained: 1-5 mm in diameter or length;

coarse-grained: 5-50 mm in diameter or length;

very coarse-grained: > 50 mm in diameter or length;

Winter (2014) suggests that the term *very coarse*-grained be used instead of *pegmatitic*, which has been traditionally applied to rocks composed predominantly of minerals greater than 50 mm in diameter. The term *pegmatitic* carries compositional implications for many geologists because pegmatites have historically been limited to late-stage crystallization of granitic magmas. This approach is adopted here.

For intermediate and mafic lithologies in which the modal abundances of mafic minerals fall outside the IUGS recommended ranges (Fig. 11C), the prefixes *leuco*- and *mela*- are used (e.g. leucogabbro). Mafic minerals in the intermediate rocks are commonly altered or otherwise difficult to identify in the field or petrographically. For this reason, the prefix *ferro*- is used to acknowledge the presence of iron-rich phases of unknown type (Miller et al., 2002).

The lithological, textural, and mineralogical attributes of the various rocks in this study are described using the nomenclature set out by the American Geological Institute's *Glossary of Geology* (Nuendorf, 2005). Bulk rock texture terminology is based on the relative habits of pyroxene and plagioclase as recommended by Miller et al. (2002) and include:

Ophitic: defined by multiple plagioclase laths (chadacrysts) fully enclosed in poikilitic crystals of pyroxene (oikocrysts);

Subophitic: Multiple lath-shaped crystals of plagioclase partially enclosed in subpoikilitic crystals of pyroxene;

Intergranular: Composed of pyroxene and plagioclase displaying anhedral to subhedral granular habits, none enclosed by the other;

Many of the rocks in this study contain large plagioclase crystals which, depending on whether they crystallized from the same magma as the groundmass or from a foreign source, will be referred to as *phenocrysts* or *xenocrysts*, respectfully. Crystals which are noticeably larger than the surrounding groundmass crystals and whose genetic origin is unknown will be referred to as *megacrysts*.

This study uses the term *foliation* to describe the planar arrangement of elongate minerals, typically plagioclase and/or pyroxene. Modifiers used to describe the contrast (or demarcation) of foliation follow the recommendation of Miller et al. (2002) and are linked to an estimation of the abundance of elongate minerals aligned to within 10° of a common plane: *non-foliated* (< 25%), *poorly-foliated* (25-50%), *moderately-foliated* (50-75%), *well-foliated* (75-90%), *very well-foliated* (> 90%).

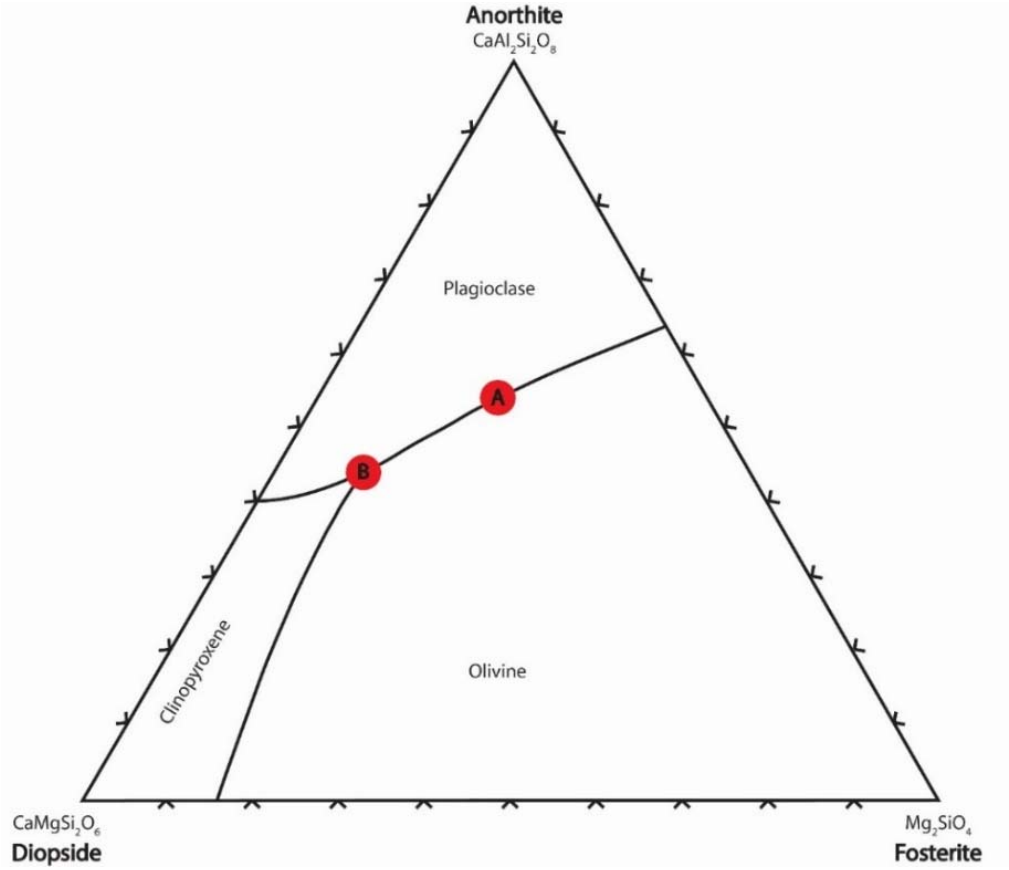

Figure 12. Phase diagram for the plagioclase anorthite-diopside-forsterite system. A magma crystallizing from point A will produce a rock with intergranular plagioclase and olivine, whereas clinopyroxene will crystallize later and interstitially after more cooling to produce ophitic to subophitic textures. For a magma corresponding to point B, all three phases will be granular.

2.2 Field Mapping and Sampling

Field mapping of the BRD-SBI and GSF exposures occurred periodically between the spring of 2013 and the summer of 2014. Field locations were chosen based on previous mapping of the BRD-SBI in northeast Minnesota (Miller, 1988; Miller et al., 1994) and the GSF on Isle Royale (Huber, 1973; Longo, 1984) and the Keweenaw Peninsula (Cornwall, 1954; Cornwall and Wright, 1954; Longo, 1984; Cannon and Nicholson, 2002). Specific field sites were chosen based on the amount and type of exposed outcrop reported in each location, as well as by accessibility by roads, trails, or

canoe. Sampling occurred in scattered locations in the southern Beaver Bay Complex (Fig. 7, area A) and along two traverses of the linear intrusions in the northern BBC (Fig. 7, area B). Transects of the GSF on the Keweenaw Peninsula were conducted near the towns of Phoenix, MI and Central, MI (Fig. 13, areas A and B, respectively). Transects of the GSF on Isle Royale were conducted in three locations: at Blake Point, along the Lookout Louise trail, and along the Tobin Harbor-Duncan Bay portage trail (Fig. 14, areas A, C, and D, respectively). Two exposures of the GSF were also mapped and sampled at Red Rock Point (Fig. 14, area B).

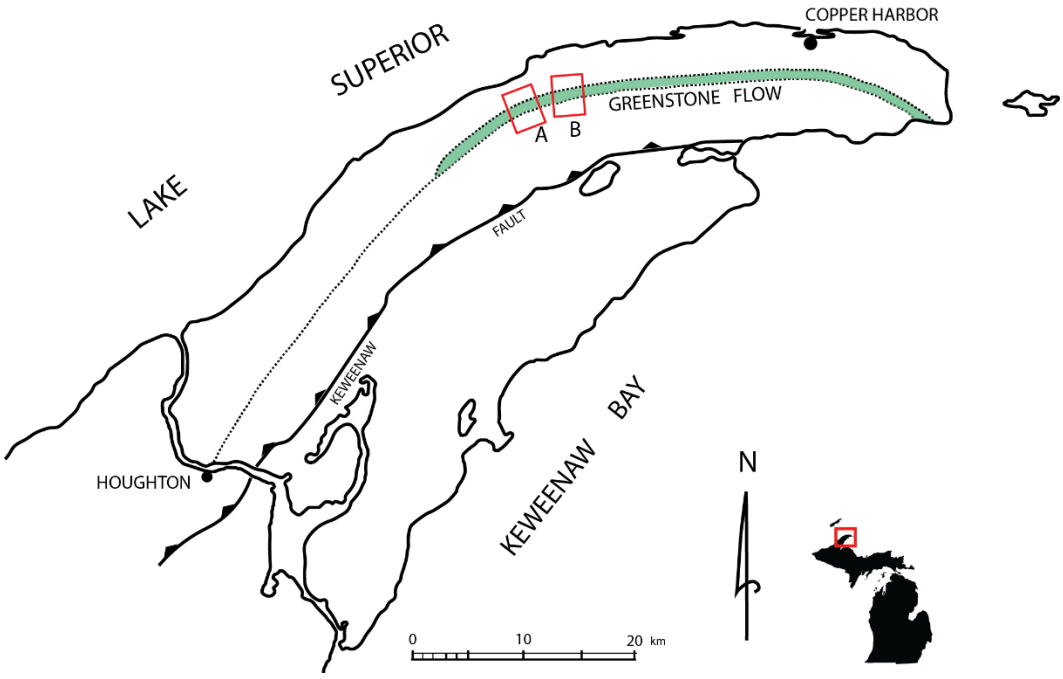

Figure 13. Locations of bedrock mapping and sampling traverses of the GSF on the Keweenaw Peninsula. A-Phoenix, MI and B-Central, MI.

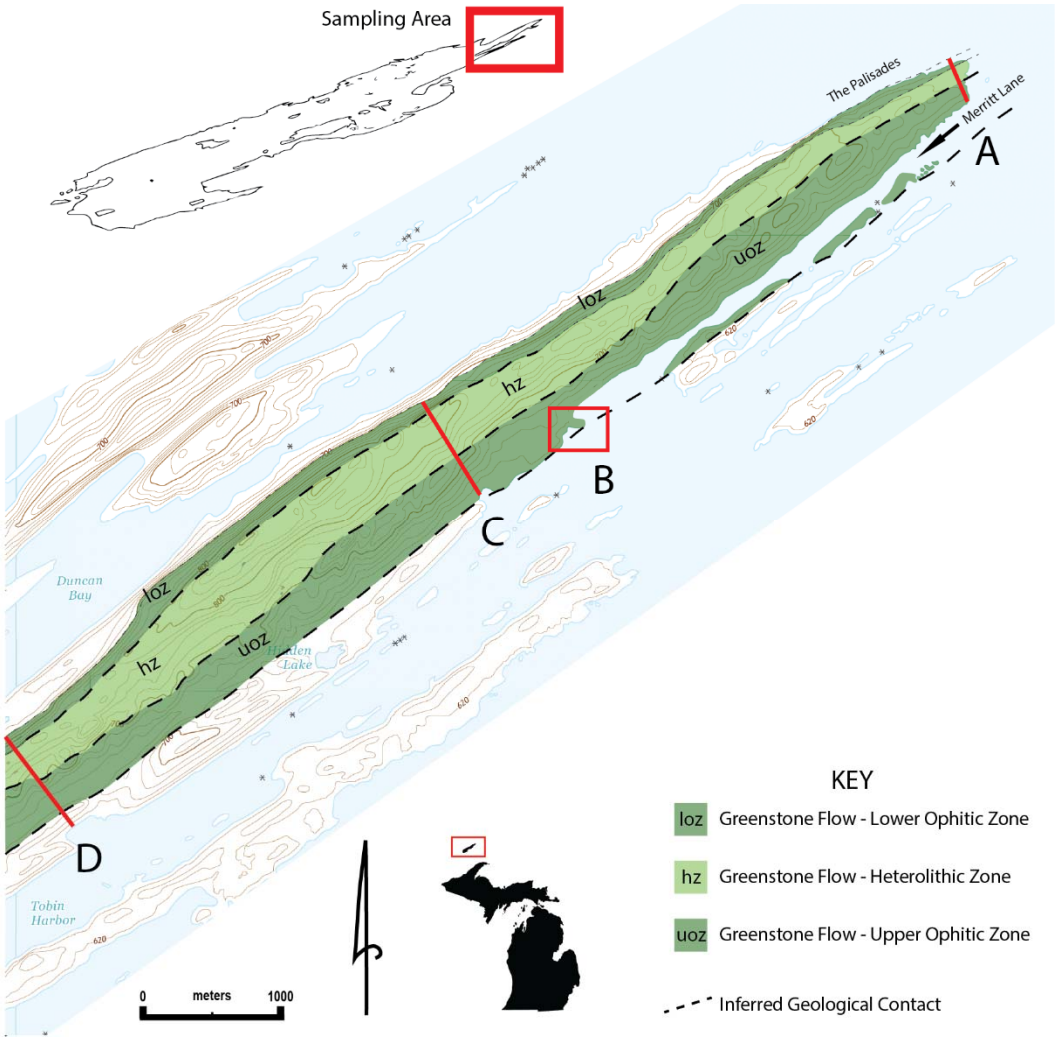

Figure 14. Locations of bedrock mapping and sampling traverses of the GSF on Isle Royale. A- Blake Point, B- Red Rock Point, C- Lookout Louise trail, and D- Tobin Harbor-Duncan Bay Portage trail.

Mapping was conducted on mylar overlays on 1:5,000 topographic basemaps of USGS 7.5-minute quadrangles with 100 meter grids in NAD83 UTM Zone 15 and NAD83 UTM Zone16 for exposures in Minnesota and Michigan, respectively. Roughly 140 outcrops were mapped in total. Outcrops were catalogued in the order in which they were visited and assigned specific field ID numbers. Outcrops were color-coded based on lithology and sketched on the mylar overlays along with any pertinent structural

measurements, lithological contacts, and traverse lines. Detailed notes were taken at each outcrop describing the following criteria: location (UTM), physical condition (exposure type, degree of weathering, etc.), lithology, grain size and textural attributes (ophitic, subophitic, etc.), orientation of structural features (foliation, layering, etc.), variation in mineralogy and/or texture, contact relationships between adjacent lithologies, general field conditions (weather, terrane, etc.), description of samples and/or photos taken.

A total of 95 hand samples were collected from the study areas, 31 from the BRD-SBI and 72 from the GSF. All samples were made into thin sections for petrographic analysis with 53 sections polished for mineral chemical analysis. Sixty-two samples were crushed and pulverized for whole rock analysis. This study also took advantage of previous mapping and sampling in the Beaver Bay Complex by the Minnesota Geological Survey (Miller, 1988; Miller et al., 1989, 1993, 1994, 2006, and Boerboom et al., 1994) as part of the USGS's COGEOMAP program. A total of 26 thin sections with descriptions, 60 lithogeochemical analyses, and mineral analyses from 27 samples acquired for the COGEOMAP project were incorporated into this study.

Samples of the BRD-SBI were collected from outcrops identified from previous mapping (Miller, 1988; Miller et al., 1994) with the goal of acquiring representative samples of the various lithologies that comprise the intrusions (Fig. 7). Samples of the GSF were collected along traverses that profile the stratigraphic sections on the Keweenaw Peninsula (Fig. 13) and Isle Royale (Fig. 14). GSF samples were collected at a roughly 20-meter interval or wherever distinct changes in grain-size, mineralogy, and/or texture were evident. Close-spaced sampling was often conducted across

lithological contacts to evaluate the mineralogical, textural, and geochemical variation between adjacent rocks types.

2.3 Petrographic Analysis

Standard thin sections of 23 BRD-SBI and 72 GSF samples were prepared by Quality Thin Sections in Tucson, Arizona for petrographic analysis. Thin sections were analyzed with transmitted light using standard petrographic techniques. Detailed petrographic descriptions were recorded describing the grain size, estimated modal mineralogy, primary texture, degree of alteration, and alteration mineral assemblage. These observational data were used both for rock classification and description, as well as to determine those samples suitable for later mineral analysis by SEM-EDS and for whole-rock lithogeochemical analyses. The criteria used for this determination included the lithological designation, abundance of unaltered primary minerals, and the occurrence of plagioclase megacrysts. Full petrographic descriptions of all 95 samples are presented in Appendix A.

Petrography was especially useful in characterizing the variation in the textures of clinopyroxene, particularly changes from ophitic, to subophitic, to anhedral granular, to prismatic granular textures. Previous field and petrographic studies of the BRD-SBI (e.g. Miller, 1988; Shank, 1989; Miller et al., 1994; Miller and Chandler, 1997) and the GSF (e.g. Lane, 1892, 1911; Cornwall, 1951; Longo, 1984) reported that the lithological variation in these units is often expressed by subtle differences in the textural relationship between plagioclase and clinopyroxene and in changes in modal mineralogy. Since it was often difficult to recognize these differences in the field, petrographic analysis was

essential to delineating the changes in textural and mineralogical attributes between adjacent rock types.

2.4 Mineral Chemistry

Mineral chemical analyses were conducted to compare the compositions of clinopyroxene, olivine, and plagioclase megacrysts in the BRD-SBI and GSF samples. A total of 53 thin sections – 22 from the BRD-SBI and 31 from the GSF – were selected during petrographic analysis for polishing at Quality Thin Sections. Chemical analyses were conducted using a JEOL JSM-6490LV scanning electron microscope equipped with an Oxford Inca X-Act energy dispersive X-ray spectrometer (SEM-EDS) at the Research Instrumentation Laboratory at UMD. Polished thin sections were coated with an approximately 20 nm carbon film. All analyses were conducted using an accelerating voltage of 15 kV for 20 seconds.

The EDS system was used to collect semi-quantitative (~0.5% error) major elements compositions of pyroxene, olivine (where fresh olivine was present), plagioclase and oxides. The EDS system was calibrated before each sample analysis using a thin strip of pure copper tape affixed atop each polished section. Numbers of spot analyses for each sample included 8 to 16 for pyroxene, 4 to 6 for olivine and 4 to 6 for oxide. An average of 12 spot analyses was collected from the cores and rims of plagioclase megacrysts and linescans were conducted to characterize the degree of zonation in each megacryst. An average of 12-16 spot analyses of groundmass plagioclase crystals was also collected from those samples containing plagioclase megacrysts for comparison with the megacryst

core and rim compositions. Mineral chemical data collected for olivine, pyroxene, oxides, and plagioclase megacrysts are compiled in Appendix B.

2.5 Whole-Rock Lithogeochemical Analysis

Whole rock lithogeochemical analyses were obtained from a total of 21 BRD-SBI and 41 GSF samples from Acme Laboratories in Vancouver, British Columbia to characterize the geochemical attributes of the various lithologies within the BRD-SBI and GSF. Representative samples of comparable lithologies from each unit were selected for chemical analysis with special emphasis on samples collected across lithological contacts. Samples of the GSF ophitic zones were chosen based on stratigraphic height in order to characterize the chemostratigraphy of the flow. Furthermore, similar sample sizes from the GSF on Isle Royale and the Keweenaw Peninsula were chosen to assess any chemical variation between the more proximal and distal locations from the proposed BRD source vent.

Samples were dried, crushed to 2 mm, and then pulverized to 75 μm using mild steel. Sample powders were fused using a lithium borate fusion and analyzed using ICP-ES and ICP-MS methods. Table 3 lists the specific elements analyzed and methods used. Complete details of the geochemical analyses are presented in Appendix C.

Table 3. Digestion and analytical techniques and chemical components analyzed by Acme Laboratories, Vancouver, BC.

Analytical Method	Chemical Constituents Measured
Four Acid Digestion followed by ICP-ES Analysis	SiO_2, Al_2O_3, CaO, Cr_2O_3, Fe_2O_3, K_2O, MgO, MnO, Na_2O, P_2O_5, TiO_2, Ba, Nb, Ni, Sc, Sr, Y, Zr, Ce, Co, Cu, Zn, LOI
Four Acid Digestion followed by ICP-MS Analysis	Ba, Be, Ce, Co, Cs, Dy, Er, Eu, Ga, Gd, Hf, Ho, La, Lu, Nb, Nd, Pr, Rb, Sm, Sn, Sr, Ta, Tb, Th, Tm, U, V, W, Y, Yb, Zr
Leucotitration	Total carbon and sulfur
Aqua Regia Digestion followed by ICP-MS Analysis	Ag, As, Au, Bi, Cd, Hg, Mo, Ni, Pb, Sb, Se, Tl, Zn

3.0 RESULTS

This chapter presents the results of the field and petrographic observations, mineral chemical analysis, and whole-rock lithogeochemical analysis on the parts of the BRD-SBI intrusive system and the GSF volcanic system studied for this project.

3.1 Geology and Lithologic Attributes of the BRD Sampling Areas

Because of the extensive bedrock mapping conducted during the COGEOMAP program, detailed field mapping of the BRD dikes and sills and composite intrusions was not conducted during this study. Rather, previous mapping by Miller and others in the northern BBC (Miller et al., 1994; Boerboom et al, 1994) and the southern BBC (Miller, 1988; Miller et al., 1989, 1993, 2006) was used to inform the sampling strategy and ensure that a representative sampling of the various lithologies in the BRD-SBI was collected. The areas selected for sampling were chosen for their exposure of a complete range of lithologies known to comprise the BRD and SBI. Sampling through the BRD-SBI lithologies in the southern BBC was conducted in the vicinity of Beaver Bay (T55N, R8W, Secs. 11, 12, 13, & 14; Fig. 15) and included samples from the Beaver Bay body of the Silver Bay intrusions. Sampling through the composite BRD intrusions of the northern BBC was conducted in a widened area of a prominent dike near Cramer Lake (T58N, R6W, Secs. 3, 10, 15, &16; Fig. 17). This section reports on the geology of the two sampling areas in the SBBC and NBBC and summarizes the lithological attributes of these samples determined from field and petrographic observations.

3.1.1 Geology of the Southern and Northern Beaver Bay Sampling Areas

In the southern BBC in the Beaver Bay area (Fig. 15), the BRD occurs as numerous dikes and sills of predominantly ophitic olivine diabase that cross-cut basalt and rhyolite flows of the NSVG. The western extent of the BRD is marked by a NNE-trending dike (FTMD, Fig. 15) which feeds a large (150-200 m thick) sill to the east that intrudes subconcordantly into the lava flows (cross section, Fig. 15). Both the flows and the sill dip between ~5-20° toward Lake Superior. Large inclusions of anorthosite (< 100 meters in diameter) are common in this area (black masses in Fig. 15) and are irregularly distributed throughout the diabase. Less commonly, inclusions of granophyric granite and rhyolite also occur in the BRD.

The SBI form smaller, generally sheet-like intrusions within and adjacent to the BRD dikes and sills. Mapping and sampling during this study focused on the largest SBI intrusion, termed the Beaver Bay body (Fig. 15). The Beaver Bay body is a large (roughly 4 km across), concentrically zoned, lens-shaped intrusion emplaced into the upper portion of the thick BRD sill (see cross section in Fig. 15). A similar, but smaller composite intrusion, called the Silver Bay body, is located to the northeast of Beaver Bay (Fig. 15), but was not sampled during this study.

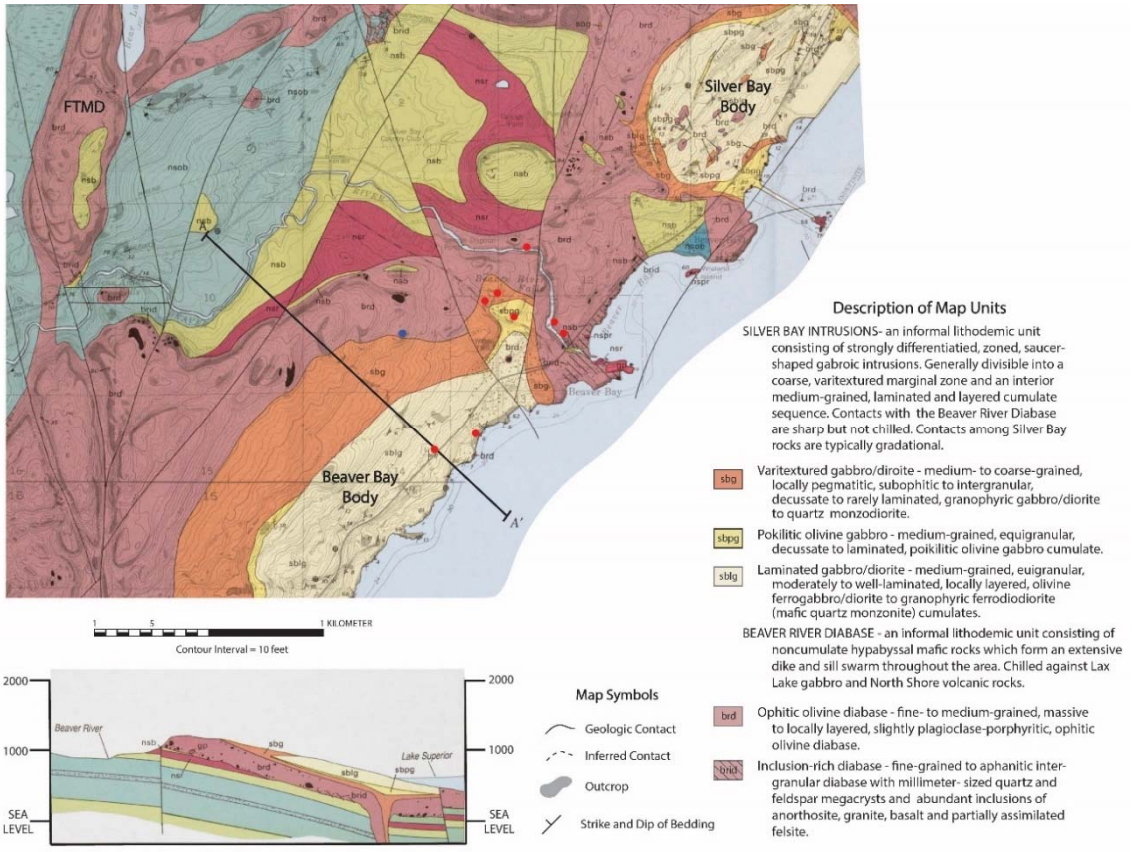

Figure 15. Geology of the Beaver River diabase and Silver Bay intrusions in the Beaver Bay area as portrayed on MGS map M-65 (Miller, 1988) and locations of samples collected during this research (red dots) and samples studied from the COGEOMAP program (blue dots). The description of BRD and SBI units shown in the figure are from the M65 map. All other map units are basalts and rhyolites from the NSVG. The Beaver Bay and Silver Bay bodies of the SBI, and the main feeder dike of the BRD, also known as the Finland Tectonomagmatic Discontinuity (FTMD), are labeled.

Bedrock mapping by Miller (1988) and follow-up petrologic studies (Shank, 1989; Miller and Chandler, 1997) concluded that the Beaver Bay intrusion is composed of two major comagmatic zones – an outer marginal zone predominantly of varitextured gabbro to ferromonzodiorite and an inner zone of ferrogabbroic/dioritic cumulates that are well foliated, locally layered and composed of systematically differentiated rocks ranging from olivine ferrogabbro to quartz ferromonzonite. Miller (1988) distinguished five

major map units as comprising the BRD-SBI intrusions in this area (Fig. 15). From youngest to oldest, these are:

sblg - Well foliated, intermittently layered, medium-grained, locally apatitic, variably granophyric, intergranular olivine ferrogabbro/diorite (mafic quartz monzonite) which forms the core of many SBI intrusions.

sbpg - Foliated, medium-grained, poikilitic olivine ferrogabbro/diorite with 1-2 centimeter olivine oikocrysts which locally occurs as a transitional unit between *sblg* and *sbg* units and as decimeter- to meter-thick layers within the *slbg* unit.

sbg - Subophitic to prismatic granular, granophyric gabbro/diorite to quartz ferromonzodiorite which comprise the marginal zone of SBI intrusions.

brd - Fine- to medium grained, ophitic olivine diabase which is in chilled contact with volcanic rocks and locally contains large inclusions of anorthosite.

brid - Fine-grained to aphanitic diabase which locally occurs near margins of the main *brd* intrusions and is host to abundant inclusions of anorthosite, granite, basalt, and rhyolite and partially resorbed quartz xenocrysts.

In the SBCC sampling area (Fig. 15), the *brd* map unit is semi-continuously exposed in the streambed and along the banks of the Beaver River roughly three kilometers inland from Lake Superior (Fig. 16A). Exposures of ophitic olivine diabase are also observed in roadcuts along Highway 61 to the northeast and southwest of the SBI-Beaver Bay body. Three samples from the *brd* unit were collected from the Beaver Bay area (Fig. 15). The inclusion-rich and obviously contaminated rocks of the *brid* occur near the margins of the diabase intrusions near the mouth of the Beaver River. Care was taken to avoid sampling these variably contaminated diabase.

Excellent, nearly continuous exposures of well foliated ferrogabbro/diorite (Fig. 16C) (map unit *sblg*) can be found as: 1) gently dipping, wave-washed ledges along the

Lake Superior shore; 2) roadcuts extending several kilometers along Highway 61 and 3) scattered outcrop knobs, ledges, and whalebacks irregularly distributed on the gently dipping hillslope up from the highway (Fig. 15). The vari-textured, granophyric ferromonzodioritic rocks of the marginal zone (map unit *sbg*) are generally poorly exposed in inland areas, but occur well exposed along the shoreline (Figs. 15 and 16D). One sample of the marginal zone was collected along Lake County Road 4 (Lax Lake Road; Fig. 15) which runs northwest from Highway 61 through the eastern margin of the intrusion. The poikilitic olivine gabbro map unit (*sbpg*), which has been mapped intermittently between the marginal gabbro and the foliated ferrodiorite, also outcrops poorly in the Beaver Bay area and was not observed along the shoreline (Fig. 15).

The ophitic diabase of map unit *brd* are strongly chilled at the contacts with the NSVG footwall rocks and earlier intrusions. The contacts between the diabase and rocks of the SBI were not directly observed during this research and are described in detail in previous studies (Miller, 1988; Shank, 1989; Miller and Chandler, 1997). Wherever exposed, the contacts between the diabase and SBI are abrupt on a centimeter scale and unchilled. Angular inclusions of altered ophitic olivine diabase are commonly found as inclusions in the ferromonzodiorites of the SBI marginal zone (Fig. 15, map unit *sbg*) of the SBI. Shank (1989) reported that the contact between the marginal zone rocks and layered gabbro/diorite unit (Fig. 15, map unit *sblg*) is typically gradational over a distance of 5-10 meters although, locally, it is very sharp, occurring over centimeter scale. The *sbg*-*sblg* contact is typically marked by a gradual or sudden decrease in the regularity of lamination and a progressive increase in the grain size in the gabbro/diorite.

The mineral habit of olivine, augite, and Fe-Ti oxides is also observed to vary across the contact, changing from granular in the layered gabbro/diorite to subpoikilitic to poikilitic in the marginal zone rocks (Shank, 1989). The distinct changes in lithology and concentrically zoned character of many SBI bodies, discussed above, led Gehman (1957) to interpret the marginal zone and layered gabbro/diorite as two separate intrusive phases. However, based on the gradational contacts between the major lithological zones and petrological studies, Miller and others (Miller, 1988; Shank, 1989; Miller and Chandler, 1997) concluded that the SBI bodies in the SBBC are the result of the emplacement and subsequent fractionation of a single pulse of highly evolved magma into the BRD dikes and sills.

In the northern BBC area sampled near Cramer Lake, the BRD occurs as two main dikes that converge to the north and cross-cut rocks of the NSVG and earlier gabbro intrusions (Fig. 7). The westernmost dike, though composed of a series of narrow anastomosing dikes, is the continuation of the main FTMD feeder dike to the BRD. The eastern dike, which was sampled for this study, is a more prominent, keel-shaped composite dike (Fig. 17). Based on the orientation of foliated rock in the interior of the eastern dike, it has an asymmetrical shape with the eastern margins dipping more steeply than the western edges (Fig. 17, cross sections). A series of progressively more differentiated composite intrusions, similar to the SBI in the southern BBC, are recognized within the axial portion of the main ophitic olivine diabase forming the margins of the dike. At its widest (~2 km across), teardrop-shaped body is composed of at least five distinct map units (Fig. 17). Based abrupt contacts between map units and

cross-cutting relationship shown in the widened area of the dike, at least three discrete composite intrusion events are evident. These units are:

brd: ophitic olivine diabase

brpg: olivine-poikilitic, ophitic to subophitic olivine gabbro

brg: subophitic to intergranular, variably granophyric olivine oxide gabbro

brfd: poorly foliated, intergranular, granophyric ferrodiorite

brld: well-laminated (foliated) intergranular ferrodiorite

Figure 16. Field photos of A) outcrop exposure of the Beaver River diabase (map unit *brd*) along the Beaver River, B) typical ophitic texture of the *brd* map unit, C) well foliated ferrogabbro of the *sblg* unit, and D) subprismatic granular granophyric ferromonzodiorite of the *sbg* unit in the southern Beaver Bay mapping area.

Two traverses of the BRD dikes were conducted in the northern BBC mapping area. The northern traverse sampled where the intrusion abruptly narrows and forms a steep-

sided ridge roughly 650 meters across and 70 meters high. Here, ophitic olivine diabase (Fig. 17, unit *brd*) typically forms a series of 1-3-meter-high ledges (Fig. 18A and B) that line the eastern and western sides of the steep hill held up by the dike. Inclusions of anorthosite, common in the diabase exposures in the southern BBC, are largely absent in the Cramer mapping area. The ophitic diabase gives way abruptly to a subophitic to intergranular olivine gabbro (Fig. 17, unit *brg*). Miller et al. (1994) reported that the sharp textural change is accompanied by a significant change in mineral composition implying that the gabbro is a composite intrusion into the ophitic diabase.

North of the northern sampling area shown in Figure 17, Miller et al. (1994) identified an ophitic gabbro with poikilitic olivine (Fig. 18B) occurring in the transition between ophitic diabase with granular olivine of the *brd* unit (Fig. 18A) and intergranular gabbro of the *brg* unit (Fig. 18C). This *brpg* unit also occurs as a lens within the *brg* unit and the southern traverse area (Fig. 17), the *brg* unit appears to cross-cut the *brpg* unit. Noting that poikilitic olivine diabase is locally found interlayered with normal granular olivine diabase of the *brd* unit in the southern BBC, Miller et al. (1994) interpreted the *brpg* unit in the Cramer Lake area to be an interior differentiated phase of the *brd* unit. The masses of *brpg* occurring within the composite intergranular gabbro (*brg*) are thus interpreted to be inclusions detached from the core of the initial BRD diabase intrusion.

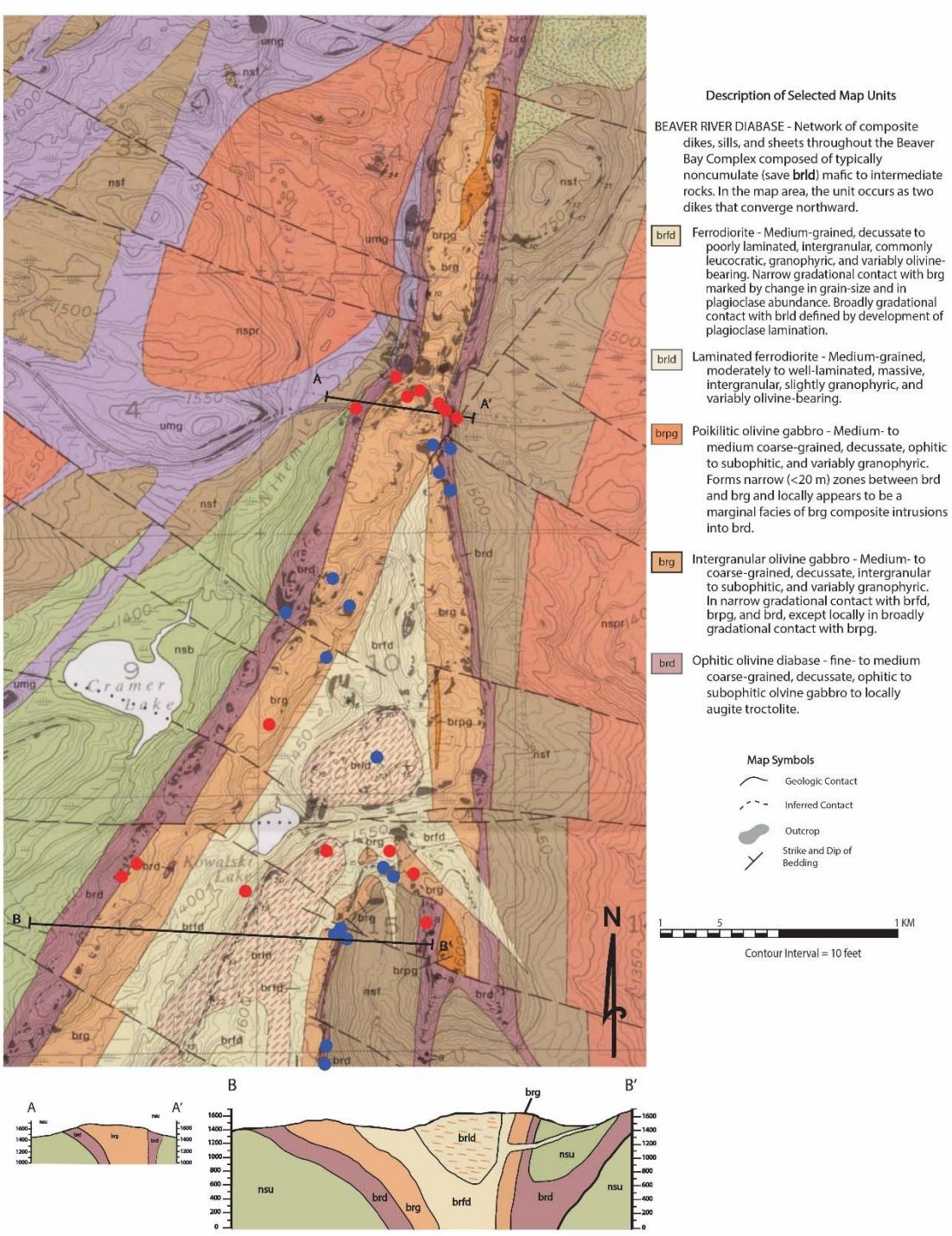

Figure 17. Geology of the Beaver River diabase and composite intrusions in the Cramer Lake area as portrayed on map M-82 (Miller et al., 1994). Locations of samples collected during this study (red dots) and during the COGEOMAP program (blue dots) are noted. Attributes of the five BRD units (*brd*, *brg*, *brpg*, *brfd*, & *brld*) are

described in the figure and in the text. Other units not defined include basalts (*nsb*), felsic volcanic (*nsf* & *nspr*), and older gabbroic intrusions (*umg*).

The ophitic diabase (*brd*) and intergranular gabbro (*brg*) units can be traced to the southern sampling area where the dike expands to accommodate more intermediate composite intrusions (Fig. 17). Clearly intrusive into the intergranular gabbros are prismatic ferrodiorites, which are distinguished into two units based on the development of foliation (Fig. 17, units *brfd* and *brld*). The marginal phase of the ferrodiorite (unit *brfd*) has a non-foliated to poorly foliated, intergranular texture with variable concentrations of olivine and granophyre. Inward from the margins, the ferrodiorite becomes moderately to very well foliated (Fig. 18D) and is distinguished as the *brld* unit. Given their similar intermediate lithologies and contact relationships to the Silver Bay intrusions in the southern BBC, Miller et al. (1994) speculate that the *brfd* and *brld* units correlate with the *sbg* and *sblg* units of the SBI.

The contacts between the BRD ophitic diabase and the volcanic footwall are not well exposed in the NBBC and it is assumed that the form topographic lows throughout the Cramer mapping area. The chilled margin of the diabase is exposed along the eastern edge of the intrusion (Fig. 17) but the physical contact is obscured. The contacts between the various composite intrusions in the BRD are also poorly exposed in the areas mapped during this research. Miller et al. (1994) reported that the BRD ophitic diabase is typically observed in narrow gradational contact with intergranular gabbro (Fig. 17, map unit *brg*) over decimeter to meter scale. *Brd-brg* contacts are typically characterized by an abrupt change in the habit of augite from ophitic to anhedral granular and a sharp increase in oxide content in the gabbro. The contacts between the gabbro and

intermediate composite intrusions (Fig. 17, map units *brfd* and *brld*) were not observed during this study as exposures were not observed in close proximity to each other. Miller et al. (1994) reported that the ferrodiorites are typically in narrow gradational contact with the *brg* gabbro. In the central teardrop-shaped body along the southern mapping traverse (Fig. 17) a broad gradation is observed between the massive and laminated ferrodiorite (map units *brfd* and *brld*, respectively) defined by the progressive alignment of plagioclase toward the center of the intrusion.

Whereas the contact relationships in the SBI bodies in the SBBC indicate that the major rock types formed by *in situ* differentiation of a single intrusive pulse of magma into the BRD dikes and sills, field relationships indicate that the northern dikes are composed of rocks formed by at least three separate intrusions (Miller and Chandler, 1997). The first pulse saw the emplacement of the marginal BRD ophitic diabase in the NSVG. Following this initial intrusion, a second pulse of more highly evolved magma created the intergranular gabbro of map unit *brg*. A third pulse created the tear-drop-shaped body of massive ferrodiorite (map unit *brfd*) which grades into well laminated ferrodiorite (map unit *brld*) in the southern end of the dike (Fig. 17).

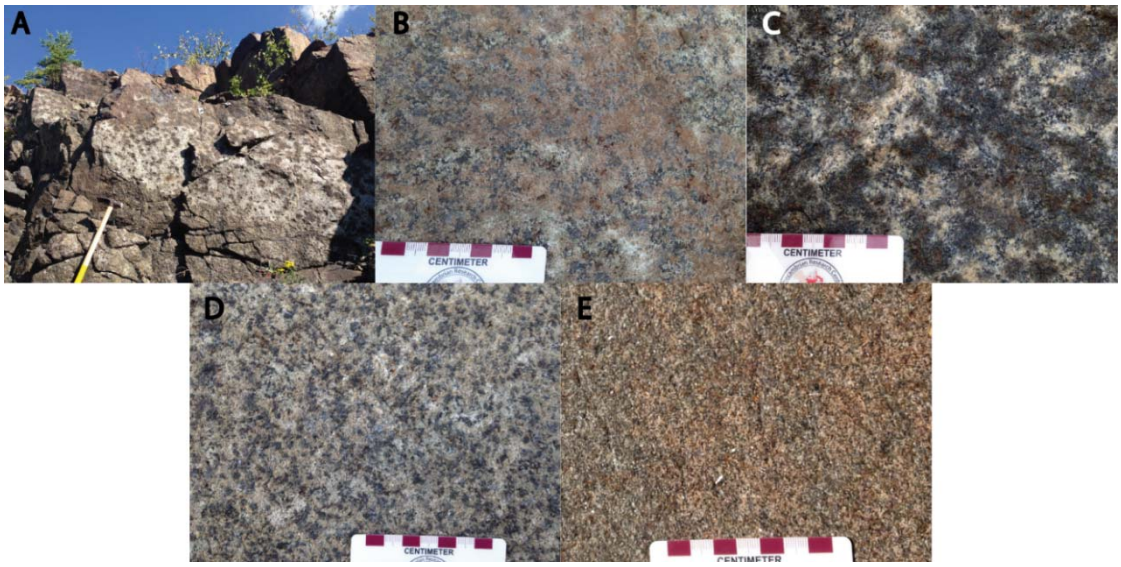

Figure 18. Field photos of A) outcrop exposure of the Beaver River diabase (map unit *brd*), B) close-up of ophitic texture of unit *brd*, C) typical olivine poikilitic texture of unit *brpg*, D) intergranular gabbro (unit *brg*), and E) massive ferrodiorite (unit *brfd*) in the northern Beaver Bay mapping area.

3.1.2 Petrographic Attributes of BRD Units in the Southern and Northern Beaver Bay Sampling Areas.

The Beaver River diabase occurs as the marginal lithology in both the southern and northern Beaver Bay Complex (Fig. 15, map units *brd and brid* and Fig. 17, map units *brd*, *brpg*) (Miller and Chandler, 1997). As such, the petrographic attributes of this unit in both the SBBC and NBCC will be discussed here. This section will be followed by discussions of the petrographic attributes of the various composite lithologies in the SBBC (Fig. 15, map units *sbpg*, *sbg*, and *sblg*) and NBBC (Fig. 17, map units *brg*, *brfd*, and *brfd*).

In general, the *brd* map unit is composed of fine- to medium-grained, ophitic olivine diabase (Fig. 19A) that coarsens away from the margins of the various intrusions. The main phase of the BRD is mineralogically and texturally homogenous between the southern and northern mapping locations although minor lithological and textural

variation occurs locally. Where it contacts the North Shore volcanics and earlier intrusions (e.g. the Lax Lake gabbro in the SBBC, Miller, 1988), the diabase is strongly chilled but retains its ophitic texture. The diabase is locally olivine rich (Fig. 19B) and displays modal layering at the margins of some intrusions (Miller, 1988; Shank, 1989; Miller et al., 1994). As discussed in the previous section, the diabase in the NBBC becomes strongly poikilitic (Fig. 17, map unit *brpg*) with olivine oikocrysts ranging up to 4 cm in diameter (Fig. 19C).

Modally, the main phase of the BRD is composed of 50-60% plagioclase laths, 15-35% subophitic to ophitic augite, 5-15% granular to poikilitic olivine, 2-10% granular to poikilitic Fe-Ti oxide, and minor amounts (<5%) subophitic hypersthene to inverted pigeonite. Olivine modes as high as 40% (Fig. 19B) can be found in the diabase near intrusive margins such that the rocks are better termed a diabasic troctolite. Near the contacts with the composite intrusions, the diabase is typically coarser-grained, oxide-rich (< 10%), and can contain anomalously high concentrations of felsic mesostasis (<10%) with associated accessory phases (e.g. apatite, zircon). Miarolitic cavities are locally abundant (< 5%) and are typically filled with fibrous chlorite and clays. Secondary alteration is generally weak and alteration assemblages typically include fibrous, interstitial chlorite, sericitic alteration of plagioclase, serpentine and iddingsite alteration of olivine, and uralite and/or amphibole alteration of augite. Several samples collected near contacts with the volcanic footwall rocks or composite intrusions (BBC1, BBC6, BBC7, SBI15, SBI16) contain trace amounts of biotite which typically occurs as thin rims on Fe-Ti oxides.

Two of the most distinctive attributes of the BRD are the ubiquitous occurrence of clustered plagioclase laths (Fig. 19A) and the local occurrence of coarse- to very coarse-grained plagioclase megacrysts (Fig. 19D), which comprise up to 5% of the mode. Clustered plagioclase grains are usually joined on their long crystallographic planes (010 or 001) and display polysynthetic or simple twinning and normal to oscillatory zoning. Plagioclase megacrysts occur as subhedral, normally zoned laths or less common equant grains and commonly display thin, zoned overgrowth rims that poikilitically extend into groundmass minerals.

Augite occurs as coarse- to very coarse-grained, ophitic to less commonly subophitic oikocrysts enclosing groundmass plagioclase laths, olivine, and Fe-Ti oxide (Fig. 19A and B). Oikocrysts range in size from a few millimeters near contacts with the lava flows or earlier intrusive rocks to over 10 centimeters in the cores of BRD intrusions. Augite is commonly zoned as evidenced by progressive extinction or a change in interference colors between the cores and rims of oikocrysts. Exsolution lamellae are rare.

Olivine usually occurs as fine- to medium-grained, subhedral, granular crystals in the *brd* but becomes coarser and more subpoikilitic near the contacts with the composite intrusions. Olivine tends to cluster into polycrystalline aggregates concentrated along the interstices between the large augite oikocrysts. Olivine is usually much more strongly altered than other primary minerals and commonly occurs as pseudomorphs completely replaced by yellowish serpentine, iddingsite, or hissengerite (Fig. 19 A and C).

Fe-Ti oxides are usually medium-grained, anhedral granular to subpoikilitic crystals enclosing or intergrown with earlier formed plagioclase and olivine (Fig. 19A). Oxides

also form skeletal crystals in areas rich in felsic mesostasis. In the finer-grained diabase and troctolitic varieties, oxides tend to form as subhedral blades (ilmenite?) and subequant grains (Ti-magnetite?).

3.1.3 Petrographic Attributes of SBI Composite Intrusions in the BRD of the Southern Beaver Bay Complex Sampling Area

In contrast to the generally uniform mineralogy and textural attributes of the *brd* unit, the Silver Bay composite intrusions (SBI) in the SBBC are quite variable (Fig. 19). Mapping in the SBBC by Miller (1988), Shank, (1989), and Miller et al., (1989, 1993, 2006) show that the SBI span a range in rock types from olivine oxide gabbro to ferrogranite (Shank, 1989).

The *sbg* unit forming the marginal zone of the SBI Beaver Bay body (Fig. 15) is composed of medium- to coarse-grained, variably granophyric rocks ranging in composition from olivine gabbro to quartz ferromonzodiorite, although very coarse-grained segregations of ferromonzonite to ferrogranite are irregularly distributed throughout the zone. As mentioned above, the contacts between the *sbg* and *brd*, though unchilled, are typically very abrupt on a centimeter scale. The main petrographic attributes that abruptly change across the *brd-sbg* contact are: 1) change in texture from ophitic to prismatic; 2) loss of plagioclase clustered texture; 3) appearance of felsic mesostasis; and 4) the absence of plagioclase xenoliths.

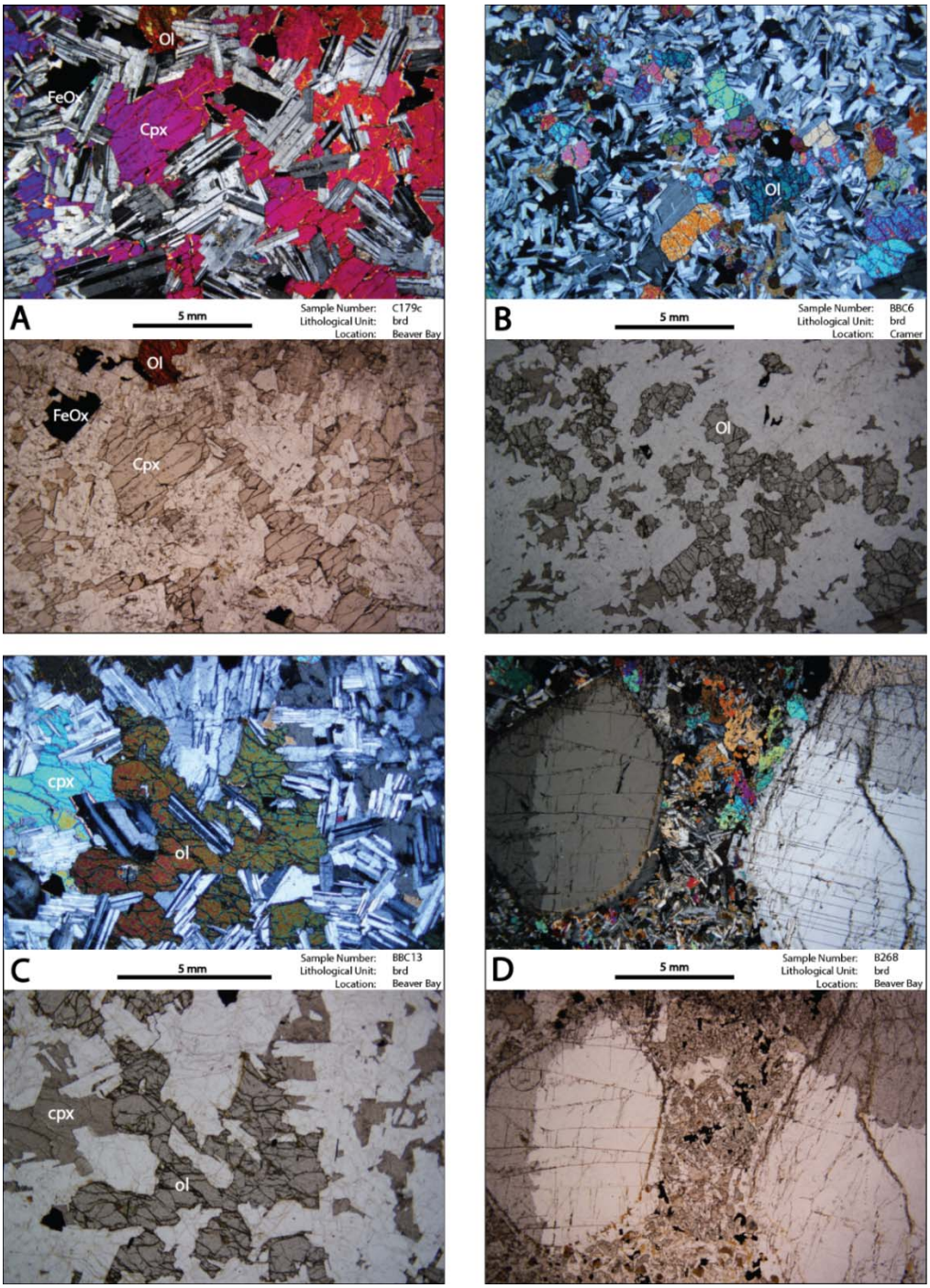

Figure 19. Crossed-polarized and plane-polarized photomicrographs of map unit *brd* showing: A) ophitic texture in olivine diabase; note subpoikilitic Fe-Ti oxide (FeOx) and altered olivine (Ol); B) diabasic troctolite phase of the *brd* unit C) poikilitic olivine gabbro of map unit *brpg*. D) very coarse-grained plagioclase megacrysts in fine-grained subophitic olivine diabase; note thin rims of more sodic plagioclase.

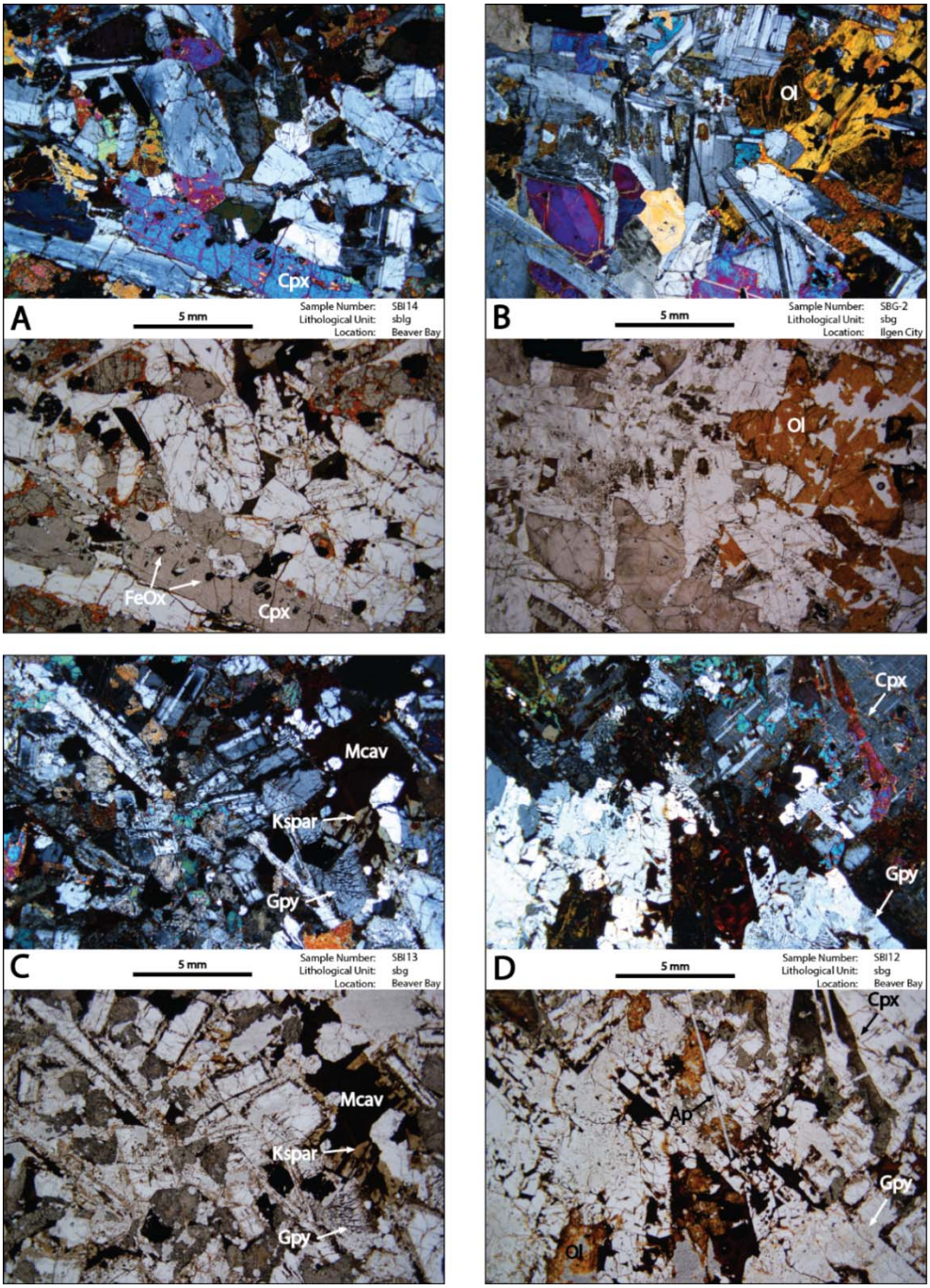

Figure 20. Crossed-polarized and plane-polarized photomicrographs of the SBI lithologies. A) well-foliated ferrodiorite of unit *sblg*; note poikiloprismatic texture of augite (Cpx) with inclusions of Fe-Ti oxides. B) intergranular oxide olivine gabbro of unit *sbg*; note altered, subpoikilitic olivine (Ol). C) prismatic ferromonzodiorite of unit *sbg*; note euhedral alkali feldspar crystals terminating in miarolitic cavity filled with opaque clay mineral (Mcav) and clots of granophyre

(Gpy). D) coarse-grained, quartz ferromonzonite segregation of unit *sbg*; note coarse-grained, bladed augite (Cpx), micrographic granophyre (Gpy), and coarse-grained, acicular apatite (Ap).

The more mafic rocks of the *sbg* unit (Fig. 20B) tend to be medium-grained, subophitic to intergranular and typically contain only minor concentrations (<5%) of felsic mesostasis. Plagioclase occurs as subhedral to euhedral, granular laths and lack the distinct clustering that marks the BRD diabase. Plagioclase grains typically display polysynthetic twinning and normal to oscillatory zoning and occasionally display thin micrographic or sodic rims when abutting felsic mesostasis. Augite is weakly subophitic to intergranular and occasionally display simple twinning. Augite commonly displays brownish amphibole overgrowths but rarely displays exsolution lamellae. Olivine is subpoikilitic to anhedral granular and is typically completely altered to iddingsite. Fe-Ti oxides usually occur as subpoikilitic crystals or skeletal overgrowths and rarely as platy laths or equant grains.

The more intermediate to felsic compositions comprising the *sbg* unit (ferromonzodiorite to quartz ferromonzonite, Fig. 20C and D, respectively) differ from the mafic lithologies by having a greater concentration of felsic mesostasis and a consistently prismatic habit of clinopyroxene. Plagioclase occurs as medium- to coarse-grained laths and equant grains and often displays complex twinning. Most grains display broad, unzoned cores surrounded by thin, strongly zoned rims and commonly have radiating micrographic overgrowths. Augite is typically poikiloprismatic (containing abundant fine-grained inclusions of Fe-Ti oxide and apatite) to bladed and is commonly highly altered to uralite and/or brownish amphibole. Olivine is rare and occurs only as

medium- to coarse-grained, granular, skeletal, or bladed relict grains which are completely altered to iddingsite, iron oxide, and chlorite. Fe-Ti oxide is typically subhedral granular to subpoikilitic and commonly display complex exsolution lamellae. Near the margins of felsic mesostasis clots, oxides also occur as skeletal, trellis-patterned intergrowths with augite and relict olivine. Miarolitic cavities are locally abundant (<5%) and are often filled with reddish-brown clay minerals and lined with euhedrally-terminating alkali feldspar laths (Fig. 20C). Accessory minerals are usually associated with felsic mesostasis or miarolitic cavities and include quartz, zircon, granular hematite, and apatite prisms and needles up to 5mm in length.

Samples of the poikilitic gabbro (Fig. 15, map unit *sbpg*) were not collected during this study but Miller (1988) and Shank (1989) give descriptions of the mineralogy and texture. The *sbpg* unit typically occurs in narrow (20-30 m) zones between the *sbg* and *sblg* units and as is gradational to both. The *sbpg* is typically medium-grained, equigranular and is distinguished from the rocks of the *sbg* by the occurrence of poikilitic olivine oikocrysts which range from 1-4 centimeters in diameter. Modally, the rocks are composed of 40-55% felty plagioclase laths, 20-30% prismatic augite, 5-15% olivine oikocrysts, 2-10% pigeonite, commonly with rims of augite, 5-10% platy ilmenite and subhedral magnetite, and up to 5% felsic mesostasis. In the interior of the SBI bodies, the gabbros are well-laminated and are locally interlayered with the rocks of the *sblg*.

The contact between the marginal *sbg* unit interior *sblg* unit of the Beaver Bay body (Fig. 15) is much more gradational on a meter to decameter scale and is defined texturally by the development of igneous foliation. The *sblg* unit is composed predominantly of

variably granophyric, well-foliated ferrogabbro/diorite. Samples of the *sblg* collected during this study are predominantly olivine ferrodiorite (Fig. 20A) and are composed of 50-60% plagioclase, 15-20% augite, 5-15% olivine, and 5-10% Fe-Ti oxides. The rocks of the *sblg* are generally similar to the rocks of the *sbg* in terms of mineralogy and texture but are distinguished by being well-foliated and by the local development of rhythmic and graded modal layering and textural layering of olivine habit near the margins of the intrusions (Miller, 1988). Plagioclase in the *sblg* unit does not display the distinctive clustering observed in the ophitic diabase of unit *brd*, and instead typically occurs as well-laminated, subprismatic laths and rarely as equant grains common in the *sbg*. Augite displays similar poikiloprismatic texture as in the *sbg* with numerous inclusions of fine-grained Fe-Ti oxide and apatite. Fe-Ti oxide is typically finer-grained and more granular in habit than in the *sbg* and generally lack the complex exsolution lamellae common in the marginal zone rocks. Olivine is more common than in the *sbg* and typically occurs as clustered, fine-grained granular crystals which are only moderately altered to serpentine or iddingsite. Apatite occurs as abundant, fine-grained euhedral inclusions in augite and Fe-Ti oxides but medium- to coarse-grained needles, common in the *sbg*, are rare. In terms of cumulate terminology, these rocks are clearly a plagioclase-augite-oxide-olivine ± apatite cumulate.

3.1.4 Petrographic Attributes of Composite Intrusions in the BRD of the Northern Beaver Bay Complex Sampling Area

Although the composite intrusions in the NBBC display evidence of more emplacement events, they show less lithological variation than the SBI bodies in the SBBC. Rocks types in the northern composite dikes range from oxide gabbro to foliated

ferrodiorite and lack the more highly differentiated lithologies – ferromonzodiorite to ferrogranite – present in the SBI.

The earliest composite unit of the in the NBBC (Fig. 17, map unit *brg*) is a generally medium-grained, intergranular to rarely subophitic, olivine oxide gabbro emplaced directly adjacent to and in abrupt contact with the *brd* ophitic diabase. Typically, the gabbro is composed of 50-65% plagioclase, 15-20% intergranular to rarely subophitic augite, 0-10% granular to subpoikilitic olivine, 5-15% granular to subpoikilitic Fe-Ti oxide, and 2-10% felsic mesostasis with associated accessory minerals. The main petrographic differences that abruptly change across the *brd-brg* contact are a change in texture of from ophitic to intergranular and the absence of plagioclase xenoliths. In contrast to the rare intergranular gabbros in the SBI intrusions in the SBBC (map unit *sblg*, Fig. 15) plagioclase in the intergranular gabbros of unit *brg* retain the distinctive clustering observed in the BRD ophitic diabase (Fig. 21A).

Plagioclase crystals commonly display thin sodic or micrographic rims and are usually slightly or moderately altered to sericite or sausserite. Augite typically displays concentric or patchy zoning and is frequently twinned. Most augite grains display exsolution lamellae and varying degrees of patchy amphibole alteration. In the subophitic gabbros, augite commonly displays mosaic texture in which larger oikocrysts appear to be composed of numerous, smaller crystals in varying optical orientation. Olivine is variably altered to yellowish serpentine or chlorite and often occurs as skeletal relict grains.

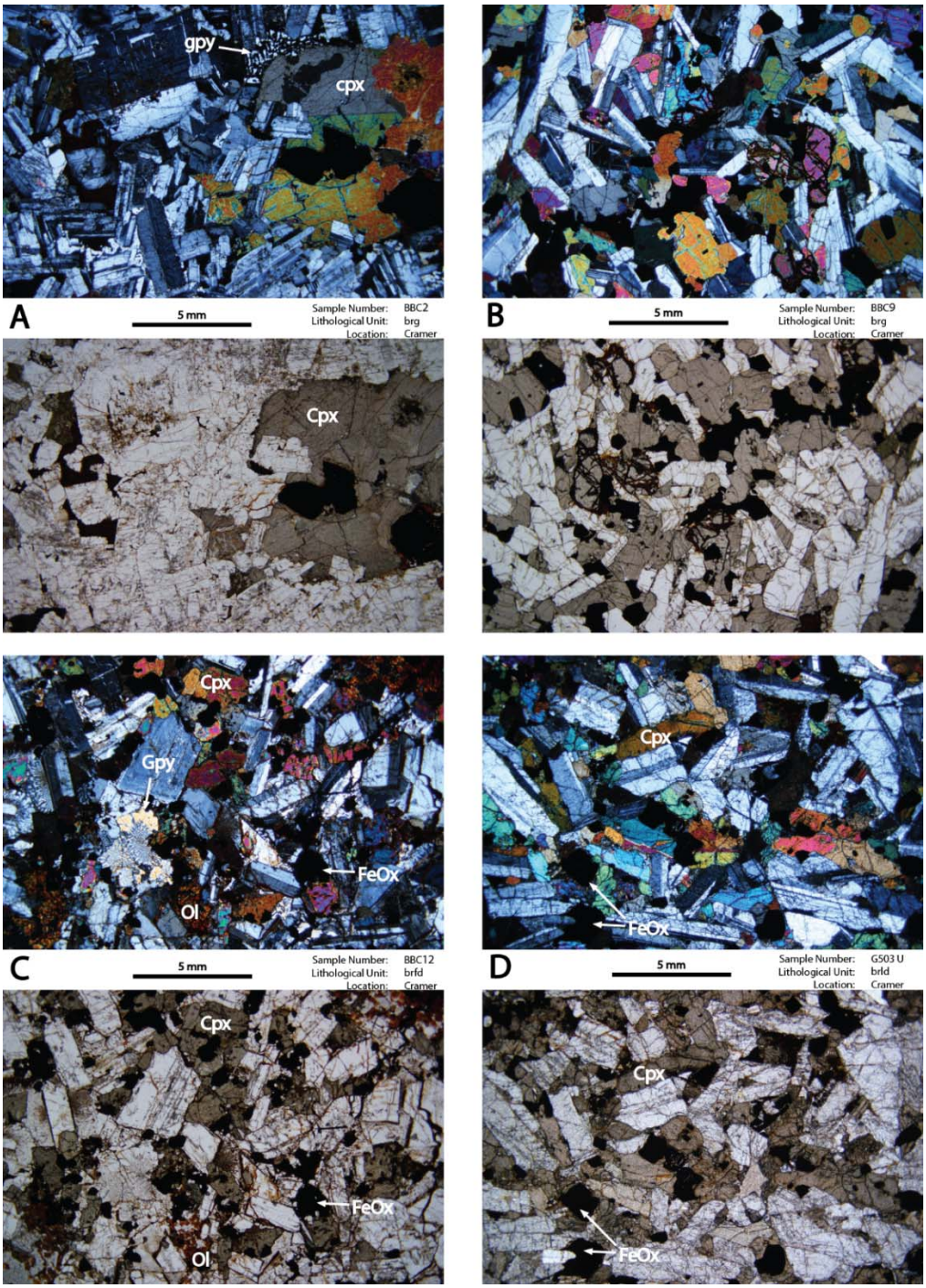

Figure 21. Crossed-polarized and plane-polarized photomicrographs of the NBBC composite intrusions showing: A) subophitic to intergranular olivine oxide gabbro of map unit *brg* with clustered plagioclase and subhedral, subophitic to granular Cpx; B) massive, prismatic ferrodiorite of map unit *brfd*; C) granophyric, massive, prismatic ferrodiorite of map unit *brfd*; D) well-laminated, prismatic ferrodiorite of map unit *brld*.

The majority of the ferrodiorites (map units *brfd* and *brld*, Fig. 17) are mineralogically and texturally similar (Fig. 21D) to the intergranular gabbros making it sometimes difficult to distinguish between the two in the field in the absence of well-developed igneous foliation. Plagioclase laths are more subhedral in habit and lack the distinctive clustered texture common in the diabase and gabbros. Plagioclase typically display broad sodic or micrographic rims, particularly when abutting clots of felsic mesostasis. Augite is typically light brown or bronzish in plane polarized light and is more prismatic or poikiloprismatic with inclusions of fine-grained Fe-Ti oxide and apatite. Fine exsolution lamellae are well-developed in the majority of the augite crystals and patchy amphibole alteration is common. Fe-Ti oxides tend to be finer-grained than in the gabbroic rocks or diabase and typically occur as subhedral laths or equant grains. Olivine is granular to subprismatic in habit and is usually extensively altered to iddingsite.

3.2 Geology and Petrographic Attributes of the GSF on the Keweenaw Peninsula and Isle Royale

3.2.1 Geology of the Keweenaw Peninsula and Isle Royale Sampling Areas

Field observations of GSF exposures along traverses on both the Keweenaw Peninsula and Isle Royale for this study show that the flow can be subdivided in both locations into four similar lithostratigraphic zones based on differences in mineralogy and textural attributes (Figs. 22 through 26). From bottom to top, these zones are:

loz - lower ophitic olivine basalt zone

hz - heterolithic zone of vari-textured mafic to intermediate rock types (ferrodiorite to ferromonzodiorite)

uoz - upper ophitic olivine basalt zone

ent – massive to amygdaloidal entablature zone

This four-fold subdivision is consistent with previous studies of the GSF by Cornwall (1951), Huber (1973), and others. As discussed previously, though the lithological variation in the GSF has long been recognized (e.g. Lane, 1893, 1911), Cornwall (1951) was the first to classify the flow into formal lithostratigraphic zones (*lower ophitic, pegmatitic, upper ophitic,* and *amygdaloidal*; Fig. 10). Although the classification of *lower ophitic* and *upper ophitic* zones is adopted for this study, the terminology used to describe the interior (*pegmatitic*) and upper (*amygdaloidal*) portions of the GSF do not seem appropriate. In the first, the term *pegmatitic* is problematic in that it has historically been limited to late-stage crystallization of granitic magmas. For this reason, the designation *heterolithic zone* will be used to describe the lithologically diverse interior portion of the GSF. The term *amygdaloidal* is also problematic because field observations and subsequent petrographic analyses show that the exposed upper portion of the flow is usually massive to only slightly amygdaloidal. For this reason, the term *entablature*, first coined by Tomkeieff (1940) and later adopted by Longo (1984), will be used to describe the uppermost portions of the flow which do not display ophitic texture.

Bedrock mapping and sampling of the GSF was conducted in two locations on the Keweenaw Peninsula (Fig. 13) near Phoenix, Michigan (T58N, R31W, Sec. 24 and 25) and Central, Michigan (T58N, R32W, Sec. 29 and 30). Figures 22 and 23 show the geological maps and cross sections compiled from this mapping. On Isle Royale, outcrop mapping and sampling was conducted in three areas that traverse the GSF (Fig. 14). The mapping areas include exposures along the northeastern end of Isle Royale at Blake Point

(T67N, R32W, Sec. 24; Fig. 24), along the Lookout Louise hiking trail (T67N, R32W, Sec. 26; Fig. 25), and along the Tobin Harbor-Duncan Bay portage trail (T67N, R32W, Sec. 27, 28, and 34; Fig. 26). Exposures of the upper part of the GSF at Red Rock Point, near the southwest entrance to Merritt Lane (Fig. 14; T67N, R32W, Sec. 26) were also investigated and sampled. Figures 24 through 26 show geological maps and cross-sections generated from the mapping traverses on Isle Royale.

The exposures near Phoenix on the Keweenaw Peninsula (Fig. 22) provide a more complete cross section of the GSF compared to the Central area (Fig. 23). At Phoenix, the GSF is estimated to have a stratigraphic thickness of approximately 300 meters. All four lithostratigraphic zones are exposed at Phoenix with individual thicknesses estimated as being approximately: *loz* – 115 meters, *hz* – 150 meters, *uoz* – 14 meters, and *ent* – 24 meters. These measurements agree with previous mapping of the GSF at Phoenix by Long (1984) and Cannon and Nicholson (2002). Because no obvious internal structure was observed during mapping, the strike and dip of the flow was not directly measured at the Phoenix location. However, Cannon and Nicholson (2002) reported a dip of roughly 25° nearly due north for flows above and below the GSF at this location, providing a reasonable dip for the flow in this area. The rocks of the *uoz* and *ent* were not observed to crop out in the Central location during this study. Previous mapping by Cannon and Nicholson (2002), however, estimated that the GSF reaches a stratigraphic thickness of approximately 448 meters at Central. The stratigraphic thicknesses of the *loz* and *hz* are estimated at 202 meters and 155 meters, respectively, based on mapping during this study. Moreover, similar to the Phoenix location, no obvious internal structure was

observed in the GSF at Central, but the trend of the zone contacts imply that the regional strike of the flow is N80°E with a moderate dip of ~25° to the north (Cannon and Nicholson, 2002). Cannon and Nicholson (2002) interpreted this abrupt change in strike of the flow to a fault inferred to occur just northeast of the Phoenix area. The lower flow contact is not exposed in either the Phoenix or Central mapping location.

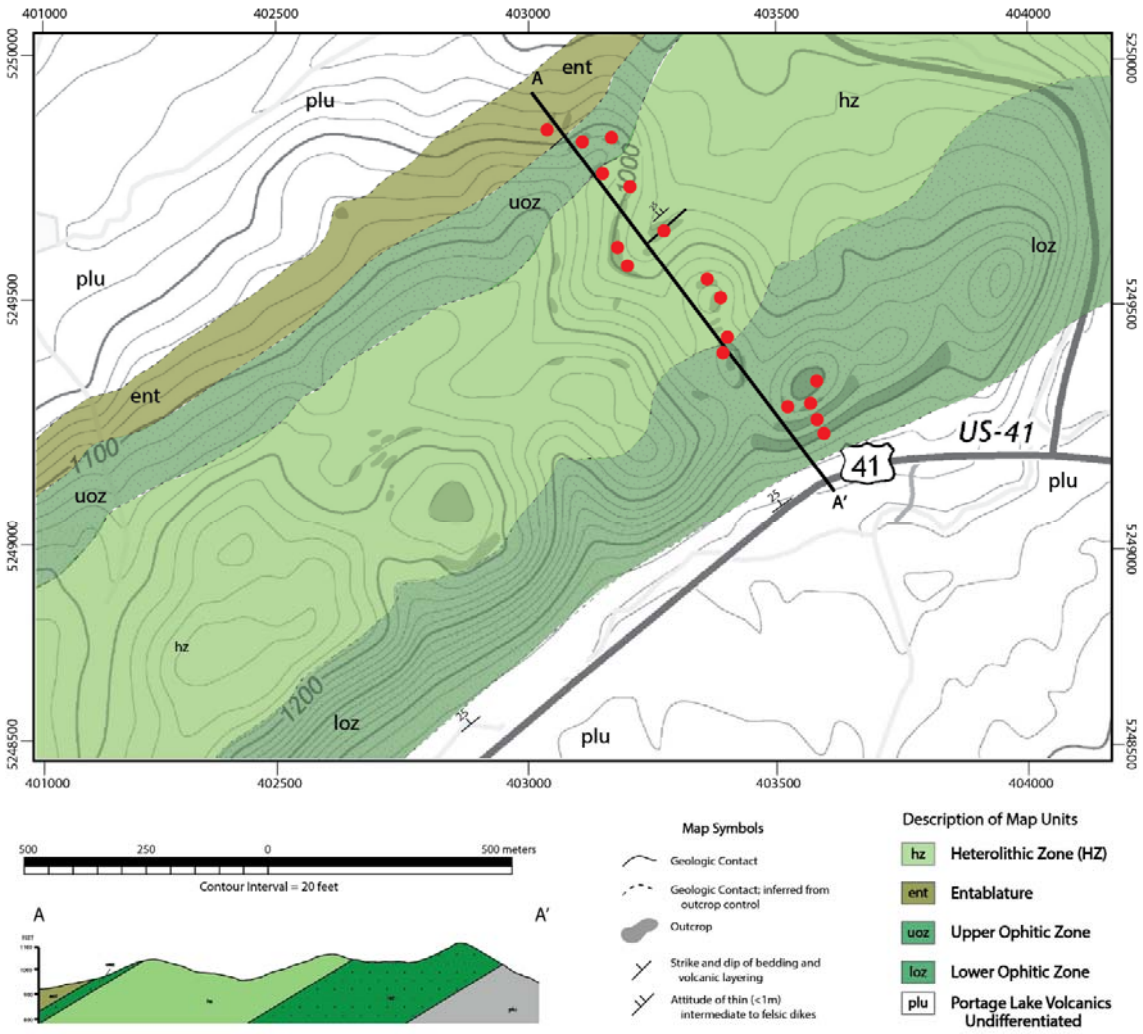

Figure 22. Geologic map of the Greenstone Flow in the Phoenix, Michigan area showing locations of samples collected during this study (red dots) and the profile line for cross section A-A'. Regional strike and dip from Cannon and Nicholson (2002).

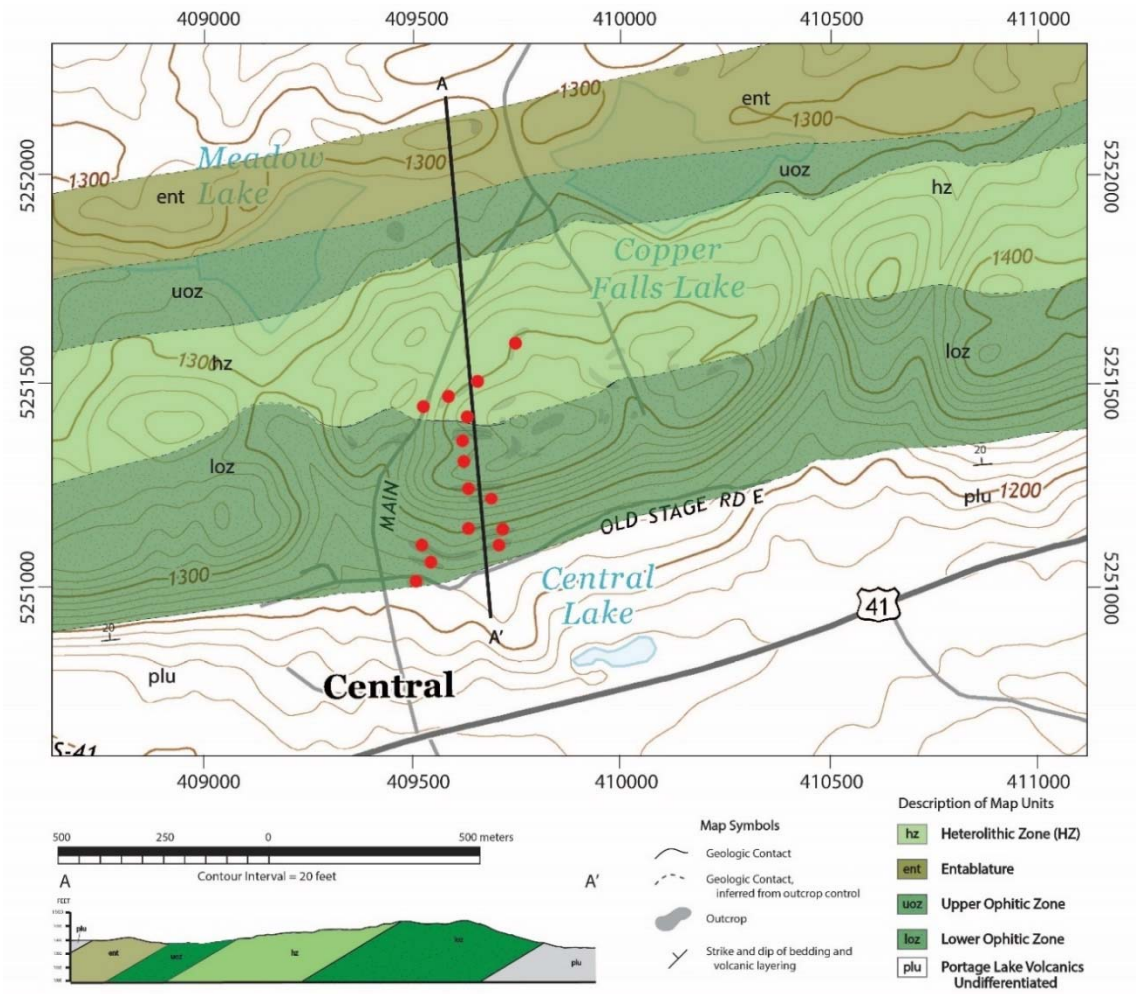

Figure 23. Geology of the Greenstone Flow in the Central, MI area and locations of samples collected during this study (red dots) and the profile line for cross section A-A'. Regional strike and dip from Cannon and Nicholson (2002).

The GSF on Isle Royale is consistently thinner and more shallowly dipping than on the Keweenaw Peninsula. Huber (1973) reported that the flow reaches a maximum stratigraphic thickness of approximately 250 meters in the central portion of the island and dips between 10-18° to the southwest. Within the Isle Royale study area, the entablature (map unit *ent*) is only exposed on the main island at Red Rock Point (Fig. 14, point B). Elsewhere, exposures are limited to a string of islands along the southeastern side of Merritt Lane (Fig. 14). These exposures could not be observed directly during this

study because of dangerous conditions on Lake Superior and all estimates of the thickness and attitude of the *ent* presented here are from Huber (1973). Neither the lower flow contact nor the *uoz-ent* contact was observed on Isle Royale and are inferred by topography.

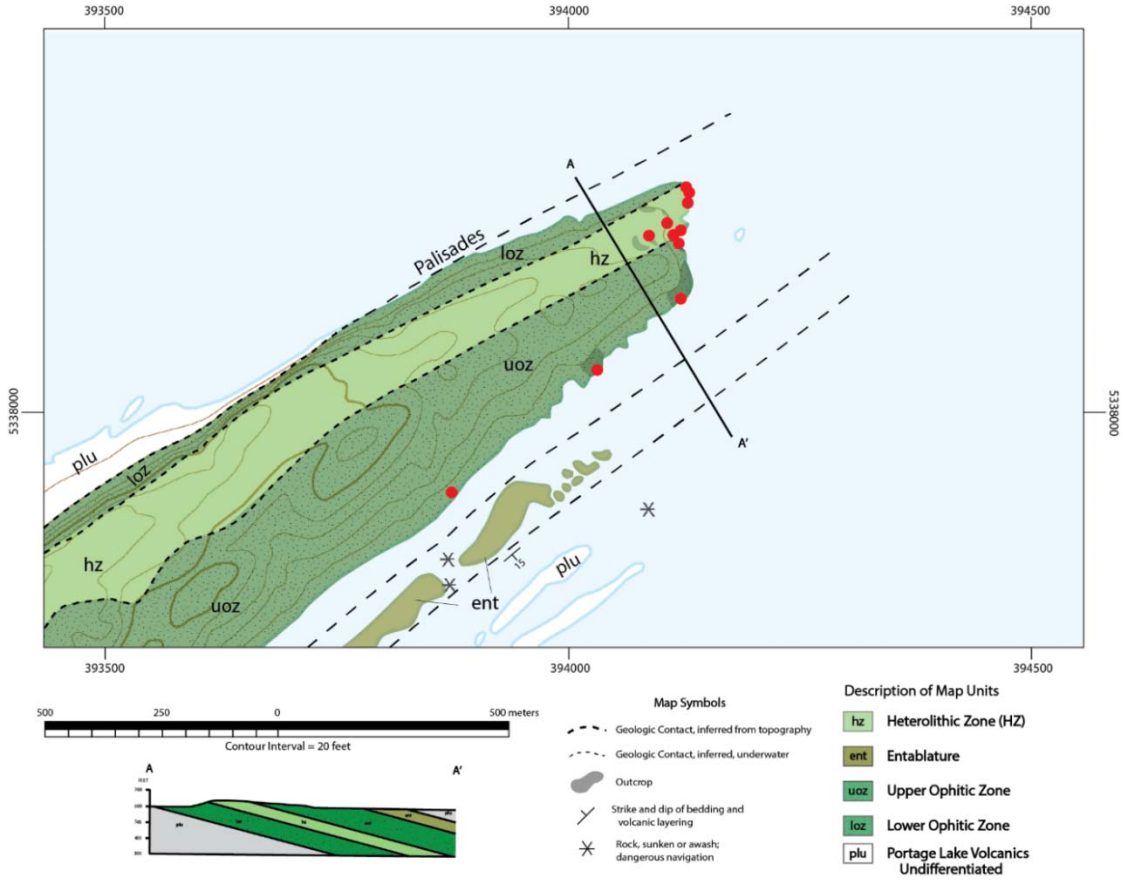

Figure 24. Geology of the Greenstone Flow on Isle Royale at Blake Point and locations of samples collected during this study (red dots) and the profile line for cross section A-A'. Regional strike and dip from Huber (1973).

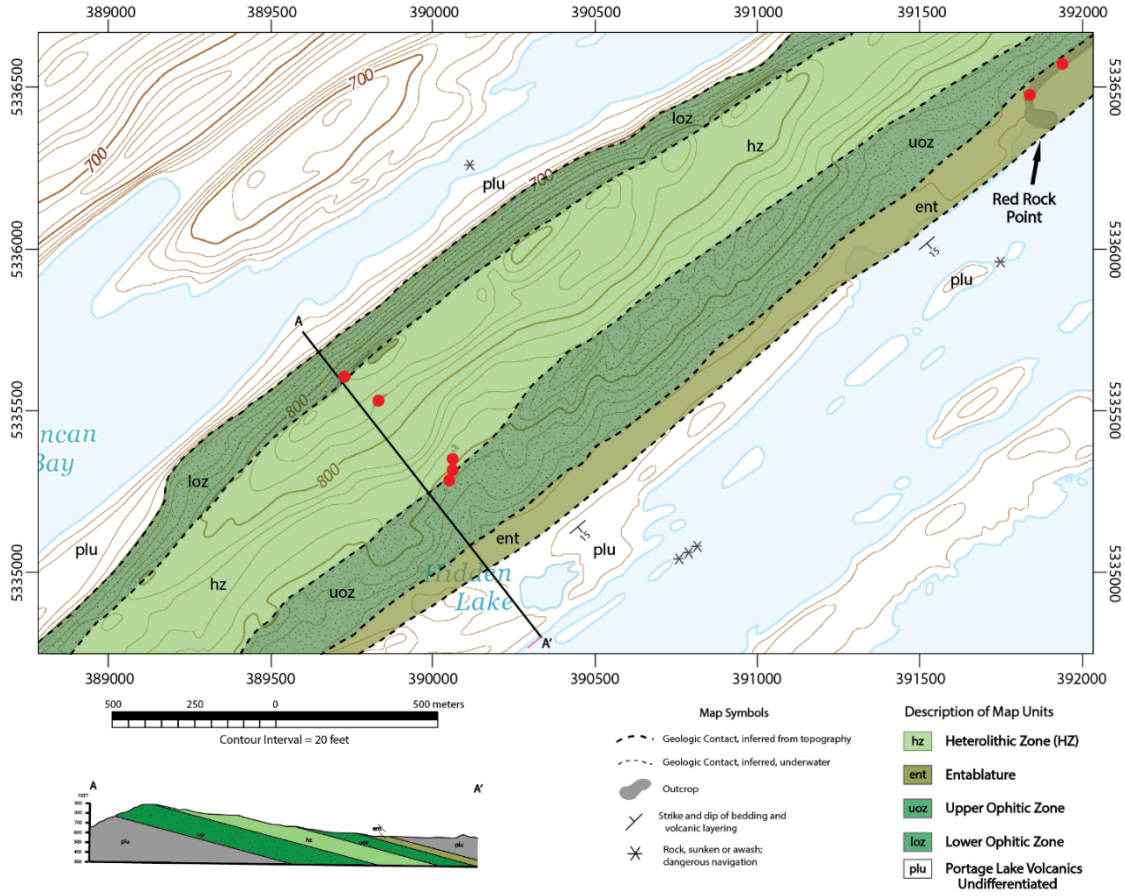

Figure 25. Geology of the Greenstone Flow on Isle Royale in the area of Lookout Louise and locations of samples collected during this study (red dots) and the profile line for cross section A-A'. Regional strike and dip from Huber (1973).

Reasonably complete cross-sections of the GSF are exposed at all three of the Isle Royale mapping locations. At Blake Point the GSF reaches a thickness of approximately 120 meters and consists of the *loz* (34 m), *hz* (22 m), and *uoz* (43 m). As discussed earlier, the *ent* basalt outcrops across Merritt Lane (Fig. 14) and reach an estimated thickness of about 23 meters (Huber, 1973). Rough waves on Lake Superior prevented direct sampling of the *loz* which occurs at the base of the steep cliff face on the northwest side of Blake Point (Fig. 24). The GSF thickens to the southwest, reaching an approximate thickness of 175 meters along the Lookout Louise trail (Fig. 25). There,

exposures consist of the *loz* (71 m), *hz* (52 m), and *uoz* (34 m). Previous mapping by Huber (1973) reported and approximate thickness of 18 meters for the *ent* at Lookout Louise. The GSF is thinnest along the Tobin Harbor-Duncan Bay portage trail (Fig. 26), reaching a maximum of approximately 100 meters and consists of the *loz* (47 m), *hz* (15 m), and *uoz* (16 m). Huber (1973) reported that the *ent* is approximately 23 meters thick at Tobin Harbor.

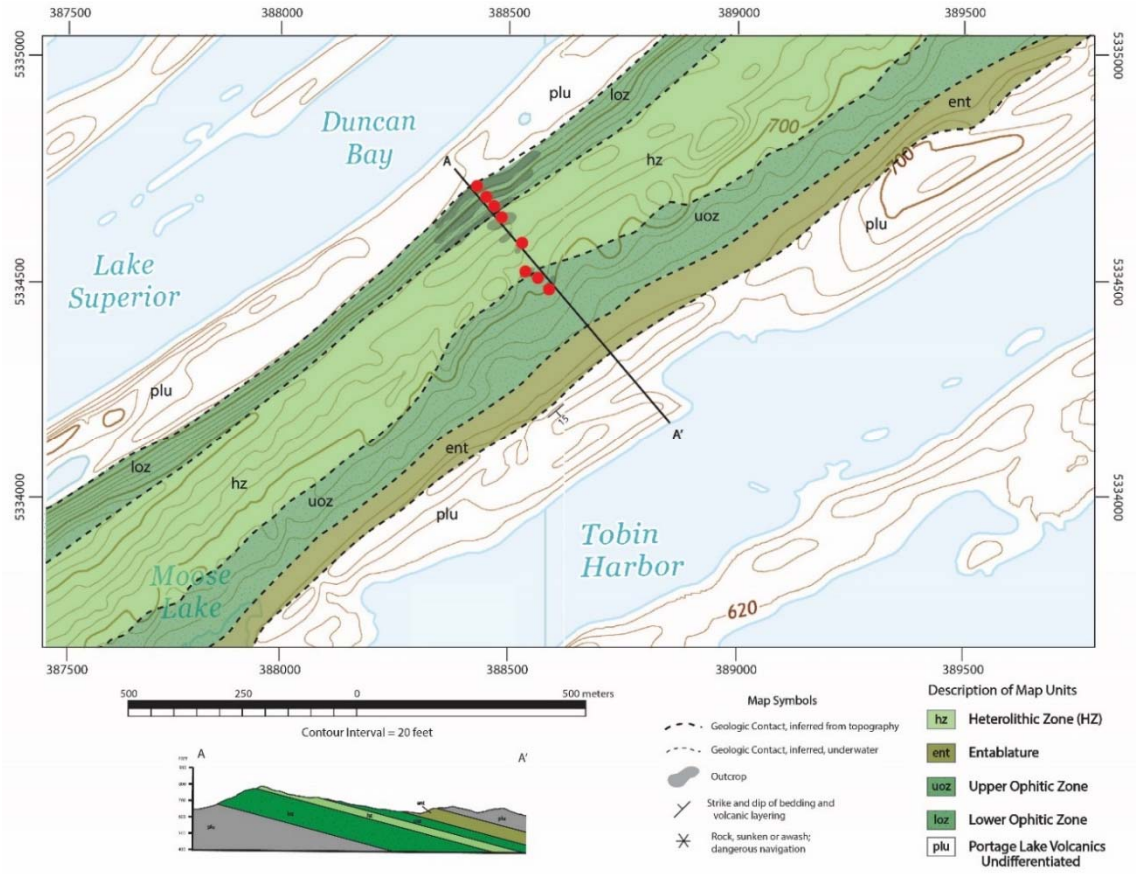

Figure 26. Geology of the Greenstone Flow on Isle Royale in the Tobin Harbor-Duncan Bay portage trail area and locations of samples collected during this study (red dots) and the profile line for cross section A-A'. Regional strike and dip from Huber (1973).

The ophitic basalts of the *loz* on Isle Royale and the Keweenaw Peninsula (Fig. 27A and B) display well-developed columnar jointing which supports prominent cliff faces in both locations. On the Keweenaw Peninsula, the *loz* holds up a precipitous, nearly 75-meter-high, south-facing cliff along the peninsula. Similarly, the *loz* on Isle Royale forms a distinctive north-facing cliff southwest of Blake Point (the Palisades, Fig. 24) that can be followed to the southwest to Lookout Louise (Fig. 25) and beyond. At the Tobin Harbor-Duncan Bay portage trail area (Fig. 26), the *loz* holds up a moderately inclined slope with outcrop occurring as 3-4-meter-high northeast-trending ledges.

Exposures of ophitic basalt of the *uoz* (Fig. 27E) are typically exposed as small pavements or whalebacks scattered along the gently to moderately inclined dip slope of the flow. At Blake Point (Fig. 24), exposures of the *uoz* form a series of wave-washed ledges that gently dip to the southeast beneath Lake Superior. Augite oikocrysts, ranging up to 2 centimeters in diameter in the *loz* and up to 1.5 centimeters in the *uoz*, give exposures of the *loz* and *uoz* a distinctive mottled texture similar to that of the BRD ophitic diabase (Figs. 16A and 18A).

The rocks of the *hz* occupy the central highlands portions of the GSF on both Isle Royale and the Keweenaw Peninsula. Near the contacts with the *hz*, the ophitic basalts of the *loz* and *uoz* display a gradation into coarser-grained and more subophitic basalt. Since exposures of ophitic basalt are commonly observed scattered throughout the interior of the flow, the *loz-hz* and *hz-uoz* transitions are defined for this study by the first and last, respectively, occurrence of intergranular gabbro or prismatic ferrodiorite/ ferromonzodiorite along transects of the flow. Exposures of the *hz* are predominantly

large rounded knobs of subophitic basalt to intergranular gabbro which are best exposed near the summit of the flow where the rocks contact the ophitic basalt of the *loz*. Scattered exposures of ophitic basalt are commonly intermingled with or capping exposures of the *hz* throughout the unit. Smaller, less-common exposures of subprismatic ferrodiorite to ferromonzodiorite (Fig. 27D) are commonly intermingled with the mafic *hz* rocks and occur as low, deeply-weathered exposures (< 1-meter-high) beneath more prominent outcrop ledges of basalt or gabbro.

Several exposures of the *ent* unit (Fig. 27F) occur at the Phoenix location on the Keweenaw Peninsula (Fig. 22). These exposures typically form 2-3 meter-high, columnar jointed ridges of generally massive basalt which project along strike for a few tens of meters before being buried under glacial cover. On Isle Royale, the *ent* unit is best represented at Red Rock Point (Fig. 14, point B) where it forms spectacular shoreline exposures of massive basalt displaying fanning columnar jointing (Fig. 27G).

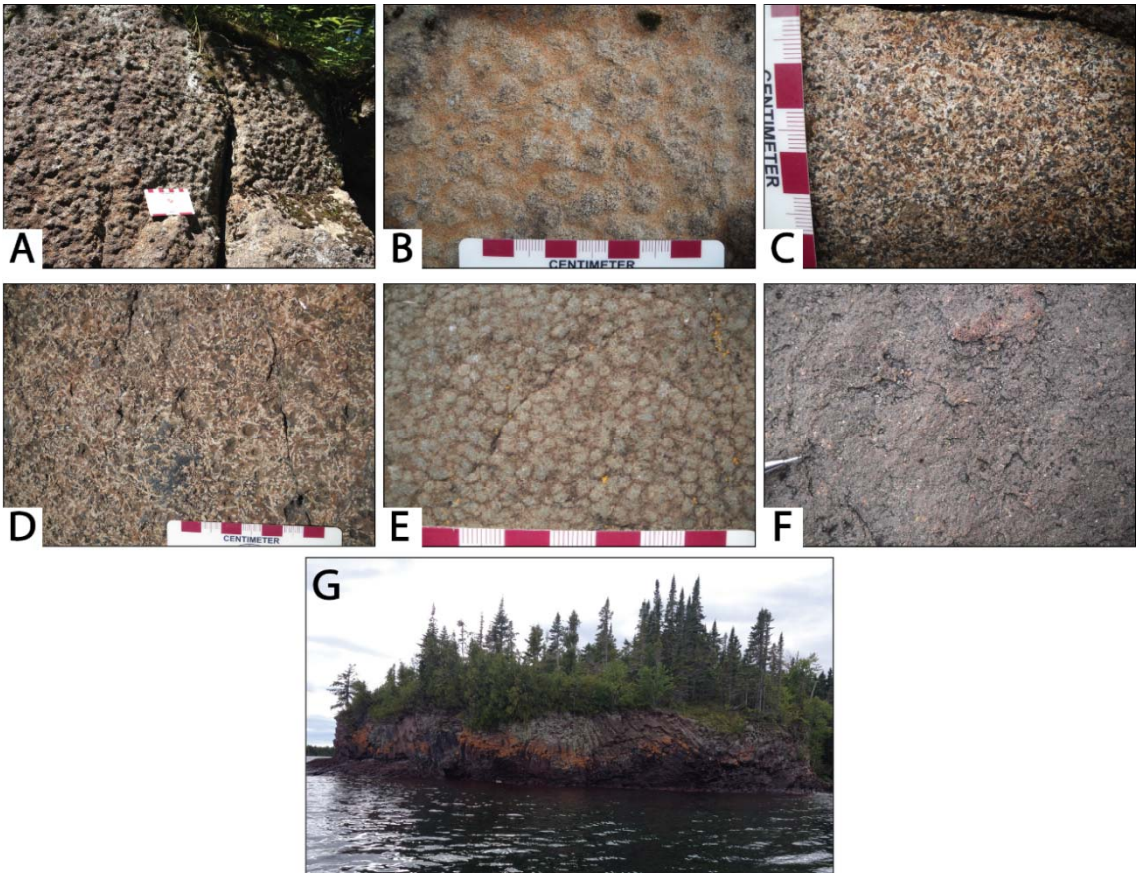

Figure 27. Field occurrences of the GSF lithologies on the Keweenaw Peninsula and Isle Royale. A) typical mottled appearance of ophitic basalt of map unit *loz* at the Central location on the Keweenaw Peninsula, B) typical texture of ophitic basalt of map unit *loz* at the Phoenix location on the Keweenaw Peninsula , C) intergranular gabbro of map unit *hz* at the Phoenix location on the Keweenaw Peninsula, D) prismatic ferromonzodiorite of map unit *hz* at Blake Point on Isle Royale, E) typical texture of ophitic basalt of map unit *uoz* at Blake Point on Isle Royale, F) amygdaloidal texture of basalt of map unit *ent* at Red Rock Point on Isle Royale, and G) shoreline exposure at Red Rock Point on Isle Royale of massive basalt displaying fanning columnar jointing characteristic of the *ent* unit.

3.2.2 Contact Relationships of the GSF on the Keweenaw Peninsula and Isle Royale

The contacts between the various lithologies in the GSF are poorly exposed on both the Keweenaw Peninsula and Isle Royale but, where observed, the contacts are consistently abrupt on a centimeter to meter scale. The base of the flow was not observed on either the Keweenaw Peninsula or Isle Royale but previous studies of drill core (e.g.

Lane, 1893, 1911; Broderick, 1935) have reported that the basalt is strongly chilled and vesicular where it contacts the underlying conglomerate rocks.

On the Keweenaw Peninsula, the contact between the ophitic basalt unit (*loz* and *uoz*) and the rocks of the *hz* are consistently abrupt but the nature of the changes differs between the two mapping locations. At Phoenix, although the actual contacts are not exposed, they can be inferred to be abrupt over a stratigraphic thickness of less than 3 meters and can be projected between exposures throughout most of the mapping location (Fig. 22). Outcrops of prismatic ferrodiorite of the *hz* were observed to be separated from exposures of ophitic basalt of the *loz* by stratigraphic thicknesses of less than a meter. Contrasting lithologies typically display little, if any, mineralogical or textural heterogeneity with proximity to the contacts. Within the *hz*, outcrops of subophitic basalt or intergranular gabbro are commonly observed separated from exposures of prismatic ferrodiorite or ferromonzodiorite by stratigraphic thicknesses of one to two meters.

At the Central mapping location (Fig. 23), however, the *loz-hz* contact is more complex and occurs over a roughly 3-meter interval containing significant intermingling of rocks types (Fig. 28A). Large exposures of ophitic basalt are often found capping exposures of intergranular *hz* gabbro near the *loz-hz* transition. Figure 28 shows the heterogeneous contact interval between the *loz* and *hz* gabbro in the eastern part of the Central mapping location (Fig. 23). The basalt is medium-grained and grades from ophitic to subophitic. Figure 28A shows the heterogeneous contact interval between a medium-grained ophitic to subophitic basalt and coarse-grained intergranular gabbro of the *hz*. Subrounded blocks of subophitic basalt occur as inclusions hosted within the

coarse-grained intergranular gabbro (Fig. 28A). The contacts between intergranular gabbro and both the ophitic basalt (Fig. 28B) and subophitic basalt inclusions (Fig. 28C) are very sharp and unchilled.

Exposures of the *loz* near the *loz-hz* contact are commonly heterogeneous and locally contain small (< 1meter), amoeboid lenses and stringers of coarse-grained, poorly to moderately foliated gabbroic rock (modally a leucogabbro) (Fig. 29A) oriented subparallel to the base of the flow. Elsewhere near the *loz-hz* transition, very coarse-grained, oxide-rich gabbroic segregations occur (Fig. 29B) which contain radiating plagioclase laths up to 2 centimeters in length. As mentioned previously, exposures of the *uoz* were not observed in the Central mapping location and, as such, the nature of the *hz-uoz* contact is unknown.

On Isle Royale, the contact between the ophitic basalt of the *loz* and the rocks of the *hz* are exposed only at Blake Point where it is observed to be abruptly gradational over less than a meter scale. Along the Lookout Louise trail, the *loz-hz* contact is buried under glacial debris but at one location along the Tobin Harbor-Duncan Bay portage trail (Fig. 30), abrupt transitions from *loz* ophitic basalt to *hz* intergranular gabbro to *hz* prismatic ferromonzodiorite are observed within a roughly 1.5-meter stratigraphic thickness.

Contacts between the rocks of the *hz* and ophitic basalt of the *uoz* are also inferred to be abrupt at several locations on Isle Royale. At Blake Point, the *hz-uoz* contact and the adjacent lithologies are well exposed across a roughly 2-meter-wide, rubble-strewn depression on the Lake Superior shoreline. Small-scale, NE-SW trending shearing is evident throughout this contact interval though the amount of offset, if any, is not

apparent. The ophitic basalt above the contact is homogenous and forms a roughly 10-meter high cliff along which there is abundant sheet jointing aligned subparallel to the base of the flow. Below the contact, the *hz* rocks are vari-textured ferromonzodiorite (Fig. 31A) and contain numerous inclusions of amygdaloidal or vuggy basalt ranging from a few centimeters to several meters across (Fig. 31B, C, and D). The basalt inclusions are generally aphanitic to fine-grained and do not display evidence of ophitic texture in outcrop, suggesting that they may be brecciated pieces of the Entablature.

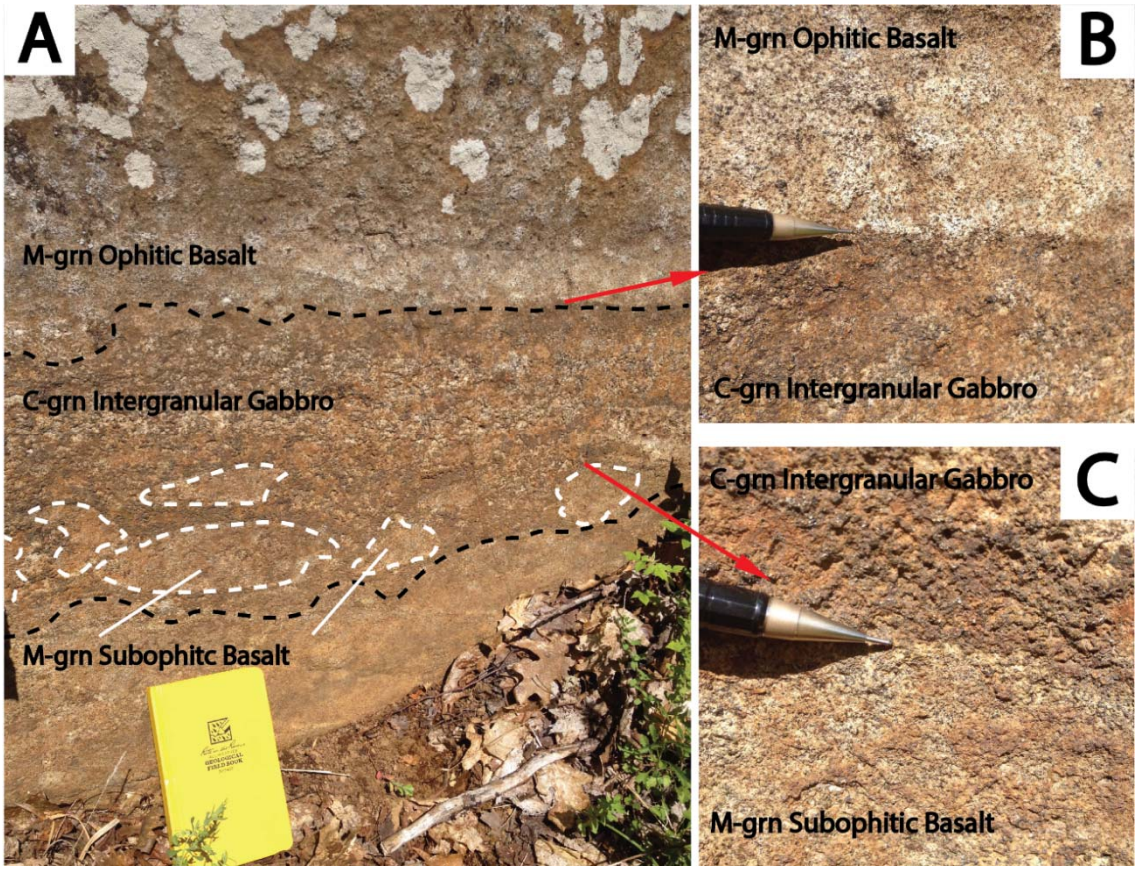

Figure 28. Exposure of *loz-hz* contacts in the GSF at the Central mapping location on the Keweenaw Peninsula. A) Subangular inclusions of medium-grained, ophitic to subophitic olivine basalt of map unit *loz* hosted by coarse-grained, intergranular olivine oxide gabbro of map unit *hz*. B) Sharp and unchilled contacts between

ophitic basalt and intergranular gabbro. C) Sharp and unchilled contacts between subophitic basalt inclusions and intergranular gabbro.

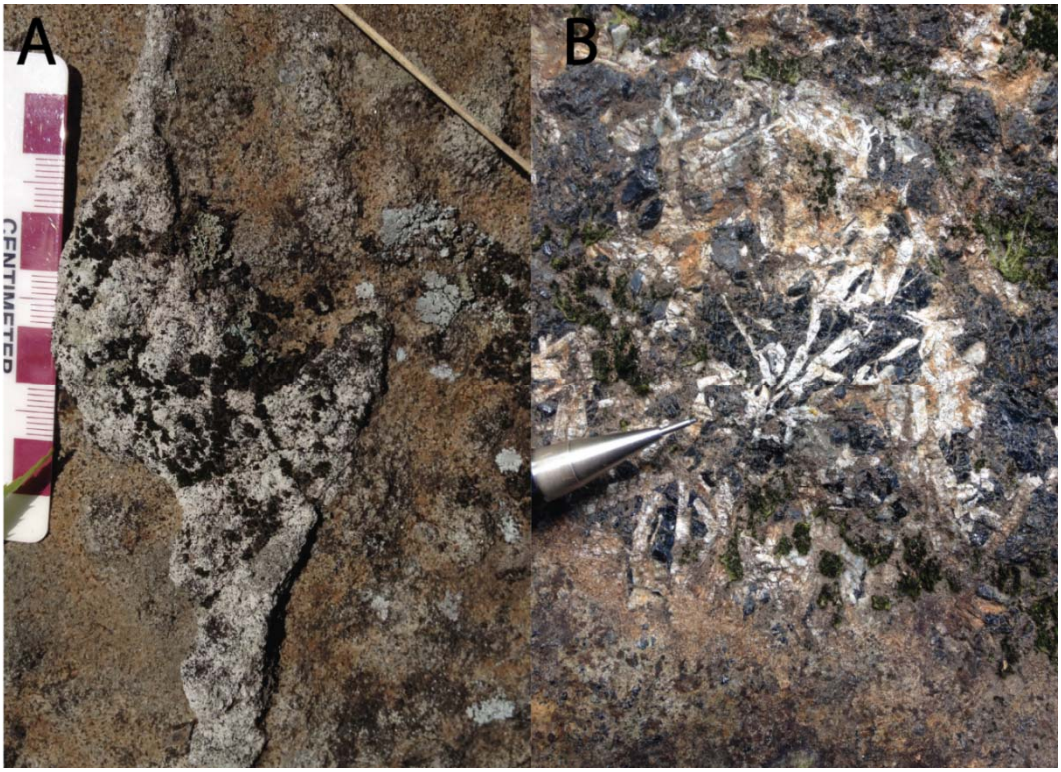

Figure 29. Coarse gabbroic patches in ophitic basalt of the GSF (map unit *loz*) near contacts with the overlying *hz* unit in the Central mapping location. A) amoeboid stringers of moderately foliated, coarse-grained leucogabbro and B) very coarse-grained segregations of oxide-rich gabbro with radiating, clustered plagioclase laths.

Similar to the contacts with the ophitic basalts of the *loz* and *uoz*, distinct changes in mineralogy and/or texture are evident in *hz* outcrops separated be a few meters or less. The internal contacts between *hz* lithologies are poorly exposed throughout most of the Isle Royale and Keweenaw Peninsula mapping areas but abrupt contacts between *hz* rocks were observed in several locations. At Blake Point, sharp, unchilled contacts between fine- and medium-grained ferromonzodiorite (Fig. 31A) are exposed along the Lake Superior shoreline. Similarly, along the Tobin Harbor-Duncan Bay portage trail, an abrupt transition between intergranular gabbro and prismatic ferromonzodiorite (Fig. 30)

occurs over a stratigraphic thickness of less than half a meter. On the Keweenaw Peninsula, sharp, unchilled contacts between medium-grained ophitic basalt and coarse-grained, prismatic ferromonzodiorite (Fig. 31E) were observed at the Phoenix mapping location. The grain sizes of both lithologies in Figure 31E increase slightly toward the contact and a small, 4-5-centimeter-thick aplite dike can be seen cutting the southwestern end of the exposure, occurring just below and running subparallel to the lithological contact.

Figure 30. Inferred abrupt to sharp contacts between ophitic olivine basalt of the *loz*, intergranular olivine oxide gabbro of the *hz* unit, and prismatic ferromonzodiorite of the *hz* unit within a roughly 3-meter interval along the Tobin Harbor-Duncan Bay portage trail on Isle Royale.

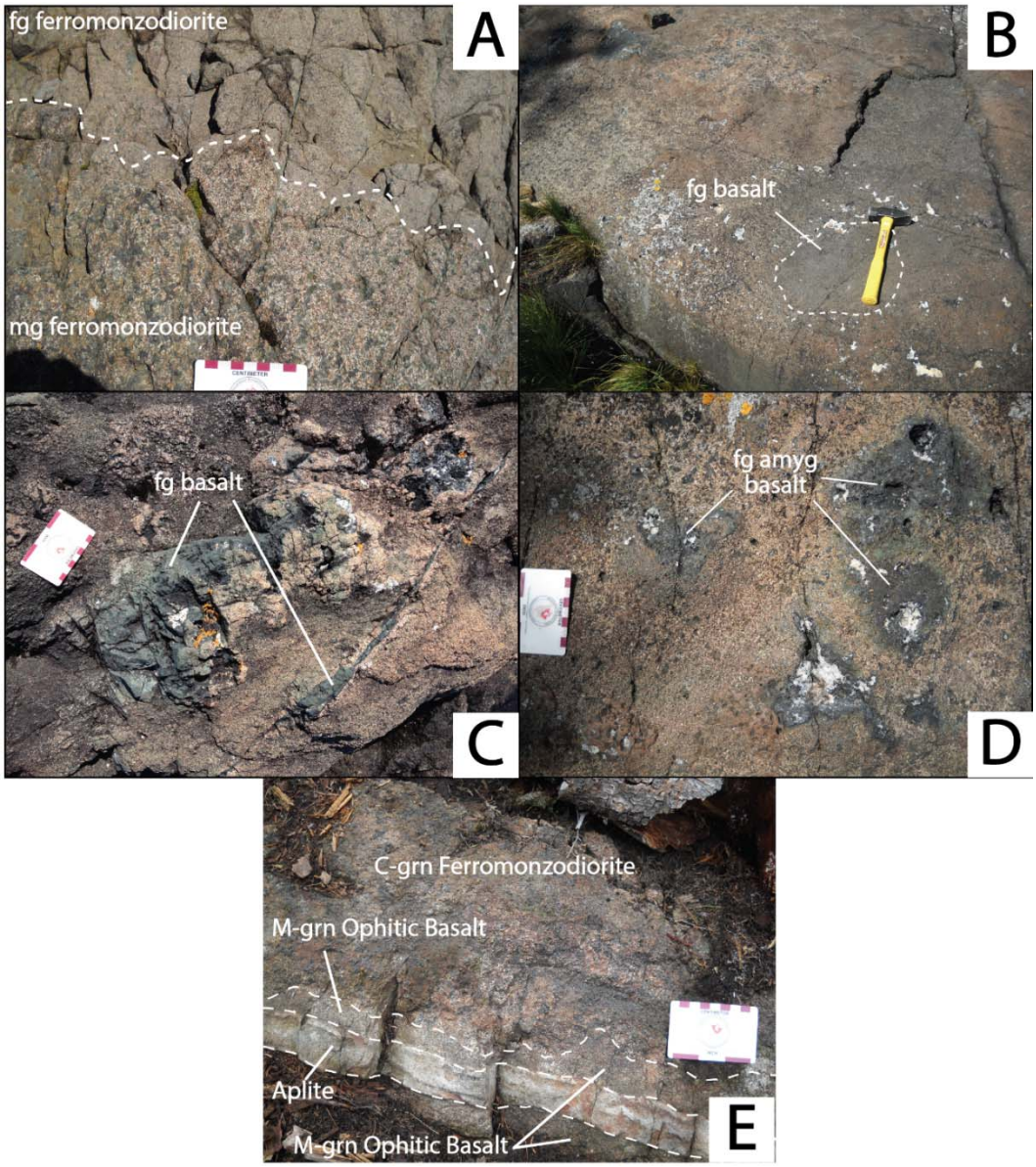

Figure 31. Lithologic variations of the Heterolithic Zone (map unit *hz*) on Isle Royale. A) varitextured ferromonzodiorite exposure at Blake Point on Isle Royale; B-D) inclusions of massive to amygdaloidal basalt in varitextured ferromonzodiorite exposure at Blake Point on Isle Royale; E) sharp, unchilled contact between medium-grained ophitic basalt and coarse-grained, prismatic ferromonzodiorite in *hz* exposure at Phoenix mapping location on the Keweenaw Peninsula, note aplite dike cutting exposure subparallel to contact.

The *uoz-ent* contact does not crop out in any of the mapping locations on the Keweenaw Peninsula or Isle Royale. On the Keweenaw Peninsula, exposures of the *ent*

and *uoz* are separated by less than a few meters at the Phoenix location, but the physical contact is buried beneath glacial debris. On the northeastern tip of Isle Royale, this contact runs along an erosional feature known as Merritt Lane (Figure 14; Huber, 1973). At Red Rock Point, the *uoz-ent* contact is buried beneath talus and glacial debris but exposures of the two are separated by just a few meters.

3.2.3 Petrographic Attributes of the GSF Ophitic Basalt Zones

The *loz* and *uoz* units at both the Keweenaw Peninsula and Isle Royale are indistinguishable petrographically and are composed predominantly of fine- to medium-grained ophitic olivine basalt (Fig. 32A and B). On average, the rocks of the *loz* tend to be coarser-grained than those of the *uoz*, however the basalt in each unit tends to coarsen away from the flow margins toward the center of the flow. Plagioclase ranges from 0.3-2.0 mm in the *loz* and from 0.4-1.0 mm in the *uoz*. Augite oikocrysts range from 0.5-20 mm in the *loz* and from 0.5-15 mm in the *uoz*. Olivine grains sizes range from 0.3-4.0 mm in the *loz* and from 0.3-0.8 mm in the *uoz*. Modally, the basalts are typically composed of 40-60% plagioclase laths, 15-45% ophitic augite, 10-15% olivine (locally up to 25% in the *loz*), 5-10% Fe-Ti oxides, and 0-5% hypersthene or inverted pigeonite. Devitrified volcanic glass, felsic mesostasis, and amygdules constitute a minor component of the basalts (<5%). The basalts of the *loz* and *uoz* are typically weakly to moderately altered but are much more highly altered on Isle Royale, particularly at Blake Point, making field and petrographic identification problematic. Alteration of the basalts is typically characterized by sericitization and sausseritization of plagioclase, uralite and

amphibole alteration of augite, iddingsite alteration of olivine, and interstitial patches of fibrous chlorite and zeolites.

Similar to the BRD ophitic diabase, two of the most distinctive features of the GSF ophitic basalts are the occurrence of clustered plagioclase laths and the local occurrence of medium- to coarse-grained plagioclase megacrysts (Fig. 32C and D). Clustered plagioclase are usually joined on their long crystallographic planes (010 or 001) and less commonly form radiating clusters. Plagioclase grains typically display polysynthetic or simple twinning and normal or oscillatory zoning. Plagioclase megacrysts occur as subhedral to euhedral laths and rare equant grains and commonly display zoned overgrowth rims that occasionally poikilitically enclose groundmass minerals.

Augite occurs as medium- to coarse-grained poikilitic oikocrysts enclosing chadacrysts of plagioclase and, less-commonly, olivine and Fe-Ti oxide (Fig. 32C and D). Augite is typically unzoned and only rarely altered. Exsolution lamellae on augite are rare but thin rims of hypersthene are locally developed on the edges of augite oikocrysts. In the finer-grained basalt near the flow margins, olivine occurs as fine-grained, clustered, granular crystals which are typically concentrated in the interstices between augite oikocrysts (Fig. 32A and B). In the coarser-grained ophitic basalt near the *loz-hz* contact, olivine increases in modal abundance (up to 25% locally) and becomes more subpoikilitic in habit, partially enclosing plagioclase laths and augite (Fig. 32D). Olivine is typically heavily to completely replaced by iddingsite and/or chlorite with serpentine alteration or deep-red hematite staining along fractures and grain boundaries. Similar to olivine, the habit of Fe-Ti oxides is also variable throughout the ophitic zones. In the

finer-grained basalt, Fe-Ti oxide typically occurs as fine-grained, subhedral laths (ilmenite?) and equant grains (Ti-magnetite?) but becomes coarser-grained and more poikilitic in the coarser-grained basalt near the contacts with the *hz* (Fig. 32D).

3.2.4 Petrographic Attributes of the GSF Heterolithic Zone

In contrast to the ophitic zones, the mineralogy and textures of the *hz* are quite variable with rock types ranging from ophitic basalt to ferromonzodiorite. Nearly all of the rocks are medium-grained but more intermediate lithologies tend to be coarse-grained. Moreover, the intermediate rocks in the *hz* also contain up to 35% felsic mesostasis of micrographic quartz and K-feldspar with prismatic mafic minerals. Scattered amygdules, usually filled with translucent to opaque clay minerals, chlorite, or concentrically banded zeolite minerals, are also common. Similar to the ophitic basalt, *hz* rocks from Isle Royale, particularly at Blake Point, are typically more heavily altered than those on the Keweenaw Peninsula.

The ophitic basalts in the *hz* are generally coarser-grained but otherwise petrographically indistinct from those in the *loz* and *uoz*. In addition to similar modal mineralogies the basalts in the *hz* share distinct textural attributes with those in the ophitic zones, including: ophitic to locally subophitic texture, the occurrence of clustered plagioclase laths usually joined along their long crystallographic axes (010 or 001), and the local occurrence of plagioclase megacrysts.

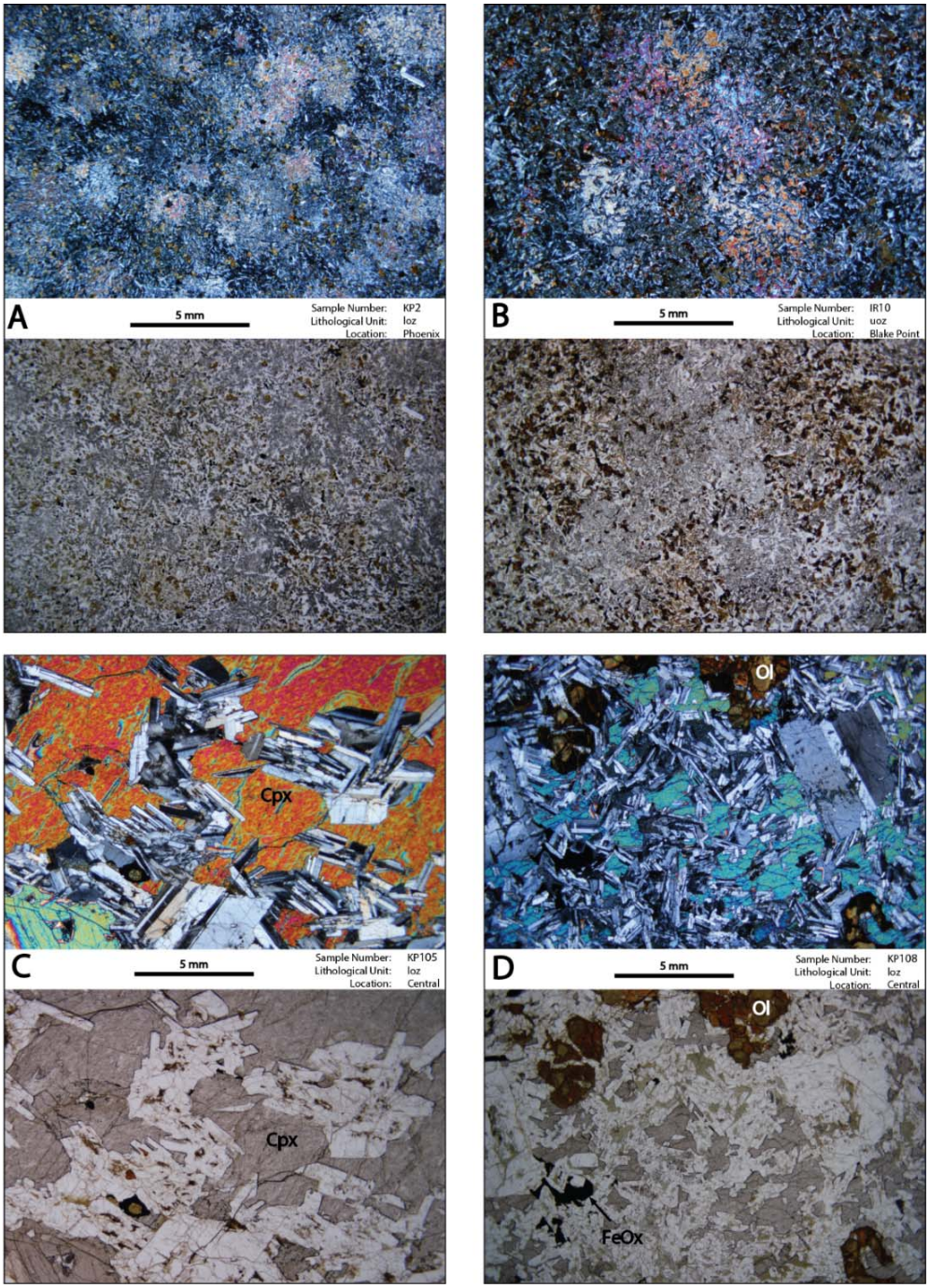

Figure 32. Crossed-polarized and plane-polarized photomicrographs of the GSF Ophitic Zones showing A) fine-grained ophitic basalt of unit *loz* at Phoenix on the Keweenaw Peninsula, B) fine-grained ophitic olivine basalt of unit *uoz* at Blake Point on Isle Royale, C) clustered plagioclase laths in medium-grained ophitic olivine basalt of unit *loz* at Central on the Keweenaw Peninsula, and D) plagioclase-megacrysts in medium-grained ophitic olivine basalt of unit *loz* at Central on the

Keweenaw Peninsula. Altered, granular olivine and interstitial Fe-Ti oxide are noted.

The gabbros in the *hz* are distinguished from the basalts by the development of intergranular texture, an absence of plagioclase megacrysts, and the ubiquitous occurrence of felsic mesostasis (< 5%). The gabbros are nearly all medium-grained and display intergranular to locally subophitic textures (Fig. 33A), Modally, the gabbros are composed of 40-60% plagioclase, 10-30% augite, 0-15% olivine, 2-10% Fe-Ti oxide, and up to 5% felsic mesostasis. Hypersthene is largely absent from the gabbros and pigeonite occurs only rarely as thin rims developed on augite and olivine. Miarolitic cavities are common and are typically filled with greenish-yellow, concentrically zoned zeolite minerals.

Plagioclase primarily occurs as medium-grained, clustered, subhedral laths to less-common equant grains (Fig. 33A). Many plagioclase crystals display thin sodic or micrographic rims, particularly those abutting felsic mesostasis or miarolitic cavities. Plagioclase in the *hz* gabbroic rocks is more altered than in the ophitic basalts and usually shows strong sericitization or sausseritization with small clots of epidote and/or zeolite minerals in pits and along microfractures. Augite typically occurs as medium- to coarse-grained, subophitic crystals and less commonly as medium-grained anhedral granular crystals (Fig. 33A). It typically shows broad normal zonation and patchy uralite alteration. Olivine is invariably altered to iddingsite and/or serpentine and pseudomorphs are typically medium- to coarse-grained and subpoikilitic (Fig. 33A). Fe-Ti oxides typically occur as subpoikilitic, interstitial equant grains (Fig. 33A) that commonly display complex ilmenite exsolution lamellae. Exsolution lamellae are typically altered to

a cloudy, greyish mineral (possibly leucoxene) and deep red haloes of hematite are commonly observed radiating from the exsolved oxides along the grain boundaries of adjacent minerals. Accessory minerals are usually associated with felsic mesostasis and include epidote, zircon, titanite, and apatite needles up to 5 millimeters in length.

The intermediate lithologies of the *hz* unit typically classify as ferrodiorites to more granophyric ferromonzodiorites. The ferrodiorites (Fig. 33B and C) are distinguished from the gabbroic rocks primarily by a change in the habit of augite from subophitic/granular to prismatic and an increase in the abundance of felsic mesostasis (up to 15%). Plagioclase crystals do not display the distinctive clustered texture that characterizes the ophitic basalt and intergranular gabbro and instead occurs as felty, laminated, subprismatic laths. Plagioclase is typically heavily altered to sericite. Augite occurs as typically subprismatic to poikiloprismatic containing abundant inclusions of fine-grained, granular Fe-Ti oxides and apatite. Prismatic plagioclase and augite commonly show varied degrees of planar alignment, locally displaying a well-foliated texture (Fig. 33C). Olivine, where present, is always completely altered to iddingsite and pseudomorphs are typically rounded, granular grains or rare, coarse-grained poikilitic crystals. Fe-Ti oxides are typically fine-grained and occur as bladed to subequant grains and less-commonly as coarse-grained, subpoikilitic grains.

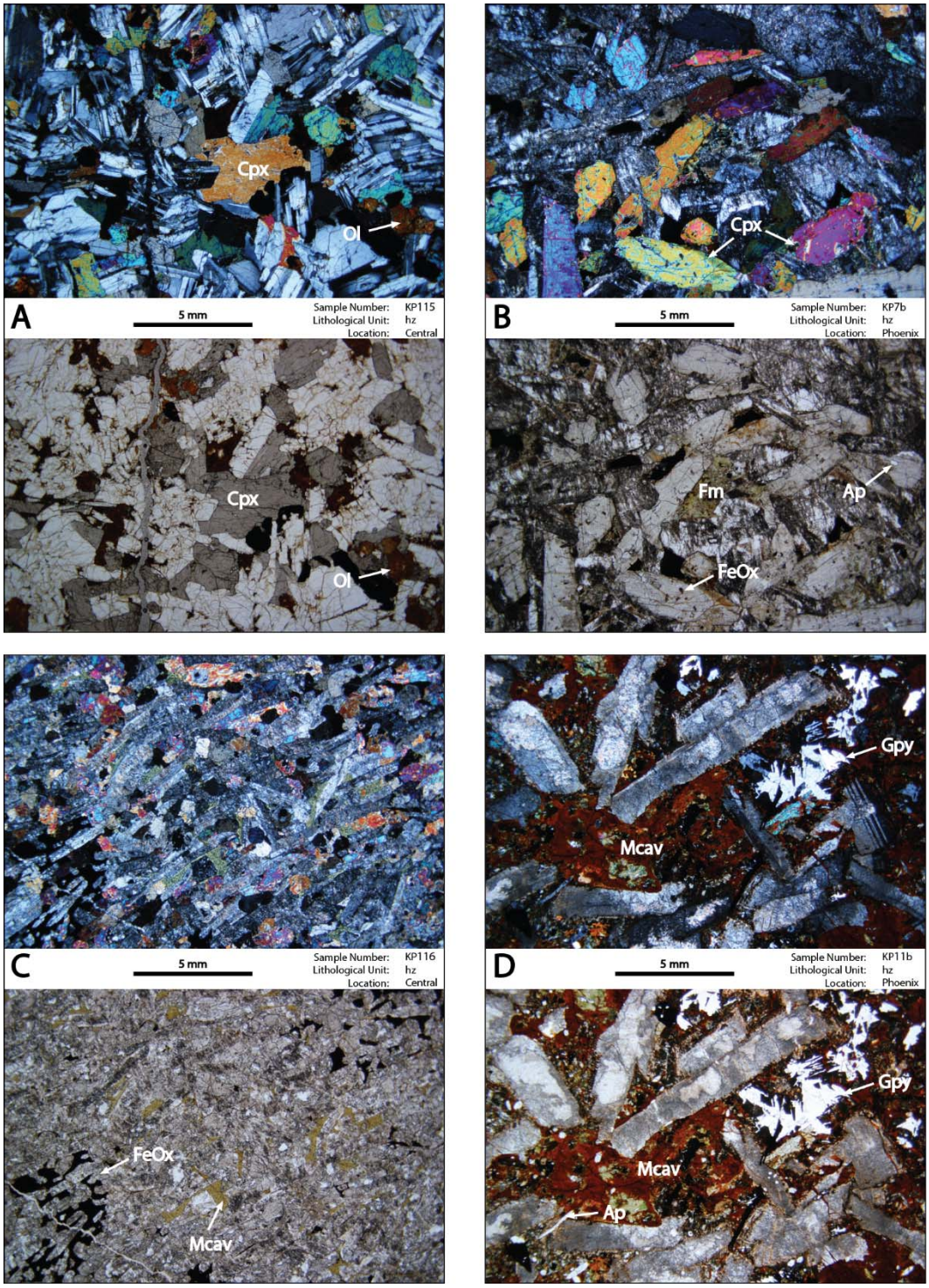

Figure 33. Crossed-polarized and plane-polarized photomicrographs showing the mineralogy and textures of the GSF Heterolithic Zone lithologies. A) medium-grained, intergranular oxide olivine gabbro from Central on the Keweenaw Peninsula, B) medium-grained, prismatic ferrodiorite from Phoenix on the

Keweenaw Peninsula; note poikiloprismatic texture of augite with inclusions of fine-grained Fe-Ti oxide and apatite; C) medium-grained, foliated ferrodiorite from Central on the Keweenaw Peninsula, and D) coarse-grained, prismatic ferromonzodiorite from Phoenix on the Keweenaw Peninsula; note miarolitic cavities filled with opaque clay minerals and greenish zeolites.

The ferromonzodiorites (Fig. 33D) are distinguished from the ferrodiorites by an increase in the abundance of felsic mesostasis (up to 35%) and a decrease in the abundance of mafic minerals. Ferromonzodiorites are typically coarser-grained and well-laminated but lack the foliation observed in the ferrodiorites. Plagioclase laths are typically medium- to coarse-grained, subprismatic, and display extensive sericite, sausserite, and/or epidote alteration. Most crystals have broad sodic or micrographic rims, particularly when abutting felsic mesostasis or miarolitic cavities (Fig. 33D). Augite occurs as strongly zoned, subhedral prisms and becomes coarser and almost acicular in habit in more highly fractionated samples. Most augite is also heavily altered to hematitic uralite and often occurs only as skeletal, relict grains. Rare olivine is completely altered to iddingsite or chlorite and pseudomorphs occur as rounded, granular or prismatic grains. Fe-Ti oxides occur predominantly as fine- to medium-grained, subhedral to euhedral blades and subequant grains, but in the vicinity of granophyre patches, oxide tends to occur as long (≤ 7 mm) acicular needles and skeletal, trellis textured overgrowths in the coarser-grained varieties. Apatite is typically abundant and occurs as prismatic to acicular needles (≤ 1cm long) (Fig. 33D) and stubby, euhedral prisms which occur as inclusions in the mafic minerals and felsic mesostasis. Other accessory phases are generally associated with felsic mesostasis and include zircon, titanite, granular hematite, and epidote.

3.2.5 Petrographic Attributes of the GSF Entablature

Only two samples of the *ent* unit were collected during this study: a fine-grained, weakly amygdaloidal basalt (Fig. 34A) from the Phoenix mapping location on the Keweenaw Peninsula (Fig. 22) and a hematite-rich, intersertal basalt (Fig. 34B) from Red Rock Point on Isle Royale (Fig. 25). Modally, the sample from the Keweenaw Peninsula is an olivine basalt composed of 40% plagioclase, 20% augite, 20% olivine, 5% Fe-Ti oxides, 10% devitrified volcanic glass, and 5% amygdules. Plagioclase occurs as radiating clusters of subhedral microlites often displaying swallow-tailed edges. Augite is typically subhedral granular in habit, but also occurs as clusters of coarser-grained, elongated prismatic and acicular crystals. Olivine occurs as rounded, granular crystals that are completely altered. Fe-Ti oxides typically occur as subrounded equant grains (Ti-magnetite?) and blades (ilmenite?).

The *ent* sample collected from Isle Royale is fine-grained, and very hematite-rich (Fig. 34B). Modally, it is composed of roughly equal proportions of slender, clustered plagioclase microlites and fine-grained, hematized mafic phases (pyroxene and olivine?). Plagioclase microlites form radiating clusters such as in the sample from the Keweenaw Peninsula but are more commonly joined on their long crystallographic axes (010 or 001) as in the GSF ophitic basalts and BRD ophitic diabase. Rare plagioclase megacrysts are subhedral laths which display thin overgrowth rims and variable sericite and hematite alteration in pits and along microfractures. The interstices between plagioclase and hematite grains are typically replaced by fibrous chlorite and/or zeolites and comprise up to 10% of the rock. Amygdules, filled with chlorite and/or zeolite minerals, are a minor component, constituting 1-2% of the sample.

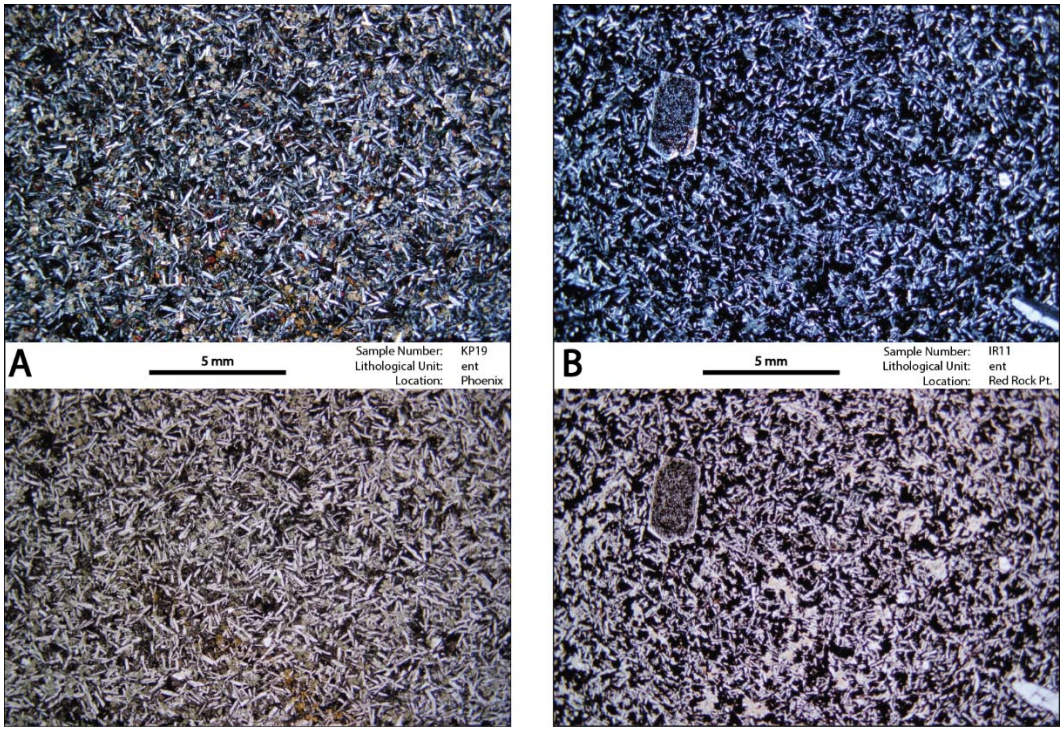

Figure 34. Crossed-polarized and plane-polarized photomicrographs of the Entablature of the GSF (map unit *ent*). A) Fine-grained, weakly amygdaloidal basalt from Phoenix on the Keweenaw Peninsula. B) Fine-grained, very hematite-rich, intersertal basalt with altered plagioclase megacrysts from Red Rock Point on Isle Royale.

3.3 Mineral Chemistry

The chemical compositions of pyroxene, olivine, plagioclase and Fe-Ti oxides were analyzed in 22 samples of the BRD-SBI and 31 samples of the GSF. Because olivine is particularly susceptible to deuteric alteration, analyses of fresh olivine was limited to 13 samples of the BRD-SBI and seven samples of ophitic basalt of the GSF, five from the *loz,* one from the *hz*, and one from the *uoz*. Mineral chemical data collected during this study is supplemented by unpublished microprobe analyses conducted on BRD-SBI samples during the COGEOMAP program by Dr. Jim Miller. These data include analyses of pyroxene compositions from 36 samples and olivine compositions from 16 samples.

Plagioclase analyses focused exclusively on samples containing megacrysts. The compositions of plagioclase megacrysts were analyzed in two samples of the BRD-SBI and four samples of the GSF. Because of the pervasive and commonly complex compositional zoning of groundmass plagioclase, many analyses would be required to acquire a statistically valid average composition. Moreover, attempts to measure and compare just the core compositions of groundmass plagioclase were made difficult by the clustered nature of the plagioclase (e.g. Figs. 19A and 32C). This texture of co-parallel to randomly oriented interlocking laths makes it nearly impossible to distinguish the grain boundaries between adjacent crystals in backscattered electron microscope images. For these reasons, as well as the often extensive alteration displayed by plagioclase crystals, groundmass plagioclase was analyzed only in the six samples containing unaltered megacrysts. In these samples, an average of 12-16 randomly chosen spot analyses of groundmass plagioclase were conducted to provide a qualitative comparison with megacrysts compositions.

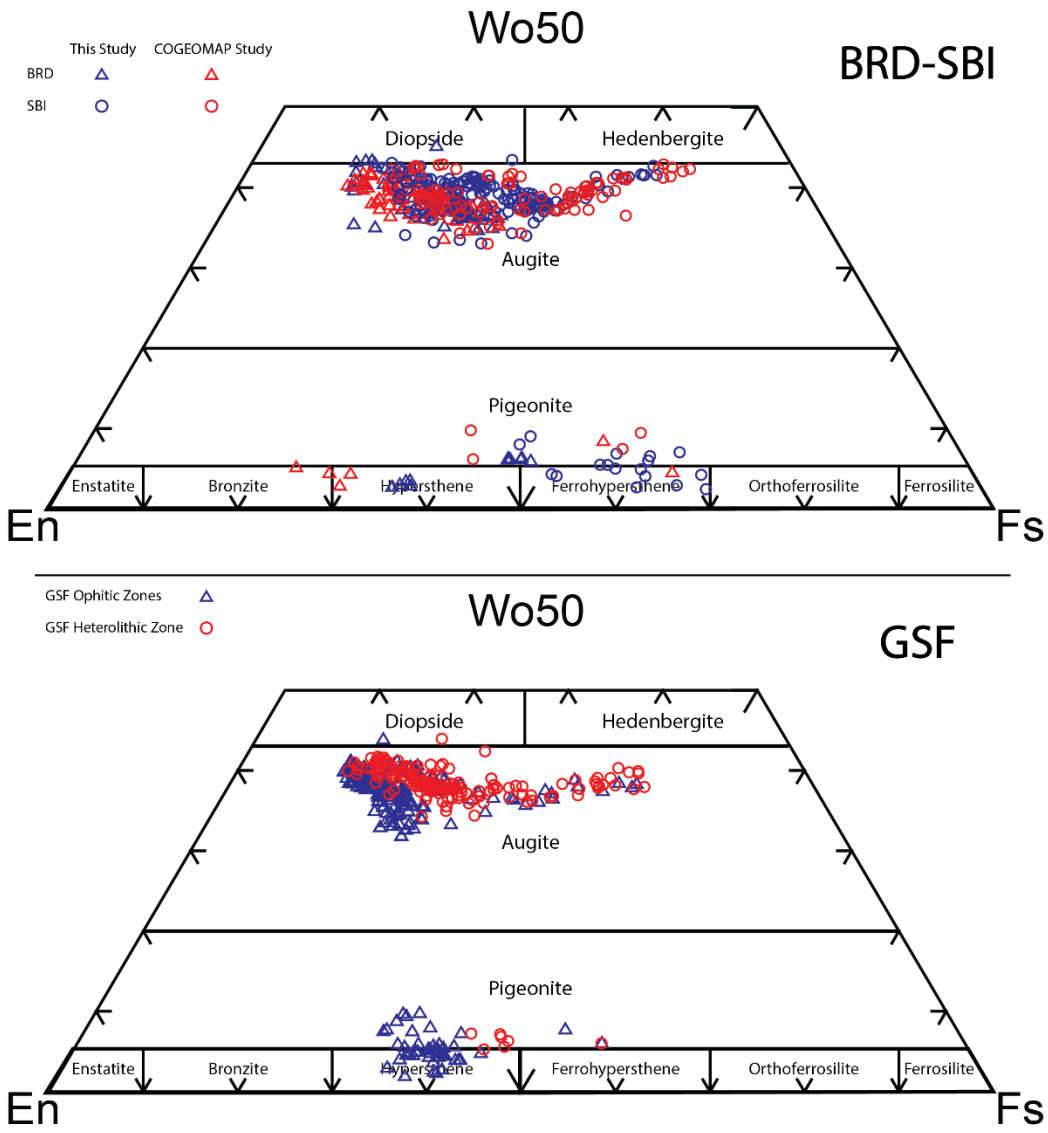

Figure 35. Pyroxene compositions of BRD-SBI (top) and GSF (bottom) lithologies in terms of En-Fs-Wo components (cation%). Pyroxene compositions for this study analyzed by SEM-EDS (Appendix B). COGEOMAP analyses are microprobe analyses from Miller (unpublished data). Pyroxene field names based on Deer et al., 1992.

SEM-EDS mineral chemical data are/ reported for pyroxene, olivine, Fe-Ti oxides, and plagioclase in Appendix B. All data are reported in weight percent oxide and converted to cation proportions to calculate stoichiometry. The compositional components of En-Fs-Wo (En=Mg/(Mg + Fe + Ca), Fs=Fe/(Mg + Fe + Ca), Wo=Ca/(Mg

+ Fe + Ca), cation %) were calculated for pyroxenes and are plotted on ternary diagrams in Figure 35. Magnesium numbers (mg# = Mg/(Mg + Fe)*100, cation %) were calculated from the cation proportions for pyroxene (En') and olivine (Fo). The distribution of En' content in augite in BRD-SBI and GSF rocks are plotted as histograms with bin sizes of 5% En' in Figure 36. En' contents in augite range from and from En'_{53-82} (average = En'_{70}) and from En'_{19-73} (average = En'_{53}) in BRD ophitic and composite lithologies, respectively. In the GSF, En' contents in augite range from En'_{46-81} (average = En'_{69}) in the ophitic lithologies and from En'_{18-76} (average = En'_{54}) in the composite lithologies. The distribution in Fo contents in olivine in BRD-SBI and GSF lithologies are plotted as histograms with bin sizes of 5% Fo in Figure 37. Fo contents in olivine range from Fo_{43-75} (average = Fo_{61}) and from Fo_{15-57} (average = Fo_{29}) in BRD-SBI ophitic and composite lithologies, respectively. Fo contents in olivine in GSF ophitic rocks range from Fo_{45-73} (average = Fo_{55}). Fresh olivine was not observed in any samples of the composite lithologies in the GSF and, thus, Fo contents were not analyzed in those lithologies. The anorthite contents (An = Ca/(Ca + Na + K)*100; cation %) were calculated for plagioclase megacrysts and groundmass crystals. The distribution of An content in the megacrystic and groundmass plagioclase is plotted as histograms using bin sizes of 5% An in Figure 38. An contents in plagioclase megacryst cores range from An_{45-81} (average = An_{70}) and from An_{52-81} (average = An_{69}) in BRD and GSF samples, respectively. An contents of megacryst rims are generally lower than in megacryst cores with averages of An_{59} in BRD samples and An_{58} in GSF samples. Groundmass plagioclase crystals have average An contents of An_{56} and An_{54} in BRD and GSF samples, respectively.

The implications of the chemical variation in BRD-SBI and GSF samples will be discussed in the following chapter.

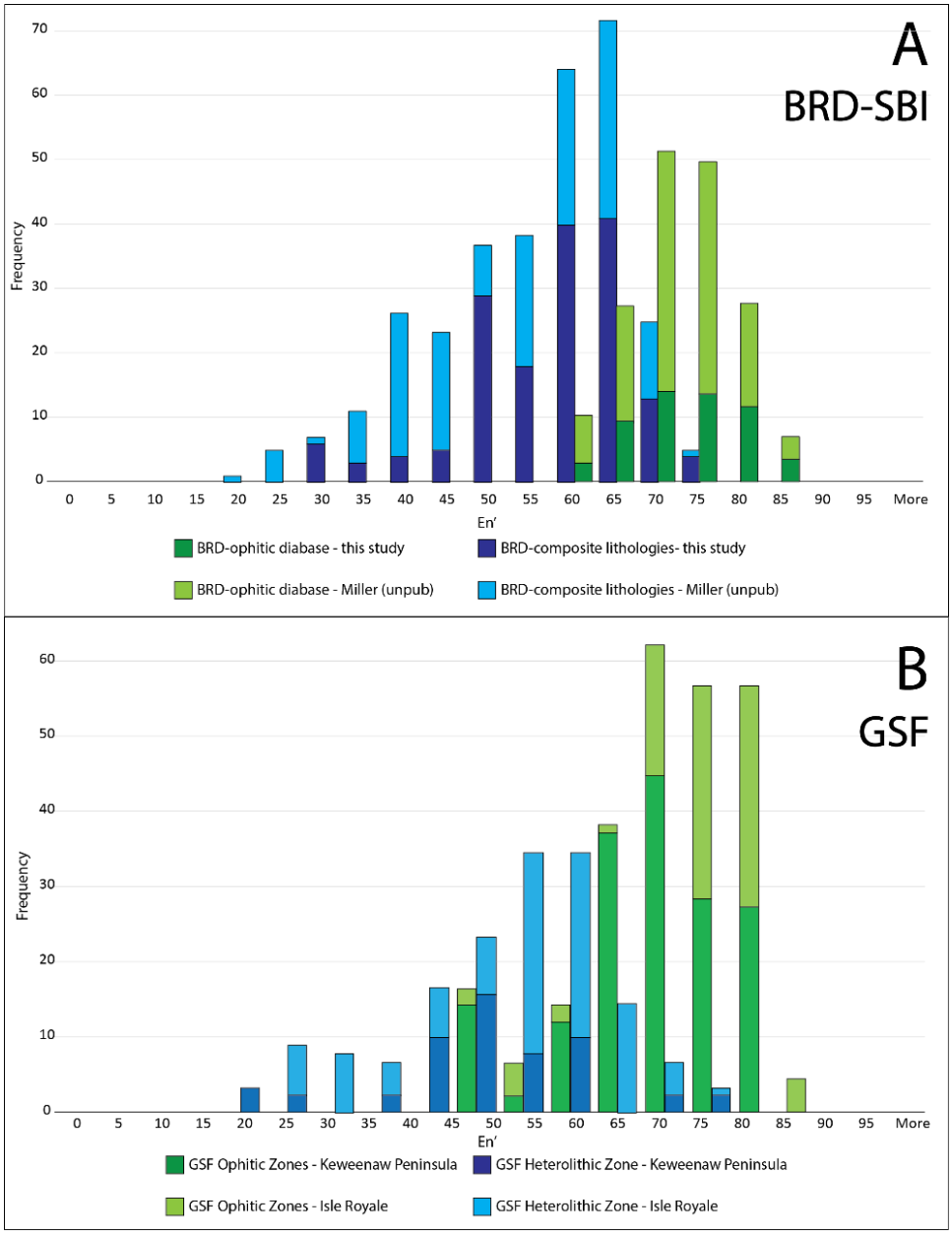

Figure 36. Histograms of En' content (=Mg/(Mg+Fe), cation %) from spot analyses of augite in BRD-SBI (A) and GSF (B) samples. Pyroxene compositions measured in this study analyzed by SEM-EDS (Appendix B); BRD data from Miller (unpublished data) measured by electron microprobe.

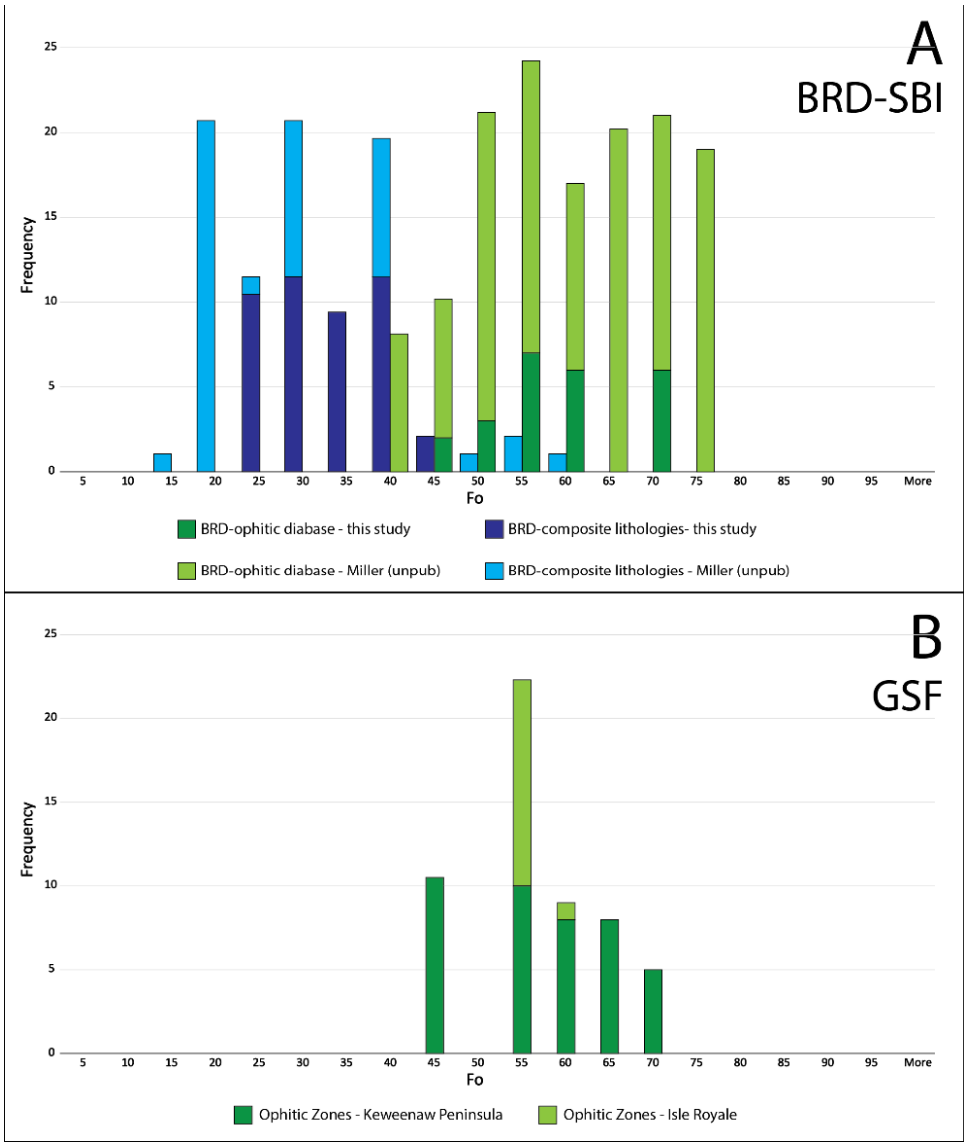

Figure 37. Histograms of Fo contents in olivine from spot analyses of BRD (A) and GSF (B) samples. Olivine compositions measured in this study analyzed by SEM-EDS (Appendix B); BRD data from Miller (unpublished data) measured by electron microprobe.

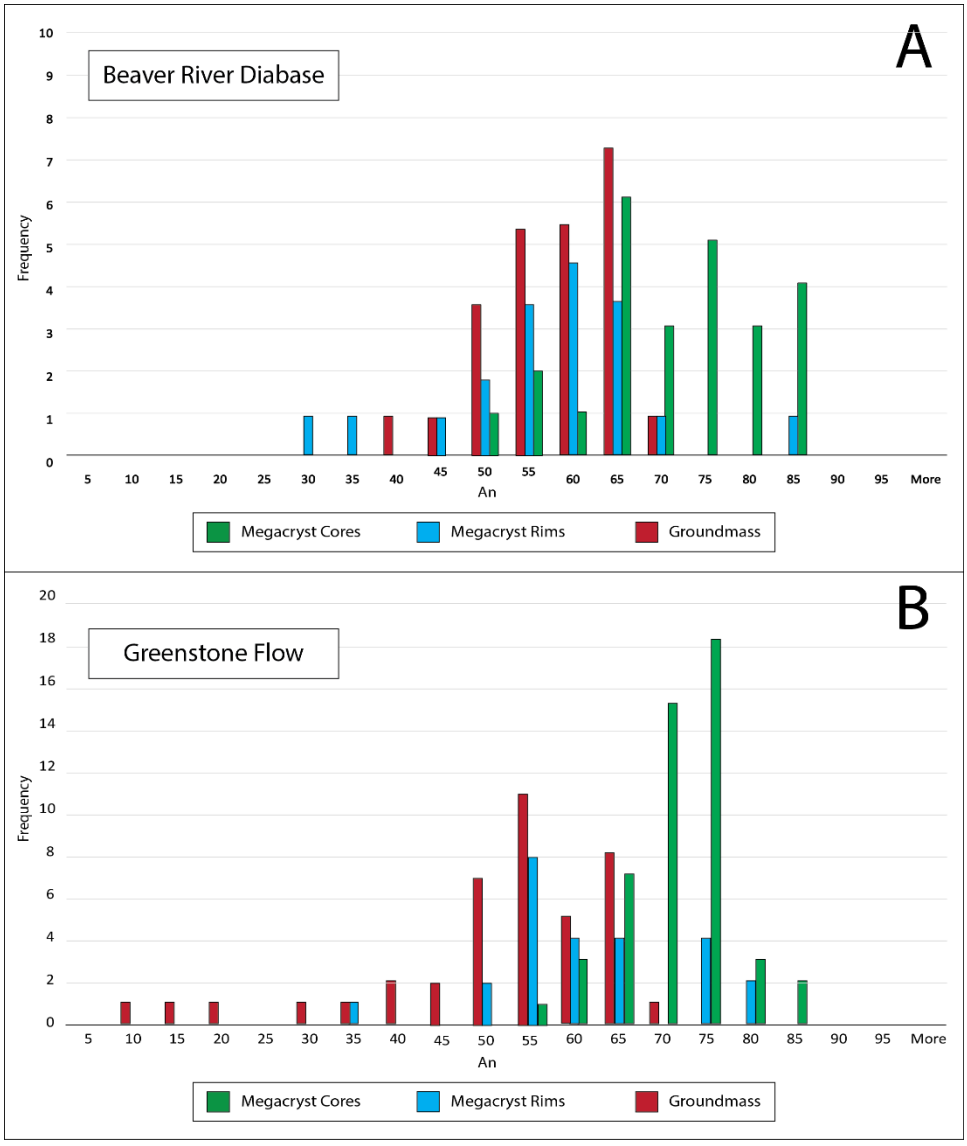

Figure 38. Histograms of An contents (= Ca/(Ca+Na+K), cation %) measured by spot SEM-EDS analyses of plagioclase megacrysts and groundmass plagioclase in A) BRD (ophitic diabase) and B) GSF samples.

3.4 Whole-rock Lithogeochemistry

Whole-rock lithogeochemical analyses were obtained for 21 samples of the BRD-SBI intrusive suite and 40 samples of the GSF volcanic suite from Acme Laboratories in Vancouver, British Columbia. All samples were analyzed for major and minor element oxides and trace elements (Table 3). Samples were also analyzed for a suite of base and

precious metals (Table 3). Major oxide data obtained for BRD samples during this study is supplemented by unpublished geochemical data obtained by Dr. Jim Miller during the COGEOMAP program. Trace element and base metal data collected during the COGEOMAP program were not used in this research because the suite of elements analyzed differed considerably from those analyzed for this study. Complete analytical and quality control data are presented in Appendix C. Major elements, select trace elements, and select base metals are summarized for the BRD in Table 4 and for the GSF in Table 5. A number of trace elements, base metals, and precious metals (Be, Sn, W, U, As, Cd, Sb, Bi, Ag, Au, Hg, Tl, Se) were consistently at or below detection limits and were thus excluded from the tables.

The standard method of graphically presenting and comparing trace and minor element concentrations is to plot normalized variation diagrams (or spider diagrams) (Rollinson, 1993). Elements are normalized to a standard composition, such as MORB, C1 chondrite, or primitive mantle, and then are plotted in order of increasing incompatibility to the left of the diagram. Chondrite-normalized REE spider diagrams were constructed using the IgPet modelling program (Carr, 1997) and the normalizing values of C1 chondrite reported by Sun and McDonough (1989). REE spider diagrams for the BRD and GSF samples suites are presented in Figure 39A and B, respectively. The various rock types in both suites display similar, co-parallel patterns which gently slope to the right side of the diagram. The lithological variations described previously for the BRD composite intrusions and GSF Heterolithic Zone are reflected by the wide range of REE normalized abundances displayed on the diagrams. A pronounced negative Eu

anomaly is evident among more enriched sampled (those with higher normalized values), whereas other samples generally display slightly negative, neutral, or slightly positive Eu anomalies. Negative Eu anomalies are generally attributed to depletion by fractionation of plagioclase (Rollinson, 1993). One sample of diabasic troctolite from the margin of the BRD in the NBBC (sample BBC6, unit *brd*; Fig. 39A) displays a significantly lower overall abundance in REEs and a pronounced positive Eu anomaly. This likely reflects high abundances of olivine contained in this sample (Fig. 19B).

Multi-element chondrite-normalized spider diagrams were also plotted for the BRD and GSF sample suites (Fig. 40A and B, respectively) using Thompson's (1982) order of incompatible and minor elements. The various rock types in each unit display similar parallel patterns as are observed in the REE diagrams. Complementary to the Eu anomaly in the REE plots (Fig. 39), a distinct negative Sr anomaly pattern is observed for more enriched samples of the GSF and BRD (Fig. 40). Sr, like Eu, is compatible in plagioclase and thus likely reflects the fractionation of plagioclase in more evolved compositions. Similar to the REE diagram (Fig. 39A), sample BBC 6 shows much less enrichment than the rest of the samples. Other notable patterns evident in the Thomson plots are the negative anomalies in both P and Nb, which are similarly expressed in all samples. The petrologic significance of the patterns displayed on these diagrams will be discussed in the next chapter.

Table 4. Selected whole-rock lithogeochemical data for BRD sample suite lithologies. Major and minor element oxides reported as weight percent, all others in ppm.

	Sample	MDL	BBC1	BBC2	BBC4	BBC5	BBC6	BBC7	BBC8	BBC10	BBC11-A	BBC11-B	BBC12	BBC13	BBC14	SB10	SB11	SB12	SB13	SB14	SB15	SB16	SB17
	Mapunit		brg	brg	brg	brg	brd	brg	brg	brg	brfd	brfd	brfd	brpg	brd	brd	sbg	sbg	sbg	sbld	sbg	sbg	sbld
Major-minor element (%)	SiO2	0.01	49.02	50.65	49.21	51.01	45.53	49.53	50.69	45.26	46.32	47.11	47.32	47.77	47.20	48.12	51.11	50.40	51.19	44.55	48.08	47.68	46.01
	Al2O3	0.01	16.95	17.55	16.53	19.94	19.77	17.60	16.85	13.36	11.55	11.55	11.60	17.77	16.95	18.12	18.47	11.80	11.03	12.59	18.64	18.54	12.82
	Fe2O3	0.04	13.33	11.70	12.24	9.61	10.16	11.47	9.41	17.48	21.04	20.83	19.99	11.77	11.76	11.80	10.43	16.52	17.55	20.30	11.57	11.49	18.87
	MgO	0.01	3.32	2.73	4.58	1.77	10.94	3.91	4.75	4.90	2.98	2.96	2.56	7.08	7.21	4.95	2.49	3.72	2.47	3.75	4.02	4.27	3.06
	CaO	0.01	9.86	9.37	10.32	9.31	10.29	10.28	11.81	9.92	8.30	7.95	7.68	10.47	10.37	10.29	9.24	8.00	7.06	8.21	9.53	10.26	8.31
	Na2O	0.01	3.01	3.14	2.81	3.86	1.92	2.94	2.78	2.41	2.58	2.57	2.58	2.53	2.36	2.82	3.19	2.72	2.75	2.92	2.93	2.77	3.01
	K2O	0.01	0.68	0.92	0.66	0.93	0.14	0.68	0.59	0.44	1.13	1.23	1.39	0.34	0.29	0.48	1.08	1.13	1.62	0.79	0.60	0.46	0.92
	TiO2	0.01	2.72	2.16	2.06	1.84	0.40	1.73	1.39	4.82	3.77	3.61	3.52	0.85	1.58	1.56	1.83	3.17	2.45	3.79	1.64	1.67	3.37
	P2O5	0.01	0.19	0.27	0.16	0.23	0.03	0.18	0.14	0.10	1.00	1.03	1.02	0.08	0.16	0.15	0.23	0.39	1.00	1.74	0.24	0.18	1.46
	MnO	0.01	0.17	0.16	0.17	0.13	0.13	0.16	0.14	0.22	0.26	0.26	0.25	0.16	0.17	0.15	0.14	0.25	0.25	0.25	0.17	0.17	0.24
Base metals (ppm)	Sc	1	29	24	30	17	10	26	34	42	36	35	34	23	32	25	20	38	34	25	19	23	33
	V	8	346	261	312	150	73	242	257	634	108	129	85	158	241	224	190	211	11	38	169	203	24
	Co	0.2	38.6	30.5	41.6	22.6	69.0	38.3	32.5	59.3	45.3	46.5	43.1	61.0	52.7	47.9	29.3	42.7	32.0	58.1	39.7	41.7	45.8
	Ni	0.1	10.1	8.8	22.8	4.2	389.0	20.8	13.3	15.1	4.4	5.4	4.3	87.7	107.5	49.5	10.3	3.3	0.5	0.6	31.4	35.8	0.4
	Cu	0.1	166.8	136.1	124.9	151.9	27.1	117.6	88.5	90.4	442.2	413.1	367.6	75.4	126.2	125.0	118.5	185.6	342.4	729.2	138.7	119.4	669.9
	Pb	0.1	6.2	2.5	2.5	5.7	1.8	1.5	2.4	1.6	2.8	3.8	3.8	2.1	14.0	1.3	1.7	2.7	4.2	1.5	1.2	1.0	5.9
	Zn	1	150	60	58	57	55	54	40	56	123	133	123	59	64	53	54	65	102	83	50	49	101
	Mo	0.1	0.5	0.4	0.4	0.8	0.2	0.7	0.5	0.4	1.2	1.3	1.2	0.2	0.3	0.3	0.6	0.4	1.0	0.4	0.4	0.4	0.7
	Ga	0.5	24.1	23.2	21.5	24.8	17.2	22.9	20.2	21.9	25.5	25.8	25.5	18.7	19.4	22.3	24.6	24.3	23.5	23.6	23.3	21.9	26.0
LILE-HFS (ppm)	Ba	1	250	308	219	301	67	244	215	173	388	408	472	130	122	174	363	395	545	359	222	184	361
	Cs	0.1	0.7	0.5	0.9	0.8	1.6	0.4	0.3	0.3	0.8	0.9	0.8	1.2	3.2	0.3	0.5	0.4	0.6	0.3	0.2	0.2	0.3
	Hf	0.1	4.4	5.6	4.8	4.0	0.8	4.6	4.3	3.9	6.5	6.5	9.6	2.2	3.1	3.9	6.5	9.1	11.3	5.2	5.2	3.6	4.9
	Nb	0.1	12.5	15.5	12.3	14.8	2.0	12.5	9.3	13.4	17.9	18.2	26.6	5.3	8.8	10.1	17.0	25.6	29.3	17.7	13.3	10.7	17.8
	Rb	0.1	18.9	30.2	18.8	26.0	2.6	19.5	16.2	13.0	41.0	47.6	46.8	8.1	9.1	11.2	30.1	34.1	53.7	18.5	16.4	10.2	25.0
	Sr	0.5	345.8	328.5	301.8	351.6	304.0	311.2	286.8	238.6	244.5	247.7	240.9	306.5	290.4	336.0	345.5	243.3	223.1	315.0	340.8	325.9	307.3
	Ta	0.1	0.9	0.9	0.9	0.8	0.2	0.8	0.5	0.8	1.1	1.3	1.8	0.4	0.6	0.6	1.1	1.9	1.6	1.2	0.9	0.6	0.9
	Th	0.2	2.3	2.3	1.8	2.4	<0.2	2.0	1.6	1.0	3.6	3.9	5.2	0.8	1.1	1.2	3.1	4.8	6.4	2.5	2.0	1.3	3.1
	Zr	0.1	163.5	217.3	181.0	154.9	28.5	177.6	157.0	134.4	239.5	251.3	350.9	75.7	109.4	132.4	247.8	324.4	433.1	190.4	194.8	124.7	181.1
	Y	0.1	30.9	40.0	29.9	31.9	6.1	30.2	27.8	24.6	56.0	55.9	74.2	17.4	21.5	28.1	38.8	58.5	74.1	54.4	33.6	24.4	59.6
REE (ppm)	La	0.1	20.0	26.8	18.1	25.2	3.8	19.2	18.1	13.0	37.0	35.1	50.9	10.1	13.1	16.0	27.1	41.2	53.9	39.7	22.5	15.9	43.2
	Ce	0.1	43.8	57.2	40.9	51.5	8.1	42.8	38.0	28.2	83.4	80.2	108.5	21.4	26.2	34.2	62.3	86.2	122.2	90.0	48.7	33.1	95.3
	Pr	0.02	5.61	7.45	5.28	6.51	1.01	5.55	4.97	3.71	11.33	10.96	15.01	2.76	3.60	4.46	7.67	11.51	15.83	12.41	6.26	4.43	13.21
	Nd	0.3	24.1	31.4	23.6	28.3	4.7	23.0	22.2	17.0	50.7	51.7	67.8	12.6	15.9	19.1	32.9	50.1	67.5	57.9	28.4	19.9	59.4
	Sm	0.05	5.60	7.28	5.48	6.53	1.08	5.88	5.32	4.31	11.52	11.89	15.36	3.13	4.06	4.64	7.58	10.96	15.67	13.28	6.07	4.89	13.99
	Eu	0.02	2.02	1.99	1.67	1.92	0.65	1.67	1.56	1.53	3.00	2.87	3.22	1.07	1.44	1.56	2.11	3.00	3.55	3.92	1.93	1.62	3.77
	Gd	0.05	6.16	7.50	5.71	6.14	1.12	5.86	5.51	4.50	12.88	13.01	16.27	3.35	4.45	4.97	7.73	11.73	15.98	13.63	6.90	4.99	14.10
	Tb	0.01	0.98	1.18	0.96	1.02	0.19	0.98	0.94	0.79	1.97	1.97	2.57	0.57	0.73	0.85	1.26	1.88	2.50	2.01	1.06	0.84	2.09
	Dy	0.05	6.07	7.53	5.93	6.53	1.27	5.85	5.61	4.84	11.27	11.60	15.02	3.28	4.16	5.26	7.50	11.69	14.48	11.03	6.50	4.97	11.88
	Ho	0.02	1.13	1.34	1.16	1.18	0.25	1.12	1.11	1.00	2.20	2.18	2.98	0.68	0.83	0.98	1.47	2.20	2.80	1.96	1.31	1.01	2.18
	Er	0.03	3.31	3.92	3.41	3.33	0.79	3.41	3.06	2.63	5.96	5.97	7.85	1.85	2.38	2.82	4.21	6.29	7.73	5.30	3.80	2.59	5.73
	Tm	0.01	0.46	0.55	0.47	0.49	0.09	0.45	0.43	0.38	0.80	0.78	1.08	0.25	0.37	0.42	0.62	0.92	1.08	0.73	0.53	0.40	0.76
	Yb	0.05	3.02	3.55	3.07	2.95	0.54	2.98	2.80	2.56	4.98	5.00	6.72	1.79	2.32	2.61	3.77	5.70	6.75	4.11	3.30	2.41	4.39
	Lu	0.01	0.43	0.56	0.46	0.46	0.08	0.43	0.40	0.38	0.75	0.73	0.95	0.26	0.33	0.39	0.57	0.84	0.98	0.59	0.51	0.39	0.67

Table 5. Selected whole-rock lithogeochemical data for BRD sample suite lithologies. Major and minor element oxides reported as weight percent, all others in ppm. Samples arranged in order of increasing fractionation.

	Sample	KP1	KP5	KP101	KP104	KP110	IR7b	IR15	IR20	IR21	IR22	IR12	KP15	KP16	IR9	IR10	IR26b	IR27	KP19	IR11	KP10
	Mapunit	*loz*	*loz*	*loz*	*loz*	*loz*	*loz*	*loz*	*loz*	*loz*	*loz*	*uoz*	*uoz*	*uoz*	*uoz*	*uoz*	*uoz*	*uoz*	*ent*	*ent*	*hz*
Major-minor element (%)	SiO2	47.34	46.51	47.50	47.11	47.06	47.15	47.54	47.42	46.91	47.10	47.10	46.70	46.15	47.25	47.33	47.53	47.57	47.43	46.82	46.59
	Al2O3	16.15	17.22	15.96	17.42	16.99	15.58	16.02	15.76	16.53	15.83	15.80	15.84	16.34	15.77	15.65	15.96	15.80	15.89	16.06	16.26
	Fe2O3	11.64	10.74	11.57	10.64	11.55	11.58	11.50	11.48	11.37	11.76	11.13	11.68	11.10	10.90	11.13	11.92	11.41	11.58	11.29	12.80
	MgO	8.14	8.92	8.10	8.05	6.80	8.26	7.71	7.66	7.62	7.64	7.93	8.21	8.12	7.99	7.82	7.87	7.55	8.01	7.35	5.72
	CaO	10.10	10.32	9.56	10.74	10.60	9.60	9.58	9.96	9.88	10.18	9.58	9.65	10.12	9.79	9.93	10.05	9.64	10.02	10.03	10.39
	Na2O	2.18	2.00	2.25	2.07	2.35	2.24	2.30	2.24	2.19	2.25	2.38	2.17	2.11	2.25	2.28	2.34	2.26	2.20	2.42	2.58
	K2O	0.35	0.27	0.37	0.34	0.32	0.41	0.45	0.42	0.38	0.44	0.48	0.38	0.35	0.47	0.44	0.42	0.44	0.35	0.51	0.36
	TiO2	1.31	1.05	1.34	1.21	1.37	1.36	1.32	1.38	1.26	1.37	1.29	1.34	1.30	1.29	1.32	1.38	1.33	1.36	1.31	1.97
	P2O5	0.12	0.08	0.12	0.10	0.13	0.10	0.11	0.12	0.11	0.10	0.11	0.13	0.11	0.12	0.11	0.12	0.12	0.13	0.12	0.11
	MnO	0.16	0.14	0.16	0.15	0.16	0.18	0.16	0.16	0.15	0.18	0.17	0.16	0.15	0.16	0.15	0.17	0.15	0.16	0.15	0.17
Base metals (ppm)	Sc	26	21	27	22	27	28	26	26	24	28	25	27	25	25	26	27	25	27	25	33
	V	230	182	232	205	236	227	229	231	218	245	213	232	226	212	215	241	233	232	222	507
	Co	57.9	59.4	54.7	52.8	51.6	54.9	54.7	53.2	56.1	55.8	55.8	57.6	58.7	52.4	53.0	53.2	52.9	54.8	53.7	52.4
	Ni	119.0	168.8	115.4	128.8	71.7	113.1	111.0	114.6	140.3	91.8	117.1	119.9	140.5	112.0	113.0	107.9	118.4	132.6	146.6	39.9
	Cu	94.0	73.1	99.4	78.5	88.5	74.7	76.0	72.2	39.6	65.7	83.1	99.1	91.2	35.6	135.4	48.4	70.4	92.7	88.1	104.0
	Pb	5.8	1.9	6.2	1.8	1.3	1.7	5.7	1.8	1.3	2.4	1.4	3.0	1.0	1.9	1.6	1.8	1.3	1.7	4.5	1.1
	Zn	57	52	58	50	53	48	51	49	42	47	49	53	53	45	52	48	47	51	68	65
	Mo	0.3	0.3	0.1	0.2	0.1	0.2	0.2	0.2	0.1	0.3	0.6	0.1	0.2	0.2	0.2	<0.1	0.1	0.2	0.9	0.3
	Ga	17.2	16.0	16.5	16.8	16.8	16.2	19.0	17.9	18.4	18.3	19.4	16.7	16.7	18.3	16.7	18.3	18.8	18.0	19.7	18.6
LILE-HFS (ppm)	Ba	139	108	129	108	108	158	170	153	131	142	218	149	126	226	172	155	153	105	174	154
	Cs	1.7	2.0	0.9	1.6	0.9	<0.1	<0.1	0.1	0.2	0.2	<0.1	1.0	0.9	0.1	<0.1	0.2	0.2	4.9	<0.1	2.0
	Hf	2.6	2.2	2.8	2.3	2.4	2.7	3.0	3.2	2.9	3.0	3.0	2.8	2.6	2.8	2.8	3.1	3.2	2.6	3.2	2.5
	Nb	8.0	6.3	8.1	7.2	7.2	8.5	8.1	8.8	7.9	8.3	9.1	8.4	7.7	9.4	9.3	8.7	8.7	7.9	9.7	7.6
	Rb	9.9	6.5	13.0	10.9	9.3	9.7	10.9	10.6	10.2	12.6	12.0	10.7	10.2	11.8	10.3	10.8	11.5	8.9	11.5	8.7
	Sr	259.5	278.3	249.3	268.8	252.7	290.3	305.9	268.0	276.0	269.1	342.0	260.0	250.1	269.3	239.6	258.7	272.6	238.9	297.0	292.1
	Ta	0.4	0.4	0.4	0.4	0.4	0.5	0.5	0.4	0.5	0.5	0.6	0.5	0.5	0.5	0.6	0.3	0.6	0.5	0.7	0.5
	Th	1.0	0.8	1.0	0.8	0.8	1.2	1.7	1.5	0.9	1.4	2.4	1.0	0.9	2.2	1.2	1.2	1.1	0.9	3.1	0.9
	Zr	104.7	82.2	106.8	90.4	91.9	104.0	105.0	115.2	101.9	106.1	110.3	109.7	98.9	114.4	111.8	111.8	114.5	103.8	116.3	95.6
	Y	22.1	16.5	22.7	18.9	19.5	21.7	22.9	22.2	20.2	22.9	23.2	23.7	21.4	22.1	23.4	24.3	23.7	20.6	24.8	21.3
REE (ppm)	La	12.1	9.0	11.4	10.2	10.4	11.2	13.1	12.3	11.3	11.6	12.6	12.1	10.8	13.9	12.6	12.0	13.3	10.7	14.3	10.5
	Ce	25.8	19.5	24.6	22.7	22.1	23.9	28.2	27.3	25.2	25.8	28.6	27.8	24.7	29.4	28.5	27.1	28.8	24.3	31.3	23.0
	Pr	3.42	2.64	3.35	2.95	2.90	3.26	3.58	3.65	3.17	3.37	3.62	3.60	3.20	3.85	3.64	3.66	3.72	3.25	4.05	3.10
	Nd	14.9	11.6	15.1	13.2	12.7	14.1	15.4	16.5	13.2	16.0	16.7	15.8	14.1	16.6	14.9	16.4	16.6	14.1	17.5	13.7
	Sm	3.66	2.83	3.52	3.07	3.18	3.55	3.63	4.05	3.21	3.77	3.90	3.87	3.47	3.82	3.73	4.06	4.15	3.48	4.20	3.35
	Eu	1.26	1.02	1.20	1.11	1.16	1.25	1.29	1.34	1.25	1.33	1.28	1.25	1.21	1.30	1.24	1.33	1.34	1.17	1.29	1.32
	Gd	4.05	3.15	4.07	3.55	3.59	4.09	4.17	4.35	3.72	4.19	4.47	4.31	3.98	4.33	4.35	4.21	4.42	3.99	4.58	3.86
	Tb	0.68	0.52	0.68	0.57	0.59	0.67	0.72	0.75	0.66	0.71	0.74	0.70	0.65	0.75	0.71	0.76	0.75	0.66	0.78	0.65
	Dy	4.27	3.21	4.08	3.47	3.51	3.91	4.33	4.37	3.90	4.28	4.36	4.30	3.83	4.53	4.14	5.00	4.64	4.00	4.37	3.92
	Ho	0.84	0.67	0.83	0.73	0.74	0.86	0.88	0.84	0.81	0.80	0.83	0.84	0.80	0.89	0.83	0.85	0.93	0.82	0.97	0.78
	Er	2.22	1.74	2.28	1.93	2.02	2.20	2.48	2.35	2.34	2.30	2.52	2.29	2.07	2.46	2.34	2.57	2.41	2.17	2.66	2.08
	Tm	0.34	0.26	0.32	0.28	0.30	0.33	0.35	0.38	0.30	0.33	0.35	0.35	0.33	0.36	0.36	0.37	0.37	0.33	0.35	0.31
	Yb	1.94	1.61	2.01	1.73	1.76	1.99	2.14	2.20	2.03	2.20	2.31	2.02	1.94	2.28	2.14	2.32	2.30	1.98	2.43	1.88
	Lu	0.32	0.25	0.32	0.26	0.27	0.33	0.34	0.33	0.30	0.32	0.34	0.33	0.29	0.35	0.34	0.34	0.35	0.30	0.36	0.31

Table 5 continued.

	Sample	KP11a	KP14b	KP111b	KP111C	KP112	KP14a	IR1	IR7a	IR3	IR23	KP111a	KP116	IR5	IR6	IR26a	KP11b	KP12	IR24	IR7c
	Mapunit	*hz*	*hz*	*hz*	*hz*	*hz*	*hz*	*hz*	*hz*	*hz*	*hz*	*hz*	*hz*	*hz*	*hz*	*hz*	*hz*	*hz*	*hz*	*hz*
Major-minor element (%)	SiO2	46.88	47.97	49.31	47.82	47.45	48.53	48.84	47.86	48.48	48.23	48.58	47.87	48.02	51.59	49.02	53.14	51.11	58.93	48.47
	Al2O3	17.29	18.47	14.02	17.28	18.31	14.25	14.74	14.79	14.63	15.39	12.69	14.95	10.78	13.62	13.30	13.76	11.64	10.81	10.49
	Fe2O3	12.13	11.28	9.71	10.49	11.09	13.13	12.29	13.75	12.11	12.52	10.06	11.78	19.89	12.58	13.25	12.29	16.71	13.45	16.05
	MgO	4.20	3.88	5.98	5.88	4.44	4.47	5.24	5.48	5.38	5.01	7.23	5.76	3.90	5.12	4.67	1.73	2.61	1.97	2.42
	CaO	9.86	10.88	13.12	9.82	10.73	9.66	7.39	9.08	8.42	8.92	13.58	10.17	4.71	7.35	9.80	7.65	6.86	3.28	13.96
	Na2O	2.78	2.71	2.95	2.96	2.70	4.05	4.39	2.86	3.67	3.31	2.53	3.79	4.05	4.01	3.96	2.95	3.59	2.60	0.07
	K2O	0.58	0.53	0.76	0.47	0.47	0.34	0.80	1.23	1.35	1.44	0.43	0.62	0.73	1.33	0.81	2.27	1.53	2.76	0.32
	TiO2	1.92	1.77	1.71	1.28	1.77	2.06	1.94	2.47	1.84	1.84	1.76	1.42	3.71	2.22	2.11	1.53	2.99	2.16	2.74
	P2O5	0.18	0.18	0.15	0.13	0.17	0.19	0.13	0.15	0.17	0.19	0.14	0.08	0.32	0.17	0.17	0.47	0.65	0.60	0.55
	MnO	0.16	0.15	0.17	0.16	0.16	0.19	0.21	0.23	0.19	0.20	0.19	0.18	0.21	0.22	0.19	0.15	0.24	0.18	0.16
Base metals (ppm)	Sc	27	25	44	26	27	35	34	36	34	33	50	43	33	40	34	15	28	21	26
	V	237	229	346	217	233	327	319	438	304	291	389	331	240	395	385	50	129	59	86
	Co	41.9	39.7	36.4	46.3	39.0	43.3	41.4	43.8	41.6	44.3	37.2	45.5	44.3	38.6	41.0	25.7	34.2	20.2	33.6
	Ni	24.4	23.6	14.4	56.1	29.3	17.4	21.5	17.8	25.6	26.7	13.1	26.8	5.9	11.9	14.7	6.5	6.7	3.5	3.9
	Cu	145.4	137.6	161.2	99.6	124.6	114.2	149.3	176.6	33.3	92.9	102.2	56.9	112.0	140.8	192.8	147.2	214.2	651.0	26.8
	Pb	1.9	1.2	2.2	1.6	2.4	4.0	2.1	2.0	3.1	3.3	1.5	1.4	3.0	2.2	3.7	6.1	6.9	4.5	8.1
	Zn	89	58	45	53	68	77	108	69	84	96	40	45	121	87	88	96	126	120	100
	Mo	0.3	0.3	0.7	0.2	0.3	0.7	0.2	0.1	0.3	0.6	0.3	0.2	0.5	0.2	0.5	1.0	1.4	0.8	0.9
	Ga	22.7	20.5	17.0	18.0	20.6	20.2	16.5	18.9	19.0	20.2	13.8	18.2	18.9	16.3	22.5	28.1	27.5	20.7	27.4
LILE-HFS (ppm)	Ba	205	176	167	157	169	84	190	593	563	1073	128	190	101	542	246	626	299	702	52
	Cs	0.4	1.5	<0.1	0.3	0.2	0.1	<0.1	<0.1	<0.1	0.3	<0.1	0.5	<0.1	<0.1	<0.1	0.4	0.3	<0.1	<0.1
	Hf	4.9	3.8	3.3	2.4	3.5	4.4	3.3	4.4	4.3	4.0	2.9	2.1	8.3	4.2	4.9	17.4	14.5	14.5	9.1
	Nb	14.3	12.1	10.2	6.9	10.7	12.8	9.7	13.2	13.1	10.9	8.9	5.7	26.3	12.3	13.5	36.9	54.9	43.8	29.2
	Rb	15.8	14.9	10.8	11.9	13.0	8.3	15.1	29.0	31.4	37.5	6.8	13.6	9.2	32.3	14.9	43.9	36.0	55.6	4.3
	Sr	283.5	329.3	274.4	343.5	311.2	135.9	195.6	273.2	511.4	509.7	223.9	371.0	46.2	292.0	153.0	86.8	101.7	174.3	47.6
	Ta	0.9	0.8	0.6	0.4	0.7	0.9	0.5	0.8	0.8	0.7	0.6	0.4	1.5	0.8	0.8	2.2	2.9	2.6	1.7
	Th	2.2	1.7	1.1	1.0	1.4	1.6	1.3	1.6	1.8	1.5	1.1	0.6	3.1	1.5	2.0	9.2	6.2	6.5	3.9
	Zr	184.8	142.6	127.1	94.4	134.0	173.3	122.9	164.3	168.6	149.6	114.7	75.7	311.4	159.2	180.7	702.9	571.5	572.6	348.2
	Y	33.7	29.4	28.4	18.8	26.3	34.3	26.0	31.6	33.2	30.7	27.3	19.3	57.4	31.4	34.9	90.4	101.5	93.6	70.8
REE (ppm)	La	20.8	16.6	13.7	10.8	15.2	18.1	12.4	16.6	18.1	16.9	12.5	7.7	27.9	15.7	18.3	60.7	61.8	67.5	46.4
	Ce	45.9	36.7	30.7	24.6	34.4	40.2	28.6	37.7	39.7	36.9	27.9	19.1	66.7	36.3	41.4	135.1	137.6	140.0	99.4
	Pr	5.84	4.88	4.18	3.04	4.37	5.22	3.85	4.98	5.36	4.88	3.79	2.52	9.27	4.69	5.35	16.58	18.25	17.86	12.98
	Nd	24.9	21.2	19.3	13.4	19.0	21.8	16.7	20.9	23.0	21.4	16.8	11.6	40.7	20.0	24.2	69.1	80.3	75.7	55.8
	Sm	5.86	4.97	4.61	3.28	4.52	5.59	4.28	5.30	5.51	5.54	4.33	3.15	9.69	5.02	6.01	15.46	17.93	18.02	12.58
	Eu	1.80	1.63	1.53	1.25	1.51	1.75	1.45	1.63	1.73	1.82	1.34	1.35	2.69	1.59	1.85	3.25	3.73	4.11	3.49
	Gd	6.34	5.52	5.16	3.70	5.03	6.17	4.85	5.92	6.33	6.07	4.89	3.74	10.90	5.86	6.62	16.34	18.88	18.70	13.67
	Tb	1.06	0.91	0.87	0.63	0.82	1.03	0.80	0.99	1.03	1.01	0.83	0.62	1.86	0.99	1.09	2.76	3.15	3.17	2.20
	Dy	6.16	5.54	5.23	3.56	4.76	6.14	4.78	5.84	6.06	5.75	4.99	3.66	10.93	5.82	6.51	16.66	18.44	18.89	12.99
	Ho	1.29	1.08	1.04	0.73	1.00	1.28	0.99	1.22	1.24	1.22	0.98	0.76	2.25	1.19	1.33	3.57	3.80	3.69	2.60
	Er	3.46	2.93	2.80	2.06	2.71	3.47	2.62	3.22	3.33	3.34	2.76	2.02	5.67	3.22	3.86	9.46	10.29	9.97	6.86
	Tm	0.53	0.43	0.42	0.29	0.40	0.48	0.39	0.48	0.50	0.43	0.40	0.29	0.89	0.47	0.53	1.46	1.54	1.44	1.05
	Yb	3.07	2.64	2.47	1.71	2.46	2.94	2.37	2.84	2.95	2.80	2.37	1.73	5.29	2.90	3.38	8.71	8.98	9.57	6.29
	Lu	0.49	0.41	0.39	0.27	0.37	0.47	0.38	0.45	0.49	0.45	0.37	0.28	0.84	0.45	0.50	1.34	1.38	1.42	0.98

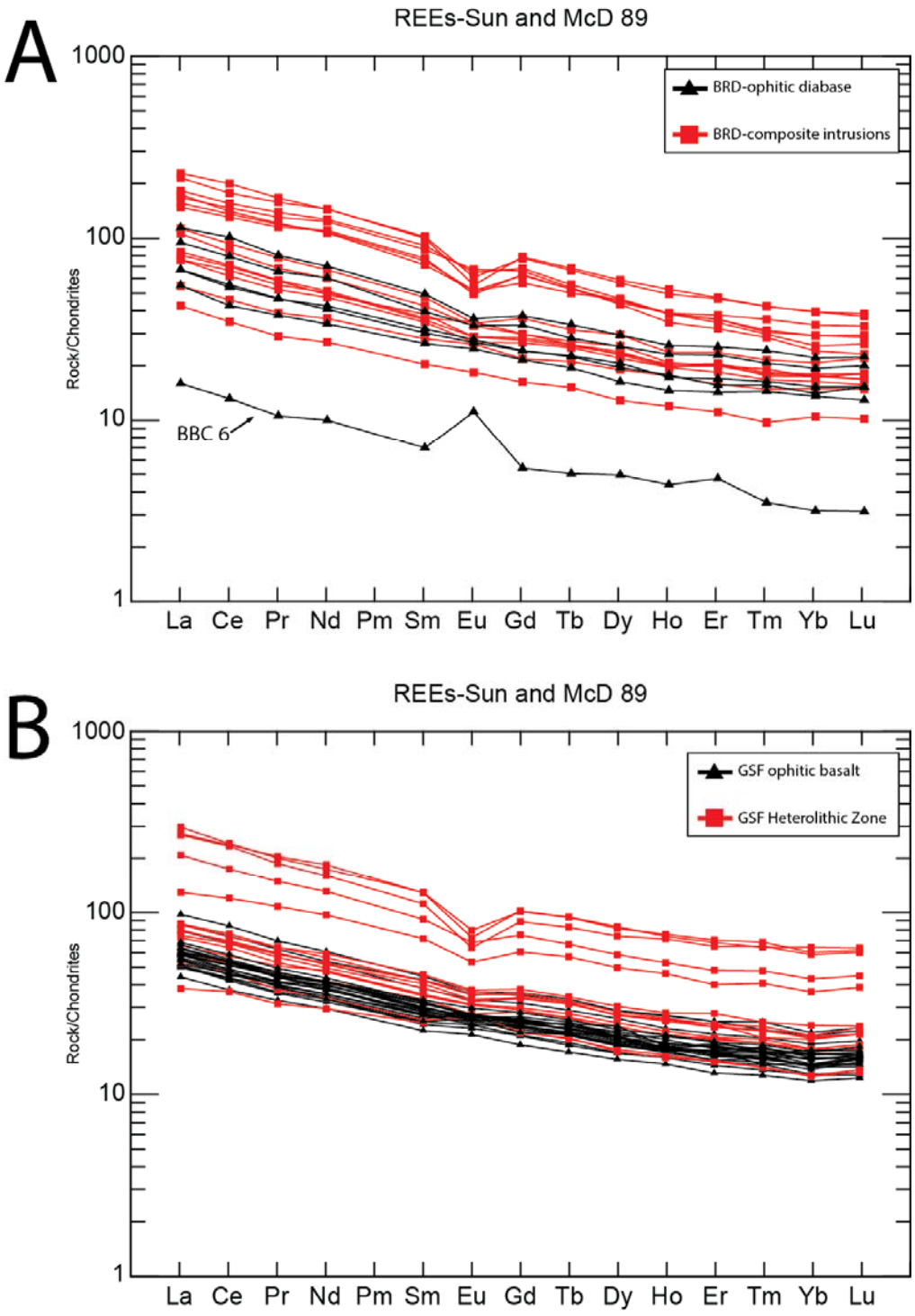

Figure 39. Chondrite-normalized spider diagram of REE concentrations for BRD and GSF sample suites. Normalizing values from Sun and McDonough (1989).

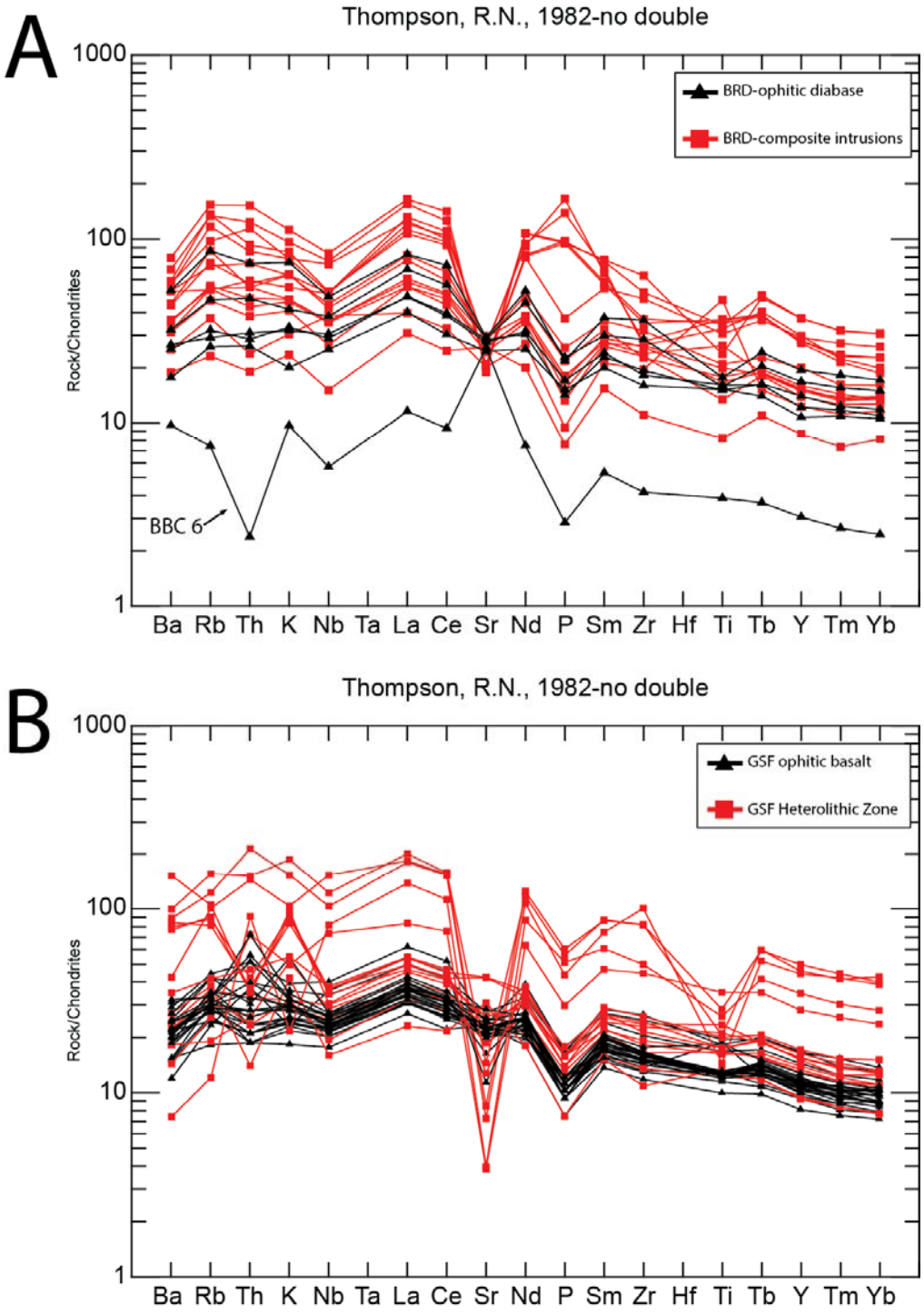

Figure 40. Multi-element spider diagram of incompatible trace element and REE concentrations from BRD-SBI and GSF samples. Chondrite normalization values are from Thompson (1982).

4.0 DISCUSSION

The field relationships, lithological attributes, mineral chemistry, and whole-rock lithogeochemistry of the BRD intrusions and GSF lava flow have been studied in order to test the validity of an intrusive-volcanic link between these two igneous systems. Several aspects of these systems will be compared, evaluated, and discussed here to test this link. Firstly, field, petrographic, and geochemical data on the various lithologies comprising the GSF will be evaluated to assess its emplacement and crystallization history. In particular, these data and field observations of contact relationships of various lithologies within the GSF will be evaluated to determine whether they were produced by *in situ* differentiation, as others have suggested (e.g. Broderick, 1935; Cornwall, 1951), or by composite emplacement of progressively more evolved magmas as has been interpreted for the BRD and its composite intrusions by Miller and coworkers (Miller, 1988; Miller et al., 1993, 1994, Miller and Chandler, 1997; Miller and Green, 2002). The second part of the discussion will compare lithologic, mineral chemical, and lithogeochemical data of both systems to evaluate the plausibility of a comagmatic link between the BRD and GSF. If such a link can be established, the final discussion will consider the implications for the BRD dikes and sills acting as the intrusive feeder system for the GSF in terms of the incredible volume of magma involved in this intrusive-volcanic event.

4.1 Emplacement and Crystallization History of the GSF

Field mapping and petrographic data, presented in the previous chapter, show that the GSF is composed of a suite of variably fractionated lithologies that are generally similar to those found in the BRD-SBI dikes and sills. While the composite nature of the

BRD-SBI has been previously demonstrated (Gehman, 1957; Shank, 1989; Miller and Chandler, 1997; Miller and Green, 2002), all previous workers have consistently championed the idea that the various lithologies comprising the interior of the GSF (Pegmatitic Zone of Cornwall, 1951; Heterolithic Zone of this study) are related to *in situ* differentiation of a single large lava eruption. Lane (1893, 1911) was the first to propose such a model, though it was Broderick (1935) and, later, Cornwall (1951), who cited geochemical evidence to show that the lithologies in the interior of the flow could be derived by the differentiation of a parental magma similar in composition to the GSF ophitic basalts and who speculated about how the coarser and more prismatic textures of this zone may have formed by *in situ* processes. Subsequent studies of the GSF by Huber (1973) and Longo (1984) accepted Cornwall's model, but did not attempt to test it further. If the GSF indeed formed from *in situ* differentiation of a singular eruption, whereas the BRD-SBI formed largely by composite emplacement of variably evolved magmas, this strongly argues that the two systems are unlikely to be comagmatic. Therefore, before evaluating the plausibility that the two systems are linked, it is first necessary to more closely examine field, petrographic, and geochemical data of the GSF to determine a plausible estimate of the GSF parent magma and whether its differentiation gave rise to the various lithologies internal to the GSF either through *in situ* processes or through fractionation in a crustal chamber that periodically vented to the surface.

4.1.1 Composition of the GSF Chilled Margin

Because basaltic lava flows cool relatively rapidly, especially at their upper and lower margins, segregation of crystals from liquid (fractionation) is unlikely. As such, analyses of chilled samples from near the lower contact that are relatively unaltered and free of amygdules or phenocrysts should yield compositions that closely approximate the composition of the initially erupted lava – the parent magma.

Fortunately, the existence of aphyric, amygdule-free, unaltered chilled margins at the upper and lower contacts of the GSF provides a reasonable proxy for the original liquid composition of the parent magma. Because the basal contact of the GSF is not observed in any of the mapping locations, four samples of the lowermost portions of the Lower Ophitic Zone on Isle Royale and the Keweenaw Peninsula and one sample of the Entablature from the Keweenaw Peninsula were chosen as close approximations of the GSF chilled margins. The major and minor element compositions of these samples and their average are listed in Table 6 (full analyses are listed in Appendix C). Samples of the Lower Ophitic Zone are a reasonable representation of the earliest erupted material given their fine grain size, relatively low stratigraphic positions, and lack of significant alteration or amygdules. The sample of the Entablature (Table 6, sample KP19) was included because of its similar chemical composition to the ophitic basalts, lack of significant alteration or amygdules (Fig. 34A).

Table 6. Major and minor element compositions use to estimate the GSF parent magma composition. Includes four Lower Ophitic Zone samples and one Entablature sample collected during this study. Also listed is the bulk composition of the GSF calculated by Broderick (1935) and a GSF chilled margin composition reported by Cornwall (1951). All compositions are normalized to 100%. Mg# = $MgO/(MgO+FeO^T)$ * 85%, mole %.

Sample	KP1 (Keweenaw Peninsula)	KP101 (Keweenaw Peninsula)	IR15 (Isle Royale)	IR20 (Isle Royale)	KP19 (Keweenaw Peninsula)	Avg. GSF Chill	Bulk GSF (Broderick, 1935)	GSF Chill (Cornwall, 1951)
SiO_2	48.6	49.0	49.2	49.1	48.8	48.9	49.2	50.7
TiO_2	1.34	1.38	1.37	1.43	1.40	1.38	1.59	2.11
Al_2O_3	16.6	16.5	16.6	16.3	16.4	16.5	17.5	14.5
FeO^T	11.9	11.9	11.9	11.9	11.9	11.9	11.1	12
MgO	8.35	8.36	7.97	7.93	8.25	8.17	6.9	7.95
CaO	10.4	9.9	9.9	10.3	10.3	10.2	10.2	7.26
Na_2O	2.24	2.32	2.38	2.32	2.27	2.30	2.73	2.36
K_2O	0.36	0.38	0.47	0.43	0.36	0.40	0.5	2.73
P_2O_5	0.12	0.12	0.11	0.12	0.13	0.12	0.19	0.24
MnO	0.16	0.17	0.17	0.17	0.16	0.17	0.18	0.18
Total	100	100	100	100	100	100	100	100
mg#	59.4	59.5	58.4	58.3	59.2	59.0	56.6	58.1

Table 6 also shows the bulk composition of the GSF as calculated by Broderick (1935). The bulk composition was calculated by averaging the chemical compositions of 154 samples taken at regular intervals from drill core profiling the entire flow. Each sample was weighted according to the stratigraphic thickness of its representative lithological unit and by its specific gravity. Although the composition of the GSF chilled margin and the bulk GSF composition calculated by Broderick are generally similar, there are several notable inconsistencies between the two. These inconsistencies will be discussed in the following section and include an overall enrichment in TiO_2, Na_2O, K_2O, and P_2O_5 and depletion in MgO in the bulk composition relative to that of the chilled

margin (Table 6). The table also shows the composition of a chilled margin sample analyzed by Cornwall (1951), however, there are several discrepancies between this composition and that of the estimated GSF chilled margin. Although the differences in Al_2O_3, TiO_2, CaO, and P_2O_5 in Cornwall's chilled sample are inexplicable, the elevated concentrations of SiO_2 and K_2O suggest that this sample likely experienced some dueteric alteration or contamination from underlying conglomerate country rocks. Cornwall (1951) did not provide a petrographic description of the sample but, based on the anomalous geochemical signature, excluded it from his study.

4.1.2 Differentiation of the GSF from a Single Parent Magma

Before assessing whether the ophitic basalts and intermediate rocks in the GSF interior formed by *in situ* differentiation or composite intrusions from a staging chamber, it is first necessary to more rigorously establish whether the various rock types can be related to a common parent magma corresponding to the GSF chill composition (Table 6). Broderick's (1935) and Cornwall's (1951) interpretation that the variably evolved lithologies in the interior of the GSF can be produced by *in situ* differentiation of the magma parental to the ophitic basalts was based largely on general evaluations of the mineralogy and major and minor element compositions of the various rock types. The lithogeochemical data collected for this study lead to similar conclusions of comagmatism.

A comparison of the basic geochemical attributes of the proposed GSF parent magma (Table 6) to other MCR volcanic compositions is shown on an AFM diagram in Figure 41. Green (2002) compiled the compositions of several hundred North Shore

Volcanic Group lavas and subdivided the data into seven tholeiitic compositional fields: primitive olivine basalt, olivine tholeiite, transitional basalt, andesite, ferroandesite, icelandite, and rhyolite. Also plotted on Figure 41 are the AFM compositions of 47 Portage Lake Volcanic Group lava flows collected on the Keweenaw Peninsula and reported by Paces (1988).

The proposed GSF parent magma composition plots at the median position of the olivine tholeiite field of the NSVG and the olivine tholeiitic basalts of the PLV (Fig. 41). This shows that the GSF magma was significantly evolved from the most primitive olivine tholeiites generated by the MCR plume. The compositions of the various GSF rock types define a tholeiitic differentiation trend typical of MCR basalts with compositions ranging from olivine tholeiite to transitional basalt to ferroandesite. One sample from Isle Royale (sample IR7C; Fig. 41), displays extreme Fe-enrichment and very low concentrations of alkalis. This sample was collected from a heterogeneous ferromonzodiorite outcrop at the Blake Point mapping location which contained abundant inclusions of amygdaloidal basalt (Fig. 31B and D). Petrographic analysis shows that this sample was highly altered and contained high abundances of chlorite and quartz-filled amygdules which may explain the anomalous major element chemistry.

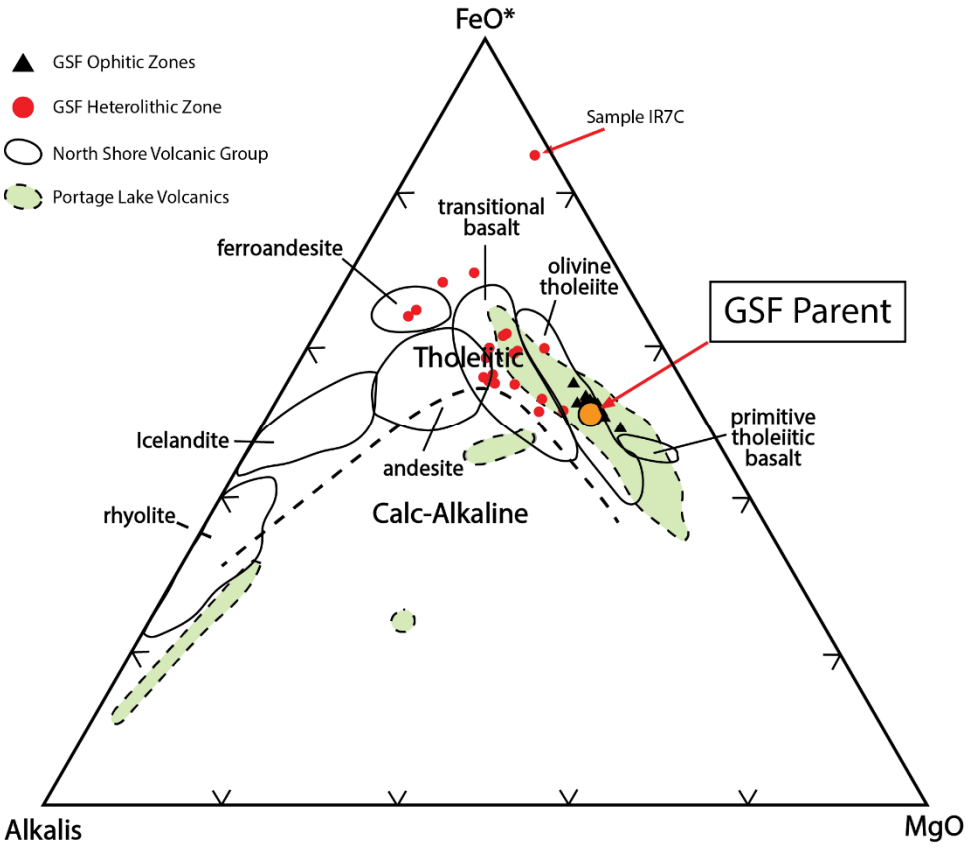

Figure 41. AFM diagram comparing the compositions of the proposed GSF parent magma to average compositions of tholeiitic lavas of the North Shore Volcanic Group and the Portage Lake Volcanic Group (PLV). Tholeiite and calc-alkaline composition boundary (heavy solid curve) after Irvine and Baragar (1971). Compositional fields for NSVG lavas are from Green (2002) and composition fields for the PLV volcanics (green shaded areas) are from Paces (1988). Also plotted are compositions of GSF samples from the ophitic and heterolithic zones analyzed for this study. FeO* = FeO+0.9*Fe2O3 as mole%.

The differentiation trend evident in the AFM compositions of GSF lithologies (Fig. 41) is also evident in plots of P_2O_5 and TiO_2 vs. mg# shown in Figure 42. The ophitic basalts of the *loz* and *uoz* plot in tight clusters around the proposed GSF parent magma composition while the variably evolved rocks of the *hz* show a distinct negative correlation between mg# and P_2O_5 and TiO_2 (Fig. 42). Several samples of ophitic basalt (samples KP10, KP11A, KP14B, KP112, and IR1) collected within the *hz* show elevated

abundances of both TiO_2 and P_2O_5 relative to the basalts collected from the Ophitic Zones (Figure 42) and overlap with the *hz* gabbros and ferrodiorites. Each of these samples was collected in close stratigraphic proximity to more evolved lithologies within the *hz* and the elevated levels of both TiO_2 and P_2O_5, as well as the lower mg#'s, of these samples compared to ophitic basalts from the *loz* and *uoz* might indicate some degree of assimilation of the more evolved magmas which would have created the intermediate rocks. The distribution of both TiO_2 and P_2O_5 suggests that the various rocks in the GSF are related by differentiation of a magma similar in composition to the proposed GSF parent magma composition. However, had this differentiation occurred *in situ*, a more continuous, linear trend would be expected in the data plots. Instead, the non-linear, clustered data distributions, particularly the distribution of P_2O_5 vs mg# (Fig. 42B), suggest that this differentiation occurred at depth and the different compositions were compositely emplaced.

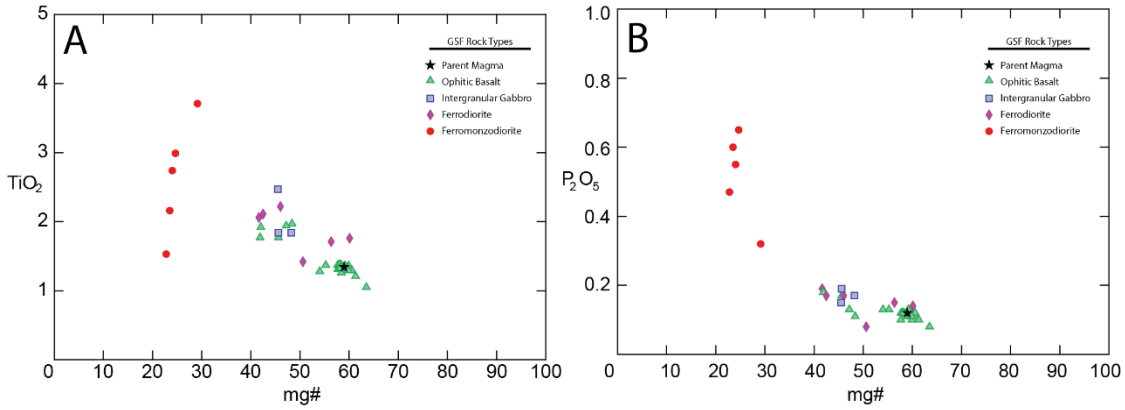

Figure 42. Plots of TiO2 (A) and P2O5 (B) versus mg# showing the subdivision of ophitic basalt and evolved lithologies in the Heterolithic Zone of the GSF.

A comagmatic relationship of GSF lithologies to the proposed parent magma is even more evident when evaluating trace element data and REE data in particular. By being

incompatible in primary mafic minerals (save Eu in plagioclase), the absolute abundances of REE increase with differentiation, while the relative abundances of REE are minimally affected. In Figure 43, the REE compositions of the various GSF lithologies are normalized to the proposed parent magma composition. As such, the REE patterns of the various GSF lithologies, if derived from the same parent magma, will retain a near-horizontal slope despite increasing in overall concentration. Not surprisingly, ophitic basalt samples generally cluster close and parallel to the unity line indicating little differentiation within the ophitic zones. The occurrence of normalized ophitic basalt values below the unity line is likely related to the presence of REE-poor olivine phenocrysts and/or plagioclase megacrysts. The presence of plagioclase megacrysts is implied by the slightly positive Eu normalized abundance in some ophitic basalt samples. One sample of ophitic basalt from the *hz* on the Keweenaw Peninsula (sample KP11A; Fig. 43) displays significant REE-enrichment relative to the other ophitic basalt samples. As discussed above, this sample was collected very near the contact with more intermediate rocks in the *hz* and contains high abundances of felsic mesostasis (~5%) which may indicate assimilation of evolved liquid from the intermediate magma.

The rocks of the *hz* show much greater variation in enrichment of REE relative to the parent magma (Fig. 43). However, that the REE patterns remain horizontal to slightly LREE-enriched and coparallel is consistent with their being related to the proposed parent magma by magmatic differentiation. Subophitic to intergranular gabbro samples from the *hz* cluster just above the unity line and display slightly positive Eu anomalies. This implies that they crystallized from magma only marginally evolved from the ophitic

zone magma. The increasingly negative Eu anomalies and greater overall REE enrichment in ferrodiorites and ferromonzodiorites is also consistent with differentiation of the proposed parent magma which involved the fractional crystallization of plagioclase. A notable exception to these observations of coparallel REE patterns of *hz* samples is sample KP116 (Fig. 43), a well-foliated olivine ferrodiorite (Fig. 33C), which shows overall depletion in REEs relative to the parent magma composition, especially LREE, and a moderately positive Eu anomaly. This result can be attributed to the presence of abundant plagioclase (~60%), as well as the occurrence of coarse-grained olivine phenocrysts (Fig. 33C), which incorporate only negligible concentrations of LREE (Rollinson, 1993).

In summary, the geochemical data presented in this study are qualitatively consistent with the conclusion of earlier workers that the various rock types in the Ophitic and Heterolithic zones are related by differentiation of a single parent magma corresponding to the chilled margin of the GSF (Table 6). However, the geochemical data alone cannot be used to evaluate whether that differentiation occurred *in situ* or in a crustal chamber that periodically vented to inflate the lava sheet.

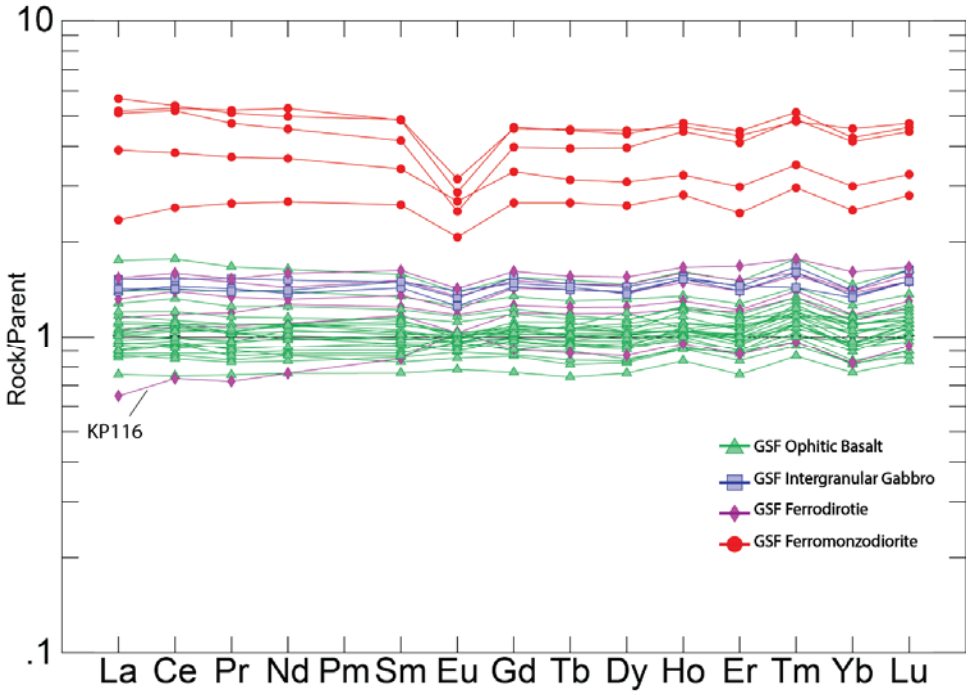

Figure 43. REE data of GSF lithologies normalized to the proposed GSF parent magma composition.

4.1.3 Evidence for Composite Emplacement of the GSF

Having established that the various lithologies of the GSF can be related to differentiation of a common parent magma, the question remains of whether this differentiation occurred *in situ* or in a periodically tapped crustal staging chamber. Three lines of evidence will be discussed below which imply that the latter is the case.

1) Compositional incongruence of the bulk composition of the GSF and parent magma chilled at the GSF margins.
2) The abrupt changes in mineralogy, texture, mineral compositions, and lithogeochemistry observed at the narrow *loz/uoz-hz* contacts; and
3) The occurrence of ophitic olivine basalt inclusions in intermediate rocks of the *hz*.

The method employed by Broderick (1935) to evaluate differentiation of the GSF was governed by the assumption that a quantitative redistribution of the flow constituents could be calculated by comparing the chemical compositions of individual samples of the various GSF lithologies to that of the weighted average composition of the flow, discussed in the previous section. This weighted average presents a convenient, if not quantitatively rigorous, way to perform a mass balance calculation of the GSF to determine if differentiation occurred under closed- or open-system conditions (i.e. *in situ* differentiation or differentiation at depth).

Since closed-system *in situ* differentiation implies that constituents are neither added to nor subtracted from the system, this requires that the GSF parent magma composition, inferred from the chilled margins, and the bulk composition of the GSF, calculated by Broderick (1935), should be the same. Although the compositions of the GSF parent magma and bulk GSF composition calculated by Broderick (1935) are generally similar (Table 6), there are some systematic differences that suggest there is more evolved rock component in the GSF than could be produced by the chilled composition. Comparing the two compositions in Table 6 shows that Broderick's (1935) bulk composition is significantly enriched (> 10%) in incompatible element oxides (TiO, Na_2O, K_2O, and P_2O_5) relative to the proposed parent magma and is significantly depleted (by 19%) in MgO. This result argues that the GSF contains an excess amount of highly evolved magma compositions relative to the parent magma composition implied by the chilled margin.

In an open system, even one fed by a common source that is differentiating as a closed system, the bulk composition of the flow is not required to be equivalent to the parent magma composition. Rather, the bulk composition will depend on the number, volume, and compositions of the various composite units. That the bulk composition is actually close to the parental composition is remarkable and implies that the volcanic system received a rather representative sampling of its deeper evolving staging chamber.

A more compelling argument in favor of open system evolution of the GSF comes from abrupt contact relationships between the major lithologies comprising the GSF. The processes expected from *in situ* differentiation cannot explain, and are in fact inconsistent with, the sharpness and dramatic contrast in mineralogy, texture, and chemistry across the fundamental contacts between major rock types in the GSF in all investigated locations. If *in situ* differentiation of a single large eruption had indeed formed the transition between ophitic basalt to evolved gabbro to intermediate rocks in the core of the GSF, one would expect to observe broadly gradational contact intervals separating these distinct lithological zones over meter to decameter scale. Such gradational contacts are well documented even in well differentiated mafic layered intrusions that cooled very slowly at depth (e.g. Skaergaard, Wagner and Brown, 1968; Sonju Lake, Miller and Ripley, 1996; Kiglapait, Morse, 1969). Given the extensive thickness and aerial extent of the GSF, it is not unreasonable to assume that it would have behaved in a similar fashion were it formed as a single eruption.

Yet, in the locations where the contacts between the major rock types in the GSF have been observed, they are consistently characterized by dramatic changes in texture,

mineralogy, mineral chemistry, and lithogeochemistry over a narrow (centimeter to decimeter) interval. The changes in the attributes across eight well-constrained contacts are summarized in Table 7. Collectively, these attributes are consistent with these being intrusive contacts resulting from the composite intrusion of evolved magma into the semi-crystalline core of an olivine tholeiitic basalt. Figure 45 shows photomicrographs highlighting the contrasting mineralogy and textures of the rocks collected across the lithological contacts listed in Table 7. In each instance, bulk textures are observed to transition from fine- to medium-grained, ophitic in the *loz* and *uoz* basalts to medium- to coarse-grained, anhedral granular to prismatic in the *hz* rocks. The distinctive clustered texture of plagioclase in the ophitic basalt and intergranular gabbro is not exhibited by plagioclase in the intermediate rocks of the *hz*. Olivine, which constitutes 10-20% of the basalts, is virtually absent in the more highly fractionated *hz* rocks. The abundance of felsic mesostasis is also greatly increased in the *hz* rocks relative to the basalts as is the degree of deuteric alteration.

Distinct changes in the mineral chemistry and lithogeochemistry in the rocks across the *loz/uoz-hz* lithological contacts are also noted (Table 7). The En' of augite is observed to decrease form an average of En'_{72} in the *loz* and *uoz* to an average of En'_{55} in the *hz* lithologies. The most dramatic change in En' is between the ophitic basalts and ferromonzodiorites at Blake Point (sample IR7B and IR7C) and Lookout Louise (samples IR19A and IR19B) which show a decrease in the values of En' of 26 and 19, respectively, between the basalts and intermediate rocks. Across all of the lithological contacts, the rocks of the *hz* also have lower mg#'s and are more highly enriched in Zr

and P than in the *loz* and *uoz* basalts. These changes are in stark contrast to the relatively constant La/Sm and Gd/Yb ratios in the rocks across lithological contacts (see also Figure 43). Since the ratio of a pair of highly incompatible elements with similar bulk partition coefficients will not vary in the course of fractional crystallization, the slope of the correlation line between two such highly incompatible elements will reflect the concentration of the elements in the source (Rollinson, 1993). The constant ratios between the LREEs (La/Sm) and HREEs (Gd/Yb) indicates that the contrasting lithologies across contacts share a common source, despite the variation in mineralogy, texture, and mineral chemistry.

Finally, one of the most definitive pieces of evidence supporting the composite intrusive nature of the GSF is the inclusion relationships exposed at the contact between the *loz* and *hz* in the Central mapping location on the Keweenaw Peninsula (Fig. 28A). Here, medium-grained ophitic to subophitic basalt is in abrupt and complex contact with coarse-grained intergranular gabbro of the *hz*. Subangular inclusions of subophitic basalt and a large included block of ophitic basalt of the *loz* occur within coarser-grained, intergranular gabbro host rock. The angular but unchilled contacts (Fig. 28B and C) indicate that sufficient cooling has occurred between the initial eruption and subsequent intrusive pulse of more highly evolved magma to result in the basalt to behaving in a brittle manner, but not enough to cause the intrusive magma to quench. Similar field relationships were used by Miller and others (e.g. Miller, 1988; Miller et al., 1994; Shank, 1989; Miller and Chandler, 1997) as evidence of the composite nature of the BRD-SBI dikes and sills.

Table 7. Mineralogical, textural, mineral chemical, and lithogeochemical attributes of samples collected across contacts between major GSF rock types.

	KEWEENAW PENINSULA				ISLE ROYALE			
	Phoenix *hz / loz*	Phoenix *hz/hz*	Phoenix *hz/uoz*	Central *hz/loz*	Blake Point *hz/uoz*	L.O. Louise *hz/uoz*	Tobin Harbor *hz/loz*	Tobin Harbor *hz/uoz*
Samples	KP7B/KP7A	KP11A/KP11B	KP14A/KP15	KP111A/KP111C	IR7C/IR7B	IR19A/IR19B	IR23/IR22	IR26A/IR26B
Spacing	~1m	1-2cm	~1.5m	~1.5m	~1m	~1m	~1m	~1m
Modal Rock Types	*hz*: olivine ferrodiorite *loz*: olivine basalt	*hz*1: olivine basalt (incl) *hz*2: ferro-monzodiorite	*hz*: alt ferrodiorite *uoz*: olivine basalt	*hz*: olivine ferrodiorite *loz*: olivine basalt	*hz*: qtz ferromonzonite *uoz*: olivine basalt	*hz*: ferro-monzodiorite *uoz*: olivine basalt	*hz*: oxide olivine gabbro *loz*: olivine basalt	*hz*: olivine ferrodiorite *uoz*: olivine basalt
Bulk Texture	*hz*: mcrs, prismatic *loz*: mfine, ophitic (5mm oiks)	*hz*1: med, ophitic *hz*2: crs, prismatic	*hz*: mcrs, prismatic *uoz*: fine, ophitic (5mm oiks)	*hz*: mcrs, prismatic *loz*: med, ophitic (10mm oiks)	*hz*: med, prismatic *uoz*: fine, ophitic (10mm oiks)	*hz*: med, prismatic *uoz*: fine, ophitic (6mm oiks)	*hz*: crs, intergranular *loz*: fine, ophitic (8mm oiks)	*hz*: med, subprismatic *uoz*: fine, ophitic (9mm oiks)
Primary Modal Mineralogy	*hz /loz* Pl:40/50 Ol:0/10 Cpx:45/35 Gpy:5/0	*hz*1/ *hz*2 Pl: 50/35 Ol: 15/0 Cpx: 25/7 Gpy:3/30	*hz /uoz* Pl:40/40 Ol: 0/20 Cp:15/40 Gp:15/0	*hz /loz* Pl:45/55 Ol:0/10 Cpx:40/30 Gpy:7/0	*hz /uoz* Pl:35/40 Ol:0/15 Cpx:25/40 Gpy:40/3	*hz/uoz* Pl:35/40 Ol:5/15 Cpx:10/35 Gpy:0/35	*hz/loz* Pl:40/40 Ol:10/10 Cpx:30/40 Gpy:3/0	*hz/uoz* Pl:50/40 Ol:5/10 Cpx:25/40 Gpy:2/0
En' of Augite	*hz*: 61.4 +/- 2.6 *loz*: 73.5 +/- 5.3	*hz*: 62.0 +/- 7.5 HZ2: 54.6 +/- 2.6	*hz*: 47.8 +/- 0.8 *uoz*: 67.3 +/- 5.0	*hz*: 52.3 +/- 4.8 *loz*: 69.5 +/- 3.7	*hz*: 46.7 +/- 3.5 *uoz*: 72.8 +/- 3.5	*hz*: 54.4 +/- 2.1 *uoz*: 73.3 +/- 3.4	*hz*: 65.4 +/- 4.5 *loz*: 73.2 +/- 5.0	*hz*: 58.8 +/- 3.0 *uoz*: 76.1 +/- 4.6
Lithogeochem	N/A	*hz / hz* mg#:42/23 Zr:185/703 P:786/2051 La/Sm:0.54/0.60 Gd/Yb:0.35/0.32	*hz /uoz* mg#:42/60 Zr: 173/110 P: 829/567 La/Sm:0.50/0.48 Gd/Yb:0.36/0.36	*hz / loz* mg#:54/60 Zr:115/94 P:611/567 La/Sm:0.44/0.50 Gd/Yb:0.35/0.37	*hz /uoz* mg#:24/60 Zr:348/104 P:2400/436 La/Sm:0.56/0.58 Gd/Yb:0.37/0.35	N/A	*hz / loz* mg#:46/58 Zr:150/106 P:829/436 La/Sm:0.47/0.47 Gd/Yb:0.37/0.32	*hz /uoz* mg#:43/58 Zr:181/112 P:742/524 La/Sm:0.47/0.45 Gd/Yb:0.33/0.31

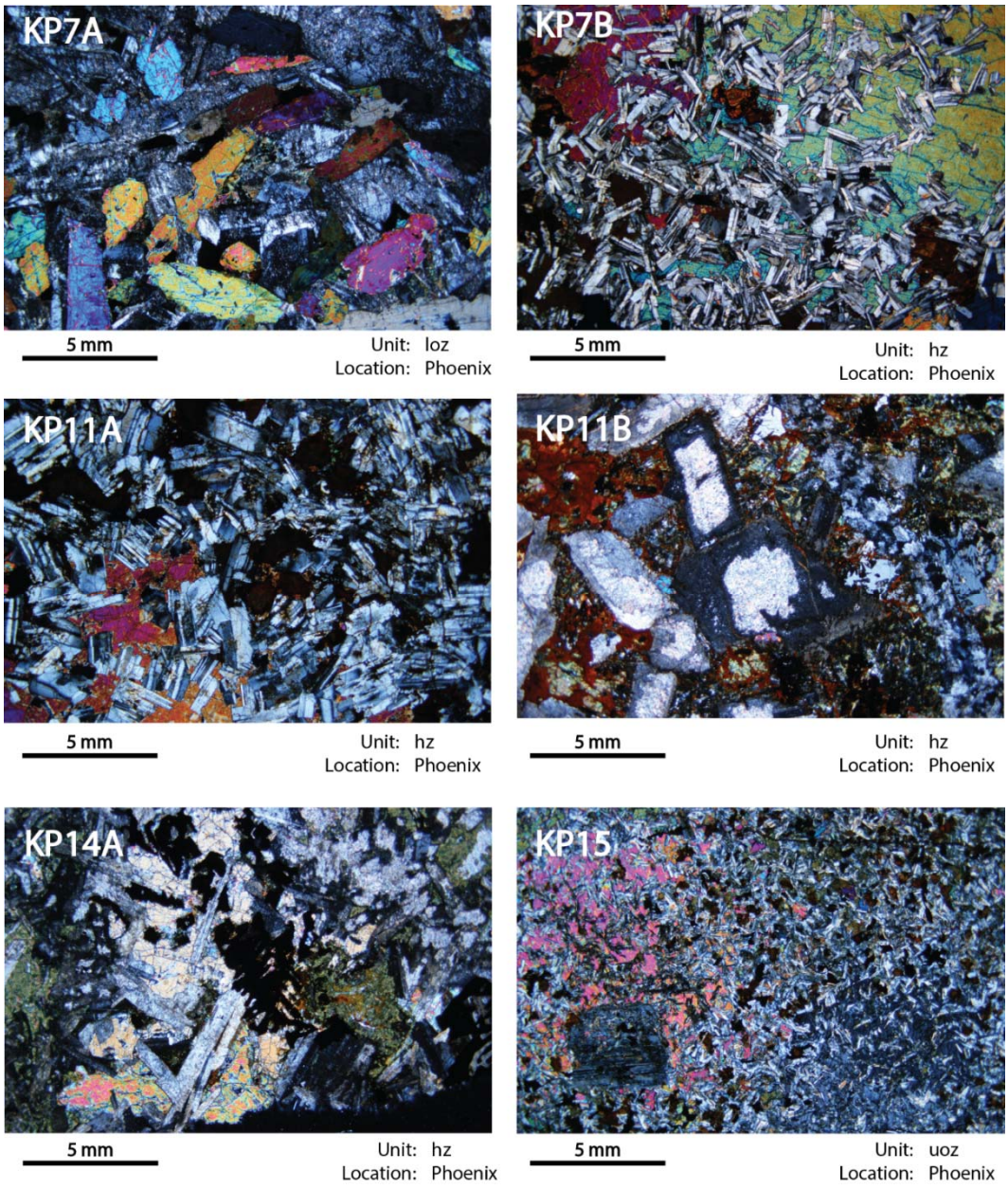

Figure 44. Crossed-polarized photomicrographs showing contrast in mineralogy and textural attributes of rocks across abrupt lithological contacts in the GSF listed in Table 7.

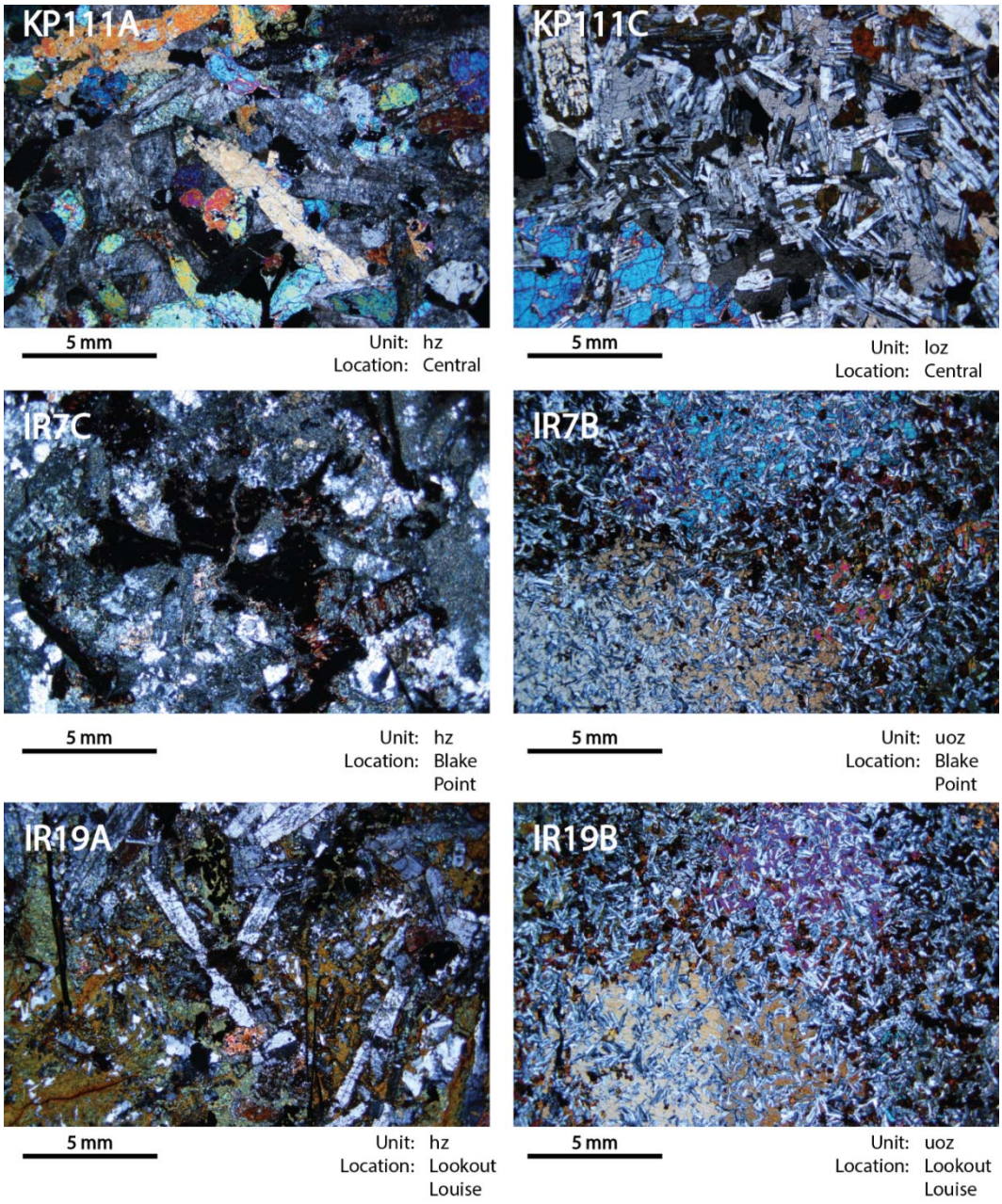

Figure 44 continued.

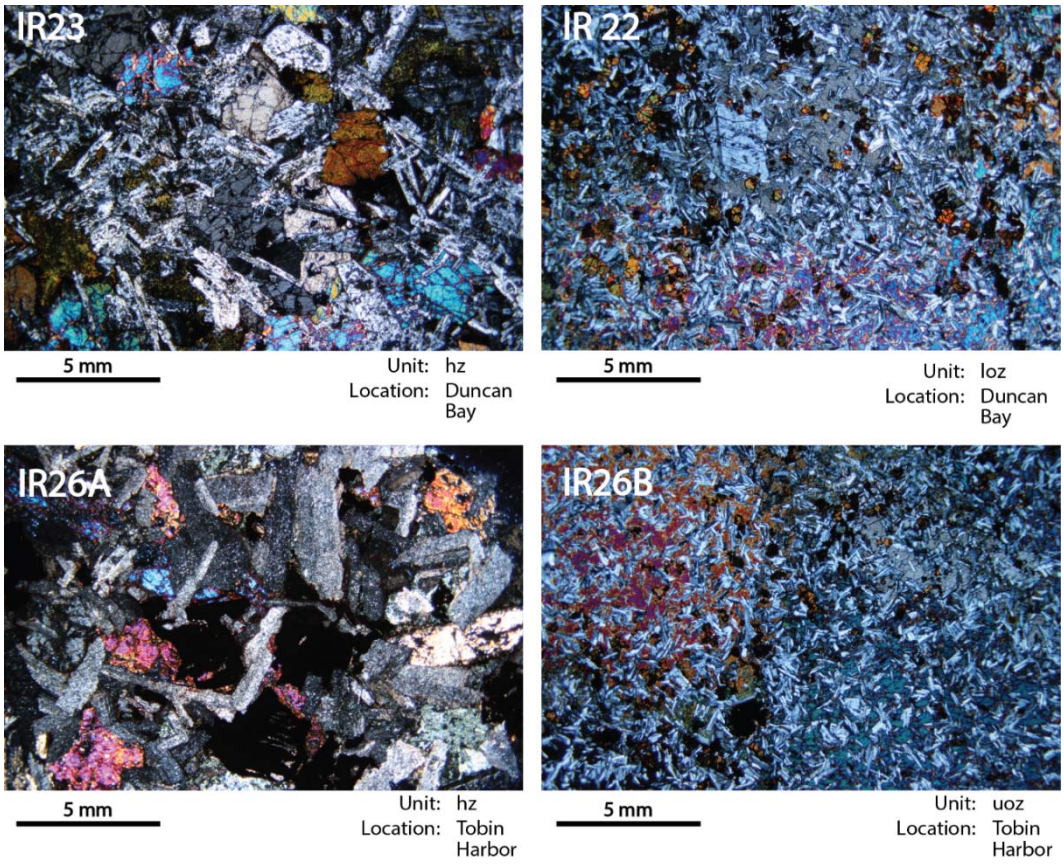

Figure 44 continued.

4.1.4 Composite Emplacement Model for the GSF

The recognition of at least three mineralogically and texturally distinct rock types in abrupt and often complex contact strongly implies that the rocks of the GSF were emplaced sequentially by multiple pulses of magma. The characteristics of the rocks within the *hz*, as well as their abrupt contact relationships to the ophitic basalts of the *loz* and *uoz* (Table 7), are inconsistent with their formation by *in situ* fractional crystallization. Rather, the characteristics and lithological relationships of the GSF on the Keweenaw Peninsula and Isle Royale are better explained by the composite emplacement of progressively evolved magma generated by periodic tapping of a differentiating magma chamber. A three stage model for the emplacement of the GSF is proposed (Fig. 45).

1) **Voluminous Eruption of Olivine Tholeiitic Basalt** – A very large volume of olivine tholeiitic lava erupted across an expansive area of the central MCR rift basin, locally reaching thicknesses of up to 450 meters (Central mapping location; Fig. 23). Rapid cooling at the subaerial contact produced a vesicular (now amygdaloidal), aphanitic basalt that became strongly columnar-jointed – Zone A in Figure 10 from Cornwall (1951). Early crystallization of olivine and plagioclase and later poikilitic augite and Fe-Ti oxide from the olivine tholeiitic magma produced an ophitic texture throughout the early crystallized basalt. However, rapid cooling at the upper and lower contacts produced a strong zoning in the grain size of plagioclase and olivine chadacrysts and augite oikocrysts. Progressive crystallization of the lava produced a gradation in the habit of augite from ophitic to subophitic from the margins to near the still-molten interior of the flow.

2) **Intrusion of Evolved Basalt and Inflation of the GSF** – After crystallization of the initial basalt had created fully crystallized upper and lower ophitic basalt intervals but was still partially molten in its interior, the GSF was intruded and inflated by one or possibly two pulses of more highly evolved basaltic magma. This pulse was emplaced into the semi-molten core of the initial basalt to form the intergranular gabbro in the *hz*. Upon emplacement, this pulse would have incompletely displaced the semi-crystalline interior of the flow to produce the remnant blocks of ophitic basalt scattered throughout the *hz* and the inclusion relationships observed in exposures of the *loz-hz* contact observed at in Central mapping location (Fig. 28A) discussed in the previous section.

The question of whether the variably evolved intermediate rocks in the *hz* (ferrodiorite to ferromonzodiorite) formed by the subsequent *in situ* fractionation of this intrusive magma or were instead emplaced by a separate pulse of more highly evolved magma is problematic due to a scarcity of exposed lithological contacts between the evolved rocks in the *hz*. The inclusions relationships and sharp lithological contacts exposed in the Central mapping location (Fig. 28A) strongly indicate that the first intrusive pulse into the core of the GSF produced a coarse-grained, intergranular gabbroic rock. Although it is reasonable to suppose that the ferrodiorites and ferromonzodiorites could represent the products of *in situ* fractionation of this gabbroic magma, the well-foliated texture (Fig. 33C) and depletion in trace elements (Figs. 39 and 40) observed in ferrodiorite samples suggest that these rocks are cumulates formed by interstitial magma from a mush. Because generating a ferrodioritic cumulate rock from fractionation of a gabbroic magma is contradictory to what is expected to occur during magmatic differentiation, it is reasonable to suppose that the intermediate rocks in the *hz* represent a second intrusive pulse of magma into the GSF.

There is similar uncertainty regarding the formation of the more highly evolved ferromonzodiorite in the *hz*. Although sharp lithological contacts are observed between remnant blocks of subophitic basalt and ferromonzodiorite at the Phoenix mapping location on the Keweenaw Peninsula (Fig. 31E), no physical contacts are exposed between the ferromonzodiorites and the other intrusive lithologies in any of the mapping locations. Abrupt lithological breaks between

intergranular gabbro and ferromonzodiorite are observed in many of the mapping locations (e.g. at Duncan Bay on Isle Royale; Fig. 30), however, such changes in lithology are generally observed over meter scale. Given the cumulate textures observed in the *hz* ferrodiorites and the lack of exposed lithological contacts between the ferromonzodiorites and other intrusive *hz* rocks, it seems most reasonable to assume that the ferromonzodiorites represent highly fractionated residual liquid generated by the earlier formation of the ferrodiorites.

3) **Late Stage Evolved Magma Migration** – When solidification of the GSF was largely complete, with the exception of some localized pockets of evolved, volatile-rich melts, compaction and contraction of the nearly-solid lava sheet likely opened fractures throughout the flow. Into these, the silica- and volatile-rich residual liquids could migrate to form the aplite dikes (Fig. 31E) and coarse-grained segregations (Fig. 29B) scattered throughout the lava sheet. Cornwall (1951) suggested that during this stage of the evolution of the GFS, vapor-rich residual liquids would react with crystalline material to form miarolitic cavity fillings in the rocks of the *hz*. Longo (1984) reported a large (1-2 meter-thick) dike of coarse-grained "pegmatitic" rock (ferromonzodiorite?) cross-cutting the stratigraphy of the Entablature on Isle Royale which he attributed to the accumulation of late-stage, intermediate to felsic magma into sub-vertical gash fractures opened by compaction of the nearly-solid GSF.

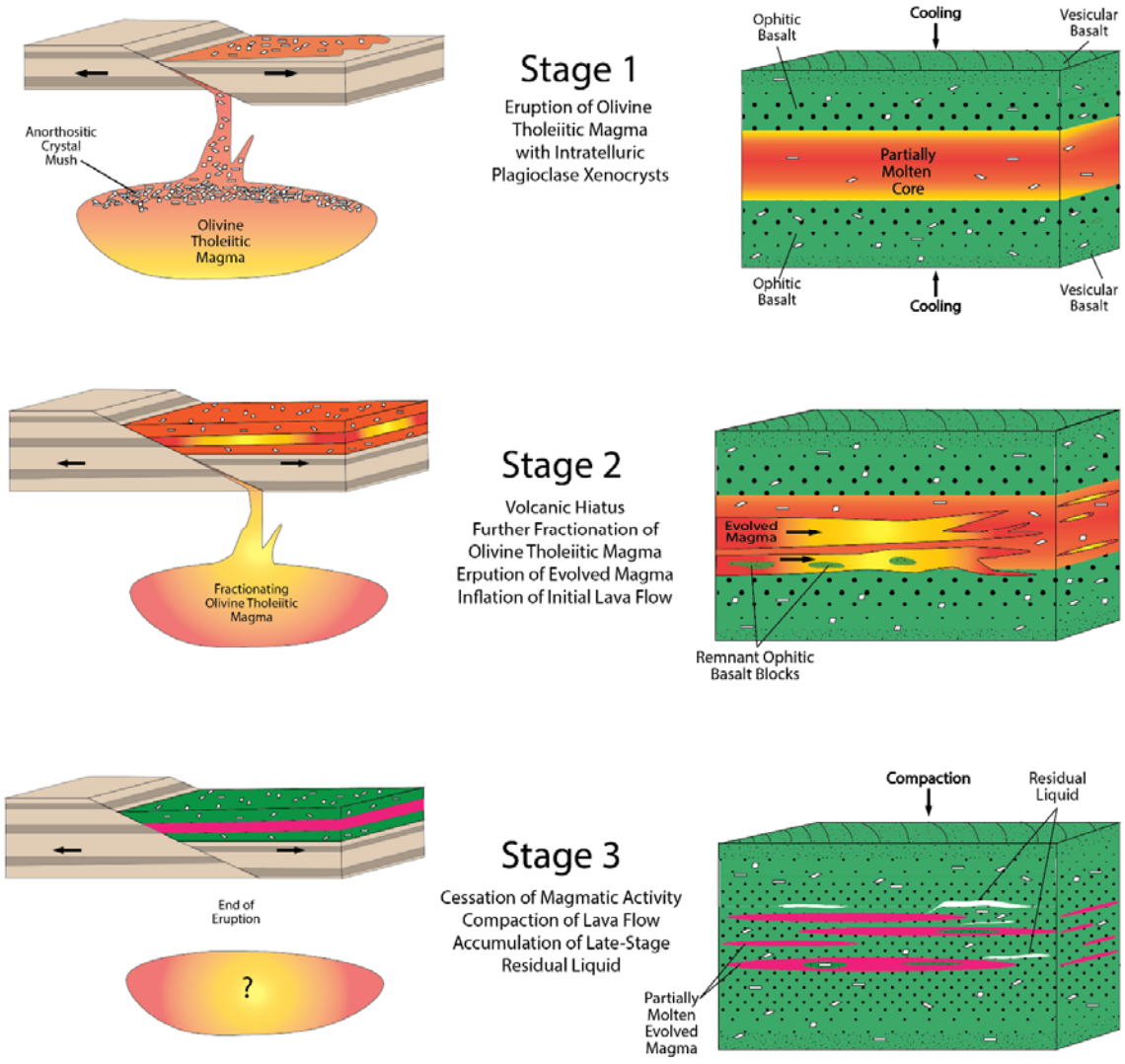

Figure 45. Schematic Diagram illustrating the hypothesized three-stage model eruption and emplacement of GSF flood basalt from proposed BRD feeder system.

4.2 Comparison of BRD-SBI and GSF Lithologies

Concluding that the GSF was formed by the intrusive emplacement of more highly evolved magma into the core of a large olivine tholeiitic lava flow, similar to the intrusive processes interpreted for the composite BRD dikes and sills (Miller, 1988, 1989; Miller et al., 1994; Shank, 1989; Miller and Chandler, 1997; Miller and Green, 2002), now permits a

more direct comparison of the lithological and geochemical attributes of the two systems to test their petrogenetic linkage.

As has been discussed in the previous chapter, the BRD and GSF are composed of a similar continuum of differentiated lithologies. In both the intrusive and volcanic systems, the initial magmatic episode created a relatively homogenous, ophitic olivine tholeiitic rock – olivine diabase in the BRD and olivine basalt in the GSF. Following this initial phase, a subsequent pulse of more highly evolved magma intruded both the diabase dikes and sills and lava flow.

As has been discussed in the previous chapter, the BRD and GSF are composed predominantly of ophitic olivine diabase/basalt. Moreover, the composite intrusions throughout the BRD are composed of a similar differentiated continuum of lithologies as observed in the Heterolithic Zone of the GSF with rock types ranging from intergranular gabbro to ferromonzodiorite. In the southern BBC, this pulse subsequently differentiated *in situ* to form the well-laminated gabbro/diorite (map unit *sblg*, Fig. 15) and a marginal phase of vari-textured ferromonzodiorite (map unit *sbg*, Fig. 15) (Shank, 1989; Miller and Chandler, 1997). Field relationships and textural attributes of the rocks in the GSF-HZ, however, suggest a formation which more closely resembles that of the composite intrusions in the northern BRD. In the northern BRD dikes, two subsequent intrusive pulses are evident (Miller et al., 1994; Miller and Chandler, 1997). The first produced the variably granophyric, intergranular gabbro of map unit *brg* (Fig. 17) and was followed by a second intrusive phase of more highly evolved magma to create the massive to well-laminated ferrodiorites of map units *brfd* and *brld* (Fig. 17), respectively. Similar

occurrences of intergranular gabbro in the GSF-HZ, which is texturally similar to that of the *brg* unit in the NBBC (Fig. 17) observed in abrupt and complex contact with ophitic basalt of the *loz*, suggest that evolved lithologies in this unit were also emplaced during at least two successive intrusive pulses.

In this section, we compare the petrographic attributes, primary mineral chemistry, and whole-rock lithogeochemistry within these intrusive and volcanic systems. In addition, the compositions of plagioclase megacrysts in the GSF will be compared to the compositions of anorthosite inclusions hosted by the BRD. The result of these comparisons supports a comagmatic link between the BRD and GSF.

4.2.1 Comparison of Petrographic Attributes

The petrographic attributes of samples collected from the BRD and GSF for this study and for samples of the BRD collected during the COGEOMAP program are tabulated in Appendix A. In nearly every instance, comparable rock types show only minor, if any, mineralogical or textural differences between the intrusive and volcanic systems (Fig. 46). Such differences are typically limited to the finer grain size and higher degree of deuteric alteration of the GSF rocks.

The primary mineralogy and modal abundances of the BRD ophitic diabase (Fig. 46A) and GSF ophitic basalt (Fig. 46B) are essentially the same, being composed of plagioclase, ophitic augite, olivine, Fe-Ti oxides, and minor abundances (< 5%) of orthopyroxene (hypersthene to inverted pigeonite) and accessory phases such as zircon and titanite. The mode of augite oikocrysts is relatively the same in the diabase (15-35%) and basalt (15-40%); however, the size range of the oikocrysts is distinctly greater in the BRD

(0.5-10 cm) than in the basalt (0.2-2 cm). Locally, both the diabase and basalt (particularly remnant blocks within the *hz*) display more evolved modal mineralogies indicated by minor amounts (< 5%) of felsic mesostasis (micrographic quartz and alkali feldspar) and trace amounts (< 1%) of hornblende and biotite. The occurrence of hornblende and biotite overgrowth rims and as subpoikilitic masses, suggests that these phases are primary and may represent slower cooling experienced by the diabase in the hypabyssal environment and the remnant basalts in the interior of the thick lava sheet which would be more conducive to migration of evolved interstitial melts late in the crystallization period. The ophitic basalts in the *loz* and *uoz* of the GSF contain small amounts of altered volcanic glass (< 10%), which is only rarely observed in the fine-grained, chilled margins of the BRD ophitic diabase. The GSF basalt also tends to be much more highly altered (particularly at Blake Point on Isle Royale) than the diabase which would be expected from hydrothermal processes and weathering in the surficial environment. A similar gradation in the texture of augite from ophitic to subophitic is observed in both the medial portions of BRD dikes and sills (Fig. 46C) and GSF lava sheet (Fig. 46D). Near the contacts with the composite intrusions, the ophitic lithologies in both systems display increased abundances of felsic mesostasis, presumably from filter-pressing of evolved liquids from the composite magma pulses into the semi-crystallized diabase and basalt. Olivine-rich compositions are found near the margins of both the intrusive and volcanic systems, with olivine abundances ranging up to 35% in the diabase and up to 25% in the basalt.

Textural and compositional characteristics of megacrystic and groundmass plagioclase in the diabase and basalt provide the most compelling evidence of their comagmatic

relationship. Although the GSF lacks the large anorthosite xenoliths found in the BRD (Fig. 8), the diabase and basalt both contain centimeter-sized plagioclase megacrysts to polycrystalline aggregates of plagioclase (Fig. 46A and B). The megacrysts in the diabase are generally coarser-grained (<3 cm) than those in the GSF (<1 cm), but single megacryst crystals are typically at least an order of magnitude coarser-grained than the surrounding groundmass crystals in both systems. As will be discussed below, the compositions of these megacrysts correlate well with the calcic compositions of the anorthosite inclusions in the BRD as reported by Miller and others (e.g. Morrison 1983; Miller, 1988, 1989; Miller et al., 1994).

Perhaps the most significant textural characteristic observed in both the BRD ophitic diabase and GSF ophitic basalt is the subparallel clustering of groundmass plagioclase crystals displayed in both systems (Fig. 46A and B). This texture is seemingly unique to the BRD diabase and has not been previously recognized in other intrusive or volcanic rocks in the MCR (Miller, personal communication). The occurrence of this characteristic texture in the GSF ophitic basalt is one of the most compelling pieces of evidence that the BRD and GSF crystallized from a common parent magma.

The commonality of mineralogy and texture extends to the composite lithologies which contain a suite of variably fractionated rocks in both systems with major rock types ranging from intergranular gabbro to ferromonzodiorite (Fig. 46). Intergranular gabbro represents only a minor phase in the SBI composite intrusions in the BRD of the southern Beaver Bay Complex (Fig. 15, map unit *sblg*) and GSF Heterolithic Zone, but comprises a significant portion of the composite intrusions in the BRD in the northern Beaver Bay

Complex. Additionally, the intergranular gabbros in the NBBC are texturally distinct from those in the SBBC by the occurrence of clustered plagioclase laths similar to the texture of plagioclase in the BRD ophitic diabase. The gabbros in both the NBBC and GSF display similar modal mineralogies as the BRD diabase and GSF basalt, but are distinctive in texture in both systems with the abrupt change in the habit of augite from ophitic/subophitic to intergranular (Fig. 46E and F). Plagioclase megacrysts are absent from the intergranular gabbros in each system but groundmass plagioclase crystals retain the distinctive clustering which marks the ophitic lithologies in both the intrusive and volcanic systems (Fig. 46E and F).

As in the case of the mafic lithologies, samples of comparable intermediate rocks from the BRD and GSF are nearly identical in terms of mineralogy and texture (Fig. 46). Ferrodiorite (Fig. 46G and H) and ferromonzodiorite (Fig. 46I and J) comprise the bulk of the intermediate rocks in each system and are composed of tabular to subprismatic plagioclase, prismatic to bladed augite, subhedral to euhedral Fe-Ti oxides, and varying abundances (15-35%) of felsic mesostasis. Olivine is rare in the intermediate rocks in both the BRD and GSF and is typically subhedral and poikilitic in habit. Plagioclase, augite, and olivine in the intermediate lithologies are typically more highly altered than in the mafic lithologies. Augite commonly occurs as poikiloprismatic crystals with abundant inclusions of fine-grained Fe-Ti oxide in the ferrodiorites of each system. Most notably, rather than showing the distinctive clustered textures observed in the ophitic lithologies and intergranular gabbros of the NBBC (*brg* unit, Fig. 46E) and GSF (Fig. 46F), plagioclase in the intermediate rocks in both systems typically displays isolated, subprismatic crystals

that impart a felty texture. Furthermore, as in the gabbroic lithologies, plagioclase megacrysts are absent from the intermediate rocks in both the BRD and GSF. In both the BRD and GSF intermediate rocks, Fe-Ti oxides are finer-grained and more commonly subhedral granular relative to the subpoikilitic oxide in the gabbroic rocks. In the more granophyre-rich monzodioritic rock types in both systems, oxide textures become more variable, occurring as fine-grained subhedral granular crystals, coarse-grained bladed to acicular crystals, and medium- to coarse-grained, skeletal to trellis-patterned overgrowths and interstitial clots.

Figure 46. Crossed-polarized photomicrographs showing similar mineralogy and textural attributes of sample from correlative units of the BRD and GSF systems. A-B) ophitic olivine diabase/basalt, C-D) intergranular olivine oxide gabbro, E-F) well-

foliated prismatic ferrodiorite, and G-H) prismatic ferromonzodiorite between the BRD-SBI composite dikes and sills and GSF composite lava flow. The map unit of each sample is indicated.

4.2.2 Comparison of Mineral Chemistry

Despite the similarities in the field relationships implying composite emplacement and petrographic attributes implying a common range of magma types, these observational data alone are not sufficient to validate an interpretation of a comagmatic link between the BRD and GSF. To provide a more robust evaluation of a link, the geochemical attributes of the various rocks in each system must be compared. If the two systems are comagmatic, the chemical compositions of the primary solid-solution minerals in the BRD-SBI and GSF should reflect the intrinsic chemical characteristics of the magmas from which the various lithologies in each system crystallized.

The range in En-Fs-Wo compositions of pyroxenes in the ophitic and composite lithologies in both the BRD-SBI and GSF, shown in Figure 35, indicate that augite is the dominant pyroxene species in all of the rocks in each system. Since the main variation in pyroxene composition is in the Mg:Fe ratio, an ideal way to evaluate the dominant clinopyroxene compositions in each system is to compare their mg#'s (where mg# = Mg/(Mg+Fe), cation %). Histograms comparing the mg# of augite (termed the En' content) between the ophitic and composite rocks in the BRD and GSF are shown in Figure 47.

The En' contents of augite in the BRD ophitic diabase (En'_{53-82}; average = En'_{70}) and the GSF ophitic basalt (En'_{46-81}; average = En'_{69}) show considerable overlap over a narrow compositional range (Fig. 47A). Similar compositional overlap is displayed by augite in the composite lithologies of the BRD and GSF systems (Fig. 47B). The compositional

range of augite in the composite units of the intrusive and volcanic systems (En'$_{19\text{-}73}$ and En'$_{18\text{-}76}$, respectively) is remarkably similar and much wider than the ophitic lithologies. This broader range is consistent with the greater lithologic diversity in the composite units and makes it all the more remarkable that the average En' compositions for BRD and GSF composite lithologies are nearly identical – En'$_{53}$ and En'$_{54}$, respectively.

Figure 48 shows a histogram comparing the mg# in olivine (termed the Fo content) between BRD ophitic diabase and GSF ophitic basalt. Olivine displays compositional overlap similar to augite between the BRD ophitic diabase ($Fo_{43\text{-}75}$; average = Fo_{61}) and GSF ophitic basalt ($Fo_{45\text{-}73}$; average = Fo_{55}). As was discussed in the previous chapter, fresh olivine was not found in any of the composite lithologies in the GSF making a comparison of Fo contents in olivine between the composite units in the two systems impossible.

Despite the lack of olivine data for the GSF composite rocks, the remarkable similarities in the average and range of En' in augite between the BRD-SBI and GSF and Fo in olivine in the ophitic lithologies provides compelling evidence that the parental and derivative magmas which formed the BRD were virtually identical in composition to those which formed the GSF.

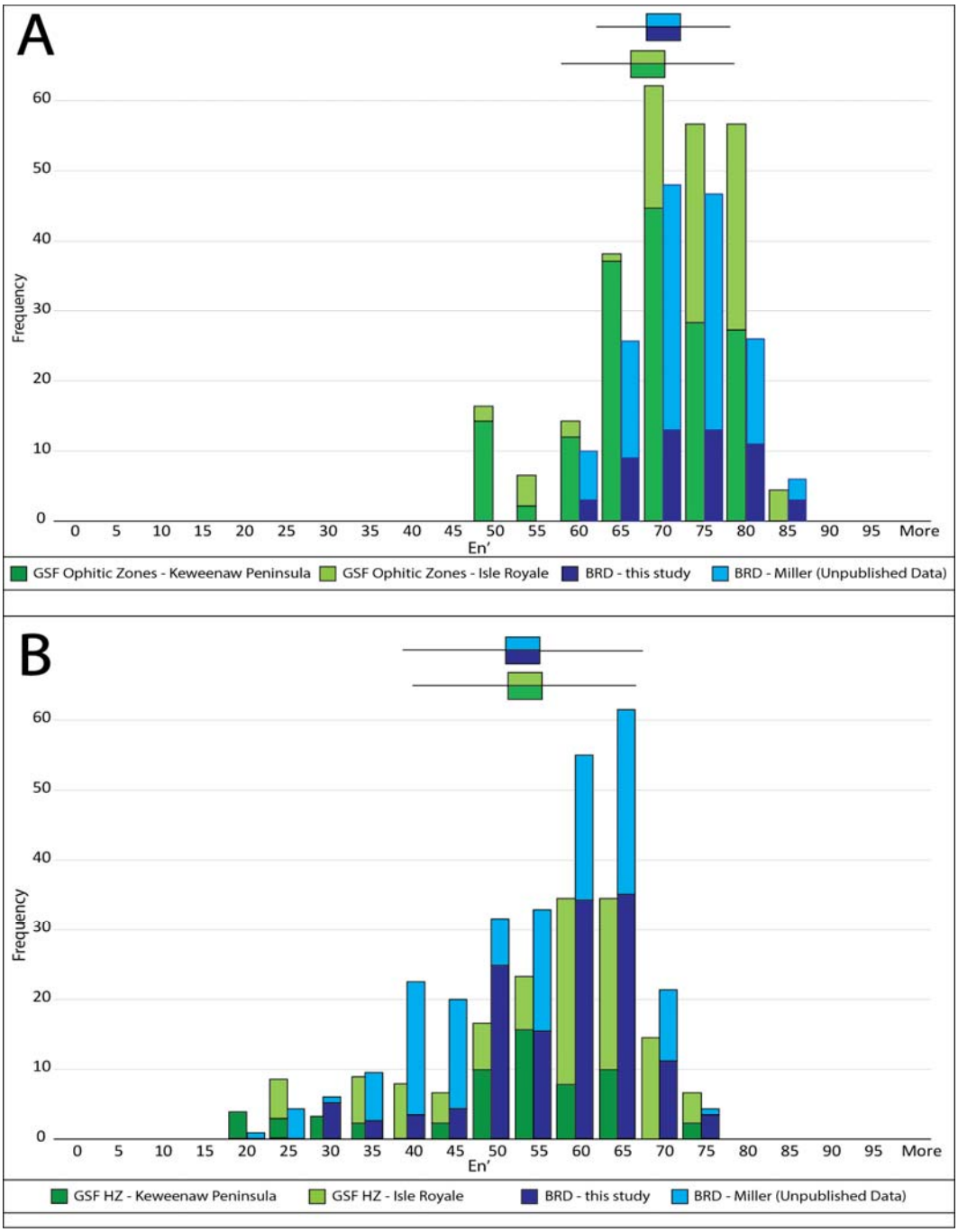

Figure 47. Histograms comparing the En' content in augite in the A) ophitic and B) composite lithologies in the BRD and GSF. Box and whisker plots represent average and standard deviation of measurements.

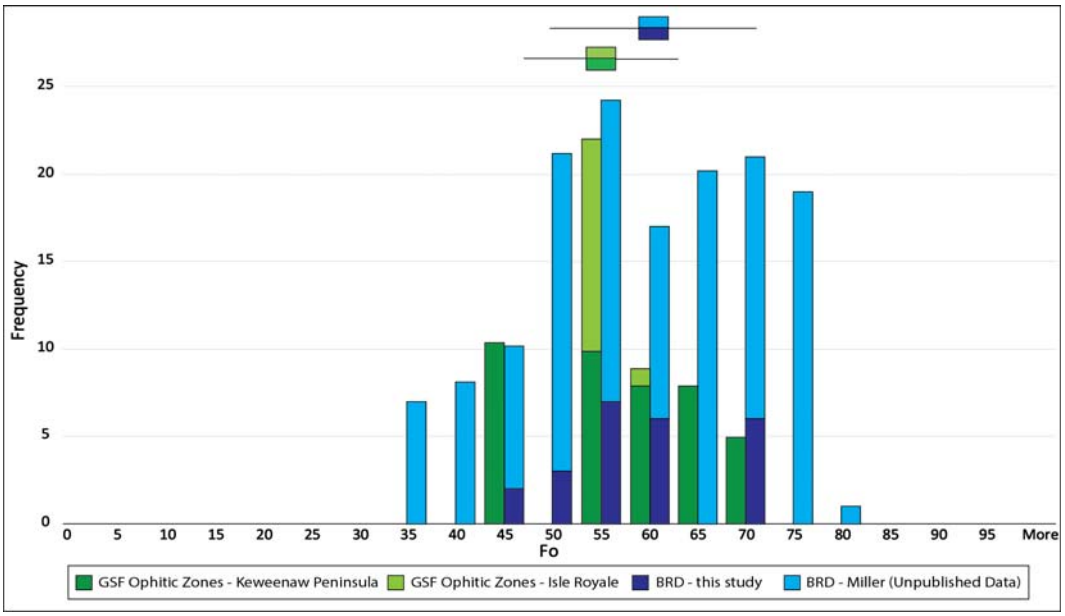

Figure 48. Histogram comparing the Fo content in olivine in the BRD ophitic diabase and GSF ophitic basalt. Box and whisker plots represent average and standard deviation of measurements.

4.2.3 Plagioclase Megacrysts

The occurrence of numerous lower crustal inclusions of nearly pure anorthosite, discussed in Section 1.15, is one of the most distinctive features of the BRD dikes and sills. Inclusions such as these do not occur in any of the composite lithologies within the BRD and have not been observed in any other intrusive phase of the BBC. The inclusions range from polycrystalline aggregates of coarse-grained plagioclase laths that are typically less than a centimeter in length to enormous blocks of anorthosite over 400 meters across (Fig. 8). Morrison et al. (1983) characterized the textural and geochemical attributes of the large inclusions and determined that the consist of four types: 1) *igneous-textured* with distinctively interlocking plagioclase textures; 2) *tectonites* with unambiguously metamorphic textures; 3) *intermediate-textured* displaying both interlocking and metamorphic textures; and 4) *cataclastites* displaying brecciated textures. Morrison et al.

(1983) reported a much wider range in An contents (where An=Ca/(Ca+Na+K), cation %) in plagioclase in the *igneous-textured* anorthosites (An_{54-80}) than in the *tectonites* (An_{76-78}). Previous studies by Miller and others (e.g. Miller, 1988; Miller et al, 1989; Miller and Chandler, 1997) reported plagioclase megacrysts in the ophitic olivine diabase of the BRD with An contents spanning a similar range (An_{60-75}) as the anorthosite inclusions reported by Morrison et al (1983). Miller and Chandler (1997) noted that the An content in the cores of the megacrysts are consistently higher than in the surrounding groundmass plagioclase crystals and thereby interpreted them to be xenocrysts derived from the anorthosite xenoliths.

Although anorthosite inclusions are not reported in this study, the occurrence of plagioclase megacrysts in the GSF raises the question as to whether they are xenocrysts derived from the An-rich anorthosite xenoliths in the BRD or whether they are phenocrysts in equilibrium with the groundmass plagioclase of the GSF ophitic basalt. If the former is the case, this provides perhaps the strongest evidence yet of a comagmatic relationship between the BRD and GSF. To address this question, the An content of plagioclase megacrysts and groundmass phase were analyzed along linear profiles (Fig. 49). Figure 50 displays histograms comparing the An contents in the cores and rims of plagioclase megacrysts in the GSF and BRD.

From the An profiles shown in Figure 49, it is evident that most plagioclase megacrysts in both the BRD and GSF ophitic basalt display normal zoning characterized by nearly uniform calcium concentrations across their cores and either sharp or subtle depletion across their rims. The sharp compositional breaks displayed internally in some

megacrysts (e.g. Fig. 49D and E) correlate with alteration along microfractures or in surficial pits, rather than changes in An composition during crystal growth.

As shown in Figure 50, anorthite contents in the cores of plagioclase megacrysts range from An_{45} to An_{81} (average = An_{70}) in the BRD and from An_{52} to An_{81} (average = An_{69}) in the GSF. These values are not only similar between the BRD and GSF systems, but are also similar to the maximum and range of An contents reported by Morrison et al. (1983) from anorthosite xenoliths in the BRD (An_{54-80}; red shaded areas on the histograms in Figure 50) and those reported for megacrysts in the BRD by Miller and others (An_{60-75}; e.g. Miller, 1988; Miller et al, 1989; Miller and Chandler, 1997). The An content of the megacryst cores is significantly greater than that measured in the groundmass plagioclase crystals in the BRD (average = An_{56}) and GSF (average = An_{54}). The average An content in the zoned rims of most plagioclase megacrysts is around An_{60} which closely matches that in the groundmass crystals.

The measured An content in the cores of plagioclase megacrysts in the GSF ophitic basalt, which display remarkably similar maximums and ranges (Fig. 50B) as the anorthosite xenoliths in the BRD ophitic diabase, strongly implies that these crystals are not phenocrysts that crystallized in equilibrium with the GSF parent magma, but are rather xenocrysts derived from a similar source as those in the BRD ophitic diabase. Furthermore, the compositions of megacryst rims, which closely match those of the groundmass plagioclase crystals, implies that the rims are overgrowths developed on previously crystallized megacryst cores. This result provides perhaps the most compelling evidence of a comagmatic link between the intrusive BRD and volcanic GSF systems.

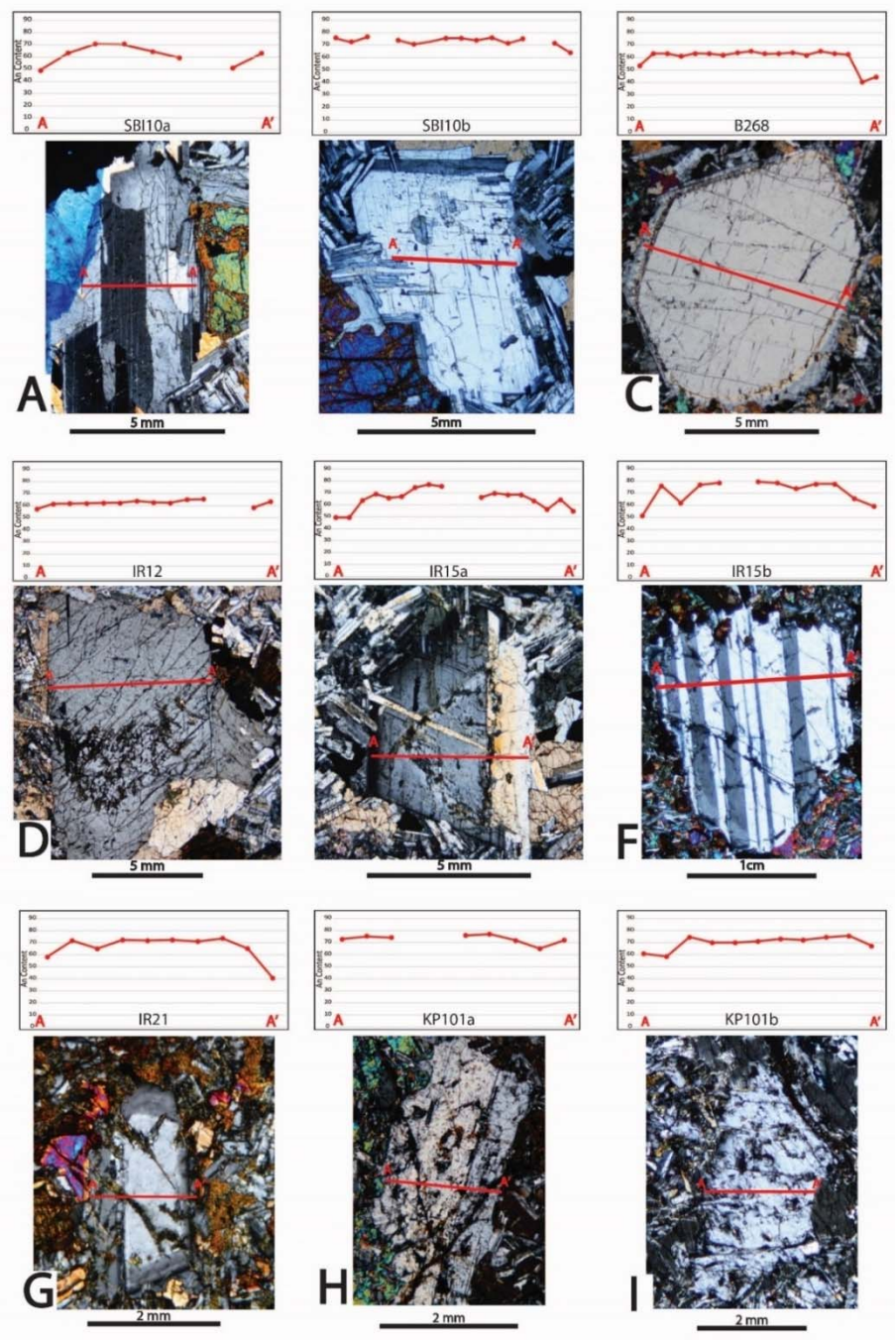

Figure 49. Crossed-polarized photomicrographs of plagioclase megacrysts in BRD ophitic diabase (A-C) and GSF ophitic basalt (D-I) analyzed at points along profile lines. Graphs illustrate the An content of megacrysts from edge to edge. Compositional breaks displayed on graphs represent areas of alteration which were excluded from An profiles. Sample numbers noted in figure.

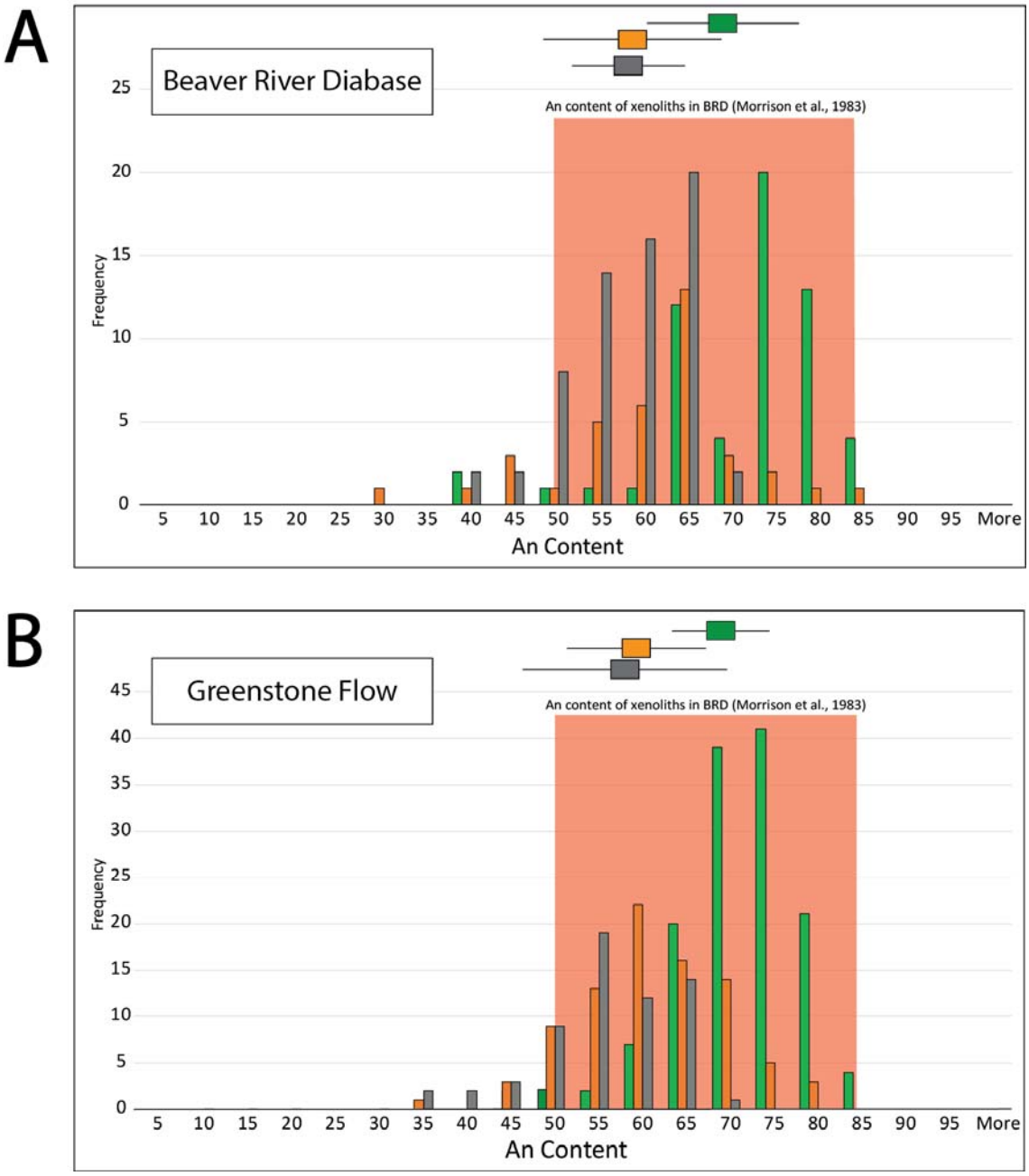

Figure 50. Histograms showing the range in An content in plagioclase megacrysts and groundmass plagioclase crystals in samples of A) BRD ophitic diabase and B) GSF ophitic basalt. Red shaded area represents range in An content reported for anorthosite xenoliths in BRD (Morrison et al., 1983). Box and whisker plots represent mean and standard deviation of measurements.

4.2.4 Whole-Rock Lithogeochemistry

Trace element and REE compositions offer another important test of a possible comagmatic link between the BRD-SBI and GSF. Figure 51 compares the chondrite-normalized REE abundances in the ophitic and composite lithologies in each system. The plots compare the patterns displayed by BRD ophitic and composite lithologies (Fig. 51A, C, D and E) with the GSF data (Fig. 51B and F). One sample of the BRD diabase from the northern BBC (sample BBC6; Fig. 17) was found to have anomalously low REE abundances and was excluded from the BRD dataset. Sample BBC6 was collected near the margin of the BRD dike in the northern BBC (Fig. 17) and contains a high abundance of olivine which is known to incorporate only negligible amounts of REEs.

The chondrite-normalized abundances in the BRD ophitic diabase and GSF ophitic basalt (Fig. 51B) plot in a dense cluster with a moderately negative slope. The ophitic rocks in both systems are moderately enriched in LREE relative to HREE, which is a common pattern displayed by tholeiitic rocks throughout the world (Rollinson, 1993). Ophitic diabase samples display a greater spread in overall REE abundances than the diabase, however the abundances of most diabase and basalt samples are observed to overlap. The greater spread in the diabase can be attributed to two factors. Firstly, several samples of BRD ophitic diabase with the highest REE abundances (samples BBC7, SBI11, and SBI15; Fig. 51A) have anomalously high abundances of felsic mesostasis (> 5%), which likely represents the accumulation of late-stage, incompatible element-rich liquid as would be expected due to a longer period of crystallization in the hypabyssal environment. It is also possible that the elevated abundances of felsic mesostasis are the result of contamination of the diabase by evolved BRD composite magmas or country rocks.

Sample BBC7 was collected close to the contact with the composite lithologies in the BRD in the northern BBC (Fig. 17) and may have experienced infiltration and contamination by evolved melts during emplacement of the evolved magma. Samples SBI11 and SBI15 were both collected near contacts with NSVG rhyolite (Fig. 15) and the high abundance of felsic mesostasis may reflect contamination from partially melted and assimilated country rock. Conversely, one sample of the marginal poikilitic gabbro phase of the *brd* unit in the northern BBC (sample BBC13, map unit *brpg*; Fig. 17) contains a high abundance (~30%) of olivine oikocrysts and thus displays lower overall REE abundances.

The patterns displayed by the composite lithologies of the BRD and GSF (Fig. 51C,D, and E) are much more variable and display a much wider spread in overall REE abundances than the ophitic rocks, as would be expected given the wider range in rock types contained in those units. Despite this variability, comparable rock types in the BRD composite intrusions and the Heterolithic Zone of the GSF display generally overlapping and similar, coparallel patterns. One sample of HZ ferrodiorite (sample KP116; Fig. 51F) has lower REE abundances and a shallower slope than other samples in both systems. Petrography shows that this rock displays well-foliated, cumulate texture (Fig. 33C) and, thus, is not expected to reflect the original liquid composition of the HZ magma. In each system, the patterns fall into two distinct clusters based on the degree of REE enrichment relative to chondrite. Curiously, however, the lithologies comprising the clusters are not consistent between the intrusive and volcanic systems. In the BRD composite intrusions, ferrodioritic rocks (Fig. 51C and D) display considerable REE enrichment and are observed to overlap with the ferromonzodiorite samples from the SBI intrusions in the

southern BBC (Fig. 51C) and the GSF (Fig. 51F). In the GSF-HZ, however, ferrodiorites display much less REE enrichment than in the monzodioritic rocks and are observed to overlap with the intergranular gabbros. The reason for this is unclear, but the disparity indicates a closer petrological relationship between the gabbros and ferrodiorites in the GSF-HZ than in the BRD composite intrusions. One plausible explanation is that the longer period of cooling and crystallization expected for the intrusive rocks in the BRD composite intrusions allowed for a higher degree of *in situ* fractionation. Evidence of this is given by the petrographic attributes which show that the ferrodiorites in the BRD composite intrusions typically contain higher abundances of felsic mesostasis (~5-10%) and visible quartz (1-2%) which is generally absent from the ferrodiorites in the GSF-HZ. Despite this disparity, the intermediate rocks in both the BRD and GSF composite lithologies display generally overlapping and similar, coparallel chondrite-normalized patterns with moderate negative Eu anomalies relative to the generally neutral Eu normalized abundances in the gabbroic rocks in each system.

Chondrite-normalized multi-element diagrams are also plotted to compare a broader spectrum of trace element concentrations in the BRD and GSF (Fig. 52). The multi-element diagrams are constructed in a similar fashion as the REE data (Fig. 51), and with the same exclusion of samples of the BRD-SBI. As in the REE diagrams, samples of the BRD ophitic diabase and GSF ophitic basalt plot along tight, coparallel, and generally overlapping trends (Fig. 52B). The diabase samples display a slightly wider spread in overall trace element abundances; however, samples of the ophitic rocks in each system

display consistent concave-downward, overlapping patterns, characterized by weakly negative Sr anomalies and negative Hf-Ta anomalies.

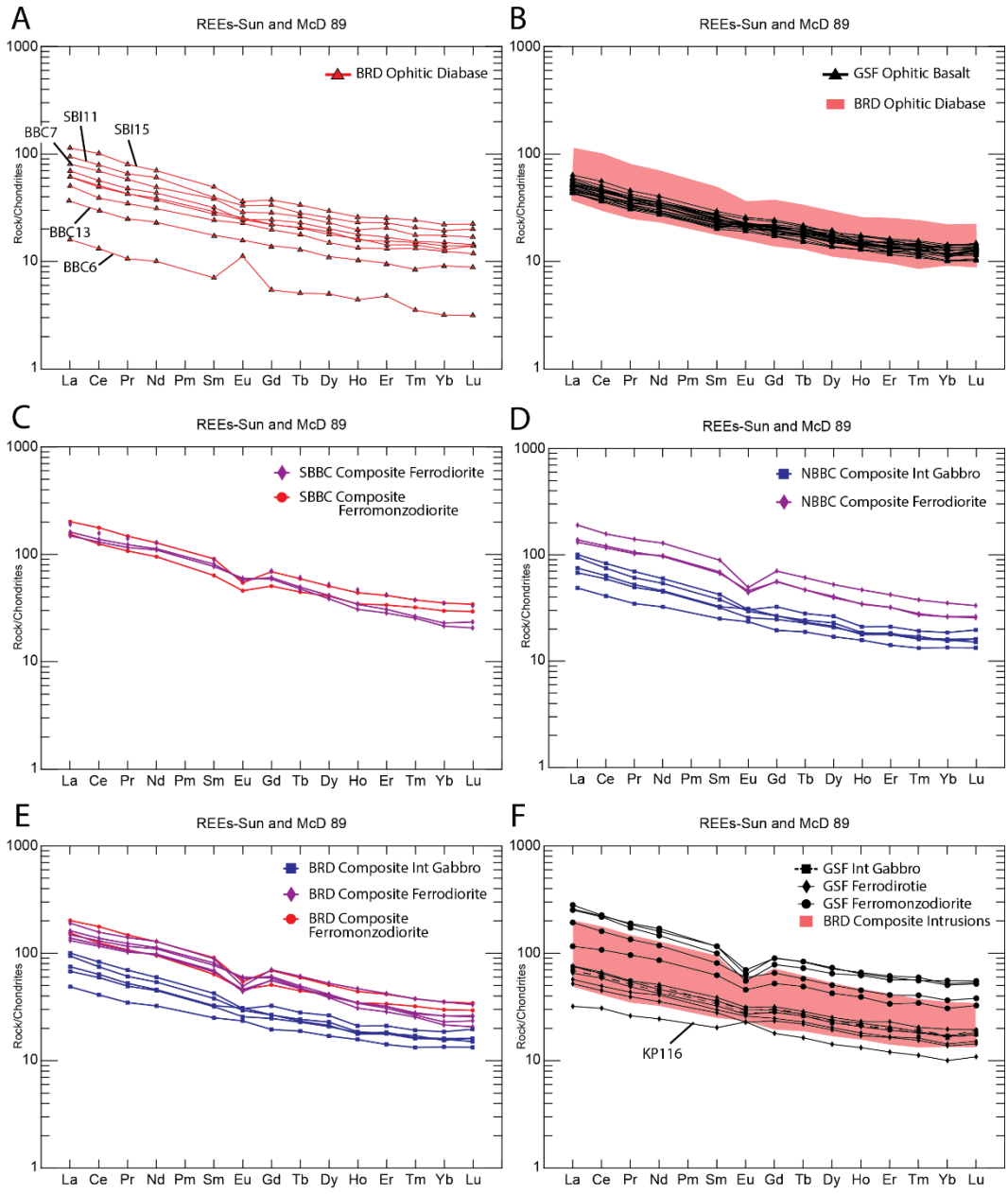

Figure 51. Chondrite-normalized diagrams comparing the REE abundances between the rocks of the BRD-SBI and GSF. Panel A shows individual analyses of BRD ophitic diabase. Panel B compares BRD ophitic diabase and GSF ophitic basalt. Panels C and D show individual analyses of the composite intrusions in the SBBC and NBBC,

respectively. Panel E shows total analyses of the composite intrusions in the BRD. Panel F compares the composite lithologies in the BRD and GSF. Chondrite normalizing values are from Sun and McDonough, 1989.

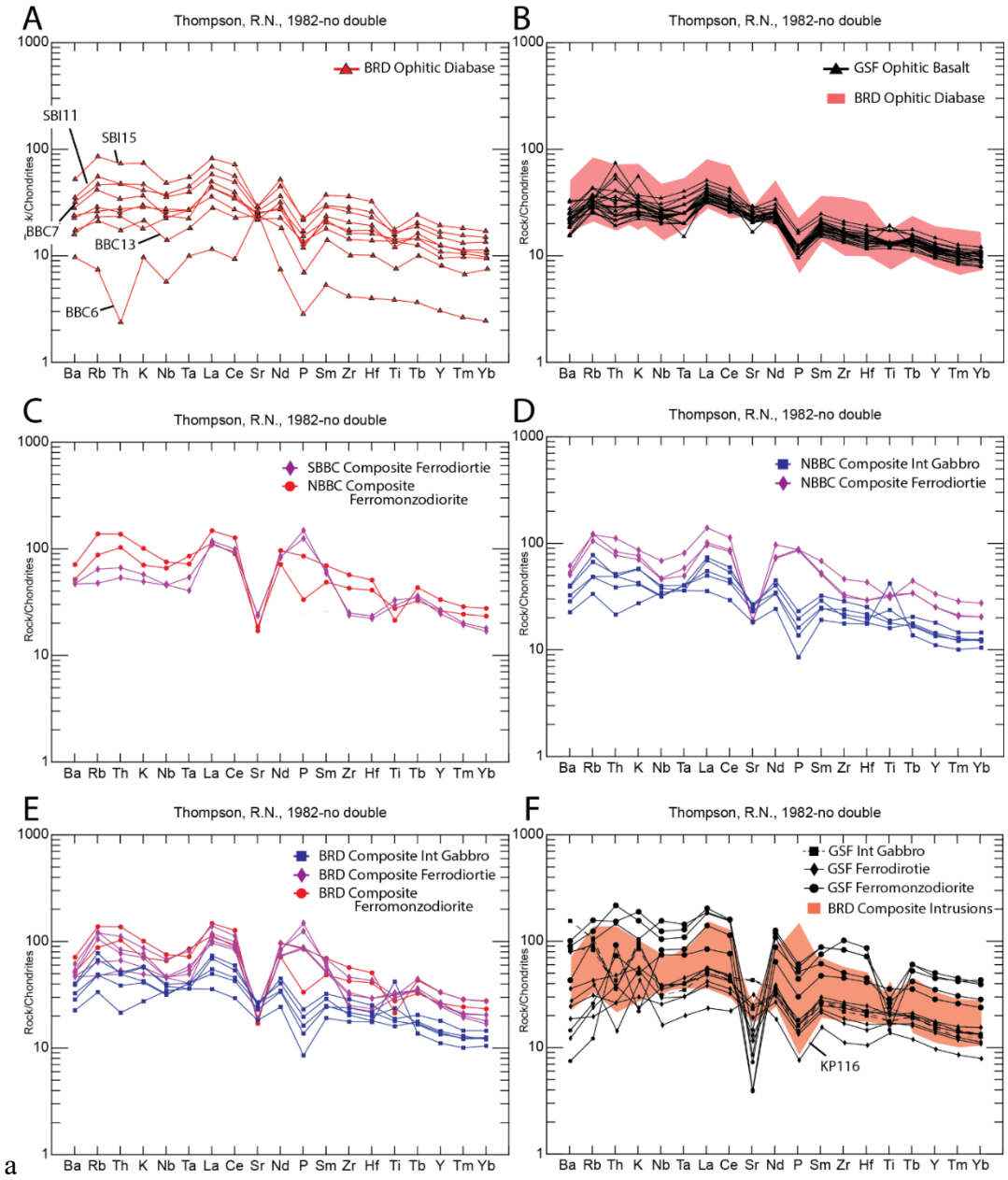

a

Figure 52. Chondrite-normalized diagrams comparing trace element abundances between the rocks of the BRD-SBI and GSF. Panels arranged as in Figure 51. Chondrite normalizing values are from Thompson (1982).

Similar to the ophitic lithologies, the composite rocks in each system display generally overlapping, coparallel trace element abundances (Fig. 52F). As observed on the REE diagram (Fig. 51D), sample KP116 of the HZ displays significant depletion in trace elements, reflecting its cumulate texture. The composite rocks in the GSF display a greater range in overall trace element abundances and, as in the case of REE abundances (Fig. 51C, D, and E), the ferrodiorites in the BRD composite intrusions are more highly enriched in overall trace element abundances than those in the GSF-HZ and plot with the ferromonzodiorites in the SBI intrusions in the southern BBC (Fig. 52C) and GSF-HZ (Fig. 52F). The patterns displayed by the composite lithologies in both the BRD and GSF systems are characterized by strong depletions in Sr which is consistent with the earlier removal of plagioclase during crystallization of the mafic lithologies. One exception to this is given by the two samples of intergranular gabbro in the GSF from Isle Royale (samples IR3 and IR23; Fig. 52F) that display roughly neutral Sr anomalies. One obvious deviation from the generally coparallel patterns displayed by each system is given by the differences in LILE abundance (Ba, Rb, K) and Th which show considerable variation in GSF-HZ samples. LILEs and Th are generally mobile during hydrothermal and metamorphic alteration (Rollinson, 1993), and the highly variable concentrations of these elements in the HZ is likely attributable to the greater degree of alteration experienced by these rocks.

Despite the minor differences observed in the chondrite-normalized REE and multi-element diagrams, the similarities in the overall abundances of incompatible elements and coparallel patterns indicate that the ophitic and composite lithologies in the BRD and GSF crystallized from magmas with remarkably similar chemical compositions. This result

lends further compelling evidence of a comagmatic link between the intrusive BRD and volcanic GSF systems.

4.2.5 Summary Evidence of BRD-GSF Comagmatism

Based on the field, petrographic, mineral chemical, and lithogeochemical evidence presented above, a comagmatic origin for the intrusive BRD and volcanic GSF systems seems highly evident. To summarize, evidence of this link is given by the following:

- Similar two- to three-stage composite emplacement histories implied by abrupt contact relationships between distinct lithologies comprising both the BRD and GSF during the composite intrusion of evolved tholeiitic magma into the core of a tholeiitic dike and sill network and extensive tholeiitic lava flow.
- Similar range in rock types, which define a continuum of differentiated tholeiitic compositions from ophitic olivine diabase/basalt to intergranular gabbro to ferrodiorite to ferromonzodiorite.
- Nearly identical modal mineralogies and textural attributes between comparable rock types in each system, most notably the occurrence of the distinctive clustered texture of plagioclase in the ophitic lithologies in each system.
- Overlapping En' contents in augite and Fo contents in olivine between comparable rock types in each system.
- The occurrence of plagioclase megacrysts in the GSF ophitic basalt with similar, anomalously-high anorthite content as compared to the plagioclase megacrysts and anorthosite xenoliths in the ophitic diabase of the BRD.

- Similar chondrite-normalized REE and trace element concentrations between the comparable rock types in each system.

Although no single piece of evidence proves conclusively a comagmatic and petrologic linkage between the BRD and GSF, collectively the data presented above strongly suggest that the BRD dike and sill network served as the intrusive feeder system for the GSF – one of the largest lava eruptions on Earth.

4.3 Estimate of the Areal Extent and Volume of the GSF

Having established the likely comagmatic relationship between the BRD and GSF by their field, lithologic, and geochemical attributes, we can now discuss how these two systems could have been structurally connected and what this implies about the extent and volume of the GSF lava flow. Interpreting the BRD dike and sill network as the feeder system for the GSF is supported by several aspects of the BBC (Figs. 1 and 7). As discussed in Section 1.2.1, the flood basalts of the Portage Lake Volcanic Group were erupted during the latter part of the main stage of MCR activity (Fig. 3) and were focused as flows into a rapidly subsiding central basin bounded by the Keweenaw and Isle Royale faults (Figs. 1 and 53). Although these faults are now recognized as reverse faults, geophysical interpretations of the Portage Lake Volcanics confined within them and accumulating to thicknesses of up to 12 kilometers (Fig. 2), indicate that these were graben-bounding normal faults during main-stage volcanic activity. This lava-filled graben, termed the Portage Lake Volcanic Basin, extends under much of western Lake Superior (Fig. 53). The shape of the western extent of the Portage Lake Volcanic Basin, historically termed the Lake Superior Syncline (White, 1960), is strongly controlled by two

large, isolated blocks of pre-Keweenawan crust (White's Ridge and the Grand Marais ridge, Fig. 1), against which volcanic rocks are observed to pinch out (Allen et al., 1994). Allen et al. (1994) interpreted gravity, aeromagnetic, and seismic data to indicate that the Portage Lake Volcanic Basin is centered along the main rift axis between the Keweenaw Peninsula and Isle Royale, curves around the Grand Marais ridge, and projects onto the Minnesota shore into the cusp of the Finland Tectonomagmatic Discontinuity (FTMD) – the bounding dike of the BRD (Fig. 1). As discussed in Section 1.2.5, Miller et al. (1995) interpreted the FTMD to have been a normal growth fault into which multiple magmas were intruded and along which an estimated vertical displacement of up to 6.5 kilometers of the riftward blocks occurred.

Given the offset along the FTMD and the projection of the Lake Superior syncline into the cusp of that dike, it is possible to conceive how the BRD could have acted as the lava supply system for the GSF and possible other PLV lava flows. Furthermore, assuming that the BRD did in fact breach the surface and vent, the positioning of White's ridge and the Grand Marais ridge likely served as ramparts to the Portage Lake Volcanic Basin (Figure 1) and acted to funnel lava erupted from the FTMD into the basin. Miller and Chandler (1997) speculated that the Schroeder-Lutsen basalts, which hug the Minnesota shoreline (Fig. 4), may be correlative with the upper part of the Portage Lake Volcanics (Fig. 5) and were themselves fed by the BRD dike and sill network. A lack of dateable material in the Schroeder-Lutsen basalts leaves this speculation unproven.

Given the preponderance of evidence that the BRD dikes and sills fed the GSF lava sheet, previous calculations of both the areal extent and overall volume of the GSF appear

to be grossly underestimated. Based on exposure limits of the GSF on Isle Royale and the Keweenaw Peninsula, several workers reported estimates of the volume of the flow (Table 8). White (1960) used estimates of the areal extent (~5,000 km^2) and average thickness (~170 m) of Lane (1893, 1911) and Cornwall (1951) to calculate a conservative estimate of the volume of the flow as approximately 850 km^3. Longo (1984), using similar exposure limits between Isle Royale and the Keweenaw Peninsula, provided an estimate of 1,650 km^3 using a geometric reconstruction of the syncline.

Accepting the model that the GSF was fed by BRD dikes and the speculation by Miller and Chandler (1997) that the Schroeder-Lutsen basalts correlate with the Portage Lake Volcanics, any volume estimate of the GSF must extend the flow from the exposure on Isle Royale and the Keweenaw Peninsula under Lake Superior and onto the Minnesota shore. A simple, rough calculation of the areal extent of the GSF, incorporating this newly interpreted stretch between Isle Royale and the Minnesota shore, shows that the GSF has an areal extent of roughly 20,000 km^2. Speculating that the thickness of the flow increases between Isle Royale and the Keweenaw Peninsula (maximum = ~220 meters and 450 meters, respectively (Figs. 23 and 25, respectively)) and the flow thins as it approaches the Minnesota coast, it seems reasonable to assume an average thickness of between 100-300 meters for the flow. The result is an estimated volume of between 2,000 km^3 and 6,000 km^3 which greatly exceeds previous estimates (Table 8).

In summary, if the BRD intrusions and GSF lava flow are indeed comagmatic, the total volume of the GSF is much larger than previously thought and rivals, or exceeds, the largest known lava flows on Earth (Table 8). The areal extent of the GSF, based on the

proposed BRD feeder system, is shown in Figure 53. It can be seen that the size of the flow is much greater than previous estimates based on exposures on Isle Royale and the Keweenaw Peninsula. Table 8 lists the largest known lava flows from their respective provinces in comparison to the volume of the GSF. This evidence suggests that the GSF is possibly the single most voluminous lava flow in the world.

Table 8. Comparison of the proposed and previous volumetric estimates of the Greenstone Flow and several large lava flows from the Columbia River Basalt Group and Iceland.

Flow	Location	Volume (km^3)	Author
Greenstone	PLV - Northern Michigan	2,000-6,000	This Study
		1,650	Longo (1984)
		850	White (1960)
Canyon Flow - Sentinel Bluffs member	CRBG – Columbia Plateau	4,278	Hooper (1982)
Umtanum	CRBG – Columbia Plateau	2,350	Bryan et al. (2010)
Monaree Dacite	Gawler Range Volcanics - Australia	2050	Bryan et al. (2010)

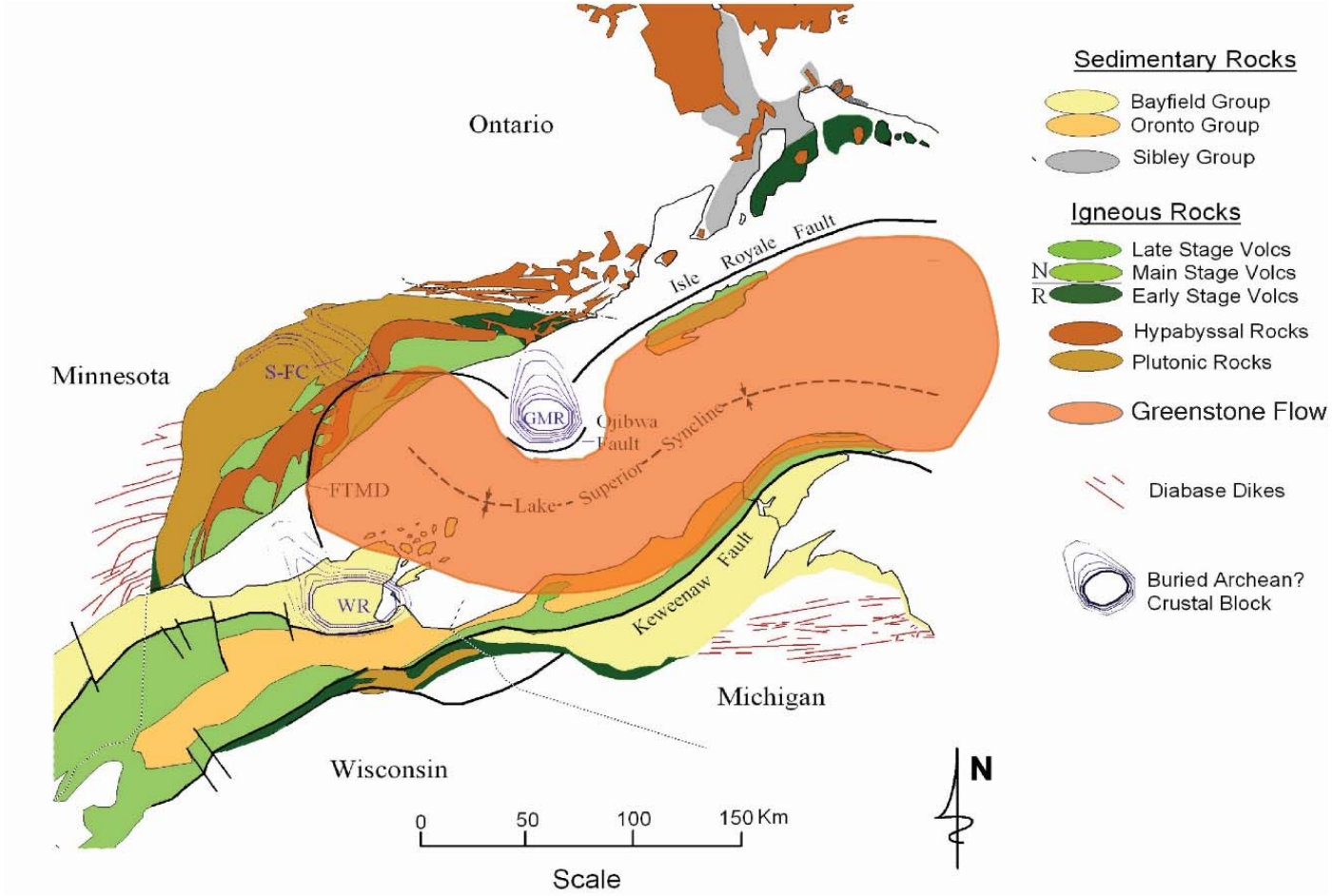

Figure 53. Regional geology of the Midcontinent Rift in the western Lake Superior region showing the estimated areal extent of the Greenstone Flow based on the proposed correlation with the BRD dike and sill network.

5.0 CONCLUSIONS

The main observations and conclusions made during this study are as follows:

- The Beaver River diabase (BRD) is an extensive, composite dike and sill network exposed throughout a roughly 600 km^2 area in northeast Minnesota. BRD dikes and sills are composed predominantly of ophitic to locally subophitic olivine diabase. One of the most distinctive features of the BRD is the occurrence of anorthosite xenoliths which range in size from polycrystalline aggregates less than a centimeter in diameter to large blocks up to 400 meters across. Within the cores of BRD ophitic diabase dikes and sills are smaller, composite intrusions of variably fractionated rocks which include intergranular gabbro, prismatic ferrodiorite, foliated ferrodiorite, and quartz ferromonzodiorite. These composite intrusions were emplaced into the diabase dikes and sills by sequential injections of progressively evolved magmas generated in deeper crustal staging chambers. In the southern BBC, these intrusions, which are termed the Silver Bay Intrusions (SBI), are generally saucer-shaped bodies emplaced into the medial portions of larger BRD sheets and sills from magma pulses of various size. The larger intrusions, such as the Beaver Bay and Silver Bay bodies subsequently fractionated in place to produce a range of rock types that include varitextured gabbro/diorite, foliated ferrodiorite, and prismatic ferromonzodiorite with local occurrences of coarse-grained felsic segregations. In the northern BBC, the composite intrusions were formed by at least two major intrusive pulses emplaced into the axial portions of keel-shaped BRD dikes. The first pulse created an

intergranular gabbro with variable concentrations of interstitial felsic mesostasis. The second pulse formed a sequence of massive to foliated ferrodiorite to quartz ferromonzodiorite, similar to the SBI.

- The Greenstone Flow (GSF) is an enormous, compositely emplaced lava flow exposed on Isle Royale and the Keweenaw Peninsula in northern Michigan. The flow is divided into four lithostratigraphic zones – Lower Ophitic, Heterolithic, Upper Ophitic, and Entablature – based on differences in the dominant lithologies in each. The Lower and Upper Ophitic Zones are similarly composed of ophitic to locally subophitic basalt. The Heterolithic Zone is composed of complexly interlayered ophitic to subophitic basalt, intergranular gabbro, ferrodiorite, and ferromonzodiorite with local occurrences of coarse-grained intermediate to felsic segregations and aplite. The Entablature represents the flow top of the GSF and is composed of massive to amygdaloidal basalt.
- Field relationships between the dominant lithological zones in the GSF, characterized by abrupt and complex lithological contacts, indicate that the GSF formed from the composite intrusion of evolved basaltic magma into the semi-crystalline core of an ophitic olivine basalt flow. Sharp, unchilled contacts between major rock types and the occurrence of subangular inclusions of subophitic basalt hosted by HZ intergranular gabbro indicate that sufficient cooling had occurred between the initial eruption and subsequent intrusive magmatic pulse to result in the basalt to behave in a brittle fashion, but not enough to cause the intrusive magma to quench. Mineralogical and textural

evidence, including the occurrence of plagioclase megacrysts and subparallel clustering of groundmass plagioclase, indicate that the ophitic to subophitic basalts scattered throughout the GSF Heterolithic Zone are remnant blocks of the initial ophitic basalt eruption which became isolated by the incomplete displacement of the semi-molten core of the GSF by the pulse of evolved magma. Well-foliated, cumulate textures observed in HZ ferrodiorites suggest that the initial intrusive pulse of magma was likely followed by a second, more highly evolved pulse of magma into the core of the GSF. The second intrusive pulse likely fractionated *in situ* to produce the well-foliated ferrodiorite cumulates, ferromonzodiorite, coarse-grained segregations, and aplite in the HZ.

- Field and petrographic observations show that the comparable rocks types in the BRD and GSF are nearly indistinguishable in terms of mineralogy and textural attributes. Of particular interest are the occurrences of coarse-grained plagioclase megacrysts, similar to the xenoliths in the BRD, and the distinctive, subparallel clustering of groundmass plagioclase laths in both the BRD ophitic diabase and GSF ophitic basalt. This distinctive texture has not been reported in any other intrusive or volcanic rocks of the MCR. Based on the occurrence of intergranular gabbro which displays clustered plagioclase laths, the sequence of emplacement of the rocks in the GSF seems to more closely resemble that of the BRD dikes in the northern BBC, which are interpreted to have formed from the composite emplacement of at least two magmatic intrusions into the semi-crystalline core of a tholeiitic olivine diabase dike.

- Compositions of primary solid-solution minerals in the BRD and GSF indicate that they formed from parent magmas with similar chemical attributes. This result is most evident by the overlap in En' contents in augite and Fo contents in olivine between comparable rock types in each system.
- Similar chemical profiles and anomalously high anorthite content (> 75 mole%) in the cores of plagioclase megacrysts in the GSF ophitic basalt and xenocrysts in the BRD ophitic diabase indicate that they share a common source.
- Regional field evidence that the BRD dike and sill network acted as the intrusive feeder system for the GFS lava flow are given by 1) evidence of multiple injections of magma along the FTMD – the main bounding dike of the BRD – and an estimated riftward offset of up to 6.5 kilometers along the FTMD, 2) the interpretation that the Schroeder-Lutsen basalts are correlative with the upper portions of the Portage Lake Volcanics, 3) the complex shape of the Portage Lake Volcanic basin in the western Lake Superior region, which is interpreted to wrap tightly around the Grand Marais ridge and project onto the Minnesota shore, terminating within the cusp of the FTMD.
- Based on the proposed correlation of the BRD and GSF, previous calculations of the areal extent and volume of the Greenstone Flow are underestimated. Projecting the flow onto the Minnesota shore and assuming an average thickness of 100-300 meters, the total volume of the Greenstone Flow is estimated to be between 2,000 km^3 and 6,000 km^3, making it possibly the most voluminous single lava flow in the world.

The field, petrographic, mineral chemical, and lithogeochemical evidence cited in this study as confirmation of a comagmatic link between the intrusive BRD and volcanic GSF systems provides more robust support for the circumstantial evidence which prompted this study – overlapping U-Pb ages, similar range of lithologies, and the occurrence of large lower crustal anorthosite xenoliths at a shallow crustal level. The conclusion that an enormous amount of lava was generated by multiple venting events from the BRD begs the question of whether this extensive dike and sill network fed other flood basalts in the MCR. Indeed, this correlation lends further support to the interpretation by Miller and Chandler (1997) that the Schroder-Lutsen basalts are correlative with the upper portions of the PLV. Furthermore, mineralogical and geochemical similarities between the Greenstone Flow and other flows of the PLV reported by several authors (e.g. Cornwall, 1951; Paces, 1988) are intriguing in that they may indicate a similar correlation with the BRD. Further research, including detailed geochemical and geochronological studies of the Schroder-Lutsen basalts and other flows within the PLV, are needed to answer this question.

In addition to further studies of the Schroder-Lutsen and PLV basalts, the full areal extent and volume of the GSF remains speculative due to an inability to map the flow from the proposed BRD feeder vent to its termination, presumably on Isle Royale and the Keweenaw Peninsula. To more fully constrain the extent of the GSF under western Lake Superior, a reexamination of seismic reflection profiles (GLIMPCE line C and Grant-Norpac lines 57, 53, 47, 45, and 43, Fig. 54) may provide more evidence that the western

extension of the GSF projects onto the Minnesota shore, allowing for a more precise calculation of its volume.

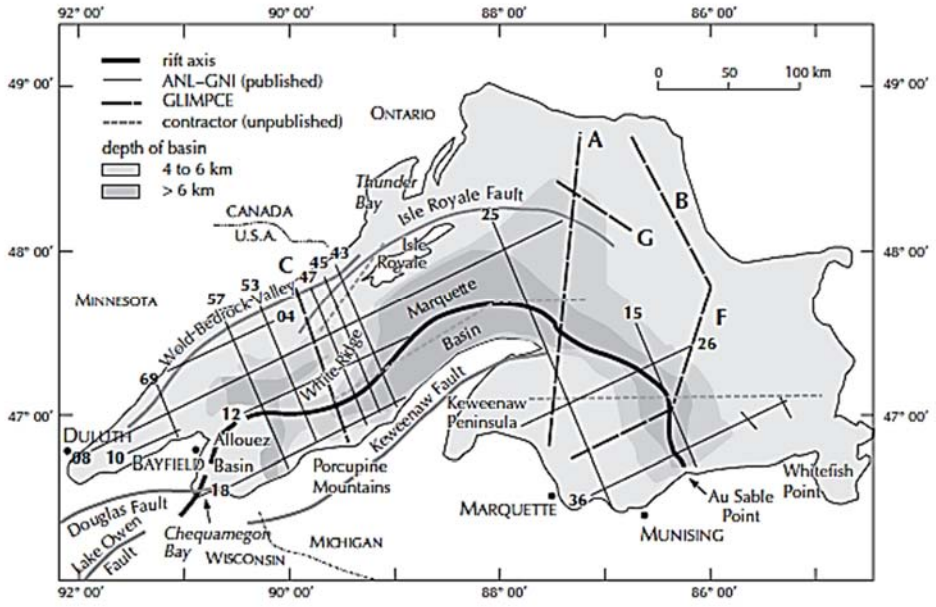

Figure 54. Outline map of Lake Superior showing locations of Argonne-Grant Norpac seismic reflection lines (numbered) and GLIMPCE seismic reflection lines (alphabetic). From McGinnis and Mudrey, 1991.

REFERENCES

Allen, D. J., Hinze, W. J., Dikas, A. B., and Mudrey Jr, M. G., 1994, Geophysical investigations of the Midcontinent Rift System: a new model for western Lake Superior and northern Wisconsin. In: Proceedings, Institute on Lake Superior Geology, 40th, Program and Abstracts, 1-2.

Allen, D.J., Hinze, W.J., Dickas, A.B., and Mudrey, M.G., Jr., 1997, Integrated geophysical modeling of the North American Midcontinent Rift System: New interpretations for western Lake Superior, northwestern Wisconsin, and eastern Minnesota. In: Ojakangas, R.J., Dickas, A.B., Green, J.C., eds. Middle Proterozoic to Cambrian Rifting, Central North America: Geological Society of America Special Paper 312, p.47-72.

Annells, R.N., 1974, Keweenawan volcanic rocks of Michipicoten Island, Lake Superior, Ontario: Geological Survey of Canada Bulletin 218, 141p.

Boerboom, T. B., 1994, Archean crustal xenoliths in a Keweenawan hypabyssal sill, northeastern Minnesota. White was right!. In: Proceedings Annual Meeting, Houghton, MI. Institute on Lake Superior Geology, 40th, Part 1, Program and Abstracts, p. 5-6.

Boerboom, T. J., and Miller Jr, J. D., 1994, Bedrock geologic map of the Silver Island Lake, Wilson Lake, and western Toohey Lake quadrangles, Cook and Lake Counties, Minnesota: Minnesota Geological Survey Miscellaneous Map Series, M-81, scale 1:24,000.

Books, K. G., 1972, Paleomagnetism of some Lake Superior Keweenawan rocks. United States Geological Survey, Professional Paper 760, 42p.

Broderick, T. M., 1935, Differentiation in lavas of the Michigan Keweenawan. Geological Society of America Bulletin, 46(4), p. 503-558.

Broderick, T. M., Hohl, C. D., and Eidemiller, H. N., 1946, Recent contributions to the geology of the Michigan copper district. Economic Geology, 41(7), p. 675-725.

Bryan, S. E., Peate, I. U., Peate, D. W., Self, S., Jerram, D. A., Mawby, M. R., Marsh, J.S., and Miller, J.A., 2010, The largest volcanic eruptions on Earth. Earth-Science Reviews, 102(3), p. 207-229.

Butler, B. S., and Burbank, W. S, 1929, The copper deposits of Michigan. United States Geological Survey, Professional Paper 144, 238p.

Campbell, I.H. and Griffiths, R.W., 1990, Implications of mantle plume structure for the evolution of flood basalts: Earth and Planetary Science Letters 99, p. 79-93.

Cannon, W.F., Green, A.C., Hutchinson, D.R., Lee, M.W., Milkereit, B., Behrendt, J.C., Halls, H.C., Green, J.C., Dickas, A.B., Morey, G.B., Sutcliffe, R.H., and Spencer, C., 1989. The North American Midcontinent rift beneath Lake Superior from GLIMPCE seismic reflection profiling. Tectonics 8, p. 305-332.

Cannon, W.F., 1992, The Midcontinent rift in the Lake Superior region with emphasis on its geodynamic evolution: Tectonophysics 213, p. 41-48.

Cannon, W.F., and Hinze, W.J., 1992, Speculations on the origin of the North American Midcontinent rift. Tectonophysics, v. 213, p. 49-55.

Cannon, W.F., 1994, Closing of the Midcontinent rift—A far-field effect of Grenvillian compression. Geology 22, p. 155-158.

Cannon, W. F., and Nicholson, S. W., 2001, Geologic map of the Keweenaw Peninsula and adjacent area, Michigan. United States Geological Survey, IMAP 2696.

Carr, M. J. (1997). IGPET for Windows. Terra Softa Inc., Somerset, NJ.

Chandler, V.W., McSwiggen, P.L., Morey, G.B., Hinze, W.J., and Anderson, R.R., 1989, Interpretation of seismic reflection, gravity and magnetic data across Middle Proterozoic Mid-Continent Rift, northwestern Wisconsin, eastern Minnesota and central Iowa. American Association of Petroleum Geology Bulletin 73, p. 261-275.

Cornwall, H. R., 1951, Differentiation in lavas of the Keweenawan series and the origin of the copper deposits of Michigan. Geological Society of America Bulletin, 62(2), p. 159-202.

Cornwall, H. R., 1954a, Bedrock geology of the Phoenix quadrangle, Michigan. United States Geological Survey Geological Quadrangle Map GQ-34, scale 1:24,000.

Cornwall, H. R., 1954b, Bedrock geology of the Eagle Harbor quadrangle, Michigan. United States Geological Survey Geological Quadrangle Map GQ-36, scale 1:24,000.

Courtillot, V., Besse, J., Vandamme, D., Montigny, R., Jaeger, J. J., and Cappetta, H., 1986, Deccan flood basalts at the Cretaceous/Tertiary boundary?. Earth and Planetary Science Letters, 80(3), p. 361-374.

Davis, D.W. and Sutcliffe, R.H., 1985, U-Pb ages from the Nipigon Plate and northern Lake Superior. Geological Society of America Bulletin, v.96, p.1572-1579.

Davis, D.W. and Paces, J.B., 1990, Time resolution of geologic events on the Keweenaw Peninsula and implications for development of the Midcontinent Rift system. Earth Planetary Science Letters 97, p. 54-64.

Davis, D.W., and Green, J.C., 1997, Geochronology of the North American Midcontinent rift in western Lake Superior and implications for its geodynamic evolution. Canadian Journal of Earth Science, v. 34, p. 476-488.

Dickas, A.B., and Mudrey, M.G., Jr., 1997, Segmented structure of the Middle Proterozoic Midcontinent Rift System, North America: In: Ojakangas, R.J., Dickas, A.B., Green, J.C., (eds.) Middle Proterozoic to Cambrian Rifting, Central North America. Geological Society of America Special Paper 312, p.37-46.

Ding, X., Li, C., Ripley, E.M., Rossell, D., and Kamo, S., 2010, The Eagle and East Eagle sulfide ore-bearing mafic-ultramafic intrusions in the Midcontinent Rift System, upper Michigan: Geochronology and petrologic evolution. G3-Geochemistry, Geophysics and Geosystems, V. 11, 22p.

Gehman, H. M., 1957, The petrology of the Beaver Bay Complex, Lake County, Minnesota. [Ph.D. thesis]: Minneapolis, Minnesota, University of Minnesota, 300 p.

Golder, B.D., 2011 Igneous petrology of the Ni-Cu-PGE-mineralized Tamarack Intrusion, Aitkin and Carlton Counties, Minnesota. MS thesis, University of Minnesota Duluth, 253p.

Green, J.C., 1972, North Shore Volcanic Group, *in* Sims, P.K., and Morey, G.B., eds., Geology of Minnesota—A centennial volume: Minnesota Geological Survey, p. 294-332.

Green, J. C., 1983, Geologic and geochemical evidence for the nature and development of the Middle Proterozoic (Keweenawan) Midcontinent Rift of North America. Tectonophysics, 94(1), p. 413-437.

Green, J.C., 2002, Volcanic and sedimentary rocks of the Keweenawan Supergroup in northeastern Minnesota. *In* Miller, J.D. Jr., Green, J.C., Severson, M.J., Chandler, V.W., Hauck, S.A., Peterson, D.E., and Wahl, T.E., Geology and mineral potential of the Duluth Complex and related rocks of northeastern Minnesota. Minnesota Geological Survey Report of Investigations 58, p. 94-105.

Grout, F. F., and Schwartz, G. M, 1939, The geology of anorthosites of the Minnesota Coast of Lake Superior: Minnesota Geological Survey Bulletin, v. 28, 119 p.

Halls, H. C., and West, G. F., 1971, A seismic refraction survey in Lake Superior. Canadian Journal of Earth Sciences, *8*(6), p. 610-630.

Heaman, L.M. and Machado, 1992, Timing and origin of Midcontinent Rift alkaline magmatism, North America: evidence from the Coldwell Complex. Contributions to Mineralogy and Petrology, V. 110, p. 289-303.

Hinze, W.J., Allen, D.J., Fox, A.J., Sunwood, D., Woelk, T., and Green, A.J., 1992, Geophysical investigations and crustal structure of the North American Midcontinent Rift system. Tectonophysics 213, p. 17-32.

Hoaglund, S.A., 2010, U-Pb geochronology of the Duluth Complex and related hypabyssal intrusions: investigating the emplacement history of a large multiphase intrusive complex related to the 1.1 Ga Midcontinent Rift. M.S. thesis, University of Minnesota Duluth, 103p.

Hollings, P., Fralick, P., and Cousens, B., 2007a, Early history of the Midcontinent Rift inferred from geochemistry and sedimentology of the Mesoproterozoic Osler Group, northwestern Ontario. Canadian Journal of Earth Sciences, V. 44, p. 389-412.

Hollings, P. Hart, T., Richardson, A., and MacDonald C.A., 2007b, Geochemistry of the Mesoproterozoic intrusive rocks of the Nipigon Embayment, northwestern Ontario: evaluating the earliest phases of rift development. Canadian Journal of Earth Sciences, V. 44, p. 1087-1110.

Hollings, P., Smyk, M., Heaman, L,M., and Halls, H., 2010, The geochemistry, geochronology, and paleomagnetism of dikes and sills associated with the Mesoproterozoic Midcontinent Rift near Thunder Bay, Ontario, Canada. Precambrian Research, V. 183, p. 553-571.

Hollings, P., Smyk, M., and Cousens, B., 2012, The radiogenic isotope characteristics of dikes and sills associated with the Mesoproterozoic Midcontinent Rift near Thunder Bay, Ontario, Canada. Precambrian Research 214-215, p. 269-279.

Hollings, P. and Heggie, G, 2014, Rethinking the Midcontinent Rift – puncturing the "plume paradigm". In: Proceedings, Institute on Lake Superior Geology, 60th, Part 1, p.57.

Hooper, P. R., 1982, The Columbia river basalts. Science, 215(4539), p. 1463-1468.

Huber, N.K., 1973, The Portage Lake Volcanics (Middle Keweenawan) on Isle Royale, Michigan. United States Geological Survey, Professional Paper 754-C, p. C1 - C32.

Hutchinson, D.R., White, R.S., Cannon, W.F., and Schulz, K.J., 1990, Keweenawan hot spot: Geophysical evidence for a 1.1 Ga mantle plume beneath the Midcontinent Rift system. Journal of Geophysical Research, v. 95, 10,869-10, p. 844.

Irvine, T., and Baragar, W., 1971, A guide to the chemical classification of the common volcanic rocks. Canadian journal of earth sciences, 8(5), p. 523-548.

Klewin, K.W. and Berg, J.H., 1990, Geochemistry of the Mamainse Point volcanics, Ontario, and implications for the Keweenawan paleomagnetic record. Canadian Journal of Earth Sciences 27, p. 1194-1199.

King, E. R., and Zietz, I., 1971, Aeromagnetic study of the midcontinent gravity high of central United States. Geological Society of America Bulletin,82(8), p. 2187-2208.

Kushiro, I., 1980, Viscosity, density, and structure of silicate melts at high pressures, and their petrological applications, In: Hargraves, R.B., ed., Physics of magmatic processes. Princeton University Press, Princeton, p. 93-120.

Lane, A. C., 1898, Geological report on Isle Royale, Michigan. Geological Survey of Michigan, v. 6, 265p.

Lane, A. C. (1911). The Keweenaw series of Michigan. Michigan Geological and Biological Survey Publications 6, Geological Survey No. 4, 2 volumes, 983p.

Lawson, A. C., 1893, The anorthosytes of the Minnesota Coast of Lake Superior. Geological and Natural History Survey of Minnesota, Bulletin 8, Part 1, p. 1–23.

Longo, A.A., 1984, A correlation for a middle Keweenawan flood basalt: The Greenstone flow, Isle Royale and Keweenaw Peninsula, Michigan, M.S. thesis, Michigan Technological University, Houghton, MI, 198 pp.

Mariano, J. and Hinze, W.J., 1994a, Structural interpretation of the Midcontinent rift in eastern Lake Superior from seismic reflection and potential-field studies. Canadian Journal of Earth Sciences 31, p. 619-628.

Mariano, J. and Hinze, W.J., 1994b, Gravity and magnetic models of the Midcontinent Rift in eastern Lake Superior. Canadian Journal of Earth Sciences 31, p. 661-674.

Martin, Susan R., 1995, The state of our knowledge about ancient copper mining in Michigan. The Michigan Archaeologist, 41(2-3), p. 119-138.

McGinnis, L.D. and Mudrey, M.G., Jr., 1991, Seismic reflection profiling and tectonic evolution of the Midcontinent rift in Lake Superior: Wisconsin Geological and Natural History Survey Misc. Paper 91-2.

Miller, J. D., Jr., 1988, Geologic map of the Split Rock Point NE and Silver Bay quadrangles, Lake County, Minnesota. Minnesota Geological Survey, Miscellaneous Map Series, M-68, scale 1:24,000.

Miller, J. D. Jr., 1989. Geology of the Beaver Bay Complex, northeastern Minnesota: In: Proceedings and Abstracts, 35th, Institute on Lake Superior Geology, v. 35, p. 56-57.

Miller, J. D., Jr., Green, J. C., and Boerboom, T. B., 1989, Geology of the Illgen City Quadrangle, Lake County, Minnesota. Minnesota Geological Survey Miscellaneous Map Series, M-69, scale 1:24,000.

Miller, J.D., Jr., and Weiblen, P.W., 1990, Anorthositic rocks of the Duluth Complex: Examples of rocks formed from plagioclase crystal mush. Journal of Petrology, v. 31, p. 295–339.

Miller, J. D., Jr., Green, J. C., Boerboom, T. B., and Chandler, V. W., 1993, Geology of the Doyle Lake and Finland quadrangles, Lake County, Minnesota. Minnesota Geological Survey Miscellaneous Map Series M-73, scale 1:24,000.

Miller, J. D., Jr., Boerboom, T. B., and Jerde, E. A., 1994, Bedrock geologic map of the Cabin Lake and Cramer 7.5-minute quadrangles, Lake and Cook Counties, Minnesota. Minnesota Geological Survey Miscellaneous Map Series, M-82, scale 1:24,000.

Miller, J.D., Jr., Nicholson, S.W., and Cannon, W.F., 1995, The Midcontinent rift in the Lake Superior region, *in* Miller, J.D., Jr., ed., Field trip guidebook for the geology and ore deposits of the Midcontinent rift in the Lake Superior region. Minnesota Geological Survey Guidebook Series, no. 20, p. 1-22.

Miller, J.D., Jr., and Ripley, E.M., 1996, Layered intrusions of the Duluth Complex, Minnesota, USA. In Cawthorne, R.G., ed., Layered Intrusions: Amsterdam, Elsevier Science, p. 257-301.

Miller, J.D., Jr., and Vervoort, J.D., 1996, The latent magmatic stage of the Midcontinent rift: A period of magmatic underplating and melting of the lower crust. In: Proceedings, Institute on Lake Superior Geology, 40th, Part I – Program and Abstracts, p. 33-35.

Miller, J.D., Jr., and Chandler, V.W., 1997, Geology, petrology, and tectonic significance of the Beaver Bay Complex, northeastern Minnesota. In: Ojakangas, R.J., Dickas, A.B., Green, J.C., (eds.) Middle Proterozoic to Cambrian Rifting, Central North America. Geological Society of America Special Paper 312, p. 73-96.

Miller, J.D., Green, J.C., and Severson, M.J., 2002, Terminology, nomenclature, and classification of Keweenawan igneous rocks of northeastern Minnesota. *In* Miller, J.D. Jr., Green, J.C., Severson, M.J., Chandler, V.W., Hauck, S.A., Peterson, D.E., and Wahl, T.E., Geology and mineral potential of the Duluth Complex and related rocks of northeastern Minnesota. Minnesota Geological Survey Report of Investigations 58, p. 5-20.

Miller, J.D., and Green, J.C., 2002a, Geology of the Beaver Bay Complex and related hypabyssal intrusions. *In* Miller, J.D. Jr., Green, J.C., Severson, M.J., Chandler, V.W., Hauck, S.A., Peterson, D.E., and Wahl, T.E., Geology and mineral potential of the Duluth Complex and related rocks of northeastern Minnesota. Minnesota Geological Survey Report of Investigations 58, p. 144-163.

Miller, J.D., and Severson, M.J., 2002b, Geology of the Duluth Complex. *In* Miller, J.D. Jr., Green, J.C., Severson, M.J., Chandler, V.W., Hauck, S.A., Peterson, D.E., and Wahl, T.E., Geology and mineral potential of the Duluth Complex and related rocks of northeastern Minnesota. Minnesota Geological Survey Report of Investigations 58, p. 106-143.

Miller Jr, J. D., Green, J. C., and Jerde, E. A., 2006, Bedrock geology of the Little Marais quadrangle, Lake County, Minnesota. Minnesota Geological Survey Miscellaneous Map M-172, scale 1:24,000.

Miller, J., Nicholson, S. W., Easton, R. M., Ripley, E. M., and Feinberg, J. M. (2013). Geology and mineral deposits of the 1.1 Ga Midcontinent Rift in the Lake Superior region–an overview. Field guide to the copper-nickel-platinum group element deposits of the Lake Superior Region. Edited by Miller, J. Precambrian Research Center Guidebook, 13-01.

Morse, S. A. (1969). The Kiglapait layered intrusion, Labrador. Geological Society of America Memoirs, 112, p. 1-198.

Morey, G.B., and Green, J.C., 1982, Status of the Keweenawan as a stratigraphic unit in the Lake Superior region, *in* Wold, R.J., and Hinze, W.J., eds., Geology and tectonics of the Lake Superior basin. Geological Society of America Memoir v. 156, p. 15-26.

Nicholson, S.W., and Shirey, S.B., 1990, Midcontinent Rift volcanism in the Lake Superior region: Sr, Nd, and Pb isotopic evidence for a mantle plume origin. Journal of Geophysical Research, v. 95, 10,851-10,868.

Nicholson, S.W., Schulz, K.J., Shirey, S.B., and Green, J.C., 1997, Rift-wide correlation of 1.1 Ga Midcontinent rift system basalts: implications for multiple mantle sources during rift development: Canadian Journal of Earth Sciences, v. 34, p. 504-520.

Neuendorf, J. P. Mehl Jr and J. A. Jackson (eds) 2005. Glossary of Geology, 5th ed. Berlin, Heidelberg, New York: Springer-Verlag.

Paces, J. B., 1988, Magmatic processes, evolution and mantle source characteristics contributing to the petrogenesis of Midcontinent Rift basalts: Portage Lake Volcanics, Keweenaw Peninsula, Michigan [Ph.D. thesis]: Houghton, Michigan, Michigan Technological University, 413 p.

Paces, J.B. and Miller, J.D., 1993, Precise U-Pb ages of Duluth Complex and related mafic intrusions, northeastern, Minnesota: new insights for physical, petrogenetic, paleomagnetic and tectono-magmatic processes associated with 1.1 Ga Midcontinent rifting. Journal of Geophysical Research v.98, No B8, 13,997-14,013.

Palmer, H.C. and Davis, D.W., 1987, Paleomagnetism and U-Pb geochronology of volcanic rocks from Michipicoten Island, Lake Superior, Canada: Precise calibration of the Keweenawan polar wander track. Precambrian Research 37, p. 157-171.

Peterson, D.M., and Severson, M.J., 2002, Archean and Paleoproterozoic rocks that form the footwall of the Duluth Complex. *In* Miller, J.D. Jr., Green, J.C., Severson, M.J., Chandler, V.W., Hauck, S.A., Peterson, D.E., and Wahl, T.E., Geology and mineral potential of the Duluth Complex and related rocks of northeastern Minnesota. Minnesota Geological Survey Report of Investigations 58, p. 76-93.

Rollinson, H., 1993. Using Geochemical Data: evaluation, presentation, interpretation: Longman Singapore Publishers (Pte) Ltd., Singapore. Sinitsin, A., 2001.

Sen, G., 2001, Generation of Deccan trap magmas. Journal of Earth System Science, 110(4), p. 409-431.

Sexton, J.L. and Henson, H., Jr., 1994, Interpretation of seismic reflection and gravity profile data in western Lake Superior. Canadian Journal of Earth Sciences 31, p. 652-660.

Shank, S. G., 1989, The petrology of the Beaver Bay Complex near Silver Bay, northeastern Minnesota [M.S. thesis]: Minneapolis, Minnesota, University of Minnesota, 127 p.

Shirey, S.B., Klewin, K.W., Berg, J.H., and Carlson, R.W., 1994, Temporal changes in the sources of flood basalts: Isotopic and trace element evidence from the 1100 Ma old Keweenawan Mamainse Point Formation, Ontario, Canada. Geochimica Cosmochimica Acta 58, p. 4475-4490.

Smyk, M.C., Hollings, P., Heaman, L.M., 2006. Preliminary investigations of the petrology, geochemistry and geochronology of the St. Ignace Island Complex, Midcontinent Rift, northern Lake Superior, Ontario. 52nd Institute on Lake Superior Geology, Sault Ste. Marie, ON, Program with Abstracts, v.52, p. 61–62.

Streckeisen, A. L., 1974, Classification and nomenclature of plutonic rocks. Geologische Rundschau, 63(2), p. 773-786.

Streckeisen, A.L., 1976, Classification and nomenclature of igneous rocks. Earth-Science Reviews, v. 12, p. 1-35.

Sun S. and McDonough W. F, 1989, Chemical and isotopic systematics of oceanic basalts: implications for mantle compositions and processes. In: A. D. Saunders and M. J. Norry (editors). Magmatism in the ocean basins. Geological Society. London. p. 313-345.

Thomas, M.D. and Teskey, D.J., 1994, An interpretation of gravity anomalies over the Midcontinent rift, Lake Superior, constrained by GLIMPCE seismic and aeromagnetic data. Canadian Journal of Earth Sciences 31, p. 682-697.

Thompson, R. N., 1982, Magmatism of the British Tertiary volcanic province. Scottish Journal of Geology, 18(1), p. 49-107.

Tomkeieff, S. I., 1940, The basalt lavas of the Giant's Causeway district of Northern Ireland. Bulletin volcanologique, 6(1), p. 89-143.

Trehu, A., and 15 others., 1991. Imaging the Midcontinent Rift beneath Lake Superior using large aperture seismic data. Geophysical Research Letters, V. 18, p. 625-628.

Van Hise, C. R., and Leith, C. K., 1911, The geology of the Lake Superior region. United States Geological Survey Mon. 52, 641 p.

Vervoort, J. D., and Wirth, K. R., 2004, Origin of the rhyolite and granophyres of the Midcontinent Rift, northeast Minnesota. In: Proceedings, Institute on Lake Superior Geology, 50th, Part, 1, p. 158-159.

Vervoort, J.D., Wirth, K., Kennedy, B., Sandland, T., and Harpp, K.S., 2007, The magmatic evolution of the Midcontinent Rift: New geochronological and geochemical evidence from felsic magmatism. Precambrian Research, v. 157, p. 235-268.

Wager, L. R., and Brown, G. M., 1968, Layered igneous rocks: San Francisco, W. H. Freeman, 588 p.

Weiblen, P.W., and Morey, G. B., 1980, A summary of the stratigraphy, petrology and structure of the Duluth Complex. American Journal of Science, v. 280-A, p. 88–133.

White, W. S., 1960, The Keweenawan lavas of Lake Superior, an example of flood basalts. American Journal of Science, 258, p. 367-374.

Winter, J. D. (2014). *Principles of igneous and metamorphic petrology*. Pearson.

Wright, T. L., Mangan, M. T., and Swanson, D. A., 1989, Chemical data for flows and feeder dikes of the Yakima basalt subgroup, Columbia River basalt group, Washington, Oregon, and Idaho, and their bearing on a petrogenetic model. United States Geological Survey Bulletin No. 1821, 71p.

Zartman, R.E., Nicholson, S.W., Cannon, W.F., and Morey, G.B., 1997, U-Th-Pb zircon ages of some Keweenawan Supergroup rocks from the south shore of Lake Superior. Canadian Journal of Earth Sciences, V. 34, p. 549-561.

Appendices

Appendix A – Petrography

Project NameAppendix A - Petrography

BULK MAFIC INTRUSIVE ROCK DESCRIPTION

Sample ID	Strat Unit	Field Description	Petrographic Description	Modal Rock Type	Cumuate Type	Absolute Grain Size	Relative Grain Size	Relative Grain Size 2	CPX-based Texture	Non-granular Texture 1	Non-granular Texture 2	Mineral Alignment	Late Magmatic Features				Intensity	Distribution	Deuteric Alteration Assemblage						
KP1	loz	ophitic basalt - 2mm OPH CPX	FF ophitic olivine basalt	OOBS	NA	FF	GP	WP	OPH	OSP	FSP	FT	AG				W	ED	SER	URL	ZEO	IDD*			
KP2	loz	ophitic basalt- 2-3mm OPH CPX	FF ophitic olivine basalt	OOBS	NA	FF	GP	WP	OPH	OSP	FSP	FT	AG				W	ED	SER	URL	ZEO	IDD*			
KP3	loz	ophitic basalt - 3-4mm OPH CPX	FF ophitic olivine basalt	OOBS	NA	FF	GP	WP	OPH	OSP		FT	AG				W	ED	SER	URL	ZEO	IDD*			
KP4	loz	ophitic basalt - 5-6mm OPH CPX	FF ophitic olivine basalt	OOBS	NA	FF	GP	WP	OPH	FSP		FT	AG				W	ED	SER	URL	ZEO	IDD*			
KP5	loz	ophitic basalt - 10mm OPH CPX	MF ophitic olivine basalt	OOBS	NA	FF	GP	WP	OPH	OSP	FSP	FT	AG				W	ED	SER	URL	ZEO	IDD*			
KP6	loz	ophitic basalt - 10mm OPH CPX	FF ophitic olivine basalt	OOBS	NA	FF	GP	WP	OPH	OPK	FPK	FT	AG				M	PD	SER	SSR	URL	ZEO	IDD*		
KP7a	loz	subophitic basalt - 5mm OPH CPX	MF ophitic olivine basalt	OOBS	NA	FM	GP	WP	OPH	OPK	FPK	FT	AG				W	ED	SER	URL	ZEO	IDD*			
KP7b	hz	intergranular oxide olivine gabbro	MM laminated prismatic olivine ferrodiorite	FDRT	OPCf	MM	EG		SPG	FPS		NF	AM	AP	OC	IG	M	ED	SER	SSR	URL	ZEO	CHL		
KP8a	hz	ophitic basalt - 4-5mm OPH CPX	FF ophitic olivine basalt	OOBS	NA	FF	GP	WP	OPH	OPK	FSP	FT	OC				W	ED	SER	ZEO	CHL	IDD*			
KP8b	hz	ophitic basalt - 5mm OPH CPX	FM ophitic olivine basalt	OOBS	NA	FM	GP	WP	OPH	OPK	FSP	FT	AG				W	ED	SER	SSR	URL	CHL	IDD*		
KP9a	hz	subophitic oxide olivine gabbro	MM intergranular olivine oxide gabbro	IOOG	OPCf	MM	GP		SOP	FSP		FT	AM				W	ED	SER	SSR	URL	IDD*			
KP9b	hz	laminated subophitic oxide olivine gabbro	FM laminated subprismatic ferrodiorite	FDRT	PCf	FM	EG		SPG	FSP		LM	AP				S	ED	SER	SSR	URL	ZEO	LXN		
KP10	hz	subophitic oxide olivine gabbro	MM ophitic olivine basalt	OOGB	oPcf	MM	GP		SOP	OSP	FSP	FT	MO	AM			W	ED	SER	SSR	CHL	ZEO	IDD*		
KP11a	hz	subophitic/intergranular oxide olivine gabbro	MM ophitic olivine basalt	OOGB	oPcf	MM	GP	WP	SOP	OSP	FSP	FT	AP	AM	OC		W	ED	SER	SSR	CHL	ZEO	IDD*		
KP11b	hz	granophyric oxide olivine gabbro	CC prismatic laminated ferromonzodiorite	FMZD	PCF	CC	ED		PRG	PPS		LM	AM	AP	IG		S	ED	SER	SSR	CHL	ZEO	LXN		
KP12	hz	heterogeneous ferromonzodiorite	MM prismatic laminated ferromonzodiorite	FMZD	PCF	MM	ED		PRG	PPS		LM	AM	AP	IG		S	ED	SER	SSR	CHL	ZEO	URL	LXN	
KP13	hz	subophitic granophyric oxide olivine gabbro	FM subophitic olivine basalt	OOGB	Opcf	FM	GP	WP	SOP	FSP		FT	AM	OC			S	ED	SER	SSR	CHL	ZEO	LXN		
KP14a	hz	ferromonzodiorite	MC, altered, subophitic olivine basalt	FRDT	PCF	MC	ED		SPG	FSP		LM	AM	Ap	KP	IG	S	ED	SER	SSR	CHL	ZEO	LXN	IDD*	
KP14b	uoz	ophitic olivine basalt (5 mm oikocrytsts)	MM ophitic olivine basalt	OOGB	Opcf	MM	GP		SOP	FSP		FT	AM				M	ED	SER	SSR	CHL	ZEO	URL	LXN	
KP15	uoz	ophitic basalt - 5-6mm OPH CPX	FF ophitic olivine basalt	OOBS	NA	FF	GP	WP	OPH	FSP		FT	AG				W	ED	SER	SSR	CHL	ZEO	URL	IDD*	
KP16	uoz	ophitic basalt - 2-3mm OPH CPX	FF ophitic olivine basalt	OOBS	NA	FF	GP		OPH	FSP		FT	AG				W	ED	SER	SSR	CHL	ZEO	URL	IDD*	
KP19	ent	amygdaloidal basalt	FF, intersertal, weakly amygdaloidal basalt	AMBS	NA	FF	GP		SOP			FT	AG				M	ED	SER	URL	CHL	ZEO	IDD*		
KP101	loz	ophitic basalt - 5-6mm OPH CPX	FF ophitic olivine basalt	OOBS	NA	FF	GP	WP	OPH	OSP	FSP	FT	AG				W	ED	SER	CHL	ZEO	IDD*			
KP102a	loz	ophitic basalt - 7-8mm OPH CPX	FF ophitic olivine basalt	OOBS	NA	FF	GP	WP	OPH	FPK		FT	AG				W	ED	SER	CHL	ZEO	IDD			
KP102b	loz	ophitic basalt - 10mm OPH CPX	FF ophitic olivine basalt	OOBS	NA	FF	GP	WP	OPH	FSP		FT	AG				W	ED	SER	CHL	ZEO	IDD*			
KP103	loz	ophitic basalt - 10mm OPH CPX	FM ophitic olivine basalt	OOBS	NA	FM	GP	WP	OPH			FT	AG				M	PD	SER	SSR	URL	CHL	ZEO	IDD*	
KP104	loz	ophitic bsalt - 8-9mm OPH CPX	FM ophitic olivine basalt	OOBS	NA	FM	GP	WP	OPH			FT	AG				W	ED	SER	URL	CHL	ZEO	IDD*		
KP105	loz	ophitic basalt - 10-11mm OPH CPX	FM ophitic olivine basalt	OOBS	NA	FM	GP	WP	OPH	FSP		FT	AG				W	ED	SER	SSR	URL	CHL	ZEO	IDD	
KP106	loz	ophitic basalt - 15mm OPH CPX	M ophitic olivine basalt	OOBS	NA	FM	GP	WP	OPH	FSP		FT	AG				M	PD	SER	SSR	URL	CHL	ZEO	IDD	
KP108	loz	ophitic basalt - 20mm OPH CPX	FM ophitic olivine basalt	OOBS	NA	FM	GP	WP	OPH	OSP	FSP	FT	AG				W	ED	SER	SSR	URL	CHL	ZEO	IDD	
KP109	loz	ophitic basalt - 20mm OPH CPX	FF ophitic olivine basalt	OOBS	NA	FF	GP	WP	OPH	OSP		FT	AG				W	ED	SER	SSR	URL	CHL	ZEO	IDD	
KP110a	loz	ophitic basalt - 20mm OPH CPX	MM ophitic olivine basalt	OOBS	NA	MM	GP	WP	OPH	OSP		FT	AG				M	ED	SER	URL	CHL	IDD	SRP		
KP110b	loz	ophitic basalt - 6-7mm OPH CPX	FF ophitic olivine basalt	OOBS	NA	FF	GP	WP	OPH			FT	AG				W	ED	SER	URL	CHL*	IDD*			
KP110c	loz	ophitic basalt - 2mm OPH CPX	MM plagioclase-porphyritic, ophitic troctolitic basalt	TRBS	NA	MM	GP	MP	OPH			FT	AG	OC	AP		W	ED	SER	SSR	URL	CHL	ZEO	IDD	
KP111a	hz	laminated ferrodiorite	MC moderately-foliated, prismatic ferrodiorite	FRDT	PCf	MC	EG		PRG	PPS	FSP	PF	AM	IG	AP		M	ED	SER	SSR	CHL	ZEO			
KP111b	hz	laminated ferrodiorite	MM laminated, subprismatic ferrodiorite	FRDT	PCF	MM	EG		SPG			LM	AM	IG	AP		M	ED	SER	SSR	URL	CHL	ZEO		
KP111c	loz	ophitic olivine gabbro - 10mm OPH CPX	MM ophitic olivine basalt	OOGB	Opcf	MM	GP	MP	OPH	FSP		FT	AM	OC	AP		W	ED	SER	URL	CHL	ZEO	IDD*		
KP112	hz	subophitic basalt	MM ophitic olivine basalt	OOGB	oPcf	MM	GP	WP	SOP	OSP	FSP	FT	AM				W	ED	SER	URL	CHL*	ZEO	IDD*		
KP113	hz	subophitic basalt	MM subophitic olivine basalt	OOGB	oPcF	MM	GP		SOP	OSP		FT	AG				W	ED	SER	URL	CHL	ZEO	IDD*		
KP114	hz	subophitic basalt	MM ophitic olivine baasalt	OOGB	OPcf	MM	GP	MP	SOP	FSP		FT	AG				W	ED	SER	SSR	URL	CHL	ZEO	IDD*	
KP115	hz	intergranular to subophitic gabbro	MM intergranular oxide olivine gabbro	OOGB	OPCF	MM	GP	WP	IGR			FT	AG	AM	OC		W	ED	SER	URL	CHL	ZEO	IDD*		
KP116	hz	laminated ferrodiorite	MM prismatic, foliated olivine ferrodiorite	FRDT	OPCf	MM	WP		SPG	FPK		WF	AM	IG			M	ED	SER	SSR	URL	CHL	ZEO	IDD*	
IR1	hz	ferromonzonite or granitic inclusion	MM altered, ophitic olivine basalt	OOGB	oPcf	MM	GP		SOP	OSP	FSP	FT	AM	AG	AP		S	ED	SER	SSR	URL	CHL	ZEO	IDD*	
IR2a	hz	heterogeneous, inclusion-rich outcrop	MM subprismatic, olivine ferromonzodiorite	FMZT	OPCF	MM	EG		PRG			FT	AM	IG	AP	KP	C	ED	SER	SSR	URL	CHL	ZEO	IDD	LXN
IR2b	hz	heterogeneous, inclusion-rich outcrop	FM altered, subophitic oxide olivine gabbro	OOGB	oPcf	FM	GP		SOP	OPK	FSP	FT	AM	AG			C	ED	SER	SSR	URL	CHL	ZEO	IDD	LXN
IR3	hz	subophitic/intergranular gabbro with 5 mm gpy	MM intergranular oxide olivine gabbro	IOOG	oPcf	MM	GP		SOP	OSP	FSP	FT	AM	AG	AP		S	ED	SER	SSR	URL	CHL	ZEO	IDD	LXN
IR4	hz	prismatic ferromonzodiorite	MM subprismatic, amygdaloidal olivine ferrodiorite	FMZD	OPCF	MM	EG		PRG			NF	AM	IG	AP	KP	S	ED	SER	SSR	URL	CHL	ZEO	IDD*	LXN
IR5a	hz	taxtitic ferromonzodiorite outcrop	FF altered, amygdaloidal, subprismatic olivine ferrodiorite	OOGB	OPCF	FF	GP		IGR			FT	AG	IG	AP	KP	S	ED	SER	SSR	URL	CHL	ZEO	IDD*	
IR5b	hz	taxtitic ferromonzodiorite outcrop	MM prismatic olivine ferromonzodiorite	FMZD	OPCF	MM	EG		PRG	PPS		NF	AM	IG	AP	KP	S	ED	SER	SSR	URL	CHL	ZEO	IDD*	LXN
IR6	hz	heterogeneous, inclusion-rich outcrop	MM subprismatic olivine ferrodiorite	FRDT	oPcf	MM	EG		SPG	OSP	FSP	NF	AM	IG	AP	KP	S	ED	SER	SSR	URL	CHL	ZEO	IDD*	LXN
IR7a	hz	heterogeneous outcrop	MM subophitic oxide olivine basalt	OOBS	oPcf	MM	GP		SOP	OSP	FSP	FT	AM	IG	AP		M	ED	SER	SSR	URL	CHL	ZEO	IDD*	
IR7b	uoz (incl)	heterogeneous outcrop	FF ophitic olivine basalt	OOBS	NA	FF	GP	WP	OPH	FSP		FT	AG				W	ED	SER	URL	CHL	ZEO	IDD*		
IR7c	hz	heterogeneous outcrop	MM altered, prismatic olivine quartz ferromonzonite	FMZN	OPCF	MM	EG		PRG			NF	AM	IG	AP	KP	C	ED	SER	SSR	URL	CHL	ZEO	IDD	LZN
IR8	uoz	ophitic basalt	FF ophitic olivine basalt	OOBS	NA	FF	GP	WP	OPH	FSP		FT	AG				W	ED	SER	URL	CHL	ZEO	IDD*		
IR9	uoz	ophitic basalt	FF ophitic olivine basalt	OOBS	NA	FF	GP		OPH	FSP		FT	AG				W	ED	SER	URL	CHL	ZEO	IDD*		

Appendix A - Petrography

BULK MAFIC INTRUSIVE ROCK DESCRIPTION

Sample ID	Strat Unit	Field Description	Petrographic Description	Modal Rock Type	Cumulate Type	Absolute Grain Size	Relative Grain Size	Relative Grain Size 2	CPX-based Texture	Non-granular Texture 1	Non-granular Texture 2	Mineral Alignment	Late Magmatic Features				Intensity	Distribution	Deuteric Alteration Assemblage						
IR10	uoz	ophitic basalt	FF ophitic olivine basalt	OOBS	NA	FF	GP		OPH			FT	AG				W	ED	SER	URL	CHL	ZEO	IDD*		
IR11	ent	columnar-jointed, massive Fe-rich basalt	FF hematite-rich, intersertal basalt	OOBS	NA	FF	GP	WP	NA	INS		FT	AG				M	ED	SER	CHL	ZEO				
IR12	uoz	ophitic basalt	FF ophitic olivine basalt	OOBS	NA	FF	GP	WP	OPH			FT	AG				W	ED	SER	URL	CHL	ZEO	IDD*		
IR13	NA	amygdaloidal basalt - not GSF	---	---	---	---	---	---	---	---	---	---	---	---	---	---	---	---	---	---	---	---	---	---	---
IR15	loz	ophitic basalt - 10mm OPH CPX	FF ophitic olivine basalt	OOBS	NA	FF	GP	WP	OPH			FT	AG				W	ED	SER	URL	CHL	ZEO	IDD*		
IR16	hz	intergranular oxide olivine gabbro	MM subophitic oxide olivine gabbro	OOGB	oPcf	MM	GP	WP	SOP	OSP	FSP	FT	AM	AP			S	ED	SER	SSR	URL	CHL	ZEO	IDD*	LXN
IR17	hz	intergranular gabbro with lenses of prismatic fmd	CC subprismatic olivine ferromonzodiorite	FMZD	oPCf	CC	EG		SPG	OPK	FPK	FT	AM	IG	AP	KP	M	ED	SER	SSR	URL	CHL	ZEO	IDD	LXN
IR18	hz	intergranular gabbro	MM intergranular oxide olivine gabbro	OOGB	oPcf	MM	GP		SOP	OSP	FSP	FT	AM	AP	MO		S	ED	SER	SSR	URL	CHL	ZEO	IDD*	
IR19a	hz	ferromonzodiorite	MM subprismatic olivine ferromonzodiorite	FMZD	oPCF	MM	EG		SPG	OSP		FT	AM	IG	AP	KP	S	ED	SER	SSR	URL	CHL	ZEO	IDD	
IR19b	uoz	ophitic basalt	FF ophitic olivine basalt	OOBS	NA	FF	GP	WP	OPH	FSP		FT	AG				W	ED	SER	URL	CHL	ZEO	IDD*		
IR20	loz	ophitic basalt - 5mm OPH CPX	FF ophitic olivine basalt	OOBS	NA	FF	GP		OPH	FSP		FT	AG				W	ED	SER	URL	CHL	ZEO	IDD*		
IR21	loz	ophitic basalt - 6mm OPH CPX	FF ophitic olivine basalt	OOBS	NA	FF	GP	WP	OPH	FSP		FT	AG	AP			W	ED	SER	URL	CHL	ZEO	IDD*		
IR22	loz	ophitic basalt - 8mm OPH CPX	FF ophitic olivine basalt	OOBS	NA	FM	GP	WP	OPH	FSP		FT	AG	AP			W	ED	SER	SSR	URL	CHL	ZEO	IDD*	LXN
IR23	hz	intergranular gabbro	FM intergranular oxide olivine gabbro	IOOG	oPcf	FM	GP		SOP	OSP	FSP	FT	AG	AM	KP		W	ED	SER	SSR	URL	CHL	ZEO	IDD*	LXN
IR24	hz	ferromonzodiorite	CC prismatic olivine ferromonzodiorite	FMZD	OPCF	CC	EG		PRG			NF	AM	IG	KP	AP	S	ED	SER	SSR	URL	CHL	ZEO	IDD*	LXN
IR25	hz	ferromonzodiorite	CC subprismatic olivine ferromonzodiorite	FMZD	OPCF	CC	EG		SPG	PPS		NF	AM	IG	KP	AP	S	ED	SER	SSR	URL	CHL	ZEO	IDD*	LXN
IR26a	hz	ferromonzodiorite	MM subpprismatic olivine ferrodiorite	FRDT	OPCf	MM	GP		SPG	PPS	FSP	NF	AM	IG	KP	AP	S	ED	SER	SSR	URL	CHL	ZEO	IDD*	LXN
IR26b	uoz	ophitic basalt - 9mm OPH CPX	FF ophitic olivine basalt	OOBS	NA	FF	GP	WP	OPH	FSP		FT	AG				W	ED	SER	URL	CHL	ZEO	IDD*	LXN	
IR27	uoz	ophitic basalt - 0.5mm OPH CPX	FF ophitic olivine basalt	OOBS	NA	FF	GP	WP	OPH	FSP		FT	AG				W	ED	SER	URL	CHL	ZEO	IDD*		
BBC1	brpg	oxide-rich olivine gabbro	MC subophitic, poikilitic oxide olivine gabbro	POOG	oPcf	MC	GP		SOP	OPK	FSP	FT	IG	AP	KP		W	ED	SER	URL	CHL	IDD			
BBC2	brg	oxide-rich, intergranular gabbro	MM subophitic oxide gabbro	OOGB	oPcf	MM	GP		SOP	OPK	FSP	FT	IG	AP	OC	KP	W	ED	SER	CHL	IDD*				
BBC3	brg	ubophitic/ophitic olivine gabbro - 2-3mm OPH CPX	MM subophitic oxide olivine gabbro	OOGB	oPcf	MM	GP		SOP	OSP	FSP	FT	IG	AP	OC	AM	W	ED	SER	SSR	URL	CHL	IDD		
BBC4	brg	hitic olivine gabbro - 10mm OPH CPX/2-3mm GP	MM subophitic oxide olivine gabbro	OOBG	oPcf	MM	GP		SOP	OSP	FSP	FT	IG	OC			W	ED	SER	SSR	URL	CHL	IDD		
BBC5	brpg	ophitic olivine gabbro - 3-4mm OPH CPX	MC subophitic, poikilitic quartz oxide olivine gabbro	POOG	oPcf	MM	GP		SOP	OPK	FSP	FT	IG	AP	OC	KP	W	ED	SER	URL	CHL	IDD*			
BBC6	brd	ophitic diabase - 1-2mm OPH CPX	FF subophitic augite troctolite	AGTR	Opcf	FF	GP		SOP	FSP	PPK	FT					W	ED	SER	CHL	IDD				
BBC7	brd	ophitic olivine gabbro - 5mm OPH CPX	MM ophitic quartz oxide olivine gabbro	OOGB	oPcf	MM	GP		OPH	OSP	FSP	FT	IG	OC	KP		W	ED	SER	SSR	URL	CHL	IDD		
BBC8	brd	intergranular gabbro	plagioclase-porphyritic, granophyric, ophitic oxide olivine gab	OOGB	oPcf	MM	GP	MP	OPH	OSP	FSP	FT	IG	OC	AP		W	ED	SER	SSR	URL	CHL	IDD	LXN	
BBC9	brg	intergranular olivine gabbro	MM laminated, intergranular oxide olivine gabbro	IOOG	oPCf	MM	GP		IGR	OSP	FSP	FT	IG	AP	OC		W	ED	SER	URL	IDD*				
BBC10	brfd	intergranular olivine gabbro	MM laminated, intergranular oxide olivine gabbro	IOOG	oPCf	MM	GP		IGR	OSP	FSP	FT	IG	AP	OC		W	ED	SER	URL	IDD*				
BBC11a	brld	intergranular olivine gabbro	MM laminated, subprismatic olivine-bearing quartz ferrodiorite	FRDT	oPCF	MM	EG		SPG	PPS	OSP	PF	IG	AP	OC	KP	M	ED	SER	SSR	URL	IDD	SRP		
BBC11b	brld	ferromonzodiorite	MM subprismatic quartz ferrodiorite	FRDT	PCF	MM	EG		SPG	PPS		NF	IG	AP	OC	KP	M	ED	SER	SSR	IDD	SRP			
BBC12	brfd	intergranular olivine gabbro	MM subprismatic, olivine-bearing quartz ferrodiorite	FRDT	oPCF	MM	EG		SPG	PPS	OSP	NF	IG	AP	OC		M	ED	SER	SSR	URL	IDD	SRP		
BBC13	brpg	ophitic olivine gabbro	MM poikilitic oxide olivine gabbro	POOG	oPcF	MM	EG		SOP	PPS	OPK	FT	IG	AP	OC		W	ED	SER	CHL	URL	IDD	SRP		
BBC14	brd	ophitic olivine diabase	FF ophitic olivine diabase	OODB	Opcf	FF	GP		OPH	FSP		FT	AP	OC			W	ED	SER	URL	CHL				
SBI10	brd	ophitic olivine diaabase - 20mm OPH CPX	MM ophitic olivine diabase	OODB	oPcf	MM	GP	WP	OPH	OSP	FSP	FT	AP				W	ED	SER	URL	CHL	SRP			
SBI11	brd	intergranular gabbro	MM plagioclase-porphyritic, ophitic oxide olivine gabbro	OOGB	oPcf	MM	GP	MP	OPH	OSP	FSP	FT	IG	AM			W	ED	SER	URL	CHL	IDD			
SBI12	sbg	oxide-rich ferrogabbro	CC prismatic olivine quartz ferromonzonite	FMZN	OPCF	CC	EG		PRG	PPS	PPK	NF	IG	AM	AP	KP	M	ED	SER	URL	CHL	IDD			
SBI13	sbg	intergranular gabbro	MC prismatic quartz ferromonzodiorite	FMZD	oPCF	MC	EG		PGR	PPS	OSP	NF	IG	AM	AP	KP	M	ED	SER	URL	CHL	IDD			
SBI14	sbld	laminated ferrodiorite	MC foliated, prismatic olivine-bearing quartz ferrodiorite	FRDT	OPCF	MC	EG		PRG	PPS	PPK	PF	IG	AP	AM		W	ED	SER	URL	CHL	IDD	SRP		
SBI15	brd	ophitic olivine gabbro - 10mm OPH CPX	MM ophitic oxide olivine gabbro	OOGB	oPcf	MM	GP	WP	OPH	OSP	FSP	FT	AG	IG	AP		W	ED	SER	URL	CHL	IDD	SRP		
SBI16	brd	ophitic olivine diabase - 30mm OPH CPX	MM ophitic olivine diabase	OODB	oPcf	MM	GP	WP	OPH	OSP	FSP	FT	AG	AP	OC		W	ED	SER	URL	CHL	IDD	SRP		
SBI17	sbld	laminated ferrodiorite	CC laminated, prismatic, olivine-bearing quartz ferrodiorite	FRDT	OPCF	CC	EG		PRG	PPS	PPK	NF	IG	AP	OC	KP	W	ED	SER	URL	CHL	IDD			

Appendix B – Mineral Chemistry

Appendix B - CPX - SBBC Sample Suite

Sample	Na2O	CaO	Al2O3	Cr2O3	FeO	MgO	K2O	SiO2	TiO2	MnO	Total
SBI10-CPX-1	0.30	16.06	1.20	0.00	16.96	11.83	0.00	52.65	0.67	0.32	100.0
SBI10-CPX-2	0.27	17.99	1.07	0.00	12.19	13.62	0.00	53.57	0.93	0.35	100.0
SBI10-CPX-3	0.27	17.47	0.95	0.00	15.28	11.49	0.00	53.37	0.71	0.45	100.0
SBI10-CPX-4	0.24	16.92	1.38	0.00	14.86	12.64	0.00	52.61	0.90	0.44	100.0
SBI10-CPX-5	0.33	17.11	1.75	0.00	12.99	13.39	0.00	52.94	1.14	0.35	100.0
SBI10-CPX-6	0.38	17.98	2.13	0.00	10.83	14.13	0.00	53.05	1.09	0.42	100.0
SBI10-CPX-7	0.22	17.54	1.24	0.00	14.21	12.39	0.00	53.08	0.95	0.37	100.0
SBI10-CPX-8	0.33	17.19	0.87	0.00	14.88	12.25	0.00	53.34	0.84	0.29	100.0
SBI10-CPX-9	0.32	17.80	1.97	0.00	11.86	13.55	0.00	52.68	1.40	0.42	100.0
SBI10-CPX-10	0.37	17.91	1.71	0.00	12.27	13.39	0.00	52.58	1.39	0.38	100.0
SBI10-CPX-11	0.32	17.23	1.40	0.00	14.03	12.97	0.00	52.60	0.93	0.51	100.0
SBI10-CPX-12	0.36	17.43	1.26	0.00	12.55	13.59	0.00	53.49	0.93	0.39	100.0
Average	**0.31**	**17.39**	**1.41**	**0.00**	**13.58**	**12.94**	**0.00**	**53.00**	**0.99**	**0.39**	**100.0**
SBI11-CPX-1	0.34	16.61	1.07	0.00	16.70	11.12	0.00	53.00	0.69	0.46	100.0
SBI11-CPX-2	0.19	16.77	1.01	0.00	16.10	11.67	0.00	53.06	0.79	0.41	100.0
SBI11-CPX-3	0.24	16.57	1.01	0.00	16.74	11.37	0.00	53.06	0.59	0.42	100.0
SBI11-CPX-4	0.24	17.16	1.45	0.00	12.46	14.00	0.00	53.31	1.01	0.37	100.0
SBI11-CPX-5	0.28	16.68	1.21	0.00	15.26	12.41	0.00	52.82	0.93	0.40	100.0
SBI11-CPX-6	0.20	16.46	1.16	0.00	15.64	11.98	0.00	53.25	0.75	0.56	100.0
SBI11-CPX-7	0.00	16.06	1.11	0.00	16.14	12.49	0.00	53.08	0.69	0.43	100.0
SBI11-CPX-8	0.34	16.63	1.02	0.00	15.20	12.47	0.00	53.51	0.83	0.00	100.0
SBI11-CPX-9	0.21	16.84	0.97	0.00	15.83	12.05	0.00	52.97	0.63	0.50	100.0
SBI11-CPX-10	0.28	16.66	1.12	0.00	14.18	13.06	0.00	53.29	0.77	0.65	100.0
Average	**0.23**	**16.64**	**1.11**	**0.00**	**15.43**	**12.26**	**0.00**	**53.14**	**0.77**	**0.42**	**100.0**
SBI12-CPX-1	0.24	18.20	0.68	0.00	22.49	5.92	0.00	51.46	0.54	0.46	100.0
SBI12-CPX-2	0.24	18.26	0.84	0.00	21.86	5.99	0.00	51.49	0.87	0.47	100.0
SBI12-CPX-3	0.30	18.24	0.51	0.00	23.31	5.07	0.00	51.40	0.53	0.62	100.0
SBI12-CPX-4	0.25	18.82	0.32	0.00	23.82	4.61	0.00	51.77	0.00	0.42	100.0
SBI12-CPX-5	0.23	17.92	0.81	0.00	21.35	6.87	0.00	51.76	0.57	0.50	100.0
SBI12-CPX-6	0.30	17.72	0.63	0.00	21.96	6.74	0.00	51.16	0.66	0.83	100.0
SBI12-CPX-7	0.20	18.21	0.45	0.00	23.26	5.08	0.00	51.69	0.52	0.58	100.0
SBI12-CPX-8	0.35	18.14	0.66	0.00	22.70	5.63	0.00	51.50	0.67	0.35	100.0
SBI12-CPX-9	0.45	18.20	0.61	0.00	23.14	5.10	0.00	51.18	0.62	0.70	100.0
SBI12-CPX-10	0.22	18.32	0.60	0.00	23.03	5.18	0.00	51.32	0.60	0.73	100.0
SBI12-CPX-11	0.29	18.21	0.36	0.00	24.19	4.66	0.00	51.54	0.36	0.39	100.0
Average	**0.28**	**18.20**	**0.59**	**0.00**	**22.83**	**5.53**	**0.00**	**51.48**	**0.54**	**0.55**	**100.0**

Appendix B - CPX - SBBC Sample Suite

Sample	CAT SUM	Si	Al	Na	Ca	Cr	Fe	Mg	K	Ti	Mn	Total	Mg#
SBI10-CPX-1	2.28	2.00	0.05	0.02	0.65	0.00	0.54	0.67	0.00	0.02	0.01	3.97	55.4
SBI10-CPX-2	2.24	2.00	0.05	0.02	0.72	0.00	0.38	0.76	0.00	0.03	0.01	3.96	66.6
SBI10-CPX-3	2.27	2.02	0.04	0.02	0.71	0.00	0.48	0.65	0.00	0.02	0.01	3.95	57.3
SBI10-CPX-4	2.27	1.99	0.06	0.02	0.68	0.00	0.47	0.71	0.00	0.03	0.01	3.97	60.3
SBI10-CPX-5	2.25	1.98	0.08	0.02	0.69	0.00	0.41	0.75	0.00	0.03	0.01	3.96	64.7
SBI10-CPX-6	2.23	1.97	0.09	0.03	0.72	0.00	0.34	0.78	0.00	0.03	0.01	3.97	69.9
SBI10-CPX-7	2.26	2.00	0.06	0.02	0.71	0.00	0.45	0.69	0.00	0.03	0.01	3.96	60.8
SBI10-CPX-8	2.27	2.01	0.04	0.02	0.69	0.00	0.47	0.69	0.00	0.02	0.01	3.96	59.5
SBI10-CPX-9	2.24	1.97	0.09	0.02	0.71	0.00	0.37	0.75	0.00	0.04	0.01	3.96	67.1
SBI10-CPX-10	2.25	1.97	0.08	0.03	0.72	0.00	0.38	0.75	0.00	0.04	0.01	3.97	66.0
SBI10-CPX-11	2.26	1.98	0.06	0.02	0.70	0.00	0.44	0.73	0.00	0.03	0.02	3.97	62.2
SBI10-CPX-12	2.24	2.00	0.06	0.03	0.70	0.00	0.39	0.76	0.00	0.03	0.01	3.96	65.9
Average	**2.26**	**1.99**	**0.06**	**0.02**	**0.70**	**0.00**	**0.43**	**0.72**	**0.00**	**0.03**	**0.01**	**3.96**	**63.0**
SBI11-CPX-1	2.28	2.01	0.05	0.03	0.68	0.00	0.53	0.63	0.00	0.02	0.01	3.96	54.3
SBI11-CPX-2	2.28	2.01	0.05	0.01	0.68	0.00	0.51	0.66	0.00	0.02	0.01	3.95	56.4
SBI11-CPX-3	2.28	2.01	0.05	0.02	0.67	0.00	0.53	0.64	0.00	0.02	0.01	3.96	54.8
SBI11-CPX-4	2.24	1.99	0.06	0.02	0.69	0.00	0.39	0.78	0.00	0.03	0.01	3.96	66.7
SBI11-CPX-5	2.27	1.99	0.05	0.02	0.67	0.00	0.48	0.70	0.00	0.03	0.01	3.96	59.2
SBI11-CPX-6	2.27	2.01	0.05	0.01	0.67	0.00	0.49	0.67	0.00	0.02	0.02	3.95	57.7
SBI11-CPX-7	2.27	2.00	0.05	0.00	0.65	0.00	0.51	0.70	0.00	0.02	0.01	3.95	58.0
SBI11-CPX-8	2.26	2.01	0.05	0.02	0.67	0.00	0.48	0.70	0.00	0.02	0.00	3.95	59.4
SBI11-CPX-9	2.28	2.01	0.04	0.02	0.68	0.00	0.50	0.68	0.00	0.02	0.02	3.96	57.6
SBI11-CPX-10	2.26	2.00	0.05	0.02	0.67	0.00	0.45	0.73	0.00	0.02	0.02	3.96	62.1
Average	**2.27**	**2.01**	**0.05**	**0.02**	**0.67**	**0.00**	**0.49**	**0.69**	**0.00**	**0.02**	**0.01**	**3.96**	**58.6**
SBI12-CPX-1	2.36	2.02	0.03	0.02	0.77	0.00	0.74	0.35	0.00	0.02	0.02	3.96	31.9
SBI12-CPX-2	2.35	2.02	0.04	0.02	0.77	0.00	0.72	0.35	0.00	0.03	0.02	3.95	32.8
SBI12-CPX-3	2.37	2.03	0.02	0.02	0.77	0.00	0.77	0.30	0.00	0.02	0.02	3.95	27.9
SBI12-CPX-4	2.38	2.05	0.01	0.02	0.80	0.00	0.79	0.27	0.00	0.00	0.01	3.95	25.6
SBI12-CPX-5	2.34	2.02	0.04	0.02	0.75	0.00	0.70	0.40	0.00	0.02	0.02	3.95	36.4
SBI12-CPX-6	2.36	2.01	0.03	0.02	0.75	0.00	0.72	0.39	0.00	0.02	0.03	3.97	35.4
SBI12-CPX-7	2.37	2.04	0.02	0.02	0.77	0.00	0.77	0.30	0.00	0.02	0.02	3.94	28.0
SBI12-CPX-8	2.36	2.02	0.03	0.03	0.76	0.00	0.75	0.33	0.00	0.02	0.01	3.95	30.7
SBI12-CPX-9	2.37	2.02	0.03	0.03	0.77	0.00	0.76	0.30	0.00	0.02	0.02	3.96	28.2
SBI12-CPX-10	2.37	2.03	0.03	0.02	0.77	0.00	0.76	0.30	0.00	0.02	0.02	3.95	28.6
SBI12-CPX-11	2.38	2.04	0.02	0.02	0.77	0.00	0.80	0.27	0.00	0.01	0.01	3.95	25.6
Average	**2.37**	**2.03**	**0.03**	**0.02**	**0.77**	**0.00**	**0.75**	**0.32**	**0.00**	**0.02**	**0.02**	**3.95**	**30.1**

Appendix B - CPX - SBBC Sample Suite

Sample	Na2O	CaO	Al2O3	Cr2O3	FeO	MgO	K2O	SiO2	TiO2	MnO	Total
SBI13-CPX-1	0.27	17.72	0.98	0.00	18.07	9.44	0.00	52.48	0.66	0.38	100.0
SBI13-CPX-2	0.23	17.60	1.13	0.00	17.66	9.95	0.00	52.38	0.65	0.41	100.0
SBI13-CPX-3	0.24	17.16	0.90	0.00	19.68	8.73	0.00	52.13	0.77	0.38	100.0
SBI13-CPX-4	0.25	17.71	0.91	0.00	17.27	9.80	0.00	52.85	0.79	0.42	100.0
SBI13-CPX-5	0.00	17.51	0.69	0.00	20.25	8.11	0.00	52.23	0.53	0.67	100.0
SBI13-CPX-6	0.24	17.66	0.88	0.00	16.78	10.64	0.00	52.67	0.75	0.37	100.0
SBI13-CPX-7	0.27	16.08	0.89	0.00	19.12	9.95	0.00	52.49	0.77	0.43	100.0
SBI13-CPX-8	0.00	17.38	0.77	0.00	21.25	7.65	0.00	51.83	0.64	0.48	100.0
SBI13-CPX-9	0.21	17.08	0.69	0.00	20.24	8.58	0.00	51.89	0.86	0.46	100.0
SBI13-CPX-10	0.00	17.14	0.89	0.00	19.32	9.08	0.00	52.49	0.75	0.34	100.0
SBI13-CPX-11	0.00	17.26	0.93	0.00	18.80	9.11	0.00	52.87	0.71	0.32	100.0
SBI13-CPX-12	0.35	17.07	1.05	0.00	18.63	9.52	0.00	52.05	0.65	0.67	100.0
Average	**0.17**	**17.28**	**0.89**	**0.00**	**18.92**	**9.21**	**0.00**	**52.36**	**0.71**	**0.44**	**100.0**
SBI14-CPX-1	0.29	17.88	0.87	0.00	16.21	10.66	0.00	53.02	0.75	0.31	100.0
SBI14-CPX-2	0.18	18.07	1.08	0.00	15.06	11.41	0.00	52.96	0.78	0.46	100.0
SBI14-CPX-3	0.26	18.18	1.04	0.00	15.18	11.20	0.00	52.93	0.71	0.50	100.0
SBI14-CPX-4	0.26	18.18	1.04	0.00	15.18	11.20	0.00	52.93	0.71	0.50	100.0
SBI14-CPX-5	0.24	18.74	0.97	0.00	14.43	11.28	0.00	53.14	0.84	0.36	100.0
SBI14-CPX-6	0.00	18.56	0.94	0.00	15.10	11.32	0.00	52.96	0.82	0.31	100.0
SBI14-CPX-7	0.22	17.07	0.98	0.00	15.88	11.36	0.00	53.29	0.80	0.40	100.0
SBI14-CPX-8	0.34	16.90	1.01	0.00	16.53	11.18	0.00	52.71	0.90	0.42	100.0
SBI14-CPX-9	0.18	15.59	1.00	0.00	18.38	10.98	0.00	52.88	0.66	0.34	100.0
Average	**0.22**	**17.69**	**0.99**	**0.00**	**15.77**	**11.18**	**0.00**	**52.98**	**0.77**	**0.40**	**100.0**
SBI15-CPX-1	0.21	16.88	0.97	0.00	15.45	12.42	0.00	53.72	0.34	0.00	100.0
SBI15-CPX-2	0.28	17.69	1.27	0.00	14.65	12.00	0.00	53.13	0.70	0.29	100.0
SBI15-CPX-3	0.00	18.45	1.36	0.00	13.85	12.02	0.00	53.57	0.75	0.00	100.0
SBI15-CPX-4	0.25	18.75	1.55	0.00	13.21	12.34	0.00	52.97	0.92	0.00	100.0
SBI15-CPX-5	0.32	15.64	1.34	0.00	15.76	13.07	0.00	52.85	0.77	0.26	100.0
SBI15-CPX-6	0.22	16.98	1.32	0.00	14.68	13.37	0.00	52.62	0.80	0.00	100.0
SBI15-CPX-7	0.21	17.97	1.72	0.00	12.71	13.24	0.00	52.76	0.98	0.42	100.0
Average	**0.21**	**17.48**	**1.36**	**0.00**	**14.33**	**12.64**	**0.00**	**53.09**	**0.75**	**0.14**	**100.0**

Appendix B - CPX - SBBC Sample Suite

Sample	CAT SUM	Si	Al	Na	Ca	Cr	Fe	Mg	K	Ti	Mn	Total	Mg#
SBI13-CPX-1	2.30	2.01	0.04	0.02	0.73	0.00	0.58	0.54	0.00	0.02	0.01	3.96	48.2
SBI13-CPX-2	2.30	2.00	0.05	0.02	0.72	0.00	0.57	0.57	0.00	0.02	0.01	3.96	50.1
SBI13-CPX-3	2.32	2.01	0.04	0.02	0.71	0.00	0.64	0.50	0.00	0.02	0.01	3.95	44.1
SBI13-CPX-4	2.29	2.02	0.04	0.02	0.72	0.00	0.55	0.56	0.00	0.02	0.01	3.95	50.3
SBI13-CPX-5	2.33	2.02	0.03	0.00	0.73	0.00	0.66	0.47	0.00	0.02	0.02	3.94	41.6
SBI13-CPX-6	2.29	2.01	0.04	0.02	0.72	0.00	0.54	0.60	0.00	0.02	0.01	3.96	53.1
SBI13-CPX-7	2.31	2.01	0.04	0.02	0.66	0.00	0.61	0.57	0.00	0.02	0.01	3.95	48.1
SBI13-CPX-8	2.34	2.02	0.04	0.00	0.72	0.00	0.69	0.44	0.00	0.02	0.02	3.95	39.1
SBI13-CPX-9	2.33	2.01	0.03	0.02	0.71	0.00	0.66	0.50	0.00	0.03	0.02	3.96	43.0
SBI13-CPX-10	2.31	2.02	0.04	0.00	0.71	0.00	0.62	0.52	0.00	0.02	0.01	3.94	45.6
SBI13-CPX-11	2.30	2.03	0.04	0.00	0.71	0.00	0.60	0.52	0.00	0.02	0.01	3.93	46.3
SBI13-CPX-12	2.31	2.00	0.05	0.03	0.70	0.00	0.60	0.55	0.00	0.02	0.02	3.97	47.7
Average	**2.31**	**2.01**	**0.04**	**0.01**	**0.71**	**0.00**	**0.61**	**0.53**	**0.00**	**0.02**	**0.01**	**3.95**	**46.4**
SBI14-CPX-1	2.28	2.02	0.04	0.02	0.73	0.00	0.52	0.60	0.00	0.02	0.01	3.95	54.0
SBI14-CPX-2	2.27	2.00	0.05	0.01	0.73	0.00	0.48	0.64	0.00	0.02	0.01	3.96	57.4
SBI14-CPX-3	2.28	2.01	0.05	0.02	0.74	0.00	0.48	0.63	0.00	0.02	0.02	3.96	56.8
SBI14-CPX-4	2.28	2.01	0.05	0.02	0.74	0.00	0.48	0.63	0.00	0.02	0.02	3.96	56.8
SBI14-CPX-5	2.27	2.01	0.04	0.02	0.76	0.00	0.46	0.64	0.00	0.02	0.01	3.95	58.2
SBI14-CPX-6	2.28	2.01	0.04	0.00	0.75	0.00	0.48	0.64	0.00	0.02	0.01	3.95	57.2
SBI14-CPX-7	2.27	2.02	0.04	0.02	0.69	0.00	0.50	0.64	0.00	0.02	0.01	3.95	56.0
SBI14-CPX-8	2.28	2.00	0.05	0.03	0.69	0.00	0.53	0.63	0.00	0.03	0.01	3.96	54.7
SBI14-CPX-9	2.29	2.02	0.04	0.01	0.64	0.00	0.59	0.62	0.00	0.02	0.01	3.95	51.6
Average	**2.28**	**2.01**	**0.04**	**0.02**	**0.72**	**0.00**	**0.50**	**0.63**	**0.00**	**0.02**	**0.01**	**3.95**	**55.9**
SBI15-CPX-1	2.26	2.02	0.04	0.02	0.68	0.00	0.49	0.70	0.00	0.01	0.00	3.95	58.9
SBI15-CPX-2	2.27	2.00	0.06	0.02	0.71	0.00	0.46	0.67	0.00	0.02	0.01	3.96	59.3
SBI15-CPX-3	2.25	2.01	0.06	0.00	0.74	0.00	0.43	0.67	0.00	0.02	0.00	3.94	60.7
SBI15-CPX-4	2.26	1.99	0.07	0.02	0.75	0.00	0.41	0.69	0.00	0.03	0.00	3.96	62.5
SBI15-CPX-5	2.27	1.99	0.06	0.02	0.63	0.00	0.50	0.73	0.00	0.02	0.01	3.97	59.6
SBI15-CPX-6	2.26	1.98	0.06	0.02	0.68	0.00	0.46	0.75	0.00	0.02	0.00	3.98	61.9
SBI15-CPX-7	2.25	1.98	0.08	0.02	0.72	0.00	0.40	0.74	0.00	0.03	0.01	3.97	65.0
Average	**2.26**	**2.00**	**0.06**	**0.02**	**0.70**	**0.00**	**0.45**	**0.71**	**0.00**	**0.02**	**0.00**	**3.96**	**61.1**

Appendix B - CPX - SBBC Sample Suite

Sample	Na2O	CaO	Al2O3	Cr2O3	FeO	MgO	K2O	SiO2	TiO2	MnO	Total
SBI16-CPX-1	0.25	18.41	1.60	0.00	12.65	13.29	0.00	52.66	0.82	0.32	100.0
SBI16-CPX-2	0.19	18.15	1.39	0.00	13.59	12.39	0.00	53.18	0.81	0.29	100.0
SBI16-CPX-3	0.19	18.00	1.34	0.00	13.42	12.54	0.00	53.36	0.84	0.32	100.0
SBI16-CPX-4	0.26	17.72	1.17	0.00	13.82	12.47	0.00	53.43	0.75	0.39	100.0
SBI16-CPX-5	0.00	16.48	1.34	0.00	14.17	13.77	0.00	53.01	0.92	0.31	100.0
SBI16-CPX-6	0.17	17.74	1.22	0.00	13.90	12.56	0.00	53.14	0.86	0.40	100.0
Average	**0.18**	**17.75**	**1.34**	**0.00**	**13.59**	**12.84**	**0.00**	**53.13**	**0.83**	**0.34**	**100.0**
B364-CPX-1	0.35	20.10	1.68	0.10	7.70	16.10	0.03	51.00	0.74	0.21	98.0
B364-CPX-2	0.32	20.00	2.21	0.31	7.20	16.20	0.04	50.00	0.91	0.17	97.4
B364-CPX-3	0.29	19.70	1.85	0.36	6.90	16.70	0.04	51.90	0.74	0.15	98.6
B364-CPX-4	0.33	19.00	2.54	0.14	8.00	16.20	0.04	49.60	1.39	0.18	97.4
B364-CPX-5	0.31	18.20	2.32	0.05	8.90	16.60	0.04	49.80	1.28	0.22	97.7
Average	**0.32**	**19.40**	**2.12**	**0.19**	**7.74**	**16.36**	**0.04**	**50.46**	**1.01**	**0.19**	**97.8**
D126-CPX-1	0.42	19.00	2.67	0.28	7.80	16.60	0.08	51.40	0.98	0.24	99.5
D126-CPX-2	0.46	19.40	2.54	0.15	7.80	16.40	0.06	51.20	1.23	0.25	99.5
D126-CPX-3	0.47	19.50	2.11	0.13	7.60	16.70	0.07	50.40	0.05	0.22	97.3
Average	**0.45**	**19.30**	**2.44**	**0.19**	**7.73**	**16.57**	**0.07**	**51.00**	**0.75**	**0.24**	**98.7**
E161-CPX-1	0.39	19.40	2.74	0.41	7.20	17.00	0.04	48.90	0.86	0.19	97.1
E161-CPX-2	0.37	19.80	1.74	0.29	6.80	17.50	0.06	51.50	0.54	0.21	98.8
E161-CPX-3	0.40	19.90	2.00	0.13	7.60	16.70	0.05	50.60	1.11	0.23	98.7
Average	**0.39**	**19.70**	**2.16**	**0.28**	**7.20**	**17.07**	**0.05**	**50.33**	**0.84**	**0.21**	**98.2**
D314-CPX-1	0.42	19.40	2.45	0.05	9.40	15.70	0.04	49.80	1.27	0.24	98.8
D314-CPX-2	0.43	19.40	2.34	0.06	9.50	15.70	0.05	49.50	1.17	0.24	98.4
D314-CPX-3	0.43	19.70	2.56	0.14	8.70	15.60	0.04	50.00	0.97	0.26	98.4
D314-CPX-4	0.41	18.20	1.98	0.00	10.80	15.80	0.05	51.20	0.88	0.31	99.6
D314-CPX-5	0.41	19.60	2.38	0.10	9.30	15.70	0.05	50.60	1.15	0.25	99.5
Average	**0.42**	**19.26**	**2.34**	**0.07**	**9.54**	**15.70**	**0.05**	**50.22**	**1.09**	**0.26**	**98.9**
D246-CPX-1	0.46	20.20	2.31	0.00	8.80	15.10	0.07	51.20	0.78	0.28	99.2
D246-CPX-2	0.43	20.00	2.03	0.21	7.80	16.10	0.05	51.10	0.70	0.22	98.6
D246-CPX-3	0.44	18.20	2.34	0.03	10.10	16.10	0.05	49.70	1.14	0.30	98.4
D246-CPX-4	0.41	20.00	2.21	0.34	7.70	16.00	0.04	51.70	0.69	0.24	99.3
D246-CPX-5	0.43	18.30	1.81	0.04	9.80	16.80	0.05	50.60	0.73	0.30	98.9
D246-CPX-6	0.42	18.60	2.35	0.00	9.70	15.70	0.05	49.80	1.29	0.30	98.2
D246-CPX-7	0.45	19.00	2.06	0.03	9.40	15.70	0.05	51.00	1.07	0.32	99.1
Average	**0.43**	**19.19**	**2.16**	**0.09**	**9.04**	**15.93**	**0.05**	**50.73**	**0.91**	**0.28**	**98.8**

Appendix B - CPX - SBBC Sample Suite

Sample	CAT SUM	Si	Al	Na	Ca	Cr	Fe	Mg	K	Ti	Mn	Total	Mg#
SBI16-CPX-1	2.25	1.97	0.07	0.02	0.74	0.00	0.40	0.74	0.00	0.02	0.01	3.98	65.2
SBI16-CPX-2	2.26	2.00	0.06	0.01	0.73	0.00	0.43	0.69	0.00	0.02	0.01	3.96	61.9
SBI16-CPX-3	2.25	2.00	0.06	0.01	0.72	0.00	0.42	0.70	0.00	0.02	0.01	3.95	62.5
SBI16-CPX-4	2.26	2.01	0.05	0.02	0.71	0.00	0.43	0.70	0.00	0.02	0.01	3.96	61.7
SBI16-CPX-5	2.25	1.99	0.06	0.00	0.66	0.00	0.44	0.77	0.00	0.03	0.01	3.96	63.4
SBI16-CPX-6	2.26	2.00	0.05	0.01	0.71	0.00	0.44	0.70	0.00	0.02	0.01	3.96	61.7
Average	**2.26**	**1.99**	**0.06**	**0.01**	**0.71**	**0.00**	**0.43**	**0.72**	**0.00**	**0.02**	**0.01**	**3.96**	**62.7**
B364-CPX-1	2.27	1.93	0.07	0.03	0.81	0.00	0.24	0.91	0.00	0.02	0.01	4.03	78.8
B364-CPX-2	2.29	1.90	0.10	0.02	0.82	0.01	0.23	0.92	0.00	0.03	0.01	4.03	80.0
B364-CPX-3	2.24	1.94	0.08	0.02	0.79	0.01	0.22	0.93	0.00	0.02	0.00	4.01	81.2
B364-CPX-4	2.29	1.89	0.11	0.02	0.77	0.00	0.25	0.92	0.00	0.04	0.01	4.03	78.3
B364-CPX-5	2.28	1.89	0.10	0.02	0.74	0.00	0.28	0.94	0.00	0.04	0.01	4.03	76.9
Average	**2.27**	**1.91**	**0.09**	**0.02**	**0.79**	**0.01**	**0.25**	**0.92**	**0.00**	**0.03**	**0.01**	**4.02**	**79.0**
D126-CPX-1	2.23	1.91	0.12	0.03	0.76	0.01	0.24	0.92	0.00	0.03	0.01	4.02	79.1
D126-CPX-2	2.23	1.90	0.11	0.03	0.77	0.00	0.24	0.91	0.00	0.03	0.01	4.02	78.9
D126-CPX-3	2.29	1.92	0.09	0.03	0.80	0.00	0.24	0.95	0.00	0.00	0.01	4.05	79.7
Average	**2.25**	**1.91**	**0.11**	**0.03**	**0.77**	**0.01**	**0.24**	**0.92**	**0.00**	**0.02**	**0.01**	**4.03**	**79.2**
E161-CPX-1	2.29	1.87	0.12	0.03	0.79	0.01	0.23	0.97	0.00	0.02	0.01	4.06	80.8
E161-CPX-2	2.24	1.92	0.08	0.03	0.79	0.01	0.21	0.97	0.00	0.02	0.01	4.04	82.1
E161-CPX-3	2.26	1.90	0.09	0.03	0.80	0.00	0.24	0.93	0.00	0.03	0.01	4.04	79.7
Average	**2.26**	**1.90**	**0.10**	**0.03**	**0.80**	**0.01**	**0.23**	**0.96**	**0.00**	**0.02**	**0.01**	**4.04**	**80.9**
D314-CPX-1	2.27	1.88	0.11	0.03	0.79	0.00	0.30	0.89	0.00	0.04	0.01	4.04	74.9
D314-CPX-2	2.29	1.88	0.10	0.03	0.79	0.00	0.30	0.89	0.00	0.03	0.01	4.05	74.7
D314-CPX-3	2.28	1.89	0.11	0.03	0.80	0.00	0.28	0.88	0.00	0.03	0.01	4.04	76.2
D314-CPX-4	2.25	1.92	0.09	0.03	0.73	0.00	0.34	0.88	0.00	0.02	0.01	4.03	72.3
D314-CPX-5	2.25	1.90	0.11	0.03	0.79	0.00	0.29	0.88	0.00	0.03	0.01	4.03	75.1
Average	**2.27**	**1.90**	**0.10**	**0.03**	**0.78**	**0.00**	**0.30**	**0.88**	**0.00**	**0.03**	**0.01**	**4.04**	**74.6**
D246-CPX-1	2.25	1.92	0.10	0.03	0.81	0.00	0.28	0.84	0.00	0.02	0.01	4.02	75.4
D246-CPX-2	2.26	1.92	0.09	0.03	0.81	0.01	0.25	0.90	0.00	0.02	0.01	4.03	78.6
D246-CPX-3	2.28	1.89	0.10	0.03	0.74	0.00	0.32	0.91	0.00	0.03	0.01	4.04	74.0
D246-CPX-4	2.24	1.93	0.10	0.03	0.80	0.01	0.24	0.89	0.00	0.02	0.01	4.02	78.7
D246-CPX-5	2.27	1.91	0.08	0.03	0.74	0.00	0.31	0.94	0.00	0.02	0.01	4.05	75.3
D246-CPX-6	2.28	1.89	0.11	0.03	0.76	0.00	0.31	0.89	0.00	0.04	0.01	4.03	74.3
D246-CPX-7	2.26	1.92	0.09	0.03	0.77	0.00	0.30	0.88	0.00	0.03	0.01	4.02	74.9
Average	**2.26**	**1.91**	**0.10**	**0.03**	**0.77**	**0.00**	**0.28**	**0.89**	**0.00**	**0.03**	**0.01**	**4.03**	**75.9**

Appendix B - CPX - SBBC Sample Suite

Sample	Na2O	CaO	Al2O3	Cr2O3	FeO	MgO	K2O	SiO2	TiO2	MnO	Total
B326-CPX-1	0.42	18.00	2.13	0.07	11.20	15.70	0.06	50.90	1.08	0.29	99.9
B326-CPX-2	0.44	18.30	2.65	0.36	9.20	16.10	0.06	50.60	0.86	0.23	98.8
B326-CPX-3	0.48	17.50	2.00	0.02	12.50	14.90	0.06	50.60	1.10	0.31	99.5
B326-CPX-4	0.44	18.00	2.31	0.05	12.00	14.70	0.06	49.70	1.31	0.29	98.9
B326-CPX-5	0.43	17.20	2.09	0.08	12.30	15.20	0.06	50.70	1.24	0.18	99.5
Average	**0.44**	**17.80**	**2.24**	**0.12**	**11.44**	**15.32**	**0.06**	**50.50**	**1.12**	**0.26**	**99.3**
A376-CPX-1	0.30	18.50	3.24	0.51	9.40	14.80	0.04	48.80	1.14	0.25	97.0
A376-CPX-2	0.36	18.70	3.40	0.70	9.60	14.80	0.02	49.20	1.11	0.24	98.1
A376-CPX-3	0.34	15.60	2.34	0.03	14.50	14.30	0.04	49.50	1.33	0.41	98.4
A376-CPX-4	0.30	19.10	3.06	0.56	8.90	14.70	0.04	48.90	1.06	0.22	96.8
A376-CPX-5	0.31	19.10	3.66	0.91	8.70	14.10	0.04	48.30	1.17	0.23	96.5
Average	**0.32**	**18.20**	**3.14**	**0.54**	**10.22**	**14.54**	**0.04**	**48.94**	**1.16**	**0.27**	**97.4**
A290B-CPX-1	0.28	17.30	1.52	0.13	10.40	16.10	0.06	50.70	0.70	0.32	97.5
A290B-CPX-2	0.31	20.00	2.53	0.25	9.60	15.50	0.04	50.30	1.02	0.15	99.7
A290B-CPX-3	0.25	18.60	1.56	0.44	9.20	16.60	0.04	51.40	0.62	0.27	99.0
Average	**0.28**	**18.63**	**1.87**	**0.27**	**9.73**	**16.07**	**0.05**	**50.80**	**0.78**	**0.25**	**98.7**
E217-CPX-1	0.38	18.50	2.36	0.00	10.70	15.40	0.05	51.40	1.22	0.29	100.3
E217-CPX-2	0.41	18.50	2.73	0.07	10.10	15.40	0.05	50.00	1.31	0.34	98.9
E217-CPX-3	0.43	19.40	2.46	0.09	9.40	15.50	0.04	49.60	1.22	0.29	98.4
E217-CPX-4	0.39	18.80	2.13	0.05	10.60	15.50	0.05	51.20	1.04	0.31	100.1
Average	**0.40**	**18.80**	**2.42**	**0.05**	**10.20**	**15.45**	**0.05**	**50.55**	**1.20**	**0.31**	**99.4**
E154-CPX-1	0.35	18.70	1.69	0.16	9.33	16.50	0.04	51.50	0.69	0.25	99.2
E154-CPX-2	0.40	19.00	2.60	0.03	10.20	15.40	0.04	49.80	1.11	0.24	98.8
E154-CPX-3	0.43	18.30	3.20	0.00	10.50	15.30	0.07	47.70	1.05	0.27	96.8
E154-CPX-4	0.41	17.50	2.61	0.00	11.70	15.40	0.05	48.60	1.25	0.31	97.8
E154-CPX-5	0.41	13.00	1.35	0.00	15.70	16.70	0.05	49.90	0.75	0.42	98.3
E154-CPX-6	0.39	15.50	1.27	0.00	14.00	16.00	0.05	51.00	0.77	0.44	99.4
Average	**0.40**	**17.00**	**2.12**	**0.03**	**11.91**	**15.88**	**0.05**	**49.75**	**0.94**	**0.32**	**98.4**
B413B-CPX-1	0.40	19.50	1.87	0.16	106.00	14.90	0.06	50.40	0.78	0.24	194.3
B413B-CPX-2	0.35	19.00	1.88	0.11	10.70	14.90	0.06	49.60	0.79	0.25	97.6
B413B-CPX-3	0.34	18.90	2.01	0.03	12.10	14.20	0.05	50.10	0.97	0.31	99.0
B413B-CPX-4	0.30	17.90	1.54	0.00	13.10	13.40	0.05	48.50	0.90	0.34	96.0
B413B-CPX-5	0.31	16.90	1.67	0.00	13.40	13.20	0.05	47.50	0.89	0.39	94.3
B413B-CPX-6	0.30	18.90	1.77	0.02	12.80	13.90	0.04	49.90	0.94	0.33	98.9
Average	**0.33**	**18.52**	**1.79**	**0.05**	**28.02**	**14.08**	**0.05**	**49.33**	**0.88**	**0.31**	**113.4**

Appendix B - CPX - SBBC Sample Suite

Sample	CAT SUM	Si	Al	Na	Ca	Cr	Fe	Mg	K	Ti	Mn	Total	Mg#
B326-CPX-1	2.25	1.91	0.09	0.03	0.72	0.00	0.35	0.88	0.00	0.03	0.01	4.03	71.4
B326-CPX-2	2.26	1.90	0.12	0.03	0.74	0.01	0.29	0.90	0.00	0.02	0.01	4.03	75.7
B326-CPX-3	2.27	1.91	0.09	0.04	0.71	0.00	0.40	0.84	0.00	0.03	0.01	4.03	68.0
B326-CPX-4	2.29	1.89	0.10	0.03	0.73	0.00	0.38	0.83	0.00	0.04	0.01	4.03	68.6
B326-CPX-5	2.27	1.91	0.09	0.03	0.70	0.00	0.39	0.85	0.00	0.04	0.01	4.02	68.8
Average	**2.27**	**1.91**	**0.10**	**0.03**	**0.72**	**0.00**	**0.36**	**0.86**	**0.00**	**0.03**	**0.01**	**4.03**	**70.5**
A376-CPX-1	2.31	1.88	0.15	0.02	0.76	0.02	0.30	0.85	0.00	0.03	0.01	4.02	73.7
A376-CPX-2	2.29	1.87	0.15	0.03	0.76	0.02	0.31	0.84	0.00	0.03	0.01	4.02	73.3
A376-CPX-3	2.31	1.90	0.11	0.03	0.64	0.00	0.47	0.82	0.00	0.04	0.01	4.02	63.7
A376-CPX-4	2.31	1.88	0.14	0.02	0.79	0.02	0.29	0.84	0.00	0.03	0.01	4.02	74.6
A376-CPX-5	2.32	1.87	0.17	0.02	0.79	0.03	0.28	0.81	0.00	0.03	0.01	4.01	74.3
Average	**2.31**	**1.88**	**0.14**	**0.02**	**0.75**	**0.02**	**0.33**	**0.83**	**0.00**	**0.03**	**0.01**	**4.02**	**71.9**
A290B-CPX-1	2.29	1.94	0.07	0.02	0.71	0.00	0.33	0.92	0.00	0.02	0.01	4.02	73.4
A290B-CPX-2	2.25	1.89	0.11	0.02	0.80	0.01	0.30	0.87	0.00	0.03	0.00	4.04	74.2
A290B-CPX-3	2.26	1.93	0.07	0.02	0.75	0.01	0.29	0.93	0.00	0.02	0.01	4.02	76.3
Average	**2.27**	**1.92**	**0.08**	**0.02**	**0.75**	**0.01**	**0.31**	**0.90**	**0.00**	**0.02**	**0.01**	**4.03**	**74.6**
E217-CPX-1	2.24	1.91	0.10	0.03	0.74	0.00	0.33	0.85	0.00	0.03	0.01	4.02	71.9
E217-CPX-2	2.27	1.89	0.12	0.03	0.75	0.00	0.32	0.87	0.00	0.04	0.01	4.03	73.1
E217-CPX-3	2.28	1.88	0.11	0.03	0.79	0.00	0.30	0.88	0.00	0.03	0.01	4.04	74.6
E217-CPX-4	2.25	1.91	0.09	0.03	0.75	0.00	0.33	0.86	0.00	0.03	0.01	4.03	72.3
Average	**2.26**	**1.90**	**0.11**	**0.03**	**0.76**	**0.00**	**0.32**	**0.87**	**0.00**	**0.03**	**0.01**	**4.03**	**73.0**
E154-CPX-1	2.25	1.93	0.07	0.03	0.75	0.00	0.29	0.92	0.00	0.02	0.01	4.03	75.9
E154-CPX-2	2.28	1.89	0.12	0.03	0.77	0.00	0.32	0.87	0.00	0.03	0.01	4.04	72.9
E154-CPX-3	2.33	1.85	0.15	0.03	0.76	0.00	0.34	0.89	0.00	0.03	0.01	4.06	72.2
E154-CPX-4	2.31	1.87	0.12	0.03	0.72	0.00	0.38	0.88	0.00	0.04	0.01	4.05	70.1
E154-CPX-5	2.31	1.92	0.06	0.03	0.54	0.00	0.50	0.96	0.00	0.02	0.01	4.05	65.5
E154-CPX-6	2.28	1.93	0.06	0.03	0.63	0.00	0.44	0.90	0.00	0.02	0.01	4.03	67.1
Average	**2.29**	**1.90**	**0.10**	**0.03**	**0.69**	**0.00**	**0.38**	**0.90**	**0.00**	**0.03**	**0.01**	**4.04**	**70.6**
B413B-CPX-1	1.52	1.27	0.06	0.02	0.53	0.00	2.24	0.56	0.00	0.01	0.01	4.70	20.0
B413B-CPX-2	2.31	1.91	0.09	0.03	0.78	0.00	0.34	0.85	0.00	0.02	0.01	4.04	71.3
B413B-CPX-3	2.29	1.91	0.09	0.03	0.77	0.00	0.39	0.81	0.00	0.03	0.01	4.03	67.7
B413B-CPX-4	2.38	1.92	0.07	0.02	0.76	0.00	0.43	0.79	0.00	0.03	0.01	4.03	64.6
B413B-CPX-5	2.42	1.91	0.08	0.02	0.73	0.00	0.45	0.79	0.00	0.03	0.01	4.03	63.7
B413B-CPX-6	2.30	1.91	0.08	0.02	0.78	0.00	0.41	0.79	0.00	0.03	0.01	4.03	65.9
Average	**2.20**	**1.81**	**0.08**	**0.02**	**0.72**	**0.00**	**0.71**	**0.77**	**0.00**	**0.02**	**0.01**	**4.14**	**58.9**

Appendix B - CPX - SBBC Sample Suite

Sample	Na2O	CaO	Al2O3	Cr2O3	FeO	MgO	K2O	SiO2	TiO2	MnO	Total
C505D-CPX-1	0.29	19.10	2.19	0.19	11.50	14.30	0.05	49.70	0.96	0.26	98.5
C505D-CPX-2	0.32	18.60	2.66	0.29	11.00	14.30	0.04	48.40	1.05	0.28	96.9
C505D-CPX-3	0.34	19.60	2.56	0.38	10.30	14.30	0.05	49.60	1.05	0.23	98.4
C505D-CPX-4	0.31	18.80	2.13	0.17	11.20	14.20	0.05	48.90	0.96	0.29	97.0
C505D-CPX-5	0.46	18.80	1.98	0.00	13.20	13.40	0.05	50.00	1.01	0.35	99.3
Average	**0.34**	**18.98**	**2.30**	**0.21**	**11.44**	**14.10**	**0.05**	**49.32**	**1.01**	**0.28**	**98.0**
B319-CPX-1	0.29	18.90	1.70	0.01	13.30	13.70	0.03	50.00	0.95	0.36	99.2
B319-CPX-2	0.34	19.80	2.76	0.60	9.90	14.80	0.02	50.40	0.88	0.25	99.8
B319-CPX-3	0.45	18.90	3.24	1.02	10.90	14.90	0.07	50.10	1.13	0.31	101.0
Average	**0.36**	**19.20**	**2.57**	**0.54**	**11.37**	**14.47**	**0.04**	**50.17**	**0.99**	**0.31**	**100.0**
C179B-CPX-1	0.44	18.80	2.36	0.21	12.00	14.10	0.07	50.10	1.01	0.27	99.4
C179B-CPX-2	0.40	18.20	1.59	0.10	11.90	15.00	0.06	51.00	0.74	0.28	99.3
C179B-CPX-3	0.40	18.40	2.28	0.18	12.10	14.60	0.06	50.40	0.98	0.28	99.7
C179B-CPX-4	0.43	18.90	1.80	0.08	12.00	14.30	0.06	50.30	0.88	0.30	99.1
C179B-CPX-5	0.40	18.90	2.10	0.15	11.60	14.50	0.07	51.30	397.00	0.26	496.3
C179B-CPX-6	0.42	18.70	2.16	0.17	11.80	14.30	0.06	51.30	0.99	0.25	100.2
Average	**0.42**	**18.65**	**2.05**	**0.15**	**11.90**	**14.47**	**0.06**	**50.73**	**66.93**	**0.27**	**165.6**
F261-CPX-1	0.40	18.50	2.30	0.00	12.30	14.30	0.06	50.60	1.01	0.34	99.8
F261-CPX-2	0.40	18.60	1.92	0.03	12.50	14.40	0.02	49.90	0.89	0.38	99.0
F261-CPX-3	0.36	16.60	1.99	0.00	15.10	13.90	0.05	49.60	0.91	0.43	98.9
F261-CPX-4	0.41	19.00	2.21	0.04	11.90	14.30	0.05	50.10	0.98	0.34	99.3
F261-CPX-5	0.34	17.20	1.68	0.00	14.80	13.80	0.05	50.00	1.07	0.42	99.4
Average	**0.38**	**17.98**	**2.02**	**0.01**	**13.32**	**14.14**	**0.05**	**50.04**	**0.97**	**0.38**	**99.3**
A386D-CPX-1	0.21	17.30	0.89	0.09	20.50	8.90	0.04	49.70	0.66	0.56	98.9
A386D-CPX-2	0.59	19.80	1.14	0.00	16.40	10.30	0.05	51.20	0.64	0.63	100.8
A386D-CPX-3	0.26	17.10	0.79	0.00	21.00	8.50	0.06	49.40	0.60	0.63	98.3
A386D-CPX-4	0.92	18.70	1.50	0.00	16.10	9.50	0.07	49.60	0.92	0.66	98.0
A386D-CPX-5	0.50	18.50	1.01	0.00	19.30	8.80	0.07	49.00	0.64	0.56	98.4
A386D-CPX-6	0.25	18.20	0.89	0.00	18.80	9.50	0.05	50.00	0.66	0.62	99.0
A386D-CPX-7	0.29	17.60	0.84	0.00	20.20	8.40	0.04	48.60	0.61	0.59	97.2
A386D-CPX-8	0.28	17.40	0.87	0.00	20.40	8.30	0.05	49.50	0.62	0.61	98.0
Average	**0.41**	**18.08**	**0.99**	**0.01**	**19.09**	**9.03**	**0.05**	**49.63**	**0.67**	**0.61**	**98.6**

Appendix B - CPX - SBBC Sample Suite

Sample	CAT SUM	Si	Al	Na	Ca	Cr	Fe	Mg	K	Ti	Mn	Total	Mg#
C505D-CPX-1	2.30	1.90	0.10	0.02	0.78	0.01	0.37	0.82	0.00	0.03	0.01	4.03	68.9
C505D-CPX-2	2.33	1.88	0.12	0.02	0.77	0.01	0.36	0.83	0.00	0.03	0.01	4.04	69.8
C505D-CPX-3	2.29	1.89	0.12	0.03	0.80	0.01	0.33	0.81	0.00	0.03	0.01	4.03	71.2
C505D-CPX-4	2.33	1.90	0.10	0.02	0.78	0.01	0.36	0.82	0.00	0.03	0.01	4.03	69.3
C505D-CPX-5	2.30	1.91	0.09	0.03	0.77	0.00	0.42	0.76	0.00	0.03	0.01	4.03	64.4
Average	**2.31**	**1.90**	**0.10**	**0.03**	**0.78**	**0.01**	**0.37**	**0.81**	**0.00**	**0.03**	**0.01**	**4.03**	**68.7**
B319-CPX-1	2.30	1.91	0.08	0.02	0.77	0.00	0.43	0.78	0.00	0.03	0.01	4.03	64.7
B319-CPX-2	2.26	1.89	0.12	0.02	0.80	0.02	0.31	0.83	0.00	0.02	0.01	4.03	72.7
B319-CPX-3	2.24	1.87	0.14	0.03	0.75	0.03	0.34	0.83	0.00	0.03	0.01	4.03	70.9
Average	**2.26**	**1.89**	**0.11**	**0.03**	**0.78**	**0.02**	**0.36**	**0.81**	**0.00**	**0.03**	**0.01**	**4.03**	**69.4**
C179B-CPX-1	2.28	1.90	0.11	0.03	0.76	0.01	0.38	0.80	0.00	0.03	0.01	4.03	67.7
C179B-CPX-2	2.27	1.93	0.07	0.03	0.74	0.00	0.38	0.85	0.00	0.02	0.01	4.03	69.2
C179B-CPX-3	2.27	1.90	0.10	0.03	0.75	0.01	0.38	0.82	0.00	0.03	0.01	4.03	68.3
C179B-CPX-4	2.29	1.92	0.08	0.03	0.77	0.00	0.38	0.81	0.00	0.03	0.01	4.03	68.0
C179B-CPX-5	0.48	0.41	0.02	0.01	0.16	0.00	0.08	0.17	0.00	2.37	0.00	3.22	69.0
C179B-CPX-6	2.25	1.92	0.10	0.03	0.75	0.01	0.37	0.80	0.00	0.03	0.01	4.01	68.3
Average	**1.97**	**1.66**	**0.08**	**0.03**	**0.66**	**0.00**	**0.33**	**0.71**	**0.00**	**0.42**	**0.01**	**3.89**	**68.4**
F261-CPX-1	2.27	1.91	0.10	0.03	0.75	0.00	0.39	0.80	0.00	0.03	0.01	4.03	67.4
F261-CPX-2	2.29	1.91	0.09	0.03	0.76	0.00	0.40	0.82	0.00	0.03	0.01	4.04	67.2
F261-CPX-3	2.31	1.91	0.09	0.03	0.68	0.00	0.49	0.80	0.00	0.03	0.01	4.04	62.1
F261-CPX-4	2.28	1.90	0.10	0.03	0.77	0.00	0.38	0.81	0.00	0.03	0.01	4.04	68.2
F261-CPX-5	2.30	1.91	0.08	0.03	0.71	0.00	0.47	0.79	0.00	0.03	0.01	4.03	62.4
Average	**2.29**	**1.91**	**0.09**	**0.03**	**0.73**	**0.00**	**0.43**	**0.80**	**0.00**	**0.03**	**0.01**	**4.03**	**65.5**
A386D-CPX-1	2.38	1.97	0.04	0.02	0.73	0.00	0.68	0.52	0.00	0.02	0.02	4.00	43.6
A386D-CPX-2	2.30	1.96	0.05	0.04	0.81	0.00	0.52	0.59	0.00	0.02	0.02	4.02	52.8
A386D-CPX-3	2.40	1.97	0.04	0.02	0.73	0.00	0.70	0.51	0.00	0.02	0.02	4.01	41.9
A386D-CPX-4	2.37	1.95	0.07	0.07	0.79	0.00	0.53	0.56	0.00	0.03	0.02	4.02	51.3
A386D-CPX-5	2.39	1.95	0.05	0.04	0.79	0.00	0.64	0.52	0.00	0.02	0.02	4.03	44.8
A386D-CPX-6	2.36	1.96	0.04	0.02	0.77	0.00	0.62	0.56	0.00	0.02	0.02	4.01	47.4
A386D-CPX-7	2.42	1.96	0.04	0.02	0.76	0.00	0.68	0.51	0.00	0.02	0.02	4.01	42.6
A386D-CPX-8	2.40	1.98	0.04	0.02	0.74	0.00	0.68	0.49	0.00	0.02	0.02	4.00	42.0
Average	**2.38**	**1.96**	**0.05**	**0.03**	**0.77**	**0.00**	**0.63**	**0.53**	**0.00**	**0.02**	**0.02**	**4.01**	**45.8**

Appendix B - CPX - SBBC Sample Suite

Sample	Na2O	CaO	Al2O3	Cr2O3	FeO	MgO	K2O	SiO2	TiO2	MnO	Total
A386H-CPX-1	0.25	17.80	1.15	0.03	16.00	12.00	0.04	49.00	0.75	0.44	97.5
A386H-CPX-2	0.39	20.10	1.67	0.00	12.80	12.20	0.05	50.20	0.90	0.46	98.8
A386H-CPX-3	0.41	19.40	1.10	0.00	14.90	11.00	0.05	49.20	0.64	0.53	97.2
A386H-CPX-4	0.44	19.50	1.11	0.09	14.80	11.10	0.04	49.30	0.64	0.57	97.6
Average	**0.37**	**19.20**	**1.26**	**0.03**	**14.63**	**11.58**	**0.05**	**49.43**	**0.73**	**0.50**	**97.8**
A386G-CPX-1	0.40	17.70	0.80	0.03	20.70	8.20	0.07	48.50	0.30	0.51	97.2
A386G-CPX-2	0.36	18.60	1.56	0.08	13.70	12.66	0.04	49.70	0.89	0.40	98.0
A386G-CPX-3	0.23	18.30	0.58	0.05	18.30	10.40	0.04	49.40	0.31	0.54	98.2
A386G-CPX-4	0.34	18.00	1.26	0.12	15.40	12.00	0.05	49.90	0.78	0.45	98.3
A386G-CPX-5	0.27	18.00	1.48	0.02	14.30	13.10	0.04	49.50	0.89	0.40	98.0
Average	**0.32**	**18.12**	**1.14**	**0.06**	**16.48**	**11.27**	**0.05**	**49.40**	**0.63**	**0.46**	**97.9**
A420-CPX-1	0.23	18.60	0.91	0.00	22.50	6.10	0.05	49.30	0.70	0.60	99.0
A420-CPX-2	0.20	18.60	0.96	0.01	22.00	6.40	0.04	49.40	0.73	0.54	98.9
A420-CPX-3	0.20	17.90	1.07	0.00	21.10	7.40	0.04	49.20	0.76	0.58	98.3
A420-CPX-4	0.36	18.70	0.93	0.08	22.70	6.00	0.09	50.20	0.68	0.66	100.4
A420-CPX-5	0.20	18.80	1.01	0.00	21.70	7.30	0.05	50.10	0.76	0.55	100.5
A420-CPX-6	0.19	18.40	0.87	0.01	22.60	5.90	0.05	49.30	0.68	0.60	98.6
A420-CPX-7	0.23	8.70	0.74	0.01	23.60	5.10	0.05	49.50	0.62	0.58	89.1
Average	**0.23**	**17.10**	**0.93**	**0.02**	**22.31**	**6.31**	**0.05**	**49.57**	**0.70**	**0.59**	**97.8**
A313-CPX-1	0.23	19.20	0.92	0.00	24.60	4.70	0.05	46.90	0.86	0.61	98.1
A313-CPX-2	0.22	19.40	1.14	0.04	26.50	3.90	0.05	47.10	1.06	0.63	100.0
A313-CPX-3	0.23	19.70	0.94	0.01	24.80	4.40	0.06	47.70	0.86	0.60	99.3
A313-CPX-4	0.23	19.30	0.89	0.04	25.20	4.20	0.06	47.80	0.86	0.64	99.2
A313-CPX-5	0.22	18.70	0.71	0.04	25.70	3.50	0.05	45.60	0.69	0.62	95.8
A313-CPX-6	0.22	18.00	0.95	0.00	24.40	4.20	0.04	45.80	0.86	0.62	95.1
Average	**0.23**	**19.05**	**0.93**	**0.02**	**25.20**	**4.15**	**0.05**	**46.82**	**0.87**	**0.62**	**97.9**
A386A-CPX-1	0.28	17.60	1.21	0.02	16.20	11.60	0.03	49.30	0.81	0.42	97.5
A386A-CPX-2	0.24	17.30	0.93	0.00	19.50	9.60	0.04	49.30	0.67	0.57	98.2
A386A-CPX-3	0.25	17.20	0.82	0.03	22.10	8.10	0.06	49.40	0.62	0.64	99.2
A386A-CPX-4	0.21	16.40	0.66	0.00	23.80	6.70	0.05	48.50	0.57	0.77	97.7
A386A-CPX-5	0.31	18.60	0.52	0.01	24.80	4.70	0.04	48.10	0.35	0.67	98.1
A386A-CPX-6	0.23	17.00	0.96	0.00	19.90	9.10	0.05	49.60	0.68	0.58	98.1
Average	**0.25**	**17.35**	**0.85**	**0.01**	**21.05**	**8.30**	**0.05**	**49.03**	**0.62**	**0.61**	**98.1**

Appendix B - CPX - SBBC Sample Suite

Sample	CAT SUM	Si	Al	Na	Ca	Cr	Fe	Mg	K	Ti	Mn	Total	Mg#
A386H-CPX-1	2.37	1.93	0.05	0.02	0.75	0.00	0.53	0.71	0.00	0.02	0.01	4.03	57.2
A386H-CPX-2	2.31	1.93	0.08	0.03	0.83	0.00	0.41	0.70	0.00	0.03	0.01	4.02	62.9
A386H-CPX-3	2.37	1.94	0.05	0.03	0.82	0.00	0.49	0.65	0.00	0.02	0.02	4.03	56.8
A386H-CPX-4	2.37	1.94	0.05	0.03	0.82	0.00	0.49	0.65	0.00	0.02	0.02	4.03	57.2
Average	**2.36**	**1.94**	**0.06**	**0.03**	**0.81**	**0.00**	**0.48**	**0.68**	**0.00**	**0.02**	**0.02**	**4.03**	**58.5**
A386G-CPX-1	2.43	1.96	0.04	0.03	0.77	0.00	0.70	0.49	0.00	0.01	0.02	4.03	41.4
A386G-CPX-2	2.33	1.93	0.07	0.03	0.77	0.00	0.44	0.73	0.00	0.03	0.01	4.02	62.2
A386G-CPX-3	2.38	1.96	0.03	0.02	0.78	0.00	0.61	0.61	0.00	0.01	0.02	4.03	50.3
A386G-CPX-4	2.34	1.94	0.06	0.03	0.75	0.00	0.50	0.70	0.00	0.02	0.01	4.02	58.1
A386G-CPX-5	2.34	1.92	0.07	0.02	0.75	0.00	0.46	0.76	0.00	0.03	0.01	4.03	62.0
Average	**2.36**	**1.94**	**0.05**	**0.02**	**0.76**	**0.00**	**0.54**	**0.66**	**0.00**	**0.02**	**0.02**	**4.02**	**54.8**
A420-CPX-1	2.41	1.97	0.04	0.02	0.80	0.00	0.75	0.36	0.00	0.02	0.02	3.99	32.6
A420-CPX-2	2.40	1.97	0.05	0.02	0.80	0.00	0.74	0.38	0.00	0.02	0.02	3.99	34.1
A420-CPX-3	2.40	1.97	0.05	0.02	0.77	0.00	0.71	0.44	0.00	0.02	0.02	3.99	38.5
A420-CPX-4	2.37	1.98	0.04	0.03	0.79	0.00	0.75	0.35	0.00	0.02	0.02	3.99	32.0
A420-CPX-5	2.36	1.96	0.05	0.02	0.79	0.00	0.71	0.43	0.00	0.02	0.02	4.00	37.5
A420-CPX-6	2.41	1.98	0.04	0.01	0.79	0.00	0.76	0.35	0.00	0.02	0.02	3.99	31.8
A420-CPX-7	2.60	2.14	0.04	0.02	0.40	0.00	0.85	0.33	0.00	0.02	0.02	3.83	27.8
Average	**2.42**	**2.00**	**0.04**	**0.02**	**0.73**	**0.00**	**0.75**	**0.38**	**0.00**	**0.02**	**0.02**	**3.97**	**33.5**
A313-CPX-1	2.48	1.93	0.04	0.02	0.85	0.00	0.85	0.29	0.00	0.03	0.02	4.03	25.4
A313-CPX-2	2.45	1.92	0.05	0.02	0.85	0.00	0.90	0.24	0.00	0.03	0.02	4.03	20.8
A313-CPX-3	2.44	1.94	0.05	0.02	0.86	0.00	0.84	0.27	0.00	0.03	0.02	4.02	24.0
A313-CPX-4	2.45	1.95	0.04	0.02	0.84	0.00	0.86	0.25	0.00	0.03	0.02	4.02	22.9
A313-CPX-5	2.56	1.94	0.04	0.02	0.85	0.00	0.91	0.22	0.00	0.02	0.02	4.03	19.5
A313-CPX-6	2.55	1.94	0.05	0.02	0.82	0.00	0.87	0.27	0.00	0.03	0.02	4.01	23.5
Average	**2.49**	**1.94**	**0.05**	**0.02**	**0.84**	**0.00**	**0.87**	**0.26**	**0.00**	**0.03**	**0.02**	**4.02**	**22.7**
A386A-CPX-1	2.37	1.94	0.06	0.02	0.74	0.00	0.53	0.68	0.00	0.02	0.01	4.02	56.1
A386A-CPX-2	2.39	1.96	0.04	0.02	0.74	0.00	0.65	0.57	0.00	0.02	0.02	4.01	46.7
A386A-CPX-3	2.39	1.96	0.04	0.02	0.73	0.00	0.73	0.48	0.00	0.02	0.02	4.01	39.5
A386A-CPX-4	2.45	1.97	0.03	0.02	0.72	0.00	0.81	0.41	0.00	0.02	0.03	4.00	33.4
A386A-CPX-5	2.47	1.97	0.03	0.02	0.82	0.00	0.85	0.29	0.00	0.01	0.02	4.02	25.2
A386A-CPX-6	2.39	1.97	0.04	0.02	0.72	0.00	0.66	0.54	0.00	0.02	0.02	4.00	44.9
Average	**2.41**	**1.96**	**0.04**	**0.02**	**0.74**	**0.00**	**0.71**	**0.49**	**0.00**	**0.02**	**0.02**	**4.01**	**41.0**

Appendix B - CPX - SBBC Sample Suite

Sample	Na2O	CaO	Al2O3	Cr2O3	FeO	MgO	K2O	SiO2	TiO2	MnO	Total
A412-CPX-1	0.21	18.20	1.05	0.10	21.00	7.80	0.04	48.40	0.69	0.55	98.0
A412-CPX-2	0.22	18.30	1.03	0.01	20.90	8.00	0.03	48.70	0.68	0.56	98.4
A412-CPX-3	0.24	19.00	0.97	0.01	21.60	7.80	0.05	49.20	0.68	0.55	100.1
A412-CPX-4	0.23	18.30	1.05	0.03	21.20	7.70	0.05	48.20	0.66	0.57	98.0
A412-CPX-5	0.23	19.00	0.90	0.02	22.00	7.20	0.05	48.70	0.59	0.55	99.2
A412-CPX-6	0.21	18.60	0.93	0.00	21.10	7.70	0.05	48.80	0.68	0.55	98.6
Average	**0.22**	**18.57**	**0.99**	**0.03**	**21.30**	**7.70**	**0.05**	**48.67**	**0.66**	**0.56**	**98.7**
C402-CPX-1	0.21	18.00	0.99	0.10	20.90	7.50	0.03	47.60	0.66	0.54	96.5
C402-CPX-2	0.22	17.80	0.75	0.00	21.20	7.60	0.03	46.90	0.50	0.53	95.5
C402-CPX-3	0.24	18.10	0.75	0.04	22.70	6.70	0.05	48.20	0.55	0.58	97.9
C402-CPX-4	0.22	18.20	1.06	0.10	20.30	8.30	0.05	48.20	0.72	0.58	97.7
C402-CPX-5	0.23	17.80	1.07	0.07	20.20	8.40	0.03	47.80	0.70	0.54	96.8
C402-CPX-6	0.26	17.90	1.00	0.00	20.90	7.80	0.04	48.50	0.66	0.60	97.7
Average	**0.23**	**17.97**	**0.94**	**0.05**	**21.03**	**7.72**	**0.04**	**47.87**	**0.63**	**0.56**	**97.0**
SB28-CPX-1	0.34	17.90	1.62	0.01	12.70	13.00	0.00	49.40	0.89	0.33	96.2
Average	**0.34**	**17.90**	**1.62**	**0.01**	**12.70**	**13.00**	**0.00**	**49.40**	**0.89**	**0.33**	**96.2**
B309B-CPX-1	0.63	17.90	1.76	0.01	13.60	13.80	0.02	49.80	1.03	0.26	98.8
B309B-CPX-2	0.35	17.60	1.57	0.03	15.00	13.10	0.03	49.70	1.07	0.37	98.8
B309B-CPX-3	0.31	15.80	1.25	0.02	17.80	12.80	0.02	50.40	0.83	0.46	99.7
B309B-CPX-4	0.33	16.40	0.91	0.10	19.50	11.30	0.04	47.80	0.62	0.50	97.5
Average	**0.41**	**16.93**	**1.37**	**0.04**	**16.48**	**12.75**	**0.03**	**49.43**	**0.89**	**0.40**	**98.7**
B309C-CPX-1	0.29	18.30	1.70	0.00	13.60	13.60	0.05	50.60	0.84	0.35	99.3
B309C-CPX-2	0.30	16.80	1.51	0.00	17.10	11.60	0.06	49.90	0.68	0.51	98.5
B309C-CPX-3	0.38	17.40	2.01	0.00	15.90	11.30	0.07	49.70	0.56	0.47	97.8
B309C-CPX-4	0.25	18.90	1.66	0.04	13.40	14.10	0.05	51.20	0.86	0.33	100.8
B309C-CPX-5	0.28	17.70	1.77	0.03	13.80	13.90	0.06	51.00	0.80	0.37	99.7
Average	**0.30**	**17.82**	**1.73**	**0.01**	**14.76**	**12.90**	**0.06**	**50.48**	**0.75**	**0.41**	**99.2**
C420-CPX-1	0.28	17.10	1.80	0.03	13.10	14.30	0.03	50.80	0.86	0.35	98.7
C420-CPX-2	0.29	18.50	1.83	0.00	12.10	14.10	0.05	50.80	0.95	0.32	98.9
C420-CPX-3	0.31	17.20	1.68	0.00	14.20	13.50	0.04	50.50	0.86	0.43	98.7
C420-CPX-4	0.28	16.60	1.55	0.00	17.10	11.70	0.05	50.10	0.76	0.55	98.7
C420-CPX-5	0.33	16.30	1.53	0.00	16.70	11.90	0.06	49.20	0.78	0.49	97.3
C420-CPX-6	0.29	18.20	2.30	0.00	12.10	14.20	0.04	50.20	0.95	0.32	98.6
C420-CPX-7	0.27	18.10	1.42	0.00	14.60	12.90	0.04	50.70	0.84	0.42	99.3
Average	**0.29**	**17.43**	**1.73**	**0.00**	**14.27**	**13.23**	**0.04**	**50.33**	**0.86**	**0.41**	**98.6**

Appendix B - CPX - SBBC Sample Suite

Sample	CAT SUM	Si	Al	Na	Ca	Cr	Fe	Mg	K	Ti	Mn	Total	Mg#
A412-CPX-1	2.42	1.95	0.05	0.02	0.78	0.00	0.71	0.47	0.00	0.02	0.02	4.02	39.8
A412-CPX-2	2.40	1.95	0.05	0.02	0.78	0.00	0.70	0.48	0.00	0.02	0.02	4.02	40.6
A412-CPX-3	2.37	1.94	0.05	0.02	0.80	0.00	0.71	0.46	0.00	0.02	0.02	4.02	39.2
A412-CPX-4	2.42	1.94	0.05	0.02	0.79	0.00	0.71	0.46	0.00	0.02	0.02	4.02	39.3
A412-CPX-5	2.40	1.95	0.04	0.02	0.81	0.00	0.74	0.43	0.00	0.02	0.02	4.02	36.8
A412-CPX-6	2.40	1.95	0.04	0.02	0.80	0.00	0.71	0.46	0.00	0.02	0.02	4.02	39.4
Average	**2.40**	**1.95**	**0.05**	**0.02**	**0.80**	**0.00**	**0.71**	**0.46**	**0.00**	**0.02**	**0.02**	**4.02**	**39.2**
C402-CPX-1	2.46	1.95	0.05	0.02	0.79	0.00	0.71	0.46	0.00	0.02	0.02	4.02	39.0
C402-CPX-2	2.49	1.94	0.04	0.02	0.79	0.00	0.74	0.47	0.00	0.02	0.02	4.03	39.0
C402-CPX-3	2.44	1.96	0.04	0.02	0.79	0.00	0.77	0.41	0.00	0.02	0.02	4.02	34.5
C402-CPX-4	2.42	1.94	0.05	0.02	0.78	0.00	0.68	0.50	0.00	0.02	0.02	4.02	42.1
C402-CPX-5	2.44	1.94	0.05	0.02	0.77	0.00	0.69	0.51	0.00	0.02	0.02	4.02	42.6
C402-CPX-6	2.42	1.96	0.05	0.02	0.77	0.00	0.70	0.47	0.00	0.02	0.02	4.01	39.9
Average	**2.45**	**1.95**	**0.04**	**0.02**	**0.78**	**0.00**	**0.72**	**0.47**	**0.00**	**0.02**	**0.02**	**4.02**	**39.5**
SB28-CPX-1	2.36	1.94	0.07	0.03	0.75	0.00	0.42	0.76	0.00	0.03	0.01	4.01	64.6
Average	**2.36**	**1.94**	**0.07**	**0.03**	**0.75**	**0.00**	**0.42**	**0.76**	**0.00**	**0.03**	**0.01**	**4.01**	**64.6**
B309B-CPX-1	2.31	1.91	0.08	0.05	0.74	0.00	0.44	0.79	0.00	0.03	0.01	4.04	64.4
B309B-CPX-2	2.32	1.92	0.07	0.03	0.73	0.00	0.48	0.75	0.00	0.03	0.01	4.03	60.9
B309B-CPX-3	2.31	1.94	0.06	0.02	0.65	0.00	0.57	0.73	0.00	0.02	0.01	4.02	56.2
B309B-CPX-4	2.41	1.92	0.04	0.03	0.70	0.00	0.65	0.67	0.00	0.02	0.02	4.06	50.8
Average	**2.34**	**1.92**	**0.06**	**0.03**	**0.71**	**0.00**	**0.54**	**0.74**	**0.00**	**0.03**	**0.01**	**4.04**	**58.1**
B309C-CPX-1	2.29	1.93	0.08	0.02	0.75	0.00	0.43	0.77	0.00	0.02	0.01	4.02	64.1
B309C-CPX-2	2.34	1.95	0.07	0.02	0.70	0.00	0.56	0.67	0.00	0.02	0.02	4.01	54.7
B309C-CPX-3	2.35	1.94	0.09	0.03	0.73	0.00	0.52	0.66	0.00	0.02	0.02	4.01	55.9
B309C-CPX-4	2.26	1.92	0.07	0.02	0.76	0.00	0.42	0.79	0.00	0.02	0.01	4.03	65.2
B309C-CPX-5	2.28	1.93	0.08	0.02	0.72	0.00	0.44	0.79	0.00	0.02	0.01	4.01	64.2
Average	**2.30**	**1.94**	**0.08**	**0.02**	**0.73**	**0.00**	**0.47**	**0.74**	**0.00**	**0.02**	**0.01**	**4.02**	**60.8**
C420-CPX-1	2.29	1.94	0.08	0.02	0.70	0.00	0.42	0.81	0.00	0.02	0.01	4.01	66.0
C420-CPX-2	2.28	1.93	0.08	0.02	0.75	0.00	0.38	0.80	0.00	0.03	0.01	4.01	67.5
C420-CPX-3	2.31	1.94	0.08	0.02	0.71	0.00	0.46	0.77	0.00	0.02	0.01	4.01	62.9
C420-CPX-4	2.34	1.95	0.07	0.02	0.69	0.00	0.56	0.68	0.00	0.02	0.02	4.01	54.9
C420-CPX-5	2.37	1.94	0.07	0.03	0.69	0.00	0.55	0.70	0.00	0.02	0.02	4.02	55.9
C420-CPX-6	2.29	1.92	0.10	0.02	0.74	0.00	0.39	0.81	0.00	0.03	0.01	4.02	67.7
C420-CPX-7	2.30	1.94	0.06	0.02	0.74	0.00	0.47	0.74	0.00	0.02	0.01	4.01	61.2
Average	**2.31**	**1.94**	**0.08**	**0.02**	**0.72**	**0.00**	**0.46**	**0.76**	**0.00**	**0.02**	**0.01**	**4.01**	**62.3**

Appendix B - CPX - SBBC Sample Suite

Sample	Na2O	CaO	Al2O3	Cr2O3	FeO	MgO	K2O	SiO2	TiO2	MnO	Total
B413A-CPX-1	0.25	17.50	1.20	0.00	14.60	9.30	0.04	45.30	0.71	0.69	89.6
B413A-CPX-2	0.20	17.40	1.04	0.05	18.40	10.50	0.05	49.20	0.71	0.54	98.1
B413A-CPX-3	0.25	18.00	0.76	0.00	22.50	7.30	0.06	49.60	0.58	0.67	99.7
B413A-CPX-4	0.26	17.70	1.54	0.00	15.20	9.80	0.06	46.40	0.77	0.47	92.2
B413A-CPX-5	0.22	18.00	0.92	0.02	21.00	8.80	0.06	49.60	0.65	0.63	99.9
B413A-CPX-6	0.66	18.70	1.49	0.00	15.70	10.30	0.16	49.30	0.91	0.89	98.1
B413A-CPX-7	0.24	16.90	1.20	0.00	17.50	10.30	0.04	47.20	0.80	0.50	94.7
Average	**0.30**	**17.74**	**1.16**	**0.01**	**17.84**	**9.47**	**0.07**	**48.09**	**0.73**	**0.63**	**96.0**
C505C-CPX-1	0.31	19.10	1.51	0.00	13.40	13.80	0.05	50.90	0.87	0.36	100.3
C505C-CPX-2	0.30	17.90	1.70	0.00	13.20	13.90	0.04	49.70	0.81	0.35	97.9
C505C-CPX-3	0.28	18.70	1.63	0.00	13.40	13.90	0.04	51.40	0.84	0.35	100.5
C505C-CPX-4	0.27	17.80	1.39	0.06	15.00	12.70	0.05	49.70	0.79	0.43	98.2
C505C-CPX-5	0.28	18.80	1.71	0.15	13.60	13.60	0.04	50.20	0.92	0.36	99.7
C505C-CPX-6	0.30	18.90	1.79	0.00	13.20	13.70	0.04	49.50	0.96	0.36	98.8
Average	**0.29**	**18.53**	**1.62**	**0.04**	**13.63**	**13.60**	**0.04**	**50.23**	**0.87**	**0.37**	**99.2**
C403A-CPX-1	0.43	20.70	2.27	0.03	10.10	14.00	0.05	49.70	0.76	0.51	98.6
C403A-CPX-2	0.36	20.60	2.27	0.05	10.40	13.80	0.03	50.30	0.77	0.48	99.1
C403A-CPX-3	0.40	20.80	2.31	0.01	10.30	14.10	0.04	49.80	0.77	0.45	99.0
C403A-CPX-4	0.38	20.00	2.10	0.10	10.60	13.80	0.04	49.10	0.74	0.55	97.4
Average	**0.39**	**20.53**	**2.24**	**0.05**	**10.35**	**13.93**	**0.04**	**49.73**	**0.76**	**0.50**	**98.5**
B309A-CPX-1	0.45	20.40	3.40	0.05	11.70	12.60	0.06	48.40	0.97	0.50	98.5
B309A-CPX-2	0.37	21.00	1.96	0.00	10.50	14.10	0.04	51.00	0.55	0.42	99.9
B309A-CPX-3	0.41	20.10	2.92	0.00	11.40	12.60	0.04	48.80	0.76	0.47	97.5
Average	**0.41**	**20.50**	**2.76**	**0.02**	**11.20**	**13.10**	**0.05**	**49.40**	**0.76**	**0.46**	**98.7**
C414-CPX-1	0.21	17.40	0.94	0.08	20.40	9.20	0.05	49.00	0.58	0.58	98.4
C414-CPX-2	0.23	18.00	1.71	0.00	13.00	13.90	0.04	50.40	0.91	0.35	98.5
C414-CPX-3	0.29	18.60	2.13	0.05	12.30	13.20	0.06	49.60	0.88	0.33	97.4
C414-CPX-4	0.22	17.60	1.37	0.06	16.00	12.30	0.04	49.90	0.78	0.41	98.7
C414-CPX-5	0.27	18.30	2.15	0.06	13.10	12.80	0.07	49.40	0.84	0.32	97.3
C414-CPX-6	0.30	18.40	2.45	0.09	12.00	13.40	0.05	49.20	1.07	0.27	97.2
Average	**0.25**	**18.05**	**1.79**	**0.06**	**14.47**	**12.47**	**0.05**	**49.58**	**0.84**	**0.38**	**97.9**

Appendix B - CPX - SBBC Sample Suite

Sample	CAT SUM	Si	Al	Na	Ca	Cr	Fe	Mg	K	Ti	Mn	Total	Mg#
B413A-CPX-1	2.59	1.95	0.06	0.02	0.81	0.00	0.53	0.60	0.00	0.02	0.03	4.01	53.2
B413A-CPX-2	2.38	1.95	0.05	0.02	0.74	0.00	0.61	0.62	0.00	0.02	0.02	4.02	50.4
B413A-CPX-3	2.38	1.97	0.04	0.02	0.77	0.00	0.75	0.43	0.00	0.02	0.02	4.01	36.6
B413A-CPX-4	2.51	1.94	0.08	0.02	0.79	0.00	0.53	0.61	0.00	0.02	0.02	4.01	53.5
B413A-CPX-5	2.36	1.95	0.04	0.02	0.76	0.00	0.69	0.52	0.00	0.02	0.02	4.02	42.8
B413A-CPX-6	2.36	1.94	0.07	0.05	0.79	0.00	0.52	0.60	0.01	0.03	0.03	4.03	53.9
B413A-CPX-7	2.46	1.93	0.06	0.02	0.74	0.00	0.60	0.63	0.00	0.02	0.02	4.02	51.2
Average	**2.43**	**1.95**	**0.06**	**0.02**	**0.77**	**0.00**	**0.60**	**0.57**	**0.00**	**0.02**	**0.02**	**4.02**	**48.8**
C505C-CPX-1	2.27	1.92	0.07	0.02	0.77	0.00	0.42	0.78	0.00	0.02	0.01	4.03	64.7
C505C-CPX-2	2.32	1.92	0.08	0.02	0.74	0.00	0.43	0.80	0.00	0.02	0.01	4.03	65.2
C505C-CPX-3	2.26	1.93	0.07	0.02	0.75	0.00	0.42	0.78	0.00	0.02	0.01	4.02	64.9
C505C-CPX-4	2.34	1.93	0.06	0.02	0.74	0.00	0.49	0.74	0.00	0.02	0.01	4.02	60.1
C505C-CPX-5	2.29	1.91	0.08	0.02	0.77	0.00	0.43	0.77	0.00	0.03	0.01	4.03	64.1
C505C-CPX-6	2.31	1.90	0.08	0.02	0.78	0.00	0.42	0.79	0.00	0.03	0.01	4.04	64.9
Average	**2.30**	**1.92**	**0.07**	**0.02**	**0.76**	**0.00**	**0.44**	**0.78**	**0.00**	**0.02**	**0.01**	**4.03**	**64.0**
C403A-CPX-1	2.30	1.90	0.10	0.03	0.85	0.00	0.32	0.80	0.00	0.02	0.02	4.04	71.2
C403A-CPX-2	2.28	1.91	0.10	0.03	0.84	0.00	0.33	0.78	0.00	0.02	0.02	4.03	70.3
C403A-CPX-3	2.29	1.90	0.10	0.03	0.85	0.00	0.33	0.80	0.00	0.02	0.01	4.05	70.9
C403A-CPX-4	2.33	1.90	0.10	0.03	0.83	0.00	0.34	0.80	0.00	0.02	0.02	4.04	69.9
Average	**2.30**	**1.90**	**0.10**	**0.03**	**0.84**	**0.00**	**0.33**	**0.79**	**0.00**	**0.02**	**0.02**	**4.04**	**70.6**
B309A-CPX-1	2.32	1.87	0.15	0.03	0.84	0.00	0.38	0.72	0.00	0.03	0.02	4.05	65.7
B309A-CPX-2	2.26	1.92	0.09	0.03	0.85	0.00	0.33	0.79	0.00	0.02	0.01	4.03	70.5
B309A-CPX-3	2.33	1.89	0.13	0.03	0.84	0.00	0.37	0.73	0.00	0.02	0.02	4.03	66.3
Average	**2.30**	**1.89**	**0.13**	**0.03**	**0.84**	**0.00**	**0.36**	**0.75**	**0.00**	**0.02**	**0.02**	**4.04**	**67.5**
C414-CPX-1	2.39	1.95	0.04	0.02	0.74	0.00	0.68	0.55	0.00	0.02	0.02	4.02	44.6
C414-CPX-2	2.30	1.93	0.08	0.02	0.74	0.00	0.42	0.79	0.00	0.03	0.01	4.01	65.6
C414-CPX-3	2.33	1.92	0.10	0.02	0.77	0.00	0.40	0.76	0.00	0.03	0.01	4.02	65.7
C414-CPX-4	2.33	1.94	0.06	0.02	0.73	0.00	0.52	0.71	0.00	0.02	0.01	4.02	57.8
C414-CPX-5	2.34	1.92	0.10	0.02	0.76	0.00	0.43	0.74	0.00	0.02	0.01	4.01	63.5
C414-CPX-6	2.33	1.91	0.11	0.02	0.76	0.00	0.39	0.77	0.00	0.03	0.01	4.02	66.6
Average	**2.34**	**1.93**	**0.08**	**0.02**	**0.75**	**0.00**	**0.47**	**0.72**	**0.00**	**0.02**	**0.01**	**4.02**	**60.6**

Appendix B - CPX - NBBC Sample Suite

Sample	Na2O	CaO	Al2O3	Cr2O3	FeO	MgO	K2O	SiO2	TiO2	MnO	Total
BBC1-CPX-1	0.23	18.72	0.83	0.00	13.53	11.98	0.00	53.79	0.50	0.42	100.0
BBC1-CPX-2	0.23	18.01	1.02	0.00	16.76	10.03	0.00	52.89	0.58	0.48	100.0
BBC1-CPX-3	0.28	17.65	1.20	0.00	14.24	12.29	0.00	53.23	0.69	0.40	100.0
BBC1-CPX-4	0.20	14.77	1.29	0.00	15.52	13.71	0.00	53.12	0.96	0.45	100.0
BBC1-CPX-5	0.32	18.42	1.28	0.00	13.57	12.37	0.00	52.89	0.72	0.45	100.0
BBC1-CPX-6	0.24	18.88	1.33	0.00	12.66	12.57	0.00	52.96	0.90	0.45	100.0
BBC1-CPX-7	0.29	18.33	1.12	0.00	15.60	10.72	0.00	52.86	0.71	0.38	100.0
BBC1-CPX-8	0.28	18.51	1.29	0.00	15.02	10.65	0.00	53.08	0.81	0.36	100.0
BBC1-CPX-9	0.22	14.20	1.27	0.00	15.06	14.84	0.00	53.18	0.80	0.43	100.0
Average	**0.25**	**17.50**	**1.18**	**0.00**	**14.66**	**12.13**	**0.00**	**53.11**	**0.74**	**0.42**	**100.0**
BBC2-CPX-1	0.31	17.27	1.93	0.00	11.94	14.47	0.00	53.12	0.96	0.00	100.0
BBC2-CPX-2	0.31	17.52	1.63	0.00	12.08	13.85	0.00	53.34	0.98	0.29	100.0
BBC2-CPX-3	0.00	19.31	0.58	0.00	13.94	11.78	0.00	53.85	0.00	0.53	100.0
BBC2-CPX-4	0.21	18.79	1.11	0.00	14.29	11.62	0.00	52.94	0.75	0.29	100.0
BBC2-CPX-5	0.19	19.88	0.72	0.00	15.65	9.56	0.00	53.45	0.00	0.55	100.0
BBC2-CPX-6	0.27	18.37	2.14	0.00	10.81	13.85	0.00	53.45	1.11	0.00	100.0
BBC2-CPX-7	0.21	16.69	1.51	0.00	13.22	13.71	0.00	53.37	0.87	0.43	100.0
BBC2-CPX-8	0.29	18.71	1.46	0.00	12.89	12.47	0.00	52.82	0.96	0.39	100.0
BBC2-CPX-9	0.23	18.18	1.35	0.00	13.50	12.12	0.00	53.41	0.85	0.34	100.0
BBC2-CPX-10	0.43	18.98	1.61	0.00	10.37	13.88	0.00	53.47	0.96	0.29	100.0
BBC2-CPX-11	0.24	18.84	1.65	0.00	12.30	12.58	0.00	53.05	0.92	0.41	100.0
BBC2-CPX-12	0.29	18.62	1.22	0.00	14.29	11.81	0.00	52.73	0.72	0.33	100.0
Average	**0.25**	**18.43**	**1.41**	**0.00**	**12.94**	**12.64**	**0.00**	**53.25**	**0.76**	**0.32**	**100.0**
BBC3-CPX-1	0.24	18.92	1.01	0.00	14.64	11.21	0.00	53.12	0.86	0.00	100.0
BBC3-CPX-2	0.24	18.77	1.17	0.00	13.76	12.05	0.00	52.98	0.65	0.38	100.0
BBC3-CPX-3	0.27	17.05	1.57	0.00	12.15	14.34	0.00	53.40	0.81	0.39	100.0
BBC3-CPX-4	0.26	15.29	0.87	0.00	17.12	12.46	0.00	52.91	0.72	0.37	100.0
BBC3-CPX-5	0.26	18.94	1.13	0.00	14.23	11.24	0.00	53.08	0.83	0.30	100.0
BBC3-CPX-6	0.36	18.50	1.18	0.00	15.45	10.86	0.00	52.70	0.62	0.33	100.0
BBC3-CPX-7	0.25	16.94	1.72	0.00	12.90	14.08	0.00	52.83	0.96	0.31	100.0
BBC3-CPX-8	0.19	9.42	0.69	0.00	22.92	13.57	0.00	52.16	0.54	0.50	100.0
BBC3-CPX-9	0.32	17.97	1.00	0.00	16.31	10.24	0.00	53.15	0.59	0.43	100.0
BBC3-CPX-10	0.30	19.25	1.79	0.00	9.68	14.33	0.00	53.82	0.82	0.00	100.0
Average	**0.27**	**17.11**	**1.21**	**0.00**	**14.92**	**12.44**	**0.00**	**53.02**	**0.74**	**0.30**	**100.0**

Appendix B - CPX - NBBC Sample Suite

Sample	CAT SUM	Si	Al	Na	Ca	Cr	Fe	Mg	K	Ti	Mn	Total	Mg#
BBC1-CPX-1	2.26	2.02	0.04	0.02	0.75	0.00	0.43	0.67	0.00	0.01	0.01	3.95	61.2
BBC1-CPX-2	2.29	2.02	0.05	0.02	0.74	0.00	0.53	0.57	0.00	0.02	0.02	3.95	51.6
BBC1-CPX-3	2.26	2.00	0.05	0.02	0.71	0.00	0.45	0.69	0.00	0.02	0.01	3.96	60.6
BBC1-CPX-4	2.26	1.99	0.06	0.01	0.59	0.00	0.49	0.77	0.00	0.03	0.01	3.96	61.2
BBC1-CPX-5	2.26	1.99	0.06	0.02	0.74	0.00	0.43	0.69	0.00	0.02	0.01	3.97	61.9
BBC1-CPX-6	2.26	1.99	0.06	0.02	0.76	0.00	0.40	0.70	0.00	0.03	0.01	3.97	63.9
BBC1-CPX-7	2.28	2.01	0.05	0.02	0.75	0.00	0.50	0.61	0.00	0.02	0.01	3.96	55.0
BBC1-CPX-8	2.27	2.01	0.06	0.02	0.75	0.00	0.48	0.60	0.00	0.02	0.01	3.95	55.8
BBC1-CPX-9	2.25	1.99	0.06	0.02	0.57	0.00	0.47	0.83	0.00	0.02	0.01	3.97	63.7
Average	**2.27**	**2.00**	**0.05**	**0.02**	**0.71**	**0.00**	**0.46**	**0.68**	**0.00**	**0.02**	**0.01**	**3.96**	**59.4**
BBC2-CPX-1	2.23	1.97	0.08	0.02	0.69	0.00	0.37	0.80	0.00	0.03	0.00	3.97	68.4
BBC2-CPX-2	2.24	1.99	0.07	0.02	0.70	0.00	0.38	0.77	0.00	0.03	0.01	3.96	67.1
BBC2-CPX-3	2.27	2.03	0.03	0.00	0.78	0.00	0.44	0.66	0.00	0.00	0.02	3.96	60.1
BBC2-CPX-4	2.27	2.00	0.05	0.02	0.76	0.00	0.45	0.65	0.00	0.02	0.01	3.96	59.2
BBC2-CPX-5	2.29	2.04	0.03	0.01	0.81	0.00	0.50	0.54	0.00	0.00	0.02	3.95	52.1
BBC2-CPX-6	2.23	1.98	0.09	0.02	0.73	0.00	0.33	0.76	0.00	0.03	0.00	3.95	69.5
BBC2-CPX-7	2.24	1.99	0.07	0.02	0.67	0.00	0.41	0.76	0.00	0.02	0.01	3.96	64.9
BBC2-CPX-8	2.26	1.98	0.06	0.02	0.75	0.00	0.41	0.70	0.00	0.03	0.01	3.97	63.3
BBC2-CPX-9	2.26	2.01	0.06	0.02	0.73	0.00	0.42	0.68	0.00	0.02	0.01	3.95	61.5
BBC2-CPX-10	2.23	1.99	0.07	0.03	0.76	0.00	0.32	0.77	0.00	0.03	0.01	3.97	70.5
BBC2-CPX-11	2.25	1.99	0.07	0.02	0.76	0.00	0.39	0.70	0.00	0.03	0.01	3.96	64.6
BBC2-CPX-12	2.27	1.99	0.05	0.02	0.75	0.00	0.45	0.67	0.00	0.02	0.01	3.97	59.6
Average	**2.25**	**2.00**	**0.06**	**0.02**	**0.74**	**0.00**	**0.41**	**0.71**	**0.00**	**0.02**	**0.01**	**3.96**	**63.4**
BBC3-CPX-1	2.27	2.01	0.04	0.02	0.77	0.00	0.46	0.63	0.00	0.02	0.00	3.95	57.7
BBC3-CPX-2	2.27	2.00	0.05	0.02	0.76	0.00	0.43	0.68	0.00	0.02	0.01	3.97	60.9
BBC3-CPX-3	2.24	1.99	0.07	0.02	0.68	0.00	0.38	0.80	0.00	0.02	0.01	3.96	67.8
BBC3-CPX-4	2.28	2.01	0.04	0.02	0.62	0.00	0.54	0.70	0.00	0.02	0.01	3.96	56.5
BBC3-CPX-5	2.27	2.00	0.05	0.02	0.77	0.00	0.45	0.63	0.00	0.02	0.01	3.96	58.5
BBC3-CPX-6	2.28	2.00	0.05	0.03	0.75	0.00	0.49	0.61	0.00	0.02	0.01	3.97	55.6
BBC3-CPX-7	2.25	1.97	0.08	0.02	0.68	0.00	0.40	0.78	0.00	0.03	0.01	3.97	66.0
BBC3-CPX-8	2.30	2.00	0.03	0.01	0.39	0.00	0.74	0.78	0.00	0.02	0.02	3.98	51.3
BBC3-CPX-9	2.28	2.02	0.04	0.02	0.73	0.00	0.52	0.58	0.00	0.02	0.01	3.95	52.8
BBC3-CPX-10	2.22	1.99	0.08	0.02	0.76	0.00	0.30	0.79	0.00	0.02	0.00	3.96	72.5
Average	**2.27**	**2.00**	**0.05**	**0.02**	**0.69**	**0.00**	**0.47**	**0.70**	**0.00**	**0.02**	**0.01**	**3.96**	**60.0**

Appendix B - CPX - NBBC Sample Suite

Sample	Na2O	CaO	Al2O3	Cr2O3	FeO	MgO	K2O	SiO2	TiO2	MnO	Total
BBC4-CPX-1	0.31	19.01	1.07	0.00	13.98	11.32	0.00	53.16	0.72	0.44	100.0
BBC4-CPX-2	0.23	17.68	0.45	0.00	18.31	9.58	0.00	52.97	0.33	0.45	100.0
BBC4-CPX-3	0.34	19.14	1.73	0.00	10.82	13.44	0.00	53.21	1.04	0.27	100.0
BBC4-CPX-4	0.00	18.45	1.78	0.00	10.51	14.53	0.00	53.46	0.94	0.33	100.0
BBC4-CPX-5	0.28	17.07	1.54	0.00	12.80	13.55	0.00	53.26	1.02	0.49	100.0
BBC4-CPX-6	0.29	17.51	1.84	0.00	12.10	14.25	0.00	52.80	0.95	0.26	100.0
BBC4-CPX-7	0.21	17.01	1.41	0.00	12.78	13.82	0.00	53.08	1.09	0.61	100.0
BBC4-CPX-8	0.00	16.02	1.58	0.00	12.66	15.19	0.00	53.70	0.85	0.00	100.0
BBC4-CPX-9	0.00	15.09	1.17	0.00	16.93	13.02	0.00	52.46	0.85	0.47	100.0
BBC4-CPX-10	0.28	15.39	1.45	0.00	14.12	14.14	0.00	53.20	0.98	0.44	100.0
BBC4-CPX-11	0.25	18.15	2.18	0.26	10.91	14.66	0.00	52.81	0.80	0.00	100.0
Average	**0.20**	**17.32**	**1.47**	**0.02**	**13.27**	**13.41**	**0.00**	**53.10**	**0.87**	**0.34**	**100.0**
BBC5-CPX-1	0.22	18.59	1.13	0.00	14.00	11.57	0.00	53.30	0.69	0.50	100.0
BBC5-CPX-2	0.23	18.54	1.40	0.00	14.43	11.26	0.00	53.06	0.66	0.42	100.0
BBC5-CPX-3	0.23	18.34	0.84	0.00	20.80	6.78	0.00	52.16	0.35	0.51	100.0
BBC5-CPX-4	0.00	18.20	1.37	0.00	13.12	12.62	0.00	53.37	0.80	0.51	100.0
BBC5-CPX-5	0.22	18.68	1.18	0.00	14.87	11.02	0.00	52.90	0.71	0.42	100.0
BBC5-CPX-6	0.26	18.84	1.50	0.00	12.60	12.16	0.00	53.25	0.96	0.43	100.0
BBC5-CPX-7	0.18	18.67	1.33	0.00	13.18	12.11	0.00	53.25	0.95	0.33	100.0
BBC5-CPX-8	0.19	18.60	1.15	0.00	14.79	11.18	0.00	53.38	0.71	0.00	100.0
BBC5-CPX-9	0.23	18.74	1.62	0.00	11.97	13.16	0.00	53.00	1.00	0.28	100.0
BBC5-CPX-10	0.28	19.13	1.66	0.00	11.79	13.01	0.00	52.93	0.89	0.30	100.0
BBC5-CPX-11	0.17	18.14	0.98	0.00	17.11	10.05	0.00	52.34	0.84	0.38	100.0
Average	**0.20**	**18.59**	**1.29**	**0.00**	**14.42**	**11.36**	**0.00**	**52.99**	**0.78**	**0.37**	**100.0**
BBC6-CPX-1	0.28	19.86	1.97	0.26	6.81	15.93	0.00	54.29	0.61	0.00	100.0
BBC6-CPX-2	0.23	19.14	2.06	0.54	7.19	16.10	0.00	53.91	0.84	0.00	100.0
BBC6-CPX-3	0.28	16.41	2.18	0.28	9.65	16.27	0.00	53.19	1.33	0.40	100.0
BBC6-CPX-4	0.29	20.26	2.07	0.30	7.31	14.89	0.00	53.43	1.46	0.00	100.0
BBC6-CPX-5	0.34	19.87	2.55	0.24	7.81	14.89	0.00	52.76	1.55	0.00	100.0
BBC6-CPX-6	0.23	20.44	2.37	0.43	6.44	15.70	0.00	53.47	0.92	0.00	100.0
BBC6-CPX-7	0.21	16.63	2.24	0.00	8.59	17.02	0.00	54.46	0.85	0.00	100.0
BBC6-CPX-8	0.28	19.04	1.29	0.30	7.12	16.43	0.00	54.80	0.74	0.00	100.0
BBC6-CPX-9	0.20	18.66	1.98	0.55	7.34	16.31	0.00	54.14	0.81	0.00	100.0
BBC6-CPX-10	0.34	19.97	2.75	0.48	6.81	14.91	0.00	53.87	0.86	0.00	100.0
BBC6-CPX-11	0.23	19.04	2.46	0.35	7.70	15.81	0.00	53.36	1.05	0.00	100.0
BBC6-CPX-12	0.33	20.17	2.54	0.27	7.29	14.92	0.00	52.89	1.26	0.33	100.0
Average	**0.27**	**19.12**	**2.21**	**0.33**	**7.51**	**15.77**	**0.00**	**53.71**	**1.02**	**0.06**	**100.0**

Appendix B - CPX - NBBC Sample Suite

Sample	CAT SUM	Si	Al	Na	Ca	Cr	Fe	Mg	K	Ti	Mn	Total	Mg#
BBC4-CPX-1	2.27	2.01	0.05	0.02	0.77	0.00	0.44	0.64	0.00	0.02	0.01	3.96	59.1
BBC4-CPX-2	2.31	2.03	0.02	0.02	0.73	0.00	0.59	0.55	0.00	0.01	0.01	3.96	48.2
BBC4-CPX-3	2.24	1.98	0.08	0.02	0.76	0.00	0.34	0.75	0.00	0.03	0.01	3.96	68.9
BBC4-CPX-4	2.23	1.98	0.08	0.00	0.73	0.00	0.33	0.80	0.00	0.03	0.01	3.95	71.1
BBC4-CPX-5	2.24	1.99	0.07	0.02	0.68	0.00	0.40	0.75	0.00	0.03	0.02	3.96	65.4
BBC4-CPX-6	2.24	1.97	0.08	0.02	0.70	0.00	0.38	0.79	0.00	0.03	0.01	3.97	67.7
BBC4-CPX-7	2.25	1.98	0.06	0.02	0.68	0.00	0.40	0.77	0.00	0.03	0.02	3.96	65.8
BBC4-CPX-8	2.23	1.99	0.07	0.00	0.64	0.00	0.39	0.84	0.00	0.02	0.00	3.95	68.1
BBC4-CPX-9	2.28	1.99	0.05	0.00	0.61	0.00	0.54	0.74	0.00	0.02	0.02	3.96	57.8
BBC4-CPX-10	2.25	1.99	0.06	0.02	0.62	0.00	0.44	0.79	0.00	0.03	0.01	3.96	64.1
BBC4-CPX-11	2.23	1.96	0.10	0.02	0.72	0.01	0.34	0.81	0.00	0.02	0.00	3.97	70.5
Average	**2.25**	**1.99**	**0.06**	**0.01**	**0.69**	**0.00**	**0.42**	**0.75**	**0.00**	**0.02**	**0.01**	**3.96**	**64.3**
BBC5-CPX-1	2.27	2.01	0.05	0.02	0.75	0.00	0.44	0.65	0.00	0.02	0.02	3.95	59.6
BBC5-CPX-2	2.27	2.00	0.06	0.02	0.75	0.00	0.46	0.63	0.00	0.02	0.01	3.95	58.2
BBC5-CPX-3	2.34	2.03	0.04	0.02	0.76	0.00	0.68	0.39	0.00	0.01	0.02	3.95	36.7
BBC5-CPX-4	2.25	2.00	0.06	0.00	0.73	0.00	0.41	0.70	0.00	0.02	0.02	3.95	63.2
BBC5-CPX-5	2.28	2.00	0.05	0.02	0.76	0.00	0.47	0.62	0.00	0.02	0.01	3.96	56.9
BBC5-CPX-6	2.25	2.00	0.07	0.02	0.76	0.00	0.40	0.68	0.00	0.03	0.01	3.95	63.2
BBC5-CPX-7	2.26	2.00	0.06	0.01	0.75	0.00	0.41	0.68	0.00	0.03	0.01	3.95	62.1
BBC5-CPX-8	2.27	2.01	0.05	0.01	0.75	0.00	0.47	0.63	0.00	0.02	0.00	3.95	57.4
BBC5-CPX-9	2.25	1.98	0.07	0.02	0.75	0.00	0.37	0.73	0.00	0.03	0.01	3.96	66.2
BBC5-CPX-10	2.25	1.98	0.07	0.02	0.77	0.00	0.37	0.73	0.00	0.03	0.01	3.97	66.3
BBC5-CPX-11	2.30	2.00	0.04	0.01	0.74	0.00	0.55	0.57	0.00	0.02	0.01	3.96	51.1
Average	**2.27**	**2.00**	**0.06**	**0.01**	**0.75**	**0.00**	**0.46**	**0.64**	**0.00**	**0.02**	**0.01**	**3.95**	**58.3**
BBC6-CPX-1	2.19	1.98	0.08	0.02	0.78	0.01	0.21	0.87	0.00	0.02	0.00	3.96	80.7
BBC6-CPX-2	2.20	1.97	0.09	0.02	0.75	0.02	0.22	0.88	0.00	0.02	0.00	3.96	80.0
BBC6-CPX-3	2.21	1.96	0.09	0.02	0.65	0.01	0.30	0.89	0.00	0.04	0.01	3.96	75.0
BBC6-CPX-4	2.21	1.96	0.09	0.02	0.80	0.01	0.22	0.82	0.00	0.04	0.00	3.96	78.4
BBC6-CPX-5	2.21	1.94	0.11	0.02	0.78	0.01	0.24	0.82	0.00	0.04	0.00	3.97	77.3
BBC6-CPX-6	2.20	1.96	0.10	0.02	0.80	0.01	0.20	0.86	0.00	0.03	0.00	3.97	81.3
BBC6-CPX-7	2.19	1.98	0.10	0.01	0.65	0.00	0.26	0.92	0.00	0.02	0.00	3.95	77.9
BBC6-CPX-8	2.19	2.00	0.06	0.02	0.74	0.01	0.22	0.89	0.00	0.02	0.00	3.96	80.4
BBC6-CPX-9	2.19	1.98	0.09	0.01	0.73	0.02	0.22	0.89	0.00	0.02	0.00	3.96	79.8
BBC6-CPX-10	2.20	1.97	0.12	0.02	0.78	0.01	0.21	0.81	0.00	0.02	0.00	3.95	79.6
BBC6-CPX-11	2.20	1.96	0.11	0.02	0.75	0.01	0.24	0.86	0.00	0.03	0.00	3.97	78.5
BBC6-CPX-12	2.21	1.95	0.11	0.02	0.80	0.01	0.22	0.82	0.00	0.03	0.01	3.97	78.5
Average	**2.20**	**1.97**	**0.10**	**0.02**	**0.75**	**0.01**	**0.23**	**0.86**	**0.00**	**0.03**	**0.00**	**3.96**	**79.0**

Appendix B - CPX - NBBC Sample Suite

Sample	Na2O	CaO	Al2O3	Cr2O3	FeO	MgO	K2O	SiO2	TiO2	MnO	Total
BBC7-CPX-1	0.22	18.34	0.75	0.00	16.82	10.02	0.00	53.12	0.40	0.33	100.0
BBC7-CPX-2	0.18	18.38	1.00	0.00	15.41	11.12	0.00	52.87	0.74	0.30	100.0
BBC7-CPX-3	0.20	16.72	0.99	0.00	16.85	11.40	0.00	52.83	0.66	0.36	100.0
BBC7-CPX-4	0.25	18.90	1.06	0.00	14.68	11.12	0.00	53.08	0.54	0.36	100.0
BBC7-CPX-5	0.00	17.69	0.56	0.00	18.41	9.61	0.00	52.83	0.39	0.51	100.0
BBC7-CPX-6	0.00	17.60	0.73	0.00	18.15	9.64	0.00	53.09	0.43	0.36	100.0
Average	**0.14**	**17.94**	**0.85**	**0.00**	**16.72**	**10.49**	**0.00**	**52.97**	**0.53**	**0.37**	**100.0**
BBC8-CPX-1	0.28	18.79	1.29	0.00	13.55	11.54	0.00	53.04	0.97	0.54	100.0
BBC8-CPX-2	0.30	18.69	1.28	0.00	12.98	12.46	0.00	53.15	0.83	0.31	100.0
BBC8-CPX-3	0.00	18.04	1.19	0.00	14.73	11.76	0.00	53.22	0.67	0.39	100.0
BBC8-CPX-4	0.20	18.99	1.06	0.00	13.89	11.91	0.00	52.95	0.70	0.31	100.0
BBC8-CPX-5	0.30	18.31	1.50	0.00	12.89	12.45	0.00	53.39	0.84	0.32	100.0
BBC8-CPX-6	0.21	14.94	1.46	0.00	14.34	14.57	0.00	53.41	1.07	0.00	100.0
BBC8-CPX-7	0.25	17.68	1.29	0.00	13.93	12.26	0.00	53.34	0.88	0.39	100.0
BBC8-CPX-8	0.30	18.39	1.03	0.00	14.76	11.34	0.00	53.12	0.67	0.39	100.0
Average	**0.23**	**17.98**	**1.26**	**0.00**	**13.88**	**12.29**	**0.00**	**53.20**	**0.83**	**0.33**	**100.0**
BBC9-CPX-1	0.22	17.30	1.02	0.00	14.77	12.29	0.00	53.33	0.69	0.38	100.0
BBC9-CPX-2	0.32	17.46	1.26	0.00	14.04	12.40	0.00	53.22	0.92	0.38	100.0
BBC9-CPX-3	0.33	17.69	1.32	0.00	13.94	12.38	0.00	53.03	0.87	0.43	100.0
BBC9-CPX-4	0.24	13.78	0.91	0.00	17.36	13.36	0.00	53.07	0.80	0.49	100.0
BBC9-CPX-5	0.22	15.47	1.09	0.00	15.63	13.13	0.00	53.15	0.90	0.40	100.0
BBC9-CPX-6	0.33	17.11	1.26	0.00	14.51	12.60	0.00	52.86	0.95	0.38	100.0
BBC9-CPX-7	0.18	17.89	1.14	0.00	13.34	12.46	0.00	53.74	0.80	0.44	100.0
BBC9-CPX-8	0.00	17.78	1.16	0.00	13.89	12.30	0.00	53.76	0.74	0.37	100.0
BBC9-CPX-9	0.29	17.73	1.35	0.00	13.97	12.33	0.00	53.13	0.70	0.50	100.0
Average	**0.24**	**16.91**	**1.17**	**0.00**	**14.61**	**12.58**	**0.00**	**53.25**	**0.82**	**0.42**	**100.0**
BBC10-CPX-1	0.22	17.51	1.45	0.00	13.70	13.24	0.00	52.75	0.80	0.32	100.0
BBC10-CPX-2	0.35	16.52	1.29	0.00	14.71	12.53	0.00	53.36	0.88	0.35	100.0
BBC10-CPX-3	0.65	16.78	1.41	0.00	15.63	11.99	0.00	52.44	0.66	0.45	100.0
BBC10-CPX-4	0.40	17.22	1.44	0.00	13.87	12.80	0.00	52.87	0.97	0.43	100.0
BBC10-CPX-5	0.23	17.16	1.34	0.00	13.52	13.17	0.00	53.21	0.93	0.43	100.0
BBC10-CPX-6	0.22	17.37	1.38	0.00	14.27	12.52	0.00	53.02	0.90	0.31	100.0
BBC10-CPX-7	0.19	16.79	1.29	0.00	15.38	12.08	0.00	53.36	0.60	0.30	100.0
BBC10-CPX-8	0.26	17.28	1.39	0.00	14.85	12.19	0.00	53.14	0.89	0.00	100.0
BBC10-CPX-9	0.00	16.90	1.19	0.00	15.01	12.56	0.00	53.22	0.81	0.31	100.0
Average	**0.28**	**17.06**	**1.35**	**0.00**	**14.55**	**12.56**	**0.00**	**53.04**	**0.83**	**0.32**	**100.0**

Appendix B - CPX - NBBC Sample Suite

Sample	CAT SUM	Si	Al	Na	Ca	Cr	Fe	Mg	K	Ti	Mn	Total	Mg#
BBC7-CPX-1	2.29	2.03	0.03	0.02	0.75	0.00	0.54	0.57	0.00	0.01	0.01	3.95	51.5
BBC7-CPX-2	2.28	2.01	0.04	0.01	0.75	0.00	0.49	0.63	0.00	0.02	0.01	3.96	56.3
BBC7-CPX-3	2.28	2.01	0.04	0.01	0.68	0.00	0.54	0.65	0.00	0.02	0.01	3.96	54.7
BBC7-CPX-4	2.27	2.01	0.05	0.02	0.77	0.00	0.46	0.63	0.00	0.02	0.01	3.96	57.4
BBC7-CPX-5	2.31	2.03	0.03	0.00	0.73	0.00	0.59	0.55	0.00	0.01	0.02	3.95	48.2
BBC7-CPX-6	2.30	2.03	0.03	0.00	0.72	0.00	0.58	0.55	0.00	0.01	0.01	3.94	48.6
Average	**2.29**	**2.02**	**0.04**	**0.01**	**0.73**	**0.00**	**0.53**	**0.60**	**0.00**	**0.02**	**0.01**	**3.95**	**52.8**
BBC8-CPX-1	2.26	2.00	0.06	0.02	0.76	0.00	0.43	0.65	0.00	0.03	0.02	3.96	60.3
BBC8-CPX-2	2.26	2.00	0.06	0.02	0.75	0.00	0.41	0.70	0.00	0.02	0.01	3.96	63.1
BBC8-CPX-3	2.27	2.01	0.05	0.00	0.73	0.00	0.46	0.66	0.00	0.02	0.01	3.95	58.7
BBC8-CPX-4	2.27	2.00	0.05	0.01	0.77	0.00	0.44	0.67	0.00	0.02	0.01	3.97	60.4
BBC8-CPX-5	2.25	2.00	0.07	0.02	0.73	0.00	0.40	0.69	0.00	0.02	0.01	3.95	63.3
BBC8-CPX-6	2.24	1.99	0.06	0.02	0.60	0.00	0.45	0.81	0.00	0.03	0.00	3.95	64.4
BBC8-CPX-7	2.26	2.00	0.06	0.02	0.71	0.00	0.44	0.69	0.00	0.02	0.01	3.95	61.1
BBC8-CPX-8	2.27	2.01	0.05	0.02	0.75	0.00	0.47	0.64	0.00	0.02	0.01	3.96	57.8
Average	**2.26**	**2.00**	**0.06**	**0.02**	**0.72**	**0.00**	**0.44**	**0.69**	**0.00**	**0.02**	**0.01**	**3.96**	**61.1**
BBC9-CPX-1	2.26	2.01	0.05	0.02	0.70	0.00	0.47	0.69	0.00	0.02	0.01	3.96	59.7
BBC9-CPX-2	2.26	2.00	0.06	0.02	0.70	0.00	0.44	0.69	0.00	0.03	0.01	3.96	61.1
BBC9-CPX-3	2.26	2.00	0.06	0.02	0.71	0.00	0.44	0.69	0.00	0.02	0.01	3.96	61.3
BBC9-CPX-4	2.27	2.01	0.04	0.02	0.56	0.00	0.55	0.75	0.00	0.02	0.02	3.96	57.8
BBC9-CPX-5	2.26	2.00	0.05	0.02	0.62	0.00	0.49	0.74	0.00	0.03	0.01	3.96	60.0
BBC9-CPX-6	2.26	1.99	0.06	0.02	0.69	0.00	0.46	0.71	0.00	0.03	0.01	3.97	60.7
BBC9-CPX-7	2.25	2.01	0.05	0.01	0.72	0.00	0.42	0.70	0.00	0.02	0.01	3.95	62.5
BBC9-CPX-8	2.25	2.02	0.05	0.00	0.71	0.00	0.44	0.69	0.00	0.02	0.01	3.94	61.2
BBC9-CPX-9	2.26	2.00	0.06	0.02	0.71	0.00	0.44	0.69	0.00	0.02	0.02	3.96	61.1
Average	**2.26**	**2.00**	**0.05**	**0.02**	**0.68**	**0.00**	**0.46**	**0.71**	**0.00**	**0.02**	**0.01**	**3.96**	**60.6**
BBC10-CPX-1	2.26	1.98	0.06	0.02	0.70	0.00	0.43	0.74	0.00	0.02	0.01	3.97	63.3
BBC10-CPX-2	2.26	2.01	0.06	0.03	0.67	0.00	0.46	0.70	0.00	0.02	0.01	3.95	60.3
BBC10-CPX-3	2.28	1.99	0.06	0.05	0.68	0.00	0.50	0.68	0.00	0.02	0.01	3.99	57.8
BBC10-CPX-4	2.26	1.99	0.06	0.03	0.69	0.00	0.44	0.72	0.00	0.03	0.01	3.97	62.2
BBC10-CPX-5	2.25	1.99	0.06	0.02	0.69	0.00	0.42	0.74	0.00	0.03	0.01	3.96	63.4
BBC10-CPX-6	2.26	1.99	0.06	0.02	0.70	0.00	0.45	0.70	0.00	0.03	0.01	3.96	61.0
BBC10-CPX-7	2.26	2.01	0.06	0.01	0.68	0.00	0.48	0.68	0.00	0.02	0.01	3.95	58.3
BBC10-CPX-8	2.26	2.00	0.06	0.02	0.70	0.00	0.47	0.68	0.00	0.03	0.00	3.95	59.4
BBC10-CPX-9	2.26	2.00	0.05	0.00	0.68	0.00	0.47	0.70	0.00	0.02	0.01	3.95	59.9
Average	**2.26**	**2.00**	**0.06**	**0.02**	**0.69**	**0.00**	**0.46**	**0.70**	**0.00**	**0.02**	**0.01**	**3.96**	**60.6**

Appendix B - CPX - NBBC Sample Suite

Sample	Na2O	CaO	Al2O3	Cr2O3	FeO	MgO	K2O	SiO2	TiO2	MnO	Total
BBC11A-CPX-1	0.32	17.11	1.07	0.00	18.07	9.96	0.00	52.27	0.64	0.56	100.0
BBC11A-CPX-2	0.27	16.78	1.19	0.00	18.31	9.67	0.00	52.68	0.75	0.36	100.0
BBC11A-CPX-3	0.33	17.47	1.06	0.00	17.71	9.87	0.00	52.40	0.60	0.57	100.0
BBC11A-CPX-4	0.30	16.73	1.22	0.00	18.31	9.94	0.00	52.64	0.52	0.33	100.0
BBC11A-CPX-5	0.21	16.90	0.96	0.00	20.04	9.06	0.00	51.69	0.63	0.51	100.0
BBC11A-CPX-6	0.28	17.26	1.09	0.00	19.09	9.14	0.00	52.18	0.43	0.53	100.0
BBC11A-CPX-7	0.25	17.67	0.90	0.00	16.94	10.57	0.00	52.54	0.60	0.54	100.0
BBC11A-CPX-8	0.26	17.09	1.00	0.00	19.27	9.15	0.00	52.14	0.59	0.49	100.0
BBC11A-CPX-9	0.26	17.25	0.99	0.00	17.59	10.23	0.00	52.53	0.67	0.48	100.0
BBC11A-CPX-10	0.20	17.20	1.06	0.00	18.18	9.95	0.00	52.35	0.51	0.55	100.0
Average	**0.27**	**17.15**	**1.05**	**0.00**	**18.35**	**9.75**	**0.00**	**52.34**	**0.59**	**0.49**	**100.0**
BBC12-CPX-1	0.31	16.96	1.02	0.00	18.14	9.90	0.00	52.35	0.53	0.79	100.0
BBC12-CPX-2	0.26	17.25	0.88	0.00	18.39	9.81	0.00	52.39	0.65	0.37	100.0
BBC12-CPX-3	0.34	17.19	1.21	0.00	18.74	9.26	0.00	51.84	0.74	0.69	100.0
BBC12-CPX-4	0.21	17.31	0.82	0.00	18.78	9.26	0.00	52.57	0.51	0.53	100.0
BBC12-CPX-5	0.29	16.73	1.14	0.00	19.19	9.39	0.00	52.15	0.51	0.59	100.0
BBC12-CPX-6	0.19	16.93	1.06	0.00	18.07	9.96	0.00	52.85	0.52	0.42	100.0
BBC12-CPX-7	0.21	17.05	1.06	0.00	18.28	9.89	0.00	52.36	0.58	0.57	100.0
BBC12-CPX-8	0.26	17.09	1.10	0.00	18.78	9.29	0.00	52.09	0.59	0.79	100.0
BBC12-CPX-9	0.24	16.97	1.07	0.00	19.24	9.18	0.00	52.17	0.50	0.63	100.0
BBC12-CPX-10	0.35	17.14	1.00	0.00	18.69	9.43	0.00	51.91	0.75	0.74	100.0
BBC12-CPX-11	0.35	17.11	0.97	0.00	18.59	9.61	0.00	52.53	0.48	0.36	100.0
BBC12-CPX-12	0.29	17.10	1.01	0.00	18.78	9.39	0.00	52.30	0.49	0.64	100.0
BBC12-CPX-13	0.29	16.59	1.07	0.00	19.09	9.74	0.00	51.74	0.77	0.71	100.0
Average	**0.28**	**17.03**	**1.03**	**0.00**	**18.67**	**9.55**	**0.00**	**52.25**	**0.59**	**0.60**	**100.0**
BBC13-CPX-1	0.36	18.79	2.02	0.00	10.02	14.41	0.00	52.95	1.15	0.30	100.0
BBC13-CPX-2	0.19	19.04	1.46	0.00	10.45	13.99	0.00	53.60	0.97	0.31	100.0
BBC13-CPX-3	0.31	19.89	2.68	0.30	8.97	13.92	0.00	52.96	0.97	0.00	100.0
BBC13-CPX-4	0.31	18.86	1.52	0.00	11.46	13.08	0.00	53.14	1.23	0.40	100.0
BBC13-CPX-5	0.28	19.08	1.30	0.00	11.40	13.26	0.00	53.69	1.00	0.00	100.0
BBC13-CPX-6	0.34	19.63	2.26	0.00	9.64	13.72	0.00	53.18	1.24	0.00	100.0
BBC13-CPX-7	0.29	18.84	1.44	0.00	10.94	13.43	0.00	53.80	0.83	0.43	100.0
BBC13-CPX-8	0.27	19.09	1.46	0.00	11.83	13.10	0.00	53.23	1.02	0.00	100.0
BBC13-CPX-9	0.35	19.81	1.58	0.00	8.63	14.50	0.00	54.32	0.80	0.00	100.0
BBC13-CPX-10	0.29	19.64	2.18	0.00	10.83	12.97	0.00	52.72	1.36	0.00	100.0
BBC13-CPX-11	0.29	19.50	1.74	0.00	10.00	13.55	0.00	53.22	1.30	0.39	100.0
Average	**0.30**	**19.29**	**1.79**	**0.03**	**10.38**	**13.63**	**0.00**	**53.35**	**1.08**	**0.17**	**100.0**

Appendix B - CPX - NBBC Sample Suite

Sample	CAT SUM	Si	Al	Na	Ca	Cr	Fe	Mg	K	Ti	Mn	Total	Mg#
BBC11A-CPX-1	2.30	2.00	0.05	0.02	0.70	0.00	0.58	0.57	0.00	0.02	0.02	3.96	49.6
BBC11A-CPX-2	2.30	2.01	0.05	0.02	0.69	0.00	0.59	0.55	0.00	0.02	0.01	3.95	48.5
BBC11A-CPX-3	2.30	2.01	0.05	0.02	0.72	0.00	0.57	0.56	0.00	0.02	0.02	3.96	49.8
BBC11A-CPX-4	2.30	2.01	0.06	0.02	0.69	0.00	0.59	0.57	0.00	0.01	0.01	3.95	49.2
BBC11A-CPX-5	2.33	2.00	0.04	0.02	0.70	0.00	0.65	0.52	0.00	0.02	0.02	3.97	44.6
BBC11A-CPX-6	2.32	2.01	0.05	0.02	0.71	0.00	0.62	0.52	0.00	0.01	0.02	3.96	46.0
BBC11A-CPX-7	2.29	2.01	0.04	0.02	0.72	0.00	0.54	0.60	0.00	0.02	0.02	3.97	52.6
BBC11A-CPX-8	2.32	2.01	0.05	0.02	0.71	0.00	0.62	0.53	0.00	0.02	0.02	3.96	45.8
BBC11A-CPX-9	2.30	2.01	0.04	0.02	0.71	0.00	0.56	0.58	0.00	0.02	0.02	3.96	50.9
BBC11A-CPX-10	2.30	2.01	0.05	0.01	0.71	0.00	0.58	0.57	0.00	0.01	0.02	3.96	49.4
Average	**2.31**	**2.01**	**0.05**	**0.02**	**0.70**	**0.00**	**0.59**	**0.56**	**0.00**	**0.02**	**0.02**	**3.96**	**48.6**
BBC12-CPX-1	2.31	2.01	0.05	0.02	0.70	0.00	0.58	0.57	0.00	0.02	0.03	3.96	49.3
BBC12-CPX-2	2.31	2.01	0.04	0.02	0.71	0.00	0.59	0.56	0.00	0.02	0.01	3.96	48.7
BBC12-CPX-3	2.32	2.00	0.05	0.03	0.71	0.00	0.60	0.53	0.00	0.02	0.02	3.97	46.8
BBC12-CPX-4	2.31	2.02	0.04	0.02	0.71	0.00	0.60	0.53	0.00	0.01	0.02	3.95	46.8
BBC12-CPX-5	2.31	2.01	0.05	0.02	0.69	0.00	0.62	0.54	0.00	0.01	0.02	3.96	46.6
BBC12-CPX-6	2.30	2.02	0.05	0.01	0.69	0.00	0.58	0.57	0.00	0.01	0.01	3.95	49.6
BBC12-CPX-7	2.30	2.01	0.05	0.02	0.70	0.00	0.59	0.57	0.00	0.02	0.02	3.96	49.1
BBC12-CPX-8	2.31	2.01	0.05	0.02	0.71	0.00	0.60	0.53	0.00	0.02	0.03	3.96	46.9
BBC12-CPX-9	2.32	2.01	0.05	0.02	0.70	0.00	0.62	0.53	0.00	0.01	0.02	3.96	46.0
BBC12-CPX-10	2.32	2.00	0.05	0.03	0.71	0.00	0.60	0.54	0.00	0.02	0.02	3.97	47.3
BBC12-CPX-11	2.31	2.02	0.04	0.03	0.70	0.00	0.60	0.55	0.00	0.01	0.01	3.96	47.9
BBC12-CPX-12	2.31	2.01	0.05	0.02	0.70	0.00	0.60	0.54	0.00	0.01	0.02	3.96	47.1
BBC12-CPX-13	2.32	1.99	0.05	0.02	0.69	0.00	0.62	0.56	0.00	0.02	0.02	3.97	47.6
Average	**2.31**	**2.01**	**0.05**	**0.02**	**0.70**	**0.00**	**0.60**	**0.55**	**0.00**	**0.02**	**0.02**	**3.96**	**47.7**
BBC13-CPX-1	2.23	1.96	0.09	0.03	0.75	0.00	0.31	0.80	0.00	0.03	0.01	3.97	71.9
BBC13-CPX-2	2.23	1.99	0.06	0.01	0.76	0.00	0.32	0.77	0.00	0.03	0.01	3.96	70.5
BBC13-CPX-3	2.22	1.96	0.12	0.02	0.79	0.01	0.28	0.77	0.00	0.03	0.00	3.96	73.4
BBC13-CPX-4	2.24	1.98	0.07	0.02	0.75	0.00	0.36	0.73	0.00	0.03	0.01	3.96	67.0
BBC13-CPX-5	2.24	2.00	0.06	0.02	0.76	0.00	0.35	0.74	0.00	0.03	0.00	3.96	67.5
BBC13-CPX-6	2.22	1.97	0.10	0.02	0.78	0.00	0.30	0.76	0.00	0.03	0.00	3.96	71.7
BBC13-CPX-7	2.23	2.00	0.06	0.02	0.75	0.00	0.34	0.74	0.00	0.02	0.01	3.96	68.6
BBC13-CPX-8	2.24	1.99	0.06	0.02	0.76	0.00	0.37	0.73	0.00	0.03	0.00	3.96	66.4
BBC13-CPX-9	2.21	2.00	0.07	0.02	0.78	0.00	0.27	0.80	0.00	0.02	0.00	3.96	75.0
BBC13-CPX-10	2.24	1.96	0.10	0.02	0.78	0.00	0.34	0.72	0.00	0.04	0.00	3.96	68.1
BBC13-CPX-11	2.23	1.98	0.08	0.02	0.78	0.00	0.31	0.75	0.00	0.04	0.01	3.96	70.7
Average	**2.23**	**1.98**	**0.08**	**0.02**	**0.77**	**0.00**	**0.32**	**0.75**	**0.00**	**0.03**	**0.01**	**3.96**	**70.1**

Appendix B - CPX - NBBC Sample Suite

Sample	Na2O	CaO	Al2O3	Cr2O3	FeO	MgO	K2O	SiO2	TiO2	MnO	Total
BBC14-CPX-1	0.30	18.46	1.41	0.00	12.73	13.86	0.00	51.84	1.05	0.35	100.0
BBC14-CPX-2	0.38	19.42	2.13	0.00	9.66	13.56	0.00	53.70	0.68	0.47	100.0
BBC14-CPX-3	0.38	19.42	2.13	0.00	9.66	13.56	0.00	53.70	0.68	0.47	100.0
BBC14-CPX-4	0.30	19.46	2.37	0.39	9.48	13.93	0.00	53.29	0.79	0.00	100.0
BBC14-CPX-5	0.31	19.62	2.54	0.67	8.09	14.47	0.00	53.03	0.96	0.32	100.0
BBC14-CPX-6	0.36	18.79	2.52	0.58	8.56	14.92	0.00	53.00	0.93	0.33	100.0
BBC14-CPX-7	0.21	19.75	1.28	0.00	9.27	14.43	0.00	54.35	0.39	0.32	100.0
BBC14-CPX-8	0.27	19.48	1.85	0.00	9.23	14.32	0.00	53.82	0.78	0.24	100.0
BBC14-CPX-9	0.39	20.01	1.85	0.00	9.28	14.14	0.00	53.24	0.66	0.42	100.0
BBC14-CPX-10	0.33	17.42	2.14	0.26	10.71	14.87	0.00	52.93	1.00	0.34	100.0
BBC14-CPX-11	0.17	21.20	1.05	0.00	10.92	12.33	0.00	53.77	0.55	0.00	100.0
Average	**0.31**	**19.37**	**1.93**	**0.17**	**9.78**	**14.04**	**0.00**	**53.33**	**0.77**	**0.30**	**100.0**
G500A-CPX-1	0.16	17.40	1.55	0.02	15.00	13.00	0.03	52.60	0.92	0.35	101.0
G500A-CPX-2	0.19	16.70	1.38	0.03	17.20	12.00	0.01	51.40	0.88	0.45	100.2
G500A-CPX-3	0.19	16.60	1.17	0.01	18.50	11.30	0.01	52.00	0.75	0.38	100.9
G500A-CPX-4	0.19	16.70	1.09	0.00	18.70	11.20	0.00	51.70	0.71	0.47	100.8
G500A-CPX-5	0.20	17.00	1.33	0.00	15.90	12.50	0.00	51.80	0.76	0.41	99.9
G500A-CPX-6	0.18	17.00	1.29	0.02	17.00	12.10	0.00	51.60	0.84	0.37	100.4
G500A-CPX-7	0.17	16.70	1.32	0.00	16.30	12.80	0.00	51.60	0.81	0.40	100.1
G500A-CPX-8	0.20	17.30	1.55	0.00	14.60	13.50	0.01	51.10	0.90	0.35	99.5
G500A-CPX-9	0.19	16.80	1.45	0.00	15.60	13.00	0.00	52.00	0.86	0.39	100.3
G500A-CPX-10	0.18	17.40	1.60	0.02	17.50	11.40	0.00	51.30	0.90	0.43	100.7
Average	**0.19**	**16.96**	**1.37**	**0.01**	**16.63**	**12.28**	**0.01**	**51.71**	**0.83**	**0.40**	**100.4**
G550B-CPX-1	0.24	17.90	1.86	0.01	13.10	14.00	0.00	51.30	1.04	0.30	99.8
G550B-CPX-2	0.26	18.20	2.09	0.00	12.10	14.30	0.00	51.80	1.16	0.31	100.2
G550B-CPX-3	0.27	18.60	2.06	0.02	12.10	14.30	0.01	51.80	1.06	0.23	100.5
G550B-CPX-4	0.25	18.90	1.83	0.03	11.50	14.20	0.02	52.30	1.10	0.31	100.4
G550B-CPX-5	0.21	16.10	1.61	0.00	13.90	14.80	0.02	52.10	0.74	0.32	99.8
G550B-CPX-6	0.30	19.50	1.70	0.11	10.10	14.60	0.00	52.20	0.93	0.20	99.6
G550B-CPX-7	0.26	18.20	2.39	0.06	11.30	14.10	0.00	51.70	1.22	0.26	99.5
G550B-CPX-8	0.27	19.50	2.39	0.10	11.10	13.80	0.01	51.60	1.22	0.22	100.2
G550B-CPX-9	0.27	18.60	1.69	0.05	10.60	15.10	0.00	52.40	0.96	0.23	99.9
G550B-CPX-10	0.33	19.20	2.36	0.12	10.70	14.40	0.00	51.00	1.25	0.20	99.6
G550B-CPX-11	0.25	19.00	1.99	0.05	11.30	14.30	0.01	52.40	1.16	0.21	100.7
Average	**0.26**	**18.52**	**2.00**	**0.05**	**11.62**	**14.35**	**0.01**	**51.87**	**1.08**	**0.25**	**100.0**

Appendix B - CPX - NBBC Sample Suite

Sample	CAT SUM	Si	Al	Na	Ca	Cr	Fe	Mg	K	Ti	Mn	Total	Mg#
BBC14-CPX-1	2.26	1.95	0.06	0.02	0.74	0.00	0.40	0.78	0.00	0.03	0.01	4.00	66.0
BBC14-CPX-2	2.22	1.99	0.09	0.03	0.77	0.00	0.30	0.75	0.00	0.02	0.01	3.96	71.4
BBC14-CPX-3	2.22	1.99	0.09	0.03	0.77	0.00	0.30	0.75	0.00	0.02	0.01	3.96	71.4
BBC14-CPX-4	2.22	1.97	0.10	0.02	0.77	0.01	0.29	0.77	0.00	0.02	0.00	3.96	72.4
BBC14-CPX-5	2.22	1.96	0.11	0.02	0.78	0.02	0.25	0.80	0.00	0.03	0.01	3.96	76.1
BBC14-CPX-6	2.22	1.95	0.11	0.03	0.74	0.02	0.26	0.82	0.00	0.03	0.01	3.97	75.6
BBC14-CPX-7	2.22	2.01	0.06	0.02	0.78	0.00	0.29	0.79	0.00	0.01	0.01	3.96	73.5
BBC14-CPX-8	2.22	1.99	0.08	0.02	0.77	0.00	0.29	0.79	0.00	0.02	0.01	3.96	73.4
BBC14-CPX-9	2.23	1.97	0.08	0.03	0.80	0.00	0.29	0.78	0.00	0.02	0.01	3.98	73.1
BBC14-CPX-10	2.23	1.96	0.09	0.02	0.69	0.01	0.33	0.82	0.00	0.03	0.01	3.97	71.2
BBC14-CPX-11	2.24	2.01	0.05	0.01	0.85	0.00	0.34	0.69	0.00	0.02	0.00	3.96	66.8
Average	**2.23**	**1.98**	**0.08**	**0.02**	**0.77**	**0.01**	**0.30**	**0.78**	**0.00**	**0.02**	**0.01**	**3.97**	**71.9**
G500A-CPX-1	2.25	1.97	0.07	0.01	0.70	0.00	0.47	0.72	0.00	0.03	0.01	3.98	60.7
G500A-CPX-2	2.29	1.96	0.06	0.01	0.68	0.00	0.55	0.68	0.00	0.03	0.01	3.99	55.4
G500A-CPX-3	2.28	1.98	0.05	0.01	0.68	0.00	0.59	0.64	0.00	0.02	0.01	3.98	52.1
G500A-CPX-4	2.29	1.97	0.05	0.01	0.68	0.00	0.60	0.64	0.00	0.02	0.02	3.99	51.6
G500A-CPX-5	2.29	1.97	0.06	0.01	0.69	0.00	0.51	0.71	0.00	0.02	0.01	3.99	58.3
G500A-CPX-6	2.29	1.96	0.06	0.01	0.69	0.00	0.54	0.69	0.00	0.02	0.01	3.99	55.9
G500A-CPX-7	2.28	1.96	0.06	0.01	0.68	0.00	0.52	0.73	0.00	0.02	0.01	3.99	58.3
G500A-CPX-8	2.29	1.94	0.07	0.01	0.71	0.00	0.46	0.77	0.00	0.03	0.01	4.00	62.2
G500A-CPX-9	2.27	1.96	0.06	0.01	0.68	0.00	0.49	0.73	0.00	0.02	0.01	3.99	59.8
G500A-CPX-10	2.29	1.95	0.07	0.01	0.71	0.00	0.56	0.65	0.00	0.03	0.01	3.99	53.7
Average	**2.28**	**1.96**	**0.06**	**0.01**	**0.69**	**0.00**	**0.53**	**0.69**	**0.00**	**0.02**	**0.01**	**3.99**	**56.8**
G550B-CPX-1	2.27	1.94	0.08	0.02	0.72	0.00	0.41	0.79	0.00	0.03	0.01	4.00	65.6
G550B-CPX-2	2.25	1.94	0.09	0.02	0.73	0.00	0.38	0.80	0.00	0.03	0.01	3.99	67.8
G550B-CPX-3	2.24	1.93	0.09	0.02	0.74	0.00	0.38	0.80	0.00	0.03	0.01	4.00	67.8
G550B-CPX-4	2.24	1.95	0.08	0.02	0.75	0.00	0.36	0.79	0.00	0.03	0.01	3.99	68.8
G550B-CPX-5	2.26	1.96	0.07	0.02	0.65	0.00	0.44	0.83	0.00	0.02	0.01	3.99	65.5
G550B-CPX-6	2.25	1.95	0.07	0.02	0.78	0.00	0.32	0.81	0.00	0.03	0.01	3.99	72.0
G550B-CPX-7	2.25	1.94	0.11	0.02	0.73	0.00	0.35	0.79	0.00	0.03	0.01	3.98	69.0
G550B-CPX-8	2.25	1.93	0.11	0.02	0.78	0.00	0.35	0.77	0.00	0.03	0.01	3.99	68.9
G550B-CPX-9	2.24	1.95	0.07	0.02	0.74	0.00	0.33	0.84	0.00	0.03	0.01	3.99	71.7
G550B-CPX-10	2.26	1.92	0.10	0.02	0.77	0.00	0.34	0.81	0.00	0.04	0.01	4.01	70.6
G550B-CPX-11	2.23	1.94	0.09	0.02	0.76	0.00	0.35	0.79	0.00	0.03	0.01	3.99	69.3
Average	**2.25**	**1.94**	**0.09**	**0.02**	**0.74**	**0.00**	**0.36**	**0.80**	**0.00**	**0.03**	**0.01**	**3.99**	**68.8**

Appendix B - CPX - NBBC Sample Suite

Sample	Na2O	CaO	Al2O3	Cr2O3	FeO	MgO	K2O	SiO2	TiO2	MnO	Total
G500C-CPX-1	0.17	17.60	1.01	0.01	22.10	7.70	0.01	50.40	0.70	0.51	100.2
G500C-CPX-2	0.19	17.00	1.07	0.01	21.30	8.80	0.00	50.30	0.66	0.48	99.8
G500C-CPX-3	0.18	17.80	0.92	0.00	21.60	7.80	0.00	51.60	0.67	0.58	101.2
G500C-CPX-4	0.18	16.80	1.23	0.00	23.00	7.60	0.00	48.90	0.58	0.47	98.8
G500C-CPX-5	0.16	16.10	1.26	0.00	21.50	9.40	0.01	50.30	0.64	0.63	100.0
G500C-CPX-6	0.21	17.60	0.97	0.00	22.30	7.70	0.02	51.00	0.66	0.51	101.0
G500C-CPX-7	0.18	17.80	0.97	0.00	21.70	8.00	0.00	50.50	0.60	0.57	100.3
G500C-CPX-8	0.19	17.20	0.99	0.00	22.20	8.10	0.00	50.90	0.60	0.52	100.7
Average	**0.18**	**17.24**	**1.05**	**0.00**	**21.96**	**8.14**	**0.01**	**50.49**	**0.64**	**0.53**	**100.2**
H514-CPX-1	0.29	18.80	2.19	0.02	12.50	13.40	0.00	51.90	1.24	0.25	100.6
H514-CPX-2	0.31	18.70	2.30	0.05	12.10	13.60	0.01	51.20	1.23	0.24	99.7
H514-CPX-3	0.31	18.40	2.28	0.01	12.20	13.80	0.00	51.30	1.22	0.31	99.8
H514-CPX-4	0.29	19.00	1.81	0.06	11.80	14.30	0.00	52.60	0.99	0.23	101.1
H514-CPX-5	0.28	18.20	2.12	0.03	13.30	13.50	0.01	51.10	1.23	0.27	100.0
H514-CPX-6	0.26	18.30	1.68	0.00	12.70	13.80	0.01	52.20	1.03	0.24	100.2
H514-CPX-7	0.17	16.50	1.28	0.00	17.30	12.30	0.01	51.20	0.73	0.32	99.8
H514-CPX-8	0.17	20.40	0.61	0.01	15.20	11.10	0.00	52.80	0.15	0.31	100.8
H514-CPX-9	0.20	16.90	1.29	0.01	16.10	12.50	0.00	51.50	0.74	0.34	99.6
H514-CPX-10	0.23	16.50	1.32	0.00	16.10	13.00	0.00	52.10	0.80	0.43	100.5
Average	**0.25**	**18.17**	**1.69**	**0.02**	**13.93**	**13.13**	**0.00**	**51.79**	**0.94**	**0.29**	**100.2**
H515-CPX-1	0.22	16.90	1.39	0.00	17.10	12.40	0.02	51.30	0.78	0.43	100.5
H515-CPX-2	0.24	17.70	1.66	0.03	13.70	13.80	0.01	52.20	0.97	0.34	100.7
H515-CPX-3	0.23	17.90	1.63	0.01	13.50	13.60	0.00	52.20	0.96	0.32	100.4
H515-CPX-4	0.19	17.00	1.41	0.02	16.10	12.90	0.00	51.50	0.88	0.38	100.4
H515-CPX-5	0.20	16.30	1.30	0.00	17.60	12.20	0.00	52.00	0.73	0.45	100.8
H515-CPX-6	0.16	15.80	1.07	0.00	20.00	10.60	0.00	50.70	0.69	0.49	99.5
H515-CPX-7	0.20	17.10	1.61	0.01	15.10	13.50	0.00	52.50	0.96	0.31	101.3
H515-CPX-8	0.19	17.10	1.44	0.00	15.90	13.00	0.00	51.70	0.89	0.32	100.5
H515-CPX-9	0.19	16.70	1.22	0.01	18.00	11.40	0.00	51.50	0.70	0.44	100.2
Average	**0.20**	**16.94**	**1.41**	**0.01**	**16.33**	**12.60**	**0.00**	**51.73**	**0.84**	**0.39**	**100.5**

Appendix B - CPX - NBBC Sample Suite

Sample	CAT SUM	Si	Al	Na	Ca	Cr	Fe	Mg	K	Ti	Mn	Total	Mg#
G500C-CPX-1	2.36	1.98	0.05	0.01	0.74	0.00	0.72	0.45	0.00	0.02	0.02	3.99	38.3
G500C-CPX-2	2.35	1.97	0.05	0.01	0.71	0.00	0.70	0.51	0.00	0.02	0.02	3.99	42.4
G500C-CPX-3	2.32	1.99	0.04	0.01	0.74	0.00	0.70	0.45	0.00	0.02	0.02	3.97	39.2
G500C-CPX-4	2.40	1.96	0.06	0.01	0.72	0.00	0.77	0.45	0.00	0.02	0.02	4.00	37.1
G500C-CPX-5	2.35	1.96	0.06	0.01	0.67	0.00	0.70	0.55	0.00	0.02	0.02	4.00	43.8
G500C-CPX-6	2.34	1.98	0.04	0.02	0.73	0.00	0.73	0.45	0.00	0.02	0.02	3.98	38.1
G500C-CPX-7	2.35	1.97	0.04	0.01	0.75	0.00	0.71	0.47	0.00	0.02	0.02	3.99	39.6
G500C-CPX-8	2.34	1.98	0.05	0.01	0.72	0.00	0.72	0.47	0.00	0.02	0.02	3.99	39.4
Average	**2.35**	**1.97**	**0.05**	**0.01**	**0.72**	**0.00**	**0.72**	**0.47**	**0.00**	**0.02**	**0.02**	**3.99**	**39.7**
H514-CPX-1	2.24	1.94	0.10	0.02	0.75	0.00	0.39	0.75	0.00	0.03	0.01	3.99	65.6
H514-CPX-2	2.26	1.93	0.10	0.02	0.75	0.00	0.38	0.76	0.00	0.03	0.01	4.00	66.7
H514-CPX-3	2.26	1.93	0.10	0.02	0.74	0.00	0.38	0.77	0.00	0.03	0.01	4.00	66.8
H514-CPX-4	2.23	1.95	0.08	0.02	0.75	0.00	0.37	0.79	0.00	0.03	0.01	3.99	68.3
H514-CPX-5	2.27	1.93	0.09	0.02	0.74	0.00	0.42	0.76	0.00	0.03	0.01	4.00	64.4
H514-CPX-6	2.25	1.96	0.07	0.02	0.73	0.00	0.40	0.77	0.00	0.03	0.01	3.99	65.9
H514-CPX-7	2.30	1.96	0.06	0.01	0.68	0.00	0.55	0.70	0.00	0.02	0.01	4.00	55.9
H514-CPX-8	2.28	2.00	0.03	0.01	0.83	0.00	0.48	0.63	0.00	0.00	0.01	3.99	56.5
H514-CPX-9	2.30	1.97	0.06	0.01	0.69	0.00	0.51	0.71	0.00	0.02	0.01	3.99	58.0
H514-CPX-10	2.27	1.97	0.06	0.02	0.67	0.00	0.51	0.73	0.00	0.02	0.01	3.99	59.0
Average	**2.27**	**1.95**	**0.07**	**0.02**	**0.73**	**0.00**	**0.44**	**0.74**	**0.00**	**0.03**	**0.01**	**3.99**	**62.7**
H515-CPX-1	2.29	1.95	0.06	0.02	0.69	0.00	0.54	0.70	0.00	0.02	0.01	4.00	56.4
H515-CPX-2	2.25	1.95	0.07	0.02	0.71	0.00	0.43	0.77	0.00	0.03	0.01	3.99	64.2
H515-CPX-3	2.25	1.96	0.07	0.02	0.72	0.00	0.42	0.76	0.00	0.03	0.01	3.99	64.2
H515-CPX-4	2.28	1.95	0.06	0.01	0.69	0.00	0.51	0.73	0.00	0.03	0.01	4.00	58.8
H515-CPX-5	2.28	1.97	0.06	0.01	0.66	0.00	0.56	0.69	0.00	0.02	0.01	3.99	55.3
H515-CPX-6	2.34	1.97	0.05	0.01	0.66	0.00	0.65	0.61	0.00	0.02	0.02	3.99	48.6
H515-CPX-7	2.24	1.96	0.07	0.01	0.68	0.00	0.47	0.75	0.00	0.03	0.01	3.99	61.4
H515-CPX-8	2.27	1.95	0.06	0.01	0.69	0.00	0.50	0.73	0.00	0.03	0.01	4.00	59.3
H515-CPX-9	2.30	1.97	0.06	0.01	0.69	0.00	0.58	0.65	0.00	0.02	0.01	3.99	53.0
Average	**2.28**	**1.96**	**0.06**	**0.01**	**0.69**	**0.00**	**0.52**	**0.71**	**0.00**	**0.02**	**0.01**	**3.99**	**57.9**

Appendix B - CPX - NBBC Sample Suite

Sample	Na2O	CaO	Al2O3	Cr2O3	FeO	MgO	K2O	SiO2	TiO2	MnO	Total
G549-CPX-1	0.22	17.50	1.68	0.03	14.80	13.20	0.00	52.10	0.98	0.28	100.8
G549-CPX-2	0.22	17.70	1.75	0.00	13.90	13.40	0.00	51.90	0.98	0.35	100.2
G549-CPX-3	0.20	17.20	1.65	0.00	14.70	13.30	0.01	51.90	0.92	0.33	100.2
G549-CPX-4	0.19	17.50	1.49	0.00	15.60	12.90	0.00	51.80	0.85	0.39	100.7
G549-CPX-5	0.11	14.60	1.01	0.01	22.10	10.40	0.00	50.60	0.60	0.55	100.0
G549-CPX-6	0.18	16.60	1.42	0.00	17.20	12.40	0.00	51.10	0.76	0.39	100.1
G549-CPX-7	0.25	18.20	2.19	0.03	13.40	13.40	0.00	51.70	1.12	0.26	100.6
G549-CPX-8	0.21	17.10	1.63	0.00	14.20	13.90	0.01	52.10	0.84	0.34	100.3
G549-CPX-9	0.19	17.80	1.62	0.05	13.60	13.70	0.00	52.20	0.90	0.30	100.4
G549-CPX-10	0.22	17.30	1.79	0.04	14.00	13.60	0.01	51.80	0.96	0.32	100.0
G549-CPX-11	0.19	16.50	1.38	0.00	17.20	12.60	0.00	51.70	0.80	0.38	100.8
G549-CPX-12	0.23	17.60	1.70	0.06	14.10	13.60	0.00	51.60	0.93	0.32	100.1
	0.20	**17.13**	**1.61**	**0.02**	**15.40**	**13.03**	**0.00**	**51.71**	**0.89**	**0.35**	**100.3**
G528-CPX-1	0.17	17.00	1.53	0.02	15.20	13.30	0.01	51.70	0.87	0.34	100.1
G528-CPX-2	0.22	17.90	1.78	0.04	12.80	13.90	0.01	52.80	0.94	0.27	100.7
G528-CPX-3	0.20	17.00	1.64	0.00	15.00	13.10	0.00	51.80	0.88	0.33	100.0
G528-CPX-4	0.19	17.80	1.70	0.04	14.00	13.50	0.02	51.50	0.94	0.33	100.0
G528-CPX-5	0.16	17.00	1.50	0.00	16.80	12.10	0.01	51.20	0.73	0.38	99.9
G528-CPX-6	0.20	17.10	1.63	0.00	14.70	13.60	0.00	51.90	0.90	0.33	100.4
G528-CPX-7	0.25	16.90	1.56	0.00	15.40	12.90	0.03	51.40	0.89	0.36	99.7
G528-CPX-8	0.17	16.70	1.35	0.02	17.10	12.00	0.01	51.00	0.76	0.37	99.5
G528-CPX-9	0.22	17.70	1.63	0.02	14.10	13.30	0.00	51.80	0.86	0.39	100.0
G528-CPX-10	0.24	17.30	1.57	0.00	15.10	13.30	0.00	51.50	0.94	0.40	100.4
G528-CPX-11	0.19	17.50	1.68	0.00	13.90	13.50	0.00	52.50	0.91	0.30	100.5
	0.20	**17.26**	**1.60**	**0.01**	**14.92**	**13.14**	**0.01**	**51.74**	**0.87**	**0.35**	**100.1**
G527-CPX-1	0.18	16.60	1.20	0.03	18.70	11.40	0.01	51.60	0.64	0.45	100.8
G527-CPX-2	0.18	17.70	1.60	0.00	14.70	13.10	0.01	51.60	0.89	0.33	100.1
G527-CPX-3	0.16	16.60	1.22	0.00	18.70	11.20	0.01	51.20	0.60	0.46	100.2
G527-CPX-4	0.22	17.90	1.66	0.02	13.70	13.80	0.00	52.50	0.96	0.31	101.1
G527-CPX-5	0.24	17.50	1.70	0.02	14.10	13.60	0.03	52.00	0.92	0.32	100.4
G527-CPX-6	0.20	16.80	1.59	0.04	15.40	12.90	0.00	51.90	0.86	0.37	100.1
G527-CPX-7	0.20	17.10	1.62	0.04	14.70	13.10	0.00	51.80	0.92	0.39	99.9
G527-CPX-8	0.23	17.40	1.66	0.03	13.90	13.50	0.00	52.10	0.94	0.29	100.1
G527-CPX-9	0.19	17.60	1.72	0.00	14.20	13.40	0.01	51.70	0.99	0.32	100.1
G527-CPX-10	0.13	15.80	1.54	0.02	17.20	12.80	0.00	50.80	0.81	0.47	99.6
G527-CPX-11	0.18	17.00	1.50	0.00	18.00	11.20	0.01	50.50	0.81	0.37	99.6
	0.19	**17.09**	**1.55**	**0.02**	**15.75**	**12.73**	**0.01**	**51.61**	**0.85**	**0.37**	**100.2**

Appendix B - CPX - NBBC Sample Suite

Sample	CAT SUM	Si	Al	Na	Ca	Cr	Fe	Mg	K	Ti	Mn	Total	Mg#
G549-CPX-1	2.25	1.95	0.07	0.02	0.70	0.00	0.46	0.74	0.00	0.03	0.01	3.99	61.4
G549-CPX-2	2.26	1.95	0.08	0.02	0.71	0.00	0.44	0.75	0.00	0.03	0.01	3.99	63.2
G549-CPX-3	2.27	1.96	0.07	0.01	0.69	0.00	0.46	0.75	0.00	0.03	0.01	3.99	61.7
G549-CPX-4	2.27	1.95	0.07	0.01	0.71	0.00	0.49	0.73	0.00	0.02	0.01	4.00	59.6
G549-CPX-5	2.34	1.97	0.05	0.01	0.61	0.00	0.72	0.60	0.00	0.02	0.02	3.99	45.6
G549-CPX-6	2.30	1.95	0.06	0.01	0.68	0.00	0.55	0.71	0.00	0.02	0.01	4.00	56.2
G549-CPX-7	2.25	1.94	0.10	0.02	0.73	0.00	0.42	0.75	0.00	0.03	0.01	3.99	64.1
G549-CPX-8	2.26	1.96	0.07	0.02	0.69	0.00	0.45	0.78	0.00	0.02	0.01	3.99	63.6
G549-CPX-9	2.25	1.96	0.07	0.01	0.72	0.00	0.43	0.77	0.00	0.03	0.01	3.99	64.2
G549-CPX-10	2.26	1.95	0.08	0.02	0.70	0.00	0.44	0.76	0.00	0.03	0.01	3.99	63.4
G549-CPX-11	2.28	1.96	0.06	0.01	0.67	0.00	0.54	0.71	0.00	0.02	0.01	3.99	56.6
G549-CPX-12	2.27	1.95	0.08	0.02	0.71	0.00	0.44	0.76	0.00	0.03	0.01	4.00	63.2
Average	**2.27**	**1.95**	**0.07**	**0.01**	**0.69**	**0.00**	**0.49**	**0.73**	**0.00**	**0.03**	**0.01**	**3.99**	**60.2**
G528-CPX-1	2.27	1.96	0.07	0.01	0.69	0.00	0.48	0.75	0.00	0.02	0.01	3.99	60.9
G528-CPX-2	2.24	1.96	0.08	0.02	0.71	0.00	0.40	0.77	0.00	0.03	0.01	3.98	65.9
G528-CPX-3	2.27	1.96	0.07	0.01	0.69	0.00	0.47	0.74	0.00	0.03	0.01	3.99	60.9
G528-CPX-4	2.27	1.95	0.08	0.01	0.72	0.00	0.44	0.76	0.00	0.03	0.01	4.00	63.2
G528-CPX-5	2.30	1.96	0.07	0.01	0.70	0.00	0.54	0.69	0.00	0.02	0.01	3.99	56.2
G528-CPX-6	2.26	1.95	0.07	0.01	0.69	0.00	0.46	0.76	0.00	0.03	0.01	3.99	62.2
G528-CPX-7	2.29	1.96	0.07	0.02	0.69	0.00	0.49	0.73	0.00	0.03	0.01	3.99	59.9
G528-CPX-8	2.31	1.96	0.06	0.01	0.69	0.00	0.55	0.69	0.00	0.02	0.01	3.99	55.6
G528-CPX-9	2.27	1.96	0.07	0.02	0.72	0.00	0.45	0.75	0.00	0.02	0.01	3.99	62.7
G528-CPX-10	2.27	1.95	0.07	0.02	0.70	0.00	0.48	0.75	0.00	0.03	0.01	4.00	61.1
G528-CPX-11	2.25	1.97	0.07	0.01	0.70	0.00	0.44	0.75	0.00	0.03	0.01	3.98	63.4
Average	**2.27**	**1.96**	**0.07**	**0.01**	**0.70**	**0.00**	**0.47**	**0.74**	**0.00**	**0.02**	**0.01**	**3.99**	**61.1**
G527-CPX-1	2.29	1.97	0.05	0.01	0.68	0.00	0.60	0.65	0.00	0.02	0.01	3.99	52.1
G527-CPX-2	2.27	1.95	0.07	0.01	0.72	0.00	0.47	0.74	0.00	0.03	0.01	3.99	61.4
G527-CPX-3	2.31	1.97	0.06	0.01	0.68	0.00	0.60	0.64	0.00	0.02	0.01	3.99	51.6
G527-CPX-4	2.24	1.96	0.07	0.02	0.71	0.00	0.43	0.77	0.00	0.03	0.01	3.99	64.2
G527-CPX-5	2.26	1.95	0.08	0.02	0.70	0.00	0.44	0.76	0.00	0.03	0.01	3.99	63.2
G527-CPX-6	2.27	1.96	0.07	0.01	0.68	0.00	0.49	0.73	0.00	0.02	0.01	3.98	59.9
G527-CPX-7	2.27	1.96	0.07	0.01	0.69	0.00	0.47	0.74	0.00	0.03	0.01	3.98	61.4
G527-CPX-8	2.26	1.96	0.07	0.02	0.70	0.00	0.44	0.76	0.00	0.03	0.01	3.98	63.4
G527-CPX-9	2.27	1.95	0.08	0.01	0.71	0.00	0.45	0.75	0.00	0.03	0.01	3.99	62.7
G527-CPX-10	2.30	1.95	0.07	0.01	0.65	0.00	0.55	0.73	0.00	0.02	0.02	4.00	57.0
G527-CPX-11	2.32	1.95	0.07	0.01	0.70	0.00	0.58	0.64	0.00	0.02	0.01	4.00	52.6
Average	**2.28**	**1.96**	**0.07**	**0.01**	**0.69**	**0.00**	**0.50**	**0.72**	**0.00**	**0.02**	**0.01**	**3.99**	**59.0**

Appendix B - CPX - NBBC Sample Suite

Sample	Na2O	CaO	Al2O3	Cr2O3	FeO	MgO	K2O	SiO2	TiO2	MnO	Total
G536-CPX-1	0.19	16.50	1.57	0.00	17.10	11.90	0.01	51.30	0.75	0.36	99.7
G536-CPX-2	0.20	16.80	1.32	0.00	16.70	12.00	0.02	52.10	0.79	0.42	100.4
G536-CPX-3	0.23	17.10	1.32	0.00	16.80	12.20	0.00	51.40	0.79	0.40	100.2
G536-CPX-4	0.23	16.40	1.32	0.01	16.70	12.60	0.00	52.00	0.75	0.46	100.5
G536-CPX-5	0.22	16.20	1.27	0.03	17.30	12.60	0.00	51.80	0.74	0.39	100.6
G536-CPX-6	0.23	16.50	1.37	0.02	17.10	12.00	0.00	51.70	0.80	0.37	100.1
G536-CPX-7	0.18	16.40	1.29	0.00	17.40	12.20	0.01	51.10	0.77	0.41	99.8
G536-CPX-8	0.22	17.10	1.31	0.00	17.00	12.10	0.01	51.90	0.78	0.36	100.8
G536-CPX-9	0.21	16.50	1.23	0.00	17.00	12.30	0.00	50.90	0.76	0.37	99.3
G536-CPX-10	0.20	16.90	1.26	0.04	17.00	12.10	0.00	51.40	0.80	0.32	100.0
G536-CPX-11	0.22	16.80	1.32	0.00	16.40	12.50	0.01	52.00	0.81	0.33	100.4
	0.21	**16.65**	**1.33**	**0.01**	**16.95**	**12.23**	**0.01**	**51.60**	**0.78**	**0.38**	**100.1**

Appendix B - CPX - NBBC Sample Suite

Sample	CAT SUM	Si	Al	Na	Ca	Cr	Fe	Mg	K	Ti	Mn	Total	Mg#
G536-CPX-1	2.30	1.96	0.07	0.01	0.68	0.00	0.55	0.68	0.00	0.02	0.01	3.99	55.4
G536-CPX-2	2.28	1.98	0.06	0.01	0.68	0.00	0.53	0.68	0.00	0.02	0.01	3.98	56.1
G536-CPX-3	2.29	1.96	0.06	0.02	0.70	0.00	0.54	0.69	0.00	0.02	0.01	4.00	56.4
G536-CPX-4	2.28	1.97	0.06	0.02	0.67	0.00	0.53	0.71	0.00	0.02	0.01	3.99	57.3
G536-CPX-5	2.28	1.97	0.06	0.02	0.66	0.00	0.55	0.71	0.00	0.02	0.01	3.99	56.5
G536-CPX-6	2.29	1.97	0.06	0.02	0.67	0.00	0.54	0.68	0.00	0.02	0.01	3.98	55.6
G536-CPX-7	2.30	1.96	0.06	0.01	0.67	0.00	0.56	0.70	0.00	0.02	0.01	4.00	55.5
G536-CPX-8	2.28	1.97	0.06	0.02	0.69	0.00	0.54	0.68	0.00	0.02	0.01	3.99	55.9
G536-CPX-9	2.31	1.96	0.06	0.02	0.68	0.00	0.55	0.71	0.00	0.02	0.01	4.00	56.3
G536-CPX-10	2.29	1.96	0.06	0.01	0.69	0.00	0.54	0.69	0.00	0.02	0.01	3.99	55.9
G536-CPX-11	2.28	1.97	0.06	0.02	0.68	0.00	0.52	0.71	0.00	0.02	0.01	3.99	57.6
Average	**2.29**	**1.97**	**0.06**	**0.02**	**0.68**	**0.00**	**0.54**	**0.69**	**0.00**	**0.02**	**0.01**	**3.99**	**56.2**

Appendix B - CPX - Keweenaw Sample Suite

Sample	Na2O	CaO	Al2O3	Cr2O3	FeO	MgO	K2O	SiO2	TiO2	MnO	Total
KP1-CPX-1	0.25	18.45	1.92	0.00	9.59	15.15	0.00	53.56	1.09	0.00	100.0
KP1-CPX-2	0.44	17.33	1.43	0.00	9.87	15.94	0.00	53.72	0.92	0.35	100.0
KP1-CPX-3	0.00	1.99	0.60	0.00	20.99	20.82	0.00	54.61	0.40	0.59	100.0
KP1-CPX-4	0.00	15.55	1.18	0.00	12.14	15.92	0.00	54.43	0.78	0.00	100.0
KP1-CPX-5	0.34	16.84	1.59	0.00	11.85	14.82	0.00	53.44	1.13	0.00	100.0
KP1-CPX-6	0.28	18.38	1.78	0.00	8.69	15.79	0.00	54.27	0.82	0.00	100.0
KP1-CPX-7	0.27	18.75	2.25	0.00	7.62	15.97	0.00	54.00	1.14	0.00	100.0
KP1-CPX-8	0.27	18.72	1.77	0.00	8.88	15.51	0.00	53.72	1.12	0.00	100.0
KP1-CPX-9	0.19	11.05	1.04	0.00	15.92	16.99	0.00	53.73	0.78	0.30	100.0
KP1-CPX-10	0.00	4.23	0.76	0.00	19.46	20.06	0.00	54.58	0.49	0.42	100.0
KP1-CPX-11	0.36	17.72	1.29	0.00	10.05	15.60	0.00	54.10	0.88	0.00	100.0
KP1-CPX-12	0.00	3.78	1.05	0.00	19.42	20.81	0.00	54.19	0.39	0.36	100.0
KP1-CPX-13	0.22	18.33	1.87	0.00	9.30	15.24	0.00	53.76	0.97	0.31	100.0
Average	**0.20**	**13.93**	**1.43**	**0.00**	**12.60**	**16.82**	**0.00**	**54.01**	**0.84**	**0.18**	**100.0**
KP5-CPX-1	0.22	17.09	1.80	0.00	11.23	15.13	0.00	53.33	0.87	0.32	100.0
KP5-CPX-2	0.48	16.88	1.93	0.00	10.57	15.74	0.00	53.03	1.36	0.00	100.0
KP5-CPX-3	0.00	3.72	0.37	0.00	19.30	21.18	0.00	54.42	0.50	0.52	100.0
KP5-CPX-4	0.00	5.30	0.92	0.00	17.62	20.86	0.00	54.11	0.68	0.50	100.0
KP5-CPX-5	0.30	16.22	1.80	0.00	11.34	15.70	0.00	53.37	1.01	0.26	100.0
KP5-CPX-6	0.19	16.01	1.66	0.00	11.56	15.94	0.00	53.37	0.98	0.29	100.0
KP5-CPX-7	0.29	19.06	2.33	0.39	7.23	15.98	0.00	53.63	0.81	0.27	100.0
KP5-CPX-8	0.31	18.66	2.15	0.00	8.57	15.55	0.00	53.28	1.22	0.25	100.0
KP5-CPX-9	0.21	15.77	1.26	0.00	11.59	16.13	0.00	54.21	0.83	0.00	100.0
KP5-CPX-10	0.27	18.00	2.13	0.00	8.75	15.90	0.00	53.50	1.13	0.31	100.0
KP5-CPX-11	0.31	18.78	1.95	0.00	8.13	15.83	0.00	53.52	1.14	0.34	100.0
KP5-CPX-12	0.00	20.81	0.63	0.00	8.10	14.61	0.00	55.54	0.00	0.33	100.0
Average	**0.22**	**15.53**	**1.58**	**0.03**	**11.17**	**16.55**	**0.00**	**53.78**	**0.88**	**0.28**	**100.0**
KP6-CPX-1	0.27	17.60	2.18	0.00	11.23	14.69	0.00	52.35	1.25	0.43	100.0
KP6-CPX-2	0.00	11.19	1.27	0.00	14.76	17.51	0.00	54.41	0.51	0.36	100.0
KP6-CPX-3	0.20	15.80	1.39	0.00	10.87	17.29	0.00	53.34	0.78	0.35	100.0
KP6-CPX-4	0.00	21.54	1.86	0.22	9.32	16.63	0.00	53.10	0.45	0.01	103.1
KP6-CPX-5	0.32	17.67	2.11	0.00	10.28	15.09	0.00	53.43	1.09	0.00	100.0
KP6-CPX-6	0.00	17.15	1.46	0.00	11.44	14.97	0.00	53.51	1.10	0.37	100.0
Average	**0.13**	**16.83**	**1.71**	**0.04**	**11.32**	**16.03**	**0.00**	**53.36**	**0.86**	**0.25**	**100.5**

Appendix B - CPX - Keweenaw Sample Suite

Sample	CAT SUM	Si	Al	Na	Ca	Cr	Fe	Mg	K	Ti	Mn	Total	Mg#
KP1-CPX-1	2.22	1.97	0.08	0.02	0.73	0.00	0.30	0.83	0.00	0.03	0.00	3.96	73.8
KP1-CPX-2	2.22	1.98	0.06	0.03	0.68	0.00	0.30	0.88	0.00	0.03	0.01	3.98	74.2
KP1-CPX-3	2.22	2.02	0.03	0.00	0.08	0.00	0.65	1.15	0.00	0.01	0.02	3.95	63.9
KP1-CPX-4	2.22	2.01	0.05	0.00	0.61	0.00	0.37	0.88	0.00	0.02	0.00	3.94	70.0
KP1-CPX-5	2.23	1.98	0.07	0.02	0.67	0.00	0.37	0.82	0.00	0.03	0.00	3.96	69.0
KP1-CPX-6	2.20	1.99	0.08	0.02	0.72	0.00	0.27	0.86	0.00	0.02	0.00	3.96	76.4
KP1-CPX-7	2.20	1.97	0.10	0.02	0.73	0.00	0.23	0.87	0.00	0.03	0.00	3.96	78.9
KP1-CPX-8	2.21	1.98	0.08	0.02	0.74	0.00	0.27	0.85	0.00	0.03	0.00	3.96	75.7
KP1-CPX-9	2.23	2.00	0.05	0.01	0.44	0.00	0.49	0.94	0.00	0.02	0.01	3.96	65.5
KP1-CPX-10	2.22	2.02	0.03	0.00	0.17	0.00	0.60	1.11	0.00	0.01	0.01	3.95	64.8
KP1-CPX-11	2.21	1.99	0.06	0.03	0.70	0.00	0.31	0.86	0.00	0.02	0.00	3.97	73.4
KP1-CPX-12	2.22	2.00	0.05	0.00	0.15	0.00	0.60	1.15	0.00	0.01	0.01	3.96	65.6
KP1-CPX-13	2.21	1.98	0.08	0.02	0.72	0.00	0.29	0.84	0.00	0.03	0.01	3.96	74.5
Average	**2.22**	**1.99**	**0.06**	**0.01**	**0.55**	**0.00**	**0.39**	**0.92**	**0.00**	**0.02**	**0.01**	**3.96**	**71.2**
KP5-CPX-1	2.23	1.98	0.08	0.02	0.68	0.00	0.35	0.84	0.00	0.02	0.01	3.97	70.6
KP5-CPX-2	2.22	1.96	0.08	0.03	0.67	0.00	0.33	0.87	0.00	0.04	0.00	3.98	72.6
KP5-CPX-3	2.22	2.01	0.02	0.00	0.15	0.00	0.60	1.17	0.00	0.01	0.02	3.97	66.2
KP5-CPX-4	2.21	1.99	0.04	0.00	0.21	0.00	0.54	1.15	0.00	0.02	0.02	3.97	67.8
KP5-CPX-5	2.22	1.97	0.08	0.02	0.64	0.00	0.35	0.87	0.00	0.03	0.01	3.97	71.2
KP5-CPX-6	2.22	1.97	0.07	0.01	0.63	0.00	0.36	0.88	0.00	0.03	0.01	3.97	71.1
KP5-CPX-7	2.20	1.96	0.10	0.02	0.75	0.01	0.22	0.87	0.00	0.02	0.01	3.97	79.8
KP5-CPX-8	2.21	1.96	0.09	0.02	0.74	0.00	0.26	0.85	0.00	0.03	0.01	3.97	76.4
KP5-CPX-9	2.22	2.00	0.05	0.02	0.62	0.00	0.36	0.89	0.00	0.02	0.00	3.96	71.3
KP5-CPX-10	2.21	1.97	0.09	0.02	0.71	0.00	0.27	0.87	0.00	0.03	0.01	3.97	76.4
KP5-CPX-11	2.21	1.97	0.08	0.02	0.74	0.00	0.25	0.87	0.00	0.03	0.01	3.97	77.6
KP5-CPX-12	2.21	2.04	0.03	0.00	0.82	0.00	0.25	0.80	0.00	0.00	0.01	3.95	76.3
Average	**2.21**	**1.98**	**0.07**	**0.02**	**0.61**	**0.00**	**0.34**	**0.91**	**0.00**	**0.02**	**0.01**	**3.97**	**73.1**
KP6-CPX-1	2.24	1.95	0.10	0.02	0.70	0.00	0.35	0.81	0.00	0.03	0.01	3.98	70.0
KP6-CPX-2	2.22	2.01	0.06	0.00	0.44	0.00	0.46	0.96	0.00	0.01	0.01	3.95	67.9
KP6-CPX-3	2.22	1.97	0.06	0.01	0.62	0.00	0.34	0.95	0.00	0.02	0.01	3.99	73.9
KP6-CPX-4	2.17	1.92	0.08	0.00	0.83	0.01	0.28	0.90	0.00	0.01	0.00	4.03	76.1
KP6-CPX-5	2.22	1.97	0.09	0.02	0.70	0.00	0.32	0.83	0.00	0.03	0.00	3.96	72.3
KP6-CPX-6	2.23	1.98	0.06	0.00	0.68	0.00	0.35	0.83	0.00	0.03	0.01	3.95	70.0
Average	**2.21**	**1.97**	**0.07**	**0.01**	**0.66**	**0.00**	**0.35**	**0.88**	**0.00**	**0.02**	**0.01**	**3.98**	**71.7**

Appendix B - CPX - Keweenaw Sample Suite

Sample	Na2O	CaO	Al2O3	Cr2O3	FeO	MgO	K2O	SiO2	TiO2	MnO	Total
KP7A-CPX-1	0.38	20.09	1.94	0.32	8.07	17.30	0.00	50.86	0.72	0.32	100.0
KP7A-CPX-2	0.31	19.58	2.27	0.38	8.35	16.83	0.00	51.12	0.80	0.36	100.0
KP7A-CPX-3	0.30	19.14	2.05	0.00	8.75	17.04	0.00	51.54	0.90	0.28	100.0
KP7A-CPX-4	0.00	20.09	1.86	0.32	9.08	16.63	0.00	51.10	0.92	0.00	100.0
KP7A-CPX-5	0.00	21.91	1.83	0.00	12.64	13.61	0.00	48.66	0.95	0.40	100.0
KP7A-CPX-6	0.00	20.09	1.86	0.32	9.08	16.63	0.00	51.10	0.92	0.00	100.0
KP7A-CPX-7	0.30	19.25	2.09	0.35	8.09	17.17	0.00	51.68	0.81	0.26	100.0
KP7A-CPX-8	0.25	20.14	1.95	0.27	8.68	16.79	0.00	51.35	0.57	0.00	100.0
KP7A-CPX-9	0.00	21.91	1.83	0.00	12.64	13.61	0.00	48.66	0.95	0.40	100.0
KP7A-CPX-10	0.00	21.91	1.83	0.00	12.64	13.61	0.00	48.66	0.95	0.40	100.0
KP7A-CPX-11	0.40	19.16	1.77	0.00	12.60	14.43	0.00	50.55	1.10	0.00	100.0
KP7A-CPX-12	0.25	21.24	2.25	0.56	8.51	16.13	0.00	50.33	0.73	0.00	100.0
KP7A-CPX-13	0.34	20.26	1.85	0.26	9.61	16.13	0.00	50.36	0.84	0.35	100.0
KP7A-CPX-14	0.26	19.86	1.98	0.40	8.71	16.89	0.00	51.17	0.74	0.00	100.0
KP7A-CPX-15	0.33	19.16	2.03	0.30	8.81	16.97	0.00	51.75	0.65	0.00	100.0
Average	**0.21**	**20.25**	**1.96**	**0.23**	**9.75**	**15.98**	**0.00**	**50.59**	**0.84**	**0.18**	**100.0**
KP7B-CPX-1	0.29	17.96	1.35	0.00	14.09	14.50	0.00	50.46	0.99	0.36	100.0
KP7B-CPX-2	0.29	17.77	1.34	0.00	15.73	13.56	0.00	50.18	1.13	0.00	100.0
KP7B-CPX-3	0.41	17.89	1.34	0.00	15.14	13.88	0.00	50.05	0.92	0.36	100.0
KP7B-CPX-4	0.29	19.56	1.59	0.00	15.22	12.55	0.00	49.56	0.87	0.36	100.0
KP7B-CPX-5	0.29	17.96	1.35	0.00	14.09	14.50	0.00	50.46	0.99	0.36	100.0
KP7B-CPX-6	0.41	17.89	1.34	0.00	15.14	13.88	0.00	50.05	0.92	0.36	100.0
KP7B-CPX-7	0.29	17.77	1.34	0.00	14.73	14.56	0.00	50.18	1.13	0.00	100.0
KP7B-CPX-8	0.38	18.14	1.65	0.00	15.29	13.07	0.15	50.27	0.71	0.34	100.0
KP7B-CPX-9	0.33	17.35	3.06	0.00	15.43	14.30	0.00	48.23	0.93	0.37	100.0
KP7B-CPX-10	0.30	18.44	1.29	0.00	14.66	14.25	0.00	50.18	0.87	0.00	100.0
KP7B-CPX-11	0.31	17.48	0.90	0.00	17.69	12.49	0.00	49.87	0.68	0.59	100.0
KP7B-CPX-12	0.27	16.35	0.90	0.00	17.55	13.49	0.00	50.19	0.69	0.55	100.0
Average	**0.32**	**17.88**	**1.45**	**0.00**	**15.40**	**13.75**	**0.01**	**49.97**	**0.90**	**0.30**	**100.0**
KP10-CPX-1	0.21	17.49	1.08	0.00	13.30	13.45	0.00	53.15	0.85	0.46	100.0
KP10-CPX-2	0.33	18.77	2.16	0.00	9.98	14.28	0.00	52.91	1.15	0.43	100.0
KP10-CPX-3	0.19	17.71	1.30	0.00	13.18	13.32	0.00	53.16	0.85	0.29	100.0
KP10-CPX-4	0.26	17.36	1.47	0.00	12.85	13.51	0.00	53.11	1.01	0.42	100.0
KP10-CPX-5	0.00	1.29	13.44	0.00	29.12	16.55	0.00	39.27	0.00	0.34	100.0
KP10-CPX-6	0.23	17.55	1.34	0.00	13.08	13.19	0.00	53.42	0.80	0.37	100.0
KP10-CPX-7	0.00	1.63	12.98	0.00	27.61	16.14	0.17	41.15	0.00	0.32	100.0

Appendix B - CPX - Keweenaw Sample Suite

Sample	CAT SUM	Si	Al	Na	Ca	Cr	Fe	Mg	K	Ti	Mn	Total	Mg#
KP7A-CPX-1	2.24	1.89	0.09	0.03	0.80	0.01	0.25	0.96	0.00	0.02	0.01	4.05	79.3
KP7A-CPX-2	2.23	1.90	0.10	0.02	0.78	0.01	0.26	0.93	0.00	0.02	0.01	4.04	78.2
KP7A-CPX-3	2.23	1.91	0.09	0.02	0.76	0.00	0.27	0.94	0.00	0.03	0.01	4.03	77.6
KP7A-CPX-4	2.24	1.90	0.08	0.00	0.80	0.01	0.28	0.92	0.00	0.03	0.00	4.03	76.5
KP7A-CPX-5	2.30	1.86	0.08	0.00	0.90	0.00	0.40	0.78	0.00	0.03	0.01	4.07	65.7
KP7A-CPX-6	2.24	1.90	0.08	0.00	0.80	0.01	0.28	0.92	0.00	0.03	0.00	4.03	76.5
KP7A-CPX-7	2.22	1.91	0.09	0.02	0.76	0.01	0.25	0.95	0.00	0.02	0.01	4.03	79.1
KP7A-CPX-8	2.23	1.91	0.09	0.02	0.80	0.01	0.27	0.93	0.00	0.02	0.00	4.04	77.5
KP7A-CPX-9	2.30	1.86	0.08	0.00	0.90	0.00	0.40	0.78	0.00	0.03	0.01	4.07	65.7
KP7A-CPX-10	2.30	1.86	0.08	0.00	0.90	0.00	0.40	0.78	0.00	0.03	0.01	4.07	65.7
KP7A-CPX-11	2.27	1.91	0.08	0.03	0.78	0.00	0.40	0.81	0.00	0.03	0.00	4.03	67.1
KP7A-CPX-12	2.25	1.88	0.10	0.02	0.85	0.02	0.27	0.90	0.00	0.02	0.00	4.05	77.2
KP7A-CPX-13	2.25	1.89	0.08	0.02	0.81	0.01	0.30	0.90	0.00	0.02	0.01	4.06	74.9
KP7A-CPX-14	2.23	1.90	0.09	0.02	0.79	0.01	0.27	0.94	0.00	0.02	0.00	4.04	77.6
KP7A-CPX-15	2.23	1.92	0.09	0.02	0.76	0.01	0.27	0.94	0.00	0.02	0.00	4.03	77.4
Average	**2.25**	**1.89**	**0.09**	**0.02**	**0.81**	**0.01**	**0.31**	**0.89**	**0.00**	**0.02**	**0.01**	**4.04**	**74.4**
KP7B-CPX-1	2.28	1.92	0.06	0.02	0.73	0.00	0.45	0.82	0.00	0.03	0.01	4.04	64.7
KP7B-CPX-2	2.29	1.92	0.06	0.02	0.73	0.00	0.50	0.77	0.00	0.03	0.00	4.03	60.6
KP7B-CPX-3	2.30	1.91	0.06	0.03	0.73	0.00	0.48	0.79	0.00	0.03	0.01	4.05	62.0
KP7B-CPX-4	2.31	1.90	0.07	0.02	0.80	0.00	0.49	0.72	0.00	0.03	0.01	4.05	59.5
KP7B-CPX-5	2.28	1.92	0.06	0.02	0.73	0.00	0.45	0.82	0.00	0.03	0.01	4.04	64.7
KP7B-CPX-6	2.30	1.91	0.06	0.03	0.73	0.00	0.48	0.79	0.00	0.03	0.01	4.05	62.0
KP7B-CPX-7	2.29	1.91	0.06	0.02	0.72	0.00	0.47	0.83	0.00	0.03	0.00	4.04	63.8
KP7B-CPX-8	2.30	1.92	0.07	0.03	0.74	0.00	0.49	0.74	0.01	0.02	0.01	4.04	60.4
KP7B-CPX-9	2.30	1.85	0.14	0.02	0.71	0.00	0.49	0.82	0.00	0.03	0.01	4.07	62.3
KP7B-CPX-10	2.29	1.91	0.06	0.02	0.75	0.00	0.47	0.81	0.00	0.02	0.00	4.05	63.4
KP7B-CPX-11	2.32	1.93	0.04	0.02	0.72	0.00	0.57	0.72	0.00	0.02	0.02	4.04	55.7
KP7B-CPX-12	2.31	1.93	0.04	0.02	0.67	0.00	0.56	0.77	0.00	0.02	0.02	4.04	57.8
Average	**2.30**	**1.91**	**0.07**	**0.02**	**0.73**	**0.00**	**0.49**	**0.78**	**0.00**	**0.03**	**0.01**	**4.04**	**61.4**
KP10-CPX-1	2.25	1.99	0.05	0.02	0.70	0.00	0.42	0.75	0.00	0.02	0.01	3.97	64.3
KP10-CPX-3	2.23	1.96	0.09	0.02	0.75	0.00	0.31	0.79	0.00	0.03	0.01	3.97	71.8
KP10-CPX-4	2.25	1.99	0.06	0.01	0.71	0.00	0.41	0.74	0.00	0.02	0.01	3.96	64.3
KP10-CPX-5	2.25	1.99	0.06	0.02	0.70	0.00	0.40	0.75	0.00	0.03	0.01	3.96	65.2
KP10-CPX-6	2.36	1.54	0.62	0.00	0.05	0.00	0.96	0.97	0.00	0.00	0.01	4.15	50.3
KP10-CPX-8	2.25	2.00	0.06	0.02	0.70	0.00	0.41	0.74	0.00	0.02	0.01	3.96	64.2
KP10-CPX-9	2.33	1.60	0.59	0.00	0.07	0.00	0.90	0.93	0.01	0.00	0.01	4.11	51.0

Appendix B - CPX - Keweenaw Sample Suite

Sample	Na2O	CaO	Al2O3	Cr2O3	FeO	MgO	K2O	SiO2	TiO2	MnO	Total
KP10-CPX-8	0.27	17.40	1.23	0.00	13.58	13.04	0.00	53.21	0.77	0.50	100.0
KP10-CPX-9	0.30	18.70	1.80	0.00	10.86	13.84	0.00	53.14	0.97	0.40	100.0
KP10-CPX-10	0.31	18.81	1.49	0.00	11.37	13.58	0.00	53.39	1.05	0.00	100.0
Average	**0.21**	**14.67**	**3.83**	**0.00**	**15.49**	**14.09**	**0.02**	**50.59**	**0.75**	**0.35**	**100.0**
KP11A-CPX-1	0.23	17.63	1.06	0.00	14.27	12.69	0.00	53.05	0.78	0.28	100.0
KP11A-CPX-2	0.30	16.64	1.04	0.00	16.65	11.37	0.00	52.79	0.84	0.36	100.0
KP11A-CPX-3	0.28	17.49	0.98	0.00	14.56	12.30	0.00	53.47	0.93	0.00	100.0
KP11A-CPX-4	0.30	16.63	0.63	0.00	17.95	10.75	0.00	52.92	0.35	0.47	100.0
KP11A-CPX-5	0.24	17.98	1.19	0.00	13.08	12.85	0.00	53.08	1.17	0.42	100.0
KP11A-CPX-6	0.30	17.13	1.09	0.00	15.77	11.90	0.00	52.78	0.76	0.27	100.0
KP11A-CPX-7	0.27	16.35	0.90	0.00	17.55	13.49	0.00	50.19	0.69	0.55	100.0
KP11A-CPX-8	0.00	18.01	3.19	0.00	14.26	10.33	0.00	53.08	0.00	1.14	100.0
KP11A-CPX-9	0.31	17.48	0.90	0.00	17.69	12.49	0.00	49.87	0.68	0.59	100.0
KP11A-CPX-10	0.34	20.26	1.85	0.26	16.23	9.61	0.00	50.36	0.84	0.35	100.1
KP11A-CPX-11	0.32	16.90	1.10	0.00	16.27	11.43	0.00	52.68	0.93	0.38	100.0
KP11A-CPX-12	0.22	17.33	0.71	0.00	17.60	10.29	0.00	52.43	0.95	0.45	100.0
Average	**0.26**	**17.49**	**1.22**	**0.02**	**15.99**	**11.63**	**0.00**	**52.23**	**0.74**	**0.44**	**100.0**
KP12-CPX-1	0.43	18.01	0.54	0.00	24.99	5.97	0.00	48.64	0.56	0.87	100.0
KP12-CPX-2	0.32	18.49	0.51	0.00	23.76	6.62	0.00	49.05	0.60	0.64	100.0
KP12-CPX-3	0.23	17.25	0.90	0.00	21.09	9.70	0.00	49.63	0.57	0.62	100.0
KP12-CPX-4	0.31	18.02	0.66	0.00	23.77	7.14	0.00	48.82	0.66	0.61	100.0
KP12-CPX-5	0.26	18.11	0.75	0.00	21.87	8.53	0.00	49.09	0.90	0.51	100.0
KP12-CPX-6	0.20	18.00	0.79	0.00	21.30	9.13	0.00	49.39	0.69	0.51	100.0
KP12-CPX-7	0.26	18.10	0.81	0.00	19.09	10.77	0.00	49.54	0.71	0.71	100.0
KP12-CPX-8	0.00	17.31	1.09	0.00	20.33	10.74	0.00	49.47	0.62	0.45	100.0
KP12-CPX-9	0.24	17.92	1.90	0.00	18.18	11.22	0.00	48.87	1.18	0.48	100.0
KP12-CPX-10	0.21	17.60	1.02	0.00	18.78	11.56	0.00	49.53	0.83	0.45	100.0
KP12-CPX-11	0.25	17.21	0.76	0.00	20.98	9.84	0.00	49.43	0.90	0.62	100.0
KP12-CPX-12	0.37	17.39	0.36	0.00	26.04	6.08	0.00	48.67	0.29	0.81	100.0
KP12-CPX-13	0.34	18.22	0.72	0.00	24.98	5.95	0.00	48.42	0.68	0.70	100.0
KP12-CPX-14	0.30	17.81	1.14	0.00	16.95	12.74	0.00	49.65	0.92	0.48	100.0
KP12-CPX-15	0.48	17.32	1.42	0.00	19.69	10.49	0.00	48.92	1.10	0.59	100.0
Average	**0.28**	**17.78**	**0.89**	**0.00**	**21.45**	**9.10**	**0.00**	**49.14**	**0.75**	**0.60**	**100.0**

Appendix B - CPX - Keweenaw Sample Suite

Sample	CAT SUM	Si	Al	Na	Ca	Cr	Fe	Mg	K	Ti	Mn	Total	Mg#
KP10-CPX-10	2.26	2.00	0.05	0.02	0.70	0.00	0.43	0.73	0.00	0.02	0.02	3.96	63.1
KP10-CPX-11	2.24	1.98	0.08	0.02	0.75	0.00	0.34	0.77	0.00	0.03	0.01	3.97	69.4
KP10-CPX-12	2.24	1.99	0.07	0.02	0.75	0.00	0.35	0.75	0.00	0.03	0.00	3.96	68.0
Average	**2.26**	**1.90**	**0.17**	**0.02**	**0.59**	**0.00**	**0.49**	**0.79**	**0.00**	**0.02**	**0.01**	**4.00**	**63.2**
KP11A-CPX-1	2.26	2.00	0.05	0.02	0.71	0.00	0.45	0.71	0.00	0.02	0.01	3.97	61.3
KP11A-CPX-2	2.28	2.00	0.05	0.02	0.68	0.00	0.53	0.64	0.00	0.02	0.01	3.96	54.9
KP11A-CPX-3	2.26	2.01	0.04	0.02	0.70	0.00	0.46	0.69	0.00	0.03	0.00	3.95	60.1
KP11A-CPX-4	2.30	2.02	0.03	0.02	0.68	0.00	0.57	0.61	0.00	0.01	0.02	3.96	51.6
KP11A-CPX-5	2.25	1.99	0.05	0.02	0.72	0.00	0.41	0.72	0.00	0.03	0.01	3.96	63.6
KP11A-CPX-6	2.28	2.00	0.05	0.02	0.70	0.00	0.50	0.67	0.00	0.02	0.01	3.97	57.4
KP11A-CPX-7	2.31	1.93	0.04	0.02	0.67	0.00	0.56	0.77	0.00	0.02	0.02	4.04	57.8
KP11A-CPX-8	2.26	2.00	0.14	0.00	0.73	0.00	0.45	0.58	0.00	0.00	0.04	3.93	56.3
KP11A-CPX-9	2.32	1.93	0.04	0.02	0.72	0.00	0.57	0.72	0.00	0.02	0.02	4.04	55.7
KP11A-CPX-10	2.31	1.94	0.08	0.03	0.84	0.01	0.52	0.55	0.00	0.02	0.01	4.00	51.3
KP11A-CPX-11	2.28	2.00	0.05	0.02	0.69	0.00	0.52	0.65	0.00	0.03	0.01	3.96	55.6
KP11A-CPX-12	2.30	2.01	0.03	0.02	0.71	0.00	0.56	0.59	0.00	0.03	0.01	3.96	51.0
Average	**2.28**	**1.99**	**0.05**	**0.02**	**0.71**	**0.00**	**0.51**	**0.66**	**0.00**	**0.02**	**0.01**	**3.98**	**56.4**
KP12-CPX-1	2.41	1.95	0.03	0.03	0.78	0.00	0.84	0.36	0.00	0.02	0.03	4.03	29.9
KP12-CPX-2	2.40	1.96	0.02	0.02	0.79	0.00	0.79	0.39	0.00	0.02	0.02	4.02	33.2
KP12-CPX-3	2.36	1.95	0.04	0.02	0.72	0.00	0.69	0.57	0.00	0.02	0.02	4.03	45.0
KP12-CPX-4	2.40	1.95	0.03	0.02	0.77	0.00	0.79	0.42	0.00	0.02	0.02	4.03	34.9
KP12-CPX-5	2.37	1.94	0.03	0.02	0.77	0.00	0.72	0.50	0.00	0.03	0.02	4.03	41.0
KP12-CPX-6	2.36	1.94	0.04	0.02	0.76	0.00	0.70	0.54	0.00	0.02	0.02	4.03	43.3
KP12-CPX-7	2.34	1.93	0.04	0.02	0.76	0.00	0.62	0.63	0.00	0.02	0.02	4.04	50.1
KP12-CPX-8	2.35	1.93	0.05	0.00	0.72	0.00	0.66	0.62	0.00	0.02	0.01	4.03	48.5
KP12-CPX-9	2.33	1.90	0.09	0.02	0.75	0.00	0.59	0.65	0.00	0.03	0.02	4.04	52.4
KP12-CPX-10	2.33	1.92	0.05	0.02	0.73	0.00	0.61	0.67	0.00	0.02	0.01	4.04	52.3
KP12-CPX-11	2.36	1.94	0.04	0.02	0.72	0.00	0.69	0.58	0.00	0.03	0.02	4.03	45.5
KP12-CPX-12	2.42	1.96	0.02	0.03	0.75	0.00	0.88	0.37	0.00	0.01	0.03	4.04	29.4
KP12-CPX-13	2.41	1.95	0.03	0.03	0.78	0.00	0.84	0.36	0.00	0.02	0.02	4.03	29.8
KP12-CPX-14	2.32	1.91	0.05	0.02	0.74	0.00	0.55	0.73	0.00	0.03	0.02	4.04	57.3
KP12-CPX-15	2.35	1.91	0.07	0.04	0.72	0.00	0.64	0.61	0.00	0.03	0.02	4.04	48.7
Average	**2.37**	**1.94**	**0.04**	**0.02**	**0.75**	**0.00**	**0.71**	**0.53**	**0.00**	**0.02**	**0.02**	**4.03**	**42.7**

Appendix B - CPX - Keweenaw Sample Suite

Sample	Na2O	CaO	Al2O3	Cr2O3	FeO	MgO	K2O	SiO2	TiO2	MnO	Total
KP14A-CPX-1	0.34	17.27	0.75	0.00	20.96	10.39	0.00	49.26	0.61	0.41	100.0
KP14A-CPX-2	0.25	16.93	0.85	0.00	20.52	10.64	0.00	49.51	0.78	0.52	100.0
KP14A-CPX-3	0.33	16.93	0.88	0.00	20.83	10.21	0.00	49.60	0.64	0.58	100.0
KP14A-CPX-4	0.23	17.01	0.84	0.00	20.13	10.57	0.00	49.89	0.89	0.43	100.0
KP14A-CPX-5	0.30	16.49	1.04	0.00	20.27	10.99	0.00	49.52	0.87	0.51	100.0
KP14A-CPX-6	0.39	17.31	1.00	0.00	20.24	10.27	0.00	49.33	0.75	0.72	100.0
KP14A-CPX-7	0.30	16.85	0.76	0.00	20.32	10.89	0.00	49.48	0.87	0.52	100.0
KP14A-CPX-8	0.39	17.18	0.85	0.00	20.77	10.23	0.00	49.39	0.73	0.46	100.0
KP14A-CPX-9	0.30	16.93	0.67	0.00	20.40	10.51	0.00	49.83	0.84	0.52	100.0
KP14A-CPX-10	0.28	17.02	0.79	0.00	20.41	10.30	0.00	49.82	0.85	0.52	100.0
Average	**0.31**	**16.99**	**0.84**	**0.00**	**20.49**	**10.50**	**0.00**	**49.56**	**0.78**	**0.52**	**100.0**
KP14B-CPX-1	0.32	18.47	1.80	0.00	11.16	13.64	0.00	53.00	1.29	0.32	100.0
KP14B-CPX-2	0.30	18.68	1.45	0.00	10.77	14.28	0.00	53.52	1.01	0.00	100.0
KP14B-CPX-3	0.24	18.47	1.86	0.00	11.26	13.71	0.00	53.30	1.16	0.00	100.0
KP14B-CPX-4	0.39	17.58	1.37	0.00	13.36	12.78	0.00	53.37	0.79	0.35	100.0
KP14B-CPX-5	0.28	18.18	2.14	0.00	11.42	13.85	0.00	52.58	1.23	0.33	100.0
KP14B-CPX-6	0.35	17.90	1.32	0.00	12.35	13.44	0.00	53.23	1.00	0.40	100.0
KP14B-CPX-7	0.29	18.09	1.68	0.00	12.35	13.28	0.00	52.75	1.25	0.31	100.0
KP14B-CPX-8	0.25	18.68	1.90	0.00	10.50	14.34	0.00	53.26	1.08	0.00	100.0
KP14B-CPX-9	0.36	19.09	2.37	0.26	9.60	14.26	0.00	52.70	1.03	0.34	100.0
Average	**0.31**	**18.35**	**1.77**	**0.03**	**11.42**	**13.73**	**0.00**	**53.08**	**1.09**	**0.23**	**100.0**
KP15-CPX-1	0.28	17.57	1.77	0.00	9.92	15.66	0.00	53.35	1.09	0.35	100.0
KP15-CPX-2	0.21	18.10	1.33	0.00	8.76	16.40	0.00	54.04	0.79	0.36	100.0
KP15-CPX-3	0.00	3.88	0.00	0.00	21.91	19.08	0.00	54.26	0.38	0.50	100.0
KP15-CPX-4	0.00	2.55	0.27	0.00	22.82	19.09	0.00	54.33	0.41	0.53	100.0
KP15-CPX-5	0.24	18.66	2.44	0.67	7.56	15.89	0.00	53.32	0.93	0.29	100.0
KP15-CPX-6	0.00	2.54	0.37	0.00	22.70	19.65	0.00	54.32	0.00	0.41	100.0
KP15-CPX-7	0.24	17.90	1.27	0.00	9.15	16.11	0.00	54.23	0.85	0.25	100.0
KP15-CPX-8	0.00	2.51	0.27	0.00	23.00	19.30	0.00	53.98	0.35	0.59	100.0
KP15-CPX-9	0.25	14.56	1.13	0.00	12.76	15.95	0.00	54.01	0.85	0.50	100.0
KP15-CPX-10	0.00	5.32	0.65	0.00	19.83	19.31	0.00	53.77	0.57	0.55	100.0
KP15-CPX-11	0.31	18.84	2.05	0.00	7.78	15.87	0.00	54.29	0.86	0.00	100.0
KP15-CPX-12	0.28	15.36	1.52	0.00	13.18	15.19	0.00	53.01	1.06	0.40	100.0
Average	**0.15**	**11.48**	**1.09**	**0.06**	**14.95**	**17.29**	**0.00**	**53.91**	**0.68**	**0.39**	**100.0**

Appendix B - CPX - Keweenaw Sample Suite

Sample	CAT SUM	Si	Al	Na	Ca	Cr	Fe	Mg	K	Ti	Mn	Total	Mg#
KP14A-CPX-1	2.36	1.93	0.03	0.03	0.73	0.00	0.69	0.61	0.00	0.02	0.01	4.05	46.9
KP14A-CPX-2	2.35	1.93	0.04	0.02	0.71	0.00	0.67	0.62	0.00	0.02	0.02	4.03	48.0
KP14A-CPX-3	2.35	1.94	0.04	0.03	0.71	0.00	0.68	0.60	0.00	0.02	0.02	4.03	46.6
KP14A-CPX-4	2.34	1.94	0.04	0.02	0.71	0.00	0.66	0.61	0.00	0.03	0.01	4.02	48.3
KP14A-CPX-6	2.34	1.93	0.05	0.02	0.69	0.00	0.66	0.64	0.00	0.03	0.02	4.03	49.1
KP14A-CPX-8	2.35	1.93	0.05	0.03	0.73	0.00	0.66	0.60	0.00	0.02	0.02	4.04	47.5
KP14A-CPX-9	2.35	1.93	0.03	0.02	0.71	0.00	0.66	0.63	0.00	0.03	0.02	4.04	48.8
KP14A-CPX-11	2.35	1.93	0.04	0.03	0.72	0.00	0.68	0.60	0.00	0.02	0.02	4.04	46.7
KP14A-CPX-12	2.35	1.95	0.03	0.02	0.71	0.00	0.67	0.61	0.00	0.02	0.02	4.03	47.9
KP14A-CPX-13	2.35	1.95	0.04	0.02	0.71	0.00	0.67	0.60	0.00	0.02	0.02	4.02	47.3
Average	**2.35**	**1.94**	**0.04**	**0.02**	**0.71**	**0.00**	**0.67**	**0.61**	**0.00**	**0.02**	**0.02**	**4.03**	**47.7**
KP14B-CPX-1	2.24	1.97	0.08	0.02	0.74	0.00	0.35	0.76	0.00	0.04	0.01	3.96	68.5
KP14B-CPX-2	2.23	1.99	0.06	0.02	0.74	0.00	0.33	0.79	0.00	0.03	0.00	3.97	70.3
KP14B-CPX-3	2.23	1.98	0.08	0.02	0.74	0.00	0.35	0.76	0.00	0.03	0.00	3.96	68.5
KP14B-CPX-4	2.25	2.00	0.06	0.03	0.71	0.00	0.42	0.71	0.00	0.02	0.01	3.96	63.0
KP14B-CPX-5	2.24	1.96	0.09	0.02	0.73	0.00	0.36	0.77	0.00	0.03	0.01	3.97	68.4
KP14B-CPX-6	2.25	1.99	0.06	0.03	0.72	0.00	0.39	0.75	0.00	0.03	0.01	3.97	66.0
KP14B-CPX-7	2.25	1.97	0.07	0.02	0.73	0.00	0.39	0.74	0.00	0.04	0.01	3.97	65.7
KP14B-CPX-8	2.23	1.97	0.08	0.02	0.74	0.00	0.33	0.79	0.00	0.03	0.00	3.96	70.9
KP14B-CPX-9	2.23	1.95	0.10	0.03	0.76	0.01	0.30	0.79	0.00	0.03	0.01	3.97	72.6
Average	**2.24**	**1.98**	**0.08**	**0.02**	**0.73**	**0.00**	**0.36**	**0.76**	**0.00**	**0.03**	**0.01**	**3.96**	**68.2**
KP15-CPX-1	2.22	1.97	0.08	0.02	0.70	0.00	0.31	0.86	0.00	0.03	0.01	3.97	73.8
KP15-CPX-2	2.21	1.99	0.06	0.01	0.71	0.00	0.27	0.90	0.00	0.02	0.01	3.97	76.9
KP15-CPX-3	2.25	2.03	0.00	0.00	0.16	0.00	0.69	1.06	0.00	0.01	0.02	3.96	60.8
KP15-CPX-4	2.25	2.03	0.01	0.00	0.10	0.00	0.71	1.06	0.00	0.01	0.02	3.95	59.9
KP15-CPX-5	2.20	1.96	0.11	0.02	0.73	0.02	0.23	0.87	0.00	0.03	0.01	3.97	78.9
KP15-CPX-6	2.24	2.03	0.02	0.00	0.10	0.00	0.71	1.09	0.00	0.00	0.01	3.96	60.7
KP15-CPX-7	2.21	1.99	0.06	0.02	0.70	0.00	0.28	0.88	0.00	0.02	0.01	3.96	75.8
KP15-CPX-8	2.25	2.02	0.01	0.00	0.10	0.00	0.72	1.08	0.00	0.01	0.02	3.96	59.9
KP15-CPX-9	2.23	2.00	0.05	0.02	0.58	0.00	0.40	0.88	0.00	0.02	0.02	3.96	69.0
KP15-CPX-10	2.24	2.00	0.03	0.00	0.21	0.00	0.62	1.07	0.00	0.02	0.02	3.97	63.4
KP15-CPX-11	2.20	1.98	0.09	0.02	0.74	0.00	0.24	0.86	0.00	0.02	0.00	3.96	78.4
KP15-CPX-12	2.24	1.98	0.07	0.02	0.61	0.00	0.41	0.84	0.00	0.03	0.01	3.97	67.3
Average	**2.23**	**2.00**	**0.05**	**0.01**	**0.45**	**0.00**	**0.46**	**0.96**	**0.00**	**0.02**	**0.01**	**3.96**	**68.7**

Appendix B - CPX - Keweenaw Sample Suite

Sample	Na2O	CaO	Al2O3	Cr2O3	FeO	MgO	K2O	SiO2	TiO2	MnO	Total
KP101-CPX-1	0.25	16.38	1.66	0.00	12.81	14.18	0.00	53.32	0.97	0.43	100.0
KP101-CPX-2	0.25	16.38	1.66	0.00	12.81	14.18	0.00	53.32	0.97	0.43	100.0
KP101-CPX-3	0.00	3.47	0.52	0.00	23.52	17.71	0.00	53.72	0.43	0.63	100.0
KP101-CPX-4	0.27	17.92	1.96	0.00	10.98	14.83	0.00	52.72	1.32	0.00	100.0
KP101-CPX-5	0.29	16.55	1.21	0.00	12.86	14.34	0.00	53.59	0.84	0.32	100.0
KP101-CPX-6	0.26	15.47	1.25	0.00	15.10	13.66	0.00	52.88	0.80	0.57	100.0
KP101-CPX-7	0.33	17.33	1.15	0.00	13.10	13.31	0.00	53.69	0.71	0.39	100.0
KP101-CPX-8	0.24	16.54	1.53	0.00	12.90	14.25	0.00	53.24	0.92	0.38	100.0
KP101-CPX-9	0.00	4.80	0.37	0.00	23.97	16.54	0.00	53.17	0.51	0.63	100.0
KP101-CPX-10	0.31	17.62	1.72	0.00	12.00	13.98	0.00	52.87	1.19	0.30	100.0
Average	**0.22**	**14.25**	**1.30**	**0.00**	**15.01**	**14.70**	**0.00**	**53.25**	**0.87**	**0.41**	**100.0**
KP108-CPX-1	0.27	18.38	1.16	0.00	13.97	14.50	0.00	50.86	0.57	0.28	100.0
KP108-CPX-2	0.00	21.91	1.83	0.00	12.64	13.61	0.00	48.66	0.95	0.40	100.0
KP108-CPX-3	0.29	19.56	1.59	0.00	15.22	12.55	0.00	49.56	0.87	0.36	100.0
KP108-CPX-4	0.41	17.89	1.34	0.00	15.14	13.88	0.00	50.05	0.92	0.36	100.0
KP108-CPX-5	0.00	21.91	1.83	0.00	12.64	13.61	0.00	48.66	0.95	0.40	100.0
KP108-CPX-6	0.21	17.75	1.83	0.00	12.62	15.85	0.00	50.24	1.14	0.36	100.0
KP108-CPX-7	0.35	18.22	1.64	0.00	11.43	15.97	0.00	50.99	1.02	0.38	100.0
KP108-CPX-8	0.29	17.77	1.34	0.00	14.75	14.32	0.00	51.20	1.21	0.00	100.9
KP108-CPX-9	0.00	3.64	0.63	0.00	20.66	19.76	0.00	54.27	0.38	0.67	100.0
KP108-CPX-10	0.23	16.57	1.51	0.00	15.64	14.30	0.00	50.48	0.95	0.33	100.0
Average	**0.21**	**17.36**	**1.47**	**0.00**	**14.47**	**14.84**	**0.00**	**50.50**	**0.90**	**0.35**	**100.1**
KP111A-CPX-1	0.38	17.15	1.27	0.00	13.53	13.47	0.00	53.32	0.88	0.00	100.0
KP111A-CPX-2	0.25	19.12	2.26	0.00	15.03	8.76	0.00	53.81	0.76	0.00	100.0
KP111A-CPX-3	0.00	18.63	1.65	0.00	15.63	9.07	0.00	54.44	0.59	0.00	100.0
KP111A-CPX-4	0.22	19.26	1.75	0.00	15.31	8.48	0.00	54.01	0.97	0.00	100.0
KP111A-CPX-5	0.26	19.16	1.73	0.00	15.32	8.42	0.00	54.19	0.64	0.29	100.0
KP111A-CPX-6	0.32	17.75	1.33	0.00	13.70	12.40	0.00	53.24	0.92	0.34	100.0
KP111A-CPX-7	0.24	18.76	2.01	0.00	15.51	8.74	0.00	53.60	0.87	0.27	100.0
KP111A-CPX-8	0.32	19.07	1.87	0.39	15.32	8.41	0.00	53.83	0.80	0.00	100.0
KP111A-CPX-9	0.35	19.05	1.70	0.00	15.14	8.77	0.00	53.83	0.87	0.29	100.0
KP111A-CPX-10	0.45	19.00	1.86	0.00	14.72	8.86	0.00	53.66	1.03	0.42	100.0
KP111A-CPX-11	0.32	19.33	1.77	0.00	15.03	8.31	0.00	54.51	0.72	0.00	100.0
KP111A-CPX-12	0.57	18.91	1.77	0.00	15.69	8.47	0.00	53.71	0.87	0.00	100.0
Average	**0.31**	**18.77**	**1.75**	**0.03**	**14.99**	**9.35**	**0.00**	**53.85**	**0.83**	**0.13**	**100.0**

Appendix B - CPX - Keweenaw Sample Suite

Sample	CAT SUM	Si	Al	Na	Ca	Cr	Fe	Mg	K	Ti	Mn	Total	Mg#
KP101-CPX-1	2.24	1.99	0.07	0.02	0.65	0.00	0.40	0.79	0.00	0.03	0.01	3.96	66.4
KP101-CPX-2	2.24	1.99	0.07	0.02	0.65	0.00	0.40	0.79	0.00	0.03	0.01	3.96	66.4
KP101-CPX-3	2.26	2.02	0.02	0.00	0.14	0.00	0.74	0.99	0.00	0.01	0.02	3.95	57.3
KP101-CPX-4	2.23	1.96	0.09	0.02	0.71	0.00	0.34	0.82	0.00	0.04	0.00	3.97	70.6
KP101-CPX-5	2.24	2.00	0.05	0.02	0.66	0.00	0.40	0.80	0.00	0.02	0.01	3.96	66.5
KP101-CPX-6	2.26	1.99	0.06	0.02	0.62	0.00	0.48	0.77	0.00	0.02	0.02	3.97	61.7
KP101-CPX-7	2.25	2.01	0.05	0.02	0.69	0.00	0.41	0.74	0.00	0.02	0.01	3.96	64.4
KP101-CPX-8	2.24	1.99	0.07	0.02	0.66	0.00	0.40	0.79	0.00	0.03	0.01	3.96	66.3
KP101-CPX-9	2.28	2.02	0.02	0.00	0.20	0.00	0.76	0.94	0.00	0.01	0.02	3.96	55.1
KP101-CPX-10	2.24	1.97	0.08	0.02	0.70	0.00	0.37	0.78	0.00	0.03	0.01	3.97	67.5
Average	**2.25**	**1.99**	**0.06**	**0.02**	**0.57**	**0.00**	**0.47**	**0.82**	**0.00**	**0.02**	**0.01**	**3.96**	**64.2**
KP108-CPX-1	2.28	1.93	0.05	0.02	0.75	0.00	0.44	0.82	0.00	0.02	0.01	4.04	64.9
KP108-CPX-2	2.30	1.86	0.08	0.00	0.90	0.00	0.40	0.78	0.00	0.03	0.01	4.07	65.7
KP108-CPX-3	2.31	1.90	0.07	0.02	0.80	0.00	0.49	0.72	0.00	0.03	0.01	4.05	59.5
KP108-CPX-4	2.30	1.91	0.06	0.03	0.73	0.00	0.48	0.79	0.00	0.03	0.01	4.05	62.0
KP108-CPX-5	2.30	1.86	0.08	0.00	0.90	0.00	0.40	0.78	0.00	0.03	0.01	4.07	65.7
KP108-CPX-6	2.27	1.89	0.08	0.02	0.72	0.00	0.40	0.89	0.00	0.03	0.01	4.04	69.1
KP108-CPX-7	2.25	1.91	0.07	0.03	0.73	0.00	0.36	0.89	0.00	0.03	0.01	4.04	71.3
KP108-CPX-8	2.26	1.92	0.06	0.02	0.72	0.00	0.46	0.80	0.00	0.03	0.00	4.02	63.4
KP108-CPX-9	2.23	2.02	0.03	0.00	0.14	0.00	0.64	1.09	0.00	0.01	0.02	3.96	63.0
KP108-CPX-10	2.29	1.92	0.07	0.02	0.68	0.00	0.50	0.81	0.00	0.03	0.01	4.03	62.0
Average	**2.28**	**1.91**	**0.07**	**0.02**	**0.71**	**0.00**	**0.46**	**0.84**	**0.00**	**0.03**	**0.01**	**4.03**	**64.7**
KP111A-CPX-1	2.25	2.00	0.06	0.03	0.69	0.00	0.42	0.75	0.00	0.02	0.00	3.97	64.0
KP111A-CPX-2	2.27	2.03	0.10	0.02	0.77	0.00	0.47	0.49	0.00	0.02	0.00	3.91	50.9
KP111A-CPX-3	2.26	2.05	0.07	0.00	0.75	0.00	0.49	0.51	0.00	0.02	0.00	3.90	50.8
KP111A-CPX-4	2.27	2.04	0.08	0.02	0.78	0.00	0.48	0.48	0.00	0.03	0.00	3.90	49.7
KP111A-CPX-5	2.27	2.05	0.08	0.02	0.78	0.00	0.48	0.47	0.00	0.02	0.01	3.91	49.5
KP111A-CPX-6	2.26	2.00	0.06	0.02	0.71	0.00	0.43	0.69	0.00	0.03	0.01	3.96	61.7
KP111A-CPX-7	2.27	2.03	0.09	0.02	0.76	0.00	0.49	0.49	0.00	0.02	0.01	3.91	50.1
KP111A-CPX-8	2.27	2.03	0.08	0.02	0.77	0.01	0.48	0.47	0.00	0.02	0.00	3.91	49.4
KP111A-CPX-9	2.27	2.04	0.08	0.03	0.77	0.00	0.48	0.49	0.00	0.02	0.01	3.92	50.8
KP111A-CPX-10	2.27	2.03	0.08	0.03	0.77	0.00	0.47	0.50	0.00	0.03	0.01	3.92	51.8
KP111A-CPX-11	2.26	2.05	0.08	0.02	0.78	0.00	0.47	0.47	0.00	0.02	0.00	3.90	49.6
KP111A-CPX-12	2.28	2.03	0.08	0.04	0.77	0.00	0.50	0.48	0.00	0.02	0.00	3.92	49.0
Average	**2.27**	**2.03**	**0.08**	**0.02**	**0.76**	**0.00**	**0.47**	**0.53**	**0.00**	**0.02**	**0.00**	**3.92**	**52.3**

Appendix B - CPX - Keweenaw Sample Suite

Sample	Na2O	CaO	Al2O3	Cr2O3	FeO	MgO	K2O	SiO2	TiO2	MnO	Total
KP111B-CPX-1	0.40	17.39	1.24	0.00	13.56	12.71	0.00	53.50	0.89	0.31	100.0
KP111B-CPX-2	0.25	18.89	1.89	0.25	8.92	15.24	0.00	53.73	0.82	0.00	100.0
KP111B-CPX-3	0.32	17.00	1.28	0.00	13.61	12.71	0.00	54.03	0.74	0.30	100.0
KP111B-CPX-4	0.33	18.53	2.17	0.00	15.29	8.90	0.00	53.89	0.90	0.00	100.0
KP111B-CPX-5	0.30	16.71	1.07	0.00	14.76	12.81	0.00	53.35	0.62	0.38	100.0
KP111B-CPX-6	0.29	18.09	3.01	0.00	14.10	10.41	0.00	52.79	1.31	0.00	100.0
KP111B-CPX-7	0.21	18.97	1.77	0.22	15.07	8.51	0.00	54.07	0.90	0.27	100.0
KP111B-CPX-8	0.43	16.51	10.68	0.00	11.11	11.23	0.00	48.79	0.88	0.37	100.0
KP111B-CPX-9	0.26	19.20	2.53	0.00	8.48	14.99	0.00	53.31	0.96	0.27	100.0
Average	**0.31**	**17.92**	**2.85**	**0.05**	**12.77**	**11.95**	**0.00**	**53.05**	**0.89**	**0.21**	**100.0**
KP111C-CPX-1	0.42	18.62	1.74	0.00	10.65	14.12	0.00	53.34	1.12	0.00	100.0
KP111C-CPX-2	0.34	18.58	1.52	0.00	10.63	14.18	0.00	53.36	0.97	0.42	100.0
KP111C-CPX-3	0.16	19.14	1.73	0.00	9.09	14.90	0.00	54.00	0.68	0.29	100.0
KP111C-CPX-4	0.25	18.97	1.92	0.00	9.37	14.80	0.00	53.85	0.84	0.00	100.0
KP111C-CPX-5	0.51	17.72	1.58	0.00	11.97	14.00	0.00	52.83	1.06	0.33	100.0
KP111C-CPX-6	0.33	16.62	1.40	0.00	14.07	13.17	0.00	53.05	0.95	0.42	100.0
KP111C-CPX-7	0.20	18.72	1.71	0.31	10.56	14.20	0.00	53.12	0.92	0.25	100.0
KP111C-CPX-8	0.55	17.61	1.42	0.00	12.40	13.71	0.00	53.00	0.91	0.40	100.0
Average	**0.35**	**18.25**	**1.63**	**0.04**	**11.09**	**14.14**	**0.00**	**53.32**	**0.93**	**0.26**	**100.0**
KP114-CPX-1	0.20	18.41	1.36	0.00	13.35	14.49	0.00	50.82	0.84	0.54	100.0
KP114-CPX-2	0.29	18.99	1.59	0.00	12.10	14.84	0.00	50.49	1.28	0.42	100.0
KP114-CPX-3	0.29	18.41	1.49	0.00	13.05	15.12	0.00	50.43	1.20	0.00	100.0
KP114-CPX-4	0.30	17.07	1.36	0.00	15.42	14.43	0.00	50.11	0.94	0.36	100.0
KP114-CPX-5	0.00	17.63	1.37	0.00	14.86	14.37	0.00	50.34	0.97	0.47	100.0
KP114-CPX-6	0.29	18.20	1.40	0.00	13.71	14.99	0.00	50.50	0.91	0.00	100.0
KP114-CPX-7	0.29	18.58	1.71	0.00	12.85	14.61	0.00	50.54	1.42	0.00	100.0
KP114-CPX-8	0.30	18.25	1.84	0.00	13.59	14.43	0.00	50.29	1.29	0.00	100.0
Average	**0.25**	**18.19**	**1.52**	**0.00**	**13.62**	**14.66**	**0.00**	**50.44**	**1.11**	**0.22**	**100.0**

Appendix B - CPX - Keweenaw Sample Suite

Sample	CAT SUM	Si	Al	Na	Ca	Cr	Fe	Mg	K	Ti	Mn	Total	Mg#
KP111B-CPX-1	2.25	2.01	0.05	0.03	0.70	0.00	0.43	0.71	0.00	0.03	0.01	3.96	62.6
KP111B-CPX-2	2.21	1.98	0.08	0.02	0.75	0.01	0.27	0.84	0.00	0.02	0.00	3.96	75.3
KP111B-CPX-3	2.25	2.02	0.06	0.02	0.68	0.00	0.43	0.71	0.00	0.02	0.01	3.94	62.5
KP111B-CPX-4	2.26	2.03	0.10	0.02	0.75	0.00	0.48	0.50	0.00	0.03	0.00	3.91	50.9
KP111B-CPX-5	2.26	2.01	0.05	0.02	0.67	0.00	0.46	0.72	0.00	0.02	0.01	3.96	60.7
KP111B-CPX-6	2.26	1.98	0.13	0.02	0.73	0.00	0.44	0.58	0.00	0.04	0.00	3.93	56.8
KP111B-CPX-7	2.27	2.04	0.08	0.02	0.77	0.01	0.48	0.48	0.00	0.03	0.01	3.90	50.2
KP111B-CPX-8	2.22	1.80	0.47	0.03	0.65	0.00	0.34	0.62	0.00	0.02	0.01	3.95	64.3
KP111B-CPX-9	2.21	1.96	0.11	0.02	0.76	0.00	0.26	0.82	0.00	0.03	0.01	3.97	75.9
Average	**2.24**	**1.98**	**0.12**	**0.02**	**0.72**	**0.00**	**0.40**	**0.66**	**0.00**	**0.03**	**0.01**	**3.94**	**62.1**
KP111C-CPX-1	2.23	1.98	0.08	0.03	0.74	0.00	0.33	0.78	0.00	0.03	0.00	3.97	70.3
KP111C-CPX-2	2.23	1.98	0.07	0.02	0.74	0.00	0.33	0.79	0.00	0.03	0.01	3.97	70.4
KP111C-CPX-3	2.21	1.99	0.08	0.01	0.76	0.00	0.28	0.82	0.00	0.02	0.01	3.96	74.5
KP111C-CPX-4	2.21	1.98	0.08	0.02	0.75	0.00	0.29	0.81	0.00	0.02	0.00	3.96	73.8
KP111C-CPX-5	2.24	1.97	0.07	0.04	0.71	0.00	0.37	0.78	0.00	0.03	0.01	3.98	67.6
KP111C-CPX-6	2.26	1.99	0.06	0.02	0.67	0.00	0.44	0.74	0.00	0.03	0.01	3.96	62.5
KP111C-CPX-7	2.23	1.97	0.07	0.01	0.75	0.01	0.33	0.79	0.00	0.03	0.01	3.97	70.6
KP111C-CPX-8	2.25	1.98	0.06	0.04	0.71	0.00	0.39	0.76	0.00	0.03	0.01	3.98	66.3
Average	**2.23**	**1.98**	**0.07**	**0.02**	**0.73**	**0.00**	**0.35**	**0.78**	**0.00**	**0.03**	**0.01**	**3.97**	**69.5**
KP114-CPX-1	2.28	1.92	0.06	0.01	0.75	0.00	0.42	0.82	0.00	0.02	0.02	4.03	65.9
KP114-CPX-2	2.27	1.91	0.07	0.02	0.77	0.00	0.38	0.83	0.00	0.04	0.01	4.03	68.6
KP114-CPX-3	2.27	1.91	0.07	0.02	0.75	0.00	0.41	0.85	0.00	0.03	0.00	4.04	67.4
KP114-CPX-4	2.29	1.91	0.06	0.02	0.70	0.00	0.49	0.82	0.00	0.03	0.01	4.04	62.5
KP114-CPX-5	2.29	1.92	0.06	0.00	0.72	0.00	0.47	0.81	0.00	0.03	0.02	4.03	63.3
KP114-CPX-6	2.28	1.91	0.06	0.02	0.74	0.00	0.43	0.85	0.00	0.03	0.00	4.04	66.1
KP114-CPX-7	2.27	1.91	0.08	0.02	0.75	0.00	0.41	0.82	0.00	0.04	0.00	4.02	67.0
KP114-CPX-8	2.27	1.90	0.08	0.02	0.74	0.00	0.43	0.81	0.00	0.04	0.00	4.03	65.4
Average	**2.28**	**1.91**	**0.07**	**0.02**	**0.74**	**0.00**	**0.43**	**0.83**	**0.00**	**0.03**	**0.01**	**4.03**	**65.8**

Appendix B - CPX - Isle Royale Sample Suite

Sample	Na2O	CaO	Al2O3	Cr2O3	FeO	MgO	K2O	SiO2	TiO2	MnO	Total
IR1-CPX-1	0.28	18.26	2.36	0.61	15.67	8.43	0.00	53.52	0.87	0.00	100.0
IR1-CPX-2	0.00	17.98	1.47	0.00	12.38	13.59	0.00	53.06	1.09	0.42	100.0
IR1-CPX-3	0.20	18.85	1.49	0.00	14.67	9.89	0.00	54.07	0.83	0.00	100.0
IR1-CPX-4	0.32	18.43	1.62	0.00	14.20	10.82	0.00	53.82	0.79	0.00	100.0
IR1-CPX-5	0.23	19.11	1.44	0.29	15.82	8.20	0.00	54.20	0.70	0.00	100.0
IR1-CPX-6	0.27	19.02	1.61	0.00	14.67	9.77	0.00	53.87	0.79	0.00	100.0
IR1-CPX-7	0.30	18.11	1.26	0.00	12.63	12.89	0.00	53.25	1.04	0.52	100.0
IR1-CPX-8	0.46	18.89	1.96	0.00	15.22	9.11	0.00	53.34	1.03	0.00	100.0
IR1-CPX-9	0.26	18.81	1.55	0.00	14.68	9.72	0.00	53.89	0.70	0.38	100.0
IR1-CPX-10	0.28	16.96	0.91	0.00	15.69	12.41	0.00	52.63	0.70	0.41	100.0
Average	**0.26**	**18.44**	**1.57**	**0.09**	**14.56**	**10.48**	**0.00**	**53.57**	**0.85**	**0.17**	**100.0**
IR3-CPX-1	0.27	17.60	1.35	0.00	12.76	13.62	0.00	53.21	0.93	0.26	100.0
IR3-CPX-2	0.42	17.54	1.56	0.00	12.18	13.78	0.00	53.08	1.11	0.33	100.0
IR3-CPX-3	0.42	17.54	1.56	0.00	12.18	13.78	0.00	53.08	1.11	0.33	100.0
IR3-CPX-4	0.33	17.54	1.45	0.00	12.65	13.69	0.00	52.97	1.05	0.32	100.0
IR3-CPX-5	0.30	17.34	1.17	0.00	13.80	12.94	0.00	53.71	0.75	0.00	100.0
IR3-CPX-6	0.30	17.83	1.45	0.00	12.04	13.91	0.00	53.20	0.96	0.30	100.0
IR3-CPX-7	0.28	17.23	1.39	0.00	12.88	13.73	0.00	53.37	0.88	0.25	100.0
IR3-CPX-8	0.31	17.62	1.44	0.00	12.32	13.72	0.00	53.29	0.96	0.35	100.0
IR3-CPX-9	0.25	18.58	1.79	0.00	14.71	10.13	0.13	53.33	0.79	0.29	100.0
IR3-CPX-10	0.24	18.19	1.73	0.00	15.00	9.95	0.00	54.06	0.82	0.00	100.0
Average	**0.31**	**17.70**	**1.49**	**0.00**	**13.05**	**12.93**	**0.01**	**53.33**	**0.94**	**0.24**	**100.0**
IR6-CPX-1	0.29	17.59	1.86	0.00	12.08	14.09	0.00	53.04	1.06	0.00	100.0
IR6-CPX-2	0.29	18.07	1.54	0.00	12.22	13.40	0.00	52.98	1.19	0.32	100.0
IR6-CPX-3	0.33	17.70	1.94	0.00	14.06	11.68	0.00	53.06	1.23	0.00	100.0
IR6-CPX-4	0.22	18.76	2.04	0.00	13.77	11.14	0.00	53.05	1.02	0.00	100.0
IR6-CPX-5	0.27	17.33	1.21	0.00	13.93	12.90	0.00	52.99	0.93	0.44	100.0
IR6-CPX-6	0.29	17.97	1.50	0.00	14.23	11.26	0.00	53.67	0.78	0.00	99.7
IR6-CPX-7	0.21	16.74	1.08	0.00	14.40	13.08	0.00	53.19	0.79	0.51	100.0
IR6-CPX-8	0.21	16.43	0.98	0.00	16.50	12.04	0.00	52.69	0.76	0.39	100.0
IR6-CPX-9	0.22	17.37	1.08	0.00	14.63	12.56	0.00	53.01	0.86	0.27	100.0
IR6-CPX-10	0.16	16.61	0.87	0.00	15.73	12.38	0.00	52.96	0.75	0.53	100.0
Average	**0.25**	**17.46**	**1.41**	**0.00**	**14.16**	**12.45**	**0.00**	**53.06**	**0.94**	**0.25**	**100.0**

Appendix B - CPX - Isle Royale Sample Suite

Sample	CAT SUM	Si	Al	Na	Ca	Cr	Fe	Mg	K	Ti	Mn	Total	Mg#
IR1-CPX-1	2.27	2.02	0.11	0.02	0.74	0.02	0.50	0.47	0.00	0.02	0.00	3.90	48.9
IR1-CPX-2	2.25	1.98	0.06	0.00	0.72	0.00	0.39	0.76	0.00	0.03	0.01	3.95	66.2
IR1-CPX-3	2.26	2.03	0.07	0.01	0.76	0.00	0.46	0.55	0.00	0.02	0.00	3.92	54.6
IR1-CPX-4	2.26	2.02	0.07	0.02	0.74	0.00	0.45	0.61	0.00	0.02	0.00	3.93	57.6
IR1-CPX-5	2.27	2.05	0.06	0.02	0.78	0.01	0.50	0.46	0.00	0.02	0.00	3.90	48.0
IR1-CPX-6	2.26	2.03	0.07	0.02	0.77	0.00	0.46	0.55	0.00	0.02	0.00	3.92	54.3
IR1-CPX-7	2.25	1.99	0.06	0.02	0.73	0.00	0.40	0.72	0.00	0.03	0.02	3.96	64.5
IR1-CPX-8	2.27	2.02	0.09	0.03	0.77	0.00	0.48	0.51	0.00	0.03	0.00	3.93	51.6
IR1-CPX-9	2.27	2.03	0.07	0.02	0.76	0.00	0.46	0.55	0.00	0.02	0.01	3.92	54.1
IR1-CPX-10	2.28	1.99	0.04	0.02	0.69	0.00	0.50	0.70	0.00	0.02	0.01	3.98	58.5
Average	**2.26**	**2.02**	**0.07**	**0.02**	**0.74**	**0.00**	**0.46**	**0.59**	**0.00**	**0.02**	**0.01**	**3.93**	**55.8**
IR3-CPX-1	2.25	1.99	0.06	0.02	0.70	0.00	0.40	0.76	0.00	0.03	0.01	3.96	65.5
IR3-CPX-2	2.24	1.98	0.07	0.03	0.70	0.00	0.38	0.77	0.00	0.03	0.01	3.97	66.8
IR3-CPX-3	2.24	1.98	0.07	0.03	0.70	0.00	0.38	0.77	0.00	0.03	0.01	3.97	66.8
IR3-CPX-4	2.25	1.98	0.06	0.02	0.70	0.00	0.40	0.76	0.00	0.03	0.01	3.97	65.9
IR3-CPX-5	2.25	2.01	0.05	0.02	0.70	0.00	0.43	0.72	0.00	0.02	0.00	3.95	62.6
IR3-CPX-6	2.24	1.98	0.06	0.02	0.71	0.00	0.38	0.77	0.00	0.03	0.01	3.97	67.3
IR3-CPX-7	2.24	1.99	0.06	0.02	0.69	0.00	0.40	0.76	0.00	0.02	0.01	3.96	65.5
IR3-CPX-8	2.24	1.99	0.06	0.02	0.70	0.00	0.38	0.76	0.00	0.03	0.01	3.96	66.5
IR3-CPX-9	2.27	2.01	0.08	0.02	0.75	0.00	0.46	0.57	0.01	0.02	0.01	3.94	55.1
IR3-CPX-10	2.26	2.03	0.08	0.02	0.73	0.00	0.47	0.56	0.00	0.02	0.00	3.91	54.2
Average	**2.25**	**2.00**	**0.07**	**0.02**	**0.71**	**0.00**	**0.41**	**0.72**	**0.00**	**0.03**	**0.01**	**3.96**	**63.6**
IR6-CPX-1	2.24	1.97	0.08	0.02	0.70	0.00	0.38	0.78	0.00	0.03	0.00	3.97	67.5
IR6-CPX-2	2.25	1.98	0.07	0.02	0.72	0.00	0.38	0.75	0.00	0.03	0.01	3.96	66.1
IR6-CPX-3	2.26	1.99	0.09	0.02	0.71	0.00	0.44	0.65	0.00	0.03	0.00	3.94	59.7
IR6-CPX-4	2.26	1.99	0.09	0.02	0.76	0.00	0.43	0.62	0.00	0.03	0.00	3.94	59.0
IR6-CPX-5	2.26	1.99	0.05	0.02	0.70	0.00	0.44	0.72	0.00	0.03	0.01	3.96	62.3
IR6-CPX-6	2.26	2.02	0.07	0.02	0.72	0.00	0.45	0.63	0.00	0.02	0.00	3.93	58.5
IR6-CPX-7	2.26	2.00	0.05	0.02	0.67	0.00	0.45	0.73	0.00	0.02	0.02	3.96	61.8
IR6-CPX-8	2.28	2.00	0.04	0.02	0.67	0.00	0.52	0.68	0.00	0.02	0.01	3.96	56.5
IR6-CPX-9	2.26	2.00	0.05	0.02	0.70	0.00	0.46	0.71	0.00	0.02	0.01	3.96	60.5
IR6-CPX-10	2.27	2.00	0.04	0.01	0.67	0.00	0.50	0.70	0.00	0.02	0.02	3.96	58.4
Average	**2.26**	**2.00**	**0.06**	**0.02**	**0.70**	**0.00**	**0.45**	**0.70**	**0.00**	**0.03**	**0.01**	**3.96**	**61.0**

Appendix B - CPX - Isle Royale Sample Suite

Sample	Na2O	CaO	Al2O3	Cr2O3	FeO	MgO	K2O	SiO2	TiO2	MnO	Total
IR7A-CPX-1	0.28	17.51	1.27	0.00	13.02	13.37	0.00	53.27	0.91	0.37	100.0
IR7A-CPX-2	0.19	18.61	1.49	0.00	14.50	10.59	0.00	53.58	0.80	0.24	100.0
IR7A-CPX-3	0.28	15.68	1.17	0.00	16.34	12.58	0.00	52.61	0.89	0.45	100.0
IR7A-CPX-4	0.35	16.30	1.15	0.00	15.49	12.48	0.00	52.62	1.14	0.47	100.0
IR7A-CPX-5	0.25	17.56	1.43	0.00	13.39	13.26	0.00	52.72	1.15	0.24	100.0
IR7A-CPX-6	0.35	17.06	0.96	0.00	15.13	12.49	0.00	53.20	0.82	0.00	100.0
IR7A-CPX-7	0.23	17.16	1.12	0.00	14.07	12.61	0.00	53.40	0.93	0.49	100.0
IR7A-CPX-8	0.44	17.35	1.73	0.00	13.48	12.77	0.00	52.68	1.23	0.32	100.0
IR7A-CPX-9	0.24	18.48	1.60	0.00	10.05	14.84	0.00	53.38	0.93	0.45	100.0
Average	**0.29**	**17.30**	**1.32**	**0.00**	**13.94**	**12.78**	**0.00**	**53.05**	**0.98**	**0.34**	**100.0**
IR7B-CPX-1	0.33	16.60	1.46	0.00	12.48	14.76	0.00	53.39	0.98	0.00	100.0
IR7B-CPX-2	0.17	18.78	1.89	0.00	8.10	16.03	0.00	54.37	0.65	0.00	100.0
IR7B-CPX-3	0.25	18.69	2.19	0.41	7.49	15.86	0.00	54.33	0.79	0.00	100.0
IR7B-CPX-4	0.23	17.07	1.51	0.00	10.99	15.48	0.00	53.79	0.94	0.00	100.0
IR7B-CPX-5	0.20	18.32	1.83	0.00	9.93	15.36	0.00	53.03	0.97	0.35	100.0
IR7B-CPX-6	0.29	17.43	1.82	0.00	10.05	15.83	0.00	53.56	1.03	0.00	100.0
IR7B-CPX-7	0.16	17.61	1.57	0.00	10.31	15.45	0.00	53.50	1.06	0.33	100.0
IR7B-CPX-8	0.25	18.25	1.32	0.00	8.57	16.21	0.00	54.44	0.66	0.30	100.0
Average	**0.24**	**17.84**	**1.70**	**0.05**	**9.74**	**15.62**	**0.00**	**53.80**	**0.89**	**0.12**	**100.0**
IR7C-CPX-1	0.00	17.93	0.75	0.00	20.40	9.88	0.00	49.77	0.71	0.56	100.0
IR7C-CPX-2	0.27	17.29	0.82	0.00	20.82	9.69	0.00	49.52	0.86	0.72	100.0
IR7C-CPX-3	0.34	17.56	0.90	0.00	18.51	11.28	0.00	49.87	0.93	0.62	100.0
IR7C-CPX-4	0.33	17.51	0.66	0.00	23.55	7.63	0.00	48.77	0.88	0.66	100.0
IR7C-CPX-5	0.28	18.19	0.85	0.00	24.55	6.96	0.00	47.82	0.69	0.67	100.0
IR7C-CPX-6	0.21	17.90	0.75	0.00	25.36	6.26	0.00	47.94	0.86	0.71	100.0
IR7C-CPX-7	0.24	17.59	0.81	0.00	24.96	6.44	0.00	48.41	0.83	0.73	100.0
IR7C-CPX-8	0.44	16.80	1.27	0.00	17.58	12.65	0.00	49.95	0.84	0.47	100.0
IR7C-CPX-9	0.00	17.10	0.99	0.00	20.12	10.28	0.00	50.00	0.83	0.67	100.0
IR7C-CPX-10	0.25	17.70	0.99	0.00	20.90	9.69	0.00	49.27	0.69	0.51	100.0
IR7C-CPX-11	0.00	18.33	0.73	0.00	22.52	8.69	0.00	48.32	0.82	0.60	100.0
IR7C-CPX-12	0.24	18.42	0.94	0.00	21.90	8.51	0.00	48.75	0.85	0.39	100.0
IR7C-CPX-13	0.30	17.09	0.85	0.00	19.83	10.92	0.00	49.76	0.82	0.43	100.0
Average	**0.22**	**17.65**	**0.87**	**0.00**	**21.62**	**9.14**	**0.00**	**49.09**	**0.82**	**0.60**	**100.0**

Appendix B - CPX - Isle Royale Sample Suite

Sample	CAT SUM	Si	Al	Na	Ca	Cr	Fe	Mg	K	Ti	Mn	Total	Mg#
IR7A-CPX-1	2.25	1.99	0.06	0.02	0.70	0.00	0.41	0.75	0.00	0.03	0.01	3.96	64.7
IR7A-CPX-2	2.26	2.02	0.07	0.01	0.75	0.00	0.46	0.59	0.00	0.02	0.01	3.93	56.5
IR7A-CPX-3	2.27	1.99	0.05	0.02	0.64	0.00	0.52	0.71	0.00	0.03	0.01	3.97	57.8
IR7A-CPX-4	2.27	1.99	0.05	0.03	0.66	0.00	0.49	0.70	0.00	0.03	0.02	3.97	58.9
IR7A-CPX-5	2.25	1.98	0.06	0.02	0.71	0.00	0.42	0.74	0.00	0.03	0.01	3.97	63.8
IR7A-CPX-6	2.26	2.00	0.04	0.03	0.69	0.00	0.48	0.70	0.00	0.02	0.00	3.96	59.5
IR7A-CPX-7	2.26	2.01	0.05	0.02	0.69	0.00	0.44	0.71	0.00	0.03	0.02	3.95	61.5
IR7A-CPX-8	2.26	1.98	0.08	0.03	0.70	0.00	0.42	0.71	0.00	0.03	0.01	3.97	62.8
IR7A-CPX-9	2.23	1.98	0.07	0.02	0.73	0.00	0.31	0.82	0.00	0.03	0.01	3.97	72.5
Average	**2.26**	**1.99**	**0.06**	**0.02**	**0.70**	**0.00**	**0.44**	**0.72**	**0.00**	**0.03**	**0.01**	**3.96**	**62.0**
IR7B-CPX-1	2.23	1.99	0.06	0.02	0.66	0.00	0.39	0.82	0.00	0.03	0.00	3.97	67.8
IR7B-CPX-2	2.20	1.99	0.08	0.01	0.74	0.00	0.25	0.87	0.00	0.02	0.00	3.96	77.9
IR7B-CPX-3	2.19	1.98	0.09	0.02	0.73	0.01	0.23	0.86	0.00	0.02	0.00	3.95	79.1
IR7B-CPX-4	2.22	1.99	0.07	0.02	0.68	0.00	0.34	0.85	0.00	0.03	0.00	3.96	71.5
IR7B-CPX-5	2.22	1.96	0.08	0.01	0.73	0.00	0.31	0.85	0.00	0.03	0.01	3.98	73.4
IR7B-CPX-6	2.21	1.97	0.08	0.02	0.69	0.00	0.31	0.87	0.00	0.03	0.00	3.97	73.7
IR7B-CPX-7	2.22	1.98	0.07	0.01	0.70	0.00	0.32	0.85	0.00	0.03	0.01	3.96	72.8
IR7B-CPX-8	2.20	2.00	0.06	0.02	0.72	0.00	0.26	0.89	0.00	0.02	0.01	3.97	77.1
Average	**2.21**	**1.98**	**0.07**	**0.02**	**0.70**	**0.00**	**0.30**	**0.86**	**0.00**	**0.02**	**0.00**	**3.96**	**74.2**
IR7C-CPX-1	2.35	1.95	0.03	0.00	0.75	0.00	0.67	0.58	0.00	0.02	0.02	4.02	46.3
IR7C-CPX-2	2.36	1.94	0.04	0.02	0.73	0.00	0.68	0.57	0.00	0.03	0.02	4.02	45.3
IR7C-CPX-3	2.33	1.93	0.04	0.03	0.73	0.00	0.60	0.65	0.00	0.03	0.02	4.03	52.1
IR7C-CPX-4	2.39	1.94	0.03	0.03	0.75	0.00	0.78	0.45	0.00	0.03	0.02	4.03	36.6
IR7C-CPX-5	2.41	1.92	0.04	0.02	0.78	0.00	0.82	0.42	0.00	0.02	0.02	4.05	33.6
IR7C-CPX-6	2.42	1.93	0.04	0.02	0.77	0.00	0.85	0.38	0.00	0.03	0.02	4.03	30.5
IR7C-CPX-7	2.41	1.94	0.04	0.02	0.76	0.00	0.84	0.38	0.00	0.03	0.02	4.02	31.5
IR7C-CPX-8	2.31	1.92	0.06	0.03	0.69	0.00	0.57	0.73	0.00	0.02	0.02	4.04	56.2
IR7C-CPX-9	2.34	1.95	0.05	0.00	0.71	0.00	0.66	0.60	0.00	0.02	0.02	4.01	47.7
IR7C-CPX-10	2.36	1.93	0.05	0.02	0.74	0.00	0.69	0.57	0.00	0.02	0.02	4.03	45.2
IR7C-CPX-11	2.39	1.92	0.03	0.00	0.78	0.00	0.75	0.51	0.00	0.02	0.02	4.04	40.7
IR7C-CPX-12	2.38	1.93	0.04	0.02	0.78	0.00	0.72	0.50	0.00	0.03	0.01	4.03	40.9
IR7C-CPX-13	2.34	1.94	0.04	0.02	0.71	0.00	0.65	0.63	0.00	0.02	0.01	4.03	49.5
Average	**2.37**	**1.93**	**0.04**	**0.02**	**0.75**	**0.00**	**0.71**	**0.54**	**0.00**	**0.02**	**0.02**	**4.03**	**42.8**

Appendix B - CPX - Isle Royale Sample Suite

Sample	Na2O	CaO	Al2O3	Cr2O3	FeO	MgO	K2O	SiO2	TiO2	MnO	Total
IR12-CPX-1	0.29	17.57	2.10	0.00	10.05	15.04	0.00	53.26	1.33	0.37	100.0
IR12-CPX-2	0.33	17.66	1.20	0.00	9.07	16.10	0.00	55.05	0.58	0.00	100.0
IR12-CPX-3	0.43	17.44	1.76	0.00	11.18	14.54	0.00	53.27	1.39	0.00	100.0
IR12-CPX-4	0.19	13.74	0.81	0.00	13.04	16.65	0.00	54.52	0.72	0.33	100.0
IR12-CPX-5	0.00	12.76	0.82	0.00	14.07	17.24	0.00	54.09	0.68	0.35	100.0
IR12-CPX-6	0.35	16.70	1.72	0.00	12.29	14.56	0.00	53.23	1.15	0.00	100.0
IR12-CPX-7	0.31	16.64	1.28	0.00	10.57	15.86	0.00	54.20	0.84	0.29	100.0
Average	**0.27**	**16.07**	**1.38**	**0.00**	**11.47**	**15.71**	**0.00**	**53.95**	**0.96**	**0.19**	**100.0**
IR15-CPX-1	0.27	18.05	1.63	0.00	9.62	15.46	0.00	53.78	0.85	0.34	100.0
IR15-CPX-2	0.30	17.84	2.34	0.66	7.68	16.39	0.00	54.03	0.76	0.00	100.0
IR15-CPX-3	0.28	16.80	1.28	0.00	11.87	14.72	0.00	53.75	0.94	0.36	100.0
IR15-CPX-4	0.33	17.23	1.75	0.00	10.92	15.30	0.00	53.47	1.02	0.00	100.0
IR15-CPX-5	0.38	16.97	1.61	0.00	11.22	15.03	0.00	53.44	1.09	0.27	100.0
IR15-CPX-6	0.37	17.59	1.63	0.00	11.13	14.86	0.00	53.10	0.97	0.34	100.0
IR15-CPX-7	0.22	18.50	1.41	0.00	8.36	16.08	0.00	54.76	0.66	0.00	100.0
IR15-CPX-8	0.33	18.29	1.92	0.00	8.78	15.83	0.00	53.86	0.75	0.25	100.0
IR15-CPX-9	0.33	18.80	2.21	0.63	7.30	16.18	0.00	53.81	0.74	0.00	100.0
IR15-CPX-10	0.36	16.95	1.70	0.00	11.38	15.09	0.00	52.99	1.13	0.40	100.0
Average	**0.32**	**17.70**	**1.75**	**0.13**	**9.83**	**15.49**	**0.00**	**53.70**	**0.89**	**0.20**	**100.0**
IR16-CPX-1	0.31	18.33	1.65	0.00	12.99	12.35	0.00	53.41	0.97	0.00	100.0
IR16-CPX-2	0.27	18.77	1.59	0.00	13.70	10.16	0.00	54.59	0.64	0.28	100.0
IR16-CPX-3	0.34	18.11	1.64	0.00	11.36	13.83	0.00	53.25	1.06	0.40	100.0
IR16-CPX-4	0.20	17.25	1.42	0.00	13.50	13.21	0.00	53.33	0.79	0.29	100.0
IR16-CPX-5	0.21	17.22	1.31	0.00	14.00	12.66	0.00	53.26	1.02	0.32	100.0
IR16-CPX-6	0.27	17.19	1.23	0.00	14.86	12.70	0.00	52.69	0.81	0.26	100.0
Average	**0.27**	**17.81**	**1.47**	**0.00**	**13.40**	**12.49**	**0.00**	**53.42**	**0.88**	**0.26**	**100.0**
IR17-CPX-1	0.24	17.30	0.81	0.00	22.69	8.79	0.00	48.69	0.91	0.56	100.0
IR17-CPX-2	0.26	17.93	0.83	0.00	23.04	7.79	0.00	48.87	0.78	0.50	100.0
IR17-CPX-3	0.25	17.52	0.64	0.00	22.33	8.53	0.00	49.27	0.84	0.62	100.0
IR17-CPX-4	0.21	17.32	0.94	0.00	20.13	11.01	0.00	49.34	0.78	0.28	100.0
IR17-CPX-5	0.29	17.69	0.84	0.00	23.12	7.77	0.00	49.01	0.77	0.51	100.0
IR17-CPX-6	0.00	17.87	0.68	0.00	23.86	7.64	0.00	48.72	0.79	0.43	100.0
IR17-CPX-7	0.00	17.77	0.68	0.00	23.75	7.93	0.00	48.62	0.81	0.44	100.0
IR17-CPX-8	0.29	18.20	0.82	0.00	24.51	6.31	0.00	48.73	0.66	0.47	100.0

Appendix B - CPX - Isle Royale Sample Suite

Sample	CAT SUM	Si	Al	Na	Ca	Cr	Fe	Mg	K	Ti	Mn	Total	Mg#
IR12-CPX-1	2.22	1.97	0.09	0.02	0.70	0.00	0.31	0.83	0.00	0.04	0.01	3.96	72.7
IR12-CPX-2	2.20	2.02	0.05	0.02	0.69	0.00	0.28	0.88	0.00	0.02	0.00	3.95	76.0
IR12-CPX-3	2.23	1.97	0.08	0.03	0.69	0.00	0.35	0.80	0.00	0.04	0.00	3.96	69.9
IR12-CPX-4	2.22	2.01	0.04	0.01	0.54	0.00	0.40	0.92	0.00	0.02	0.01	3.96	69.5
IR12-CPX-5	2.22	2.00	0.04	0.00	0.51	0.00	0.44	0.95	0.00	0.02	0.01	3.96	68.6
IR12-CPX-6	2.23	1.98	0.08	0.03	0.67	0.00	0.38	0.81	0.00	0.03	0.00	3.96	67.9
IR12-CPX-7	2.21	2.00	0.06	0.02	0.66	0.00	0.33	0.87	0.00	0.02	0.01	3.96	72.8
Average	**2.22**	**1.99**	**0.06**	**0.02**	**0.64**	**0.00**	**0.35**	**0.86**	**0.00**	**0.03**	**0.01**	**3.96**	**71.0**
IR15-CPX-1	2.22	1.98	0.07	0.02	0.71	0.00	0.30	0.85	0.00	0.02	0.01	3.97	74.1
IR15-CPX-2	2.19	1.97	0.10	0.02	0.70	0.02	0.23	0.89	0.00	0.02	0.00	3.96	79.2
IR15-CPX-3	2.23	2.00	0.06	0.02	0.67	0.00	0.37	0.81	0.00	0.03	0.01	3.96	68.8
IR15-CPX-4	2.22	1.98	0.08	0.02	0.68	0.00	0.34	0.84	0.00	0.03	0.00	3.97	71.4
IR15-CPX-5	2.23	1.98	0.07	0.03	0.67	0.00	0.35	0.83	0.00	0.03	0.01	3.97	70.5
IR15-CPX-6	2.23	1.97	0.07	0.03	0.70	0.00	0.35	0.82	0.00	0.03	0.01	3.98	70.4
IR15-CPX-7	2.20	2.00	0.06	0.02	0.73	0.00	0.26	0.88	0.00	0.02	0.00	3.96	77.4
IR15-CPX-8	2.21	1.98	0.08	0.02	0.72	0.00	0.27	0.87	0.00	0.02	0.01	3.97	76.3
IR15-CPX-9	2.20	1.97	0.10	0.02	0.74	0.02	0.22	0.88	0.00	0.02	0.00	3.97	79.8
IR15-CPX-10	2.23	1.97	0.07	0.03	0.67	0.00	0.35	0.84	0.00	0.03	0.01	3.98	70.3
Average	**2.22**	**1.98**	**0.08**	**0.02**	**0.70**	**0.00**	**0.30**	**0.85**	**0.00**	**0.02**	**0.01**	**3.97**	**73.8**
IR16-CPX-1	2.25	2.00	0.07	0.02	0.73	0.00	0.41	0.69	0.00	0.03	0.00	3.95	62.9
IR16-CPX-2	2.25	2.05	0.07	0.02	0.75	0.00	0.43	0.57	0.00	0.02	0.01	3.91	56.9
IR16-CPX-3	2.24	1.98	0.07	0.02	0.72	0.00	0.35	0.77	0.00	0.03	0.01	3.96	68.4
IR16-CPX-4	2.25	2.00	0.06	0.01	0.69	0.00	0.42	0.74	0.00	0.02	0.01	3.96	63.6
IR16-CPX-5	2.26	2.00	0.06	0.02	0.69	0.00	0.44	0.71	0.00	0.03	0.01	3.95	61.7
IR16-CPX-6	2.27	1.99	0.05	0.02	0.69	0.00	0.47	0.71	0.00	0.02	0.01	3.97	60.4
Average	**2.25**	**2.00**	**0.07**	**0.02**	**0.71**	**0.00**	**0.42**	**0.70**	**0.00**	**0.02**	**0.01**	**3.95**	**62.3**
IR17-CPX-1	2.38	1.93	0.04	0.02	0.73	0.00	0.75	0.52	0.00	0.03	0.02	4.03	40.8
IR17-CPX-2	2.39	1.94	0.04	0.02	0.76	0.00	0.76	0.46	0.00	0.02	0.02	4.03	37.6
IR17-CPX-3	2.37	1.95	0.03	0.02	0.74	0.00	0.74	0.50	0.00	0.02	0.02	4.02	40.5
IR17-CPX-4	2.34	1.93	0.04	0.02	0.72	0.00	0.66	0.64	0.00	0.02	0.01	4.04	49.4
IR17-CPX-5	2.38	1.94	0.04	0.02	0.75	0.00	0.77	0.46	0.00	0.02	0.02	4.02	37.5
IR17-CPX-6	2.39	1.94	0.03	0.00	0.76	0.00	0.79	0.45	0.00	0.02	0.01	4.02	36.3
IR17-CPX-7	2.39	1.94	0.03	0.00	0.76	0.00	0.79	0.47	0.00	0.02	0.01	4.02	37.3
IR17-CPX-8	2.40	1.95	0.04	0.02	0.78	0.00	0.82	0.38	0.00	0.02	0.02	4.02	31.4

Appendix B - CPX - Isle Royale Sample Suite

Sample	Na2O	CaO	Al2O3	Cr2O3	FeO	MgO	K2O	SiO2	TiO2	MnO	Total
IR17-CPX-9	0.21	18.25	0.70	0.00	23.22	7.69	0.00	48.50	0.81	0.61	100.0
IR17-CPX-10	0.39	17.75	0.62	0.00	24.54	7.18	0.00	48.23	0.59	0.70	100.0
IR17-CPX-11	0.29	17.25	0.74	0.00	25.42	6.49	0.00	48.50	0.62	0.68	100.0
IR17-CPX-12	0.25	17.77	0.77	0.00	23.64	7.81	0.00	48.68	0.68	0.39	100.0
Average	**0.22**	**17.72**	**0.76**	**0.00**	**23.35**	**7.91**	**0.00**	**48.76**	**0.75**	**0.52**	**100.0**
IR19A-CPX-1	0.31	16.92	1.03	0.00	15.62	11.83	0.00	52.95	0.93	0.41	100.0
IR19A-CPX-2	0.29	17.09	1.00	0.00	16.61	11.15	0.00	52.65	0.72	0.48	100.0
IR19A-CPX-3	0.25	17.30	0.95	0.00	16.35	11.21	0.00	52.72	0.86	0.37	100.0
IR19A-CPX-4	0.25	17.30	0.95	0.00	16.35	11.21	0.00	52.72	0.86	0.37	100.0
IR19A-CPX-5	0.22	16.70	0.73	0.00	18.44	10.38	0.00	52.42	0.78	0.33	100.0
IR19A-CPX-6	0.26	17.06	0.84	0.00	16.48	11.31	0.00	52.69	0.81	0.55	100.0
IR19A-CPX-7	0.31	17.55	1.02	0.00	15.85	11.10	0.00	52.84	0.93	0.41	100.0
IR19A-CPX-8	0.22	17.13	0.79	0.00	17.60	10.39	0.00	52.60	0.83	0.44	100.0
IR19A-CPX-9	0.32	16.90	1.10	0.00	16.27	11.43	0.00	52.68	0.93	0.38	100.0
Average	**0.27**	**17.11**	**0.93**	**0.00**	**16.62**	**11.11**	**0.00**	**52.70**	**0.85**	**0.42**	**100.0**
IR19B-CPX-1	0.00	18.21	1.78	0.00	8.78	15.84	0.00	54.22	0.93	0.24	100.0
IR19B-CPX-2	0.20	17.56	1.58	0.00	10.14	15.50	0.00	53.92	1.09	0.00	100.0
IR19B-CPX-3	0.25	18.38	1.35	0.27	8.13	16.56	0.00	54.52	0.54	0.00	100.0
IR19B-CPX-4	0.34	15.65	1.71	0.00	12.00	15.73	0.00	53.49	1.09	0.00	100.0
IR19B-CPX-5	0.29	16.47	1.76	0.00	11.06	15.41	0.00	53.42	1.15	0.44	100.0
IR19B-CPX-6	0.26	16.41	1.20	0.00	12.38	15.07	0.00	53.79	0.63	0.25	100.0
IR19B-CPX-7	0.29	18.20	1.37	0.00	8.92	15.93	0.00	54.56	0.74	0.00	100.0
IR19B-CPX-8	0.18	16.57	1.28	0.00	10.56	16.43	0.00	54.35	0.62	0.00	100.0
IR19B-CPX-9	0.23	17.92	1.96	0.25	8.49	16.19	0.00	53.89	0.75	0.33	100.0
IR19B-CPX-10	0.26	18.00	1.84	0.00	8.93	16.01	0.00	54.03	0.93	0.00	100.0
IR19B-CPX-11	0.21	14.85	1.39	0.00	12.72	15.71	0.00	53.83	1.01	0.28	100.0
Average	**0.23**	**17.11**	**1.57**	**0.05**	**10.19**	**15.85**	**0.00**	**54.00**	**0.86**	**0.14**	**100.0**
IR20-CPX-1	0.30	17.72	2.27	0.54	8.05	16.23	0.00	53.86	0.71	0.32	100.0
IR20-CPX-2	0.22	18.74	2.06	0.24	7.84	15.97	0.00	53.86	0.74	0.33	100.0
IR20-CPX-3	0.41	17.73	1.78	0.00	10.46	15.14	0.00	53.09	1.16	0.24	100.0
IR20-CPX-4	0.24	17.85	2.07	0.31	8.22	16.13	0.00	54.42	0.74	0.00	100.0
IR20-CPX-5	0.29	15.69	1.78	0.00	12.25	15.69	0.00	52.92	1.07	0.31	100.0
IR20-CPX-6	0.29	18.10	2.25	0.49	7.62	16.41	0.00	53.70	0.86	0.28	100.0
IR20-CPX-7	0.29	16.97	1.92	0.00	9.98	15.89	0.00	53.89	0.75	0.32	100.0

Appendix B - CPX - Isle Royale Sample Suite

Sample	CAT SUM	Si	Al	Na	Ca	Cr	Fe	Mg	K	Ti	Mn	Total	Mg#
IR17-CPX-9	2.39	1.93	0.03	0.02	0.78	0.00	0.77	0.46	0.00	0.02	0.02	4.04	37.1
IR17-CPX-10	2.41	1.93	0.03	0.03	0.76	0.00	0.82	0.43	0.00	0.02	0.02	4.05	34.3
IR17-CPX-11	2.41	1.95	0.04	0.02	0.74	0.00	0.85	0.39	0.00	0.02	0.02	4.03	31.3
IR17-CPX-12	2.39	1.94	0.04	0.02	0.76	0.00	0.79	0.46	0.00	0.02	0.01	4.03	37.1
Average	**2.39**	**1.94**	**0.04**	**0.02**	**0.75**	**0.00**	**0.78**	**0.47**	**0.00**	**0.02**	**0.02**	**4.03**	**37.5**
IR19A-CPX-1	2.27	2.00	0.05	0.02	0.69	0.00	0.49	0.67	0.00	0.03	0.01	3.96	57.4
IR19A-CPX-2	2.29	2.00	0.04	0.02	0.70	0.00	0.53	0.63	0.00	0.02	0.02	3.96	54.5
IR19A-CPX-3	2.28	2.00	0.04	0.02	0.70	0.00	0.52	0.63	0.00	0.02	0.01	3.96	55.0
IR19A-CPX-4	2.28	2.00	0.04	0.02	0.70	0.00	0.52	0.63	0.00	0.02	0.01	3.96	55.0
IR19A-CPX-5	2.30	2.01	0.03	0.02	0.69	0.00	0.59	0.59	0.00	0.02	0.01	3.96	50.1
IR19A-CPX-6	2.29	2.00	0.04	0.02	0.70	0.00	0.52	0.64	0.00	0.02	0.02	3.96	55.0
IR19A-CPX-7	2.28	2.00	0.05	0.02	0.71	0.00	0.50	0.63	0.00	0.03	0.01	3.96	55.5
IR19A-CPX-8	2.30	2.01	0.04	0.02	0.70	0.00	0.56	0.59	0.00	0.02	0.01	3.96	51.3
IR19A-CPX-9	2.28	2.00	0.05	0.02	0.69	0.00	0.52	0.65	0.00	0.03	0.01	3.96	55.6
Average	**2.29**	**2.00**	**0.04**	**0.02**	**0.70**	**0.00**	**0.53**	**0.63**	**0.00**	**0.02**	**0.01**	**3.96**	**54.4**
IR19B-CPX-1	2.20	1.99	0.08	0.00	0.72	0.00	0.27	0.87	0.00	0.03	0.01	3.95	76.3
IR19B-CPX-2	2.21	1.99	0.07	0.01	0.69	0.00	0.31	0.85	0.00	0.03	0.00	3.96	73.1
IR19B-CPX-3	2.20	1.99	0.06	0.02	0.72	0.01	0.25	0.90	0.00	0.01	0.00	3.97	78.4
IR19B-CPX-4	2.22	1.98	0.07	0.02	0.62	0.00	0.37	0.87	0.00	0.03	0.00	3.97	70.0
IR19B-CPX-5	2.22	1.98	0.08	0.02	0.65	0.00	0.34	0.85	0.00	0.03	0.01	3.96	71.3
IR19B-CPX-6	2.23	2.00	0.05	0.02	0.65	0.00	0.38	0.83	0.00	0.02	0.01	3.97	68.4
IR19B-CPX-7	2.20	2.00	0.06	0.02	0.72	0.00	0.27	0.87	0.00	0.02	0.00	3.96	76.1
IR19B-CPX-8	2.21	2.00	0.06	0.01	0.65	0.00	0.32	0.90	0.00	0.02	0.00	3.96	73.5
IR19B-CPX-9	2.20	1.98	0.08	0.02	0.70	0.01	0.26	0.88	0.00	0.02	0.01	3.97	77.3
IR19B-CPX-10	2.20	1.98	0.08	0.02	0.71	0.00	0.27	0.88	0.00	0.03	0.00	3.96	76.2
IR19B-CPX-11	2.22	1.99	0.06	0.02	0.59	0.00	0.39	0.87	0.00	0.03	0.01	3.96	68.8
Average	**2.21**	**1.99**	**0.07**	**0.02**	**0.67**	**0.00**	**0.31**	**0.87**	**0.00**	**0.02**	**0.00**	**3.96**	**73.6**
IR20-CPX-1	2.20	1.97	0.10	0.02	0.70	0.02	0.25	0.89	0.00	0.02	0.01	3.96	78.2
IR20-CPX-2	2.20	1.97	0.09	0.02	0.74	0.01	0.24	0.87	0.00	0.02	0.01	3.97	78.4
IR20-CPX-3	2.23	1.97	0.08	0.03	0.70	0.00	0.32	0.84	0.00	0.03	0.01	3.98	72.1
IR20-CPX-4	2.20	1.99	0.09	0.02	0.70	0.01	0.25	0.88	0.00	0.02	0.00	3.95	77.8
IR20-CPX-5	2.23	1.97	0.08	0.02	0.62	0.00	0.38	0.87	0.00	0.03	0.01	3.98	69.5
IR20-CPX-6	2.20	1.96	0.10	0.02	0.71	0.01	0.23	0.89	0.00	0.02	0.01	3.97	79.3
IR20-CPX-7	2.21	1.98	0.08	0.02	0.67	0.00	0.31	0.87	0.00	0.02	0.01	3.97	73.9

Appendix B - CPX - Isle Royale Sample Suite

Sample	Na2O	CaO	Al2O3	Cr2O3	FeO	MgO	K2O	SiO2	TiO2	MnO	Total
IR20-CPX-8	0.29	18.72	2.02	0.00	8.21	15.93	0.00	53.83	0.74	0.26	100.0
IR20-CPX-9	0.18	19.20	1.62	0.00	7.54	16.25	0.00	54.59	0.62	0.00	100.0
IR20-CPX-10	0.40	17.40	1.54	0.00	9.94	15.59	0.00	53.85	0.97	0.31	100.0
Average	**0.29**	**17.81**	**1.93**	**0.16**	**9.01**	**15.92**	**0.00**	**53.80**	**0.84**	**0.24**	**100.0**
IR22-CPX-1	0.21	16.49	1.20	0.00	11.07	16.07	0.00	53.86	0.77	0.33	100.0
IR22-CPX-2	0.39	17.54	1.73	0.00	9.93	15.51	0.00	53.57	1.34	0.00	100.0
IR22-CPX-3	0.24	18.70	1.99	0.34	8.17	15.53	0.00	53.96	0.76	0.31	100.0
IR22-CPX-4	0.29	15.29	1.57	0.00	12.82	15.49	0.00	53.29	0.93	0.31	100.0
IR22-CPX-5	0.25	16.32	1.32	0.00	13.61	15.01	0.00	52.43	0.79	0.28	100.0
IR22-CPX-6	0.20	18.96	1.56	0.55	7.03	16.53	0.00	54.34	0.58	0.24	100.0
IR22-CPX-7	0.34	19.24	2.20	0.60	6.75	16.00	0.00	53.84	0.76	0.28	100.0
IR22-CPX-8	0.32	16.16	1.55	0.00	11.78	15.33	0.00	53.63	0.88	0.35	100.0
IR22-CPX-9	0.18	17.09	1.56	0.00	11.58	14.93	0.00	53.72	0.94	0.00	100.0
Average	**0.27**	**17.31**	**1.63**	**0.17**	**10.30**	**15.60**	**0.00**	**53.63**	**0.86**	**0.23**	**100.0**
IR23-CPX-1	0.39	17.86	1.78	0.00	13.72	15.06	0.00	49.60	1.28	0.33	100.0
IR23-CPX-2	0.31	17.39	1.18	0.00	15.29	14.37	0.00	50.85	0.63	0.00	100.0
IR23-CPX-3	0.25	18.34	1.25	0.00	14.45	13.90	0.00	50.36	0.83	0.62	100.0
IR23-CPX-4	0.24	18.75	1.01	0.00	14.23	14.37	0.00	50.26	0.73	0.42	100.0
IR23-CPX-5	0.29	20.01	1.70	0.00	14.24	13.66	0.00	49.06	1.03	0.00	100.0
IR23-CPX-6	0.42	16.73	1.98	0.00	14.72	13.79	0.00	51.07	0.75	0.53	100.0
IR23-CPX-7	0.59	18.73	3.11	0.00	12.59	12.93	0.00	51.03	0.69	0.33	100.0
IR23-CPX-8	1.70	17.81	8.16	0.00	10.26	10.83	0.00	50.57	0.67	0.00	100.0
IR23-CPX-9	0.35	19.58	1.96	0.00	14.89	11.06	0.00	51.48	0.68	0.00	100.0
IR23-CPX-10	0.36	17.86	1.63	0.00	15.52	13.49	0.00	50.92	0.92	0.31	101.0
Average	**0.49**	**18.31**	**2.38**	**0.00**	**13.99**	**13.35**	**0.00**	**50.52**	**0.82**	**0.25**	**100.1**
IR26A-CPX-1	0.27	18.04	1.61	0.00	14.23	11.05	0.00	53.60	0.84	0.36	100.0
IR26A-CPX-2	0.26	17.87	2.13	0.00	14.65	10.74	0.00	53.22	1.14	0.00	100.0
IR26A-CPX-3	0.35	17.30	1.45	0.00	14.15	11.92	0.00	53.59	0.91	0.34	100.0
IR26A-CPX-4	0.26	17.40	1.28	0.00	12.91	13.65	0.00	53.31	0.87	0.33	100.0
IR26A-CPX-5	0.29	17.91	1.75	0.00	14.60	10.53	0.00	53.71	0.93	0.27	100.0
IR26A-CPX-6	0.19	18.10	1.65	0.00	14.76	10.74	0.00	53.28	0.97	0.32	100.0
IR26A-CPX-7	0.40	17.82	1.77	0.00	13.37	12.75	0.00	52.36	1.13	0.38	100.0
IR26A-CPX-8	0.37	18.07	1.74	0.00	14.15	10.97	0.00	53.50	0.96	0.25	100.0
IR26A-CPX-9	0.25	18.05	1.72	0.00	14.47	10.73	0.00	53.38	1.06	0.34	100.0
IR26A-CPX-10	0.31	17.62	1.74	0.00	14.17	12.06	0.00	53.23	0.87	0.00	100.0
IR26A-CPX-11	0.24	17.55	1.69	0.00	15.24	10.72	0.00	53.64	0.92	0.00	100.0
Average	**0.29**	**17.79**	**1.68**	**0.00**	**14.25**	**11.44**	**0.00**	**53.35**	**0.96**	**0.24**	**100.0**

Appendix B - CPX - Isle Royale Sample Suite

Sample	CAT SUM	Si	Al	Na	Ca	Cr	Fe	Mg	K	Ti	Mn	Total	Mg#
IR20-CPX-8	2.20	1.98	0.09	0.02	0.74	0.00	0.25	0.87	0.00	0.02	0.01	3.97	77.6
IR20-CPX-9	2.20	1.99	0.07	0.01	0.75	0.00	0.23	0.88	0.00	0.02	0.00	3.96	79.3
IR20-CPX-10	2.22	1.99	0.07	0.03	0.69	0.00	0.31	0.86	0.00	0.03	0.01	3.97	73.6
Average	**2.21**	**1.98**	**0.08**	**0.02**	**0.70**	**0.00**	**0.28**	**0.87**	**0.00**	**0.02**	**0.01**	**3.97**	**76.0**
IR22-CPX-1	2.22	1.99	0.05	0.02	0.65	0.00	0.34	0.89	0.00	0.02	0.01	3.97	72.1
IR22-CPX-2	2.21	1.97	0.08	0.03	0.69	0.00	0.31	0.85	0.00	0.04	0.00	3.96	73.6
IR22-CPX-3	2.21	1.98	0.09	0.02	0.74	0.01	0.25	0.85	0.00	0.02	0.01	3.96	77.2
IR22-CPX-4	2.23	1.98	0.07	0.02	0.61	0.00	0.40	0.86	0.00	0.03	0.01	3.97	68.3
IR22-CPX-5	2.25	1.96	0.06	0.02	0.66	0.00	0.43	0.84	0.00	0.02	0.01	3.99	66.3
IR22-CPX-6	2.20	1.99	0.07	0.01	0.74	0.02	0.21	0.90	0.00	0.02	0.01	3.96	80.7
IR22-CPX-7	2.20	1.97	0.09	0.02	0.75	0.02	0.21	0.87	0.00	0.02	0.01	3.97	80.9
IR22-CPX-8	2.23	1.99	0.07	0.02	0.64	0.00	0.37	0.85	0.00	0.02	0.01	3.97	69.9
IR22-CPX-9	2.23	1.99	0.07	0.01	0.68	0.00	0.36	0.82	0.00	0.03	0.00	3.96	69.7
Average	**2.22**	**1.98**	**0.07**	**0.02**	**0.68**	**0.00**	**0.32**	**0.86**	**0.00**	**0.02**	**0.01**	**3.97**	**73.2**
IR23-CPX-1	2.28	1.88	0.08	0.03	0.73	0.00	0.44	0.85	0.00	0.04	0.01	4.05	66.2
IR23-CPX-2	2.28	1.93	0.05	0.02	0.71	0.00	0.49	0.81	0.00	0.02	0.00	4.03	62.6
IR23-CPX-3	2.29	1.92	0.06	0.02	0.75	0.00	0.46	0.79	0.00	0.02	0.02	4.04	63.2
IR23-CPX-4	2.29	1.92	0.05	0.02	0.77	0.00	0.45	0.82	0.00	0.02	0.01	4.05	64.3
IR23-CPX-5	2.30	1.88	0.08	0.02	0.82	0.00	0.46	0.78	0.00	0.03	0.00	4.06	63.1
IR23-CPX-6	2.28	1.93	0.09	0.03	0.68	0.00	0.47	0.78	0.00	0.02	0.02	4.02	62.5
IR23-CPX-7	2.26	1.92	0.14	0.04	0.76	0.00	0.40	0.73	0.00	0.02	0.01	4.01	64.7
IR23-CPX-8	2.23	1.87	0.36	0.12	0.71	0.00	0.32	0.60	0.00	0.02	0.00	3.99	65.3
IR23-CPX-9	2.29	1.96	0.09	0.03	0.80	0.00	0.47	0.63	0.00	0.02	0.00	3.99	57.0
IR23-CPX-10	2.27	1.92	0.07	0.03	0.72	0.00	0.49	0.76	0.00	0.03	0.01	4.03	60.8
Average	**2.28**	**1.91**	**0.11**	**0.04**	**0.74**	**0.00**	**0.44**	**0.75**	**0.00**	**0.02**	**0.01**	**4.03**	**63.0**
IR26A-CPX-1	2.26	2.02	0.07	0.02	0.73	0.00	0.45	0.62	0.00	0.02	0.01	3.94	58.0
IR26A-CPX-2	2.26	2.00	0.09	0.02	0.72	0.00	0.46	0.60	0.00	0.03	0.00	3.93	56.6
IR26A-CPX-3	2.26	2.01	0.06	0.03	0.70	0.00	0.44	0.67	0.00	0.03	0.01	3.94	60.0
IR26A-CPX-4	2.25	1.99	0.06	0.02	0.70	0.00	0.40	0.76	0.00	0.02	0.01	3.96	65.3
IR26A-CPX-5	2.26	2.02	0.08	0.02	0.72	0.00	0.46	0.59	0.00	0.03	0.01	3.93	56.2
IR26A-CPX-6	2.27	2.01	0.07	0.01	0.73	0.00	0.47	0.60	0.00	0.03	0.01	3.93	56.5
IR26A-CPX-7	2.26	1.97	0.08	0.03	0.72	0.00	0.42	0.71	0.00	0.03	0.01	3.97	63.0
IR26A-CPX-8	2.26	2.01	0.08	0.03	0.73	0.00	0.44	0.61	0.00	0.03	0.01	3.94	58.0
IR26A-CPX-9	2.26	2.01	0.08	0.02	0.73	0.00	0.46	0.60	0.00	0.03	0.01	3.93	56.9
IR26A-CPX-10	2.26	2.00	0.08	0.02	0.71	0.00	0.44	0.67	0.00	0.02	0.00	3.95	60.3
IR26A-CPX-11	2.26	2.02	0.07	0.02	0.71	0.00	0.48	0.60	0.00	0.03	0.00	3.93	55.6
Average	**2.26**	**2.01**	**0.07**	**0.02**	**0.72**	**0.00**	**0.45**	**0.64**	**0.00**	**0.03**	**0.01**	**3.94**	**58.8**

Appendix B - CPX - Isle Royale Sample Suite

Sample	Na2O	CaO	Al2O3	Cr2O3	FeO	MgO	K2O	SiO2	TiO2	MnO	Total
IR26B-CPX-1	0.26	19.30	1.99	0.37	7.16	16.24	0.00	54.03	0.64	0.00	100.0
IR26B-CPX-2	0.30	17.44	1.59	0.00	10.60	15.19	0.00	53.63	0.97	0.28	100.0
IR26B-CPX-3	0.33	17.28	1.76	0.00	10.50	15.49	0.00	53.33	0.91	0.40	100.0
IR26B-CPX-4	0.25	15.91	1.37	0.00	13.35	14.72	0.00	52.95	1.01	0.42	100.0
IR26B-CPX-5	0.29	18.90	1.45	0.42	7.62	16.26	0.00	54.52	0.54	0.00	100.0
IR26B-CPX-6	0.30	17.90	1.37	0.00	9.17	15.69	0.00	54.45	0.78	0.34	100.0
IR26B-CPX-7	0.00	19.07	1.45	0.00	7.49	16.17	0.00	54.92	0.64	0.25	100.0
IR26B-CPX-8	0.27	18.60	1.35	0.00	7.71	16.36	0.00	54.54	0.84	0.33	100.0
IR26B-CPX-9	0.00	18.83	1.44	0.29	7.06	16.65	0.00	55.15	0.59	0.00	100.0
Average	**0.22**	**18.14**	**1.53**	**0.12**	**8.96**	**15.86**	**0.00**	**54.17**	**0.77**	**0.22**	**100.0**
IR27-CPX-1	0.29	16.72	1.79	0.00	10.59	15.88	0.00	53.39	1.04	0.30	100.0
IR27-CPX-2	0.21	16.04	1.79	0.00	11.57	15.42	0.00	53.29	1.29	0.38	100.0
IR27-CPX-3	0.35	17.07	1.64	0.00	11.84	14.62	0.00	53.40	1.08	0.00	100.0
IR27-CPX-4	0.39	16.25	1.76	0.25	11.47	15.32	0.00	52.93	1.21	0.41	100.0
IR27-CPX-5	0.32	18.60	2.26	0.55	7.60	15.85	0.00	53.51	0.99	0.31	100.0
IR27-CPX-6	0.00	18.05	2.05	0.25	8.07	16.48	0.00	54.36	0.73	0.00	100.0
IR27-CPX-7	0.27	18.67	2.08	0.00	8.14	16.11	0.00	53.99	0.75	0.00	100.0
IR27-CPX-8	0.33	15.45	1.82	0.00	11.10	16.37	0.00	53.64	1.00	0.30	100.0
Average	**0.27**	**17.11**	**1.90**	**0.13**	**10.05**	**15.76**	**0.00**	**53.56**	**1.01**	**0.21**	**100.0**

Appendix B - CPX - Isle Royale Sample Suite

Sample	CAT SUM	Si	Al	Na	Ca	Cr	Fe	Mg	K	Ti	Mn	Total	Mg#
IR26B-CPX-1	2.20	1.98	0.09	0.02	0.76	0.01	0.22	0.88	0.00	0.02	0.00	3.97	80.2
IR26B-CPX-2	2.22	1.98	0.07	0.02	0.69	0.00	0.33	0.84	0.00	0.03	0.01	3.97	71.9
IR26B-CPX-3	2.22	1.97	0.08	0.02	0.68	0.00	0.32	0.85	0.00	0.03	0.01	3.98	72.4
IR26B-CPX-4	2.25	1.98	0.06	0.02	0.64	0.00	0.42	0.82	0.00	0.03	0.01	3.97	66.3
IR26B-CPX-5	2.20	1.99	0.06	0.02	0.74	0.01	0.23	0.89	0.00	0.01	0.00	3.96	79.2
IR26B-CPX-6	2.21	2.00	0.06	0.02	0.70	0.00	0.28	0.86	0.00	0.02	0.01	3.96	75.3
IR26B-CPX-7	2.19	2.00	0.06	0.00	0.75	0.00	0.23	0.88	0.00	0.02	0.01	3.95	79.4
IR26B-CPX-8	2.20	1.99	0.06	0.02	0.73	0.00	0.24	0.89	0.00	0.02	0.01	3.96	79.1
IR26B-CPX-9	2.19	2.01	0.06	0.00	0.73	0.01	0.21	0.90	0.00	0.02	0.00	3.94	80.8
Average	**2.21**	**1.99**	**0.07**	**0.02**	**0.71**	**0.00**	**0.28**	**0.87**	**0.00**	**0.02**	**0.01**	**3.96**	**76.1**
IR27-CPX-1	2.22	1.97	0.08	0.02	0.66	0.00	0.33	0.87	0.00	0.03	0.01	3.97	72.8
IR27-CPX-2	2.22	1.97	0.08	0.02	0.64	0.00	0.36	0.85	0.00	0.04	0.01	3.96	70.4
IR27-CPX-3	2.23	1.98	0.07	0.03	0.68	0.00	0.37	0.81	0.00	0.03	0.00	3.96	68.8
IR27-CPX-4	2.23	1.96	0.08	0.03	0.65	0.01	0.36	0.85	0.00	0.03	0.01	3.97	70.4
IR27-CPX-5	2.20	1.96	0.10	0.02	0.73	0.02	0.23	0.87	0.00	0.03	0.01	3.97	78.8
IR27-CPX-6	2.19	1.98	0.09	0.00	0.71	0.01	0.25	0.90	0.00	0.02	0.00	3.95	78.4
IR27-CPX-7	2.20	1.98	0.09	0.02	0.73	0.00	0.25	0.88	0.00	0.02	0.00	3.97	77.9
IR27-CPX-8	2.21	1.98	0.08	0.02	0.61	0.00	0.34	0.90	0.00	0.03	0.01	3.97	72.4
Average	**2.21**	**1.97**	**0.08**	**0.02**	**0.68**	**0.00**	**0.31**	**0.87**	**0.00**	**0.03**	**0.01**	**3.96**	**73.7**

Appendix B - Olivine - BRD Sample Suite

Sample	MgO	SiO2	CaO	TiO2	MnO	FeO	Total
BBC6-Ol-1	33.70	38.77	0.00	0.00	0.42	27.11	100.0
BBC6-Ol-2	33.23	38.84	0.00	0.00	0.50	27.43	100.0
BBC6-Ol-3	33.71	38.70	0.00	0.00	0.37	27.21	100.0
BBC6-Ol-4	33.64	38.85	0.00	0.00	0.52	26.99	100.0
BBC6-Ol-5	33.55	39.09	0.00	0.00	0.38	26.98	100.0
BBC6-Ol-6	33.55	39.22	0.00	0.00	0.43	26.80	100.0
Average	**33.56**	**38.91**	**0.00**	**0.00**	**0.44**	**27.09**	**100.0**
BBC13-Ol-1	27.51	37.48	0.00	0.00	0.54	34.47	100.0
BBC13-Ol-2	27.28	37.46	0.19	0.00	0.32	34.75	100.0
BBC13-Ol-3	27.21	37.15	0.00	0.00	0.48	35.15	100.0
BBC13-Ol-4	25.62	37.22	0.15	0.00	0.45	36.57	100.0
BBC13-Ol-5	24.48	37.04	0.20	0.00	0.36	37.92	100.0
BBC13-Ol-6	26.86	37.47	0.00	0.00	0.60	35.06	100.0
Average	**26.49**	**37.30**	**0.09**	**0.00**	**0.46**	**35.65**	**100.0**
BBC14-Ol-1	24.79	36.99	0.00	0.00	0.65	37.57	100.0
BBC14-Ol-2	25.10	37.18	0.00	0.00	0.55	37.17	100.0
BBC14-Ol-3	24.80	36.95	0.00	0.00	0.71	37.55	100.0
BBC14-Ol-4	25.27	37.44	0.00	0.00	0.41	36.88	100.0
BBC14-Ol-5	25.51	37.34	0.00	0.00	0.53	36.63	100.0
BBC14-Ol-6	25.37	37.05	0.00	0.00	0.52	37.05	100.0
Average	**25.14**	**37.16**	**0.00**	**0.00**	**0.56**	**37.14**	**100.0**
SBI10-Ol-1	20.89	36.26	0.44	0.00	0.70	41.71	100.0
SBI10-Ol-2	19.04	35.55	0.22	0.00	0.47	44.71	100.0
SBI10-Ol-3	20.50	36.08	0.23	0.00	0.69	42.49	100.0
SBI10-Ol-4	22.73	36.87	0.21	0.00	0.59	39.59	100.0
SBI10-Ol-5	22.22	36.29	0.22	0.00	0.41	40.85	100.0
SBI10-Ol-6	19.01	35.49	0.19	0.00	0.50	44.82	100.0
Average	**20.73**	**36.09**	**0.25**	**0.00**	**0.56**	**42.36**	**100.0**
B364-Ol-1	36.10	37.10	0.14	0.00	0.33	24.70	98.4
B364-Ol-2	36.30	37.70	0.12	0.00	0.30	24.90	99.3
B364-Ol-3	35.70	36.80	0.20	0.00	0.32	24.80	97.8
B364-Ol-4	36.30	37.30	0.22	0.00	0.33	24.60	98.8
B364-Ol-5	36.60	37.30	0.16	0.00	0.30	24.50	98.9
B364-Ol-6	36.30	36.70	0.17	0.00	0.30	24.70	98.2
B364-Ol-7	36.60	37.50	0.14	0.00	0.32	25.00	99.6
Average	**36.27**	**37.20**	**0.16**	**0.00**	**0.31**	**24.74**	**98.7**
E161-Ol-1	38.30	37.50	0.34	0.08	0.34	23.50	100.1
E161-Ol-2	38.00	37.90	0.34	0.07	0.32	23.30	99.9
E161-Ol-3	38.30	38.10	0.23	0.03	0.32	23.20	100.2
E161-Ol-4	38.10	38.00	0.25	0.08	0.31	23.30	100.0
E161-Ol-5	38.50	38.30	0.29	0.08	0.29	23.30	100.8
E161-Ol-6	37.60	38.70	0.35	0.09	0.30	23.00	100.0
Average	**38.13**	**38.08**	**0.30**	**0.07**	**0.31**	**23.27**	**100.2**

Appendix B - Olivine - BRD Sample Suite

Sample	CAT sum	Si	Fe	Mg	Mn	Ca	Ti	Total	Mg#
BBC6-Ol-1	1.59	1.03	0.60	1.33	0.01	0.00	0.00	2.97	68.9
BBC6-Ol-2	1.60	1.03	0.61	1.32	0.01	0.00	0.00	2.97	68.3
BBC6-Ol-3	1.59	1.03	0.60	1.33	0.01	0.00	0.00	2.97	68.8
BBC6-Ol-4	1.59	1.03	0.60	1.33	0.01	0.00	0.00	2.97	69.0
BBC6-Ol-5	1.59	1.03	0.60	1.32	0.01	0.00	0.00	2.97	68.9
BBC6-Ol-6	1.59	1.04	0.59	1.32	0.01	0.00	0.00	2.96	69.1
Average	**1.59**	**1.03**	**0.60**	**1.33**	**0.01**	**0.00**	**0.00**	**2.97**	**68.8**
BBC13-Ol-1	1.65	1.03	0.79	1.13	0.01	0.00	0.00	2.97	58.7
BBC13-Ol-2	1.66	1.03	0.80	1.12	0.01	0.01	0.00	2.97	58.3
BBC13-Ol-3	1.66	1.03	0.81	1.12	0.01	0.00	0.00	2.97	58.0
BBC13-Ol-4	1.67	1.04	0.85	1.06	0.01	0.00	0.00	2.96	55.5
BBC13-Ol-5	1.68	1.04	0.89	1.02	0.01	0.01	0.00	2.96	53.5
BBC13-Ol-6	1.66	1.04	0.81	1.11	0.01	0.00	0.00	2.96	57.7
Average	**1.66**	**1.03**	**0.83**	**1.09**	**0.01**	**0.00**	**0.00**	**2.97**	**57.0**
BBC14-Ol-1	1.68	1.04	0.88	1.03	0.02	0.00	0.00	2.96	54.0
BBC14-Ol-2	1.68	1.04	0.87	1.04	0.01	0.00	0.00	2.96	54.6
BBC14-Ol-3	1.68	1.03	0.88	1.04	0.02	0.00	0.00	2.97	54.1
BBC14-Ol-4	1.67	1.04	0.86	1.05	0.01	0.00	0.00	2.96	55.0
BBC14-Ol-5	1.67	1.04	0.85	1.06	0.01	0.00	0.00	2.96	55.4
BBC14-Ol-6	1.68	1.03	0.86	1.06	0.01	0.00	0.00	2.97	55.0
Average	**1.68**	**1.04**	**0.87**	**1.05**	**0.01**	**0.00**	**0.00**	**2.96**	**54.7**
SBI10-Ol-1	1.72	1.04	1.00	0.89	0.02	0.01	0.00	2.96	47.2
SBI10-Ol-2	1.75	1.03	1.09	0.83	0.01	0.01	0.00	2.97	43.2
SBI10-Ol-3	1.73	1.04	1.02	0.88	0.02	0.01	0.00	2.96	46.2
SBI10-Ol-4	1.70	1.04	0.94	0.96	0.01	0.01	0.00	2.96	50.6
SBI10-Ol-5	1.71	1.03	0.97	0.94	0.01	0.01	0.00	2.97	49.2
SBI10-Ol-6	1.75	1.03	1.09	0.82	0.01	0.01	0.00	2.97	43.1
Average	**1.73**	**1.04**	**1.02**	**0.89**	**0.01**	**0.01**	**0.00**	**2.96**	**46.6**
B364-Ol-1	1.61	1.00	0.55	1.44	0.01	0.00	0.00	3.00	72.3
B364-Ol-2	1.59	1.00	0.55	1.44	0.01	0.00	0.00	3.00	72.2
B364-Ol-3	1.62	0.99	0.56	1.44	0.01	0.01	0.00	3.01	72.0
B364-Ol-4	1.60	1.00	0.55	1.44	0.01	0.01	0.00	3.00	72.5
B364-Ol-5	1.60	0.99	0.55	1.45	0.01	0.00	0.00	3.01	72.7
B364-Ol-6	1.62	0.99	0.56	1.46	0.01	0.00	0.00	3.01	72.4
B364-Ol-7	1.59	0.99	0.55	1.45	0.01	0.00	0.00	3.01	72.3
Average	**1.61**	**0.99**	**0.55**	**1.45**	**0.01**	**0.00**	**0.00**	**3.01**	**72.3**
E161-Ol-1	1.58	0.98	0.52	1.50	0.01	0.01	0.00	3.01	74.4
E161-Ol-2	1.57	0.99	0.51	1.48	0.01	0.01	0.00	3.01	74.4
E161-Ol-3	1.57	0.99	0.51	1.49	0.01	0.01	0.00	3.01	74.6
E161-Ol-4	1.57	0.99	0.51	1.49	0.01	0.01	0.00	3.00	74.5
E161-Ol-5	1.56	0.99	0.51	1.49	0.01	0.01	0.00	3.00	74.7
E161-Ol-6	1.57	1.01	0.50	1.46	0.01	0.01	0.00	2.99	74.5
Average	**1.57**	**0.99**	**0.51**	**1.48**	**0.01**	**0.01**	**0.00**	**3.00**	**74.5**

Appendix B - Olivine - BRD Sample Suite

Sample	MgO	SiO2	CaO	TiO2	MnO	FeO	Total
D126-Ol-1	37.50	37.40	0.26	0.10	0.34	24.50	100.1
D126-Ol-2	37.40	38.30	0.24	0.05	0.34	24.50	100.8
D126-Ol-3	37.40	38.70	0.28	0.08	0.35	24.80	101.6
D126-Ol-4	37.20	37.30	0.25	0.09	0.35	24.70	99.9
D126-Ol-5	37.40	38.00	0.26	0.08	0.35	24.60	100.7
Average	**37.38**	**37.94**	**0.26**	**0.08**	**0.35**	**24.62**	**100.6**
D314-Ol-1	33.10	35.60	0.23	0.00	0.41	30.20	99.5
D314-Ol-2	33.50	36.30	0.29	0.00	0.40	30.10	100.6
D314-Ol-3	34.80	36.20	0.24	0.00	0.32	28.50	100.1
D314-Ol-4	34.50	34.80	0.30	0.00	0.42	29.60	99.6
D314-Ol-5	33.80	35.40	0.37	0.00	0.44	29.80	99.8
Average	**33.94**	**35.66**	**0.29**	**0.00**	**0.40**	**29.64**	**99.9**
D246-Ol-1	35.50	36.40	0.28	0.00	0.38	26.80	99.4
D246-Ol-2	35.80	36.70	0.25	0.00	0.38	26.90	100.0
D246-Ol-3	36.90	35.80	0.26	0.00	0.34	26.60	99.9
D246-Ol-4	35.40	36.70	0.22	0.00	0.35	28.10	100.8
D246-Ol-5	34.60	35.90	0.25	0.00	0.41	28.90	100.1
D246-Ol-6	35.20	36.40	0.22	0.00	0.40	28.70	100.9
D246-Ol-7	34.70	36.00	0.21	0.00	0.41	29.20	100.5
Average	**35.44**	**36.27**	**0.24**	**0.00**	**0.38**	**27.89**	**100.2**
B326-Ol-1	26.60	34.40	0.34	0.00	0.52	36.30	98.2
B326-Ol-2	28.00	34.50	0.40	0.00	0.47	35.10	98.5
B326-Ol-3	27.30	34.20	0.35	0.00	0.46	35.70	98.0
B326-Ol-4	26.90	34.30	0.36	0.00	0.51	36.20	98.3
Average	**27.20**	**34.35**	**0.36**	**0.00**	**0.49**	**35.83**	**98.2**
E217-Ol-1	31.40	36.70	0.30	0.00	0.48	31.40	100.3
E217-Ol-2	32.10	36.50	0.30	0.00	0.39	31.00	100.3
E217-Ol-3	32.80	36.00	0.30	0.00	0.41	31.00	100.5
E217-Ol-4	31.90	36.10	0.29	0.00	0.44	30.90	99.6
E217-Ol-5	32.10	36.80	0.29	0.00	0.44	31.30	100.9
Average	**32.06**	**36.42**	**0.30**	**0.00**	**0.43**	**31.12**	**100.3**
E159A-Ol-1	28.10	35.20	0.41	0.00	0.55	35.70	100.0
E159A-Ol-2	31.00	35.70	0.42	0.00	0.48	32.30	99.9
E159A-Ol-3	31.40	35.80	0.41	0.00	0.44	32.60	100.7
E159A-Ol-4	25.50	34.20	0.42	0.01	0.59	38.30	99.0
E159A-Ol-5	20.60	34.00	0.49	0.05	0.72	44.60	100.5
E159A-Ol-6	23.80	34.40	0.34	0.00	0.65	41.70	100.9
E159A-Ol-7	23.20	34.80	0.41	0.01	0.69	42.10	101.2
E159A-Ol-8	23.60	34.50	0.40	0.01	0.66	41.70	100.9
E159A-Ol-9	21.30	34.20	0.29	0.00	0.72	43.90	100.4
Average	**25.39**	**34.76**	**0.40**	**0.01**	**0.61**	**39.21**	**100.4**

Appendix B - Olivine - BRD Sample Suite

Sample	CAT sum	Si	Fe	Mg	Mn	Ca	Ti	Total	Mg#
D126-Ol-1	1.58	0.98	0.54	1.47	0.01	0.01	0.00	3.01	73.2
D126-Ol-2	1.57	1.00	0.53	1.45	0.01	0.01	0.00	3.00	73.1
D126-Ol-3	1.55	1.00	0.54	1.44	0.01	0.01	0.00	3.00	72.9
D126-Ol-4	1.59	0.99	0.55	1.47	0.01	0.01	0.00	3.01	72.9
D126-Ol-5	1.57	0.99	0.54	1.46	0.01	0.01	0.00	3.01	73.0
Average	**1.57**	**0.99**	**0.54**	**1.46**	**0.01**	**0.01**	**0.00**	**3.01**	**73.0**
D314-Ol-1	1.64	0.97	0.69	1.35	0.01	0.01	0.00	3.03	66.1
D314-Ol-2	1.62	0.98	0.68	1.35	0.01	0.01	0.00	3.02	66.5
D314-Ol-3	1.62	0.97	0.64	1.40	0.01	0.01	0.00	3.03	68.5
D314-Ol-4	1.64	0.95	0.68	1.40	0.01	0.01	0.00	3.05	67.5
D314-Ol-5	1.64	0.96	0.68	1.37	0.01	0.01	0.00	3.04	66.9
Average	**1.63**	**0.97**	**0.67**	**1.37**	**0.01**	**0.01**	**0.00**	**3.03**	**67.1**
D246-Ol-1	1.62	0.98	0.60	1.42	0.01	0.01	0.00	3.02	70.2
D246-Ol-2	1.60	0.98	0.60	1.42	0.01	0.01	0.00	3.02	70.3
D246-Ol-3	1.61	0.96	0.60	1.47	0.01	0.01	0.00	3.04	71.2
D246-Ol-4	1.60	0.98	0.63	1.41	0.01	0.01	0.00	3.02	69.2
D246-Ol-5	1.62	0.97	0.65	1.39	0.01	0.01	0.00	3.03	68.1
D246-Ol-7	1.60	0.97	0.64	1.40	0.01	0.01	0.00	3.03	68.6
D246-Ol-8	1.62	0.97	0.66	1.39	0.01	0.01	0.00	3.03	67.9
Average	**1.61**	**0.97**	**0.62**	**1.42**	**0.01**	**0.01**	**0.00**	**3.03**	**69.4**
B326-Ol-1	1.72	0.99	0.87	1.14	0.01	0.01	0.00	3.01	56.6
B326-Ol-2	1.71	0.98	0.83	1.18	0.01	0.01	0.00	3.02	58.7
B326-Ol-3	1.72	0.98	0.85	1.17	0.01	0.01	0.00	3.02	57.7
B326-Ol-4	1.72	0.98	0.87	1.15	0.01	0.01	0.00	3.02	57.0
Average	**1.72**	**0.98**	**0.86**	**1.16**	**0.01**	**0.01**	**0.00**	**3.02**	**57.5**
E217-Ol-1	1.63	1.00	0.71	1.27	0.01	0.01	0.00	3.00	64.1
E217-Ol-2	1.63	0.99	0.70	1.30	0.01	0.01	0.00	3.01	64.9
E217-Ol-3	1.63	0.98	0.70	1.33	0.01	0.01	0.00	3.02	65.4
E217-Ol-4	1.64	0.99	0.71	1.30	0.01	0.01	0.00	3.01	64.8
E217-Ol-5	1.62	0.99	0.71	1.29	0.01	0.01	0.00	3.01	64.6
Average	**1.63**	**0.99**	**0.71**	**1.30**	**0.01**	**0.01**	**0.00**	**3.01**	**64.7**
E159A-Ol-1	1.68	0.98	0.83	1.17	0.01	0.01	0.00	3.02	58.4
E159A-Ol-2	1.65	0.98	0.74	1.27	0.01	0.01	0.00	3.02	63.1
E159A-Ol-3	1.64	0.98	0.74	1.28	0.01	0.01	0.00	3.02	63.2
E159A-Ol-4	1.72	0.98	0.92	1.09	0.01	0.01	0.00	3.02	54.3
E159A-Ol-5	1.75	0.99	1.09	0.90	0.02	0.02	0.00	3.01	45.2
E159A-Ol-6	1.72	0.98	1.00	1.01	0.02	0.01	0.00	3.02	50.4
E159A-Ol-7	1.71	0.99	1.00	0.99	0.02	0.01	0.00	3.01	49.6
E159A-Ol-8	1.72	0.99	1.00	1.00	0.02	0.01	0.00	3.01	50.2
E159A-Ol-9	1.74	0.99	1.07	0.92	0.02	0.01	0.00	3.01	46.4
Average	**1.70**	**0.99**	**0.93**	**1.07**	**0.01**	**0.01**	**0.00**	**3.01**	**53.4**

Appendix B - Olivine - BRD Sample Suite

Sample	MgO	SiO2	CaO	TiO2	MnO	FeO	Total
A290B-Ol-1	29.30	35.80	0.38	0.00	0.48	33.20	99.2
A290B-Ol-2	30.50	36.00	0.37	0.00	0.45	32.00	99.3
A290B-Ol-3	26.70	35.20	0.35	0.03	0.59	36.50	99.4
A290B-Ol-4	29.80	35.70	0.41	0.00	0.45	33.40	99.8
A290B-Ol-5	28.00	35.50	0.34	0.01	0.47	34.50	98.8
A290B-Ol-6	30.00	36.50	0.37	0.00	0.45	32.90	100.2
Average	**29.05**	**35.78**	**0.37**	**0.01**	**0.48**	**33.75**	**99.4**
B319-Ol-1	28.50	35.40	0.31	0.01	0.51	33.80	98.5
B319-Ol-2	26.50	34.90	0.37	0.02	0.57	36.90	99.3
B319-Ol-3	24.00	34.20	0.45	0.00	0.64	40.30	99.6
B319-Ol-4	25.70	35.40	0.43	0.00	0.57	38.10	100.2
B319-Ol-5	22.70	34.30	0.41	0.02	0.63	42.40	100.5
B319-Ol-6	22.80	34.30	0.40	0.02	0.61	42.00	100.1
B319-Ol-7	25.70	35.00	0.36	0.03	0.57	38.10	99.8
B319-Ol-8	26.00	35.30	0.35	0.00	0.56	38.80	101.0
Average	**25.24**	**34.85**	**0.39**	**0.01**	**0.58**	**38.80**	**99.9**
C179B-Ol-1	22.60	34.40	0.34	0.00	0.61	41.50	99.5
C179B-Ol-2	22.80	34.90	0.38	0.04	0.60	40.80	99.5
C179B-Ol-3	23.10	34.50	0.34	0.00	0.62	40.80	99.4
C179B-Ol-4	23.50	34.00	0.37	0.01	0.63	40.50	99.0
C179B-Ol-5	19.80	33.20	0.41	0.02	0.72	44.90	99.1
C179B-Ol-6	21.20	34.00	0.42	0.01	0.70	43.00	99.3
Average	**22.17**	**34.17**	**0.38**	**0.01**	**0.65**	**41.92**	**99.3**
B190-Ol-1	17.10	32.60	0.36	0.02	0.74	48.00	98.8
B190-Ol-2	16.70	33.30	0.34	0.02	0.77	48.00	99.1
B190-Ol-3	16.10	32.80	0.37	0.00	0.80	48.80	98.9
Average	**16.63**	**32.90**	**0.36**	**0.01**	**0.77**	**48.27**	**98.9**
C442A-Ol-1	14.30	32.20	0.35	0.00	0.82	51.50	99.2
C442A-Ol-2	14.40	32.40	0.39	0.02	0.81	51.60	99.6
C442A-Ol-3	14.10	33.60	0.33	0.05	0.77	51.20	100.1
C442A-Ol-4	14.20	33.00	0.34	0.01	0.81	51.50	99.9
C442A-Ol-5	14.00	31.90	0.36	0.02	0.80	51.80	98.9
Average	**14.20**	**32.62**	**0.35**	**0.02**	**0.80**	**51.52**	**99.5**
D193-Ol-1	18.80	32.60	0.36	0.02	0.81	47.30	99.9
D193-Ol-2	18.70	32.80	0.38	0.00	0.74	47.00	99.6
D193-Ol-3	14.00	32.40	0.36	0.03	0.87	52.40	100.1
D193-Ol-4	13.40	32.20	0.33	0.03	0.90	52.80	99.7
Average	**16.23**	**32.50**	**0.36**	**0.02**	**0.83**	**49.88**	**99.8**
F261-Ol-1	17.90	32.50	0.43	0.00	0.73	48.80	100.4
F261-Ol-2	17.40	33.10	0.42	0.10	0.73	49.10	100.9
F261-Ol-3	17.90	32.10	0.43	0.00	0.71	49.00	100.1
Average	**17.73**	**32.57**	**0.43**	**0.03**	**0.72**	**48.97**	**100.5**

Appendix B - Olivine - BRD Sample Suite

Sample	CAT sum	Si	Fe	Mg	Mn	Ca	Ti	Total	Mg#
A290B-Ol-1	1.67	1.00	0.77	1.21	0.01	0.01	0.00	3.00	61.1
A290B-Ol-2	1.66	0.99	0.74	1.25	0.01	0.01	0.00	3.01	62.9
A290B-Ol-3	1.70	0.99	0.86	1.12	0.01	0.01	0.00	3.01	56.6
A290B-Ol-4	1.66	0.99	0.77	1.23	0.01	0.01	0.00	3.01	61.4
A290B-Ol-5	1.69	1.00	0.81	1.17	0.01	0.01	0.00	3.00	59.1
A290B-Ol-6	1.65	1.00	0.75	1.23	0.01	0.01	0.00	3.00	61.9
Average	**1.67**	**0.99**	**0.78**	**1.20**	**0.01**	**0.01**	**0.00**	**3.01**	**60.5**
B319-Ol-1	1.69	0.99	0.79	1.19	0.01	0.01	0.00	3.00	60.0
B319-Ol-2	1.70	0.99	0.87	1.12	0.01	0.01	0.00	3.01	56.1
B319-Ol-3	1.73	0.98	0.97	1.03	0.02	0.01	0.00	3.02	51.5
B319-Ol-4	1.69	1.00	0.90	1.08	0.01	0.01	0.00	3.00	54.6
B319-Ol-5	1.73	0.99	1.02	0.97	0.02	0.01	0.00	3.01	48.8
B319-Ol-6	1.73	0.99	1.01	0.98	0.01	0.01	0.00	3.01	49.2
B319-Ol-7	1.70	0.99	0.90	1.09	0.01	0.01	0.00	3.01	54.6
B319-Ol-8	1.68	0.99	0.91	1.09	0.01	0.01	0.00	3.01	54.4
Average	**1.71**	**0.99**	**0.92**	**1.07**	**0.01**	**0.01**	**0.00**	**3.01**	**53.7**
C179B-Ol-1	1.74	1.00	1.01	0.98	0.01	0.01	0.00	3.00	49.3
C179B-Ol-2	1.73	1.01	0.98	0.98	0.01	0.01	0.00	2.99	49.9
C179B-Ol-3	1.74	1.00	0.99	0.99	0.02	0.01	0.00	3.00	50.2
C179B-Ol-4	1.74	0.99	0.98	1.02	0.02	0.01	0.00	3.01	50.8
C179B-Ol-5	1.79	0.99	1.12	0.88	0.02	0.01	0.00	3.01	44.0
C179B-Ol-6	1.76	1.00	1.05	0.93	0.02	0.01	0.00	3.00	46.8
Average	**1.75**	**0.99**	**1.02**	**0.96**	**0.02**	**0.01**	**0.00**	**3.01**	**48.5**
B190-Ol-1	1.82	0.99	1.22	0.77	0.02	0.01	0.00	3.01	38.8
B190-Ol-2	1.81	1.00	1.21	0.75	0.02	0.01	0.00	3.00	38.3
B190-Ol-3	1.83	1.00	1.24	0.73	0.02	0.01	0.00	3.00	37.0
Average	**1.82**	**1.00**	**1.22**	**0.75**	**0.02**	**0.01**	**0.00**	**3.00**	**38.1**
C442A-Ol-1	1.85	0.99	1.33	0.66	0.02	0.01	0.00	3.01	33.1
C442A-Ol-2	1.84	0.99	1.32	0.66	0.02	0.01	0.00	3.01	33.2
C442A-Ol-3	1.82	1.02	1.30	0.64	0.02	0.01	0.00	2.98	32.9
C442A-Ol-4	1.83	1.01	1.31	0.64	0.02	0.01	0.00	2.99	33.0
C442A-Ol-5	1.86	0.99	1.34	0.65	0.02	0.01	0.00	3.01	32.5
Average	**1.84**	**1.00**	**1.32**	**0.65**	**0.02**	**0.01**	**0.00**	**3.00**	**32.9**
D193-Ol-1	1.80	0.97	1.18	0.84	0.02	0.01	0.00	3.03	41.5
D193-Ol-2	1.80	0.98	1.17	0.83	0.02	0.01	0.00	3.02	41.5
D193-Ol-3	1.84	0.99	1.34	0.64	0.02	0.01	0.00	3.01	32.3
D193-Ol-4	1.85	0.99	1.36	0.62	0.02	0.01	0.00	3.01	31.1
Average	**1.82**	**0.98**	**1.27**	**0.73**	**0.02**	**0.01**	**0.00**	**3.01**	**36.6**
F261-Ol-1	1.80	0.97	1.22	0.80	0.02	0.01	0.00	3.03	39.5
F261-Ol-2	1.79	0.98	1.22	0.77	0.02	0.01	0.00	3.01	38.7
F261-Ol-3	1.81	0.97	1.23	0.80	0.02	0.01	0.00	3.03	39.4
Average	**1.80**	**0.97**	**1.23**	**0.79**	**0.02**	**0.01**	**0.00**	**3.02**	**39.2**

Appendix B - Olivine - BRD Sample Suite

Sample	MgO	SiO2	CaO	TiO2	MnO	FeO	Total
G500A-Ol-1	12.40	32.70	0.25	0.00	0.70	53.90	100.0
G500A-Ol-2	12.40	32.50	0.28	0.00	0.76	53.80	99.7
G500A-Ol-3	12.20	32.90	0.28	0.00	0.89	55.00	101.3
G500A-Ol-4	11.80	32.80	0.28	0.00	0.90	52.90	98.7
G500A-Ol-5	12.00	33.20	0.31	0.00	0.80	54.20	100.5
G500A-Ol-6	12.00	32.60	0.28	0.00	0.80	53.90	99.6
Average	**12.13**	**32.78**	**0.28**	**0.00**	**0.81**	**53.95**	**100.0**
G500B-Ol-1	25.20	35.70	0.15	0.00	0.55	38.40	100.0
G500B-Ol-2	25.10	35.80	0.18	0.00	0.49	38.30	99.9
G500B-Ol-3	25.50	36.00	0.16	0.00	0.59	37.60	99.9
G500B-Ol-4	25.50	35.70	0.17	0.00	0.51	37.50	99.4
G500B-Ol-5	24.70	36.10	0.14	0.00	0.44	39.30	100.7
G500B-Ol-6	24.80	35.70	0.17	0.00	0.44	39.20	100.3
G500B-Ol-7	24.80	35.90	0.14	0.00	0.50	38.40	99.7
G500B-Ol-8	24.90	35.70	0.16	0.00	0.47	39.00	100.2
G500B-Ol-9	25.30	35.70	0.18	0.00	0.43	37.80	99.4
G500B-Ol-10	24.90	35.90	0.15	0.00	0.49	38.70	100.1
Average	**25.07**	**35.82**	**0.16**	**0.00**	**0.49**	**38.42**	**100.0**
G500C-Ol-1	7.50	32.10	0.30	0.00	1.08	60.40	101.4
G500C-Ol-2	7.40	31.30	0.29	0.00	0.98	60.10	100.1
G500C-Ol-3	7.20	31.30	0.30	0.00	1.07	60.20	100.1
G500C-Ol-4	7.50	31.60	0.31	0.00	0.98	59.30	99.7
G500C-Ol-5	7.30	31.50	0.28	0.00	1.02	60.10	100.2
G500C-Ol-6	7.50	31.60	0.35	0.00	1.03	59.10	99.6
G500C-Ol-7	7.30	31.40	0.33	0.00	1.04	60.30	100.4
Average	**7.39**	**31.54**	**0.31**	**0.00**	**1.03**	**59.93**	**100.2**
H515-Ol-1	10.70	32.60	0.23	0.00	0.79	55.70	100.0
H515-Ol-2	10.60	32.50	0.26	0.00	0.84	55.80	100.0
H515-Ol-3	9.80	32.30	0.18	0.00	0.99	56.80	100.1
H515-Ol-4	10.80	32.40	0.17	0.00	0.86	56.00	100.2
H515-Ol-5	6.60	31.60	0.20	0.00	0.79	61.70	100.9
H515-Ol-6	6.60	31.70	0.19	0.00	0.82	61.20	100.5
H515-Ol-7	6.60	31.60	0.17	0.00	0.87	61.70	100.9
Average	**8.81**	**32.10**	**0.20**	**0.00**	**0.85**	**58.41**	**100.4**
G536-Ol-1	16.10	33.20	0.27		0.69	49.30	99.6
G536-Ol-2	15.40	33.70	0.26	0.00	0.76	50.10	100.2
G536-Ol-3	16.10	33.50	0.28	0.00	0.67	49.20	99.8
G536-Ol-4	16.20	33.40	0.24	0.00	0.69	49.20	99.7
G536-Ol-5	16.20	33.80	0.28	0.00	0.57	49.40	100.3
Average	**16.00**	**33.52**	**0.27**	**0.00**	**0.68**	**49.44**	**99.9**

Appendix B - Olivine - BRD Sample Suite

Sample	CAT sum	Si	Fe	Mg	Mn	Ca	Ti	Total	Mg#
G500A-Ol-1	1.85	1.01	1.39	0.57	0.02	0.01	0.00	2.99	29.1
G500A-Ol-2	1.86	1.00	1.39	0.57	0.02	0.01	0.00	3.00	29.1
G500A-Ol-3	1.83	1.00	1.40	0.56	0.02	0.01	0.00	3.00	28.3
G500A-Ol-4	1.87	1.02	1.38	0.55	0.02	0.01	0.00	2.98	28.5
G500A-Ol-5	1.84	1.02	1.39	0.55	0.02	0.01	0.00	2.98	28.3
G500A-Ol-6	1.86	1.01	1.40	0.55	0.02	0.01	0.00	2.99	28.4
Average	**1.85**	**1.01**	**1.39**	**0.56**	**0.02**	**0.01**	**0.00**	**2.99**	**28.6**
G500B-Ol-1	1.70	1.01	0.91	1.06	0.01	0.00	0.00	2.99	53.9
G500B-Ol-2	1.70	1.01	0.90	1.06	0.01	0.01	0.00	2.99	53.9
G500B-Ol-3	1.69	1.01	0.88	1.07	0.01	0.00	0.00	2.99	54.7
G500B-Ol-4	1.70	1.01	0.89	1.08	0.01	0.01	0.00	2.99	54.8
G500B-Ol-5	1.69	1.01	0.92	1.03	0.01	0.00	0.00	2.99	52.8
G500B-Ol-6	1.70	1.01	0.93	1.04	0.01	0.01	0.00	2.99	53.0
G500B-Ol-7	1.70	1.02	0.91	1.05	0.01	0.00	0.00	2.98	53.5
G500B-Ol-8	1.70	1.01	0.92	1.05	0.01	0.00	0.00	2.99	53.2
G500B-Ol-9	1.70	1.01	0.89	1.07	0.01	0.01	0.00	2.99	54.4
G500B-Ol-10	1.69	1.01	0.91	1.05	0.01	0.00	0.00	2.99	53.4
Average	**1.70**	**1.01**	**0.91**	**1.05**	**0.01**	**0.00**	**0.00**	**2.99**	**53.8**
G500C-Ol-1	1.89	1.01	1.59	0.35	0.03	0.01	0.00	2.99	18.1
G500C-Ol-2	1.92	1.00	1.61	0.35	0.03	0.01	0.00	3.00	18.0
G500C-Ol-3	1.92	1.00	1.61	0.34	0.03	0.01	0.00	3.00	17.6
G500C-Ol-4	1.92	1.01	1.59	0.36	0.03	0.01	0.00	2.99	18.4
G500C-Ol-5	1.92	1.01	1.60	0.35	0.03	0.01	0.00	2.99	17.8
G500C-Ol-6	1.92	1.01	1.58	0.36	0.03	0.01	0.00	2.99	18.4
G500C-Ol-7	1.92	1.00	1.61	0.35	0.03	0.01	0.00	3.00	17.7
Average	**1.92**	**1.01**	**1.60**	**0.35**	**0.03**	**0.01**	**0.00**	**2.99**	**18.0**
H515-Ol-1	1.87	1.01	1.45	0.50	0.02	0.01	0.00	2.99	25.5
H515-Ol-2	1.87	1.01	1.45	0.49	0.02	0.01	0.00	2.99	25.3
H515-Ol-3	1.88	1.01	1.49	0.46	0.03	0.01	0.00	2.99	23.5
H515-Ol-4	1.87	1.01	1.46	0.50	0.02	0.01	0.00	2.99	25.6
H515-Ol-5	1.91	1.01	1.64	0.31	0.02	0.01	0.00	2.99	16.0
H515-Ol-6	1.92	1.01	1.63	0.31	0.02	0.01	0.00	2.99	16.1
H515-Ol-7	1.91	1.01	1.64	0.31	0.02	0.01	0.00	2.99	16.0
Average	**1.89**	**1.01**	**1.54**	**0.41**	**0.02**	**0.01**	**0.00**	**2.99**	**21.2**
G536-Ol-1	1.81	1.00	1.24	0.72	0.02	0.01	0.00	3.00	36.8
G536-Ol-2	1.80	1.01	1.26	0.69	0.02	0.01	0.00	2.99	35.4
G536-Ol-3	1.81	1.01	1.24	0.72	0.02	0.01	0.00	2.99	36.8
G536-Ol-4	1.81	1.00	1.24	0.73	0.02	0.01	0.00	3.00	37.0
G536-Ol-5	1.80	1.01	1.23	0.72	0.01	0.01	0.00	2.99	36.9
Average	**1.81**	**1.01**	**1.24**	**0.72**	**0.02**	**0.01**	**0.00**	**2.99**	**36.6**

Appendix B - Olivine GSF Sample Suite

Sample	MgO	SiO2	CaO	TiO2	MnO	FeO	Total
KP1-Ol-1	28.15	38.59	0.18	0.00	0.00	33.08	100.0
KP1-Ol-2	27.77	37.73	0.00	0.00	0.48	34.02	100.0
KP1-Ol-3	26.36	37.36	0.00	0.00	0.44	35.84	100.0
KP1-Ol-4	25.42	37.40	0.16	0.00	0.53	36.50	100.0
KP1-Ol-5	25.98	37.42	0.00	0.00	0.44	36.16	100.0
KP1-Ol-6	25.73	37.23	0.00	0.22	0.51	36.31	100.0
KP1-Ol-7	25.41	37.14	0.00	0.00	0.60	36.84	100.0
KP1-Ol-8	25.61	36.99	0.00	0.00	0.53	36.87	100.0
KP1-Ol-9	25.25	36.96	0.00	0.00	0.42	37.36	100.0
Average	**26.19**	**37.42**	**0.04**	**0.02**	**0.44**	**35.89**	**100.0**
KP5-Ol-1	29.24	37.78	0.00	0.30	0.57	32.11	100.0
KP5-Ol-2	29.30	37.72	0.25	0.00	0.53	32.20	100.0
KP5-Ol-3	28.51	38.00	0.00	0.00	0.32	33.17	100.0
KP5-Ol-4	28.92	37.75	0.17	0.00	0.55	32.61	100.0
KP5-Ol-5	32.12	38.06	0.15	0.00	0.33	29.33	100.0
KP5-Ol-6	23.62	44.56	4.88	0.61	0.38	25.94	100.0
KP5-Ol-7	30.83	38.12	0.15	0.00	0.46	30.44	100.0
KP5-Ol-8	31.11	38.46	0.00	0.00	0.53	29.91	100.0
Average	**29.21**	**38.81**	**0.70**	**0.11**	**0.46**	**30.71**	**100.0**
KP101-Ol-1	22.91	36.22	0.26	0.00	0.56	40.04	100.0
KP101-Ol-2	24.59	37.00	0.21	0.00	0.47	37.73	100.0
KP101-Ol-3	25.13	37.07	0.21	0.00	0.66	36.93	100.0
KP101-Ol-4	23.74	36.89	0.21	0.00	0.46	38.71	100.0
KP101-Ol-5	25.21	37.42	0.29	0.00	0.36	36.72	100.0
KP101-Ol-6	23.55	36.70	0.23	0.00	0.62	38.92	100.0
Average	**24.19**	**36.88**	**0.24**	**0.00**	**0.52**	**38.18**	**100.0**
KP108-Ol-1	24.50	58.72	0.48	0.00	0.00	16.31	100.0
KP108-Ol-2	24.06	57.08	0.79	0.00	0.00	18.07	100.0
KP108-Ol-3	28.87	34.09	0.16	0.00	0.53	36.35	100.0
KP108-Ol-4	28.72	34.35	0.16	0.00	0.71	36.05	100.0
KP108-Ol-5	28.11	34.28	0.15	0.00	0.61	36.84	100.0
KP108-Ol-6	28.63	34.32	0.20	0.00	0.56	36.30	100.0
Average	**27.15**	**42.14**	**0.32**	**0.00**	**0.40**	**29.99**	**100.0**
KP114-Ol-1	20.82	32.93	0.29	0.00	0.79	45.18	100.0
KP114-Ol-2	21.57	33.06	0.22	0.00	0.92	44.24	100.0
KP114-Ol-3	21.39	32.67	0.21	0.00	0.76	44.97	100.0
KP114-Ol-4	21.51	33.07	0.20	0.00	0.72	44.50	100.0
KP114-Ol-5	21.03	32.52	0.23	0.00	0.35	45.88	100.0
KP114-Ol-6	22.09	32.97	0.22	0.00	0.72	44.00	100.0
KP114-Ol-7	22.59	33.12	0.17	0.00	0.66	43.46	100.0
KP114-Ol-8	22.02	32.88	0.20	0.00	0.62	44.28	100.0
KP114-Ol-9	22.60	33.20	0.00	0.00	0.61	43.58	100.0
KP114-Ol-10	22.28	33.43	0.21	0.00	0.64	43.44	100.0
KP114-Ol-11	22.28	33.05	0.22	0.00	0.71	43.74	100.0
KP114-Ol-12	22.37	33.29	0.22	0.00	0.70	43.42	100.0
Average	**21.88**	**33.02**	**0.20**	**0.00**	**0.68**	**44.22**	**100.0**

Appendix B - Olivine GSF Sample Suite

Sample	CAT sum	Si	Fe	Mg	Mn	Ca	Ti	Total	Mg#
KP1-Ol-1	1.63	1.05	0.75	1.14	0.00	0.01	0.00	2.95	60.3
KP1-Ol-2	1.65	1.04	0.78	1.14	0.01	0.00	0.00	2.96	59.3
KP1-Ol-3	1.66	1.04	0.83	1.09	0.01	0.00	0.00	2.96	56.7
KP1-Ol-4	1.67	1.04	0.85	1.05	0.01	0.00	0.00	2.96	55.4
KP1-Ol-5	1.67	1.04	0.84	1.07	0.01	0.00	0.00	2.96	56.2
KP1-Ol-6	1.67	1.03	0.84	1.07	0.01	0.00	0.00	2.96	55.8
KP1-Ol-7	1.68	1.04	0.86	1.06	0.01	0.00	0.00	2.96	55.1
KP1-Ol-8	1.68	1.03	0.86	1.06	0.01	0.00	0.00	2.97	55.3
KP1-Ol-9	1.68	1.03	0.87	1.05	0.01	0.00	0.00	2.97	54.6
Average	**1.67**	**1.04**	**0.83**	**1.08**	**0.01**	**0.00**	**0.00**	**2.96**	**56.5**
KP5-Ol-1	1.64	1.03	0.73	1.19	0.01	0.00	0.01	2.97	61.9
KP5-Ol-2	1.64	1.03	0.73	1.19	0.01	0.01	0.00	2.97	61.9
KP5-Ol-3	1.64	1.04	0.76	1.16	0.01	0.00	0.00	2.96	60.5
KP5-Ol-4	1.64	1.03	0.74	1.18	0.01	0.00	0.00	2.97	61.3
KP5-Ol-5	1.61	1.02	0.66	1.29	0.01	0.00	0.00	2.98	66.1
KP5-Ol-6	1.58	1.17	0.57	0.92	0.01	0.14	0.01	2.82	61.9
KP5-Ol-7	1.62	1.03	0.69	1.24	0.01	0.00	0.00	2.97	64.4
KP5-Ol-8	1.62	1.03	0.67	1.25	0.01	0.00	0.00	2.97	65.0
Average	**1.62**	**1.05**	**0.69**	**1.18**	**0.01**	**0.02**	**0.00**	**2.95**	**62.9**
KP101-Ol-1	1.71	1.03	0.95	0.97	0.01	0.01	0.00	2.97	50.5
KP101-Ol-2	1.68	1.04	0.88	1.03	0.01	0.01	0.00	2.96	53.7
KP101-Ol-3	1.68	1.03	0.86	1.05	0.02	0.01	0.00	2.97	54.8
KP101-Ol-4	1.69	1.04	0.91	1.00	0.01	0.01	0.00	2.96	52.2
KP101-Ol-5	1.67	1.04	0.85	1.05	0.01	0.01	0.00	2.96	55.0
KP101-Ol-6	1.69	1.04	0.92	0.99	0.01	0.01	0.00	2.96	51.9
Average	**1.69**	**1.04**	**0.90**	**1.01**	**0.01**	**0.01**	**0.00**	**2.96**	**53.0**
KP108-Ol-1	1.43	1.40	0.32	0.87	0.00	0.01	0.00	2.60	72.8
KP108-Ol-2	1.45	1.38	0.36	0.86	0.00	0.02	0.00	2.62	70.4
KP108-Ol-3	1.69	0.96	0.85	1.21	0.01	0.00	0.00	3.04	58.6
KP108-Ol-4	1.69	0.96	0.85	1.20	0.02	0.00	0.00	3.04	58.7
KP108-Ol-5	1.69	0.97	0.87	1.18	0.01	0.00	0.00	3.03	57.6
KP108-Ol-6	1.69	0.96	0.85	1.20	0.01	0.01	0.00	3.04	58.4
Average	**1.61**	**1.10**	**0.69**	**1.09**	**0.01**	**0.01**	**0.00**	**2.90**	**62.8**
KP114-Ol-1	1.77	0.97	1.11	0.92	0.02	0.01	0.00	3.03	45.1
KP114-Ol-2	1.76	0.97	1.09	0.94	0.02	0.01	0.00	3.03	46.5
KP114-Ol-3	1.77	0.96	1.11	0.94	0.02	0.01	0.00	3.04	45.9
KP114-Ol-4	1.76	0.97	1.09	0.94	0.02	0.01	0.00	3.03	46.3
KP114-Ol-5	1.78	0.96	1.13	0.93	0.01	0.01	0.00	3.04	45.0
KP114-Ol-6	1.76	0.97	1.08	0.96	0.02	0.01	0.00	3.03	47.2
KP114-Ol-7	1.75	0.97	1.06	0.98	0.02	0.01	0.00	3.03	48.1
KP114-Ol-8	1.76	0.96	1.09	0.96	0.02	0.01	0.00	3.04	47.0
KP114-Ol-9	1.75	0.97	1.06	0.98	0.02	0.00	0.00	3.03	48.0
KP114-Ol-10	1.75	0.97	1.06	0.97	0.02	0.01	0.00	3.03	47.8
KP114-Ol-11	1.76	0.97	1.07	0.97	0.02	0.01	0.00	3.03	47.6
KP114-Ol-12	1.75	0.97	1.06	0.97	0.02	0.01	0.00	3.03	47.9
Average	**1.76**	**0.97**	**1.08**	**0.96**	**0.02**	**0.01**	**0.00**	**3.03**	**46.9**

Appendix B - Olivine GSF Sample Suite

Sample	MgO	SiO2	CaO	TiO2	MnO	FeO	Total
IR15-Ol-1	25.02	36.97	0.00	0.00	0.35	37.67	100.0
IR15-Ol-2	24.55	37.02	0.00	0.00	0.56	37.87	100.0
IR15-Ol-3	24.83	37.00	0.16	0.00	0.45	37.55	100.0
IR15-Ol-4	25.25	37.10	0.22	0.00	0.46	36.97	100.0
IR15-Ol-5	24.26	36.99	0.24	0.00	0.39	38.12	100.0
IR15-Ol-6	23.86	37.21	0.00	0.00	0.36	38.58	100.0
Average	**24.63**	**37.05**	**0.10**	**0.00**	**0.43**	**37.79**	**100.0**
IR19B-Ol-1	24.05	36.81	0.16	0.00	0.48	38.51	100.0
IR19B-Ol-2	27.49	38.10	0.00	0.00	0.61	33.80	100.0
IR19B-Ol-3	24.75	37.49	0.00	0.00	0.49	37.28	100.0
IR19B-Ol-4	24.87	37.22	0.18	0.00	0.36	37.37	100.0
IR19B-Ol-5	24.05	37.14	0.00	0.00	0.40	38.41	100.0
IR19B-Ol-6	24.44	36.69	0.15	0.00	0.41	38.30	100.0
Average	**24.94**	**37.24**	**0.08**	**0.00**	**0.46**	**37.28**	**100.0**

Appendix B - Olivine GSF Sample Suite

Sample	CAT sum	Si	Fe	Mg	Mn	Ca	Ti	Total	Mg#
IR15-Ol-1	1.68	1.03	0.88	1.04	0.01	0.00	0.00	2.97	54.2
IR15-Ol-2	1.68	1.04	0.89	1.03	0.01	0.00	0.00	2.96	53.6
IR15-Ol-3	1.68	1.04	0.88	1.04	0.01	0.00	0.00	2.96	54.1
IR15-Ol-4	1.68	1.03	0.86	1.05	0.01	0.01	0.00	2.97	54.9
IR15-Ol-5	1.69	1.04	0.89	1.01	0.01	0.01	0.00	2.96	53.1
IR15-Ol-6	1.69	1.04	0.91	1.00	0.01	0.00	0.00	2.96	52.4
Average	**1.68**	**1.04**	**0.88**	**1.03**	**0.01**	**0.00**	**0.00**	**2.96**	**53.7**
IR19B-Ol-1	1.69	1.04	0.91	1.01	0.01	0.00	0.00	2.96	52.7
IR19B-Ol-2	1.65	1.04	0.77	1.12	0.01	0.00	0.00	2.96	59.2
IR19B-Ol-3	1.68	1.05	0.87	1.03	0.01	0.00	0.00	2.95	54.2
IR19B-Ol-4	1.68	1.04	0.87	1.04	0.01	0.01	0.00	2.96	54.3
IR19B-Ol-5	1.69	1.04	0.90	1.01	0.01	0.00	0.00	2.96	52.7
IR19B-Ol-6	1.69	1.03	0.90	1.02	0.01	0.00	0.00	2.97	53.2
Average	**1.68**	**1.04**	**0.87**	**1.04**	**0.01**	**0.00**	**0.00**	**2.96**	**54.4**

Appendix B - Plagioclase Megacrysts

Sample	Na2O	CaO	Al2O3	FeO	MgO	K2O	SiO2	Total
KP101a-Core-1	4.30	13.26	30.30	0.63	0.00	0.17	51.34	100.00
KP101a-Core-2	4.31	13.32	30.77	0.55	0.00	0.14	50.92	100.01
KP101a-Core-3	4.07	13.06	30.92	0.63	0.19	0.00	51.13	100.00
KP101a-Core-4	4.26	13.30	30.85	0.57	0.00	0.16	50.85	99.99
KP101a-Core-5	4.09	12.77	30.34	0.73	0.00	0.22	51.85	100.00
KP101a-Core-6	3.59	12.09	29.55	0.77	0.00	0.00	54.00	100.00
KP101a-Core-7	3.75	13.24	30.20	0.60	0.00	0.18	52.04	100.01
KP101a-Core-8	2.22	11.54	27.43	0.83	0.24	0.00	57.74	100.00
KP101a-Core-9	3.26	10.32	27.05	6.79	4.33	0.00	48.24	99.99
KP101a-Core-10	3.95	12.51	30.22	1.52	0.80	0.16	50.84	100.00
KP101a-Core-11	3.75	12.66	32.01	0.65	0.00	0.00	50.93	100.00
KP101a-Core-12	3.90	14.03	30.82	0.72	0.00	0.00	50.52	99.99
KP101a-Core-13	2.13	16.43	33.22	0.65	0.00	0.00	47.57	100.00
KP101a-Core-14	1.88	12.16	23.99	10.39	4.91	0.00	46.67	100.00
KP101a-Core-15	3.91	12.29	29.63	0.83	0.00	0.00	53.33	99.99
KP101a-Core-16	4.24	13.43	30.42	0.57	0.00	0.17	51.18	100.01
KP101a-Core-17	1.34	11.29	27.41	3.88	2.43	0.15	53.50	100.00
KP101a-Core-18	4.40	13.10	30.27	0.70	0.00	0.15	51.38	100.00
Average	**3.52**	**12.82**	**29.74**	**1.78**	**0.72**	**0.08**	**51.34**	**100.00**
KP101a-Rim-1	4.46	11.11	29.82	0.93	0.00	0.19	53.48	99.99
KP101a-Rim-2	3.96	11.48	28.49	1.08	0.24	0.00	54.74	99.99
KP101a-Rim-3	4.42	12.92	30.86	0.66	0.00	0.00	51.13	99.99
KP101a-Rim-4	4.31	13.12	30.48	0.68	0.00	0.20	51.21	100.00
KP101a-Rim-5	5.78	10.30	27.90	0.88	0.00	0.29	54.86	100.01
KP101a-Rim-6	4.29	11.27	28.14	0.62	0.20	0.15	55.33	100.00
KP101a-Rim-7	4.25	13.31	31.34	0.56	0.00	0.00	50.55	100.01
KP101a-Rim-8	4.09	13.14	29.72	0.68	0.00	0.14	52.23	100.00
KP101a-Rim-9	6.52	9.94	27.48	0.00	0.00	0.49	55.58	100.01
KP101a-Rim-10	4.29	13.01	30.25	0.75	0.00	0.18	51.52	100.00
Average	**4.64**	**11.96**	**29.45**	**0.68**	**0.04**	**0.16**	**53.06**	**100.00**
KP101b-Core-1	3.84	13.43	30.47	0.44	0.00	0.00	51.82	100.00
KP101b-Core-2	3.56	13.09	29.79	1.22	0.49	0.00	51.83	99.98
KP101b-Core-3	2.43	13.30	29.23	0.88	0.29	0.14	53.73	100.00
KP101b-Core-4	2.59	15.76	32.74	0.76	0.00	0.00	48.15	100.00
KP101b-Core-5	2.81	15.60	32.74	0.74	0.00	0.00	48.11	100.00
KP101b-Core-6	2.42	10.73	25.92	3.95	2.54	0.20	54.24	100.00
KP101b-Core-7	3.65	14.35	31.42	0.38	0.00	0.00	50.19	99.99
KP101b-Core-8	3.62	14.38	31.91	0.59	0.00	0.00	49.50	100.00
KP101b-Core-9	2.39	7.99	28.34	0.42	0.00	0.21	60.64	99.99
KP101b-Core-10	4.13	13.66	30.76	0.65	0.00	0.00	50.79	99.99
KP101b-Core-11	5.13	11.67	28.90	0.53	0.00	0.33	53.44	100.00
Average	**3.32**	**13.09**	**30.20**	**0.96**	**0.30**	**0.08**	**52.04**	**100.00**
KP101b-Rim-1	4.73	8.74	26.18	0.80	0.00	0.29	59.26	100.00
KP101b-Rim-2	5.76	10.59	28.13	0.65	0.00	0.36	54.51	100.00
KP101b-Rim-3	4.06	13.22	30.58	0.68	0.00	0.12	51.34	100.00
KP101b-Rim-4	2.90	12.09	28.33	1.18	0.54	0.13	54.84	100.01
KP101b-Rim-5	4.68	11.56	28.47	0.46	0.22	0.20	54.41	100.00

Appendix B - Plagioclase Megacrysts

Sample	Cat Sum	Si	Al	Na	Ca	Fe	Mg	K	Total	An
KP101a-Core-1	2.74	2.34	1.63	0.38	0.65	0.02	0.00	0.01	5.04	62.4
KP101a-Core-2	2.74	2.32	1.66	0.38	0.65	0.02	0.00	0.01	5.04	62.6
KP101a-Core-3	2.74	2.33	1.66	0.36	0.64	0.02	0.01	0.00	5.02	63.9
KP101a-Core-4	2.74	2.32	1.66	0.38	0.65	0.02	0.00	0.01	5.04	62.7
KP101a-Core-5	2.74	2.36	1.63	0.36	0.62	0.03	0.00	0.01	5.01	62.5
KP101a-Core-6	2.71	2.44	1.57	0.31	0.58	0.03	0.00	0.00	4.94	65.0
KP101a-Core-7	2.73	2.37	1.62	0.33	0.65	0.02	0.00	0.01	4.99	65.4
KP101a-Core-8	2.68	2.57	1.44	0.19	0.55	0.03	0.02	0.00	4.80	74.2
KP101a-Core-9	2.82	2.26	1.49	0.30	0.52	0.27	0.30	0.00	5.14	63.6
KP101a-Core-10	2.75	2.33	1.63	0.35	0.61	0.06	0.05	0.01	5.04	63.0
KP101a-Core-11	2.73	2.31	1.71	0.33	0.62	0.02	0.00	0.00	5.00	65.1
KP101a-Core-12	2.75	2.31	1.66	0.35	0.69	0.03	0.00	0.00	5.03	66.5
KP101a-Core-13	2.76	2.19	1.80	0.19	0.81	0.02	0.00	0.00	5.01	81.0
KP101a-Core-14	2.89	2.24	1.36	0.18	0.63	0.42	0.35	0.00	5.17	78.1
KP101a-Core-15	2.72	2.41	1.58	0.34	0.60	0.03	0.00	0.00	4.97	63.5
KP101a-Core-16	2.74	2.34	1.64	0.38	0.66	0.02	0.00	0.01	5.04	63.0
KP101a-Core-17	2.73	2.43	1.47	0.12	0.55	0.15	0.16	0.01	4.89	81.3
KP101a-Core-18	2.74	2.35	1.63	0.39	0.64	0.03	0.00	0.01	5.04	61.7
Average	**2.75**	**2.35**	**1.60**	**0.31**	**0.63**	**0.07**	**0.05**	**0.00**	**5.01**	**67.0**
KP101a-Rim-1	2.72	2.42	1.59	0.39	0.54	0.04	0.00	0.01	4.99	57.2
KP101a-Rim-2	2.71	2.47	1.52	0.35	0.56	0.04	0.02	0.00	4.94	61.6
KP101a-Rim-3	2.74	2.33	1.66	0.39	0.63	0.03	0.00	0.00	5.04	61.8
KP101a-Rim-4	2.74	2.34	1.64	0.38	0.64	0.03	0.00	0.01	5.04	62.0
KP101a-Rim-5	2.72	2.48	1.49	0.51	0.50	0.03	0.00	0.02	5.03	48.8
KP101a-Rim-6	2.71	2.49	1.49	0.37	0.54	0.02	0.01	0.01	4.95	58.7
KP101a-Rim-7	2.74	2.31	1.69	0.38	0.65	0.02	0.00	0.00	5.04	63.4
KP101a-Rim-8	2.74	2.38	1.60	0.36	0.64	0.03	0.00	0.01	5.01	63.5
KP101a-Rim-9	2.72	2.51	1.46	0.57	0.48	0.00	0.00	0.03	5.06	44.5
KP101a-Rim-10	2.74	2.35	1.63	0.38	0.64	0.03	0.00	0.01	5.03	62.0
Average	**2.73**	**2.41**	**1.58**	**0.41**	**0.58**	**0.03**	**0.00**	**0.01**	**5.01**	**58.3**
KP101b-Core-1	2.73	2.36	1.63	0.34	0.65	0.02	0.00	0.00	5.00	65.9
KP101b-Core-2	2.74	2.36	1.60	0.31	0.64	0.05	0.03	0.00	5.00	67.0
KP101b-Core-3	2.72	2.43	1.56	0.21	0.64	0.03	0.02	0.01	4.90	74.5
KP101b-Core-4	2.76	2.21	1.77	0.23	0.78	0.03	0.00	0.00	5.02	77.1
KP101b-Core-5	2.76	2.21	1.77	0.25	0.77	0.03	0.00	0.00	5.03	75.4
KP101b-Core-6	2.74	2.47	1.39	0.21	0.52	0.15	0.17	0.01	4.94	69.9
KP101b-Core-7	2.74	2.29	1.69	0.32	0.70	0.01	0.00	0.00	5.02	68.5
KP101b-Core-8	2.75	2.26	1.72	0.32	0.71	0.02	0.00	0.00	5.03	68.7
KP101b-Core-9	2.63	2.65	1.46	0.20	0.37	0.02	0.00	0.01	4.72	63.6
KP101b-Core-10	2.74	2.32	1.66	0.37	0.67	0.02	0.00	0.00	5.04	64.6
KP101b-Core-11	2.73	2.43	1.55	0.45	0.57	0.02	0.00	0.02	5.03	54.7
Average	**2.73**	**2.36**	**1.62**	**0.29**	**0.64**	**0.04**	**0.02**	**0.00**	**4.98**	**68.2**
KP101b-Rim-1	2.68	2.64	1.37	0.41	0.42	0.03	0.00	0.02	4.89	49.5
KP101b-Rim-2	2.72	2.47	1.50	0.51	0.51	0.02	0.00	0.02	5.04	49.4
KP101b-Rim-3	2.74	2.34	1.64	0.36	0.65	0.03	0.00	0.01	5.02	63.8
KP101b-Rim-4	2.71	2.47	1.51	0.25	0.58	0.04	0.04	0.01	4.90	69.1
KP101b-Rim-5	2.72	2.46	1.52	0.41	0.56	0.02	0.01	0.01	4.99	57.0

Appendix B - Plagioclase Megacrysts

Sample	Na2O	CaO	Al2O3	FeO	MgO	K2O	SiO2	Total
KP101b-Rim-6	6.15	10.07	27.71	0.61	0.00	0.36	55.11	100.01
KP101b-Rim-7	3.85	14.01	31.21	0.32	0.00	0.14	50.47	100.00
KP101b-Rim-8	2.74	6.61	19.16	0.46	0.00	0.16	70.87	100.00
Average	**4.36**	**10.86**	**27.47**	**0.65**	**0.10**	**0.22**	**56.35**	**100.00**
KP101-gm-1	4.61	11.01	27.91	0.75	0.00	0.42	55.30	100.00
KP101-gm-2	4.12	11.89	28.53	0.68	0.00	0.35	54.44	100.01
KP101-gm-3	4.30	12.26	28.94	0.61	0.00	0.25	53.65	100.01
KP101-gm-4	4.61	10.81	27.19	0.77	0.00	0.47	56.15	100.00
KP101-gm-5	4.43	11.21	27.70	0.40	0.00	0.37	55.88	99.99
KP101-gm-6	4.05	12.16	28.64	0.73	0.00	0.27	54.16	100.01
KP101-gm-7	4.20	11.99	28.23	0.93	0.00	0.36	54.29	100.00
KP101-gm-8	4.05	12.12	28.93	0.47	0.00	0.30	54.13	100.00
KP101-gm-9	5.36	8.62	25.17	0.51	0.00	0.75	59.59	100.00
KP101-gm-10	4.62	10.37	28.59	0.82	0.25	0.36	54.99	100.00
KP101-gm-11	7.11	6.24	23.46	0.42	0.00	0.85	61.92	100.00
Average	**4.68**	**10.79**	**27.57**	**0.64**	**0.02**	**0.43**	**55.86**	**100.00**
IR12b-Core-1	4.35	13.24	31.15	0.66	0.00	0.14	50.45	99.99
IR12b-Core-2	2.64	15.94	33.19	0.87	0.00	0.00	47.36	100.00
IR12b-Core-3	2.44	16.34	33.49	0.63	0.00	0.00	47.09	99.99
IR12b-Core-4	3.69	15.08	32.81	0.58	0.00	0.00	47.83	99.99
IR12b-Core-5	2.30	16.29	33.56	0.65	0.00	0.00	47.20	100.00
IR12b-Core-6	2.47	16.33	33.27	0.62	0.00	0.00	47.31	100.00
IR12b-Core-7	3.01	15.19	32.74	0.81	0.00	0.00	48.24	99.99
IR12b-Core-8	2.54	16.16	33.25	0.82	0.00	0.00	47.23	100.00
IR12b-Core-9	2.53	16.10	33.14	0.61	0.00	0.00	47.61	99.99
IR12b-Core-10	2.57	16.05	32.43	0.69	0.00	0.17	48.10	100.01
IR12b-Core-11	2.60	16.15	33.07	0.79	0.00	0.00	47.39	100.00
IR12b-Core-12	2.30	16.36	33.33	0.80	0.00	0.00	47.22	100.01
Average	**2.79**	**15.77**	**32.95**	**0.71**	**0.00**	**0.03**	**47.75**	**100.00**
IR12b-Rim-1	5.65	11.14	28.80	0.88	0.00	0.32	53.20	99.99
IR12b-Rim-2	2.73	15.95	32.88	0.83	0.00	0.00	47.61	100.00
IR12b-Rim-3	3.97	13.70	31.17	0.61	0.00	0.00	50.55	100.00
IR12b-Rim-4	4.66	12.58	29.66	0.71	0.00	0.17	52.22	100.00
IR12b-Rim-5	3.03	15.07	32.31	0.80	0.00	0.15	48.65	100.01
IR12b-Rim-6	3.90	14.80	33.35	0.70	0.00	0.00	47.25	100.00
IR12b-Rim-7	6.46	9.57	27.36	1.03	0.00	0.39	55.19	100.00
IR12b-Rim-8	4.27	13.43	30.73	0.97	0.00	0.28	50.32	100.00
IR12b-Rim-9	5.14	11.23	28.39	0.89	0.00	0.24	54.12	100.01
Average	**4.42**	**13.05**	**30.52**	**0.82**	**0.00**	**0.17**	**51.01**	**100.00**
IR12-gm-1	8.14	5.14	29.88	0.00	0.00	0.00	56.84	100.00
IR12-gm-2	5.39	9.67	26.32	0.74	0.00	0.40	57.49	100.01
IR12-gm-3	3.69	12.87	30.05	0.72	0.00	0.00	52.66	99.99
IR12-gm-4	7.64	2.52	20.01	0.38	0.00	2.87	66.57	99.99
IR12-gm-5	5.39	9.67	26.32	0.74	0.00	0.40	57.49	100.01
IR12-gm-6	11.28	4.60	29.21	0.28	0.00	0.00	54.63	100.00

Appendix B - Plagioclase Megacrysts

Sample	Cat Sum	Si	Al	Na	Ca	Fe	Mg	K	Total	An
KP101b-Rim-6	2.72	2.49	1.48	0.54	0.49	0.02	0.00	0.02	5.05	46.6
KP101b-Rim-7	2.74	2.30	1.68	0.34	0.69	0.01	0.00	0.01	5.03	66.3
KP101b-Rim-8	2.59	3.05	0.97	0.23	0.30	0.02	0.00	0.01	4.58	56.2
Average	**2.70**	**2.53**	**1.46**	**0.38**	**0.53**	**0.02**	**0.01**	**0.01**	**4.94**	**57.2**
KP101-gm-1	2.71	2.50	1.49	0.40	0.53	0.03	0.00	0.02	4.97	55.5
KP101-gm-2	2.72	2.46	1.52	0.36	0.58	0.03	0.00	0.02	4.97	60.2
KP101-gm-3	2.72	2.43	1.55	0.38	0.60	0.02	0.00	0.01	4.99	60.3
KP101-gm-4	2.71	2.53	1.45	0.40	0.52	0.03	0.00	0.03	4.96	54.8
KP101-gm-5	2.71	2.52	1.47	0.39	0.54	0.02	0.00	0.02	4.95	57.0
KP101-gm-6	2.72	2.45	1.53	0.36	0.59	0.03	0.00	0.02	4.97	61.4
KP101-gm-7	2.72	2.46	1.51	0.37	0.58	0.04	0.00	0.02	4.98	59.9
KP101-gm-8	2.72	2.45	1.54	0.36	0.59	0.02	0.00	0.02	4.97	61.2
KP101-gm-9	2.69	2.66	1.33	0.46	0.41	0.02	0.00	0.04	4.93	44.9
KP101-gm-10	2.71	2.48	1.52	0.40	0.50	0.03	0.02	0.02	4.97	54.1
KP101-gm-11	2.67	2.76	1.23	0.61	0.30	0.02	0.00	0.05	4.96	31.0
Average	**2.71**	**2.52**	**1.47**	**0.41**	**0.52**	**0.02**	**0.00**	**0.02**	**4.97**	**54.6**
IR12b-Core-1	2.75	2.31	1.68	0.39	0.65	0.03	0.00	0.01	5.05	62.2
IR12b-Core-2	2.77	2.18	1.80	0.24	0.79	0.03	0.00	0.00	5.04	76.9
IR12b-Core-3	2.77	2.17	1.82	0.22	0.81	0.02	0.00	0.00	5.03	78.7
IR12b-Core-4	2.76	2.20	1.78	0.33	0.74	0.02	0.00	0.00	5.07	69.3
IR12b-Core-5	2.76	2.17	1.82	0.21	0.80	0.02	0.00	0.00	5.02	79.6
IR12b-Core-6	2.76	2.18	1.80	0.22	0.81	0.02	0.00	0.00	5.03	78.5
IR12b-Core-7	2.76	2.21	1.77	0.27	0.75	0.03	0.00	0.00	5.03	73.6
IR12b-Core-8	2.77	2.17	1.81	0.23	0.80	0.03	0.00	0.00	5.04	77.9
IR12b-Core-9	2.76	2.19	1.80	0.23	0.79	0.02	0.00	0.00	5.03	77.9
IR12b-Core-10	2.76	2.21	1.76	0.23	0.79	0.03	0.00	0.01	5.03	76.8
IR12b-Core-11	2.77	2.18	1.80	0.23	0.80	0.03	0.00	0.00	5.04	77.4
IR12b-Core-12	2.77	2.17	1.81	0.21	0.81	0.03	0.00	0.00	5.02	79.7
Average	**2.76**	**2.20**	**1.79**	**0.25**	**0.78**	**0.03**	**0.00**	**0.00**	**5.04**	**75.7**
IR12b-Rim-1	2.74	2.42	1.55	0.50	0.54	0.03	0.00	0.02	5.06	51.2
IR12b-Rim-2	2.77	2.19	1.78	0.24	0.79	0.03	0.00	0.00	5.04	76.4
IR12b-Rim-3	2.74	2.31	1.68	0.35	0.67	0.02	0.00	0.00	5.03	65.6
IR12b-Rim-4	2.74	2.38	1.59	0.41	0.61	0.03	0.00	0.01	5.04	59.3
IR12b-Rim-5	2.76	2.23	1.75	0.27	0.74	0.03	0.00	0.01	5.03	72.7
IR12b-Rim-6	2.77	2.18	1.81	0.35	0.73	0.03	0.00	0.00	5.09	67.7
IR12b-Rim-7	2.73	2.50	1.46	0.57	0.47	0.04	0.00	0.02	5.06	44.1
IR12b-Rim-8	2.75	2.31	1.66	0.38	0.66	0.04	0.00	0.02	5.06	62.5
IR12b-Rim-9	2.73	2.46	1.52	0.45	0.55	0.03	0.00	0.01	5.02	53.9
Average	**2.75**	**2.33**	**1.64**	**0.39**	**0.64**	**0.03**	**0.00**	**0.01**	**5.05**	**61.5**
IR12-gm-1	2.67	2.53	1.57	0.70	0.24	0.00	0.00	0.00	5.04	25.9
IR12-gm-2	2.70	2.58	1.39	0.47	0.47	0.03	0.00	0.02	4.96	48.6
IR12-gm-3	2.72	2.39	1.61	0.32	0.63	0.03	0.00	0.00	4.97	65.8
IR12-gm-4	2.66	2.95	1.04	0.66	0.12	0.01	0.00	0.16	4.94	12.8
IR12-gm-5	2.70	2.58	1.39	0.47	0.47	0.03	0.00	0.02	4.96	48.6
IR12-gm-6	2.72	2.47	1.56	0.99	0.22	0.01	0.00	0.00	5.25	18.4

Appendix B - Plagioclase Megacrysts

Sample	Na2O	CaO	Al2O3	FeO	MgO	K2O	SiO2	Total
IR12-gm-7	6.06	1.22	18.46	1.34	0.89	5.43	66.59	99.99
IR12-gm-8	5.33	9.74	26.70	0.90	0.00	0.32	57.01	100.00
IR12-gm-9	6.57	7.20	24.00	0.98	0.00	0.43	60.82	100.00
Average	**6.61**	**6.96**	**25.66**	**0.68**	**0.10**	**1.09**	**58.90**	**100.00**
IR15a-Core-1	3.21	15.15	32.55	0.40	0.00	0.00	48.68	99.99
IR15a-Core-2	3.12	14.83	32.41	0.81	0.00	0.13	48.70	100.00
IR15a-Core-3	3.08	15.00	32.54	0.77	0.00	0.14	48.46	99.99
IR15a-Core-4	3.28	15.03	32.18	0.62	0.00	0.17	48.71	99.99
IR15a-Core-5	3.17	15.93	31.35	2.44	0.00	0.00	47.11	100.00
IR15a-Core-6	3.20	15.24	32.16	0.45	0.00	0.00	48.94	99.99
IR15a-Core-7	3.22	14.82	32.62	0.37	0.00	0.00	48.97	100.00
IR15a-Core-8	3.11	14.69	32.59	0.84	0.00	0.00	48.77	100.00
IR15a-Core-9	3.21	15.01	32.45	0.80	0.00	0.00	48.54	100.01
IR15a-Core-10	2.20	15.97	33.85	0.87	0.00	0.00	47.11	100.00
IR15a-Core-11	3.21	14.80	32.52	0.65	0.00	0.19	48.63	100.00
IR15a-Core-12	3.12	15.06	32.07	0.53	0.00	0.00	49.22	100.00
IR15a-Core-13	2.96	14.01	30.13	0.47	0.00	0.13	52.30	100.00
IR15a-Core-14	2.62	14.52	30.63	0.53	0.00	0.16	51.54	100.00
IR15a-Core-15	4.47	11.60	28.02	0.48	0.00	0.35	55.08	100.00
IR15a-Core-16	2.09	15.81	31.88	0.43	0.00	0.00	49.79	100.00
IR15a-Core-17	3.19	13.92	30.13	0.55	0.00	0.20	52.00	99.99
IR15a-Core-18	3.17	14.06	30.63	0.59	0.00	0.20	51.35	100.00
IR15a-Core-19	2.88	14.30	30.63	0.51	0.00	0.19	51.49	100.00
Average	**3.08**	**14.72**	**31.65**	**0.69**	**0.00**	**0.10**	**49.76**	**100.00**
IR15a-Rim-1	4.67	12.27	29.13	0.97	0.00	0.26	52.71	100.01
IR15a-Rim-2	3.21	15.12	32.13	0.76	0.00	0.13	48.64	99.99
IR15a-Rim-3	4.18	14.16	31.82	0.37	0.00	0.00	49.46	99.99
IR15a-Rim-4	3.92	13.92	31.10	0.60	0.00	0.29	50.17	100.00
IR15a-Rim-5	6.91	8.97	26.60	0.68	0.00	0.50	56.33	99.99
IR15a-Rim-6	5.06	11.35	29.03	0.78	0.00	0.49	53.29	100.00
IR15a-Rim-7	4.71	12.52	29.84	0.88	0.00	0.36	51.70	100.01
IR15a-Rim-8	2.98	15.24	32.22	1.08	0.00	0.23	48.25	100.00
IR15a-Rim-9	4.80	12.00	32.77	0.50	0.25	0.00	49.68	100.00
IR15a-Rim-10	5.68	10.71	27.90	0.76	0.29	0.39	54.26	99.99
IR15a-Rim-11	7.49	7.54	25.35	0.85	0.00	0.94	57.82	99.99
IR15a-Rim-12	6.01	11.91	27.40	0.62	0.00	0.99	53.07	100.00
IR15a-Rim-13	4.63	12.80	30.24	0.65	0.00	0.36	51.33	100.01
Average	**4.94**	**12.19**	**29.66**	**0.73**	**0.04**	**0.38**	**52.05**	**100.00**
IR15b-Core-1	2.20	15.97	33.85	0.87	0.00	0.00	47.11	100.00
IR15b-Core-2	6.37	9.67	27.02	0.82	0.00	0.65	55.46	99.99
IR15b-Core-3	5.70	8.71	28.58	1.77	0.60	0.39	54.24	99.99
IR15b-Core-4	4.61	12.40	29.96	0.94	0.00	0.22	51.87	100.00
IR15b-Core-5	5.12	11.92	28.84	0.89	0.00	0.37	52.86	100.00
IR15b-Core-6	5.28	11.27	28.54	0.86	0.00	0.42	53.63	100.00
IR15b-Core-7	2.32	16.30	33.16	0.86	0.00	0.16	47.20	100.00
IR15b-Core-8	4.69	12.08	29.51	0.70	0.00	0.42	52.60	100.00
IR15b-Core-9	4.75	12.50	30.28	0.86	0.00	0.32	51.29	100.00
IR15b-Core-10	4.17	13.06	30.35	0.76	0.00	0.28	51.38	100.00

Appendix B - Plagioclase Megacrysts

Sample	Cat Sum	Si	Al	Na	Ca	Fe	Mg	K	Total	An
IR12-gm-7	2.69	2.98	0.97	0.53	0.06	0.05	0.06	0.31	4.95	6.5
IR12-gm-8	2.70	2.57	1.42	0.47	0.47	0.03	0.00	0.02	4.97	49.3
IR12-gm-9	2.68	2.71	1.26	0.57	0.34	0.04	0.00	0.02	4.95	36.7
Average	**2.69**	**2.64**	**1.36**	**0.57**	**0.34**	**0.03**	**0.01**	**0.06**	**5.00**	**34.7**
IR15a-Core-1	2.75	2.23	1.76	0.29	0.74	0.02	0.00	0.00	5.03	72.3
IR15a-Core-2	2.76	2.23	1.75	0.28	0.73	0.03	0.00	0.01	5.03	71.9
IR15a-Core-3	2.76	2.22	1.76	0.27	0.74	0.03	0.00	0.01	5.04	72.3
IR15a-Core-4	2.76	2.24	1.74	0.29	0.74	0.02	0.00	0.01	5.04	71.0
IR15a-Core-5	2.80	2.19	1.72	0.29	0.79	0.10	0.00	0.00	5.09	73.5
IR15a-Core-6	2.75	2.24	1.74	0.28	0.75	0.02	0.00	0.00	5.03	72.5
IR15a-Core-7	2.75	2.24	1.76	0.29	0.73	0.01	0.00	0.00	5.02	71.8
IR15a-Core-8	2.75	2.23	1.76	0.28	0.72	0.03	0.00	0.00	5.02	72.3
IR15a-Core-9	2.76	2.23	1.76	0.29	0.74	0.03	0.00	0.00	5.04	72.1
IR15a-Core-10	2.76	2.17	1.83	0.20	0.79	0.03	0.00	0.00	5.02	80.0
IR15a-Core-11	2.76	2.23	1.76	0.29	0.73	0.02	0.00	0.01	5.04	71.0
IR15a-Core-12	2.75	2.25	1.73	0.28	0.74	0.02	0.00	0.00	5.02	72.7
IR15a-Core-13	2.73	2.37	1.61	0.26	0.68	0.02	0.00	0.01	4.95	71.8
IR15a-Core-14	2.73	2.34	1.64	0.23	0.71	0.02	0.00	0.01	4.95	74.6
IR15a-Core-15	2.71	2.49	1.49	0.39	0.56	0.02	0.00	0.02	4.97	57.7
IR15a-Core-16	2.74	2.27	1.72	0.18	0.77	0.02	0.00	0.00	4.96	80.7
IR15a-Core-17	2.73	2.37	1.62	0.28	0.68	0.02	0.00	0.01	4.97	69.8
IR15a-Core-18	2.74	2.34	1.64	0.28	0.69	0.02	0.00	0.01	4.98	70.2
IR15a-Core-19	2.73	2.34	1.64	0.25	0.70	0.02	0.00	0.01	4.97	72.4
Average	**2.75**	**2.28**	**1.71**	**0.27**	**0.72**	**0.03**	**0.00**	**0.01**	**5.01**	**72.1**
IR15a-Rim-1	2.74	2.40	1.56	0.41	0.60	0.04	0.00	0.02	5.03	58.3
IR15a-Rim-2	2.76	2.23	1.74	0.29	0.74	0.03	0.00	0.01	5.04	71.7
IR15a-Rim-3	2.75	2.26	1.72	0.37	0.69	0.01	0.00	0.00	5.06	65.2
IR15a-Rim-4	2.75	2.30	1.68	0.35	0.68	0.02	0.00	0.02	5.05	65.2
IR15a-Rim-5	2.72	2.55	1.42	0.61	0.43	0.03	0.00	0.03	5.06	40.6
IR15a-Rim-6	2.73	2.42	1.56	0.45	0.55	0.03	0.00	0.03	5.04	53.8
IR15a-Rim-7	2.75	2.36	1.61	0.42	0.61	0.03	0.00	0.02	5.05	58.3
IR15a-Rim-8	2.77	2.22	1.75	0.27	0.75	0.04	0.00	0.01	5.04	72.9
IR15a-Rim-9	2.74	2.26	1.76	0.42	0.59	0.02	0.02	0.00	5.07	58.0
IR15a-Rim-10	2.73	2.46	1.49	0.50	0.52	0.03	0.02	0.02	5.05	49.9
IR15a-Rim-11	2.71	2.61	1.35	0.66	0.36	0.03	0.00	0.05	5.07	33.9
IR15a-Rim-12	2.76	2.44	1.48	0.53	0.59	0.02	0.00	0.06	5.12	49.7
IR15a-Rim-13	2.75	2.34	1.63	0.41	0.63	0.02	0.00	0.02	5.06	59.2
Average	**2.74**	**2.37**	**1.60**	**0.44**	**0.60**	**0.03**	**0.00**	**0.02**	**5.06**	**56.7**
IR15b-Core-1	2.76	2.17	1.83	0.20	0.79	0.03	0.00	0.00	5.02	80.0
IR15b-Core-2	2.73	2.52	1.45	0.56	0.47	0.03	0.00	0.04	5.06	44.0
IR15b-Core-3	2.72	2.46	1.53	0.50	0.42	0.07	0.04	0.02	5.04	44.7
IR15b-Core-4	2.74	2.37	1.61	0.41	0.61	0.04	0.00	0.01	5.04	59.0
IR15b-Core-5	2.74	2.41	1.55	0.45	0.58	0.03	0.00	0.02	5.05	55.1
IR15b-Core-6	2.73	2.44	1.53	0.47	0.55	0.03	0.00	0.02	5.04	52.8
IR15b-Core-7	2.77	2.18	1.80	0.21	0.80	0.03	0.00	0.01	5.03	78.8
IR15b-Core-8	2.74	2.39	1.58	0.41	0.59	0.03	0.00	0.02	5.03	57.3
IR15b-Core-9	2.75	2.34	1.63	0.42	0.61	0.03	0.00	0.02	5.06	58.2
IR15b-Core-10	2.74	2.35	1.63	0.37	0.64	0.03	0.00	0.02	5.03	62.4

Appendix B - Plagioclase Megacrysts

Sample	Na2O	CaO	Al2O3	FeO	MgO	K2O	SiO2	Total
IR15b-Core-11	4.83	12.10	29.75	0.61	0.00	0.29	52.42	100.00
IR15b-Core-12	5.38	11.21	28.84	0.75	0.00	0.38	53.43	99.99
IR15b-Core-13	4.95	11.98	29.20	0.74	0.00	0.30	52.83	100.00
IR15b-Core-14	5.03	12.00	29.49	0.61	0.00	0.31	52.57	100.01
Average	**4.67**	**12.23**	**29.81**	**0.86**	**0.04**	**0.32**	**52.06**	**100.00**
IR15b-Core-1	2.79	14.49	30.63	0.62	0.00	0.14	51.34	100.01
IR15b-Core-2	2.79	14.36	31.18	0.62	0.00	0.17	50.88	100.00
IR15b-Core-3	2.41	14.79	31.14	0.68	0.00	0.13	50.84	99.99
IR15b-Core-4	2.72	14.60	30.87	0.46	0.00	0.00	51.35	100.00
IR15b-Core-5	2.85	14.52	30.90	0.61	0.00	0.16	50.95	99.99
IR15b-Core-6	2.79	14.37	30.70	0.57	0.00	0.13	51.43	99.99
IR15b-Core-7	2.61	14.68	30.89	0.45	0.00	0.21	51.17	100.01
IR15b-Core-8	2.87	14.45	30.81	0.68	0.00	0.00	51.19	100.00
Average	**2.73**	**14.53**	**30.89**	**0.59**	**0.00**	**0.12**	**51.14**	**100.00**
IR15b-Rim-1	4.91	11.96	29.64	0.86	0.00	0.29	52.35	100.01
IR15b-Rim-2	4.47	12.56	30.47	0.75	0.00	0.22	51.54	100.01
IR15b-Rim-3	4.28	13.04	30.28	0.68	0.00	0.28	51.44	100.00
IR15b-Rim-4	5.00	11.78	28.68	1.02	0.00	0.40	53.11	99.99
IR15b-Rim-5	4.92	12.37	29.79	0.62	0.00	0.26	52.04	100.00
IR15b-Rim-6	4.69	12.23	29.98	0.81	0.00	0.22	52.08	100.01
IR15b-Rim-7	5.11	11.80	29.47	0.50	0.00	0.20	52.92	100.00
IR15b-Rim-8	4.27	12.66	31.53	1.78	1.12	0.17	48.47	100.00
IR15b-Rim-9	2.95	14.72	31.79	1.78	0.63	0.00	48.14	100.01
Average	**4.51**	**12.57**	**30.18**	**0.98**	**0.19**	**0.23**	**51.34**	**100.00**
IR15-gm-1	5.33	9.50	26.12	0.73	0.00	0.46	57.86	100.00
IR15-gm-2	4.71	10.24	26.72	0.81	0.25	0.45	56.81	99.99
IR15-gm-3	4.02	12.11	28.17	0.87	0.00	0.23	54.60	100.00
IR15-gm-4	4.94	10.12	26.96	0.65	0.00	0.56	56.77	100.00
IR15-gm-5	4.99	10.31	27.07	0.72	0.00	0.52	56.39	100.00
IR15-gm-6	4.33	11.71	28.20	0.73	0.00	0.21	54.83	100.01
IR15-gm-7	5.33	9.50	26.12	0.73	0.00	0.46	57.86	100.00
IR15-gm-8	4.71	10.24	26.72	0.81	0.25	0.45	56.81	99.99
IR15-gm-9	4.02	12.11	28.17	0.87	0.00	0.23	54.60	100.00
IR15-gm-10	4.94	10.12	26.96	0.65	0.00	0.56	56.77	100.00
IR15-gm-11	4.99	10.31	27.07	0.72	0.00	0.52	56.39	100.00
IR15-gm-12	4.33	11.71	28.20	0.73	0.00	0.21	54.83	100.01
Average	**4.72**	**10.67**	**27.21**	**0.75**	**0.04**	**0.41**	**56.21**	**100.00**
IR21-Core-1	2.83	15.09	33.36	0.49	0.00	0.00	48.22	99.99
IR21-Core-2	3.31	14.38	32.39	0.53	0.00	0.14	49.26	100.01
IR21-Core-3	3.30	14.41	32.01	0.42	0.00	0.17	49.70	100.01
IR21-Core-4	3.24	14.39	32.74	0.46	0.00	0.00	49.17	100.00
IR21-Core-5	2.78	13.65	32.85	0.82	0.20	0.00	49.70	100.00
IR21-Core-6	2.61	12.88	42.64	0.10	0.00	0.21	42.59	101.03
IR21-Core-7	2.57	14.31	30.48	0.73	0.00	0.24	51.66	99.99
IR21-Core-8	2.63	14.83	33.25	0.70	0.00	0.00	48.59	100.00
IR21-Core-9	2.97	14.86	33.05	0.67	0.00	0.00	48.45	100.00

Appendix B - Plagioclase Megacrysts

Sample	Cat Sum	Si	Al	Na	Ca	Fe	Mg	K	Total	An
IR15b-Core-11	2.73	2.39	1.60	0.43	0.59	0.02	0.00	0.02	5.04	57.1
IR15b-Core-12	2.73	2.43	1.55	0.47	0.55	0.03	0.00	0.02	5.05	52.4
IR15b-Core-13	2.74	2.40	1.57	0.44	0.58	0.03	0.00	0.02	5.04	56.3
IR15b-Core-14	2.74	2.39	1.58	0.44	0.59	0.02	0.00	0.02	5.05	55.9
Average	**2.74**	**2.37**	**1.60**	**0.41**	**0.60**	**0.03**	**0.00**	**0.02**	**5.04**	**58.2**
IR15b-Core-1	2.74	2.34	1.64	0.25	0.71	0.02	0.00	0.01	4.97	73.5
IR15b-Core-2	2.74	2.32	1.67	0.25	0.70	0.02	0.00	0.01	4.97	73.2
IR15b-Core-3	2.74	2.32	1.67	0.21	0.72	0.03	0.00	0.01	4.96	76.6
IR15b-Core-4	2.73	2.33	1.65	0.24	0.71	0.02	0.00	0.00	4.96	74.8
IR15b-Core-5	2.74	2.32	1.66	0.25	0.71	0.02	0.00	0.01	4.98	73.1
IR15b-Core-6	2.73	2.34	1.65	0.25	0.70	0.02	0.00	0.01	4.96	73.4
IR15b-Core-7	2.74	2.33	1.66	0.23	0.72	0.02	0.00	0.01	4.96	74.7
IR15b-Core-8	2.74	2.33	1.65	0.25	0.70	0.03	0.00	0.00	4.97	73.6
Average	**2.74**	**2.33**	**1.66**	**0.24**	**0.71**	**0.02**	**0.00**	**0.01**	**4.97**	**74.1**
IR15b-Rim-1	2.74	2.39	1.59	0.43	0.58	0.03	0.00	0.02	5.04	56.4
IR15b-Rim-2	2.74	2.35	1.64	0.40	0.61	0.03	0.00	0.01	5.04	60.1
IR15b-Rim-3	2.74	2.35	1.63	0.38	0.64	0.03	0.00	0.02	5.04	61.7
IR15b-Rim-4	2.74	2.42	1.54	0.44	0.58	0.04	0.00	0.02	5.04	55.3
IR15b-Rim-5	2.74	2.37	1.60	0.43	0.60	0.02	0.00	0.02	5.05	57.3
IR15b-Rim-6	2.74	2.37	1.61	0.41	0.60	0.03	0.00	0.01	5.04	58.3
IR15b-Rim-7	2.73	2.40	1.58	0.45	0.57	0.02	0.00	0.01	5.04	55.4
IR15b-Rim-8	2.77	2.23	1.71	0.38	0.62	0.07	0.08	0.01	5.11	61.5
IR15b-Rim-9	2.77	2.22	1.73	0.26	0.73	0.07	0.04	0.00	5.05	73.4
Average	**2.74**	**2.34**	**1.63**	**0.40**	**0.62**	**0.04**	**0.01**	**0.01**	**5.05**	**59.9**
IR15-gm-1	2.70	2.60	1.38	0.46	0.46	0.03	0.00	0.03	4.96	48.2
IR15-gm-2	2.70	2.56	1.42	0.41	0.49	0.03	0.02	0.03	4.95	53.1
IR15-gm-3	2.72	2.47	1.50	0.35	0.59	0.03	0.00	0.01	4.96	61.6
IR15-gm-4	2.70	2.56	1.43	0.43	0.49	0.02	0.00	0.03	4.96	51.3
IR15-gm-5	2.71	2.54	1.44	0.44	0.50	0.03	0.00	0.03	4.97	51.7
IR15-gm-6	2.72	2.48	1.50	0.38	0.57	0.03	0.00	0.01	4.97	59.2
IR15-gm-7	2.70	2.60	1.38	0.46	0.46	0.03	0.00	0.03	4.96	48.2
IR15-gm-8	2.70	2.56	1.42	0.41	0.49	0.03	0.02	0.03	4.95	53.1
IR15-gm-9	2.72	2.47	1.50	0.35	0.59	0.03	0.00	0.01	4.96	61.6
IR15-gm-10	2.70	2.56	1.43	0.43	0.49	0.02	0.00	0.03	4.96	51.3
IR15-gm-11	2.71	2.54	1.44	0.44	0.50	0.03	0.00	0.03	4.97	51.7
IR15-gm-12	2.72	2.48	1.50	0.38	0.57	0.03	0.00	0.01	4.97	59.2
Average	**2.71**	**2.53**	**1.45**	**0.41**	**0.52**	**0.03**	**0.00**	**0.02**	**4.96**	**54.2**
IR21-Core-1	2.75	2.21	1.80	0.25	0.74	0.02	0.00	0.00	5.02	74.7
IR21-Core-2	2.75	2.25	1.75	0.29	0.70	0.02	0.00	0.01	5.03	70.0
IR21-Core-3	2.75	2.27	1.72	0.29	0.71	0.02	0.00	0.01	5.02	70.0
IR21-Core-4	2.74	2.25	1.76	0.29	0.70	0.02	0.00	0.00	5.02	71.1
IR21-Core-5	2.73	2.26	1.76	0.25	0.67	0.03	0.01	0.00	4.98	73.1
IR21-Core-6	2.71	1.92	2.27	0.23	0.62	0.00	0.00	0.01	5.06	72.1
IR21-Core-7	2.73	2.35	1.64	0.23	0.70	0.03	0.00	0.01	4.95	74.4
IR21-Core-8	2.75	2.22	1.79	0.23	0.73	0.03	0.00	0.00	5.00	75.7
IR21-Core-9	2.75	2.22	1.78	0.26	0.73	0.03	0.00	0.00	5.02	73.4

Appendix B - Plagioclase Megacrysts

Sample	Na2O	CaO	Al2O3	FeO	MgO	K2O	SiO2	Total
IR21-Core-10	3.42	14.17	32.56	0.74	0.00	0.00	49.10	99.99
IR21-Core-11	4.67	11.43	31.23	0.67	0.00	0.15	51.85	100.00
IR21-Core-12	3.22	14.25	32.67	0.53	0.00	0.00	49.34	100.01
Average	**3.13**	**14.05**	**33.27**	**0.57**	**0.02**	**0.08**	**48.97**	**100.09**
IR21-Rim-1	4.17	12.05	30.50	0.85	0.00	0.19	52.24	100.00
IR21-Rim-2	4.71	12.26	30.32	0.65	0.00	0.16	51.90	100.00
IR21-Rim-3	3.72	13.87	32.02	0.43	0.00	0.00	49.96	100.00
IR21-Rim-4	4.77	12.08	30.20	0.69	0.00	0.18	52.07	99.99
IR21-Rim-5	4.46	12.18	30.19	0.77	0.28	0.19	51.92	99.99
IR21-Rim-6	4.48	12.33	30.52	0.71	0.00	0.00	51.97	100.01
IR21-Rim-7	4.44	12.44	30.84	0.78	0.00	0.15	51.35	100.00
IR21-Rim-8	3.39	14.03	32.40	0.59	0.00	0.13	49.46	100.00
Average	**4.27**	**12.66**	**30.87**	**0.68**	**0.04**	**0.13**	**51.36**	**100.00**
IR21-gm-1	5.87	8.43	25.80	0.43	0.00	0.41	59.06	100.00
IR21-gm-2	4.19	11.92	28.78	0.36	0.00	0.18	54.57	100.00
IR21-gm-3	3.93	12.31	29.01	0.00	0.00	0.22	54.52	99.99
IR21-gm-4	5.03	10.23	27.44	0.00	0.00	0.40	56.90	100.00
IR21-gm-5	5.69	9.14	26.50	0.00	0.00	0.39	58.28	100.00
IR21-gm-6	5.22	10.11	27.13	0.00	0.00	0.33	57.21	100.00
IR21-gm-7	5.60	9.19	26.34	0.00	0.00	0.50	58.37	100.00
IR21-gm-8	5.82	6.68	24.92	0.48	0.00	0.57	61.52	99.99
IR21-gm-9	4.93	10.34	28.06	0.00	0.00	0.30	56.38	100.01
Average	**5.14**	**9.82**	**27.11**	**0.14**	**0.00**	**0.37**	**57.42**	**100.00**
SBI10a-Core-1	2.36	16.37	33.24	0.34	0.00	0.00	47.70	100.01
SBI10a-Core-2	3.08	14.92	32.10	0.62	0.00	0.00	49.28	100.00
SBI10a-Core-3	2.70	15.69	32.77	0.68	0.00	0.00	48.15	99.99
SBI10a-Core-4	4.17	11.19	26.51	0.63	0.00	0.00	57.50	100.00
SBI10a-Core-5	5.58	11.16	29.27	0.00	0.00	0.45	53.53	99.99
SBI10a-Core-6	3.35	15.25	31.59	0.46	0.00	0.23	49.12	100.00
SBI10a-Core-7	3.44	14.66	31.92	0.59	0.00	0.00	49.39	100.00
SBI10a-Core-8	4.14	14.01	30.85	0.56	0.00	0.00	50.44	100.00
SBI10a-Core-9	3.41	13.03	30.31	0.71	0.00	0.00	51.55	99.01
SBI10a-Core-10	4.05	13.99	31.00	0.41	0.00	0.00	50.55	100.00
SBI10a-Core-11	3.09	13.72	28.70	0.74	0.00	0.00	53.75	100.00
SBI10a-Core-12	3.35	15.25	31.59	0.46	0.00	0.23	49.12	100.00
SBI10a-Core-13	3.44	14.66	31.92	0.59	0.00	0.00	49.39	100.00
SBI10a-Core-14	2.18	15.14	32.01	0.32	0.00	0.00	50.36	100.01
SBI10a-Core-15	2.37	15.30	31.49	0.50	0.00	0.00	50.34	100.00
SBI10a-Core-16	4.09	12.29	28.54	0.81	0.00	0.15	54.12	100.00
SBI10a-Core-17	1.69	13.12	28.16	6.24	1.72	0.00	49.07	100.00
SBI10a-Core-18	2.05	16.10	32.07	0.42	0.00	0.00	49.37	100.01
SBI10a-Core-19	2.03	15.77	32.08	0.66	0.00	0.13	49.33	100.00
Average	**3.19**	**14.30**	**30.85**	**0.83**	**0.09**	**0.06**	**50.63**	**99.95**
SBI10a-Rim-1	4.67	12.78	30.43	0.70	0.00	0.21	51.21	100.00
SBI10a-Rim-2	4.18	13.30	30.35	0.99	0.20	0.00	50.98	100.00
SBI10a-Rim-3	4.31	12.95	29.71	0.58	0.00	0.00	52.45	100.00
SBI10a-Rim-4	4.41	13.03	30.31	0.71	0.00	0.00	51.55	100.01
SBI10a-Rim-5	4.05	13.99	31.00	0.41	0.00	0.00	50.55	100.00

Appendix B - Plagioclase Megacrysts

Sample	Cat Sum	Si	Al	Na	Ca	Fe	Mg	K	Total	An
IR21-Core-10	2.75	2.25	1.76	0.30	0.69	0.03	0.00	0.00	5.03	69.6
IR21-Core-11	2.73	2.35	1.67	0.41	0.56	0.03	0.00	0.01	5.02	57.0
IR21-Core-12	2.74	2.25	1.76	0.28	0.70	0.02	0.00	0.00	5.01	71.0
Average	**2.74**	**2.23**	**1.79**	**0.28**	**0.69**	**0.02**	**0.00**	**0.00**	**5.01**	**71.0**
IR21-Rim-1	2.73	2.37	1.63	0.37	0.59	0.03	0.00	0.01	5.00	60.8
IR21-Rim-2	2.73	2.36	1.63	0.42	0.60	0.02	0.00	0.01	5.04	58.5
IR21-Rim-3	2.74	2.28	1.72	0.33	0.68	0.02	0.00	0.00	5.02	67.3
IR21-Rim-4	2.73	2.37	1.62	0.42	0.59	0.03	0.00	0.01	5.04	57.7
IR21-Rim-5	2.73	2.36	1.62	0.39	0.59	0.03	0.02	0.01	5.03	59.5
IR21-Rim-6	2.73	2.36	1.63	0.39	0.60	0.03	0.00	0.00	5.02	60.3
IR21-Rim-7	2.74	2.34	1.66	0.39	0.61	0.03	0.00	0.01	5.03	60.2
IR21-Rim-8	2.75	2.26	1.75	0.30	0.69	0.02	0.00	0.01	5.02	69.0
Average	**2.74**	**2.34**	**1.66**	**0.38**	**0.62**	**0.03**	**0.00**	**0.01**	**5.03**	**61.7**
IR21-gm-1	2.68	2.64	1.36	0.51	0.40	0.02	0.00	0.02	4.95	43.1
IR21-gm-2	2.71	2.46	1.53	0.37	0.58	0.01	0.00	0.01	4.96	60.5
IR21-gm-3	2.71	2.46	1.54	0.34	0.59	0.00	0.00	0.01	4.95	62.5
IR21-gm-4	2.69	2.55	1.45	0.44	0.49	0.00	0.00	0.02	4.95	51.6
IR21-gm-5	2.69	2.60	1.40	0.49	0.44	0.00	0.00	0.02	4.95	45.9
IR21-gm-6	2.69	2.56	1.43	0.45	0.49	0.00	0.00	0.02	4.96	50.7
IR21-gm-7	2.69	2.61	1.39	0.49	0.44	0.00	0.00	0.03	4.95	46.1
IR21-gm-8	2.66	2.72	1.30	0.50	0.32	0.02	0.00	0.03	4.89	37.3
IR21-gm-9	2.69	2.53	1.48	0.43	0.50	0.00	0.00	0.02	4.95	52.7
Average	**2.69**	**2.57**	**1.43**	**0.45**	**0.47**	**0.01**	**0.00**	**0.02**	**4.95**	**50.1**
SBI10a-Core-1	2.76	2.19	1.80	0.21	0.81	0.01	0.00	0.00	5.02	79.3
SBI10a-Core-2	2.75	2.26	1.73	0.27	0.73	0.02	0.00	0.00	5.02	72.8
SBI10a-Core-3	2.76	2.21	1.77	0.24	0.77	0.03	0.00	0.00	5.02	76.3
SBI10a-Core-4	2.69	2.58	1.40	0.36	0.54	0.02	0.00	0.00	4.90	59.7
SBI10a-Core-5	2.72	2.43	1.56	0.49	0.54	0.00	0.00	0.03	5.05	51.2
SBI10a-Core-6	2.76	2.26	1.71	0.30	0.75	0.02	0.00	0.01	5.05	70.6
SBI10a-Core-7	2.75	2.26	1.72	0.31	0.72	0.02	0.00	0.00	5.03	70.2
SBI10a-Core-8	2.75	2.31	1.66	0.37	0.69	0.02	0.00	0.00	5.05	65.2
SBI10a-Core-9	2.75	2.36	1.64	0.30	0.64	0.03	0.00	0.00	4.97	67.9
SBI10a-Core-10	2.74	2.31	1.67	0.36	0.68	0.02	0.00	0.00	5.04	65.6
SBI10a-Core-11	2.72	2.44	1.53	0.27	0.67	0.03	0.00	0.00	4.93	71.0
SBI10a-Core-12	2.76	2.26	1.71	0.30	0.75	0.02	0.00	0.01	5.05	70.6
SBI10a-Core-13	2.75	2.26	1.72	0.31	0.72	0.02	0.00	0.00	5.03	70.2
SBI10a-Core-14	2.73	2.29	1.72	0.19	0.74	0.01	0.00	0.00	4.95	79.3
SBI10a-Core-15	2.74	2.30	1.69	0.21	0.75	0.02	0.00	0.00	4.96	78.1
SBI10a-Core-16	2.72	2.45	1.52	0.36	0.60	0.03	0.00	0.01	4.97	61.9
SBI10a-Core-17	2.80	2.29	1.55	0.15	0.66	0.24	0.12	0.00	5.01	81.1
SBI10a-Core-18	2.75	2.26	1.73	0.18	0.79	0.02	0.00	0.00	4.97	81.3
SBI10a-Core-19	2.75	2.26	1.73	0.18	0.77	0.03	0.00	0.01	4.97	80.5
Average	**2.75**	**2.31**	**1.66**	**0.28**	**0.70**	**0.03**	**0.01**	**0.00**	**5.00**	**71.2**
SBI10a-Rim-1	2.74	2.34	1.64	0.41	0.63	0.03	0.00	0.01	5.05	59.5
SBI10a-Rim-2	2.75	2.33	1.64	0.37	0.65	0.04	0.01	0.00	5.04	63.7
SBI10a-Rim-3	2.73	2.38	1.59	0.38	0.63	0.02	0.00	0.00	5.01	62.4
SBI10a-Rim-4	2.74	2.35	1.63	0.39	0.64	0.03	0.00	0.00	5.03	62.0
SBI10a-Rim-5	2.74	2.31	1.67	0.36	0.68	0.02	0.00	0.00	5.04	65.6

Appendix B - Plagioclase Megacrysts

Sample	Na2O	CaO	Al2O3	FeO	MgO	K2O	SiO2	Total
SBI10a-Rim-6	4.72	8.63	23.30	0.61	0.00	0.28	62.46	100.00
SBI10a-Rim-7	4.09	12.72	28.70	0.74	0.00	0.00	53.75	100.00
SBI10a-Rim-8	4.17	11.19	26.51	0.63	0.00	0.00	57.50	100.00
SBI10a-Rim-9	6.84	8.13	25.32	0.74	0.00	0.49	58.48	100.00
SBI10a-Rim-10	5.58	11.16	29.27	0.00	0.00	0.45	53.53	99.99
SBI10a-Rim-11	4.31	12.95	29.71	0.58	0.00	0.00	52.45	100.00
SBI10a-Rim-12	4.14	14.01	30.85	0.56	0.00	0.00	50.44	100.00
Average	**4.62**	**12.07**	**28.79**	**0.60**	**0.02**	**0.12**	**53.78**	**100.00**
SBI10b-Core-1	6.68	10.04	28.01	0.48	0.00	0.00	54.79	100.00
SBI10b-Core-2	2.86	15.49	32.99	0.42	0.00	0.00	48.23	99.99
SBI10b-Core-3	3.29	15.06	32.27	0.60	0.00	0.12	48.65	99.99
SBI10b-Core-4	2.69	15.38	32.52	1.41	0.32	0.00	47.68	100.00
SBI10b-Core-5	3.02	15.41	32.66	0.68	0.00	0.00	48.22	99.99
SBI10b-Core-6	2.83	15.80	33.01	0.54	0.00	0.00	47.82	100.00
SBI10b-Core-7	2.77	15.84	33.04	0.00	0.00	0.12	48.23	100.00
SBI10b-Core-8	3.14	15.02	32.56	0.34	0.00	0.00	48.94	100.00
SBI10b-Core-9	3.41	14.81	32.01	0.50	0.00	0.00	49.27	100.00
SBI10b-Core-10	2.98	15.29	32.72	0.54	0.00	0.00	48.48	100.01
SBI10b-Core-11	7.07	7.85	24.69	0.62	0.00	0.42	59.34	99.99
SBI10b-Core-12	2.68	15.66	32.80	0.62	0.00	0.00	48.24	100.00
SBI10b-Core-13	2.49	12.29	28.27	2.84	0.90	0.19	53.02	100.00
SBI10b-Core-14	2.48	13.75	28.92	3.85	1.27	0.00	49.74	100.01
SBI10b-Core-15	2.89	15.72	33.00	0.53	0.00	0.00	47.85	99.99
SBI10b-Core-16	3.24	14.37	31.29	2.07	0.63	0.00	48.39	99.99
SBI10b-Core-17	3.30	15.08	31.76	0.69	0.00	0.00	49.16	99.99
SBI10b-Core-18	3.13	15.23	32.47	0.42	0.00	0.20	48.54	99.99
SBI10b-Core-19	2.58	12.57	28.60	6.19	2.05	0.15	47.86	100.00
SBI10b-Core-20	2.54	16.09	33.28	0.35	0.00	0.00	47.73	99.99
SBI10b-Core-21	3.09	14.95	32.65	0.52	0.00	0.00	48.79	100.00
SBI10b-Core-22	3.16	15.31	31.67	0.40	0.00	0.00	49.45	99.99
SBI10b-Core-23	2.02	15.68	32.40	0.43	0.00	0.00	49.48	100.01
SBI10b-Core-24	2.87	14.38	30.97	0.39	0.00	0.15	51.25	100.01
SBI10b-Core-25	2.17	15.26	30.87	0.52	0.00	0.00	51.18	100.00
Average	**3.18**	**14.49**	**31.42**	**1.04**	**0.21**	**0.05**	**49.61**	**100.00**
SBI10b-Rim-1	4.16	13.70	31.12	0.52	0.00	0.18	50.32	100.00
SBI10b-Rim-2	1.96	8.99	32.62	0.57	0.00	0.00	55.86	100.00
SBI10b-Rim-3	6.59	9.50	27.62	0.46	0.00	0.37	55.45	99.99
SBI10b-Rim-4	4.98	10.37	26.26	0.88	0.26	0.29	56.97	100.01
SBI10b-Rim-5	2.80	14.42	29.87	0.64	0.00	0.00	52.27	100.00
SBI10b-Rim-6	2.85	15.71	32.80	0.37	0.00	0.00	48.27	100.00
SBI10b-Rim-7	3.87	12.53	28.98	0.66	0.00	0.20	53.77	100.01
SBI10b-Rim-8	5.00	10.72	27.19	0.63	0.00	0.40	56.06	100.00
SBI10b-Rim-9	7.44	5.60	23.03	0.00	0.00	0.90	63.03	100.00
Average	**4.41**	**11.28**	**28.83**	**0.53**	**0.03**	**0.26**	**54.67**	**100.00**
SBI10-gm-1	4.37	11.68	28.13	0.59	0.00	0.16	55.07	100.00
SBI10-gm-2	4.29	11.46	27.83	0.78	0.24	0.28	55.11	99.99
SBI10-gm-3	3.79	11.31	28.48	2.63	0.48	0.00	53.29	99.98
SBI10-gm-4	3.67	12.69	29.46	0.40	0.00	0.19	53.59	100.00
SBI10-gm-5	3.22	13.14	29.08	1.33	0.30	0.14	52.79	100.00

Appendix B - Plagioclase Megacrysts

Sample	Cat Sum	Si	Al	Na	Ca	Fe	Mg	K	Total	An
SBI10a-Rim-6	2.66	2.77	1.22	0.41	0.41	0.02	0.00	0.02	4.84	49.3
SBI10a-Rim-7	2.72	2.44	1.53	0.36	0.62	0.03	0.00	0.00	4.98	63.2
SBI10a-Rim-8	2.69	2.58	1.40	0.36	0.54	0.02	0.00	0.00	4.90	59.7
SBI10a-Rim-9	2.70	2.63	1.34	0.60	0.39	0.03	0.00	0.03	5.01	38.5
SBI10a-Rim-10	2.72	2.43	1.56	0.49	0.54	0.00	0.00	0.03	5.05	51.2
SBI10a-Rim-11	2.73	2.38	1.59	0.38	0.63	0.02	0.00	0.00	5.01	62.4
SBI10a-Rim-12	2.75	2.31	1.66	0.37	0.69	0.02	0.00	0.00	5.05	65.2
Average	**2.72**	**2.44**	**1.54**	**0.41**	**0.59**	**0.02**	**0.00**	**0.01**	**5.00**	**58.6**
SBI10b-Core-1	2.72	2.48	1.49	0.59	0.49	0.02	0.00	0.00	5.07	45.4
SBI10b-Core-2	2.75	2.21	1.78	0.25	0.76	0.02	0.00	0.00	5.02	75.0
SBI10b-Core-3	2.76	2.23	1.75	0.29	0.74	0.02	0.00	0.01	5.04	71.2
SBI10b-Core-4	2.77	2.20	1.77	0.24	0.76	0.05	0.02	0.00	5.04	76.0
SBI10b-Core-5	2.76	2.21	1.77	0.27	0.76	0.03	0.00	0.00	5.04	73.8
SBI10b-Core-6	2.76	2.20	1.79	0.25	0.78	0.02	0.00	0.00	5.04	75.5
SBI10b-Core-7	2.75	2.21	1.78	0.25	0.78	0.00	0.00	0.01	5.02	75.4
SBI10b-Core-8	2.75	2.24	1.76	0.28	0.74	0.01	0.00	0.00	5.02	72.6
SBI10b-Core-9	2.75	2.26	1.73	0.30	0.73	0.02	0.00	0.00	5.03	70.6
SBI10b-Core-10	2.75	2.22	1.77	0.26	0.75	0.02	0.00	0.00	5.03	73.9
SBI10b-Core-11	2.69	2.66	1.31	0.61	0.38	0.02	0.00	0.02	5.01	37.1
SBI10b-Core-12	2.76	2.21	1.77	0.24	0.77	0.02	0.00	0.00	5.02	76.4
SBI10b-Core-13	2.74	2.42	1.52	0.22	0.60	0.11	0.06	0.01	4.94	72.2
SBI10b-Core-14	2.78	2.30	1.58	0.22	0.68	0.15	0.09	0.00	5.02	75.4
SBI10b-Core-15	2.76	2.20	1.79	0.26	0.77	0.02	0.00	0.00	5.04	75.0
SBI10b-Core-16	2.77	2.23	1.70	0.29	0.71	0.08	0.04	0.00	5.06	71.0
SBI10b-Core-17	2.76	2.25	1.72	0.29	0.74	0.03	0.00	0.00	5.03	71.6
SBI10b-Core-18	2.76	2.23	1.76	0.28	0.75	0.02	0.00	0.01	5.04	72.1
SBI10b-Core-19	2.82	2.24	1.58	0.23	0.63	0.24	0.14	0.01	5.09	72.2
SBI10b-Core-20	2.76	2.19	1.80	0.23	0.79	0.01	0.00	0.00	5.02	77.8
SBI10b-Core-21	2.75	2.23	1.76	0.27	0.73	0.02	0.00	0.00	5.02	72.8
SBI10b-Core-22	2.75	2.26	1.71	0.28	0.75	0.02	0.00	0.00	5.02	72.8
SBI10b-Core-23	2.74	2.26	1.74	0.18	0.77	0.02	0.00	0.00	4.96	81.1
SBI10b-Core-24	2.73	2.33	1.66	0.25	0.70	0.01	0.00	0.01	4.97	72.8
SBI10b-Core-25	2.73	2.33	1.66	0.19	0.74	0.02	0.00	0.00	4.94	79.5
Average	**2.75**	**2.27**	**1.70**	**0.28**	**0.71**	**0.04**	**0.01**	**0.00**	**5.02**	**71.6**
SBI10b-Rim-1	2.75	2.30	1.68	0.37	0.67	0.02	0.00	0.01	5.05	63.9
SBI10b-Rim-2	2.65	2.46	1.70	0.17	0.42	0.02	0.00	0.00	4.77	71.7
SBI10b-Rim-3	2.72	2.51	1.47	0.58	0.46	0.02	0.00	0.02	5.06	43.4
SBI10b-Rim-4	2.71	2.57	1.39	0.43	0.50	0.03	0.02	0.02	4.96	52.6
SBI10b-Rim-5	2.73	2.38	1.60	0.25	0.70	0.02	0.00	0.00	4.95	74.0
SBI10b-Rim-6	2.76	2.21	1.77	0.25	0.77	0.01	0.00	0.00	5.03	75.3
SBI10b-Rim-7	2.72	2.44	1.55	0.34	0.61	0.02	0.00	0.01	4.97	63.4
SBI10b-Rim-8	2.71	2.53	1.45	0.44	0.52	0.02	0.00	0.02	4.98	53.0
SBI10b-Rim-9	2.66	2.79	1.20	0.64	0.27	0.00	0.00	0.05	4.95	27.8
Average	**2.71**	**2.46**	**1.53**	**0.39**	**0.55**	**0.02**	**0.00**	**0.01**	**4.97**	**58.3**
SBI10-gm-1	2.71	2.49	1.50	0.38	0.56	0.02	0.00	0.01	4.96	59.1
SBI10-gm-2	2.71	2.49	1.48	0.38	0.55	0.03	0.02	0.02	4.96	58.6
SBI10-gm-3	2.74	2.43	1.53	0.33	0.55	0.10	0.03	0.00	4.98	62.3
SBI10-gm-4	2.72	2.42	1.57	0.32	0.61	0.02	0.00	0.01	4.96	64.9
SBI10-gm-5	2.73	2.40	1.56	0.28	0.64	0.05	0.02	0.01	4.96	68.7

Appendix B - Plagioclase Megacrysts

Sample	Na2O	CaO	Al2O3	FeO	MgO	K2O	SiO2	Total
SBI10-gm-6	6.46	8.33	24.80	0.53	0.00	0.49	59.37	99.98
SBI10-gm-7	3.73	12.75	29.17	0.48	0.00	0.18	53.69	100.00
SBI10-gm-8	5.21	10.17	26.80	0.46	0.00	0.25	57.12	100.01
SBI10-gm-9	3.67	12.69	29.73	0.26	0.00	0.17	53.47	99.99
Average	**4.27**	**11.58**	**28.16**	**0.83**	**0.11**	**0.21**	**54.83**	**99.99**
B268a-Core-1	3.69	14.73	31.27	0.38	0.00	0.00	49.94	100.01
B268a-Core-2	3.48	15.41	31.46	0.43	0.00	0.00	49.21	99.99
B268a-Core-3	3.62	14.87	31.54	0.00	0.00	0.00	49.98	100.01
B268a-Core-4	3.54	15.49	31.26	0.47	0.00	0.00	49.24	100.00
B268a-Core-5	5.27	13.60	30.89	0.58	0.20	0.31	49.13	99.98
B268a-Core-6	3.39	15.24	31.25	0.75	0.00	0.00	49.37	100.00
B268a-Core-7	3.95	14.07	31.55	0.48	0.00	0.00	49.94	99.99
B268a-Core-8	3.43	15.42	31.46	0.48	0.00	0.00	49.20	99.99
B268a-Core-9	3.87	14.94	31.53	0.51	0.00	0.13	49.01	99.99
B268a-Core-10	3.59	15.11	31.66	0.00	0.00	0.00	49.65	100.01
B268a-Core-11	3.54	14.98	31.08	0.64	0.29	0.00	49.46	99.99
B268a-Core-12	3.69	14.03	31.81	0.50	0.00	0.00	49.97	100.00
B268a-Core-13	3.60	14.82	31.71	0.39	0.00	0.00	49.47	99.99
B268a-Core-14	3.65	14.48	30.18	1.46	1.03	0.00	49.19	99.99
B268a-Core-15	4.60	14.69	30.89	0.59	0.00	0.20	49.02	99.99
B268a-Core-16	3.59	15.01	31.59	0.00	0.00	0.00	49.81	100.00
B268a-Core-17	4.69	14.36	30.68	0.32	0.00	0.26	49.68	99.99
B268a-Core-18	3.55	15.30	31.29	0.58	0.00	0.14	49.12	99.98
B268a-Core-19	3.65	14.93	31.47	0.70	0.00	0.00	49.25	100.00
B268a-Core-20	3.82	14.55	31.21	0.43	0.00	0.00	49.98	99.99
B268a-Core-21	3.98	12.03	29.58	0.91	0.68	1.12	51.71	100.01
B268a-Core-22	3.73	14.34	31.56	0.00	0.00	0.00	50.37	100.00
B268a-Core-23	3.25	15.14	31.19	0.00	0.00	0.14	50.28	100.00
B268a-Core-24	3.50	14.57	31.18	0.37	0.24	0.00	50.14	100.00
B268a-Core-25	3.69	14.56	31.07	0.42	0.00	0.00	50.26	100.00
B268a-Core-26	3.83	14.32	31.49	0.00	0.00	0.15	50.22	100.01
B268a-Core-27	3.70	13.75	31.48	0.45	0.00	0.12	50.49	99.99
Average	**3.77**	**14.62**	**31.23**	**0.44**	**0.09**	**0.10**	**49.74**	**100.00**
B268a-Rim-1	3.96	14.17	31.48	0.57	0.00	0.00	49.82	100.00
B268a-Rim-2	3.71	14.83	31.09	0.31	0.00	0.17	49.88	99.99
B268a-Rim-3	3.40	15.66	31.19	0.55	0.00	0.17	49.03	100.00
B268a-Rim-4	3.63	14.68	31.25	0.35	0.00	0.00	50.09	100.00
Average	**3.68**	**14.84**	**31.25**	**0.45**	**0.00**	**0.09**	**49.71**	**100.00**
B268b-Core-1	4.43	12.76	29.98	0.89	0.41	0.15	51.38	100.00
B268b-Core-2	4.36	13.68	30.21	0.45	0.00	0.00	51.30	100.00
B268b-Core-3	4.27	13.60	30.36	0.54	0.00	0.20	51.03	100.00
B268b-Core-4	4.28	12.94	30.21	0.36	0.00	0.19	52.01	99.99
B268b-Core-5	4.17	13.24	30.69	0.37	0.00	0.00	51.53	100.00
B268b-Core-6	4.11	13.85	30.27	0.00	0.00	0.00	51.78	100.01
B268b-Core-7	4.26	13.04	30.77	0.45	0.00	0.00	51.48	100.00
B268b-Core-8	4.42	13.70	30.61	0.00	0.00	0.00	51.27	100.00

Appendix B - Plagioclase Megacrysts

Sample	Cat Sum	Si	Al	Na	Ca	Fe	Mg	K	Total	An
SBI10-gm-6	2.69	2.66	1.31	0.56	0.40	0.02	0.00	0.03	4.98	40.4
SBI10-gm-7	2.72	2.43	1.56	0.33	0.62	0.02	0.00	0.01	4.96	64.7
SBI10-gm-8	2.70	2.57	1.42	0.45	0.49	0.02	0.00	0.01	4.96	51.1
SBI10B-BG-5	2.72	2.42	1.58	0.32	0.61	0.01	0.00	0.01	4.96	65.0
Average	**2.72**	**2.48**	**1.50**	**0.37**	**0.56**	**0.03**	**0.01**	**0.01**	**4.96**	**59.4**
B268a-Core-1	2.75	2.28	1.69	0.33	0.72	0.01	0.00	0.00	5.04	68.8
B268a-Core-2	2.76	2.26	1.70	0.31	0.76	0.02	0.00	0.00	5.05	71.0
B268a-Core-3	2.74	2.28	1.70	0.32	0.73	0.00	0.00	0.00	5.03	69.4
B268a-Core-4	2.76	2.26	1.69	0.32	0.76	0.02	0.00	0.00	5.05	70.7
B268a-Core-5	2.77	2.26	1.68	0.47	0.67	0.02	0.01	0.02	5.14	57.9
B268a-Core-6	2.76	2.27	1.69	0.30	0.75	0.03	0.00	0.00	5.04	71.3
B268a-Core-7	2.75	2.28	1.70	0.35	0.69	0.02	0.00	0.00	5.04	66.3
B268a-Core-8	2.76	2.26	1.70	0.31	0.76	0.02	0.00	0.00	5.04	71.3
B268a-Core-9	2.76	2.25	1.71	0.34	0.74	0.02	0.00	0.01	5.07	67.6
B268a-Core-10	2.75	2.27	1.71	0.32	0.74	0.00	0.00	0.00	5.04	69.9
B268a-Core-11	2.76	2.27	1.68	0.31	0.74	0.02	0.02	0.00	5.05	70.0
B268a-Core-12	2.74	2.28	1.71	0.33	0.69	0.02	0.00	0.00	5.03	67.8
B268a-Core-13	2.75	2.27	1.71	0.32	0.73	0.01	0.00	0.00	5.04	69.5
B268a-Core-14	2.77	2.27	1.64	0.33	0.72	0.06	0.07	0.00	5.08	68.7
B268a-Core-15	2.77	2.26	1.68	0.41	0.73	0.02	0.00	0.01	5.11	63.2
B268a-Core-16	2.75	2.28	1.70	0.32	0.74	0.00	0.00	0.00	5.03	69.8
B268a-Core-17	2.76	2.28	1.66	0.42	0.71	0.01	0.00	0.02	5.10	62.0
B268a-Core-18	2.76	2.26	1.70	0.32	0.75	0.02	0.00	0.01	5.06	69.9
B268a-Core-19	2.76	2.26	1.70	0.32	0.73	0.03	0.00	0.00	5.05	69.3
B268a-Core-20	2.75	2.29	1.68	0.34	0.71	0.02	0.00	0.00	5.04	67.8
B268a-Core-21	2.75	2.36	1.59	0.35	0.59	0.03	0.05	0.07	5.05	58.5
B268a-Core-22	2.74	2.30	1.70	0.33	0.70	0.00	0.00	0.00	5.02	68.0
B268a-Core-23	2.74	2.30	1.68	0.29	0.74	0.00	0.00	0.01	5.01	71.5
B268a-Core-24	2.75	2.29	1.68	0.31	0.71	0.01	0.02	0.00	5.02	69.7
B268a-Core-25	2.75	2.30	1.67	0.33	0.71	0.02	0.00	0.00	5.03	68.6
B268a-Core-26	2.74	2.29	1.69	0.34	0.70	0.00	0.00	0.01	5.03	66.8
B268a-Core-27	2.74	2.30	1.69	0.33	0.67	0.02	0.00	0.01	5.02	66.8
Average	**2.75**	**2.28**	**1.69**	**0.34**	**0.72**	**0.02**	**0.01**	**0.01**	**5.05**	**67.9**
B268a-Rim-1	2.75	2.28	1.70	0.35	0.69	0.02	0.00	0.00	5.05	66.4
B268a-Rim-2	2.75	2.29	1.68	0.33	0.73	0.01	0.00	0.01	5.04	68.2
B268a-Rim-3	2.76	2.26	1.69	0.30	0.77	0.02	0.00	0.01	5.05	71.1
B268a-Rim-4	2.75	2.29	1.68	0.32	0.72	0.01	0.00	0.00	5.03	69.1
Average	**2.75**	**2.28**	**1.69**	**0.33**	**0.73**	**0.02**	**0.00**	**0.00**	**5.04**	**68.7**
B268b-Core-1	2.74	2.35	1.61	0.39	0.62	0.03	0.03	0.01	5.05	60.9
B268b-Core-2	2.74	2.34	1.63	0.39	0.67	0.02	0.00	0.00	5.04	63.4
B268b-Core-3	2.75	2.33	1.64	0.38	0.67	0.02	0.00	0.01	5.04	63.1
B268b-Core-4	2.73	2.37	1.62	0.38	0.63	0.01	0.00	0.01	5.02	61.9
B268b-Core-5	2.73	2.34	1.65	0.37	0.65	0.01	0.00	0.00	5.02	63.7
B268b-Core-6	2.73	2.35	1.62	0.36	0.67	0.00	0.00	0.00	5.01	65.1
B268b-Core-7	2.73	2.34	1.65	0.38	0.64	0.02	0.00	0.00	5.02	62.8
B268b-Core-8	2.74	2.34	1.64	0.39	0.67	0.00	0.00	0.00	5.04	63.1

Appendix B - Plagioclase Megacrysts

Sample	Na2O	CaO	Al2O3	FeO	MgO	K2O	SiO2	Total
B268b-Core-9	4.28	13.75	30.32	0.47	0.00	0.00	51.19	100.01
B268b-Core-10	4.42	13.10	30.43	0.52	0.19	0.00	51.34	100.00
B268b-Core-11	4.05	13.59	29.67	0.31	0.00	0.00	52.38	100.00
B268b-Core-12	4.28	13.51	30.18	0.37	0.00	0.13	51.54	100.01
Average	**4.28**	**13.40**	**30.31**	**0.39**	**0.05**	**0.06**	**51.52**	**100.00**
B268b-Rim-1	5.36	11.56	29.24	0.60	0.00	0.29	52.95	100.00
B268b-Rim-2	4.15	13.27	30.68	0.41	0.00	0.15	51.34	100.00
B268b-Rim-3	4.19	13.33	30.51	0.55	0.00	0.17	51.26	100.01
B268b-Rim-4	4.35	13.34	30.37	0.43	0.00	0.17	51.34	100.00
B268b-Rim-5	7.50	9.22	26.73	0.00	0.00	0.00	56.55	100.00
Average	6.47	9.71	26.83	1.02	0.20	0.32	55.46	100.01
	5.34	**11.74**	**29.06**	**0.50**	**0.03**	**0.18**	**53.15**	**100.00**
B268-gm-1	4.42	13.11	30.79			0.26	51.42	100.00
B268-gm-2	2.25	5.51	16.21	18.14	8.18	0.27	49.45	100.01
B268-gm-3	5.01	12.14	29.96			0.30	52.59	100.00
B268-gm-4	5.47	10.93	28.96			0.45	54.19	100.00
B268-gm-5	5.70	10.26	27.22	0.57		0.50	55.74	99.99
B268-gm-6	4.68	12.97	30.85				51.49	99.99
B268-gm-7	5.66	10.61	28.33	0.51		0.55	54.35	100.01
B268-gm-8	5.30	11.04	29.32			0.41	53.93	100.00
B268-gm-9	5.54	10.80	28.72			0.56	54.38	100.00
B268-gm-10	3.42	9.78	33.79	0.63			52.37	99.99
B268-gm-11	4.81	12.08	30.12				52.99	100.00
B268-gm-12	5.75	9.30	26.47	2.87	1.22	0.39	53.99	99.99
B268-gm-13	5.15	11.88	29.27			0.45	53.26	100.01
B268-gm-14	4.00	13.70	31.44	0.52		0.23	50.11	100.00
B268-gm-15	6.05	10.47	28.45			0.37	54.66	100.00
B268-gm-16	4.99	10.37	27.53	0.26	0.00	0.21	56.63	99.99
B268-gm-17	4.12	11.98	28.96	0.35	0.00	0.25	54.35	100.01
B268-gm-18	4.58	11.53	28.34	0.28	0.00	0.30	54.96	99.99
B268-gm-19	4.46	11.62	28.37	0.00	0.00	0.20	55.35	100.00
B268-gm-20	4.02	12.17	28.81	0.32	0.00	0.19	54.49	100.00
B268-gm-21	6.61	7.99	26.25	0.00	0.00	0.13	59.01	99.99
B268-gm-22	4.31	11.97	29.01	0.00	0.00	0.20	54.50	99.99
Average	**4.83**	**11.01**	**28.51**	**1.88**	**1.04**	**0.33**	**53.83**	**100.00**

Appendix B - Plagioclase Megacrysts

Sample	Cat Sum	Si	Al	Na	Ca	Fe	Mg	K	Total	An
B268b-Core-9	2.74	2.34	1.63	0.38	0.67	0.02	0.00	0.00	5.04	64.0
B268b-Core-10	2.74	2.34	1.64	0.39	0.64	0.02	0.01	0.00	5.04	62.1
B268b-Core-11	2.73	2.38	1.59	0.36	0.66	0.01	0.00	0.00	5.00	65.0
B268b-Core-12	2.74	2.35	1.62	0.38	0.66	0.01	0.00	0.01	5.03	63.1
Average	**2.74**	**2.35**	**1.63**	**0.38**	**0.65**	**0.02**	**0.00**	**0.00**	**5.03**	**63.2**
B268b-Rim-1	2.73	2.41	1.57	0.47	0.56	0.02	0.00	0.02	5.05	53.5
B268b-Rim-2	2.74	2.34	1.65	0.37	0.65	0.02	0.00	0.01	5.03	63.3
B268b-Rim-3	2.74	2.34	1.64	0.37	0.65	0.02	0.00	0.01	5.03	63.1
B268b-Rim-4	2.74	2.34	1.63	0.38	0.65	0.02	0.00	0.01	5.04	62.3
B268b-Rim-5	2.71	2.55	1.42	0.66	0.45	0.00	0.00	0.00	5.07	40.5
B268b-Rim-6	2.73	2.52	1.43	0.57	0.47	0.04	0.01	0.02	5.06	44.5
Average	**2.73**	**2.42**	**1.56**	**0.47**	**0.57**	**0.02**	**0.00**	**0.01**	**5.05**	**54.5**
B268-gm-1	2.73	2.34	1.65	0.39	0.64	0.00	0.00	0.02	5.04	61.2
B268-gm-2	2.95	2.42	0.94	0.21	0.29	0.74	0.60	0.02	5.22	55.6
B268-gm-3	2.73	2.39	1.60	0.44	0.59	0.00	0.00	0.02	5.04	56.3
B268-gm-4	2.72	2.45	1.54	0.48	0.53	0.00	0.00	0.03	5.03	51.2
B268-gm-5	2.72	2.52	1.45	0.50	0.50	0.02	0.00	0.03	5.02	48.5
B268-gm-6	2.73	2.34	1.65	0.41	0.63	0.00	0.00	0.00	5.04	60.5
B268-gm-7	2.72	2.46	1.51	0.50	0.52	0.02	0.00	0.03	5.04	49.3
B268-gm-8	2.72	2.44	1.56	0.46	0.53	0.00	0.00	0.02	5.02	52.3
B268-gm-9	2.72	2.46	1.53	0.49	0.52	0.00	0.00	0.03	5.03	50.3
B268-gm-10	2.69	2.34	1.78	0.30	0.47	0.02	0.00	0.00	4.91	61.2
B268-gm-11	2.72	2.40	1.61	0.42	0.59	0.00	0.00	0.00	5.01	58.1
B268-gm-12	2.75	2.47	1.43	0.51	0.46	0.11	0.08	0.02	5.08	46.1
B268-gm-13	2.73	2.42	1.57	0.45	0.58	0.00	0.00	0.03	5.04	54.7
B268-gm-14	2.75	2.29	1.69	0.35	0.67	0.02	0.00	0.01	5.05	64.6
B268-gm-15	2.72	2.47	1.52	0.53	0.51	0.00	0.00	0.02	5.05	47.9
B268-gm-16	2.70	2.54	1.46	0.43	0.50	0.01	0.00	0.01	4.95	52.8
B268-gm-17	2.71	2.45	1.54	0.36	0.58	0.01	0.00	0.01	4.96	60.7
B268-gm-18	2.71	2.48	1.51	0.40	0.56	0.01	0.00	0.02	4.97	57.2
B268-gm-19	2.70	2.49	1.51	0.39	0.56	0.00	0.00	0.01	4.96	58.3
B268-gm-20	2.71	2.46	1.53	0.35	0.59	0.01	0.00	0.01	4.96	61.9
B268-gm-21	2.68	2.63	1.38	0.57	0.38	0.00	0.00	0.01	4.97	39.7
B268-gm-22	2.71	2.46	1.54	0.38	0.58	0.00	0.00	0.01	4.97	59.8
Average	**2.73**	**2.44**	**1.52**	**0.42**	**0.53**	**0.04**	**0.03**	**0.02**	**5.02**	**54.9**

Appendix C – Whole-Rock Lithogeochemistry

Appendix - C - Whole-Rock Lithogeochemistry

	Method	WGHT	LF200	LF200	LF200	LF200	LF200	LF200	LF200	LF200	LF200	LF200	LF200	LF200	LF200	LF200	LF200	LF200
	Analyte	**Wgt**	**SiO2**	**Al2O3**	**Fe2O3**	**MgO**	**CaO**	**Na2O**	**K2O**	**TiO2**	**P2O5**	**MnO**	**Cr2O3**	**Ni**	**Sc**	**LOI**	**Sum**	**Ba**	**Be**
	Unit	**KG**	**%**	**%**	**%**	**%**	**%**	**%**	**%**	**%**	**%**	**%**	**%**	**PPM**	**PPM**	**%**	**%**	**PPM**	**PPM**
	MDL	**0.01**	**0.01**	**0.01**	**0.04**	**0.01**	**0.01**	**0.01**	**0.01**	**0.01**	**0.01**	**0.01**	**0.002**	**20**	**1**	**-5.1**	**0.01**	**1**	**1**
Sample	**Type**																		
KP1	Rock	0.31	47.34	16.15	11.64	8.14	10.10	2.18	0.35	1.31	0.12	0.16	0.026	185	26	2.2	99.74	139	1
KP5	Rock	0.39	46.51	17.22	10.74	8.92	10.32	2.00	0.27	1.05	0.08	0.14	0.020	221	21	2.4	99.74	108	1
KP10	Rock	0.79	46.59	16.26	12.80	5.72	10.39	2.58	0.36	1.97	0.11	0.17	0.014	67	33	2.8	99.73	154	<1
KP11a	Rock	0.54	46.88	17.29	12.13	4.20	9.86	2.78	0.58	1.92	0.18	0.16	0.012	48	27	3.8	99.75	205	2
KP11b	Rock	0.36	53.14	13.76	12.29	1.73	7.65	2.95	2.27	1.53	0.47	0.15	<0.002	<20	15	3.8	99.70	626	2
KP12	Rock	0.90	51.11	11.64	16.71	2.61	6.86	3.59	1.53	2.99	0.65	0.24	<0.002	<20	28	1.8	99.70	299	3
KP14a	Rock	0.81	48.53	14.25	13.13	4.47	9.66	4.05	0.34	2.06	0.19	0.19	0.021	41	35	2.9	99.79	84	<1
KP14b	Rock	0.76	47.97	18.47	11.28	3.88	10.88	2.71	0.53	1.77	0.18	0.15	0.013	47	25	1.9	99.78	176	3
KP15	Rock	0.96	46.70	15.84	11.68	8.21	9.65	2.17	0.38	1.34	0.13	0.16	0.026	182	27	3.4	99.74	149	<1
KP16	Rock	0.61	46.15	16.34	11.10	8.12	10.12	2.11	0.35	1.30	0.11	0.15	0.025	200	25	3.8	99.74	126	<1
KP101	Rock	0.80	47.50	15.96	11.57	8.10	9.56	2.25	0.37	1.34	0.12	0.16	0.025	182	27	2.8	99.75	129	<1
KP104	Rock	0.52	47.11	17.42	10.64	8.05	10.74	2.07	0.34	1.21	0.10	0.15	0.019	183	22	1.9	99.76	108	<1
KP110	Rock	0.64	47.06	16.99	11.55	6.80	10.60	2.35	0.32	1.37	0.13	0.16	0.029	109	27	2.4	99.78	108	<1
KP111	Rock	0.72	48.58	12.69	10.06	7.23	13.58	2.53	0.43	1.76	0.14	0.19	0.050	59	50	2.5	99.74	128	1
KP111-B	Rock	1.20	49.31	14.02	9.71	5.98	13.12	2.95	0.76	1.71	0.15	0.17	0.040	46	44	1.8	99.75	167	<1
KP111-C	Rock	1.32	47.82	17.28	10.49	5.88	9.82	2.96	0.47	1.28	0.13	0.16	0.012	87	26	3.5	99.77	157	<1
KP112	Rock	0.87	47.45	18.31	11.09	4.44	10.73	2.70	0.47	1.77	0.17	0.16	0.013	56	27	2.5	99.78	169	<1
KP116	Rock	0.94	47.87	14.95	11.78	5.76	10.17	3.79	0.62	1.42	0.08	0.18	0.018	54	43	3.1	99.76	190	1
KP19	Rock	0.62	47.43	15.89	11.58	8.01	10.02	2.20	0.35	1.36	0.13	0.16	0.026	183	27	2.6	99.75	105	<1
IR1	Rock	0.58	48.84	14.74	12.29	5.24	7.39	4.39	0.80	1.94	0.13	0.21	0.022	35	34	3.7	99.75	190	<1
IR3	Rock	0.71	48.48	14.63	12.11	5.38	8.42	3.67	1.35	1.84	0.17	0.19	0.023	49	34	3.4	99.67	563	<1

Appendix - C - Whole-Rock Lithogeochemistry

	LF200	LF200	LF200	LF200	LF200	LF200	LF200	LF200	LF200	LF200	LF200	LF200	LF200	LF200	LF200	LF200	LF200	LF200	LF200
	Co	**Cs**	**Ga**	**Hf**	**Nb**	**Rb**	**Sn**	**Sr**	**Ta**	**Th**	**U**	**V**	**W**	**Zr**	**Y**	**La**	**Ce**	**Pr**	**Nd**
	PPM	**PPM**	**PPM**	**PPM**	**PPM**	**PPM**	**PPM**	**PPM**	**PPM**	**PPM**	**PPM**	**PPM**	**PPM**	**PPM**	**PPM**	**PPM**	**PPM**	**PPM**	**PPM**
	0.2	**0.1**	**0.5**	**0.1**	**0.1**	**0.1**	**1**	**0.5**	**0.1**	**0.2**	**0.1**	**8**	**0.5**	**0.1**	**0.1**	**0.1**	**0.1**	**0.02**	**0.3**
Sample																			
KP1	57.9	1.7	17.2	2.6	8.0	9.9	1	259.5	0.4	1.0	0.2	230	<0.5	104.7	22.1	12.1	25.8	3.42	14.9
KP5	59.4	2.0	16.0	2.2	6.3	6.5	<1	278.3	0.4	0.8	0.1	182	<0.5	82.2	16.5	9.0	19.5	2.64	11.6
KP10	52.4	2.0	18.6	2.5	7.6	8.7	<1	292.1	0.5	0.9	0.1	507	<0.5	95.6	21.3	10.5	23.0	3.10	13.7
KP11a	41.9	0.4	22.7	4.9	14.3	15.8	2	283.5	0.9	2.2	0.5	237	<0.5	184.8	33.7	20.8	45.9	5.84	24.9
KP11b	25.7	0.4	28.1	17.4	36.9	43.9	4	86.8	2.2	9.2	1.7	50	<0.5	702.9	90.4	60.7	135.1	16.58	69.1
KP12	34.2	0.3	27.5	14.5	54.9	36.0	5	101.7	2.9	6.2	1.2	129	<0.5	571.5	101.5	61.8	137.6	18.25	80.3
KP14a	43.3	0.1	20.2	4.4	12.8	8.3	1	135.9	0.9	1.6	0.3	327	<0.5	173.3	34.3	18.1	40.2	5.22	21.8
KP14b	39.7	1.5	20.5	3.8	12.1	14.9	<1	329.3	0.8	1.7	0.4	229	<0.5	142.6	29.4	16.6	36.7	4.88	21.2
KP15	57.6	1.0	16.7	2.8	8.4	10.7	<1	260.0	0.5	1.0	0.2	232	<0.5	109.7	23.7	12.1	27.8	3.60	15.8
KP16	58.7	0.9	16.7	2.6	7.7	10.2	<1	250.1	0.5	0.9	0.2	226	<0.5	98.9	21.4	10.8	24.7	3.20	14.1
KP101	54.7	0.9	16.5	2.8	8.1	13.0	<1	249.3	0.4	1.0	0.1	232	<0.5	106.8	22.7	11.4	24.6	3.35	15.1
KP104	52.8	1.6	16.8	2.3	7.2	10.9	<1	268.8	0.4	0.8	0.1	205	<0.5	90.4	18.9	10.2	22.7	2.95	13.2
KP110	51.6	0.9	16.8	2.4	7.2	9.3	<1	252.7	0.4	0.8	0.1	236	<0.5	91.9	19.5	10.4	22.1	2.90	12.7
KP111	37.2	<0.1	13.8	2.9	8.9	6.8	<1	223.9	0.6	1.1	0.2	389	<0.5	114.7	27.3	12.5	27.9	3.79	16.8
KP111-B	36.4	<0.1	17.0	3.3	10.2	10.8	<1	274.4	0.6	1.1	0.2	346	<0.5	127.1	28.4	13.7	30.7	4.18	19.3
KP111-C	46.3	0.3	18.0	2.4	6.9	11.9	<1	343.5	0.4	1.0	0.1	217	<0.5	94.4	18.8	10.8	24.6	3.04	13.4
KP112	39.0	0.2	20.6	3.5	10.7	13.0	<1	311.2	0.7	1.4	0.2	233	<0.5	134.0	26.3	15.2	34.4	4.37	19.0
KP116	45.5	0.5	18.2	2.1	5.7	13.6	<1	371.0	0.4	0.6	<0.1	331	<0.5	75.7	19.3	7.7	19.1	2.52	11.6
KP19	54.8	4.9	18.0	2.6	7.9	8.9	<1	238.9	0.5	0.9	0.2	232	<0.5	103.8	20.6	10.7	24.3	3.25	14.1
IR1	41.4	<0.1	16.5	3.3	9.7	15.1	<1	195.6	0.5	1.3	0.2	319	<0.5	122.9	26.0	12.4	28.6	3.85	16.7
IR3	41.6	<0.1	19.0	4.3	13.1	31.4	1	511.4	0.8	1.8	0.3	304	<0.5	168.6	33.2	18.1	39.7	5.36	23.0

Appendix - C - Whole-Rock Lithogeochemistry

	LF200	LF200	LF200	LF200	LF200	LF200	LF200	LF200	LF200	LF200	TC000	TC000	AQ200	AQ200	AQ200	AQ200	AQ200	AQ200	AQ200
	Sm	**Eu**	**Gd**	**Tb**	**Dy**	**Ho**	**Er**	**Tm**	**Yb**	**Lu**	**TOT/C**	**TOT/S**	**Mo**	**Cu**	**Pb**	**Zn**	**Ni**	**As**	**Cd**
	PPM	**PPM**	**PPM**	**PPM**	**PPM**	**PPM**	**PPM**	**PPM**	**PPM**	**PPM**	**%**	**%**	**PPM**	**PPM**	**PPM**	**PPM**	**PPM**	**PPM**	**PPM**
	0.05	**0.02**	**0.05**	**0.01**	**0.05**	**0.02**	**0.03**	**0.01**	**0.05**	**0.01**	**0.02**	**0.02**	**0.1**	**0.1**	**0.1**	**1**	**0.1**	**0.5**	**0.1**
Sample																			
KP1	3.66	1.26	4.05	0.68	4.27	0.84	2.22	0.34	1.94	0.32	0.07	<0.02	0.3	94.0	5.8	57	119.0	0.7	<0.1
KP5	2.83	1.02	3.15	0.52	3.21	0.67	1.74	0.26	1.61	0.25	0.04	<0.02	0.3	73.1	1.9	52	168.8	0.5	<0.1
KP10	3.35	1.32	3.86	0.65	3.92	0.78	2.08	0.31	1.88	0.31	0.02	<0.02	0.3	104.0	1.1	65	39.9	0.7	<0.1
KP11a	5.86	1.80	6.34	1.06	6.16	1.29	3.46	0.53	3.07	0.49	0.02	<0.02	0.3	145.4	1.9	89	24.4	<0.5	<0.1
KP11b	15.46	3.25	16.34	2.76	16.66	3.57	9.46	1.46	8.71	1.34	0.08	<0.02	1.0	147.2	6.1	96	6.5	1.3	0.3
KP12	17.93	3.73	18.88	3.15	18.44	3.80	10.29	1.54	8.98	1.38	0.08	<0.02	1.4	214.2	6.9	126	6.7	0.7	0.2
KP14a	5.59	1.75	6.17	1.03	6.14	1.28	3.47	0.48	2.94	0.47	0.05	<0.02	0.7	114.2	4.0	77	17.4	0.7	0.1
KP14b	4.97	1.63	5.52	0.91	5.54	1.08	2.93	0.43	2.64	0.41	0.05	<0.02	0.3	137.6	1.2	58	23.6	<0.5	<0.1
KP15	3.87	1.25	4.31	0.70	4.30	0.84	2.29	0.35	2.02	0.33	0.05	<0.02	0.1	99.1	3.0	53	119.9	<0.5	<0.1
KP16	3.47	1.21	3.98	0.65	3.83	0.80	2.07	0.33	1.94	0.29	0.03	<0.02	0.2	91.2	1.0	53	140.5	<0.5	<0.1
KP101	3.52	1.20	4.07	0.68	4.08	0.83	2.28	0.32	2.01	0.32	0.06	<0.02	0.1	99.4	6.2	58	115.4	0.5	<0.1
KP104	3.07	1.11	3.55	0.57	3.47	0.73	1.93	0.28	1.73	0.26	0.02	<0.02	0.2	78.5	1.8	50	128.8	<0.5	<0.1
KP110	3.18	1.16	3.59	0.59	3.51	0.74	2.02	0.30	1.76	0.27	0.02	<0.02	0.1	88.5	1.3	53	71.7	<0.5	<0.1
KP111	4.33	1.34	4.89	0.83	4.99	0.98	2.76	0.40	2.37	0.37	0.02	<0.02	0.3	102.2	1.5	40	13.1	<0.5	<0.1
KP111-B	4.61	1.53	5.16	0.87	5.23	1.04	2.80	0.42	2.47	0.39	<0.02	<0.02	0.7	161.2	2.2	45	14.4	0.7	<0.1
KP111-C	3.28	1.25	3.70	0.63	3.56	0.73	2.06	0.29	1.71	0.27	0.03	<0.02	0.2	99.6	1.6	53	56.1	<0.5	<0.1
KP112	4.52	1.51	5.03	0.82	4.76	1.00	2.71	0.40	2.46	0.37	<0.02	<0.02	0.3	124.6	2.4	68	29.3	<0.5	<0.1
KP116	3.15	1.35	3.74	0.62	3.66	0.76	2.02	0.29	1.73	0.28	0.03	<0.02	0.2	56.9	1.4	45	26.8	<0.5	<0.1
KP19	3.48	1.17	3.99	0.66	4.00	0.82	2.17	0.33	1.98	0.30	0.04	<0.02	0.2	92.7	1.7	51	132.6	<0.5	<0.1
IR1	4.28	1.45	4.85	0.80	4.78	0.99	2.62	0.39	2.37	0.38	0.09	<0.02	0.2	149.3	2.1	108	21.5	<0.5	<0.1
IR3	5.51	1.73	6.33	1.03	6.06	1.24	3.33	0.50	2.95	0.49	0.03	<0.02	0.3	33.3	3.1	84	25.6	<0.5	<0.1

Appendix - C - Whole-Rock Lithogeochemistry

	AQ200	AQ200	AQ200	AQ200	AQ200	AQ200	AQ200
	Sb	**Bi**	**Ag**	**Au**	**Hg**	**Tl**	**Se**
	PPM	**PPM**	**PPM**	**PPB**	**PPM**	**PPM**	**PPM**
	0.1	**0.1**	**0.1**	**0.5**	**0.01**	**0.1**	**0.5**
Sample							
KP1	0.2	<0.1	<0.1	0.9	<0.01	<0.1	<0.5
KP5	<0.1	<0.1	<0.1	<0.5	<0.01	<0.1	<0.5
KP10	<0.1	<0.1	<0.1	<0.5	<0.01	<0.1	0.5
KP11a	<0.1	<0.1	<0.1	<0.5	<0.01	<0.1	<0.5
KP11b	<0.1	<0.1	<0.1	<0.5	<0.01	<0.1	<0.5
KP12	<0.1	<0.1	<0.1	<0.5	<0.01	<0.1	0.7
KP14a	<0.1	<0.1	<0.1	<0.5	<0.01	<0.1	<0.5
KP14b	<0.1	<0.1	<0.1	<0.5	<0.01	<0.1	<0.5
KP15	<0.1	<0.1	<0.1	<0.5	<0.01	<0.1	<0.5
KP16	<0.1	<0.1	<0.1	<0.5	<0.01	<0.1	<0.5
KP101	0.1	<0.1	<0.1	<0.5	<0.01	<0.1	<0.5
KP104	<0.1	<0.1	<0.1	0.9	<0.01	<0.1	<0.5
KP110	<0.1	<0.1	<0.1	<0.5	<0.01	<0.1	<0.5
KP111	<0.1	<0.1	<0.1	<0.5	<0.01	<0.1	<0.5
KP111-B	<0.1	<0.1	<0.1	<0.5	<0.01	<0.1	<0.5
KP111-C	<0.1	<0.1	<0.1	<0.5	<0.01	<0.1	<0.5
KP112	<0.1	<0.1	<0.1	1.7	<0.01	<0.1	<0.5
KP116	<0.1	<0.1	<0.1	<0.5	<0.01	<0.1	<0.5
KP19	<0.1	<0.1	<0.1	<0.5	<0.01	<0.1	<0.5
IR1	<0.1	<0.1	<0.1	<0.5	<0.01	<0.1	<0.5
IR3	<0.1	<0.1	<0.1	<0.5	<0.01	<0.1	<0.5

Appendix - C - Whole-Rock Lithogeochemistry

	Method	WGHT	LF200	LF200	LF200	LF200	LF200	LF200	LF200	LF200	LF200	LF200	LF200	LF200	LF200	LF200	LF200	LF200
	Analyte	**Wgt**	**SiO2**	**Al2O3**	**Fe2O3**	**MgO**	**CaO**	**Na2O**	**K2O**	**TiO2**	**P2O5**	**MnO**	**Cr2O3**	**Ni**	**Sc**	**LOI**	**Sum**	**Ba**	**Be**
	Unit	**KG**	**%**	**%**	**%**	**%**	**%**	**%**	**%**	**%**	**%**	**%**	**%**	**PPM**	**PPM**	**%**	**%**	**PPM**	**PPM**
	MDL	**0.01**	**0.01**	**0.01**	**0.04**	**0.01**	**0.01**	**0.01**	**0.01**	**0.01**	**0.01**	**0.01**	**0.002**	**20**	**1**	**-5.1**	**0.01**	**1**	**1**
IR5	Rock	0.42	48.02	10.78	19.89	3.90	4.71	4.05	0.73	3.71	0.32	0.21	<0.002	<20	33	3.4	99.74	101	1
IR6	Rock	0.89	51.59	13.62	12.58	5.12	7.35	4.01	1.33	2.22	0.17	0.22	0.010	36	40	1.5	99.69	542	<1
IR7-A	Rock	0.62	47.86	14.79	13.75	5.48	9.08	2.86	1.23	2.47	0.15	0.23	0.017	37	36	1.7	99.66	593	1
IR7-B	Rock	0.79	47.15	15.58	11.58	8.26	9.60	2.24	0.41	1.36	0.10	0.18	0.026	175	28	3.2	99.73	158	<1
IR7-C	Rock	0.85	48.47	10.49	16.05	2.42	13.96	0.07	0.32	2.74	0.55	0.16	<0.002	<20	26	4.6	99.81	52	2
IR9	Rock	0.68	47.25	15.77	10.90	7.99	9.79	2.25	0.47	1.29	0.12	0.16	0.024	177	25	3.7	99.75	226	<1
IR10	Rock	0.76	47.33	15.65	11.13	7.82	9.93	2.28	0.44	1.32	0.11	0.15	0.024	175	26	3.5	99.73	172	1
IR11	Rock	0.63	46.82	16.06	11.29	7.35	10.03	2.42	0.51	1.31	0.12	0.15	0.024	172	25	3.6	99.73	174	<1
IR12	Rock	1.17	47.10	15.80	11.13	7.93	9.58	2.38	0.48	1.29	0.11	0.17	0.025	170	25	3.7	99.73	218	<1
IR15	Rock	1.05	47.54	16.02	11.50	7.71	9.58	2.30	0.45	1.32	0.11	0.16	0.026	177	26	3.0	99.74	170	<1
IR20	Rock	0.70	47.42	15.76	11.48	7.66	9.96	2.24	0.42	1.38	0.12	0.16	0.024	171	26	3.1	99.74	153	<1
IR21	Rock	0.68	46.91	16.53	11.37	7.62	9.88	2.19	0.38	1.26	0.11	0.15	0.026	202	24	3.3	99.76	131	<1
IR22	Rock	0.72	47.10	15.83	11.76	7.64	10.18	2.25	0.44	1.37	0.10	0.18	0.026	155	28	2.9	99.75	142	<1
IR23	Rock	0.74	48.23	15.39	12.52	5.01	8.92	3.31	1.44	1.84	0.19	0.20	0.024	52	33	2.6	99.63	1073	<1
IR24	Rock	0.67	58.93	10.81	13.45	1.97	3.28	2.60	2.76	2.16	0.60	0.18	<0.002	<20	21	2.9	99.63	702	1
IR26-A	Rock	0.82	49.02	13.30	13.25	4.67	9.80	3.96	0.81	2.11	0.17	0.19	0.010	33	34	2.4	99.74	246	<1
IR26-B	Rock	1.09	47.53	15.96	11.92	7.87	10.05	2.34	0.42	1.38	0.12	0.17	0.026	210	27	1.9	99.73	155	2
IR27	Rock	1.23	47.57	15.80	11.41	7.55	9.64	2.26	0.44	1.33	0.12	0.15	0.024	177	25	3.4	99.74	153	2
BBC1	Rock	1.09	49.02	16.95	13.33	3.32	9.86	3.01	0.68	2.72	0.19	0.17	<0.002	<20	29	0.5	99.75	250	<1
BBC2	Rock	0.51	50.65	17.55	11.70	2.73	9.37	3.14	0.92	2.16	0.27	0.16	0.003	<20	24	1.1	99.75	308	3
BBC4	Rock	0.54	49.21	16.53	12.24	4.58	10.32	2.81	0.66	2.06	0.16	0.17	0.015	41	30	1.0	99.75	219	<1
BBC5	Rock	0.83	51.01	19.94	9.61	1.77	9.31	3.86	0.93	1.84	0.23	0.13	<0.002	<20	17	1.2	99.80	301	4

Appendix - C - Whole-Rock Lithogeochemistry

	LF200	LF200	LF200	LF200	LF200	LF200	LF200	LF200	LF200	LF200	LF200	LF200	LF200	LF200	LF200	LF200	LF200	LF200	LF200
	Co	**Cs**	**Ga**	**Hf**	**Nb**	**Rb**	**Sn**	**Sr**	**Ta**	**Th**	**U**	**V**	**W**	**Zr**	**Y**	**La**	**Ce**	**Pr**	**Nd**
	PPM	**PPM**	**PPM**	**PPM**	**PPM**	**PPM**	**PPM**	**PPM**	**PPM**	**PPM**	**PPM**	**PPM**	**PPM**	**PPM**	**PPM**	**PPM**	**PPM**	**PPM**	**PPM**
	0.2	**0.1**	**0.5**	**0.1**	**0.1**	**0.1**	**1**	**0.5**	**0.1**	**0.2**	**0.1**	**8**	**0.5**	**0.1**	**0.1**	**0.1**	**0.1**	**0.02**	**0.3**
IR5	44.3	<0.1	18.9	8.3	26.3	9.2	3	46.2	1.5	3.1	0.8	240	<0.5	311.4	57.4	27.9	66.7	9.27	40.7
IR6	38.6	<0.1	16.3	4.2	12.3	32.3	1	292.0	0.8	1.5	0.3	395	<0.5	159.2	31.4	15.7	36.3	4.69	20.0
IR7-A	43.8	<0.1	18.9	4.4	13.2	29.0	1	273.2	0.8	1.6	0.3	438	<0.5	164.3	31.6	16.6	37.7	4.98	20.9
IR7-B	54.9	<0.1	16.2	2.7	8.5	9.7	<1	290.3	0.5	1.2	0.2	227	<0.5	104.0	21.7	11.2	23.9	3.26	14.1
IR7-C	33.6	<0.1	27.4	9.1	29.2	4.3	3	47.6	1.7	3.9	0.8	86	<0.5	348.2	70.8	46.4	99.4	12.98	55.8
IR9	52.4	0.1	18.3	2.8	9.4	11.8	1	269.3	0.5	2.2	0.2	212	<0.5	114.4	22.1	13.9	29.4	3.85	16.6
IR10	53.0	<0.1	16.7	2.8	9.3	10.3	1	239.6	0.6	1.2	0.2	215	<0.5	111.8	23.4	12.6	28.5	3.64	14.9
IR11	53.7	<0.1	19.7	3.2	9.7	11.5	2	297.0	0.7	3.1	0.2	222	0.5	116.3	24.8	14.3	31.3	4.05	17.5
IR12	55.8	<0.1	19.4	3.0	9.1	12.0	1	342.0	0.6	2.4	0.2	213	<0.5	110.3	23.2	12.6	28.6	3.62	16.7
IR15	54.7	<0.1	19.0	3.0	8.1	10.9	<1	305.9	0.5	1.7	0.1	229	<0.5	105.0	22.9	13.1	28.2	3.58	15.4
IR20	53.2	0.1	17.9	3.2	8.8	10.6	<1	268.0	0.4	1.5	0.2	231	<0.5	115.2	22.2	12.3	27.3	3.65	16.5
IR21	56.1	0.2	18.4	2.9	7.9	10.2	<1	276.0	0.5	0.9	0.1	218	0.6	101.9	20.2	11.3	25.2	3.17	13.2
IR22	55.8	0.2	18.3	3.0	8.3	12.6	<1	269.1	0.5	1.4	0.2	245	<0.5	106.1	22.9	11.6	25.8	3.37	16.0
IR23	44.3	0.3	20.2	4.0	10.9	37.5	<1	509.7	0.7	1.5	0.4	291	<0.5	149.6	30.7	16.9	36.9	4.88	21.4
IR24	20.2	<0.1	20.7	14.5	43.8	55.6	4	174.3	2.6	6.5	1.6	59	<0.5	572.6	93.6	67.5	140.0	17.86	75.7
IR26-A	41.0	<0.1	22.5	4.9	13.5	14.9	3	153.0	0.8	2.0	0.5	385	<0.5	180.7	34.9	18.3	41.4	5.35	24.2
IR26-B	53.2	0.2	18.3	3.1	8.7	10.8	<1	258.7	0.3	1.2	0.4	241	1.9	111.8	24.3	12.0	27.1	3.66	16.4
IR27	52.9	0.2	18.8	3.2	8.7	11.5	<1	272.6	0.6	1.1	0.2	233	<0.5	114.5	23.7	13.3	28.8	3.72	16.6
BBC1	38.6	0.7	24.1	4.4	12.5	18.9	1	345.8	0.9	2.3	0.5	346	<0.5	163.5	30.9	20.0	43.8	5.61	24.1
BBC2	30.5	0.5	23.2	5.6	15.5	30.2	1	328.5	0.9	2.3	0.6	261	<0.5	217.3	40.0	26.8	57.2	7.45	31.4
BBC4	41.6	0.9	21.5	4.8	12.3	18.8	1	301.8	0.9	1.8	0.5	312	<0.5	181.0	29.9	18.1	40.9	5.28	23.6
BBC5	22.6	0.8	24.8	4.0	14.8	26.0	1	351.6	0.8	2.4	0.6	150	<0.5	154.9	31.9	25.2	51.5	6.51	28.3

Appendix - C - Whole-Rock Lithogeochemistry

	LF200	LF200	LF200	LF200	LF200	LF200	LF200	LF200	LF200	LF200	TC000	TC000	AQ200	AQ200	AQ200	AQ200	AQ200	AQ200	AQ200
	Sm	**Eu**	**Gd**	**Tb**	**Dy**	**Ho**	**Er**	**Tm**	**Yb**	**Lu**	**TOT/C**	**TOT/S**	**Mo**	**Cu**	**Pb**	**Zn**	**Ni**	**As**	**Cd**
	PPM	**PPM**	**PPM**	**PPM**	**PPM**	**PPM**	**PPM**	**PPM**	**PPM**	**PPM**	**%**	**%**	**PPM**	**PPM**	**PPM**	**PPM**	**PPM**	**PPM**	**PPM**
	0.05	**0.02**	**0.05**	**0.01**	**0.05**	**0.02**	**0.03**	**0.01**	**0.05**	**0.01**	**0.02**	**0.02**	**0.1**	**0.1**	**0.1**	**1**	**0.1**	**0.5**	**0.1**
IR5	9.69	2.69	10.90	1.86	10.93	2.25	5.67	0.89	5.29	0.84	0.07	<0.02	0.5	112.0	3.0	121	5.9	<0.5	<0.1
IR6	5.02	1.59	5.86	0.99	5.82	1.19	3.22	0.47	2.90	0.45	0.02	<0.02	0.2	140.8	2.2	87	11.9	<0.5	<0.1
IR7-A	5.30	1.63	5.92	0.99	5.84	1.22	3.22	0.48	2.84	0.45	0.02	<0.02	0.1	176.6	2.0	69	17.8	<0.5	<0.1
IR7-B	3.55	1.25	4.09	0.67	3.91	0.86	2.20	0.33	1.99	0.33	0.03	<0.02	0.2	74.7	1.7	48	113.1	<0.5	<0.1
IR7-C	12.58	3.49	13.67	2.20	12.99	2.60	6.86	1.05	6.29	0.98	0.06	<0.02	0.9	26.8	8.1	100	3.9	0.7	0.3
IR9	3.82	1.30	4.33	0.75	4.53	0.89	2.46	0.36	2.28	0.35	0.02	<0.02	0.2	35.6	1.9	45	112.0	<0.5	<0.1
IR10	3.73	1.24	4.35	0.71	4.14	0.83	2.34	0.36	2.14	0.34	0.05	<0.02	0.2	135.4	1.6	52	113.0	<0.5	<0.1
IR11	4.20	1.29	4.58	0.78	4.37	0.97	2.66	0.35	2.43	0.36	0.10	<0.02	0.9	88.1	4.5	68	146.6	0.7	<0.1
IR12	3.90	1.28	4.47	0.74	4.36	0.83	2.52	0.35	2.31	0.34	0.04	<0.02	0.6	83.1	1.4	49	117.1	<0.5	<0.1
IR15	3.63	1.29	4.17	0.72	4.33	0.88	2.48	0.35	2.14	0.34	0.03	<0.02	0.2	76.0	5.7	51	111.0	<0.5	<0.1
IR20	4.05	1.34	4.35	0.75	4.37	0.84	2.35	0.38	2.20	0.33	<0.02	<0.02	0.2	72.2	1.8	49	114.6	0.6	<0.1
IR21	3.21	1.25	3.72	0.66	3.90	0.81	2.34	0.30	2.03	0.30	0.06	<0.02	0.1	39.6	1.3	42	140.3	<0.5	<0.1
IR22	3.77	1.33	4.19	0.71	4.28	0.80	2.30	0.33	2.20	0.32	<0.02	<0.02	0.3	65.7	2.4	47	91.8	0.8	<0.1
IR23	5.54	1.82	6.07	1.01	5.75	1.22	3.34	0.43	2.80	0.45	0.07	<0.02	0.6	92.9	3.3	96	26.7	1.2	0.2
IR24	18.02	4.11	18.70	3.17	18.89	3.69	9.97	1.44	9.57	1.42	0.11	<0.02	0.8	651.0	4.5	120	3.5	1.3	<0.1
IR26-A	6.01	1.85	6.62	1.09	6.51	1.33	3.86	0.53	3.38	0.50	0.03	<0.02	0.5	192.8	3.7	88	14.7	1.1	0.2
IR26-B	4.06	1.33	4.21	0.76	5.00	0.85	2.57	0.37	2.32	0.34	0.03	<0.02	<0.1	48.4	1.8	48	107.9	0.7	<0.1
IR27	4.15	1.34	4.42	0.75	4.64	0.93	2.41	0.37	2.30	0.35	0.05	<0.02	0.1	70.4	1.3	47	118.4	1.0	<0.1
BBC1	5.60	2.02	6.16	0.98	6.07	1.13	3.31	0.46	3.02	0.43	<0.02	<0.02	0.5	166.8	6.2	150	10.1	0.7	<0.1
BBC2	7.28	1.99	7.50	1.18	7.53	1.34	3.92	0.55	3.55	0.56	0.07	<0.02	0.4	136.1	2.5	60	8.8	1.0	<0.1
BBC4	5.48	1.67	5.71	0.96	5.93	1.16	3.41	0.47	3.07	0.46	0.03	<0.02	0.4	124.9	2.5	58	22.8	0.6	<0.1
BBC5	6.53	1.92	6.14	1.02	6.53	1.18	3.33	0.49	2.95	0.46	<0.02	<0.02	0.8	151.9	5.7	57	4.2	0.9	<0.1

Appendix - C - Whole-Rock Lithogeochemistry

	AQ200	AQ200	AQ200	AQ200	AQ200	AQ200	AQ200
	Sb	**Bi**	**Ag**	**Au**	**Hg**	**Tl**	**Se**
	PPM	**PPM**	**PPM**	**PPB**	**PPM**	**PPM**	**PPM**
	0.1	**0.1**	**0.1**	**0.5**	**0.01**	**0.1**	**0.5**
IR5	<0.1	<0.1	<0.1	3.6	<0.01	<0.1	<0.5
IR6	<0.1	<0.1	<0.1	<0.5	<0.01	<0.1	0.5
IR7-A	<0.1	<0.1	<0.1	0.5	<0.01	<0.1	<0.5
IR7-B	<0.1	<0.1	<0.1	1.5	<0.01	<0.1	<0.5
IR7-C	0.2	<0.1	<0.1	<0.5	<0.01	<0.1	<0.5
IR9	<0.1	<0.1	<0.1	4.1	<0.01	<0.1	<0.5
IR10	<0.1	<0.1	<0.1	<0.5	0.01	<0.1	<0.5
IR11	0.1	<0.1	1.0	10966.8	4.49	<0.1	<0.5
IR12	<0.1	<0.1	<0.1	8.4	0.01	<0.1	<0.5
IR15	0.1	<0.1	<0.1	4.8	0.02	<0.1	<0.5
IR20	<0.1	<0.1	<0.1	3.1	<0.01	<0.1	<0.5
IR21	<0.1	<0.1	<0.1	4.9	<0.01	<0.1	0.6
IR22	<0.1	<0.1	<0.1	3.5	<0.01	<0.1	<0.5
IR23	<0.1	<0.1	<0.1	<0.5	<0.01	<0.1	<0.5
IR24	<0.1	<0.1	0.1	2.2	0.01	<0.1	
IR26-A	<0.1	<0.1	0.1	1.6	<0.01	<0.1	<0.5
IR26-B	<0.1	<0.1	<0.1	0.8	<0.01	<0.1	<0.5
IR27	<0.1	<0.1	<0.1	2.1	<0.01	<0.1	<0.5
BBC1	<0.1	<0.1	<0.1	4.0	<0.01	<0.1	<0.5
BBC2	<0.1	<0.1	<0.1	4.1	<0.01	<0.1	<0.5
BBC4	<0.1	<0.1	<0.1	<0.5	<0.01	<0.1	<0.5
BBC5	<0.1	<0.1	<0.1	4.4	<0.01	<0.1	<0.5

Appendix - C - Whole-Rock Lithogeochemistry

	Method	WGHT	LF200	LF200	LF200	LF200	LF200	LF200	LF200	LF200	LF200	LF200	LF200	LF200	LF200	LF200	LF200	LF200	LF200
	Analyte	**Wgt**	**SiO2**	**Al2O3**	**Fe2O3**	**MgO**	**CaO**	**Na2O**	**K2O**	**TiO2**	**P2O5**	**MnO**	**Cr2O3**	**Ni**	**Sc**	**LOI**	**Sum**	**Ba**	**Be**
	Unit	**KG**	**%**	**%**	**%**	**%**	**%**	**%**	**%**	**%**	**%**	**%**	**%**	**PPM**	**PPM**	**%**	**%**	**PPM**	**PPM**
	MDL	**0.01**	**0.01**	**0.01**	**0.04**	**0.01**	**0.01**	**0.01**	**0.01**	**0.01**	**0.01**	**0.01**	**0.002**	**20**	**1**	**-5.1**	**0.01**	**1**	**1**
BBC6	Rock	0.37	45.53	19.77	10.16	10.94	10.29	1.92	0.14	0.40	0.03	0.13	0.017	384	10	0.4	99.75	67	<1
BBC7	Rock	0.83	49.53	17.60	11.47	3.91	10.28	2.94	0.68	1.73	0.18	0.16	0.012	36	26	1.3	99.77	244	<1
BBC8	Rock	0.88	50.69	16.85	9.41	4.75	11.81	2.78	0.59	1.39	0.14	0.14	0.040	48	34	1.2	99.78	215	1
BBC10	Rock	1.00	45.26	13.36	17.48	4.90	9.92	2.41	0.44	4.82	0.10	0.22	<0.002	37	42	0.8	99.72	173	1
BBC11-A	Rock	1.01	46.32	11.55	21.04	2.98	8.30	2.58	1.13	3.77	1.00	0.26	<0.002	<20	36	0.8	99.72	388	<1
BBC11-B	Rock	0.70	47.11	11.55	20.83	2.96	7.95	2.57	1.23	3.61	1.03	0.26	<0.002	<20	35	0.6	99.71	408	<1
BBC12	Rock	0.69	47.32	11.60	19.99	2.56	7.68	2.58	1.39	3.52	1.02	0.25	<0.002	<20	34	1.8	99.70	472	<1
BBC13	Rock	1.04	47.77	17.77	11.77	7.08	10.47	2.53	0.34	0.85	0.08	0.16	0.026	97	23	0.9	99.77	130	2
BBC14	Rock	1.62	47.20	16.95	11.76	7.21	10.37	2.36	0.29	1.58	0.16	0.17	0.029	164	32	1.7	99.82	122	<1
SB10	Rock	1.02	48.12	18.12	11.80	4.95	10.29	2.82	0.48	1.56	0.15	0.15	0.014	69	25	1.3	99.77	174	<1
SB11	Rock	1.21	51.11	18.47	10.43	2.49	9.24	3.19	1.08	1.83	0.23	0.14	0.005	<20	20	1.5	99.77	363	<1
SB12	Rock	1.08	50.40	11.80	16.52	3.72	8.00	2.72	1.13	3.17	0.39	0.25	<0.002	<20	38	1.6	99.72	395	2
SB13	Rock	0.87	51.19	11.03	17.55	2.47	7.06	2.75	1.62	2.45	1.00	0.25	<0.002	<20	34	2.3	99.70	545	2
SB14	Rock	1.04	44.55	12.59	20.30	3.75	8.21	2.92	0.79	3.79	1.74	0.25	<0.002	<20	25	0.8	99.68	359	5
SB15	Rock	0.78	48.08	18.64	11.57	4.02	9.53	2.93	0.60	1.64	0.24	0.17	0.004	41	19	2.3	99.77	222	<1
SB16	Rock	1.02	47.68	18.54	11.49	4.27	10.26	2.77	0.46	1.67	0.18	0.17	0.008	53	23	2.3	99.76	184	<1
SB17	Rock	1.02	46.01	12.82	18.87	3.06	8.31	3.01	0.92	3.37	1.46	0.24	<0.002	<20	33	1.6	99.70	361	1

Appendix - C - Whole-Rock Lithogeochemistry

	LF200	LF200	LF200	LF200	LF200	LF200	LF200	LF200	LF200	LF200	LF200	LF200	LF200	LF200	LF200	LF200	LF200	LF200	LF200
	Co	**Cs**	**Ga**	**Hf**	**Nb**	**Rb**	**Sn**	**Sr**	**Ta**	**Th**	**U**	**V**	**W**	**Zr**	**Y**	**La**	**Ce**	**Pr**	**Nd**
	PPM	**PPM**	**PPM**	**PPM**	**PPM**	**PPM**	**PPM**	**PPM**	**PPM**	**PPM**	**PPM**	**PPM**	**PPM**	**PPM**	**PPM**	**PPM**	**PPM**	**PPM**	**PPM**
	0.2	**0.1**	**0.5**	**0.1**	**0.1**	**0.1**	**1**	**0.5**	**0.1**	**0.2**	**0.1**	**8**	**0.5**	**0.1**	**0.1**	**0.1**	**0.1**	**0.02**	**0.3**
BBC6	69.0	1.6	17.2	0.8	2.0	2.6	<1	304.0	0.2	<0.2	<0.1	73	<0.5	28.5	6.1	3.8	8.1	1.01	4.7
BBC7	38.3	0.4	22.9	4.6	12.5	19.5	1	311.2	0.8	2.0	0.4	242	<0.5	177.6	30.2	19.2	42.8	5.55	23.0
BBC8	32.5	0.3	20.2	4.3	9.3	16.2	<1	286.8	0.5	1.6	0.4	257	<0.5	157.0	27.8	18.1	38.0	4.97	22.2
BBC10	59.3	0.3	21.9	3.9	13.4	13.0	<1	238.6	0.8	1.0	0.3	634	<0.5	134.4	24.6	13.0	28.2	3.71	17.0
BBC11-A	45.3	0.8	25.5	6.5	17.9	41.0	2	244.5	1.1	3.6	0.9	108	0.9	239.5	56.0	37.0	83.4	11.33	50.7
BBC11-B	46.5	0.9	25.8	6.5	18.2	47.6	2	247.7	1.3	3.9	1.0	129	0.7	251.3	55.9	35.1	80.2	10.96	51.7
BBC12	43.1	0.8	25.5	9.6	26.6	46.8	3	240.9	1.8	5.2	1.2	85	<0.5	350.9	74.2	50.9	108.5	15.01	67.8
BBC13	61.0	1.2	18.7	2.2	5.3	8.1	<1	306.5	0.4	0.8	0.2	158	0.6	75.7	17.4	10.1	21.4	2.76	12.6
BBC14	52.7	3.2	19.4	3.1	8.8	9.1	<1	290.4	0.6	1.1	0.2	241	<0.5	109.4	21.5	13.1	26.2	3.60	15.9
SB10	47.9	0.3	22.3	3.9	10.1	11.2	<1	336.0	0.6	1.2	0.2	224	<0.5	132.4	28.1	16.0	34.2	4.46	19.1
SB11	29.3	0.5	24.6	6.5	17.0	30.1	<1	345.5	1.1	3.1	0.8	190	<0.5	247.8	38.8	27.1	62.3	7.67	32.9
SB12	42.7	0.4	24.3	9.1	25.6	34.1	2	243.3	1.9	4.8	1.2	211	1.0	324.4	58.5	41.2	86.2	11.51	50.1
SB13	32.0	0.6	23.5	11.3	29.3	53.7	3	223.1	1.6	6.4	1.4	11	1.1	433.1	74.1	53.9	122.2	15.83	67.5
SB14	58.1	0.3	23.6	5.2	17.7	18.5	1	315.0	1.2	2.5	0.6	38	<0.5	190.4	54.4	39.7	90.0	12.41	57.9
SB15	39.7	0.2	23.3	5.2	13.3	16.4	<1	340.8	0.9	2.0	0.5	169	<0.5	194.8	33.6	22.5	48.7	6.26	28.4
SB16	41.7	0.2	21.9	3.6	10.7	10.2	<1	325.9	0.6	1.3	0.2	203	<0.5	124.7	24.4	15.9	33.1	4.43	19.9
SB17	45.8	0.3	26.0	4.9	17.8	25.0	2	307.3	0.9	3.1	0.6	24	1.1	181.1	59.6	43.2	95.3	13.21	59.4

Appendix - C - Whole-Rock Lithogeochemistry

	LF200	LF200	LF200	LF200	LF200	LF200	LF200	LF200	LF200	LF200	TC000	TC000	AQ200	AQ200	AQ200	AQ200	AQ200	AQ200	AQ200
	Sm	**Eu**	**Gd**	**Tb**	**Dy**	**Ho**	**Er**	**Tm**	**Yb**	**Lu**	**TOT/C**	**TOT/S**	**Mo**	**Cu**	**Pb**	**Zn**	**Ni**	**As**	**Cd**
	PPM	**PPM**	**PPM**	**PPM**	**PPM**	**PPM**	**PPM**	**PPM**	**PPM**	**PPM**	**%**	**%**	**PPM**	**PPM**	**PPM**	**PPM**	**PPM**	**PPM**	**PPM**
	0.05	**0.02**	**0.05**	**0.01**	**0.05**	**0.02**	**0.03**	**0.01**	**0.05**	**0.01**	**0.02**	**0.02**	**0.1**	**0.1**	**0.1**	**1**	**0.1**	**0.5**	**0.1**
BBC6	1.08	0.65	1.12	0.19	1.27	0.25	0.79	0.09	0.54	0.08	<0.02	<0.02	0.2	27.1	1.8	55	389.0	0.7	<0.1
BBC7	5.88	1.67	5.86	0.98	5.85	1.12	3.41	0.45	2.98	0.43	0.06	<0.02	0.7	117.6	1.5	54	20.8	0.9	<0.1
BBC8	5.32	1.56	5.51	0.94	5.61	1.11	3.06	0.43	2.80	0.40	0.03	<0.02	0.5	88.5	2.4	40	13.3	1.3	<0.1
BBC10	4.31	1.53	4.50	0.79	4.84	1.00	2.63	0.38	2.56	0.38	0.06	<0.02	0.4	90.4	1.6	56	15.1	0.5	<0.1
BBC11-A	11.52	3.00	12.88	1.97	11.27	2.20	5.96	0.80	4.98	0.75	0.05	<0.02	1.2	442.2	2.8	123	4.4	0.7	0.1
BBC11-B	11.89	2.87	13.01	1.97	11.60	2.18	5.97	0.78	5.00	0.73	0.14	<0.02	1.3	413.1	3.8	133	5.4	1.4	0.2
BBC12	15.36	3.22	16.27	2.57	15.02	2.98	7.85	1.08	6.72	0.95	0.05	<0.02	1.2	367.6	3.8	123	4.3	2.8	0.1
BBC13	3.13	1.07	3.35	0.57	3.28	0.68	1.85	0.25	1.79	0.26	<0.02	<0.02	0.2	75.4	2.1	59	87.7	0.5	<0.1
BBC14	4.06	1.44	4.45	0.73	4.16	0.83	2.38	0.37	2.32	0.33	0.02	<0.02	0.3	126.2	14.0	64	107.5	1.9	<0.1
SB10	4.64	1.56	4.97	0.85	5.26	0.98	2.82	0.42	2.61	0.39	0.02	<0.02	0.3	125.0	1.3	53	49.5	0.8	<0.1
SB11	7.58	2.11	7.73	1.26	7.50	1.47	4.21	0.62	3.77	0.57	0.06	<0.02	0.6	118.5	1.7	54	10.3	1.0	<0.1
SB12	10.96	3.00	11.73	1.88	11.69	2.20	6.29	0.92	5.70	0.84	<0.02	<0.02	0.4	185.6	2.7	65	3.3	1.0	<0.1
SB13	15.67	3.55	15.98	2.50	14.48	2.80	7.73	1.08	6.75	0.98	0.11	<0.02	1.0	342.4	4.2	102	0.5	1.1	0.2
SB14	13.28	3.92	13.63	2.01	11.03	1.96	5.30	0.73	4.11	0.59	0.04	0.02	0.4	729.2	1.5	83	0.6	0.9	<0.1
SB15	6.07	1.93	6.90	1.06	6.50	1.31	3.80	0.53	3.30	0.51	0.02	<0.02	0.4	138.7	1.2	50	31.4	<0.5	<0.1
SB16	4.89	1.62	4.99	0.84	4.97	1.01	2.59	0.40	2.41	0.39	0.02	<0.02	0.4	119.4	1.0	49	35.8	0.9	<0.1
SB17	13.99	3.77	14.10	2.09	11.88	2.18	5.73	0.76	4.39	0.67	<0.02	0.02	0.7	669.9	5.9	101	0.4	1.9	0.2

Appendix - C - Whole-Rock Lithogeochemistry

	AQ200	AQ200	AQ200	AQ200	AQ200	AQ200	AQ200
	Sb	**Bi**	**Ag**	**Au**	**Hg**	**Tl**	**Se**
	PPM	**PPM**	**PPM**	**PPB**	**PPM**	**PPM**	**PPM**
	0.1	**0.1**	**0.1**	**0.5**	**0.01**	**0.1**	**0.5**
BBC6	<0.1	<0.1	<0.1	<0.5	<0.01	<0.1	<0.5
BBC7	<0.1	<0.1	<0.1	1.1	<0.01	<0.1	<0.5
BBC8	<0.1	<0.1	<0.1	3.5	<0.01	<0.1	<0.5
BBC10	<0.1	<0.1	<0.1	<0.5	<0.01	<0.1	<0.5
BBC11-A	<0.1	<0.1	0.1	2.6	<0.01	<0.1	<0.5
BBC11-B	0.1	<0.1	0.1	0.8	<0.01	<0.1	
BBC12	0.1	<0.1	<0.1	2.1	<0.01	<0.1	0.5
BBC13	<0.1	<0.1	<0.1	1.2	<0.01	<0.1	<0.5
BBC14	<0.1	<0.1	<0.1	<0.5	<0.01	0.1	<0.5
SB10	<0.1	<0.1	<0.1	1.9	<0.01	<0.1	<0.5
SB11	<0.1	<0.1	<0.1	2.5	<0.01	<0.1	<0.5
SB12	<0.1	<0.1	<0.1	3.0	<0.01	<0.1	<0.5
SB13	<0.1	<0.1	<0.1	<0.5	<0.01	<0.1	0.8
SB14	<0.1	<0.1	0.3	<0.5	<0.01	<0.1	
SB15	<0.1	<0.1	<0.1	2.6	<0.01	<0.1	
SB16	<0.1	<0.1	<0.1	3.6	0.01	<0.1	
SB17	<0.1	<0.1	0.2	0.9	<0.01	<0.1	